

The Textile Institute and Woodhead Publishing

The Textile Institute is a unique organisation in textiles, clothing and footwear. Incorporated in England by a Royal Charter granted in 1925, the Institute has individual and corporate members in over 90 countries. The aim of the Institute is to facilitate learning, recognise achievement, reward excellence and disseminate information within the global textiles, clothing and footwear industries.

Historically, The Textile Institute has published books of interest to its members and the textile industry. To maintain this policy, the Institute has entered into partnership with Woodhead Publishing Limited to ensure that Institute members and the textile industry continue to have access to high calibre titles on textile science and technology.

Most Woodhead titles on textiles are now published in collaboration with The Textile Institute. Through this arrangement, the Institute provides an Editorial Board which advises Woodhead on appropriate titles for future publication and suggests possible editors and authors for these books. Each book published under this arrangement carries the Institute's logo.

Woodhead books published in collaboration with The Textile Institute are offered to Textile Institute members at a substantial discount. These books, together with those published by The Textile Institute that are still in print, are offered on the Elsevier website at: <http://store.elsevier.com/>. Textile Institute books still in print are also available directly from the Institute's web site at: www.textileinstitutebooks.com/.

A list of Woodhead books on textiles science and technology, most of which have been published in collaboration with the Textile Institute, can be found towards the end of the contents pages.

Related titles

Functional Finishes for Textiles

(ISBN 978-0-85709-839-9)

Advances in Shape Memory Polymers

(ISBN 978-0-85709-852-8)

Woodhead Publishing

(ISBN 978-0-85709-843-6)

Woodhead Publishing Series in Textiles:
Number 176

Active Coatings for Smart Textiles

Edited by

Jinlian Hu



The Textile Institute



ELSEVIER

AMSTERDAM • BOSTON • CAMBRIDGE • HEIDELBERG
LONDON • NEW YORK • OXFORD • PARIS • SAN DIEGO
SAN FRANCISCO • SINGAPORE • SYDNEY • TOKYO

Woodhead Publishing is an imprint of Elsevier



Woodhead Publishing is an imprint of Elsevier
The Officers' Mess Business Centre, Royston Road, Duxford, CB22 4QH, UK
50 Hampshire Street, 5th Floor, Cambridge, MA 02139, USA
The Boulevard, Langford Lane, Kidlington, OX5 1GB, UK

Copyright © 2016 Elsevier Ltd. All rights reserved.

No part of this publication may be reproduced or transmitted in any form or by any means, electronic or mechanical, including photocopying, recording, or any information storage and retrieval system, without permission in writing from the publisher. Details on how to seek permission, further information about the Publisher's permissions policies and our arrangements with organizations such as the Copyright Clearance Center and the Copyright Licensing Agency, can be found at our website: www.elsevier.com/permissions.

This book and the individual contributions contained in it are protected under copyright by the Publisher (other than as may be noted herein).

Notices

Knowledge and best practice in this field are constantly changing. As new research and experience broaden our understanding, changes in research methods, professional practices, or medical treatment may become necessary.

Practitioners and researchers must always rely on their own experience and knowledge in evaluating and using any information, methods, compounds, or experiments described herein. In using such information or methods they should be mindful of their own safety and the safety of others, including parties for whom they have a professional responsibility.

To the fullest extent of the law, neither the Publisher nor the authors, contributors, or editors, assume any liability for any injury and/or damage to persons or property as a matter of products liability, negligence or otherwise, or from any use or operation of any methods, products, instructions, or ideas contained in the material herein.

British Library Cataloguing-in-Publication Data

A catalogue record for this book is available from the British Library

Library of Congress Cataloguing-in-Publication Data

A catalog record for this book is available from the Library of Congress

ISBN: 978-0-08-100263-6 (print)

ISBN: 978-0-08-100265-0 (online)

For information on all Woodhead Publishing publications
visit our website at <https://www.elsevier.com/>



Working together
to grow libraries in
developing countries

www.elsevier.com • www.bookaid.org

Publisher: Matthew Deans

Acquisition Editor: David Jackson

Editorial Project Manager: Edward Payne

Production Project Manager: Debasish Ghosh

Designer: Vicky Pearson Esser

Typeset by TNQ Books and Journals

List of contributors

- R. Alagirusamy** Indian Institute of Technology Delhi, Delhi, India
- F. Alimohammadi** Clarkson University, Potsdam, NY, USA; Young Researchers and Elites Club, Islamic Azad University, South Tehran Branch, Tehran, Iran
- H. Cao** University of Delaware, Newark, DE, United States
- A. Das** Indian Institute of Technology Delhi, Delhi, India
- I. De Vilder** Centexbel, Textile Competence Centre, Ghent, Belgium
- H. Fan** Research Institute for Biomimetics and Soft Matter, Fujian Provincial Key Lab for Soft Functional Materials Research, Xiamen University, Xiamen, China
- P. Heyse** Centexbel, Textile Competence Centre, Ghent, Belgium
- J.L. Hu** Institute of Textiles and Clothing, The Hong Kong Polytechnic University, Hung Hom, Hong Kong
- D. Jovic** University of Belgrade, Belgrade, Serbia
- C.-W. Kan** The Hong Kong Polytechnic University, Kowloon, Hong Kong
- A. Kaynak** Deakin University, Geelong, VIC, Australia
- J. Kiwi** Ecole Polytechnique Fédérale de Lausanne, Lausanne, Switzerland
- L. Leclercq** Lille University, Science and Technology, Villeneuve d'Ascq Cedex, France
- N. Lin** Research Institute for Biomimetics and Soft Matter, Fujian Provincial Key Lab for Soft Functional Materials Research, Xiamen University, Xiamen, China
- G. Liu** Zhejiang Sci-Tech University, Hangzhou, China
- X.Y. Liu** Research Institute for Biomimetics and Soft Matter, Fujian Provincial Key Lab for Soft Functional Materials Research, Xiamen University, Xiamen, China; Department of Physics, FOS, National University of Singapore, Singapore
- J. Lu** Institute of Textiles and Clothing, The Hong Kong Polytechnic University, Hung Hom, Hong Kong
- M. Manshahia** Amity University, Noida, Uttar Pradesh, India
- R.E. Meirowitz** RnD Technical Solutions Inc., San Diego, CA, United States

- V.K. Midha** National Institute of Technology Jalandhar, Punjab, India
- A. Mukhopadhyay** National Institute of Technology Jalandhar, Punjab, India
- E. Pakdel** Deakin University, Geelong, VIC, Australia
- M. Parvinezadeh Gashti** Young Researchers and Elites Club, Yadegar-e-Imam Khomeini (RAH) Branch, Islamic Azad University, Tehran, Iran
- A. Ritter** Ritter Architekten, Germany
- S. Rtimi** Ecole Polytechnique Fédérale de Lausanne, Lausanne, Switzerland
- F. Salaün** University of Lille Nord de France, Lille, France; ENSAIT, GEMTEX, Roubaix, France
- J. Shao** Zhejiang Sci-Tech University, Hangzhou, China
- M. Vanneste** Centexbel, Textile Competence Centre, Ghent, Belgium
- C. Wang** Jiangnan University, Wuxi, China
- Y. Yin** Jiangnan University, Wuxi, China
- L. Zhou** Zhejiang Sci-Tech University, Hangzhou, China

Woodhead Publishing Series in Textiles

- 1 **Watson's textile design and colour** Seventh edition
Edited by Z. Grosicki
- 2 **Watson's advanced textile design**
Edited by Z. Grosicki
- 3 **Weaving** Second edition
P. R. Lord and M. H. Mohamed
- 4 **Handbook of textile fibres Volume 1: Natural fibres**
J. Gordon Cook
- 5 **Handbook of textile fibres Volume 2: Man-made fibres**
J. Gordon Cook
- 6 **Recycling textile and plastic waste**
Edited by A. R. Horrocks
- 7 **New fibers** Second edition
T. Hongu and G. O. Phillips
- 8 **Atlas of fibre fracture and damage to textiles** Second edition
J. W. S. Hearle, B. Lomas and W. D. Cooke
- 9 **Ecotextile '98**
Edited by A. R. Horrocks
- 10 **Physical testing of textiles**
B. P. Saville
- 11 **Geometric symmetry in patterns and tilings**
C. E. Horne
- 12 **Handbook of technical textiles**
Edited by A. R. Horrocks and S. C. Anand
- 13 **Textiles in automotive engineering**
W. Fung and J. M. Hardcastle
- 14 **Handbook of textile design**
J. Wilson
- 15 **High-performance fibres**
Edited by J. W. S. Hearle
- 16 **Knitting technology** Third edition
D. J. Spencer
- 17 **Medical textiles**
Edited by S. C. Anand
- 18 **Regenerated cellulose fibres**
Edited by C. Woodings
- 19 **Silk, mohair, cashmere and other luxury fibres**
Edited by R. R. Franck

-
- 20 **Smart fibres, fabrics and clothing**
Edited by X. M. Tao
- 21 **Yarn texturing technology**
J. W. S. Hearle, L. Hollick and D. K. Wilson
- 22 **Encyclopedia of textile finishing**
H.-K. Rouette
- 23 **Coated and laminated textiles**
W. Fung
- 24 **Fancy yarns**
R. H. Gong and R. M. Wright
- 25 **Wool: Science and technology**
Edited by W. S. Simpson and G. Crawshaw
- 26 **Dictionary of textile finishing**
H.-K. Rouette
- 27 **Environmental impact of textiles**
K. Slater
- 28 **Handbook of yarn production**
P. R. Lord
- 29 **Textile processing with enzymes**
Edited by A. Cavaco-Paulo and G. Gübitz
- 30 **The China and Hong Kong denim industry**
Y. Li, L. Yao and K. W. Yeung
- 31 **The World Trade Organization and international denim trading**
Y. Li, Y. Shen, L. Yao and E. Newton
- 32 **Chemical finishing of textiles**
W. D. Schindler and P. J. Hauser
- 33 **Clothing appearance and fit**
J. Fan, W. Yu and L. Hunter
- 34 **Handbook of fibre rope technology**
H. A. McKenna, J. W. S. Hearle and N. O'Hear
- 35 **Structure and mechanics of woven fabrics**
J.L. Hu
- 36 **Synthetic fibres: Nylon, polyester, acrylic, polyolefin**
Edited by J. E. McIntyre
- 37 **Woollen and worsted woven fabric design**
E. G. Gilligan
- 38 **Analytical electrochemistry in textiles**
P. Westbroek, G. Priniotakis and P. Kiekens
- 39 **Bast and other plant fibres**
R. R. Franck
- 40 **Chemical testing of textiles**
Edited by Q. Fan
- 41 **Design and manufacture of textile composites**
Edited by A. C. Long
- 42 **Effect of mechanical and physical properties on fabric hand**
Edited by H. M. Behery
- 43 **New millennium fibers**
T. Hongu, M. Takigami and G. O. Phillips

-
- 44 **Textiles for protection**
Edited by R. A. Scott
- 45 **Textiles in sport**
Edited by R. Shishoo
- 46 **Wearable electronics and photonics**
Edited by X. M. Tao
- 47 **Biodegradable and sustainable fibres**
Edited by R. S. Blackburn
- 48 **Medical textiles and biomaterials for healthcare**
Edited by S. C. Anand, M. MirafTAB, S. Rajendran and J. F. Kennedy
- 49 **Total colour management in textiles**
Edited by J. Xin
- 50 **Recycling in textiles**
Edited by Y. Wang
- 51 **Clothing biosensory engineering**
Y. Li and A. S. W. Wong
- 52 **Biomechanical engineering of textiles and clothing**
Edited by Y. Li and D. X.-Q. Dai
- 53 **Digital printing of textiles**
Edited by H. Ujiie
- 54 **Intelligent textiles and clothing**
Edited by H. R. Mattila
- 55 **Innovation and technology of women's intimate apparel**
W. Yu, J. Fan, S. C. Harlock and S. P. Ng
- 56 **Thermal and moisture transport in fibrous materials**
Edited by N. Pan and P. Gibson
- 57 **Geosynthetics in civil engineering**
Edited by R. W. Sarsby
- 58 **Handbook of nonwovens**
Edited by S. Russell
- 59 **Cotton: Science and technology**
Edited by S. Gordon and Y.-L. Hsieh
- 60 **Ecotextiles**
Edited by M. MirafTAB and A. R. Horrocks
- 61 **Composite forming technologies**
Edited by A. C. Long
- 62 **Plasma technology for textiles**
Edited by R. Shishoo
- 63 **Smart textiles for medicine and healthcare**
Edited by L. Van Langenhove
- 64 **Sizing in clothing**
Edited by S. Ashdown
- 65 **Shape memory polymers and textiles**
J.L. Hu
- 66 **Environmental aspects of textile dyeing**
Edited by R. Christie
- 67 **Nanofibers and nanotechnology in textiles**
Edited by P. Brown and K. Stevens

-
- 68 **Physical properties of textile fibres Fourth edition**
W. E. Morton and J. W. S. Hearle
- 69 **Advances in apparel production**
Edited by C. Fairhurst
- 70 **Advances in fire retardant materials**
Edited by A. R. Horrocks and D. Price
- 71 **Polyesters and polyamides**
Edited by B. L. Deopura, R. Alagirusamy, M. Joshi and B. S. Gupta
- 72 **Advances in wool technology**
Edited by N. A. G. Johnson and I. Russell
- 73 **Military textiles**
Edited by E. Wilusz
- 74 **3D fibrous assemblies: Properties, applications and modelling of three-dimensional textile structures**
J.L. Hu
- 75 **Medical and healthcare textiles**
Edited by S. C. Anand, J. F. Kennedy, M. MirafTAB and S. Rajendran
- 76 **Fabric testing**
Edited by J.L. Hu
- 77 **Biologically inspired textiles**
Edited by A. Abbott and M. Ellison
- 78 **Friction in textile materials**
Edited by B. S. Gupta
- 79 **Textile advances in the automotive industry**
Edited by R. Shishoo
- 80 **Structure and mechanics of textile fibre assemblies**
Edited by P. Schwartz
- 81 **Engineering textiles: Integrating the design and manufacture of textile products**
Edited by Y. E. El-Mogahzy
- 82 **Polyolefin fibres: Industrial and medical applications**
Edited by S. C. O. Ugbolue
- 83 **Smart clothes and wearable technology**
Edited by J. McCann and D. Bryson
- 84 **Identification of textile fibres**
Edited by M. Houck
- 85 **Advanced textiles for wound care**
Edited by S. Rajendran
- 86 **Fatigue failure of textile fibres**
Edited by M. MirafTAB
- 87 **Advances in carpet technology**
Edited by K. Goswami
- 88 **Handbook of textile fibre structure Volume 1 and Volume 2**
Edited by S. J. Eichhorn, J. W. S. Hearle, M. Jaffe and T. Kikutani
- 89 **Advances in knitting technology**
Edited by K.-F. Au
- 90 **Smart textile coatings and laminates**
Edited by W. C. Smith
- 91 **Handbook of tensile properties of textile and technical fibres**
Edited by A. R. Bunsell

-
- 92 **Interior textiles: Design and developments**
Edited by T. Rowe
- 93 **Textiles for cold weather apparel**
Edited by J. T. Williams
- 94 **Modelling and predicting textile behaviour**
Edited by X. Chen
- 95 **Textiles, polymers and composites for buildings**
Edited by G. Pohl
- 96 **Engineering apparel fabrics and garments**
J. Fan and L. Hunter
- 97 **Surface modification of textiles**
Edited by Q. Wei
- 98 **Sustainable textiles**
Edited by R. S. Blackburn
- 99 **Advances in yarn spinning technology**
Edited by C. A. Lawrence
- 100 **Handbook of medical textiles**
Edited by V. T. Bartels
- 101 **Technical textile yarns**
Edited by R. Alagirusamy and A. Das
- 102 **Applications of nonwovens in technical textiles**
Edited by R. A. Chapman
- 103 **Colour measurement: Principles, advances and industrial applications**
Edited by M. L. Gulrajani
- 104 **Fibrous and composite materials for civil engineering applications**
Edited by R. Figueiro
- 105 **New product development in textiles: Innovation and production**
Edited by L. Horne
- 106 **Improving comfort in clothing**
Edited by G. Song
- 107 **Advances in textile biotechnology**
Edited by V. A. Nierstrasz and A. Cavaco-Paulo
- 108 **Textiles for hygiene and infection control**
Edited by B. McCarthy
- 109 **Nanofunctional textiles**
Edited by Y. Li
- 110 **Joining textiles: Principles and applications**
Edited by I. Jones and G. Stylios
- 111 **Soft computing in textile engineering**
Edited by A. Majumdar
- 112 **Textile design**
Edited by A. Briggs-Goode and K. Townsend
- 113 **Biotextiles as medical implants**
Edited by M. W. King, B. S. Gupta and R. Guidoin
- 114 **Textile thermal bioengineering**
Edited by Y. Li
- 115 **Woven textile structure**
B. K. Behera and P. K. Hari

- 116 **Handbook of textile and industrial dyeing Volume 1: Principles, processes and types of dyes**
Edited by M. Clark
- 117 **Handbook of textile and industrial dyeing Volume 2: Applications of dyes**
Edited by M. Clark
- 118 **Handbook of natural fibres Volume 1: Types, properties and factors affecting breeding and cultivation**
Edited by R. Kozłowski
- 119 **Handbook of natural fibres Volume 2: Processing and applications**
Edited by R. Kozłowski
- 120 **Functional textiles for improved performance, protection and health**
Edited by N. Pan and G. Sun
- 121 **Computer technology for textiles and apparel**
Edited by J.L. Hu
- 122 **Advances in military textiles and personal equipment**
Edited by E. Sparks
- 123 **Specialist yarn and fabric structures**
Edited by R. H. Gong
- 124 **Handbook of sustainable textile production**
M. I. Tobler-Rohr
- 125 **Woven textiles: Principles, developments and applications**
Edited by K. Gandhi
- 126 **Textiles and fashion: Materials design and technology**
Edited by R. Sinclair
- 127 **Industrial cutting of textile materials**
I. Viļumsone-Nemes
- 128 **Colour design: Theories and applications**
Edited by J. Best
- 129 **False twist textured yarns**
C. Atkinson
- 130 **Modelling, simulation and control of the dyeing process**
R. Shamey and X. Zhao
- 131 **Process control in textile manufacturing**
Edited by A. Majumdar, A. Das, R. Alagirusamy and V. K. Kothari
- 132 **Understanding and improving the durability of textiles**
Edited by P. A. Annis
- 133 **Smart textiles for protection**
Edited by R. A. Chapman
- 134 **Functional nanofibers and applications**
Edited by Q. Wei
- 135 **The global textile and clothing industry: Technological advances and future challenges**
Edited by R. Shishoo
- 136 **Simulation in textile technology: Theory and applications**
Edited by D. Veit
- 137 **Pattern cutting for clothing using CAD: How to use Lectra Modaris pattern cutting software**
M. Stott

-
- 138 **Advances in the dyeing and finishing of technical textiles**
M. L. Gulrajani
- 139 **Multidisciplinary know-how for smart textiles developers**
Edited by T. Kirstein
- 140 **Handbook of fire resistant textiles**
Edited by F. Selcen Kilinc
- 141 **Handbook of footwear design and manufacture**
Edited by A. Luximon
- 142 **Textile-led design for the active ageing population**
Edited by J. McCann and D. Bryson
- 143 **Optimizing decision making in the apparel supply chain using artificial intelligence (AI): From production to retail**
Edited by W. K. Wong, Z. X. Guo and S. Y. S. Leung
- 144 **Mechanisms of flat weaving technology**
V. V. Choogin, P. Bandara and E. V. Chepelyuk
- 145 **Innovative jacquard textile design using digital technologies**
F. Ng and J. Zhou
- 146 **Advances in shape memory polymers**
J.L. Hu
- 147 **Design of clothing manufacturing processes: A systematic approach to planning, scheduling and control**
J. Gersak
- 148 **Anthropometry, apparel sizing and design**
D. Gupta and N. Zakaria
- 149 **Silk: Processing, properties and applications**
Edited by K. Murugesh Babu
- 150 **Advances in filament yarn spinning of textiles and polymers**
Edited by D. Zhang
- 151 **Designing apparel for consumers: The impact of body shape and size**
Edited by M.-E. Faust and S. Carrier
- 152 **Fashion supply chain management using radio frequency identification (RFID) technologies**
Edited by W. K. Wong and Z. X. Guo
- 153 **High performance textiles and their applications**
Edited by C. A. Lawrence
- 154 **Protective clothing: Managing thermal stress**
Edited by F. Wang and C. Gao
- 155 **Composite nonwoven materials**
Edited by D. Das and B. Pourdeyhimi
- 156 **Functional finishes for textiles: Improving comfort, performance and protection**
Edited by R. Paul
- 157 **Assessing the environmental impact of textiles and the clothing supply chain**
S. S. Muthu
- 158 **Braiding technology for textiles**
Y. Kyosev
- 159 **Principles of colour appearance and measurement**
Volume 1: Object appearance, colour perception and instrumental measurement
A. K. R. Choudhury

-
- 160 **Principles of colour appearance and measurement**
Volume 2: Visual measurement of colour, colour comparison and management
A. K. R. Choudhury
- 161 **Ink jet textile printing**
C. Cie
- 162 **Textiles for sportswear**
Edited by R. Shishoo
- 163 **Advances in silk science and technology**
Edited by A. Basu
- 164 **Denim: Manufacture, finishing and applications**
Edited by R. Paul
- 165 **Fabric structures in architecture**
Edited by J. Ignasi de Llorens
- 166 **Electronic textiles: Smart fabrics and wearable technology**
Edited by T. Dias
- 167 **Advances in 3D textiles**
Edited by X. Chen
- 168 **Garment manufacturing technology**
Edited by R. Nayak and R. Padhye
- 169 **Handbook of technical textiles Second edition Volume 1: Technical textile processes**
Edited by A. R. Horrocks and S. C. Anand
- 170 **Handbook of technical textiles Second edition Volume 2: Technical applications**
Edited by A. R. Horrocks and S. C. Anand
- 171 **Sustainable apparel**
Edited by R. S. Blackburn
- 172 **Handbook of life cycle assessment (LCA) of textiles and clothing**
Edited by S. S. Muthu
- 173 **Advances in smart medical textiles: Treatments and health monitoring**
Edited by L. van Langenhove
- 174 **Medical textile materials**
Y. Qin
- 175 **Geotextiles**
Edited by R. M. Koerner
- 176 **Active coatings for smart textiles**
Edited by J.L. Hu
- 177 **Advances in braiding technology: Specialized techniques and applications**
Edited by Y. Kyosev
- 178 **Smart textiles and their applications**
Edited by V. Koncar

Introduction to active coatings for smart textiles

1

J.L. Hu

Institute of Textiles and Clothing, The Hong Kong Polytechnic University, Hung Hom, Hong Kong

1.1 Introduction

The coating, finishing, and lamination of textiles are old arts and traditional technologies and are used in almost every area of industry and our lives. Laminating combines a fabric and a prepared film by adhesive, heat, and mechanical bonding, which replaces or supplements sewing to obtain laminated fabrics with enhanced function and more consistent qualities. However, it is easy to confuse the definitions of coating and finishing. The term “finishing” is usually used in a broad sense to refer to operations for improving the appearance or usefulness of a textile after it leaves the loom or knitting machine (Tomasino, 1992). These operations include washing, bleaching, coloring, and all kinds of chemical and mechanical steps that may comprise coating. In this book, “finishing” is used in its narrow definition (Schindler and Hauser, 2004), which is the final step in the textile manufacturing process (Fig. 1.1), which distinguishes it from a coating according to film continuity or morphology in processing technologies. Under this definition, finishing and coating both create the characteristics of textiles and endow them with special performance such as the final hand feeling. The coating also can complete yarn preparation such as warp sizing. In coating, a thick liquid chemical or paste is used that forms a continuous film on the yarn or textile surface, formed in situ. Gaps between fibers and yarns may disappear or narrow to varying degrees. In finishing, the light liquid chemical paste is applied and penetrates into the fibers and yarns to make up the textile, after which the gaps cannot be altered between the yarns and fibers (Fung, 2002).

Traditional textile coatings are commonly passive protections or decorations for the substrate for which they are designed and are applied by providing a barrier on the surface. Some advanced coatings include functional materials that enable the textiles to exhibit increased functionalities such as wrinkle free, flame retardant, etc. Furthermore, an active coating is to be considered smart. It is able to sense a change in conditions and respond to it in a predictable and conspicuous manner. Generally speaking, an active coating gives textiles intelligent properties more than just functional performance (Smith, 2010). The active coating senses the environment changing, responds to it, and does something by itself.

Active coatings can be categorized in many different ways based on the smart ingredients, fabrication technologies, and applications. For intelligent textiles or

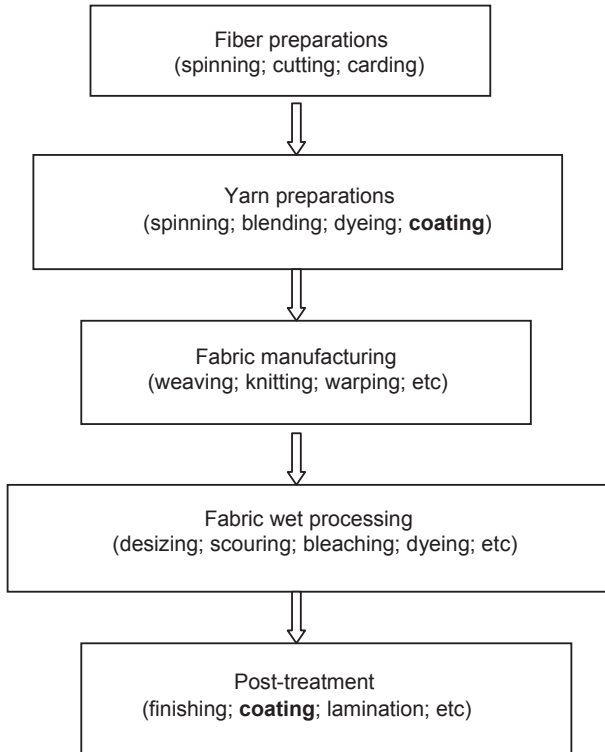


Figure 1.1 Coating positions in textile processing.

systems, there are normally three parts: a sensor, a processor, and an actuator (Tao, 2001; Mattila, 2006). Therefore, besides response, active coatings can consciously trace performance, for instance by remotely monitoring.

Intelligent materials contained in the coating layer can sense and respond to the environment, such as phase-change materials (Ghosh, 2006; Jyothi Sris et al., 2012), memory materials, and chromic materials. Active coatings by these intelligent materials acting as sensors can respond to changes in heat, light, chemicals, electronics, liquid, humidity, pressure, or bioactivity. Response may involve color change, shape adaptation, surface cleaning and healing, energy harvest and release, textile structure dimensional variance or drug release, and so on.

The smart ingredient within the active coating can be the polymer or resin itself, such as a memory polymer or a variety of additives consisting of nanoparticles for self-cleaning, pigments for color changing, microcapsules of phase-change materials for thermal regulation, microelectromechanical devices for wearable electronics, or antimicrobial agents for biomedical textiles. The successful combination of smart material science with advanced processing technology makes the active coating possible.

1.2 Functions and applications of active coating

Functions of textile coating are usually summarized according to their applied chemical properties, such as antibacterial, water resistance, etc. In this chapter, however, their functions are classified into three major categories; examples are listed in [Table 1.1](#) based on the type of common or active coating.

Applications of textile coating are listed only partially based on industrial and civilian uses. This is a good place to begin understanding common coatings and discuss potential applications for active coatings, which also have occurred or been applied in these areas and products: for example, in breathable garments with a water-responsive, variable-sized opening fabric structure; in antibacterial bedding; and in impact-active protection ([Table 1.2](#)).

Table 1.1 Functions of common and active textile coating

Categories	Common coating	Active coating
Aesthetic	Wrinkle free; flat appearance; dimensional stability; antistain; water or oil repellent; leather; color resistance	Color change; appearance retention; self-cleaning;
Comfort	Windproof; thermal resistance; water resistance; moisture management	Thermal adjustability; breathability
Protection	Humidity resistance; flame retardant; antiimpact; ultraviolet protection; antistatic; reflective; chemical resistance; blood resistance; anticorrosion; safety airbag; thermal insulating; aging resistance	Antibacterial; wearable electronics for biomedical use; self-healing; chemical odor absorbing and decomposing
Others	Filtration; stiffness	

Table 1.2 Applications of textile coatings

Areas	Examples
Clothing	Garments; footwear; accessories
Home furnishings	Upholstery; bedding; carpet
Medicals	Implants; barrier materials; bandages; hygiene products; health monitor
Industrial	Belts; hoses; filtration; screens; covers; liners; barriers; tents; separation; building reinforcement layer

1.3 Development of smart materials for active coating

Smart materials for active coating are mostly active materials which transport the sensing and responding properties to textiles by traditional coating technologies (Singha, 2012). Adaptive polymers can exhibit distinct and great changes when responding to a small stimulus. Accordingly, adaptive coating textiles have preprogrammed responses to small environmental changes. Different stimulations of active materials are listed; these have been applied in active coating textiles:

- heat and temperature
- pH value
- chemical and ionic strength
- electromagnetic radiation (ultraviolet, visible light)
- electrical and magnetic fields
- mechanical stress, strain, and pressure
- water and humidity

A number of active materials exist for textile coating, such as smart and polymeric hydrogels, memory polymers, phase-change materials, color-change materials, and functional nanomaterials.

Smart or polymeric hydrogels as a special classification of hydrogels display different changes under specific stimuli such as temperature, pH sensitivity, light, salt, and stress. Responses include swelling/collapsing and hydrophilic/hydrophobic changes in shape. The most commonly used hydrogels in active coating are temperature-active hydrogels with a transition temperature adjusted by additives, a modifying monomer structure, or copolymerization. The widely applied and known hydrogel active coating application is temperature-dependent water vapor permeability textiles, based on their swelling and integrity characteristics below and above the switch temperature.

Memory polymers can sense thermal, mechanical, electric, and magnetic stimuli and respond by changing shape, position, stiffness, and other static and dynamical characteristics. Memory polymers have found wide applications in textiles and other fields. Their low cost, good processing ability, and controllable responses make them more suitable for industrial production than memory alloy (Maria Rosa Aguilar, 2014; Hu, 2010). The functions of memory polymers can be achieved in many systems such as a molecular structure with covalent and noncovalent bonding or a supramolecular structure with novel quadruple hydrogen bonding. As a group of the most applicable smart materials, memory polymers have developed rapidly in both academics and industry areas in past decades.

Adaptive polymeric particles include nanoparticles and microcapsules. The benefits of smart materials combined with particle materials give an integrated and unique property to textile coating owing to their tiny forms and responsive characteristics, which are different from normal particles. The morphology, shape, size, light reflection/diffraction, and solvent ability are the important chemical and physical parameters of adaptive polymeric particles. The surface properties of nanoparticles are more essential than those of microcapsules. The surface energy, surface structure, and

reaction ability can be modified to serve the active requirements of coating textiles. There are different methods for obtaining adaptive polymer particles, such as the core–shell structure microencapsulation technique and surface modification. Applications of active coating of these particles include self-cleaning textiles, phase-change microencapsulation textiles, and hydrophilic/hydrophobic textiles.

1.4 Development of processing technologies for active coating

Many traditional coating techniques have been applied in the active textiles industry (Sen, 2007). These may include, but not limited to:

- yarn coating
- spread coating
- dipping
- calendaring
- extrusion coating
- foam coating
- rotary screen coating

Coating processes vary, but the objective of all of the technologies is to produce stable films with desired adhesion and designed functions on the substrate surface. Some new technologies such as microencapsulation, plasma technology, nanotechnology, and sol–gel technology have been applied in the coating process to achieve functional and active textiles.

Plasma offers a uniquely effective surface treatment effects because of its physical and chemical range and low temperature, low energy cost, and environmentally friendly nature (Shishoo, 2007). The study or potential use of the plasma finishing of textiles may achieve futuristic results such as the hydrophilic/hydrophobic enhancement of water and oil-repellent textiles, antibacterial textiles by coating functional particles in the plasma, a flame-retardant coating using monomer vapor, and the electroconductivity of textiles by surface plasma coating.

Nanotechnology-based coating is different from traditional coating methods such as dipping and soaking. The thickness of nanocoating film is less than 100 nm and is formed and processed by atomistic or molecular deposition technology such as chemical vapor deposition, physical vapor deposition, electroplating, and self-assembly (Schindler and Hauser, 2004; Hyde, 2008). The most commonly used ones are nanoparticles and nanocomposites. Nanotechnology-based coatings not only achieve the active properties of textiles but ensure that the fabrics have the ability to breath and drape and have hand characteristics comparable to untreated fabric (Chow et al., 2000). Because of the higher surface energy between the nanocoating layer and the fabric surface, the durability of these textiles is better than traditional finishes.

Sol–gel coating is also an effective technology to obtain active textiles. The sol–gel technique offers a low-temperature method for material synthesis with totally

inorganic or both inorganic and organic results. Several methods can be applied to obtain sol–gel coatings with the sol–gel process (Huang et al., 2001). Spin coating, dip coating, and roll coating are basic techniques used to deposit sol–gel coatings.

Microencapsulation has been proven as a successful technology in the pharmaceutical and agrochemical industries. The technology allows combinations to be made of the properties of different materials that will achieve various active performances from the smart textiles.

1.5 Outline of the book

This edited book is intended to provide an overview and review of the latest developments in active coating materials and the technologies of textiles for smart clothing, protective clothing, and equipment, and biomedical and industrial applications. It targets readers including researchers in materials science textile processing; engineers in the area of smart textiles product developments; architects, medical scientists, equipment developers, and students in colleges and universities.

The book has been contributed to by a panel of international researchers and experts in the field and covers various aspects of active coating research and development. It is composed of 18 chapters, which can be divided into three parts except this chapter, the introduction, which provides background information on active coating technology for textiles including a brief overview of active and smart materials, coating technologies, and the book's structure. The first part involves a classification of main active coatings from Chapters 2 to 8. Chapter 2 is concerned with memory polymers and their smart coating for appearance and structure retention, and hydrophobic/hydrophilic textiles. Chapter 3 deals with active coating by nanoparticles for self-cleaning textiles. Chapter 4 presents self-healing and durable textile coatings using a specific memory material. Chapter 5 involves smart breathable textiles coated with a water vapor permeability-controlled material. Chapter 6 presents protein coatings for smart textiles, and Chapter 7 discusses natural photonic materials for textile coatings.

The second part contains six chapters from Chapters 8 to 13, with a focus on coating processes and techniques for active textiles. Chapter 8 provides an overview of the developments and key issues in coating techniques and processes which integrate smart materials and textiles. Chapters 9–13 describe advanced technologies and principles for active coating, which consist of microencapsulation technology, plasma surface treatment, nanotechnology, biomimetic coating technology, and sol–gel technology.

The third part focuses on applications of active coating textiles. Chapter 14 outlines various smart coatings for comfort clothing and Chapter 15 concentrates on smart coatings for sportswear. Chapter 16 describes the applications of smart coatings for protective clothing and equipment. Chapter 17 introduces medical applications of smart coating textiles for patient care and wound dressings. Chapter 18 describes applications in architecture textiles.

References

- Chow, G.M., Ovid'ko, I.A., Tsakalakos, T., 2000. *Nanostructured Films and Coatings*. Kluwer Academic Publishers.
- Fung, W., 2002. *Coated and Laminated Textiles*. Woodhead Publishing Ltd.
- Ghosh, S.K., 2006. *Functional Coatings: By Polymer Microencapsulation*. Wiley.
- Hu, J., 2010. *Adaptive and Functional Polymers Textiles and Applications*. Publishing With World Scientific.
- Hyde, G.K., 2008. *Functional Textiles via Self-assembled Nanoalayers and Atomic Layer Deposition*. Fiber and Polymer Science (Ph.D.). North Carolina State University.
- Huang, Y., Zheng, H., Ball, I., Luo, Z., 2001. Advances in sol-gel technology. *Ceramic Industry* 12, 17–19.
- Jyothi Sris, A.S., Suria Prabha, K., Muthprasanna, P., 2012. Microencapsulation: a review. *International Journal of Pharma and Bio Sciences* 3, 509–531.
- Maria Rosa Aguilar, J.S.R., 2014. *Smart Polymers and Their Applications*. Woodhead Publishing.
- Mattila, H., 2006. *Intelligent Textiles and Clothing*. Woodhead Publishing.
- Sen, A.K., 2007. *Coated Textiles: Principles and Applications*, second ed. CPC Press.
- Shishoo, R., 2007. *Plasma Technologies for Textiles*. Woodhead Publishing.
- Singha, K., 2012. A review on coating & lamination in textiles: processes and Applications. *American Journal of Polymer Science* 2 (3), 39–49.
- Smith, W.C., 2010. *Smart Textile Coatings and Laminates*. Woodhead Publishing Ltd.
- Schindler, W.D., Hauser, P.J., 2004. *Chemical Finishing of Textiles*. Woodhead Publishing Ltd.
- Tao, X., 2001. *Smart Fibers, Fabrics and Clothing: Fundamentals and Applications*. Elsevier Publishing Ltd.
- Tomasino, C., 1992. *Chemistry and Technology of Fabric Preparation and Finishing* (Ph.D.). College of Textiles, North Carolina State University, p. 245.

Memory polymer coatings for smart textiles

2

J.L. Hu, J. Lu

Institute of Textiles and Clothing, The Hong Kong Polytechnic University,
Hung Hom, Hong Kong

2.1 Introduction

Memory materials can respond to different external stimuli in a controlled and predictable manner (adaptive polymers and textiles) and belong to smart materials, which display a response to a narrow range of external stimuli such as heat, water, light, and pressure. The property of shape memory is a widely known characteristic for materials, particularly polymers. However, many other properties can be memorized and recovered, such as color, stiffness, and natural frequency. Over the past few decades, research into memory polymers developed rapidly. Fundamental theories have been investigated extensively and a variety of different memory materials have been applied industrially. A large variety of alloys, polymers, gels, particles, and ceramics exhibit memory properties by synthesizing functional polymers with specific compositions, blending polymers with special molecules, designing special structures, and modifying with chemical or physical treatment. By integrating memory polymers into textiles structures, we can obtain novel functional or smart textiles with profoundly significant properties in areas such as aesthetic appeal, moisture/temperature management, protection against extreme climatic conditions, skin care, fantasy designs with color changes, controlled release, and smart wetting properties on textile surfaces. Many researchers have focused on the design and discovery of materials with smart-behaving textiles using coating technologies.

Memory polymer solutions can be used directly as a finishing or coating agent to obtain valuable properties in different types of textile fabrics. Accordingly, smart memory coating textiles also display predesigned or preprogrammed responses when meeting small external changes. Research and commercialized memory materials in smart coating textiles have been based mainly on shape memory polymers and responsive hydrogels. Besides shape-changing properties, other remarkable changes in physical and mechanical properties enable the materials to show novel smart functions to adapt to external changes in temperature, moisture, friction, light, and so on. There are many kinds of memory polymers but most are not suitable for textile applications. Comfort, the process, washing durability, cost and environmental friendliness are main considerations for memory polymers in textile applications.

Memory polymers can be applied on the textile surface by traditional methods such as the direct coating method, the padding—drying—curing method, the blade—cure method, and novel methods such as sol—gel technology. The memory polymer

structure, memory polymer coating functions, and mechanism of memory performance transferred from polymer to textiles will be introduced in this chapter.

2.2 Memory polymers

As mentioned, memorial materials are composed of large quantities of structures, from metals to polymers, composites, and ceramics. For smart textile coatings, memory polymers and their composites have been widely researched. Memory polymers mainly refer to shape memory polymers such as shape memory polyurethane (PU), polyester, polyhydroxyproline, polysilamine, etc., and some responsive hydrogels including poly(*N*-isopropylacrylamide) (PNIPAAm) hydrogels, polythiophene gel, etc. They also refer to memory polymer composites composed of shape memory polymer/cellulose composites, poly(*N*-vinyl carbazole) composites, shape memory polymer/nanowhiskers, etc. Memory polymers and their composites have several advantages for textile coatings: (1) They use different stimuli and triggers which textiles commonly undergo, such as water, light, and heat; (2) they have highly flexible programming, which can be done with various stimuli by single- or multiple-step processes; (3) they possess tunable properties that can be engineered easily to be applied onto the fabric surface; and (4) they have a light and adjustable modulus that is easily identical to a textile's softness. The structure, mechanism, and classification of memory polymers and gels will be introduced next.

2.2.1 Structures and mechanisms of memory polymers

Memory behavior can be demonstrated in various polymer systems that are different in molecular structure and morphology. Common conventional memory systems are listed in [Table 2.1](#).

Several types of structure and programming models have been proposed to describe the mechanism of the memory effects. In chemically cross-linked, semicrystalline, thermally responsive polyethylene (PE), the crystalline phase with a crystal melting

Table 2.1 Forms and molecular structures of memory polymers

Forms	Molecular structure
Cross-linked	Polyethylene, polycyclooctene
Copolymer	Dodecanedioic acid and bile acid-based polyesters
Cross-linked copolymer	Ethylenevinyl acetate
Segmented	Polyurethane ionomers, polyurethane
Others	Styrene-based polymers, acrylate-based polymers, epoxy-based polymers, thiophene-based polymers

temperature is used to provide temporary memory capacity and a chemically or physically cross-linked PE network takes charge of permanent memory ability, which ensures a return to the original shape with heating (Lendlein and Kelch, 2002; Rousseau and Mather, 2003). For a light-sensitive memory polymer (Lendlein et al., 2005), the chromophores are covalently grafted onto a cross-linked polymer network and the memory effect can be obtained through photoreversible cycloaddition reactions between chromophore molecules, ie, cinnamic acid-type molecules. For a water-sensitive memory polymer composite system with nanocellulose whiskers dispersed in an elastomer matrix, the reversible formation and disorganization of a network of nanocellulose whiskers in the polymer matrix makes a distinctive switching memory effect sensitive to water (Zhu et al., 2012).

Hu and Chen (2010) proposed a simple but reasonable, overall three-dimensional (3D) memory polymer architecture based on the development of molecular mechanisms. This model can describe almost all kinds of shape memory polymers (Table 2.2). Key components of this model are the switch units and netpoints. The netpoints cover chemical or physical cross-links, with an interpenetrated or interlocked supramolecular complex, which define the permanent shape of the polymer. Similarly, the switch unit takes charge of the shape fixity and recovery upon a specific and predetermined external stimulus. To date, the known switch units have been composed of amorphous, crystalline, and liquid crystal phases, supramolecular entities, light-reversible coupling groups, and newly used percolating cellulose-whisker networks. During the strain recovery process, the entropic elasticity from the polymer network is the driving force; thus, physical or chemical netpoints via intermolecular forces and/or covalent bonding are usually required.

Table 2.2 Overall mechanism of shape memory systems

Components	Structures	Mechanisms
Switch	Crystallization Glass transition Liquid crystallization Supramolecular hydrogen bonding Light-reduced reversible network Percolating network Hydrogen bonding Isomerization	Reversible phase-changing structures for temporary memory and recovery upon specific predetermined stimulus
Net point	Physical cross-linking Chemical cross-linking Interpenetrating network CDs (cyclodextrins) interlocking	Permanent shape determined owing to entropic elastic force from intermolecular forces and/or covalent bonding among netpoints

The focus of much research on memory polymers is to enhance their thermal and mechanical characteristics and expand their smart functions by implanting switch types to meet particular requirements. The molecular design method can develop tailor-made memory polymers and composites methods and offer simple and efficient ways to obtain special triggering mechanisms and functionalities. It is necessary and helpful to study the modeling of the structure and process memory effects and their processes. The following section presents an overview of the growth of memory switches and shape memory functionalities.

The switch unit is an important component which differentiates memory polymers from others. In the earliest reports, switches were either amorphous or semicrystalline phases. Researchers have been developing more special switches since then. Besides switches on a phase-transition level, other series of switches based on reversible molecular units have been exploited, such as supramolecular, photosensitive, and mercapto units, which have led to the emergence of new types of sensitivities such as moisture sensitivity and light sensitivity (Chen, 2009a,b; Wu et al., 2011). Switches of shape memory polymers are summarized in Table 2.3. From a phase level, three kinds of switch units have been studied: semicrystalline, amorphous, and liquid crystalline. Memory polymers based on phase-level switch units are commonly thermally sensitive polymers with transition temperatures of the glass transition temperature (T_g), melting transition temperature (T_m), or liquid crystal switch temperature (T_i).

Cross-linked PE is considered the first type of memory polymer based on semicrystallinity. Current polymeric segments used as semicrystalline phase switches for memory polymers can be divided into three types. The first is polyolefins such as PE (Morshedien et al., 2003), poly(ethylene-co-1-octene) (Kolesov et al., 2009), trans-polyisoprene (Sun and Ni, 2004), trans-polycyclooctene (Liu et al., 2002), and poly(1,4-butadiene) (Sakurai et al., 1994); the second type includes polyethers such as polyethylene oxide (PEO) (Luo et al., 1997), polyethylene glycol (PEG) (Meng and Hu, 2008), and poly(tetramethylene ether glycol) (Lee et al., 2001); and the third type covers polyesters such as poly(caprolactone) (PCL) (Ji et al., 2007; Lendlein et al., 2001; Hu et al., 2005), poly(butylene adipate) (Han et al., 2007), and poly(3-hydroxyalkanoate) (Chen et al., 2007a,b).

Memory polymers with amorphous phase switch units have been investigated to show relatively slow shape recovery effects compared with other phase-level switch memory polymers owing to the broader glass transition interval. Besides the thermal stimulus, memory polymers with amorphous phase switch units can be activated by a solvent or water (Yang et al., 2004, 2006; Huang et al., 2005; Du and Zhang, 2010) but the recovery stress is often small.

Liquid crystalline elastomers (LCEs) have a first-order phase transition with an endothermic peak on heating curves which shows the material's transition from an anisotropic to an isotropic phase. Similar to the T_g - and T_m -type memory polymers, chemical or physical cross-links are also required in T_i -type memory polymers made of LCEs to exhibit shape memory effects.

Nematic phase (Ahir et al., 2006) or smectic phase (Rousseau and Mather, 2003) is commonly used as a switch for liquid crystal memory polymers. Many types of liquid crystal memory polymers are thermally sensitive based on the T_i or the combination of

Table 2.3 Switches of shape memory polymers

Switches units		Memory polymer series	Stimuli/switch
Phase level	Semicrystalline phase	Polyolefins (PE, EOC (ethylene-co-octene copolymer), <i>trans</i> -polycyclooctene, etc.)	Thermal (T_m)
		Polyethers (polyethylene glycol, poly(tertramethylene ether glycol), polyethylene oxide, etc.)	
		Polyesters (poly(caprolactone), poly(butylene adipate), poly(3-hydroxyalkanoate), etc.)	
Molecular level	Amorphous phase	Epoxy, poly(ether ether ketone), acrylate-type polymers, polynorbornene, oligo((rac)lactide)- <i>co</i> -glycolide) PLGA, and poly(glycerol- <i>co</i> -dodecanoate)	Thermal (T_g); water; solvent
	Liquid crystalline phases	Nematic/smectic	Thermal ($T_i/T_g/T_m$)
		Photoresponsive	Photo (λ)
Molecular level	Photosensitive	Cinnamic groups	Photo (λ)
		Cinnamamide	
	Supramolecular	Ureidopyridinone (UPy)	Thermal
		Cyclic UPy	Thermal
		Pyridine derivative	Thermal/water
		Metal ligand	Thermal/light/ solvents
	Other reversible molecular	Mercapto	Redox
	Furyl-telechelic; poly(1,4-butylensuccinate- <i>co</i> -1,3-propylensuccinate) prepolymer; hydrogen; isomerization; reversible ionic dissociation	Thermal (T_m); pH; light	

T_i and T_g . Apart from thermally induced memory effects, photosensitive ones such as photoinduced contractions or bending have been obtained by liquid crystals which usually contain photoresponsive moieties (Li et al., 2003). Although the molecular mechanisms of light-induced and thermally induced memory liquid crystals are different, both of their memory behaviors result from the liquid crystal phase transition. Notably, most liquid crystal memory effects exhibit two-way behaviors (Ahir et al., 2006; Yu and Ikeda, 2006; Qin and Mather, 2009) or the materials can show triple memory effects that memorize more than one shape, because liquid crystals generally possess a low T_g or T_m in addition to the T_i . However, liquid crystal memory polymers are rarely used in textiles because of their high cost.

On a molecular level, movement of the polymer chain is controlled by intermolecular interactions or reversible chemistry reactions; the kind of switch can be divided into three main types: supramolecular, mercapto, and photosensitive units. The most popular molecular switch is photosensitive. Light can be rapidly, precisely, and remotely controlled, which is attractive for medical uses and others that need temperature limitations (Lendlein, 2005; Andreopoulos et al., 1998; Jiang et al., 2006; Zhu et al., 2003).

Reversible supramolecular units have been used in memory polymers to fix temporary shapes based on the mechanism of the stabilization of H-bonds at low temperatures. H-bonding moiety, ureidopyridinone (UPy), pyridine moieties, and cyclic UPy are commonly used as the side group to attain reversible fixing of the temporary shape (Li, 2007; Zhu et al., 2009).

Memory polymers with supramolecular switches can be designed to achieve thermally sensitive, water-sensitive, light-sensitive, solvent-sensitive, and redox-sensitive effects (Kushner et al., 2009; Chen, 2009a,b, 2010, 2011). Other special supramolecular reversible cross-linking moieties have been investigated, such as metal–ligand coordination bonds (Kumpfer and Rowan, 2011) and the mercapto group (Aoki et al., 2007). Three types of stimuli (heat, light, and solvents) can soften the hard phase and increase decomplexation or the rate of exchange of the metal–ligand switch. A mercapto group with cellulose acetate derivatives (Aoki et al., 2007) can achieve switching through redox treatments. Supramolecular switch units offer a great opportunity to create diversified memory performance and unexpected properties in the resultant memory polymers. Supramolecular switches are one of the most valuable directions for investigation in the future.

2.2.2 Classifications of memory polymers

Classifications of memory polymers have been widely discussed based on different methods. As reported, memory polymers can be thermally induced, light-induced, electroactive, water/moisture/solvent-induced, pH sensitive, and magnetically sensitive based on their external stimulus. According to the nature of their netpoints, physically cross-linked and chemically cross-linked ones are divided (Liu et al., 2007a,b; Ratna and Karger-Kocsis, 2008). Sometimes memory polymers are subdivided based on their switch type into either T_g type with an amorphous phase or T_m type with a crystalline phase (Ratna and Karger-Kocsis, 2008). Behl and Lendlein (2007) used actively moving polymers to classify them into shape memory and shape-changing

polymers. These classifications only partially show the principle of memory polymers and cannot be uniformly accepted.

From an integrated insight, the classification of memory polymers includes polymerization methods, structures, stimuli, and memory functionality. The composition and structure of memory polymers is composed of block/segmented copolymers (Korley et al., 2006; Chen et al., 2007a,b; Ji et al., 2007; Ji and Hu, 2011; Ji et al., 2011), chemically cross-linked polymers (Liu et al., 2002; Safranski and Gall, 2008; Yakacki et al., 2008), interpenetrating polymer networks (IPNs) (Zhang et al., 2007)/semi-IPNs (Liu et al., 2005a,b; Ratna and Karger-Kocsis, 2011; Rodriguez et al., 2011), polymer blends (Zhang et al., 2009; Kurahashi et al., 2012; Li and Tao, 2010), polymer composites (Zheng et al., 2006; Jang et al., 2009; Ivens et al., 2011; Fan et al., 2011), and even supramolecular polymer networks (Li et al., 2007). Almost all polymerization methods can be applied in the synthesis of memory polymers, including addition (Ji and Hu, 2011), condensation (Luo et al., 1997), shape memory PU, free-radical (Li et al., 2007) and photochemical polymerization (Lendlein et al., 2001), radiation reactions such as cross-linked PE (Zhu et al., 2003), acyclic diene metathesis polymerization (Del Rio et al., 2011), and even ring-open polymerization (Yang et al., 2010).

Moreover, diverse memory functions can be achieved by controlling the composition and chemistry/polymerization, which were developed from the conventional one-way memory effect to two-way, triple, and even multiple memory effects. In addition, multifunctionality (eg, permeable, optical, biodegradable, and thermal-chromic properties) can be achieved in one memory polymer (Behl et al., 2010).

From external stimuli such as heating and light, a redox condition (Aoki et al., 2007) or moisture is currently used to trigger strain recovery after deformation. As a widely and commonly used stimulus, heating can be achieved by direct or indirect heating, such as electrically induced (Cho et al., 2005; Sahoo et al., 2005), magnetically induced (Mohr et al., 2005; Schmidt, 2006), and infrared light-induced (Leng et al., 2010) heating. Thus, memory polymers can be categorized by their stimulus into the following four groups: (1) thermally induced; (2) athermal water (molecule) sensitive; (3) athermal light sensitive; and (4) redox sensitive.

Among memory polymers, smart gels also attract attention because of the different memory effects from shape memory polymers, and they have potential application in medical and industrial textiles and apparel. The netpoints of smart gels are covalent cross-linking, physical aggregation, and mesophases. Switches include hydrogen bonding, light-reduced reversible networks, etc. Smart gels exhibit sharp changes in response to external stimuli such as pH values, solvents, photo light, temperature, ionic strength, magnetic fields, electrical fields, and pressure (Mukae et al., 1990; Brannon-peppas and Peppas, 1991; Rodriguez et al., 2003; Stromberg and Hulth, 2003; He et al., 2008). Difference types of responses of memory gels are investigated, composed of reversible precipitation, reversible adsorption on a surface, and reversible collapse of surface graft polymers and reversible collapse of hydrogels (Hoffman, 2000).

Cross-linking netpoints are key structures of polymer gels, which create a 3D structure and gel configuration (Osada and Kajiwara, 2001). Based on the type of

cross-linking, chemical and physical gels are divided. Chemical gels are formed by a chemical reaction that cannot be dissolved again and is irreversible. Physical gels are formed by the physical entanglement of polymer chains and are reversibly responsive to temperature change, pH values, etc.; they are called reversible gels.

Temperature-sensitive polymeric gels are common; one of their features is that hydrophobic and hydrophilic groups coexist in one macromolecular network. PNIPAAm is a typical temperature-responsive gel. Below the lower critical solution temperature (LCST), the molecular chains of PNIPAAm are hydrated to an expanded form and are soluble in water. Above the LCST, PNIPAAm is in an insoluble form and dehydrates to a compact form. The temperature property of PNIPAAm can be controlled by the molecular design. The volume change can be achieved up to 1000 times when changing temperature. However, after repeated swelling/deswelling, the network structure of the gels becomes loose and the mechanical strength decreases (Ilavsky et al., 1985).

The most commonly used pH-responsive functional groups are carboxyl and pyridine. At low pH, carboxyl groups are protonated and hydrophobic interactions dominate, leading to volume shrinkage of the polymer. At high pH, carboxyl groups dissociate into carboxylate ions, resulting in a high charge density in the polymer and causing it to swell. In contrast to the alkali-swellaible carboxyl group, pyridine is an acid-swellaible group. Under acidic environmental conditions, the pyridine groups are protonated, resulting in internal charge repulsions between neighboring protonated pyridine groups. Charge repulsion leads to an expansion in the overall dimensions of the polymer. At higher pH values, the groups become less ionized, the charge repulsion is reduced, and polymer–polymer interactions increase, leading to a reduction in the overall hydrodynamic diameter of the polymer (Dupin et al., 2007; Stubenrauch et al., 2009).

Light as an external stimulus has several advantages, such as scalable miniaturization, limited chemical contamination, and ability to be controlled remotely (Lim et al., 2007). Photoresponsive hydrogels are mostly based on the following functional molecules and mechanisms: (1) photoisomerizable molecules such as azobenzenes (Finkelmann and Nishikawa, 2001); (2) photoreactive molecules such as cinnamates (Lendlein et al., 2005); (3) addition–fragmentation chain transfer reaction using allyl sulfides (Scott et al., 2006); and (4) reversible photo-induced ionic dissociation such as triphenylmethane leuco. Complicated movements such as oscillating, twisting, swimming (White et al., 2008), and rotation have been obtained on photoactive polymer gels and films (Yamada et al., 2009). The well-known function of photoresponsive hydrogels is the wettability of textiles.

2.3 Functions of memory coating textiles

2.3.1 Smart wettability control

The hydrophobic surface is a structure bioinspired from lotus leaves or shark skin using periodic micro- or nanosized patterns (Sun et al., 2009). In addition to micro- or nanoparticle coating or finishing on the textile surface, memory polymer coating

provides the same effects. The micro- or nanopattern effect is forced by the phase transformation of memory polymers. Two types of methods format the pattern, called the programmable pattern memorizing surface and the nonreprogramming reversible deformation surface. Programmable pattern memorizing surface was reported to fabricate dense patterns via nanoimprint lithography (Wang et al., 2011). A Non-programming reversible memory method (Higgins et al., 2011) uses electrochemical control of the polymer redox state to conceal and temporarily store preformed nano-scale surface patterns.

Micropatterns or nanopatterns or wrinkles can be produced by a coating method based on the principle of thermal mismatch-induced buckling of a thin elastic layer on a soft substrate (Lester et al., 1941). Currently, most wrinkles or patterns made by coating methods are elastic metal coated on a prestretched T_g -type memory polymer film or coated on no-prestraining memory polymers of the T_m type. If a memory polymer coating is used on a fiber surface, it will show different shrinkage effects after heating and cooling. Microwrinkles would form. This result exhibits a potential application for textile surface treatment to achieve a water-repellent effect or control water-spreading behavior. After studying water droplet spreading and patterned substrates using memory polymers, wetting anisotropy occurred when the droplets spread on anisotropically patterned substrates. The static contact angles were different in the direction parallel to wrinkles and perpendicular to wrinkles. When the water was spread perpendicular to the wrinkles, it showed a noncircular shape and the droplets were adhesive to their edges (Wang et al., 2011).

Besides hydrophobicity, controlling the movement of water on textile surfaces is of increasing interest. The behavior of water reverting from repellency (hydrophobic) to adhesion (hydrophilic) is governed by a combination of the contact angle between the water droplet and the surface, and the angle of the surface at which the droplet slides off.

To date, research has focused on altering the liquid to change the behavior or creating an array of different surfaces that produce the required effects. Xinyu Cao, Lei Jiang, Huai Yang, etc. have developed a technology that may provide the full range of hydrophobic to hydrophilic behavior just by changing the temperature based on a memory polymer coating (Li et al., 2009).

The researchers developed their surface by spin-coating a thin film of a liquid crystal polymer of PDMS-40CB, which has amphiphilic side chains, onto a silicon wafer etched with an array of pillars. The resulting surface has micrometer- or nanometer-scale roughness, which expands the range of contact angles possible. On one particular arrangement of pillars (pillars 10 μm wide and 30 μm high, spaced 15 μm apart), the water droplets rolled off at 23°C but adhered fast at 75°C even when the surface was held upside-down. The change in the behaviors of water on the surface was attributed to the phase transition of the polymer (Fig. 2.1). At room temperature (23°C), the polymer is in a liquid crystal smectic A phase but at 74.6°C, it converts to an isotropic phase. With increasing temperature, the orientation of side chains in the polymer changes: The hydrophilic chains can turn toward the water to minimize interfacial energy, which results in a decrease in the contact angle and stronger adhesion between the droplet and the surface. The spin-coating method can be easily scaled up and has potential for use in the volume production of textiles.

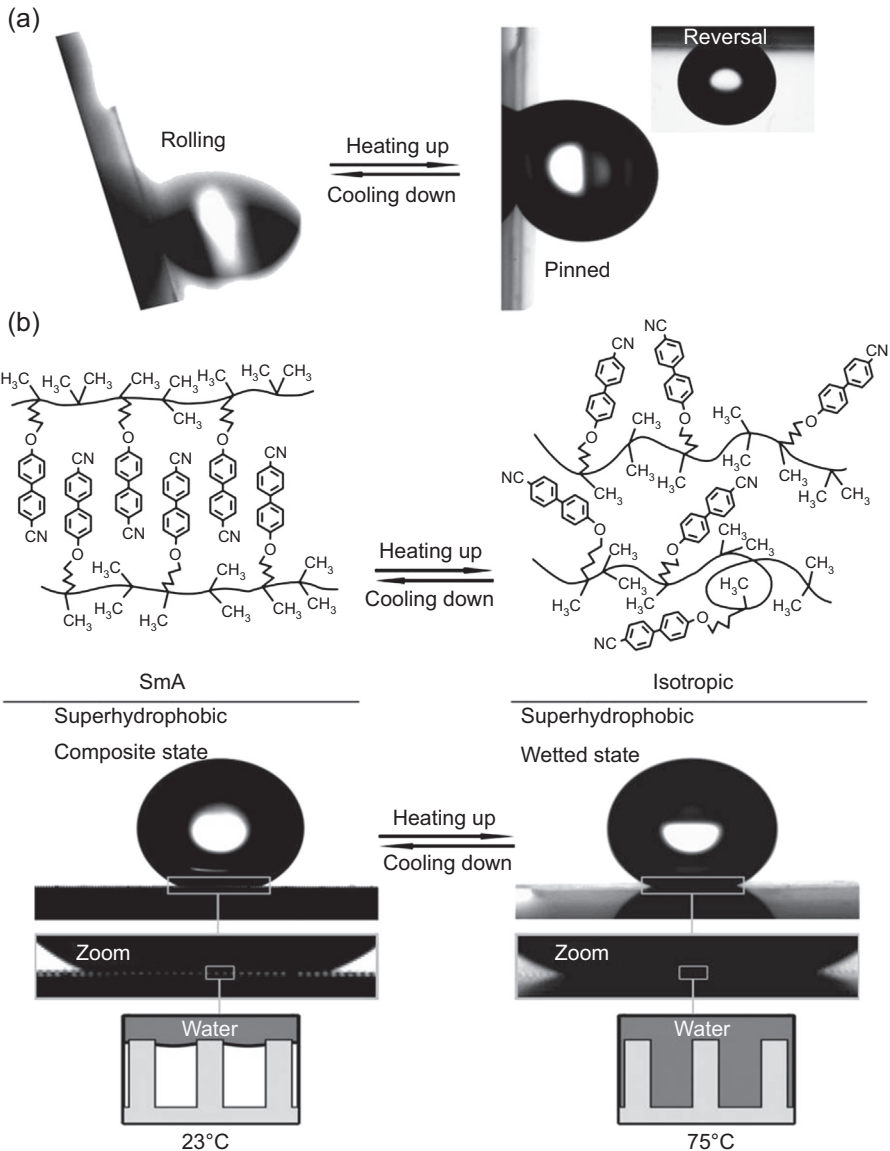


Figure 2.1 Wettability changing of a memory polymer coating surface. (a) Droplet sticks on the surface even when the substrate is turned upside down; (b) the proposed conformation rearrangement upon the phase transition.

Reproduced from Li, C., Guo, R., Jiang, X., Hu, S., Li, L., Cao, X., Yang, H., Song, Y., Ma, Y., Jiang, L., November 13, 2009. Reversible switching of water-droplet mobility on a superhydrophobic surface based on a phase transition of a side-chain liquid-crystal polymer. *Advanced Materials* 21 (42), 4254–4258.

PNIPAAm is a well-known temperature-sensitive polymer with a 32°C LCST. Below the LCST, the polymer swells and hydrophilicity occurs. Above the LCST, the polymer collapses and shows hydrophobicity. Based on this mechanism, reversible wettability can easily be achieved by changing the temperature below or above LCST.

This characteristic can be applied to a temperature-responsive drug delivery system and separation membrane (Chilkoti et al., 2002). For textiles, the hydrogel can be coated and grafted onto nonwoven fabrics for a wound dressing, which could absorb the tissue fluid, deliver drugs, and not adhere to the wound. This kind of hydrogel-coated nonwoven can also be used as a reusable facial mask. However, pure PNIPAAm is heavy above LCST, which is undesirable in a facial mask (Han and Bae, 1998). PU hydrogel is known to be biocompatible, and it exhibits elasticity and a high degree of swelling. A fabric-supported, chitosan-modified, temperature-responsive PNIPAAm (PNIPAAm/PU) hydrogel was reported for use in the preparation of facial masks; it feels tender and soft without obvious syneresis and rapidly responds to changes in temperature varying from 32°C to 35°C. Ingredients loaded in hydrogels are released slowly at body temperature; the incorporation of chitosan renders the facial mask antibacterial.

Besides temperature-active reversible wettability and water absorbency, light, pH, or redox also can control the water behavior of memory polymer coating surfaces by sol–gel method. Some inorganic oxides and memory polymers are photoresponsive materials. Under light, these materials can reversibly change their molecular conformation in solutions, crystals, and gels and then have physical property changes. As reported, the contact angle of TiO₂ polycrystalline coating can switch between 0 degree and 70 degree with the irradiation of visible light and UV. Besides the photoresponsive semiconductor inorganic oxides, azobenzene and its derivatives are widely used materials which show trans-conformation under visible light and turn to *cis*-conformation exposure to UV. When introducing low free energy groups on their side chain, the hydrophobic and hydrophilic transition can be obtained.

Poly(styrene-methyl methacrylate-acrylic acid) crystal films in the sodium dodecyl benzenesulfonate form could exhibit pH-responsive properties. At low pH, the hydrophobic long alkyl chain would be protruded outside, resulting in hydrophobic properties. At high pH, the hydrophilic groups were exposed to the outside, which led to hydrophilicity. Furthermore, polydimethylaminomethacrylate-grafted anodized alumina and some polycations could also achieve switchable wettability under pH stimulus (Fig. 2.2).

2.3.2 Self-healing liquid repellent

Self-healing means that damage is detected and repaired in situ. It is a new and innovative approach to extending the material's lifetime and durability in use. The main self-healing mechanism is the mixture of external healing agents. However, memory polymers can be used to heal damage at the structural-length scale and self-healing can be repeatable and controllable by preprogramming.

Self-healing memory polymers can be used on external scratches, surfaces, and damage to thin materials or internal cracks and flaws of an object. A blended system

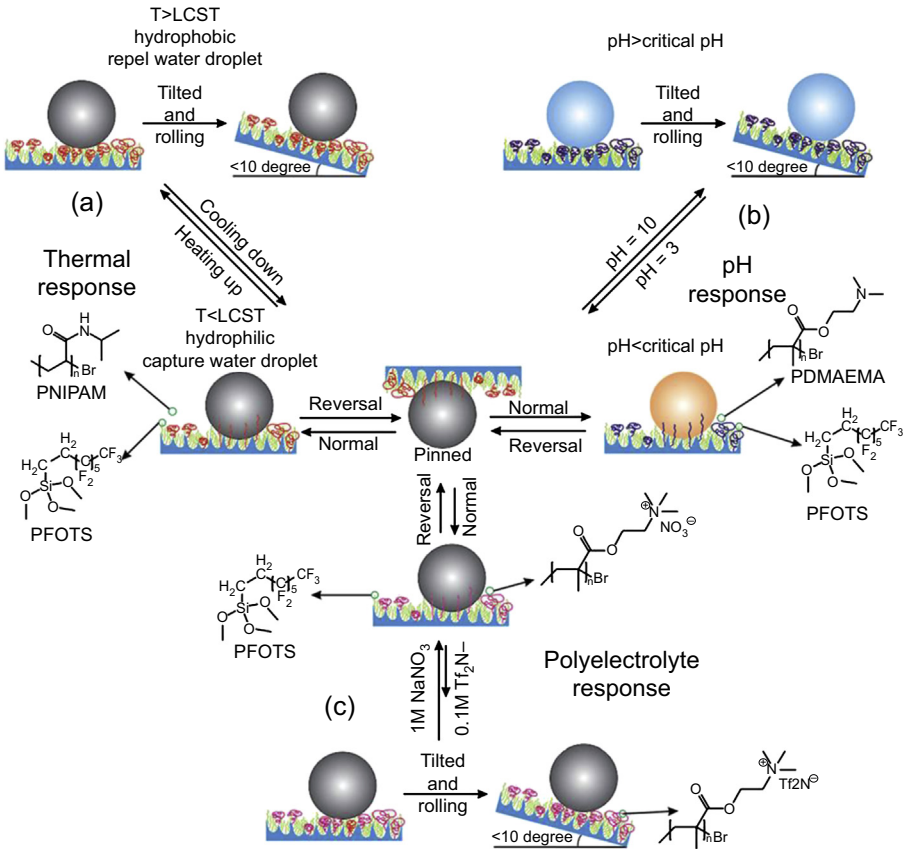


Figure 2.2 Memory polymers for wettability-changing coating.

Adapted from Extreme wettability and tunable adhesion: biomimicking beyond nature? *Soft Matter* 8, 2070–2086, 2012.

consisting of a cross-linked PCL network with linear PCL interpenetrating the network (Rodriguez et al., 2011) exhibited a combination of memory effects from network components and self-healing ability from the linear component, which is a memory self-healing mechanism. Nano-layered, graphene-filled, epoxy-based memory composites display significant property enhancements of scratch resistance and thermal healing capability under stress-free conditions more than the unfilled polymers. Segmented block shape memory PU was used as coating materials for the corrosion protection of pure aluminum and aluminum alloys (Jorcin et al., 2010; Gonzalez-Garcia et al., 2011); the coating film was capable of physically healing some defects when damaged. In this mechanism, the soft segments relaxed under higher temperature and filled in the damaged area, whereas the hard segments maintained the mechanical properties of the film.

Besides surface damage, memory polymers can self-repair large structural-scale damage. For these types of damage, two steps are needed: to close the crack close and then repair it (Li and Lettles, 2010). Confining the crack enhances the efficiency of the repair. However, without external confinement, the memory polymer matrix would recover its original shape with little or no closure of the internal cracks. A 3D-woven fabric memory polymer composite has been reported to show self-healing ability (Nji and Li, 2009).

The self-healing property of memory polymers has significant prospects and value in engineering and has been used for smart coating textiles.

Research work has reported new insight into durable, liquid-repellent coating fabrics for various applications. When a hydrolyzed fluoroalkyl silane (FAS) containing well-dispersed fluorinated-decyl polyhedral oligomeric silsesquioxane (FD-POSS) was coated onto fabrics, the fabrics showed superamphiphobicity with remarkable self-healing ability against chemical damage. When the fabric was coated with hydrophobic nanoparticles and FAS/FD-POSS, it showed a novel multiple self-healing ability against physical damage such as blade scratching, sandpapering, and abrasion and chemical damage (Fig. 2.3). Lin and his team (Wang, 2011) found that the presence of fluoroalkyl surface-modified silica nanoparticles in the coating exceptionally enhanced the liquid repellency of the coated fabric, especially against ultralow surface-tension liquids including ethanol.

Washing is an important cause of degradation to hydrophobic coatings during their practical use. During washing, fabric undergoes mechanical forces in addition to chemical agents.

However, after repeated standard machine laundering, the fabric coating is durable to withstand 200 cycles of washing and 5000 cycles of Martindale abrasion without apparently changing superamphiphobicity. Furthermore, the coating has self-healing ability against both chemical and physical damage. The FS-NP/FD-POSS/FAS-coated fabric damaged by plasma treatment became amphiphilic with a contact angle of 0 degree to both water and oil fluids. However, when the damaged fabric was heated at 140°C for just 5 min, its liquid repellency was recovered. The self-healing ability was repeatable and can be performed many times. When scratching the coated fabric with a sharp blade or subjecting it to abrasion with sandpaper and Martindale abrasion, its liquid repellency decreased. After 100 scratches were performed, the ethanol contact angle reduced to 0 degree and the contact angle for water and hexadecane reduced to 150 degree and 120 degree, respectively.

However, after heat treatment of the scratched fabric at 140°C for 30 min, the contact angle changed to 168, 156, and 146 degree for water, hexadecane, and ethanol, respectively. This thermally activated self-healing process was repeatable.

2.3.3 Coating for breathability

The breathability of textiles means the capability of allowing moisture vapor to be transmitted through the textiles. This claim has been widely made in some functional garments with waterproof performance. Traditionally, waterproof textiles are considered uncomfortable because of the relatively stiff feeling and because they do not allow

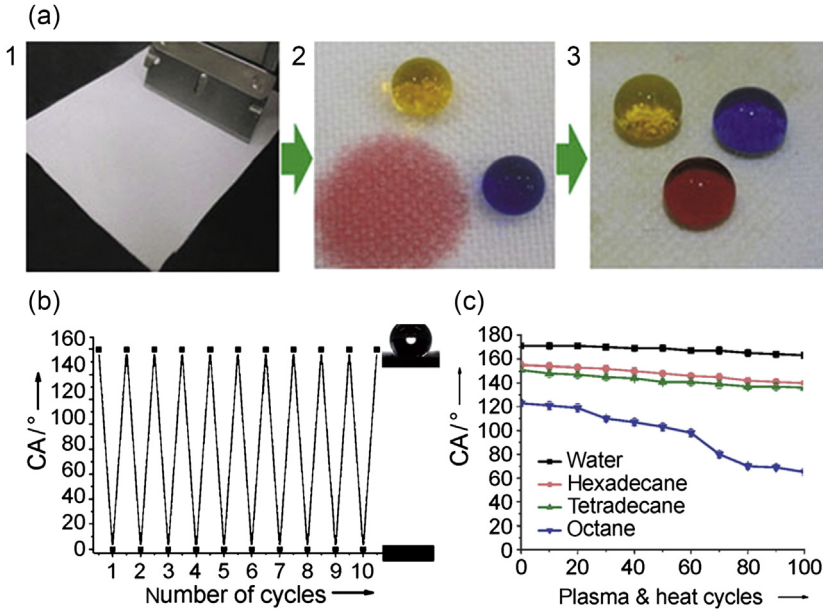


Figure 2.3 Self-healing superhydrophobic and superoleophobic surface. (a)(1) Scratching fabric; (2, 3) colored water, hexadecane, and ethanol drops on the coated fabric (b) after 100 scratches; (c) after heat treatment at 140°C.

Reproduced from Wang, H., Xue, Y., Ding, J., Feng, L., Wang, X., Lin, T., 2011. Durable, self-healing superhydrophobic and superoleophobic surfaces from fluorinated-decyl polyhedral oligomeric silsesquioxane and hydrolyzed fluorinated Alkyl Silane, *Angewandte Chemie International Edition* 50 (48), 11433–11436.

perspiration vapor to escape. However, breathable fabrics allow water vapor to diffuse and still repel liquid water penetration. Commonly, breathable fabrics are made by microporous membranes or hydrophilic membranes. The interconnected channels of microporous membranes are smaller than raindrops but larger than water vapor molecules. Most membranes are made from polytetrafluorethylene polymer, polyvinylidene fluoride. The hydrophilic membranes are made from chemically modified polyester or PU. The amorphous regions of the hydrophilic membrane allow water vapor molecules to pass by absorption, diffusion, and desorption but prevent the penetration of liquid water owing to their solid nature. Compared with breathable polymers, memory polymers can achieve adaptable water vapor permeability (WVP) for breathable textiles (Mondal and Hu, 2006) (Mondal et al., 2006), which can provide better comfort in both cold and warm climates (Jeong et al., 2000). In 2006, a Swiss company released an innovative membrane which was sensitive to heat. The structure opened to enable excess heat to escape and closed to retain heat close to the body at low temperatures. The Japanese company Mitsubishi Heavy Industries also developed breathable fabrics with memory membranes for outerwear. The resulting fabrics had excellent waterproofing and breathability and kept wearers comfortable in various environments. In addition, Toray Industries and Marmot Mountain Works developed a

PU film breathable clothing system by combining excellent WVP and shape memory polymers with microporous coatings and garment lamination technology.

Shape memory PU has become a good candidate for breathable coating nonporous fabrics owing to the sensitivity of its WVP to temperature and humidity. In 2000, Jeong et al. studied the WVP properties of shape memory PUs with an amorphous reversible phase, and water vapor-permeable fabrics were developed by coating shape memory PU membranes on them. Similarly, smart WVP was developed by the T_m -type shape memory PU with a semicrystalline reversible phase (Ding et al., 2004; Mondal and Hu, 2006). Mondal and Hu (2007) reported shape memory PU-coated fabrics with a tailored responsive room temperature and studied their WVP properties, which increased sharply when they reached the transition temperature (Mondal et al., 2006). These results confirm that memory polymer coating breathable textiles have a high WVP at higher temperatures and low WVP at lower temperatures (Fig. 2.4). In addition, by applying shape memory PUs containing a small percentage of multiwall nanotubes, the coated cotton fabric showed excellent UV protection along with desirable WVP and wear comfort (Mondal and Hu, 2007).

In addition to temperature-responsive WVP, Chen et al. (2007a,b) reported an attempt to adjust the size and shape of the free volume holes found in membrane materials. The effects of hydrophilic groups and crystalline soft segments on the WVP of shape memory PU coating film was studied by Mondal and Hu (2006, 2007). The WVP increased with the increase in PE glycol owing to the enhanced hydrophilicity. However, poly(caprolactone) glycol reduced WVP in the polytetramethylene glycol-based shape memory PU because of increased interaction among polymer chains (Mondal and Hu, 2007).

Fabrics coated with adjustable WVP film provide a breathable clothing system. By combining the excellent WVP of shape memory polymers with microporous coatings, these textiles can find broad applications such as sportswear, footwear, gloves, and socks.

2.3.4 Aesthetic surface

A variety of aesthetic surface effects can be achieved by memory polymer coatings, such as the structure color effect and 3D patterns.

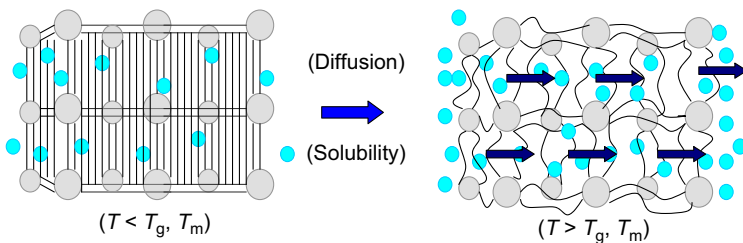


Figure 2.4 Water vapor management of memory coating.

Reproduced from Anticipating the future assessing the impact part 4: Biomimetics and smart coatings.

Xie et al. (2010) described a method using shape memory polymers to create localized structural colors. The 3D colored patterns originate from light diffraction caused by the 2D wrinkle structure under regular fluorescent light while changing only the viewing angle (less than 45°C). It is a flexible method and an arbitrary structurally colored image can be prepared as long as simple equipment for metal deposition and shape memory polymer textiles or substrates are available. The wrinkles are sensitive to strain distribution on the microscopic scale and can be controlled, which may be used for anticounterfeiting purposes.

Besides color effects, shape memory PUs are widely used for the textiles' aesthetic appearances, including the heat-responsive flat, crease, or pattern retention. Shape memory PU solutions can be used directly as a finishing or coating agent to obtain valuable properties in different types of textile fabrics such as cotton or wool (Liem et al., 2007; Li et al., 2007). Coating and finishing are important methods for producing shape memory textiles which can transfer the shape memory properties from polymers to fabrics (Liu, 2007a,b). Cotton easily becomes wrinkled and difficult to set when creases are required, such as pleated skirts. Liu et al. (Liem et al., 2007) investigated a chemical modification method for cotton through shape memory finishing and coating. The resultant cotton fabric with Fourier transform infrared spectroscopy (FTIR) and X-ray photoelectron spectroscopy revealed that when shape memory PUs are grafted onto the surface of cotton, high washability and enduring anticreasing of the treated cotton would be achieved. Hu et al. reported the recovery of wrinkles, retention of creases, and retention of patterns of different shape memory fabrics by coating them with shape memory PU (Fig. 2.5), and developed corresponding testing methods for these shape memory fabrics (Hu et al., 2008). Furthermore, Hu developed

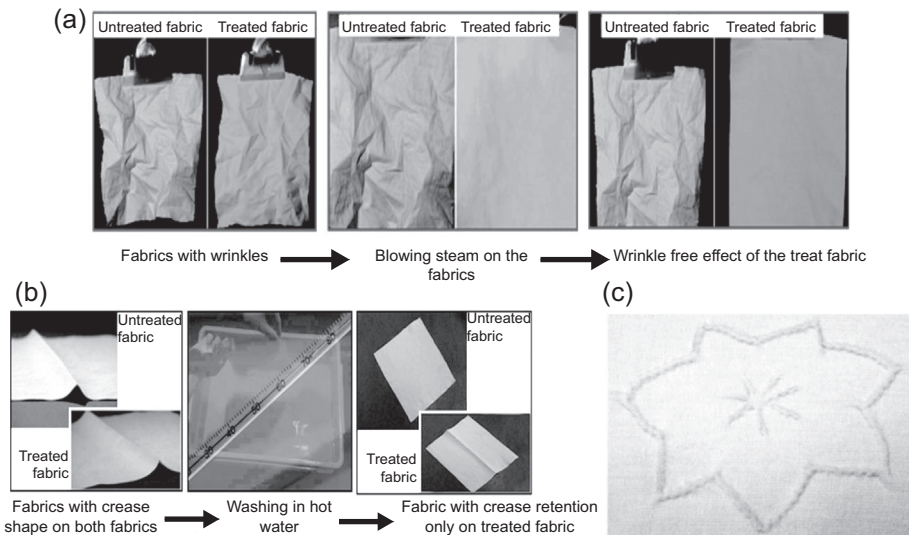


Figure 2.5 Memory coating for aesthetic appearance. (a) Flat appearance memory; (b) crease memory; and (c) pattern memory.

shape memory treatment agents for wool (Li et al., 2007; Dong et al., 2008). The thermal and hygrothermal effects of wool fabrics were studied through shape memory finishing and coating with shape memory PU. The results confirmed that synthetic shape memory polymers influenced the thermal and hygrothermal behaviors of wool fabrics.

Compared with shape memory fabrics knitted or woven with shape memory fibers, a small content of shape memory polymer is sufficient to transfer shape memory effects to the fabric during the finishing and coating process, which is highly efficient. Many interesting functionalities can be achieved in a fabric coated by shape memory PUs, such as antipilling, flexibility/strength protection, dimensional stability, shrink-proofing, a good flat appearance, crease retention, ease of 3D pattern design, and bulging recovery.

The general mechanism for memory coating is proposed in Fig. 2.6(a), in which the memory polymer switch-netpoint model (a) is applied to the fabric surface, as shown in Fig. 2.6(b). Cross-linking between the polymer network and the fabric fibers would form the netpoints, and the soft segments of the memory polymers are the switches; thus, the shape memory effect from memory polymers can be transferred to the fabric and maintain its durability after cycled washing. The FTIR spectra and

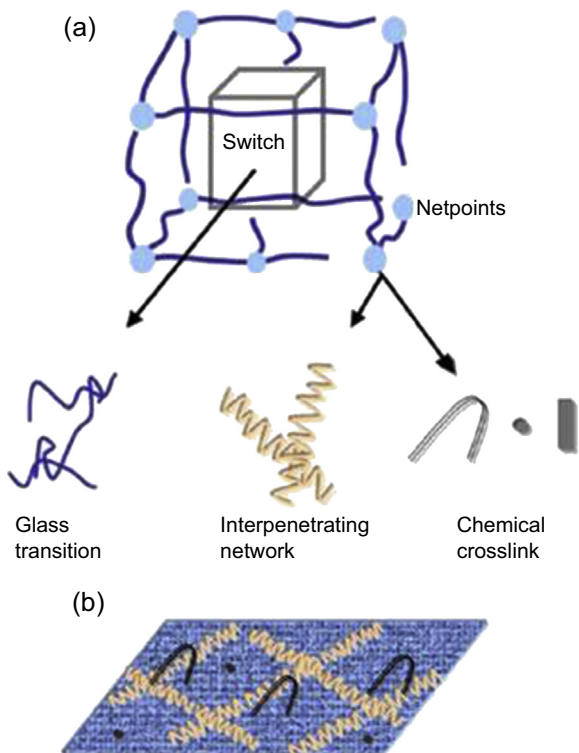


Figure 2.6 Schematic diagram of transformation of memory effect from polymer to fabric.

(a) Schematic diagram of memory polymer; (b) schematic diagram of memory polymer coating on the fabric.

scanning electron microscopy pictures confirm the existing of a layer of shape memory macromolecules that form an interpenetrating network and graft onto the fabric surface. These structures make the shape memory properties more durable and genuinely transfer the shape memory effects to the fabric. For example, the shape memory PU-coated cotton fabric shows a decrease at $3000\text{--}3500\text{ cm}^{-1}$ (O–H hydrogen bond-stretching vibration) that means an increased degree of shape memory solution grafted to the cotton fiber. The appearance of two bonds at 1725 cm^{-1} (carbonyl CO stretching) and 2950 cm^{-1} (CH stretching vibration), which are the characteristic absorption peaks of the shape memory PU (Liu, 2005a,b; Liem et al., 2007), proved the formation of a memory polymer network on the fiber surface, which has a critical role in reducing the residual stress of the weft fibers by forming a coating on the fiber surface and establishing the prerequisite for conferring memory effects to the fabrics.

2.4 Conclusions

The principles of imparting performance, prototypes, and initial industry applications are proposed and implemented for memory polymer-coated textiles. However, some problems remain to be resolved. Commonly speaking, any individual application demands specific requirements regarding the overall properties of memory polymers. For textile applications, the difficulties are satisfying the requirements for all aspects of appearance, comfortable feeling, and hand feeling, such as color, dimensional stability, comfort and tactile properties, washing durability, strength, flexibility, stretchability, easy processability, and compatibility with many other chemical, mechanical, and thermal processing requirements and low-cost production.

We have made significant progress in memory polymer technologies, such as materials, processes, and techniques, but the applications of memory polymer-coated textiles remain limited compared with their potential. Innovating memory polymers, coating technologies, and applications in practice is worth our concerted effort.

Memory polymers have a tremendous capacity for design, programmability, and functionality. Thus, the application potential for memory polymer coating appears to be nearly unlimited, and we can reasonably predict that applications in various areas will continue to prosper in future. Wearable electronics applications have been the most active area of research and they will continue to be one of the most important focuses in the near future of smart textiles. Microcircuit on the fabric surface are easily achieved by memory polymer coating technology.

Memory polymer coating is expected to be capable of providing more complex actuation structures. In particular, studies are rapidly moving toward combining different technologies for multifunctional memory coating textiles. In addition, special functions of memory polymers would be desirable to enhance their performance and tailor their properties for different coating functions, which could include, but are not limited to, antibacterial properties, UV resistance, thermal resistance, and chemical resistance.

References

- Ahir, S.V., Tajbakhsh, A.R., Terentjev, E.M., 2006. Self-assembled shape-memory fibers of triblock liquid-crystal polymers. *Advanced Functional Materials* 16, 556–560.
- Andreopoulos, F.M.B., Beckman, E.J., Russell, A.J., 1998. Light induced tailoring of PEG-hydrogel properties. *Biomaterials* 19, 1343–1352.
- Aoki, D., Teramoto, Y., Nishio, Y., 2007. SH-containing cellulose acetate derivatives: preparation and characterization as a shape memory-recovery material. *Biomacromolecules* 8, 3749–3757.
- Behl, M., Lendlein, A., 2007. Actively moving polymers. *Soft Matter* 3, 58–67.
- Behl, M., Razzag, M., Lendlein, A., 2010. Multifunctional shape-memory polymers. *Advanced Materials* 22, 3388–3410.
- Brannon-peppas, L., Peppas, N.A., 1991. Equilibrium swelling behavior of pH-sensitive hydrogels. *Chemical Engineering Science* 46 (3), 715–722.
- Chen, S.J., Hu, J., Chen, S.G., Zhang, C.L., 2011. Study on the structure and morphology of supramolecular shape memory polyurethane containing pyridine moieties. *Smart Materials and Structures* 20, 605001–605003.
- Chen, S.J., Hu, J., Liu, Y.Q., Liem, H.M., Zhu, Y., Liu, Y.J., 2007a. Effect of SSL and HSC on morphology and properties of PHA based SMPU synthesized by bulk polymerization method. *Journal of Polymer Science Part B: Polymer Physics* 45, 444–454.
- Chen, S.J., Hu, J., Yuen, C.W., Chan, L.K., 2009a. Supramolecular polyurethane networks containing pyridine moieties for shape memory materials. *Materials Letters* 63, 1462–1464.
- Chen, S.J., Hu, J., Yuen, C.W., Chan, L.K., 2009b. Novel moisture-sensitive shape memory polyurethanes containing pyridine moieties. *Polymer* 50, 4424–4428.
- Chen, S.J., Hu, J., Yuen, C.W., Chan, L.K., 2010. Fourier transform infrared study of supramolecular polyurethane networks containing pyridine moieties for shape memory materials. *Polymer International* 59, 529–538.
- Chen, Y., Liu, Y., Fan, H.J., Li, H., Shi, B., Zhou, H., Peng, B.Y., 2007b. The polyurethane membranes with temperature sensitivity for water vapor permeation. *Journal of Membrane Science* 287, 192–197.
- Chilkoti, A., Dreher, M.R., Meyer, D.E., Raucher, D., 2002. Targeted drug delivery by thermally responsive polymers. *Advanced Drug Delivery Reviews* 54, 613–630.
- Cho, J.W., Kim, J.W., Jung, Y.C., Goo, N.S., 2005. Electroactive shape-memory polyurethane composites incorporating carbon nanotubes. *Macromolecular Rapid Communications* 26, 412–416.
- Del Rio, E., Lligadas, G., Ronda, J.C., Galia, M., Cadiz, V., Meier, M.A.R., 2011. Shape memory polyurethanes from renewable polyols obtained by ATMET polymerization of glyceryl triundec-10-enoate and 10-undecenol. *Macromolecular Chemistry and Physics* 212, 1392–1399.
- Ding, X.M., Hu, J., Tao, X.M., 2004. Effect of crystal melting on water vapor permeability of shape-memory polyurethane film. *Textile Research Journal* 74, 39–43.
- Dong, Z.E., Hu, J.L., Liu, Y., Liu, Y., Chan, L.K., 2008. The performance evaluation of the woven wool fabrics treated with shape memory polymers. *International Journal of Sheep and Wool Science* 56.
- Du, H.Y., Zhang, J., 2010. Solvent induced shape recovery of shape memory polymer based on chemically cross-linked poly(vinyl alcohol). *Soft Matter* 6, 3370–3376.

- Dupin, D.R., Rosselgong, J., Armes, S.P., Routh, A.F., 2007. Swelling kinetics for a pH-induced latex-to-microgel transition. *Langmuir* 23, 4035–4041.
- Fan, K., Huang, W., Wang, C.C., Ding, Z., Zhao, Y., Purnawali, H., Liew, K.C., Zheng, L.X., 2011. Water-responsive shape memory hybrid: design concept and demonstration. *Express Polymer Letters* 5, 409–416.
- Finkelmann, H.N., Nishikawa, E., 2001. A new opto-mechanical effect in solids. *Physical Review Letters* 87, 015501–015504.
- Gonzalez-Garcia, Y., Mol, J., Muselle, T., De Graeve, I., Van Assche, G., Scheltjens, G., Van Mele, B., Terryn, H., 2011. SEM study of defect repair in self-healing polymer coatings on metals. *Electrochemistry Communications* 13, 169–173.
- Han, C.K., Bae, Y.H., 1998. Inverse thermally-reversible gelation of aqueous *N*-isopropylacrylamide copolymer solution. *Polymer* 9, 2809–2814.
- Han, S.I., Gu, B.H., Nam, K.H., Im, S.J., Kim, S.C., Im, S.S., 2007. Novel copolyester-based ionomer for a shape-memory biodegradable material. *Polymer* 48, 1830–1834.
- He, H., Li, L., Lee, L.J., 2008. Photopolymerization and structure formation of methacrylic acid based hydrogels: the effect of light intensity. *Reactive and Functional Polymers* 68 (1), 103–113.
- Higgins, M.J., Grosse, W., Wagner, K., Molino, P.J., Wallace, G.G., 2011. Reversible shape memory of nanoscale deformations in inherently conducting polymers without reprogramming. *The Journal of Physical Chemistry B* 115, 3371–3378.
- Hoffman, A.S., 2000. Bioconjugates of intelligent polymers and recognition proteins for use in diagnostics and affinity separations. *Clinical Chemistry* 46 (9), 1478–1486.
- Hu, J.L., Chen, S., 2010. A review of actively moving polymers in textile applications. *Journal of Materials Chemistry* 20, 3346–3355.
- Hu, J.L., Dong, Z.E., Liu, Y., Liu, Y.J., 2008. The investigation about the shape memory behavior of wool. *Advances in Science and Technology* 60.
- Hu, J.L., Yang, Z., Yeung, L.Y., Ji, F.L., Liu, Y.Q., 2005. Crosslinked polyurethanes with shape memory properties. *Polymer International* 54, 854–859.
- Huang, W.M., Yang, B., An, L., Li, C., Chan, Y.S., 2005. Water-driven programmable polyurethane shape memory polymer: demonstration and mechanism. *Applied Physics Letters* 86, 114101–114105.
- Ilavsky, M., Hrouz, J., Havlicek, I., 1985. Phase transition in swollen gels: 7 effect of charge concentration on the temperature collapse of poly(*N,N*-diethylacrylamide) networks in water. *Polymer* 26 (10), 1514–1518.
- Ivens, J., Urbanus, M., De Smet, C., 2011. Shape recovery in a thermoset shape memory polymer and its fabric-reinforced composites. *Express Polymer Letters* 5, 254–261.
- Jang, M.K., Hartwig, A., Kim, B.K., 2009. Shape memory polyurethanes cross-linked by surface modified silica particles. *Journal of Materials Chemistry* 19, 1166–1172.
- Jeong, H.M., Ahn, B.K., Cho, S.M., Kim, B.K., 2000. Water vapor permeability of shape memory polyurethane with amorphous reversible phase. *Journal of Polymer Science Part B: Polymer Physics* 38, 3009–3017.
- Ji, F.L., Hu, J., 2011. Comparison of shape memory polyurethanes and polyurethane-ureas having crystalline reversible phase. *High Performance Polymers* 23, 314–325.
- Ji, F.L., Hu, J.L., Han, J.P., 2011. Shape memory polyurethane-ureas based on isophorone diisocyanate. *High Performance Polymers* 23, 177–187.
- Ji, F.L., Hu, J.L., Li, T.C., Wong, Y.W., 2007. Morphology and shape memory effect of segmented polyurethanes. Part I: with crystalline reversible phase. *Polymer* 48, 5233–5243.

- Jiang, H.Y., Kelch, S., Lendlein, A., 2006. Polymers move in response to light. *Advanced Materials* 18, 1471–1475.
- Jorcin, J.B., Scheltjens, G., Van Ingelgem, Y., Tourwé, E., Van Assche, G., De Graeve, I., Van Mele, B., Terryn, H., Hubin, A., 2010. Investigation of the self-healing properties of shape memory polyurethane coatings with the ‘odd random phase multisine’ electrochemical impedance spectroscopy. *Electrochimica Acta* 55, 6195–6203.
- Kolesov, I.S., Kratz, K., Lendlein, A., Radsch, H.J., 2009. Kinetics and dynamics of thermally-induced shape-memory behavior of cross-linked short-chain branched polyethylenes. *Polymer* 50, 5490–5498.
- Korley, L.T.J., Pate, B.D., Thomas, E.L., Hammond, P.T., 2006. Effect of the degree of soft and hard segment ordering on the morphology and mechanical behavior of semicrystalline segmented polyurethanes. *Polymer* 47, 3073–3082.
- Kumpfer, J.R., Rowan, S.J., 2011. Thermo-, photo-, and chemo-responsive shape-memory properties from photo-cross-linked metallosupramolecular polymers. *Journal of the American Chemical Society* 133, 12866–12874.
- Kurahashi, E., Sugimoto, H., Nakanishi, E., Nagata, K., Inomata, K., 2012. Shape memory properties of polyurethane/poly(oxyethylene) blends. *Soft Matter* 8, 496–503.
- Kushner, A.M., Vossler, J.D., Williams, G.A., Guan, Z.B., 2009. A biomimetic modular polymer with tough and adaptive properties. *Journal of the American Chemical Society* 131, 8766–8768.
- Lee, B.S., Chun, B.C., Chung, Y.C., Sul, K.I., Cho, J.W., 2001. Structure and thermomechanical properties of polyurethane block copolymers with shape memory effect. *Macromolecules* 34, 6431–6437.
- Lendlein, A., Jiang, H., Junger, O., Langer, R., 2005. Light-induced shape-memory polymers. *Nature* 434, 879–882.
- Lendlein, A., Kelch, S., 2002. Shape-memory polymers. *Angewandte Chemie International Edition* 41, 2034–2057.
- Lendlein, A., Schmidt, A.M., Langer, R., 2001. AB-polymer networks based on oligo(epsilon-caprolactone) segments showing shape-memory properties. *Proceedings of the National Academy of Sciences of the United States of America* 98, 824–827.
- Leng, J.S., Dawei, Z., Liu, Y., Yu, K., Lan, X., 2010. Study on the activation of styrene-based shape memory polymer by medium-infrared laser light. *Applied Physics Letters* 96, 111901–111905.
- Li, Y.K., 2007. Evaluation of Shape Memory Fabrics. Hong Kong Polytechnic University (Ph.D.).
- Li, C., Guo, R., Jiang, X., Hu, S., Li, L., Cao, X., Yang, H., Song, Y., Ma, Y., Jiang, L., 2009. Reversible switching of water-droplet mobility on a superhydrophobic surface based on a phase transition of a side-chain liquid-crystal polymer. *Advance Materials* 21.
- Li, M.H., Keller, P., Li, B., Wang, X.G., Brunet, M., 2003. Light-driven side-on nematic elastomer actuators. *Advanced Materials* 15, 569–572.
- Li, G.Q., Nettles, D., 2010. Thermomechanical characterization of a shape memory polymer based self-repairing syntactic foam. *Polymer* 51, 755–762.
- Li, S.C., Tao, L., 2010. Melt rheological and thermoresponsive shape memory properties of HDPE/PA6/POE-g-MAH blends. *Polymer-Plastics Technology and Engineering* 49, 218–222.
- Li, J.H., Viveros, J.A., Wrue, M.H., Anthamatten, M., 2007. Shape-memory effects in polymer networks containing reversibly associating side-groups. *Advanced Materials* 19, 2851–2855.

- Liem, H., Yeung, L.Y., Hu, J.L., 2007. A prerequisite for the effective transfer of the shape-memory effect to cotton fibers. *Smart Materials and Structures* 16, 748.
- Lim, H.S.K., Kwak, D., Lee, D.Y., Lee, S.G., Cho, K., 2007. UV-Driven reversible switching of a roselike vanadium oxide film between superhydrophobicity and superhydrophilicity. *Journal of the American Chemical Society* 129, 4128–4129.
- Liu, C.D., Chun, S.B., Mather, P.T., Zheng, L., Haley, E.H., Coughlin, E.B., 2002. Chemically cross-linked polycyclooctene: synthesis, characterization, and shape memory behavior. *Macromolecules* 35, 9868–9874.
- Liu, Y., Chung, A., Hu, J.L., Lu, J., 2007b. Shape memory behavior of SMPU knitted fabric. *Journal of Zhejiang University Science A* 8, 830.
- Liu, G.Q., Ding, X., Cao, Y.P., Zheng, Z.H., Peng, Y.X., 2005a. Novel shape-memory polymer with two transition temperatures. *Macromolecular Rapid Communications* 26, 649–652.
- Liu, Y.Q., Hu, J., Zhu, Y., Yang, Z.H., 2005b. Surface modification of cotton fabric by grafting of polyurethane. *Carbohydrate Polymers* 61, 276–280.
- Liu, C., Qin, H., Mather, P.T., 2007a. Review of progress in shape-memory polymers. *Journal of Materials Chemistry* 17, 1543–1558.
- Luo, X.L., Zhang, X., Wang, M.T., Ma, D.Z., Xu, M., Li, F.K., 1997. Thermally stimulated shape-memory behavior of ethylene oxide-ethylene terephthalate segmented copolymer. *Journal of Applied Polymer Science* 64, 2433–2440.
- Meng, Q.H., Hu, J., 2008. A poly(ethylene glycol)-based smart phase change material. *Solar Energy Materials and Solar Cells* 92, 1260–1268.
- Mohr, R., Kratz, K., Weigel, T., Lucka-Gabor, M., Moneke, M., Lendlein, A., 2005. Initiation of shape-memory effect by inductive heating of magnetic nanoparticles in thermoplastic polymers. *Proceedings of the National Academy of Sciences of the United States of America* 103, 3540–3545.
- Mondal, S., Hu, J., 2006. Segmented shape memory polyurethane and its water vapor transport properties. *Designed Monomers and Polymers* 9, 527–550.
- Mondal, S., Hu, J., 2007. Water vapor permeability of cotton fabrics coated with shape memory polyurethane. *Carbohydrate Polymers* 67, 282–287.
- Mondal, S., Hu, J., Yong, Z., 2006. Free volume and water vapor permeability of dense segmented polyurethane membrane. *Journal of Membrane Science* 280, 427–432.
- Morshedian, J., Khonakdar, H.A., Mehrazadeh, M., Eslami, H., 2003. Preparation and properties of heat-shrinkable cross-linked low-density polyethylene. *Advances in Polymer Technology* 22, 112–119.
- Mukae, K., Bae, Y.h., Okano, T., Kim, S.W., 1990. New thermosensitive hydrogel. Poly(ethylene oxide-dimethyl siloxane-ethylene oxide)/poly(*N*-isopropyl acrylamide) interpenetrating polymer networks I. Synthesis and characterization. *Polymer Journal* 22 (3), 206–217.
- Nji, J., Li, G., 2009. A self-healing 3D woven fabric reinforced shape memory polymer composite for impact mitigation. *Smart Materials and Structures* 19, 35001–35007.
- Osada, Y., Kajiwara, K., 2001. *Gels Handbook*. Academic Press, London.
- Qin, H.H., Mather, P.T., 2009. Combined one-way and two-way shape memory in a glass-forming nematic network. *Macromolecules* 42, 273–280.
- Ratna, D., Karger-Kocsis, J., 2008. Recent advances in shape memory polymers and composites: a review. *Journal of Materials Science* 43, 254–269.
- Ratna, D., Karger-Kocsis, J., 2011. Shape memory polymer system of semi-interpenetrating network structure composed of crosslinked poly (methyl methacrylate) and poly (ethylene oxide). *Polymer* 52, 1063–1070.

- Rodriguez, R., Alvarez-Lorenzo, C., Concheiro, A., 2003. Cationic cellulose hydrogels: kinetics of the cross-linking process and characterization as pH-/ion-sensitive drug delivery systems. *Journal of Controlled Release* 86 (2–3), 253–265.
- Rodriguez, E.D., Luo, X., Mather, P.T., 2011. Linear/network poly(ϵ -caprolactone) blends exhibiting shape memory assisted self-healing (SMASH). *ACS Applied Materials & Interface* 3, 152–161.
- Rousseau, I.A., Mather, P.T., 2003. Shape memory effect exhibited by smectic liquid crystalline elastomers. *Journal of the American Chemical Society* 125, 15300–15301.
- Safranski, D.L., Gall, K., 2008. Effect of chemical structure and crosslinking density on the thermo-mechanical properties and toughness of (meth)acrylate shape memory polymer networks. *Polymer* 49, 4446–4455.
- Sahoo, N.G., Jung, Y.C., Goo, N.S., Cho, J.W., 2005. Conducting shape memory polyurethane-polypyrrole composites for an electroactive actuator. *Macromolecular Materials and Engineering* 290, 1049–1055.
- Sakurai, K., Shirakawa, Y., Kashiwagi, T., Takahashi, T., 1994. Crystal transformation of styrene-butadiene block copolymer. *Polymer* 35, 4238–4239.
- Schmidt, A.M., 2006. Electromagnetic activation of shape memory polymer networks containing magnetic nanoparticles. *Macromolecular Rapid Communications* 27, 1168–1172.
- Scott, T.F.D., Draughon, R.B., Bowman, C.N., 2006. Actuation in crosslinked polymers via photoinduced stress relaxation. *Advanced Materials* 18, 2128–2132.
- Stromberg, N., Hulth, S., 2003. A fluorescence ratiometric detection scheme for ammonium ions based on the solvent sensitive dye MC 540. *Sensors and Actuators B: Chemical* 90 (1–3), 308–318.
- Stubenrauch, K., Voets, I., Fritz-Popovski, G., Trimmel, G., 2009. PH and ionic strength responsive polyelectrolyte block copolymer micelles prepared by ring opening metathesis polymerization. *Journal of Polymer Science Part A: Polymer Chemistry* 47, 1178–1191.
- Sun, X.H., Ni, X., 2004. Block copolymer of trans-polyisoprene and urethane segment: crystallization behavior and morphology. *Journal of Applied Polymer Science* 94, 2286–2294.
- Sun, L., Zhao, Y., Huang, W.M., Tong, T.H., 2009. Formation of combined surface features of protrusion array and wrinkles atop shape-memory polymer. *Surface Review and Letters* 16, 929–933.
- Veron, L.B., Vernon, H.M., 1941. *Process of Manufacturing Articles of Thermoplastic Synthetic Resins*.
- Wang, Z., Hansen, C., Ge, Q., Maruf, S.H., Ahn, D.U., Qi, H.J., Ding, Y.F., 2011. Programmable, pattern-memorizing polymer surface. *Advanced Materials* 23, 3669–4373.
- Wang, H., Xue, Y., Ding, J., Feng, L., Wang, X., Lin, T., 2011. Durable, self-healing superhydrophobic and superoleophobic surfaces from fluorinated-decyl polyhedral oligomeric silsesquioxane and hydrolyzed fluorinated alkyl silane. *Angewandte Chemie International Edition* 50 (48), 11433–11436.
- White, T.J., Tabiryran, N.V., Tondiglia, V.P., Serak, S., Hrozhyk, V., Vaia, R.A., Bunning, T.J., 2008. High frequency photodriven polymer oscillator. *Soft Matter* 4, 1796–1798.
- Wu, L.B., Jin, C., Sun, X.Y., 2011. Synthesis, properties, and light-induced shape memory effect of multiblock polyesterurethanes containing biodegradable segments and pendant cinnamide groups. *Biomacromolecules* 12, 235–241.
- Xie, T., Xiao, X., Li, J., Wang, R., 2010. Encoding localized strain history through wrinkle based structural colors. *Advanced Materials* 22 (39), 4390–4394.

- Yakacki, C.M., Shandas, R., Safranski, D., Ortega, A.M., Sassaman, K., Gall, K., 2008. Strong, tailored, biocompatible shape-memory polymer networks. *Advanced Functional Materials* 18, 2428–2435.
- Yamada, M., Kondo, M., Miyasato, R., Naka, Y., Mamiya, J.I., Kinoshita, M., Shishido, A., Yu, Y., Barrett, C.J., Ikeda, T., 2009. Photomobile polymer materials—various three-dimensional movements. *Journal of Materials Chemistry* 19, 60–62.
- Yang, B., H, W., Li, C., Lee, C.M., Li, L., 2004. On the effects of moisture in a polyurethane shape memory polymer. *Smart Materials and Structures* 13, 191–195.
- Yang, B., Huang, W.M., Li, C., Li, L., 2006. Effects of moisture on the thermal mechanical properties of a polyurethane shape memory polymer. *Polymer* 47, 1348–1356.
- Yang, D., Huang, W., Yu, J.H., Jiang, J.S., Zhang, L.Y., Xie, M.R., 2010. A novel shape memory polynorbornene functionalized with poly(*ε*-caprolactone) side chain and cyano group through ring-opening metathesis polymerization. *Polymer* 51, 5100–5106.
- Yu, Y.L., Ikeda, T., 2006. Soft actuators based on liquid-crystalline elastomers. *Angewandte Chemie International Edition* 45, 5416–5418.
- Zhang, S.F., Feng, Y., Zhang, L., Sun, J.F., Xu, X.K., Xu, Y.S., 2007. Novel interpenetrating networks with shape-memory properties. *Journal of Polymer Science Part A: Polymer Chemistry* 45, 768–775.
- Zhang, H., Wang, H., Zhong, W., Du, Q., 2009. A novel type of shape memory polymer blend and the shape memory mechanism. *Polymer* 50, 1596–1601.
- Zheng, X.T., Zhou, S., Li, X.H., Weng, H., 2006. Shape memory properties of poly(D,L-lactide)/hydroxyapatite composites. *Biomaterials* 27, 4288–4295.
- Zhu, Y., Hu, J., Liu, Y.J., 2009. Shape memory effect of thermoplastic segmented polyurethanes with self-complementary quadruple hydrogen bonding in soft segments. *European Physical Journal* 28, 3–10.
- Zhu, Y., Hu, J., Luo, H.S., Young, R.J., Deng, L.B., Zhang, S., Fan, Y., Ye, G.D., 2012. Rapidly switchable water-sensitive shape-memory cellulose/elastomer nano-composites. *Soft Matter* 8, 2509–2517.
- Zhu, G., Liang, G., Xu, Q., Yu, Q., 2003. Shape-memory effects of radiation crosslinked poly(*ε*-caprolactone). *Journal of Applied Polymer Science* 90, 1589–1595.

Environmentally mild self-cleaning processes on textile surfaces under daylight irradiation: critical issues

3

J. Kiwi, S. Rtimi

Ecole Polytechnique Fédérale de Lausanne, Lausanne, Switzerland

3.1 Introduction: self-cleaning of textiles by mild environmental sunlight-activated processes

Photocatalysis as a useful tool for the self-cleaning of glass, polymer thin films, and textile fabric surfaces was reported by Afzal et al. (2011), Bozzi et al. (2005a), Qiu et al. (2012), Fujishima et al. (2008), Zhang et al. (2012), Mihailovic et al. (2011), and Kasanen et al. (2009). TiO_2 has been chosen as the standard photocatalyst used in the field of environmental photochemistry owing to its stability, the effective separation of charges under band-gap irradiation, and the availability of fairly pure samples. Self-cleaning by TiO_2 -modified surfaces is basically a photooxidative process requiring sunlight, O_2 (air), and water vapor in the air that produces highly oxidative radicals able to destroy organic compounds, as reported by Qiu et al. (2012) and Patrocínio et al. (2014). Interest in developing more efficient self-cleaning textiles and polymer films has grown as a result of the higher world population and increased production of fabrics. These self-cleaning textile/polymer surfaces also provide protection against infection because under low-intensity solar radiation, they inactivate bacteria, viruses, and fungus-based biofilms. In this chapter, we address some aspects of work related to the concept, scientific bases, nanotechnology, and environmental impacts of actual and future self-cleaning fabrics. Self-cleaning has benefits for the environment; it avoids energy-intensive and polluting processes resulting from traditional cleaning processes that involve detergents, chemicals, and bleaches. The subject of photo-induced hydrophilicity was addressed in relation to TiO_2 -modified surfaces by Rtimi et al. (2015), Patrocínio et al. (2014) and Mills (2012) addressed the method of depositing the coating onto the selected substrate, and examined TiO_2 superhydrophilicity induced under light irradiation and the photocatalytic mechanism of reaction. Yuranova et al. (2005) and Fateh et al. (2011) reported dip-coating methods to deposit TiO_2 coating onto the underlayers of SiO_2 to protect the textile or polymer substrate against corrosion by the highly oxidative valence band hole (vbh^+) of TiO_2 at +3.1 eV.

3.2 Pretreatment by and functionalization of surfaces by radiofrequency plasma and ultraviolet-C (184 nanomoles)

Pretreatment of textile surfaces by radiofrequency (RF) plasma or ultraviolet-C (UVC) light is intended to increase the amount of TiO_2 complexing or chelating binding sites on textile surfaces. This is necessary to induce photodiscoloration proceeding at acceptable kinetics.

1. RF-plasma pretreatment of polyamides and polyesters (PES): The first study specifically reporting RF-plasma pretreatment enhancing and modifying textile surfaces on artificial fibers was reported in detail by [Bozzi et al. \(2005b\)](#). A schematic for the production of oxygen active resulting from RF plasma under vacuum and up to atmospheric pressure is shown in [Fig. 3.1](#). TiO_2 subsequently attaches to the modified textile surface by exchange, impregnation, or electrostatic binding of positively loaded Ti^{4+} (TiO_2) with the negatively charged $-\text{COO}^-$ and $-\text{O}-\text{O}^-$ functional groups introduced onto the textile surface. In the plasma, the ions, molecules, and electrons attain temperatures up to a few hundred degrees and have energies corresponding to these high temperatures lasting only nanoseconds or microseconds. In this way, the plasma species activate textiles stable up to $150\text{--}160^\circ\text{C}$ pretreated without damaging the textile. In the RF cavity, the intense local heat resulting from to RF plasma breaks the H and intermolecular bonds in the textile. Intermolecular C–C bond scissions occur and the O_2 -containing hydrophilic functional groups increase, improving the textile's wettability as a result of surface hydrophilic $-\text{COO}^-$, $-\text{O}-\text{O}-$, phenolic, and lactam groups, as detected by X-ray photoelectron spectroscopy (XPS), as reported by [Wagner et al. \(1979\)](#) and [Nogier et al. \(1994\)](#).

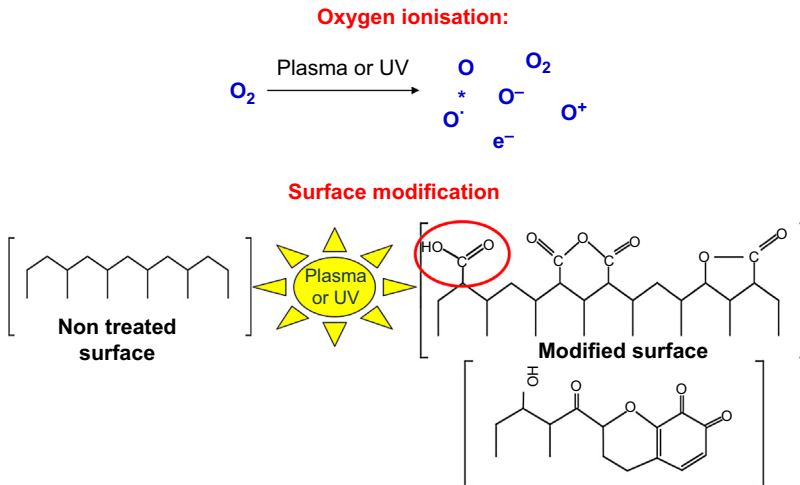


Figure 3.1 Schema of pretreatment of textiles by RF plasma and UVC to generate surface functionalities and complex, chelate, and bind electrostatically TiO_2 . For other details, see text. Modified from [Bozzi, A., Yuranova, T., Guasaquillo, I., Laub D., Kiwi, J., 2005b](#). Self-cleaning of modified cotton textiles by TiO_2 at low temperatures under daylight irradiation. *Journal of Photochemistry and Photobiology A* 174, 156–164.

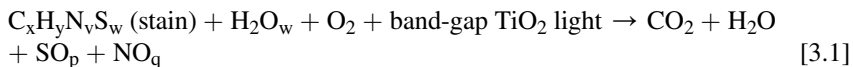
2. UVC light for surface pretreatment: Light excitation at 185 nm does not have the energy content to produce cationic O^+ and anionic oxygen O^- species as it does in the case of RF plasma. Only atomic and excited species of O_2 are produced in Fig. 3.1. UVC light below 241 nm/5.1 eV is equivalent to the $O=O$ binding energy of 495 kJ/mol. When this bond energy is broken, the dissociation $O=O \rightarrow 2O^*$ occurs. The light at 185 nm has an energy content of 6.70 eV. The optical absorption of O_2 in the atmosphere for solar light was reported by Brasseur and Solomon (1986). No radiation (at 185 nm) is lost in the optical pathway between the light source and the textile sample even at atmospheric pressures owing to the low molar absorption coefficient of O_2 at 185 nm.

3.3 Coating by colloidal titanium dioxide of artificial fibers such as polyamide and polyester: evaluation of self-cleaning performance under low-intensity solar irradiation

3.3.1 Photodiscoloration/self-cleaning of polyamide, polyester, and nylon fabrics

Artificial fibers such as polyamide, PES, and nylon can be pretreated by RF plasma or UVC, as described in the preceding section. PES (100% Trevira), wool (90%)–polyamide (10%), and nylon were impregnated with Ti colloids in acid media after an optimized pretreatment procedure, as reported by Bozzi et al. (2005a,b) and Mejia et al. (2009a,b). Titanium tetrachloride, titanium tetra-isopropoxide (TTIP), nitric acid, and hydrochloric acid (HCl) were Fluka p.a. reagents and were used as received. For coating, the pretreated textiles were immersed in the TiO_2 suspension/colloidal solutions for 30 min. Then, samples were dried in air at 22–25°C for 24 h and heated at 100°C for 15 min. The samples were washed with distilled water under sonication to remove TiO_2 particles that did not attach to the fabric surface.

The self-cleaning kinetics for artificial fibers and polymers under solar-simulated irradiation were evaluated after the evolution of CO_2 induced by solar-simulated light, because satin mineralization proceeds according to Eq. [3.1]; the reaction is shown in Fig. 3.2. CO_2 evolution was proportional to the decomposition of the stain and formed a small amount of cations and anions, as shown in Eq. [3.1]



The amount of CO_2 produced in the photochemical reactor was injected in a thermal conductivity detector equipped with Poropak Q column as a function of time. In this way, mineralization of coffee, food, makeup, and wine was monitored during discoloration. Blank experiments were run on unloaded textile samples. No CO_2 was observed in the absence of TiO_2 on polyester and wool–polyamide textiles. This type of analysis allows the selection of the best pretreatment time and loading procedures of TiO_2 on the textile to obtain the fastest stain mineralization kinetics. Samples pretreated by UVC for

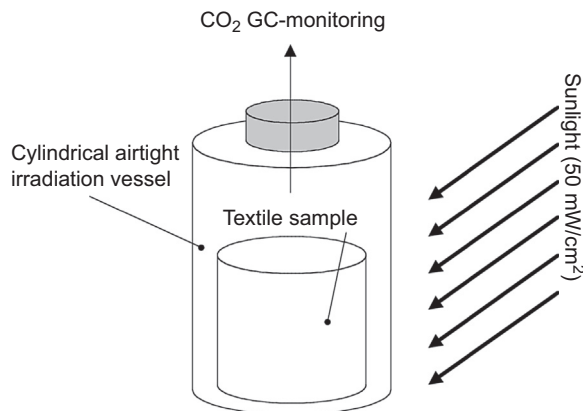


Figure 3.2 CO₂ determination reactor under light irradiation during the irradiation of stained textile samples by gas chromatography-TCD.

Reused from Bozzi, A., Yuranova, T., Kiwi, J., 2005a. Self-cleaning of wool-polyamide and polyester textiles by TiO₂-rutile modification under daylight irradiation at ambient temperature. *Journal of Photochemistry and Photobiology A* 172, 27–34 under license No. 3686380899875 from Elsevier.

10 min at 0.1 Torr (trace g) presented the highest CO₂ evolution (3532 μL) after 24 h irradiation. Samples pretreated by vacuum UVC for 30 min at 0.1 mbar produced the second highest amount of CO₂ (2607 μL). Samples with UVC pretreatment at atmospheric pressure produce 2353 μL of CO₂ after 24 h of irradiation. The result in the absence of vacuum makes the UVC highly convenient for industrial applications; it reduced cost because no vacuum is required. Very small amounts of CO₂ were found for nylon fabrics stained with red wine in the absence of TiO₂ and for nylon irradiated in the absence of TiO₂ and wine.

The mechanism of stain discoloration under light irradiation is shown for transparent stains (grease) absorbing below 390 nm in Fig. 3.3(a) and for colored stains under TiO₂ band-gap irradiation in Fig. 3.3(b). The mechanism will not be further explained in detail in this chapter. It has been fully reported in references by our laboratory and other research groups. “R” stands for organic radical in Fig. 3.3. Peroxides and highly oxidative radicals HO₂[•], OH[•], RO[•], and RO₂[•] adsorbed onto the TiO₂ surface, mineralizing the stain up to CO₂ (see Eq. [3.1]). An alternative mechanism is stain decomposition by a direct reaction between the oxidative hole of TiO₂ (h⁺_{vb}) with the organic compound. The oxidative radicals originating from O₂^{•-} lead to long-lived intermediates. These intermediates then decompose to carboxylic acids, ultimately generating CO₂. The vbh⁺ also reacts with carboxylic acids under light irradiation, leading to CO₂ through the well-known photo-Kolbe reaction:



Stain self-cleaning of textiles is based on the continuous generation of highly oxidative radicals on the surface of TiO₂ under continuous light irradiation in the presence of

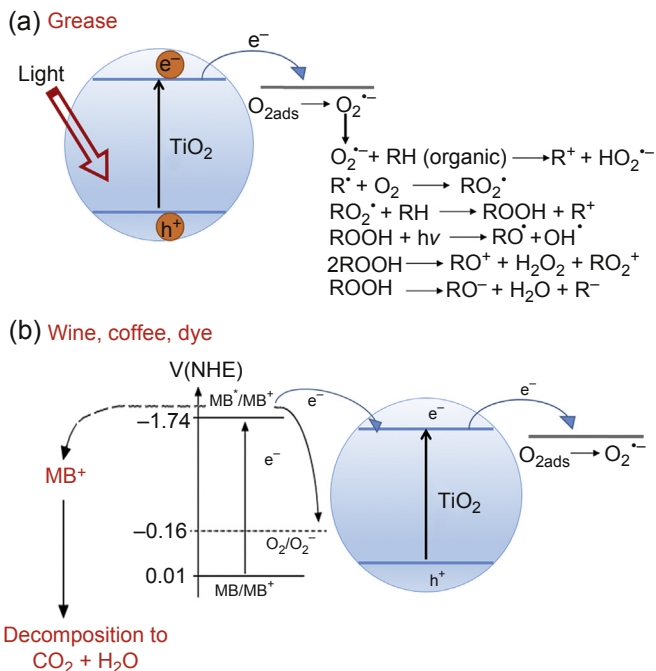


Figure 3.3 Mechanism for the production of oxidative radicals on TiO_2 by a textile substrate with (a) transparent stains in which the TiO_2 absorbs incoming light and (b) a textile stained with color stains such as wine, coffee, or dye.

air (O_2) and H_2O -vapor (H_2Ov). Therefore, a mild environmental green chemistry process sets in that does not need chemicals, solvents, and expensive composites. The highly oxidative radicals produced at the TiO_2 surface leading to stains that discolor the nylon pump radicals on a continual basis.

3.3.2 Surface characterization of photocatalytically modified titanium dioxide artificial textiles

A high-resolution electron microscopic image (HRTEM) of nylon- TiO_2 shown in Fig. 3.4 shows an almost continuous coating of TiO_2 on the nylon surface. The thickness of the TiO_2 layer was between 35 and 115 nm and remained stable after 24 h discoloration. The TiO_2 nanoparticles making up the coating were 8–20 nm, as determined by HRTEM. The TiO_2 size was small enough to produce transparent films and keep the original handling touch of the nylon. This is important for the potential application of nylon- TiO_2 self-cleaning fabrics. No atomic force microscopy could be carried out on these samples because of the rough nylon- TiO_2 surface.

Next, we addressed X-ray diffraction imaging (XRD) of nylon- TiO_2 prepared at 100°C . The XRD spectra confirmed the presence of TiO_2 anatase on the nylon surface. Peaks at 20.32 degree, 21.36 degree, and 23.8 degree were seen and were attributed to

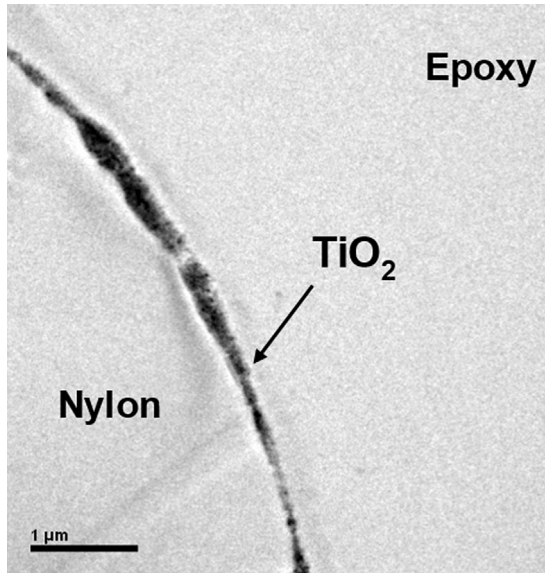


Figure 3.4 Transmission electron microscopic image of nylon–TiO₂ fabric at time 0. Reused from “Catalysis Today 122 (2007) 109–117” under the license No. 3686380482120 from Elsevier Mejia, M.I., Marin, J.M., Restrepo, G., Pulgarin, C., Mielczarski, E., Mielczarski, J., Stolitchnov, I., Kiwi, J., 2009b. Innovative UVC light (185 nm) and radio-frequency-plasma pretreatment of nylon surfaces at atmospheric pressure and their implications in photocatalytic processes. *ACS Applied Materials and Interface* 1, 2190–2198.

the nylon fibers. The brookite orthorhombic TiO₂ phase is shown at 30.81 degree. At the work condition temperatures at which we deposited TiO₂ on the nylon, we expected the formation of amorphous titania after hydrolyzing the TTIP precursor. Anatase formation from TTIP suspensions requires temperatures of 300°C for several hours. The formation of anatase at about 100°C implies that nylon has a structure-forming function on the TTIP colloid that produces crystallographic forms of TiO₂ at very low temperatures, in this case anatase.

Another important surface feature we investigated by XPS was the binding energy of the peaks found at the topmost catalyst layers of the nylon–TiO₂, containing about 2% TiO₂. We found a Ti2p peak at 458.4 eV, as shown in Fig. 3.5. At time 0, the Ti2p peak of the TiO₂ signal was high before coming into contact with red wine. At 3 h the Ti2p peak was lower owing to the addition of the wine. The addition of the wine spot attenuated the signal from the TiO₂ on nylon. However, after 3 or 6 h reaction, the Ti2p signals again reached the initial peak intensity when the wine stain (and organic residues) was eliminated under light irradiation. Furthermore, redox catalysis in the TiO₂ seemed to take place during Orange II dye discoloration. The initial Ti2p peak at 458.4 eV shifted to 458.0 eV, providing evidence for a Ti⁴⁺/Ti³⁺ reduction concomitant to the photooxidation of Orange II, as reported by Mejia et al. (2009a,b). An XPS binding energy peak shift >0.2 eV is accepted as proof for the generation of a new species or changes in the oxidation state of a component in the XPS signal, according to Wagner et al. (1979).

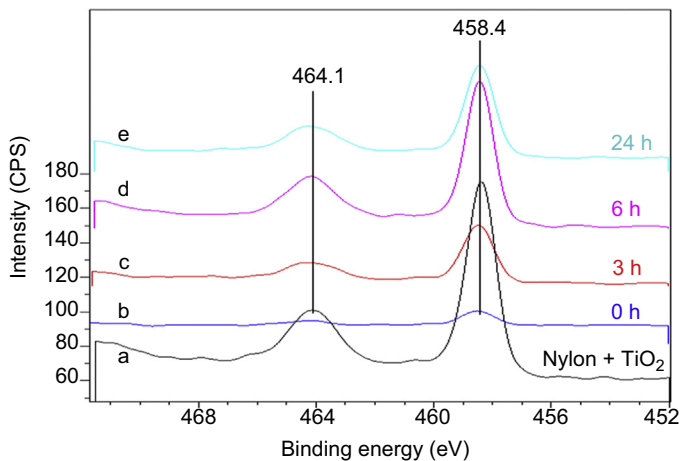


Figure 3.5 XPS spectrum of Ti2p peaks of (a) nylon–TiO₂ without wine at 0 h and wine-stained nylon under Suntest light for (b) 0 h, (c) 3 h, (d) 6 h, and (e) 24 h. Reused from Mejia, M.I., Marin, J.M., Restrepo, G., Pulgarin, C., Mielczarski, E., Mielczarski, J., Stolitchnov, I., Kiwi, J., 2009b. Innovative UVC light (185 nm) and radio-frequency-plasma pretreatment of nylon surfaces at atmospheric pressure and their implications in photocatalytic processes. *ACS Applied Materials and Interface* 1, 2190–2198.

3.4 Coating by colloidal titanium dioxide of natural fibers: evaluation of self-cleaning performance under low-intensity solar irradiation

Pretreatment, the colloidal deposition of TiO₂ on cotton, and the test of their self-cleaning discoloration performance follow a pattern similar to that of the features reported for artificial fibers such as polyamides, polyester, and their combinations mentioned earlier, as reported by [Bozzi et al. \(2005a,b\)](#) and [Mejia et al. \(2009a,b\)](#). The cotton fabrics were also pretreated using the 185-nm line of low-pressure mercury lamp from Ebara Corp., Iwasaki Electric Co., Shiba, Japan with a power of 25 W. The scheme of the installation used is shown in [Fig. 3.6](#). The lamp wall consisted of synthetic silica able to transmit 184 nm light. This wavelength was composed of 25% of the total lamp output; 75% of the lamp output consisted of 254 nm bactericide radiation. Because vacuum–UV activation proceeds with lower energy than plasma activation, no cation or anionic oxygen species are formed in the gas phase. Only atomic and excited oxygen species are formed, which is the difference with the plasma pretreatment method described previously. This leads to a more defined and uniform modification of the textile surfaces, with an increased polarity, because it contains a variety of oxygen functional groups formed by the reactions of free radicals with the O₂ in the gas phase. The upper textile layers are excited by the incoming UV light up to ~ 100 Å or the equivalent of about 50 atomic layers, as stated by [Yuranova et al. \(2005\)](#). By plasma or vacuum–UV pretreatment, the residual oxygen at the chosen pressures was sufficient to modify the textile surfaces owing to the absorption cross-section of the O₂ for UVC light.

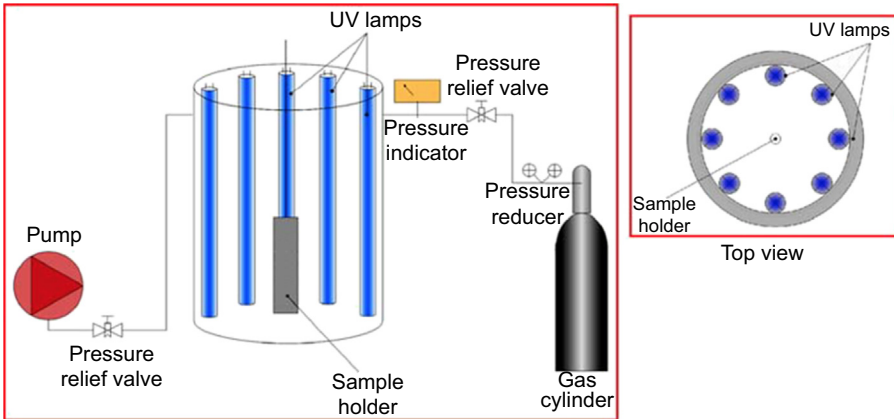
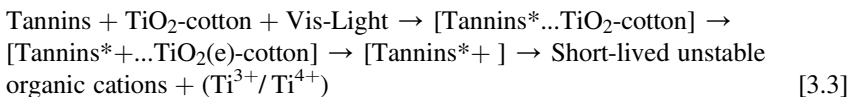


Figure 3.6 Schematic of UVC pretreatment unit used for the pretreatment of cotton fabrics. Reused from “Catalysis Today 122 (2007) 109–117” under the license No. 3686380482120 from Elsevier Bozzi, A., Yuranova, T., Guasaquillo, I., Laub D., Kiwi, J., 2005b. Self-cleaning of modified cotton textiles by TiO_2 at low temperatures under daylight irradiation. *Journal of Photochemistry and Photobiology A* 174, 156–164.

Preparation of TiO_2 colloids as applied to cotton fabrics can be summarized as follows: TTIP (20 mL) was added drop-wise to 300 mL of 2-propanol acidified with 1 mL of concentrated HNO_3 and cooled to about 0°C . This solution was stirred for about 1 h to achieve total dissolution of the polymer chains and produce a transparent solution. Hydrothermal treatment of this colloid was then carried out to grow the particles to the desired size by heating in an autoclave for 10–36 h at $100\text{--}250^\circ\text{C}$. After autoclaving, the TiO_2 particles were redispersed by stirring or sonication. Hydrolysis of TTIP as a precursor for 5-nm particles was reported by Moser and Gratzel (1983). Kiwi (1983) prepared 10- to 25-nm anatase particles. Using the hydrothermal method, particles of a few nanometers were obtained by Ovenstone (2001) from TiO_2 -sols.

The coating of textiles by colloidal and suspension layers was carried out on $4 \times 12\text{-cm}$ samples pretreated with RF plasma for 30 min. These fabrics were immersed in a TiO_2 colloid and then dried at 60°C for 24 h and cured at $100\text{--}120^\circ\text{C}$ for 10 min. A second layer of TiO_2 was then deposited by immersing the textile in a suspension of TiO_2 Degussa P25 (5 g/L).

Self-cleaning of colored stains (such as wine and tomatoes) occurs as the result of photosensitization of the unstable short-lived cation under visible light, as shown in Fig. 3.7. The discoloration reaction of the wine containing tannin or lycopene pigments is outlined in Eq. [3.3]. Redox reactions induced under light irradiation between the tannins or lycopenes and TiO_2 lead to oxidoreduction in the excited exciplex (Eq. [3.3]) by charge transfer followed by charge separation between the tannin or lycopene and TiO_2 , leading to tannin discoloration, as found by Bozzi et al. (2005a).



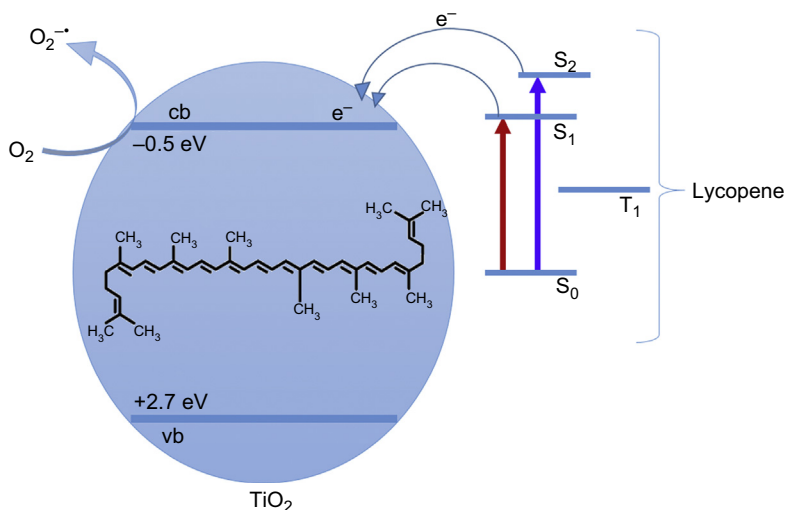


Figure 3.7 Scheme for the generation of highly oxidative species on the surface of TiO_2 under daylight irradiation (90 mW cm^{-2}) for the photodiscoloration mechanism of a red wine stain under daylight irradiation.

The surface characterization of photocatalytic TiO_2 -modified cotton showed the main results: (1) XRD diffraction of TiO_2 -cotton detected anatase peaks at 22.9 degree and 34.4 degree and (2) high-resolution transmission electron microscopy of TiO_2 -coated cotton had a homogeneous TiO_2 coating on the cotton with a thickness of about 31 nm ($\pm 10\%$) and a TiO_2 particle size of about 8–18 nm. This particle size conserved the cotton's appearance and feel.

Carboxymethylation of cotton enhancing the grafting of TiO_2 nanoparticles (NT) for self-cleaning purposes was reported by Wijesena et al. (2015). TiO_2 had a uniform distribution on the cotton surface. Methyl orange was used as the probe to follow the stain removal of the dye when irradiated by UV-A light, ensuring that the only absorber was TiO_2 . The Methyl Orange removal increased with TiO_2 loading, as followed by XPS, because the TiO_2 initial particles were no longer covered with dye. Carboxylic acid groups on the cotton bind the TiO_2 nanoparticles through a bidentate complex with Ti atoms. Carboxylic acid groups on the cotton were responsible for TiO_2 particle binding, as detected by attenuated total reflectance–infrared spectroscopy (ATR-IR).

3.5 Cotton self-cleaning by titanium dioxide clusters attached by chemical spacers under low-intensity solar irradiation

The aim of this work was to use a spacer (linker) on a cotton textile with free carboxylate moieties able to bind TiO_2 by strong electrostatic interactions by attaching maleic anhydride units on pretreated textiles at temperatures $< 140^\circ\text{C}$.

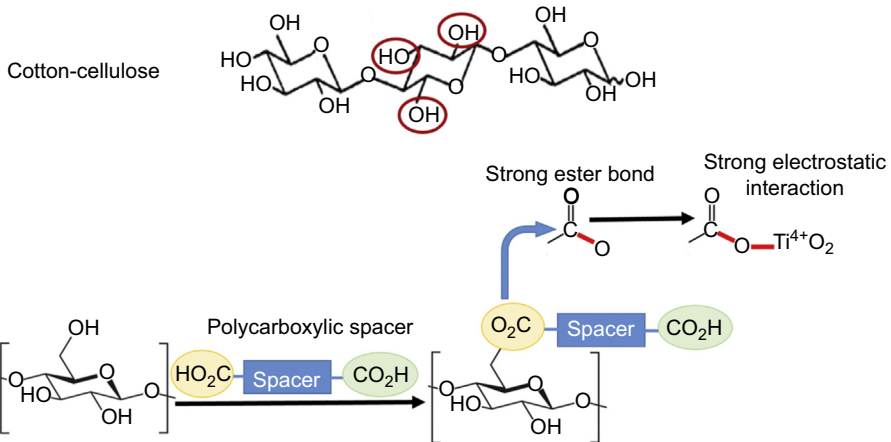


Figure 3.8 Attachment of TiO₂ to cellulose to via a chemical spacer, eg, succinic acid. Cotton is almost pure cellulose; cellulose is a polymer of glucose; the free OH groups (three per glucose unit) are potential bending sites for the spacer.

The cellulose is a polysaccharide with a high number of alcoholic-OH groups. These alcoholic-OH groups are able to link TiO₂ and cellulose through a spacer. According to Meilert et al. (2005), this leads to the formation of a covalent bond as a result of the esterification of the carboxyl groups. Succinic acid has been used as a spacer with two terminal COOH groups. The chemical inertness of the spacer is warranted by the succinic single bond. Binding of the TiO₂ to the alcoholic-OH group of cellulose through a polycarboxylic spacer is shown in Fig. 3.8. Curing was carried out by Meilert et al. (2005) at 150–170°C for 2 min and eliminated H₂O by hydrolysis and condensation of the OH-alcoholic group of the cellulose with the TiOH surface TiO₂ groups. By ATR-IR, as shown in Fig. 3.9, formation of the ester bonds could be confirmed. Because the characteristic stretching vibration of esters (RCOOR) and acids (RCOOH) is in the same region (1800–1600 cm⁻¹), the textiles were further treated in a diluted acidic solution (HCl 0.1 N) and a diluted basic solution (NaOH 0.1 N). By acidic treatment, the complete protonation of the carboxylic groups was ensured and subsequent basic treatment led to complete deprotonation. The deprotonation shifted the stretching vibration of the carbonyl function (RCOO⁻) to 1550 cm⁻¹. Hence, the newly formed ester bonds could be identified with the peaks at 1724 cm⁻¹ of carboxylates and 1575 cm⁻¹ (blue line). Discoloration of wine and coffee under sunlight was observed when TiO₂ clusters bound to the succinic acid spacer on cotton within less than 24 h.

This study showed that it was possible to bind TiO₂ to cotton textiles through chemical spacers. Elemental analysis of the TiO₂ loading on the cotton employing different spacers and different experimental conditions was determined to be around 1%. The coating procedure was straightforward and used nontoxic reagents. The TiO₂-loaded cotton textiles had stable self-cleaning properties and partially eliminated the chromophore(s) in the red wine under daylight irradiation, with long-term stable performance. ATR-IR spectroscopy showed the formation of ester bonds between the spacer and the

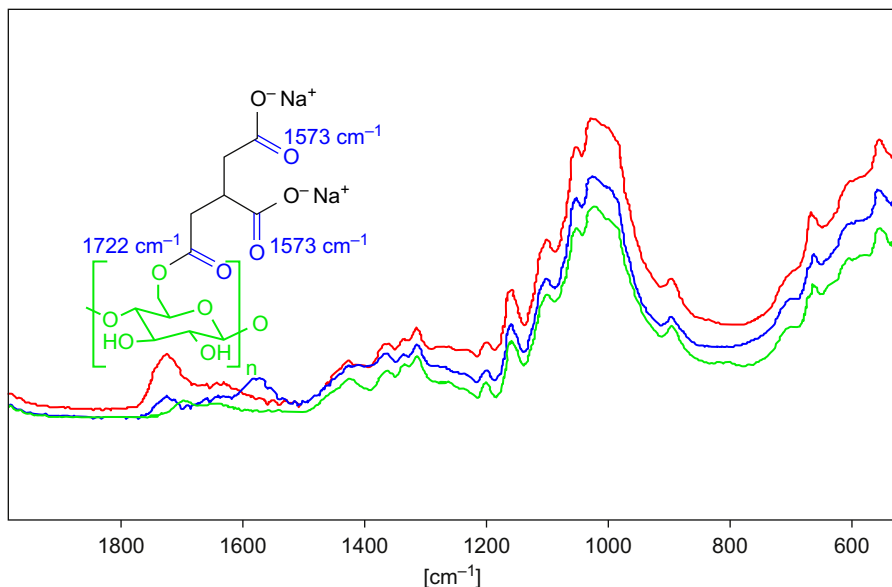


Figure 3.9 Characterization of the ester bond between the spacer and cellulose by ATR-IR. (a) Green line: cotton bleached with ammonia. (b) Red line: after immersion in a solution 4% of NaH_2PO_2 in H_2O , followed by drying (3 min at 90°C) and curing (2 min at 175°C) and final treatment in a 0.1 N solution. (c) Blue line: same as red, but final treatment in a 0.1 N solution of NaOH , same as the red line and a final treatment with TiO_2 (1 h at 75°C , 1 h drying at 100°C and washing).

cotton surface. In addition, free carboxyl units remained available to bind the TiO_2 . Without the spacer, none of the textiles bound efficiently to TiO_2 . The cellulose was not decomposed by the reactive species generated by the photocatalytic process within the dye discoloration period. Because the use of higher spacer concentrations is limited by the saturation of the solutions, multilayer loading may allow a higher space and consequently TiO_2 loading.

3.6 Self-cleaning cotton textiles titanium dioxide—modified by silicon dioxide—protective layers

To avoid the corrosion of textile by the photogenerated h^+ from irradiated TiO_2 , Yuranova et al. (2005) used SiO_2 underlayers between the textile and the TiO_2 layer. SiO_2 was selected as the TiO_2 underlayer because it is not a semiconductor and it does not decompose owing to the h^+ generated by TiO_2 . The SiO_2 layers are applied on the textile according to the procedure outlined by Yuranova et al. (2005). The corrosion of textiles can also originate from the $\text{OH}\cdot$ radicals, which are the strongest oxidant among the reactive oxygen species, as reported by Fujishima et al. (2008).

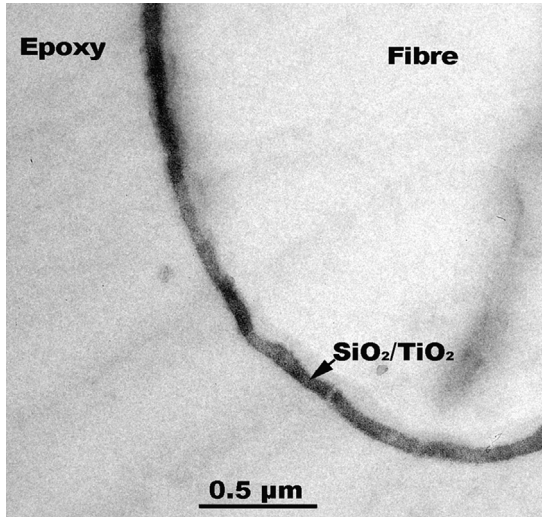


Figure 3.10 Transmission electron microscopy of a cotton fiber coated with $\text{TiO}_2\text{-SiO}_2$. Reused from “Catalysis Today 122 (2007) 109–117” under the license No. 3686380482120 from Elsevier.

The amorphous $\text{TiO}_2\text{-SiO}_2$ layer in Fig. 3.10 had sizes between 4 and 8 nm and a width of $25 \pm 10\%$ nm. This is equivalent to three to six layers of $\text{TiO}_2\text{-SiO}_2$. The Ti particles were embedded within a highly porous SiO_2 amorphous coating.

Fig. 3.11(a) shows the energy-dispersive spectroscopy (EDS) images of the cotton samples. The arrows in Fig. 3.11(a) (left-hand side) show the individual particles of Si and Ti1 and Ti2. The rectangle shows a low-resolution view of the EDS image. The high amount of C comes from the C of the grid used for the EDS observation and from the epoxy resin applied during the sample preparation. Si and Ti were observed to be everywhere on the cotton surface. The image of Ti shows a much higher resolution of the Ti1 and Ti2 particles. Ti particles were embedded in amorphous SiO_2 (see white areas in Fig. 3.11(b)). The clear areas show the SiO_2 in Fig. 3.11(b). The Ti particles always had amorphous SiO_2 surrounding them.

3.7 Coatings by binary oxides and/or promoted or enhanced copper-binary oxides leading to faster stain discoloration under low-intensity solar irradiation: reaction mechanism and surface characterization

To date, self-cleaning by TiO_2 -modified textiles has proceeded using a low kinetics under solar light irradiation. Rtimi et al. (2016), from our laboratory, addressed in a study self-cleaning polyester based on sputtered $\text{TiO}_2\text{-ZrO}_2$ and $\text{TiO}_2\text{-ZrO}_2\text{-Cu}$ at

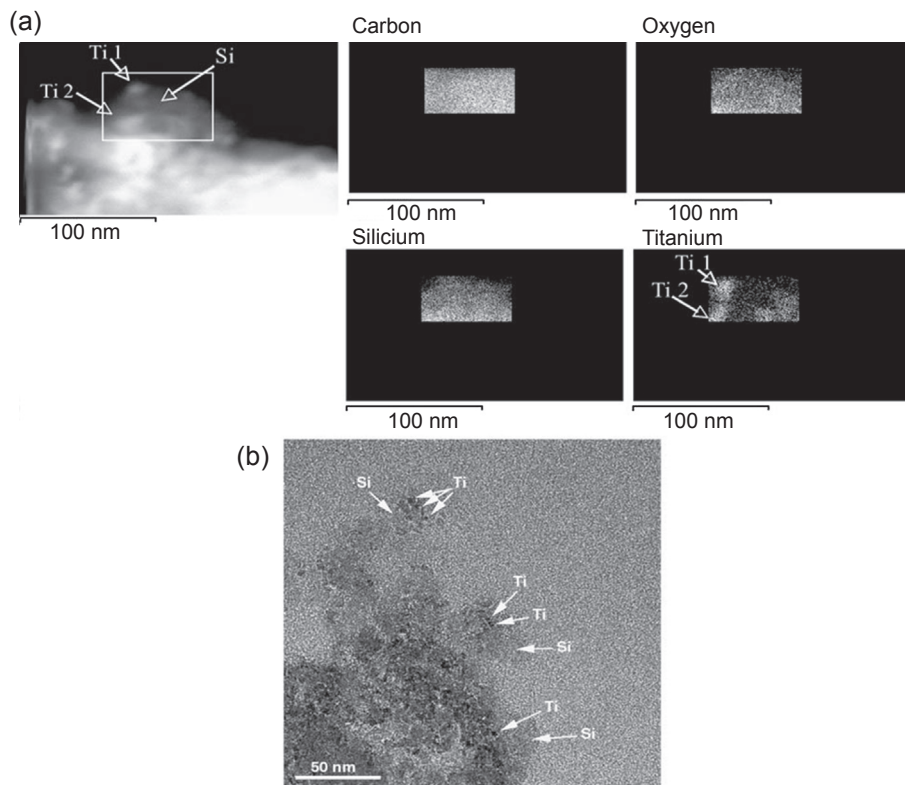


Figure 3.11 (a) EDS of the cotton $\text{TiO}_2\text{-SiO}_2$ sample. Elements Map INCA Oxford and (b) EDS spectroscopy of the cotton $\text{TiO}_2\text{-SiO}_2$ sample showing the Si and Ti particles present on the textile surface.

Reused from “Catalysis Today 122 (2007) 109–117” under the license No. 3686380482120 from Elsevier.

temperatures $< 140^\circ\text{C}$. We present a suitable film preparation and the evaluation of a photocatalytic film accelerating the discoloration kinetics and improving film uniformity and adhesion, two drawbacks observed for TiO_2 colloidal coated surfaces encountered by many research groups (Kivi and Pulgarin, 2013; Zhang et al., 2012). Sputtered $\text{TiO}_2\text{-ZrO}_2$ and $\text{TiO}_2\text{-ZrO}_2\text{-Cu}$ films on PES reduced the methylene blue (MB) self-cleaning time by TiO_2 depending on the dye stain applied to the PES. To date, $\text{TiO}_2\text{-ZrO}_2$ films prepared by sol-gel methods and used as powders or annealed on diverse substrates at a few hundred degrees have been used in industrial processes as catalysis and in electronic devices and optical applications, but they have not been reported as a photocatalyst in light-induced self-cleaning devices.

MB was used as a probe during self-cleaning; this was extensively reported by Kamat (1993) and Kumar and Devi (2011). Mills et al. (2011) reported work on MB photoinduced abatement and discoloration. The photobleaching and degradation mechanism of MB in TiO_2 suspensions and colloids is controversial. Houas et al.

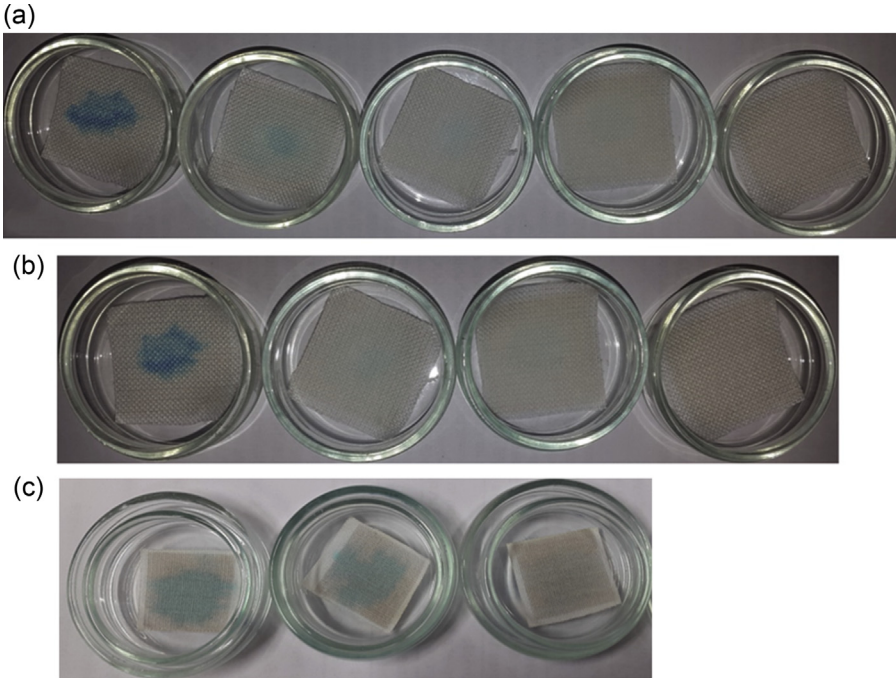
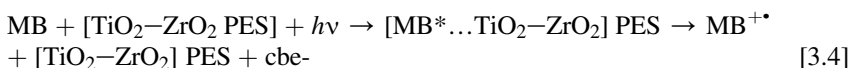


Figure 3.12 (a) MB self-cleaning under low-intensity simulated Suntest light (50 mW/cm^2) $\text{TiO}_2\text{-ZrO}_2$ sputtered samples for 8 min at 0, 5, 30, 60, and 120 min. (b) $\text{TiO}_2\text{-ZrO}_2\text{-Cu}$ sputtered for 8 min 10 s at 0, 10, 20, and 30 min. (c) $\text{TiO}_2\text{-Cu}$ sputtered for 8 min 10 s at 0, 30, and 120 min.

Reused from Rtimi, S., Pulgarin, C., Sanjines, R., Kiwi, J., 2016. Accelerated self-cleaning by Cu promoted semiconductor binary-oxides under low intensity sunlight irradiations. *Applied Catalysis B* 180, 648–655 under the license No. 3686390064812 from Elsevier.

(2001) also reported the degradation pathway and intermediates of MB in colloidal solutions under light. These studies take advantage of the fact that TiO_2 has dense-surface TiOH groups, high crystallinity, and redox properties generating highly oxidative radicals leading to MB degradation.

The discoloration of MB under light is shown in Fig. 3.12, which compares the discoloration kinetics of $\text{TiO}_2\text{-ZrO}_2$ and $\text{TiO}_2\text{-ZrO}_2\text{-Cu}$. MB discoloration induced under light on $\text{TiO}_2\text{-ZrO}_2$ samples occurs within 120 min. The discoloration time was significantly reduced by $\text{TiO}_2\text{-ZrO}_2\text{-Cu}$, taking place within 30 min. This is four times faster than for $\text{TiO}_2\text{-ZrO}_2$ films. The reaction between the $\text{TiO}_2\text{-ZrO}_2$ PES under sunlight irradiation involves charge transfer reactions from MB^* to $\text{ZrO}_2\text{-TiO}_2$:



Because of the low-energy absorption edge of MB at 720 nm or 1.75 eV, the electron transfer from the excited state of MB to TiO₂ is thermodynamically favorable. Cu accelerating MB discoloration involves: (1) acceleration of the electron transfer from the valence band to the TiO₂ conduction band by Cu-intragap states, (2) the ZrO₂cb electron transfer to the TiO₂cb, preventing electron–hole recombination in TiO₂, and (3) the presence of a Cu-promoter mediating faster TiO₂cb-electron transfer to the adsorbed O₂, as shown in Eqs. [3.5]–[3.7]. The participation of HO₂[•]/O₂⁻, OH[•] radicals and h⁺ species in the MB discoloration process is suggested:



Low levels of Cu (0.01–0.02%) sputtered for very short times on the TiO₂–ZrO₂ increased the MB discoloration rate. This may be attributed to electron intragap trapping at the TiO₂–ZrO₂ surface:



Eq. [3.8] prevents an electron–hole recombination and leads to increased radical formation, as noted in Eqs. [3.5]–[3.9]. A higher Cu-doping level would allow the OH-mediated oxidation of Cu⁽ⁿ⁻¹⁾⁺ or accelerate the reverse reaction (Eq. [3.10]). Any oxidation of Cuⁿ⁺ competes with the available hole-oxidizing species, as noted in Eqs. [3.8] and [3.9]:



ATR-IR spectroscopy was used to monitor MB degradation under solar simulated light. Fig. 3.13(a) presents the symmetric stretching vibration peak shifts for methylene (CH₂)_s by ATR-IR spectroscopy for the TiO₂–ZrO₂ samples in the range 2650–2900 cm⁻¹. The IR signals were sensitive enough to follow the spectral shifts and the reduction in amplitude during MB discoloration, as reported by Naumann et al. (1989) and Kiwi and Nadtochenko (2004). Fig. 3.13 shows a discontinuous MB IR peak shift for methylene ν_s(–CH₂) from 2829.2 cm⁻¹ at time 0 up to 2833 cm⁻¹ within 120 min, the time required for complete discoloration. Fig. 3.13(b) presents the corresponding IR shifts induced by a TiO₂–ZrO₂–Cu showing a similar trend during the accelerated MB discoloration within 30 min. The insert in Fig. 3.13(a) shows for a TiO₂–ZrO₂ sample a slower MB ν_s(–CH₂) shift up to 60 min followed by a

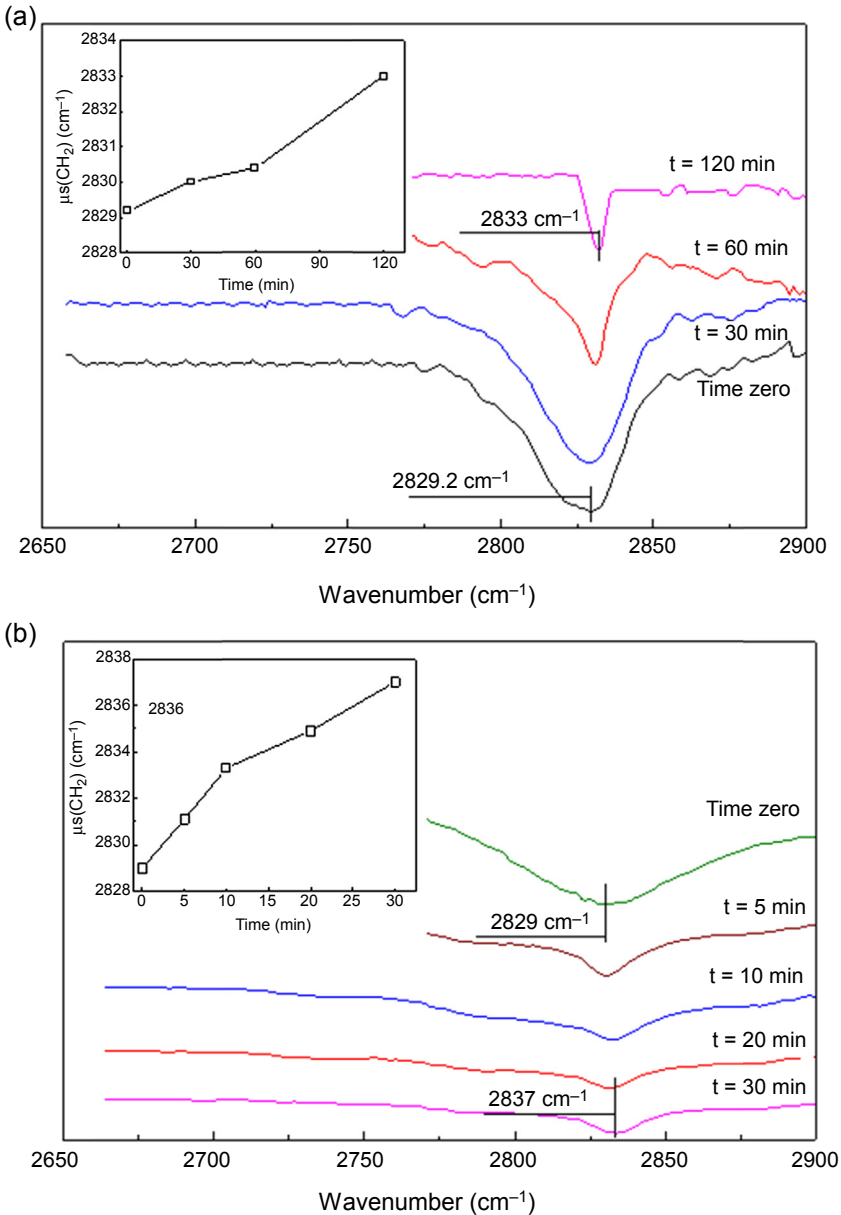


Figure 3.13 (a) Shift in the MB $\nu_s(-CH_2)$ vibrational peaks in contact with TiO_2-ZrO_2 (8 min) as function of the time of irradiation. (b) Shift in MB $\nu_s(-CH_2)$ vibrational peaks in contact with TiO_2-ZrO_2-Cu (8 min/10s) as function of the time of irradiation under solar-simulated Suntest cavity (50 mW/cm^2).

Reused from Rtimi, S., Pulgarin, C., Sanjines, R., Kiwi, J., 2016. Accelerated self-cleaning by Cu promoted semiconductor binary-oxides under low intensity sunlight irradiations. Applied Catalysis B 180, 648–655 under the license No. 3686390064812 from Elsevier.

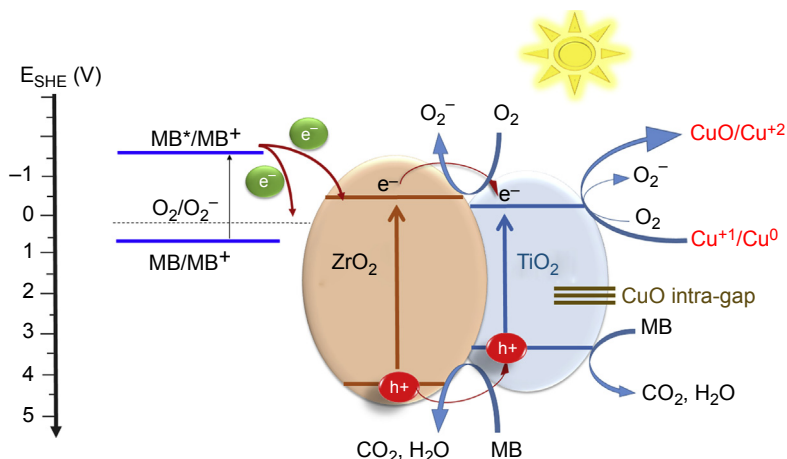


Figure 3.14 Suggested scheme for interfacial charge transfer in samples of $\text{TiO}_2\text{-ZrO}_2\text{-Cu}$ (8 min/10s) under low-intensity solar light (50 mW/cm^2) leading to MB discoloration. For further details, see text.

Reused from Rtimi, S., Pulgarin, C., Sanjines, R., Kiwi, J., 2016. Accelerated self-cleaning by Cu promoted semiconductor binary-oxides under low intensity sunlight irradiations. *Applied Catalysis B* 180, 648–655 under the license No. 3686390064812 from Elsevier.

more steep increase in the IR-stretching peaks after 60 min. The opposite trend is observed for $\text{TiO}_2\text{-ZrO}_2\text{-Cu}$ in the insert in Fig. 3.13(b) for IR-stretching of the peaks before and after 10 min.

The interfacial charge transfer mechanism presented in Fig. 3.14 follows the band model for the potential of the electronic band positions known for $\text{TiO}_2\text{-ZrO}_2\text{-Cu}$. The low-lying Cu-intragap states promote the TiO_2 $\text{vb}(h^+)$ indirect transitions to the TiO_2 cb, increasing the charge separation and decreasing the electron–hole recombination rate. The band structure modification in the $\text{TiO}_2\text{-ZrO}_2$ -coupled semiconductor may slow the recombination of the charge carriers and increase the hydrophilicity of the $\text{TiO}_2\text{-ZrO}_2$ with respect to TiO_2 and ZrO_2 acting independently. This is important because surface hydrophilicity under light irradiation is the source of the oxidative radicals leading to MB discoloration described in Eqs. [3.6]–[3.9].

Fig. 3.14 presents the electronic levels of the MB dye and the short-lived unstable MB^* produced under low-intensity Suntest-simulated light irradiation. This MB^* state injects an electron into the ZrO_2 cb owing to its higher cbe- band position, causing the reaction $\text{MB}^* \rightarrow \text{MB}^+ + e^-$ of 1.74 V NHE. Cu in Fig. 3.14 acts as a charge trap for the TiO_2 carriers and not as charge recombination centers owing to the low Cu concentration added. The $\text{Cu}^{1+/2+}$ deposited on $\text{TiO}_2\text{-ZrO}_2$ works as an electron acceptor and enhance MB removal. The potential required for the one electron oxygen reduction $\text{O}_2 + \text{H}^+ + e^- \rightarrow \text{HO}_2^\bullet$ is -0.05 V , and for the oxygen reduction $e^- + \text{O}_2 \rightarrow \text{O}_2^\bullet$ is -0.16 V . Cu^+ may also reduce O_2 -consuming electrons or be oxidized to Cu^{2+} by the photogenerated TiO_2 holes to Cu^{2+} .

3.8 Trend of work in this area: future directions

There is currently a need to develop resistant, noncorrosive, robust photocatalysts with faster self-cleaning kinetics. TiO_2 and composite- TiO_2 surfaces have self-cleaning properties that are too slow for many real and industrial applications. The second area that needs improvement is based on the fact that most self-cleaning films are deposited from colloids onto surfaces that are subsequently heated to diffuse or anneal the colloid into the surface at temperatures that fabrics and polymer films do not resist. The friction of a finger or a piece of cloth easily wipes out the deposition of these nonuniform, low-adhesive colloidal TiO_2 films because they are not mechanically stable. Direct current magnetron sputtering is used to overcome the nonuniformity and low adhesion of colloidal films in our laboratory; we have begun using high-power impulse magnetron sputtering to deposit compact thin coatings with higher self-cleaning and antibacterial activity.

In this chapter, we have addressed the deposition of thin films able to self-clean textile under light within acceptable times in a repetitive fashion. The film preparation was optimized for kinetically fastest self-cleaning kinetics. In the coming years, the synthesis of high-quality functionalized films with this objective will need a more sophisticated nanotechnological approach involving innovative composite phases. Improvement in stability will also need to be addressed before laboratory findings and new films can be scaled up to industrial production. Future work will also address toxicity effects and concomitant environmental pollution caused during the preparation and application of self-cleaning films.

Acknowledgments

We thank the EPFL, the Swiss National Science Foundation Project (SNF 200021-143283), the EC7th FP project (Grant No. 3101177), and COST Actions MP1101 and MP 1106 for interactive discussions.

References

- Afzal, S., Daoud, W., Langford, S., 2013. Photostable self-cleaning cotton by a Copper(II) Porphyrin/ TiO_2 visible-light photocatalytic system. *ACS Applied Materials and Interfaces* 5 (11), 4753–4759.
- Bozzi, A., Yuranova, T., Kiwi, J., 2005a. Self-cleaning of wool-polyamide and polyester textiles by TiO_2 -rutile modification under daylight irradiation at ambient temperature. *Journal of Photochemistry and Photobiology A* 172, 27–34.
- Bozzi, A., Yuranova, T., Guasaquillo, I., Laub, D., Kiwi, J., 2005b. Self-cleaning of modified cotton textiles by TiO_2 at low temperatures under daylight irradiation. *Journal of Photochemistry and Photobiology A* 174, 156–164.
- Brasseur, G., Solomon, S., 1986. Aeronomy of the middle atmosphere. In: Reidel, D., Dordrecht (Eds.), 2nd ed. Chapter 4.

- Fateh, R., Ismail, A., Dillert, R., Bahnemann, D., 2011. Highly active crystalline mesoporous TiO₂ films coated onto polycarbonate substrates for self-cleaning applications. *Journal of Physical Chemistry C* 115, 10405–10413.
- Fujishima, Zhang, X., Tryk, A., Donald, A., 2008. TiO₂ photocatalysis and related surface phenomena. *Surface Science Reports* 63, 515–582.
- Houas, A., Lachheb, H., Ksibi, M., El-aloui, E., Guillard, C., Herrmann, J.-M., 2001. Photocatalytic degradation pathway of methylene blue in water. *Applied Catalysis B* 31, 145–157.
- Kamat, P.V., 1993. Photochemistry on nonreactive and reactive (semiconductor) surfaces. *Chemical Reviews* 93, 267–300.
- Kasanen, J., Suvanto, M., Pakkanen, T.T., 2009. Self-cleaning, titanium dioxide based, multi-layer coating fabricated on polymer and glass surfaces. *Journal of Applied Polymer Science* 111, 2597–2602.
- Kiwi, J., 1983. Magnetic field effects on photosensitized electron transfer reactions in the presence of TiO₂ and CdS loaded particles. *Journal of Physical Chemistry* 87, 2274–2276.
- Kiwi, J., Nadochenko, V., 2004. New evidence for TiO₂ photocatalysis during bilayer lipid peroxidation. *Journal of Physical Chemistry B* 108, 17675–17684.
- Kiwi, J., Pulgarin, C., 2013. In: Daoud, W. (Ed.), *Self-cleaning Materials and Surfaces*. Woodhead Pub. Co., UK, pp. 205–224 (Chapter 7).
- Kumar, S., Devi, L., 2011. Review on modified TiO₂ photocatalysis under UV/visible light: selected results and related mechanisms on interfacial charge carrier transfer dynamics. *Journal of Physical Chemistry A* 115, 13211–13241.
- Meilert, K., Laub, D., Kiwi, J., 2005. Photocatalytic self-cleaning of modified cotton textiles by TiO₂ clusters attached by chemical spacers. *Journal of Molecular Catalysis A: Chemical* 237, 101–108.
- Mejia, M.I., Marin, J.M., Restrepo, G., Pulgarin, C., Mielczarski, E., Mielczarski, J., Arroyo, Y., Lavanchy, J.-C., Kiwi, J., 2009a. Self-cleaning modified TiO₂-cotton pretreated by UVC-light (185 nm) and RF-plasma in vacuum and also under atmospheric pressure. *Applied Catalysis B* 91, 481–488.
- Mejia, M.I., Marin, J.M., Restrepo, G., Pulgarin, C., Mielczarski, E., Mielczarski, J., Stolitchnov, I., Kiwi, J., 2009b. Innovative UVC light (185 nm) and radio-frequency-plasma pretreatment of nylon surfaces at atmospheric pressure and their implications in photocatalytic processes. *ACS Applied Materials and Interfaces* 1, 2190–2198.
- Mihailovic, D., Saponjic, Z., Radoicic, M., Lazovic, S., Baily, C.J., Jovancic, P., Nedeljkovic, J., Radetic, M., 2011. Functionalization of cotton fabrics with corona/air RF plasma and colloidal TiO₂ nanoparticles. *Cellulose* 18, 811–825.
- Mills, A., 2012. An overview of the methylene blue ISO test for assessing the activities of photocatalytic films. *Applied Catalysis B* 128, 144–149.
- Mills, A., Hazafy, D., Parkinson, J., Tuttle, T., Hitchings, M., 2011. Effect of alkali on methylene blue (C.I. Basic Blue 9) and other thiazine dyes. *Dyes and Pigments* 88, 149–155.
- Moser, J., Gratzel, M., 1983. Light-induced electron transfer in colloidal semiconductor dispersions: single vs. dielectronic reduction of acceptors by conduction-band electrons. *Journal of the American Chemical Society* 105 (1983), 6547–6555.
- Naumann, D., Schultz, C., Sabich, A., Kasrowsky, M., Labishinski, H., 1989. New insights into the phase behaviour of a complex anionic amphiphile: architecture and dynamics of bacterial deep rough lipopolysaccharide membranes as seen by FTIR, X-ray, and molecular modelling techniques. *Journal of Molecular Structure* 214, 213–246.

- Nogier, J., Delamar, M., Ruiz, P., Gratzel, M., Thampi, R., Kiwi, J., 1994. Chapter 7.1 X-ray photoelectron spectroscopy of $\text{TiO}_2/\text{V}_2\text{O}_5$ catalysts. *Catalysis Today* 20, 109–123.
- Ovenstone, J., 2001. Preparation of novel titania photocatalysts with high activity. *Journal of Materials Science* 36, 1325–1329.
- Patrocínio, A.-O., Paula, L., Paniago, R., Freitag, J., Bahnemann, D., 2014. Layer-by-Layer TiO_2/WO_3 thin films as efficient photocatalytic self-cleaning surfaces. *ACS Applied Materials and Interfaces* 6, 16859–16866.
- Qiu, X., Miyaguchi, M., Sunada, K., Minoshima, M., Liu, M., Lu, Y., Li, D., Shimodaira, Y., Hosogi, Y., Kuroda, Y., Hashimoto, K., 2012. Hybrid $\text{Cu}_x\text{O}/\text{TiO}_2$ nanocomposites as risk-reduction materials in indoor environments. *ACS Nano* 6, 1609–1618.
- Rtimi, S., Pulgarin, C., Sanjines, R., Kiwi, J., 2015. Kinetics and mechanism for transparent polyethylene- TiO_2 films mediated self-cleaning leading to MB dye discoloration under sunlight irradiation. *Applied Catalysis B* 162, 236–244.
- Rtimi, S., Pulgarin, C., Sanjines, R., Kiwi, J., 2016. Accelerated self-cleaning by Cu promoted semiconductor binary-oxides under low intensity sunlight irradiations. *Applied Catalysis B* 180, 648–655.
- Wagner, C.D., Riggs, W.M., Davis, L.E., 1979. In: Müllenberg, G.E. (Ed.), *Handbook of X-ray Photoelectron Spectroscopy*. Perkin-Elmer Corporation Physical Electronics Division, Minnesota.
- Wijesena, R., Tissera, N., Perera, R., De Silva, K., Amaratunga, G.A.J., 2015. Slightly carbomethylated cotton supported TiO_2 nanoparticles as self-cleaning fabrics. *Journal of Molecular Catalysis* 398, 107–114.
- Yuranova, T., Mosteo, R., Bandara, J., Laub, D., Kiwi, J., 2005. Self-cleaning cotton textiles surfaces modified by photoactive $\text{SiO}_2/\text{TiO}_2$ coating. *Journal of Molecular Catalysis A* 244, 160–167.
- Zhang, L., Dillert, R., Bahnemann, D., Vormoor, M., 2012. Photo-induced hydrophilicity and self-cleaning: models and reality. *Energy and Environmental Science* 5, 7491–7507.

Smart durable and self-healing textile coatings

4

P. Heyse, I. De Vilder, M. Vanneste

Centexbel, Textile Competence Centre, Ghent, Belgium

4.1 Introduction

The durability of textiles can be endangered in different ways. Abrasion or scratching, attack by bacteria or fungi, and the influence of UV or temperature impair the preservation of properties induced during the processing of textiles. Various textile treatments are used to protect against degradation or damage or even to restore or repair the initial properties. Besides conventional coating methodologies, increasing focus is put on smart coatings to comply with these demands.

In the following paragraphs an overview of some work done at Centexbel in the area of smart durable coatings is presented: Self-healing coatings active at room temperature were developed as a way to protect against scratches, coatings protect textiles against attack by bacteria or fungi, and UV and infrared (IR)-responsive coatings were developed enabling the detection of harmful chemicals in the environment, undesirable temperature changes and excessive UV levels.

4.2 Types and classifications of smart coatings for improving textile durability

4.2.1 Self-healing textile coatings

The lifetime of a coated textile can be prolonged if it can be healed at an early stage of damage formation (stage of microcracks). If the coating is able to self-heal and therefore able to repair deterioration of its functionality, the durability of the coated products can be extended. This self-healing process can occur autonomously or can be triggered by an external stimulus (eg, heat, radiation).

Various concepts have been developed over the past decade and are still being fine-tuned. A lot of emphasis is put on the use of self-healing concrete, composites and coatings for corrosion prevention. The use of self-healing coatings on textiles has been less investigated to date.

Both extrinsic and intrinsic systems have been developed.

Extrinsic approaches make use of a container which is filled with the healing agent. When damage occurs, the container breaks and the healing agent is released in the crack and reacts with the catalyst or curing agent present. These containers can be

spherical microcapsules (Fig. 4.1; White et al., 2001), hollow (Fig. 4.2; Mauldin and Kessler, 2010), or compartmented fibres (Mookhoek et al., 2012), or a vascular system can be created (Toohey et al., 2007).

In a textile coating the use of microcapsules is the most feasible extrinsic approach. Microcapsules containing a healing agent can be added to an existing coating paste and are easily applicable. A drawback of this method is the nonrecurring healing action, as damage at this particular area will be repaired only once. Also, the amount of available healing agent is limited owing to the size of the capsules.

When multiple repair actions are desired, one can use an intrinsic system based on reversible covalent chemistry, physical or supramolecular interactions (Garcia and Fischer, 2014). In this case the damaged coating is able to repair itself by means of an increase in mobility. The coating has an enhanced flow (mostly at elevated temperatures) which enables a refill of the scratch. The restored scratch gains strength because of restored bonds (chemically/physically) (García et al., 2011; Ghosh, 2009).

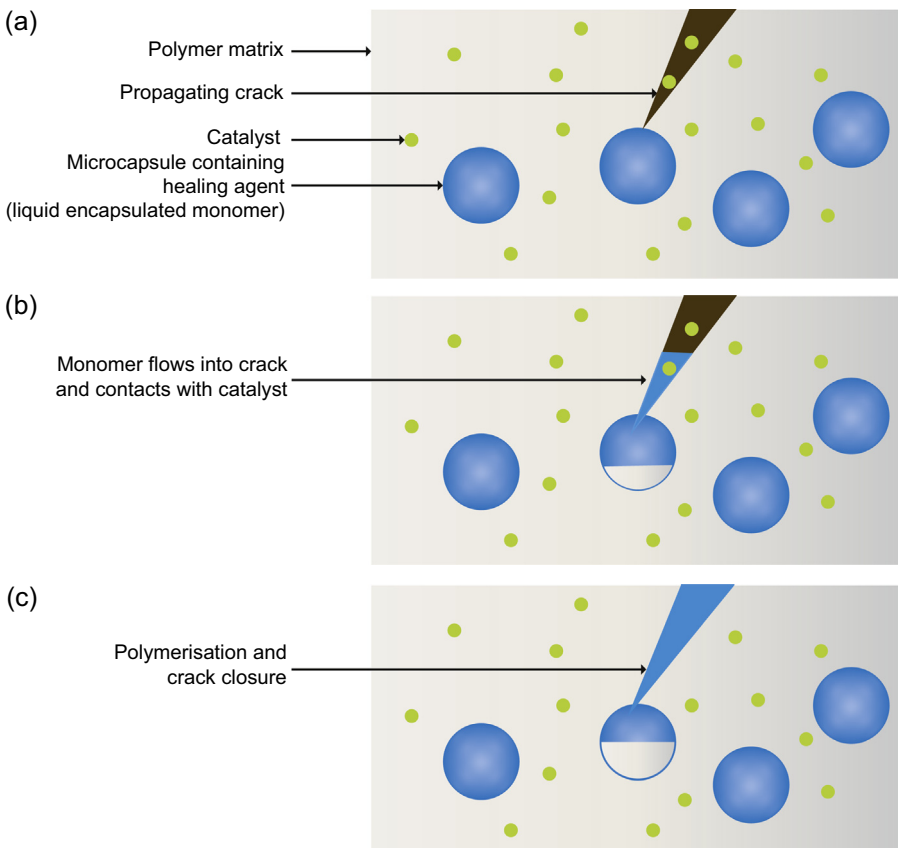


Figure 4.1 Self-healing process based on the incorporation of microcapsules. (a) Crack propagation up to healing agent capsule, (b) monomer flow, (c) crack healing by polymerization.

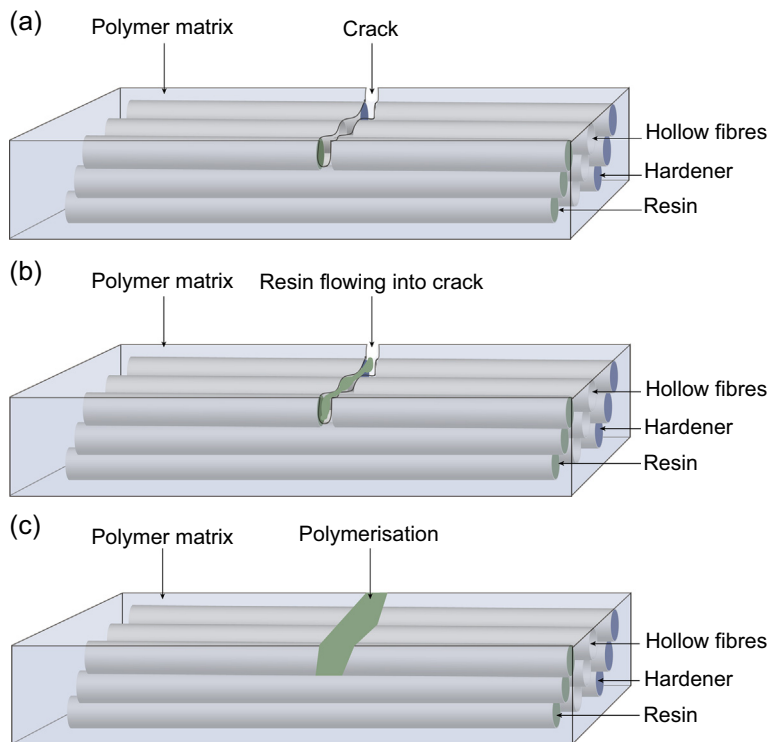


Figure 4.2 Self-healing process based on the incorporation of hollow fibres. (a) Crack propagation up to healing agent capsule, (b) monomer flow, (c) crack healing by polymerization.

This technology is already in use in the aerospace and automotive industry. Self-repairing car paints have been developed in which heat triggers the repair action.

Several companies have developed self-healing systems which possibly could be implemented on textiles. An overview is given in [Table 4.1](#).

Other companies such as BASF, AkzoNobel, Dow and DSM are also investigating the possibilities.

Table 4.1 Nonexhaustive list of suppliers of self-healing systems

Self-healing agent	Supplier
SupraB-technologies	Suprapolix
Reverlink™	Arkema
AMI technology	Autonomic Materials
Bayhydrol® U XP 2750	Bayer MaterialScience

4.2.2 *Antimicrobial and antifouling coatings*

Because of the high surface area, roughness, and ability to absorb moisture, textiles are prone to be rapidly colonised by microorganisms. These organisms affect the textile's lifetime by destroying the fibres and discolouring the fabric and they may spread unpleasant odours (Boryo, 2013; Burgess, 1954). The latter has been an important incentive to develop antimicrobial textile treatments for garments, bedding and sportswear. In addition, textiles may act as vectors for infectious diseases or spread nosocomial bacteria throughout hospital facilities (Leung and Chan, 2006; Treacle et al., 2009; Curtis White et al., 2010).

Several methods have been devised to hamper bacterial growth (bacteriostatic) or even kill bacteria (bactericide) on textiles. The treatments include releasing toxic compounds from fabric or attack microorganisms when they approach the fibre surface. Some treatments offer broad-spectrum protection whereas others are predominantly useful against bacteria or fungi. Antimicrobial compounds include metals, organometal derivatives, phenolic compounds, nitrogen and halogen compounds and nanoparticles (Coleman, 2005; Dastjerdi and Montazer, 2010; Gouveia, 2010; Shahidi and Wiener, 2012; Varesano et al., 2011; Vaun Mcarthur et al., 2012; Lacasse and Baumann, 2004; Simoncic and Tomsic, 2010). Bio-based products have gained increasing attention (Joshi et al., 2009; Simoncic and Tomsic, 2010; Yuan and Cranston, 2008).

4.2.2.1 *Metal-based antimicrobials*

Metals such as silver, titanium, zinc and copper are used in finishes and coatings and during fibre extrusion. Although silver is relatively more effective against bacteria compared with copper, which is more effective towards fungi, in both cases the metal ion needs to be released from the metal core to exert its activity. The metal ion will form complexes with vital compounds of the microorganism such as the cell membrane, enzymes and DNA. As a result, the microorganism's metabolism fails in several crucial areas (Lemire et al., 2013). Therefore, resistance against these ions is unlikely to develop because the microorganism is under attack at several targets at the same time. However, as to all antimicrobial products, also for silver and copper, resistive strains have been identified but only in very specific environments such as wastewater treatment plants and mining (Silver, 2003). The active metal ions can be released by dissolving directly from the metal, or by ion exchange. The latter is often used in silver-based products in which silver ions are bound to a ceramic matrix (Lorenz et al., 2012). Although the mobile metal ion is the active compound, metal-based antimicrobials are often not considered to be leaching out. In contrast to toxic chemical compounds, silver and copper ions easily form metal complexes with any organic substance in the vicinity. Leaching test methods such as agar diffusion tests (EN 20645 and AATCC 147) will therefore show no or only limited leaching from silver-treated fabrics.

4.2.2.2 *Halogen compounds*

Halogen-based antimicrobials from highly reactive oxides are known for strong disinfecting properties. Chlorine- and iodine-based products are well-known cleaning and

disinfectants (bleach, chlorhexidine and Betadine). Such derivatives are also used in textiles (Coleman, 2005). However, the persistence of halogens in the environment, the aggressive nature of these products (also to textile fibres) and their relation to cancer by disinfectant by-products (in particular for chlorine) limit their use in textiles. Common products are pentachlorophenol, dichlorodiphenyl methane, iodine and iodophors (Lacasse and Baumann, 2004).

4.2.2.3 Nitrogen compounds

Nitrogen compounds such as urea, amine and guanidine are used to denature proteins, hence their antimicrobial properties. One special form of nitrogen compounds for antimicrobial treatment is the so-called quats or quaternary ammonium salts (Coleman, 2005; Shahidi and Wiener, 2012; Windler et al., 2013). These molecules have a positive charge, attracting the negatively charged cell membrane of microorganisms. Mostly, the positively charged nitrogen head is followed by a long organic chain. This combination allows the molecule to puncture the cell membrane, consequently destroying the microorganisms (Curtis White et al., 2010). The advantage of the quats' molecules is their odour-free nature and the ability to add functional groups to the organic chain, which allows them to form a chemical bond to the textile fibres. In this way, leaching is limited and durability increases compared with the smaller nitrogen compounds mentioned previously.

4.2.2.4 Phenolic compounds

Phenolic compounds have a long history as disinfectants. However, the carcinogenic nature of phenols has led to the development of derivatives that are less toxic to humans. The best known is triclosan. Its relatively low toxicity to humans, effective disinfection properties and cheap production has led triclosan to become one of the highest selling disinfectants worldwide. However, its use in a wide variety of customer care products has induced the development of resistive bacteria strains (Windler et al., 2013; Lacasse and Baumann, 2004).

4.2.2.5 Aldehyde compounds

Aldehyde compounds such as formaldehyde and glutaraldehyde are commonly used for cross-linking purposes in chemistry. However, they also cross-link proteins and enzymes, rendering them useless for microorganisms (Windler et al., 2013; Lacasse and Baumann, 2004). The carcinogenic nature of these compounds has put a strict regulation on these products in textiles.

4.2.2.6 Bio-based products

One of the best known bio-based antimicrobial products is chitosan. It is a polysaccharide derived from chitin, an abundantly available waste product in shrimp farms. Although the deacetylation process to form chitosan from chitin is far from eco-friendly, it still is a renewable resource of antimicrobial products. The active groups

consist of an array of amine functionalities organised on the polysaccharide chain. Its activity is therefore similar as to the nitrogen compounds described previously.

The renewed interest in bio-based products has led to the development of new antimicrobial products in textiles (De Smet et al., 2015a). Often, these products originate from food processing, and researchers try to transfer these products in useful additives for textiles. Bio-based products are mostly plant extracts such as menthol, carvacrol (*Oregano* sp.), thymol (*Thymus* sp.), eucalyptol (*Eucalyptus* sp.), neem extract (*Azadirachta indica*), aloe vera (*Aloe barbadensis*), prickly chaff flower (*Achysanthus aspera*), eugenol (*Syzygium aromaticum*), turmeric and cumin, to name a few (Joshi et al., 2010; De Smet et al., 2015b). The antimicrobial activity of plant extracts such as peppermint, primrose and perilla oil has been explored as well. In addition, animal extracts also has potential as antimicrobial additives, such as sericin, a macromolecular protein derived from the silkworm *Bombyx mori* (Joshi et al., 2009; Shahidi and Wiener, 2012).

Although a vast number of bio-based alternatives show clear potential as antimicrobial textile treatment, the durability, applicability, availability and sometimes discolouring or unpleasant smell limit their use at an industrial level in textiles.

Alternatively, and by the grace of improved biotechnology tools for peptide production, short-chain amino acids have been reported to be useful as a bio-based antimicrobial finish for textiles (Gouveia, 2010).

4.2.2.7 Antifouling

Fouling is the result of the continuous accumulation of debris at the surface of films, rigid plates, and filters. Clearly textiles are also prone to fouling, and this chapter will focus on biofouling or biofilm formation and how it can be tackled. Fouling is a result of the stagnating flow of fluids at the surface from which debris will deposit, attracted by van der Waals forces. This process occurs within minutes after submersion. In case of biofilm formation, the first molecules depositing on the surface are proteins and polysaccharides. On the one hand, these molecules cover up any surface functionality and provide a suitable ground for bacteria to attach and develop on this new extracellular matrix (ECM). Bacteria possess surface-bound adhesion proteins designed to bind to such ECM, thus mediating colonisation of the surface. Once the bacteria and other microorganisms have gathered, exertion of more and more proteins and polysaccharides form the so-called external polysaccharide matrix in which the microorganisms thrive and form a complex ecosystem (Bixler and Bhushan, 2012; Harder and Yee, 2009). Some microorganisms and even macroorganisms are expert in colonising virgin surfaces by excreting specially designed attachment proteins such as adhesins (well known in various infectious bacteria) and mussel adhesion proteins (*Mytilus edulis*) (Klemm and Schembri, 2000; Qin and Buehler, 2014).

To overcome fouling (and biofouling in particular), surface modifications aim to (Lejars et al., 2012):

- increase shear and reduce surface energy
- limit anchoring points
- kill attaching organisms
- periodically or gradually remove the top layer of the surface

Both biofilm formation and possible antifouling strategies are illustrated in Fig. 4.3.

Increasing the shear at the surface and limiting surface energy can be achieved by creating very sleek omniphobic surfaces (Genzer and Efimenko, 2006). Usually, water- and oil-repellent fluorine-based coatings are used to reduce surface free energy as much as possible. As a result, both the static layer of fluids near the surface and the van der Waals forces are reduced (Van Zoelen et al., 2014). However, microorganisms still manage to colonise these surfaces by secreting viscous, slime-like substances that cover the entire surface and thus cover the underneath functionalities. In contrast to creating hydrophobic and oleophobic surfaces, positive results have been obtained by creating extremely hydrophilic surfaces. The reasoning behind this is that fouling (organic) molecules are partially composed of long-chain hydrocarbon segments that are strongly repelled by the superhydrophilic surface properties (Patel et al., 2010).

Protein and polysaccharide attachment can be limited by creating a dense brush-like layer at the surface. As a result, all possible anchoring points are occupied and no new (bio)polymers can attach. It has been demonstrated that polyethylene glycol (PEG) is effective in creating such surfaces (Ding et al., 2012). Unfortunately, the rigidity of such a PEG brush is low and the layer is easily damaged. Another option is not to prevent initial protein and polysaccharide attachment but to destroy any microorganism in the vicinity of the surface. This way, only a thin fouling film is developed but biofilm formation and growth of the film is significantly hampered or blocked.

Copper and heavy metal (such as mercury and tin) based products are available in coating formulations. To be effective, however, they need to leach out toxic compounds, and thus environmental concerns rise regarding the use of such coatings (Dafforn et al., 2011).

A final option is to release a small part of the coating on the surface periodically or gradually. Any biofilm developed will be removed and a new clean surface is obtained.

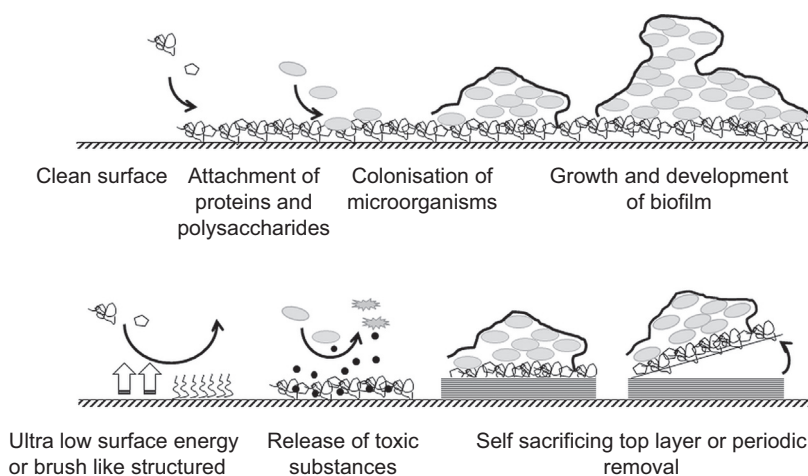


Figure 4.3 Biofilm formation (top, left to right) and possible antifouling approaches (bottom).

4.2.3 Coatings to protect against ultraviolet and infrared radiation

4.2.3.1 Ultraviolet

Fabrics exposed to UV irradiation fade in colour, strength and durability. This so-called ageing is caused by short-wavelength light that interacts with electron-rich molecules. Such molecules will absorb energy from the light waves and subsequently break down (Rabek, 1996; Alen and Edge, 1993; Andradý et al., 1998). UV rays are predominantly found in sunlight but artificial lights such as discharge lamps (tube lights, halogen bulbs) also emit UV. The problem of UV ageing is mostly recognised for outdoor textiles, leisurewear and car interiors but also indoor textiles close to windows such as upholstery, curtains and sun blinds.

UV-protective additives in finishing, dyeing, coating and extrusion focus on blocking the highly reactive UV rays from reaching sensitive pigments, binders or fibres. Some products have a high affinity for the UV waves and are preferably attacked by UV, transforming it into harmless heat (UV absorbers). Others block the propagation of free radicals initiated by UV irradiation (radical scavengers). A third mode of action is to decompose peroxides formed by UV irradiation in combination with oxygen. These products act as antioxidants but can also improve UV durability (peroxide decomposer). A final mode of action is to quench excited states and divert the energy into lower-wavelength light (fluorescence or phosphorescence) or heat (quenchers) (Patra and Gouda, 2013; Kasza, 2013; Lacasse and Baumann, 2004). The different modes of action of UV-stabilising additives are presented in Fig. 4.4 whereas Table 4.2 summarises typical light-stabilising compounds.

Although these UV stabilisers are used in numerous applications, their small molecular nature allows for easy migration throughout the polymer. Small molecule stabilisers may leach out into the environment and no longer protect the material (Scott, 1999). The current trend is to develop macromolecular UV, heat or hydrolysis stabilisers (Raching GmbH, Chemtura, Ciba and Vanderbilt). These high-molecular-weight molecules can be effective and durable and do not migrate in the polymer. However, macromolecular UV stabilisers require more synthesis, which results in more expensive additives (Kasza, 2013).

4.2.3.2 Infrared

The heat stability of coated textiles differs depending on the coating composition. Exposure of a coated textile to sunlight can have a deteriorating effect. Sunlight consists of visible light, accompanied by about 53% IR light. IR radiation with wavelengths in the range of 780 nm up to 1 mm (Fig. 4.3) is responsible for heating phenomena. Thus, coated textiles exposed to sunlight will heat up when absorbing these wavelengths. It is claimed that a lower-temperature increase in the coating will result in enhanced durability because of less polymer degradation and thermal expansion (Fang et al., 2013; Pasternack, 2013). Only limited research has been performed on the effect of reflective pigments, the related temperature rise of the coating and the durability of the coatings (Salminen, 2014).

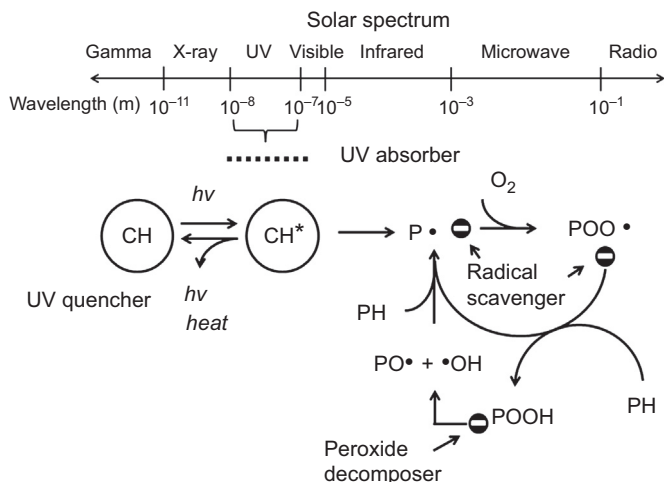


Figure 4.4 Mode of action of various UV-stabilising additives. *P*, polymer chain; *P•*, polymer with radical; *CH**, hydrocarbon chain in excited state.

Based on BASF, 2016. Light Stabilizers. Available from: http://www.dispersions-pigments.basf.com/portal/basf/en/dt.jsp?print=center&setCursor=1_556325 (accessed 08.01.2016.); Rabek, J.F., 1996. Photodegradation of Polymers, Berlin Heidelberg, Springer-Verlag, and Alen, N.S., Edge, M., 1993. Fundamentals of Polymer Degradation and Stabilization, Springer.

Table 4.2 Typical light-stabilising compounds and their mode of action

Light-stabilising compound	Mode of action
Carbon black	UV-absorbent pigment
Titanium oxide	UV-absorbent pigment
Benzophenone	UV absorber
Benzotriazole	UV absorber
Halogenated benzotriazole	UV absorber
Triazinyl	UV absorber
Hydroxyphenyltriazine	UV absorber
Metal nanoparticles (CeO, ZnO)	UV absorber
Oxalic acid derivatives	Radical scavenger
Sterically hindered amines (HALS)	Radical scavenger
Sterically hindered phenols	Radical scavenger
Copper, manganese, sulphur complexes	Peroxide decomposer
Nickel compounds	UV quencher

The reflection of this IR radiation on a coated textile can be augmented by the incorporation of IR-reflective pigments. This results in a lower absorption and transmission of IR, and therefore less heating. These coatings are denominated as low-E coatings (low emissivity).

These low-E coatings are predominantly used in architectural textiles for their thermal properties (Cremers, 2010). For example, the inside temperature of a building will be lowered when such a coating is implemented on the façade of the building. This results in lower energy consumption because of reduced air conditioning. Examples of IR-reflective coatings can also be found in the ceiling of ice tracks and on roofs and window blinds.

Several types of IR-reflecting additives have been designed based on:

- Pure metals (such as Al, Ag and Cu) with a specific size
- Metals with surface coatings (AlO[OH] or SiO₂ on Al and AgS on Ag)
- Metal oxides such as titanium dioxide and zinc oxide
- Multiple-layered structures: TiO₂/Au/TiO₂, silicon powder and metal-coated cenosphere particles
- Minerals such as mica

4.3 Properties of textiles with durability-enhancing coatings

4.3.1 Scratch resistance

Research in the field of self-healing coatings focusses on corrosion protective coatings and concrete; not much research has been performed on coated textiles.

The first self-healing experiments with polyurethane-coated fabric, in which the embedded microcapsules were filled with a PU binder, show great potential but still need to be optimised. The research was executed in the framework of the FP7 Safe@Sea project, in which improved garments for fishermen were developed (Anon, 2016a).

In experiments in which heat-triggered, self-healing polymers were evaluated on textiles, the typical open textile structure proved worrisome because the elevated temperature (up to 140°C) enhanced the flow of the polymer needed to close the crack. Owing to this enhanced flowing behaviour, the coating starts to penetrate into the textile substrate, which is not advantageous for the flexibility of the coated textile (De Vilder and Vanneste, 2013). Also, introducing these elevated temperatures to the coated textiles during the lifetime of the protective garment, technical textile, and so on is not self-evident because this can alter properties such as dimensional stability.

At Centexbel, a self-healing coating was developed which acts at room temperature. An acrylate textile coating was selected which shows the desired flowing behaviour. A supramolecular additive with a self-healing property based on hydrogen bond formation was added to the coating. This additive improves the mechanical strength of the filled crack. The coating was applied on a polyester substrate via knife-over-roll (200 µm). The coating was abraded with F2 sandpaper (Martindale, EN 510, five cycles). Most of the recovery was noticeable by 2 days at room temperature. At the stage

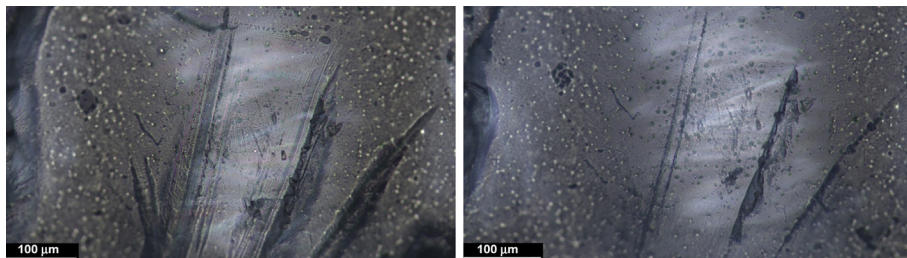


Figure 4.5 Acrylic self-healing coating on textile: (left) initial damage, (right) residual damage after 2 days at room temperature.

<http://www.vliz.be/imisdocs/publications/265822.pdf>

of microcracks, full recovery was observed (Fig. 4.5). When too much coating material is removed, the system is unable to refill the crack completely.

To evaluate the effect of different formulations, a homogeneous and uniform scratch was made with a modified motorised pencil hardness tester (De Vilder and Vanneste, 2013; Fig. 4.6). This allowed the efficacy of the self-healing properties to be compared for different formulations.

Self-healing coatings can be implemented when the textile is prone to wear and tear, cuts, abrasion and so forth. From an aesthetic point of view an intact coating is desirable, but the coating should also maintain functionality as long as possible. Prolonged barrier properties such as waterproofness, electrical (Blaiszik et al., 2012) and thermal conductivity and recovered hydrophobicity and/or oleophobicity (Wang et al., 2013; Dikić et al., 2012) can be achieved.

4.3.2 *Antibacterial and antifungal properties*

Numerous fabrics are claimed to have antimicrobial efficacy. Table 4.3 highlights several of them.

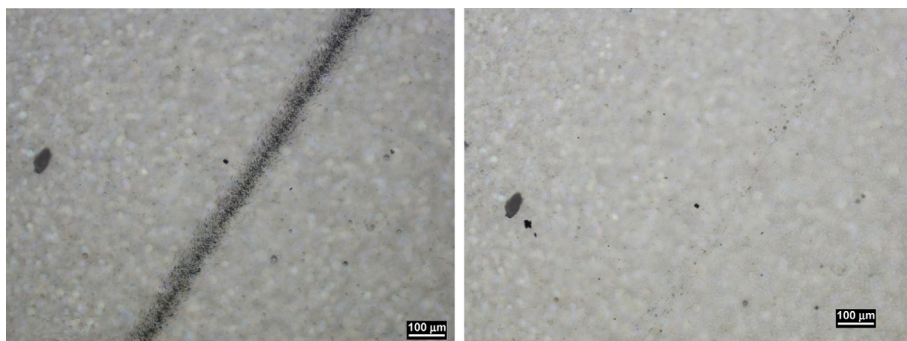


Figure 4.6 Acrylic self-healing coating on a polycarbonate plate: (left) initial damage, (right) residual damage after 2 days at room temperature.

Table 4.3 Nonexhaustive list of products claiming antimicrobial properties

Product	Origin	Claimed benefits
Agion Technologies	Zeolite agent and silver	Recognised on severe acute respiratory syndrome and H5N1
AEGIS Microbe Shield® Technology	Quaternary ammonium silane	Controls bacteria and fungus that cause objectionable odours, unsightly stains and product deterioration; friendly to environment.
Sorbtek/Amy	Silver-based antimicrobial	Characteristics: Total moisture control combined with silver-based antimicrobial. This catch, move and release technology keeps the wearer dry, comfortable and odour free. Available in comfort and performance stretch.
Thermolite freshFX	Polyester insulation with antimicrobial additive spun into fibres	Characteristics: Polyester insulation with silver-based antimicrobial additive spun into fibres to protect against odours. Provides lightweight warmth with added freshness that lasts for life of product.
VisaEndurance brand of fabrics		Characteristics: Performance active-wear fabrics that fights odours, wicks moisture away from skin, dries quickly and releases stains in wash. Knit, breathable, soft hand, wicks perspiration away from body, dries quickly, fights odours, releases stains.
iSyS AG	Dispersed silver chloride solution	Ionic form of silver has triple effect on bacteria: destruction of cell membrane, deactivation of cell metabolism, destruction of cell division. The product is based on nanotechnological sol-gel process: iSyS AG is combined with reactive organic–inorganic binder (iSyS MTX).

Sanitised T27-22	Suspension of silver chloride in water	Product has excellent wash and light fastness. Product blocks respiration and food intake of bacteria and acts on cell membrane which inhibits cell functions.
Sanitised TH22-27	Dispersion of zinc pyrithione	To obtain wash-fastness the compound needs to be linked with a binder or put into wash-resistant coating. Product acts on cell membrane of microorganism.
Ultra-Fresh Silpure FBR-5	Ultra-Fresh Silpure FBR-5 Activator (Part A) is an aqueous dispersion of a silver compound. Ultra-Fresh Silpure FBR-5 (Part B) is specifically formulated to combine with Part A.	Combined product is engineered for controlled release of silver ions providing control of bacterial growth.
Ultra-Fresh DW-56	One of the active compounds in Ultra-Fresh DW-56 is <i>bis</i> (1-hydroxy-2(1H)-pyridinethionato-O,S)-(T-4) zinc.	Aqueous suspension designed to control growth of fungi, bacteria and algae in polyurethane foams, aqueous coatings and textiles. Effective in preventing infestation of house dust mites in treated articles.

Clearly, antimicrobial effectiveness is directed not only by the product applied but also by the concentration used. Table 4.4 shows typical concentrations of antimicrobial textile additives and their limit values according to OEKO-TEX[®] 100 voluntary labeling (OEKO-TEX[®], 2015).

Antimicrobial efficiency is expressed only as a binary annotation (growth or inhibition) or the area of inhibition for leaching substances in, for example, the agar diffusion test (eg, DIN EN ISO 20645 – 2001, AATCC 147). Quantitative test methods are also possible in which the bacterial reduction is expressed in log scale (eg, JIS L 1902, DIN EN 1276, AATCC100, ASTM E 2149-01, ASTM E 2180-01). In such tests reports, negative numbers denote bacterial growth instead of a reduction of the number of bacterial colony-forming units. An overview of available test methods and their preferred use is nicely described in Pinho et al. (2011) and Llc (2010). Table 4.5 summarises some antimicrobial effectiveness results against *Staphylococcus aureus* obtained from various antimicrobial textile treatments.

4.3.3 Ultraviolet resistance

From the wealth of available UV stabilisers, it may be difficult to identify the most-suited one for a specific application. The properties and action mode of a given UV stabiliser may already point towards its usefulness as a top coating (UV absorber), as a dispersed additive in a binder (quencher or peroxide decomposer), or even chemically linked to a dye if possible (sterically hindered amines). The chart in Fig. 4.7 illustrates the effect of various types of UV stabilisers in an acrylic textile coating combined with a red pigment. This chart is not intended to discriminate between good or bad UV stabilisers; nonetheless, it shows what could happen if UV stabilisers were randomly dispersed and mixed in a typical textile coating formulation.

As an example, care must be taken when mixing UV stabilisers. Hindered amine light stabilisers combined with triazine actually accelerated UV ageing. Clearly in this case, the UV absorber (triazine) should have been applied as a top coat. The same holds for metal oxides, alleged UV absorbers. However, the mixture of CeO and ZnO in this particular case shows a synergistic acceleration of ageing. Although the mode of action of the various UV stabilisers is well known, it remains sensible to test them for your specific application and challenge them with a well-chosen test method.

4.3.4 Infrared reflection

A textile can be finished or coated with IR-reflective additives added to a binder system. Depending on the additive used, up to 70% of the incident IR radiation can be reflected. This percentage will be influenced by the binder type, colour, other additives present and the coating thickness.

At Centexbel, a two-layered PVC-coated polyester fabric was made with 15 wt% of mica pigments incorporated into the top layer. After gelling, the solar reflectance was recorded according to EN 410 (Fig. 4.8), which showed that 62% of the solar radiation was reflected.

Attention should be paid to full coverage of the surface of the coating by the additives; this will block penetration of the IR light into the polymer more efficiently (Figs 4.9 and 4.10). Lower concentrations of the pigments (less than 15 wt%) resulted in incomplete

Table 4.4 Typical concentrations of antimicrobial textile additives and their limit values according to OEKO-TEX® 100 voluntary labelling

Biocide	Typical concentration [ppm]	References	Limit value [ppm] ^a
Formaldehyde	<30 (clothing)	Piccinini et al., 2007	16–300
Organometallics	1.10 ⁴ –5.10 ⁴	Baumann et al., 2000	25.10 ⁶ –50.10 ⁶ (copper)
Silver	0.016–27.10 ⁴ ^b	Windler et al., 2013 ; Lorenz et al., 2012	–
Triclosan	7–195	Windler et al., 2013	0.2–2
Tributyltin oxide	0.1–13.3	Janssen et al., 2000	0.5–1
QUAT	2500	Windler et al., 2013	–

^aOEKO-TEX® 100 limit values are depending on the final use of the fabric under investigation.

^bHigh levels of silver indicate the use of pure silver fibres, low values point to silver ion complexes.

Table 4.5 Antimicrobial effectiveness results against *Staphylococcus aureus* obtained from various antimicrobial textile treatments

Active treatment	Bacterial log reduction (hours of exposure)		Test method	References
Quat	0.8 (6)	1.66 (24)	AATCC100	Smith et al. (2010)
Triclosan	0.68 (6)	>1.6 (24)	AATCC100	Smith et al. (2010)
AgCl	>2 (3)	>2 (24)	ASTM E 2149	Own research
Zn pyrithione	0.6 (3)	1.8 (24)	ASTM E 2149	Own research
Thymol	–	Inhibition (24)	ISO 20645	De Smet et al. (2015b)
Chitosan	–	Inhibition (24)	ISO 20645	De Smet et al. (2015b)

coverage of the surface and therefore a lower reflection rate. Augmenting the pigment concentration even more is also not advised: Once the surface is covered, this technology shows its full potential. Inserting the pigments in both the top and base layers does not improve the rate of reflection, which again shows that the predominant part of the reflection takes place at the surface.

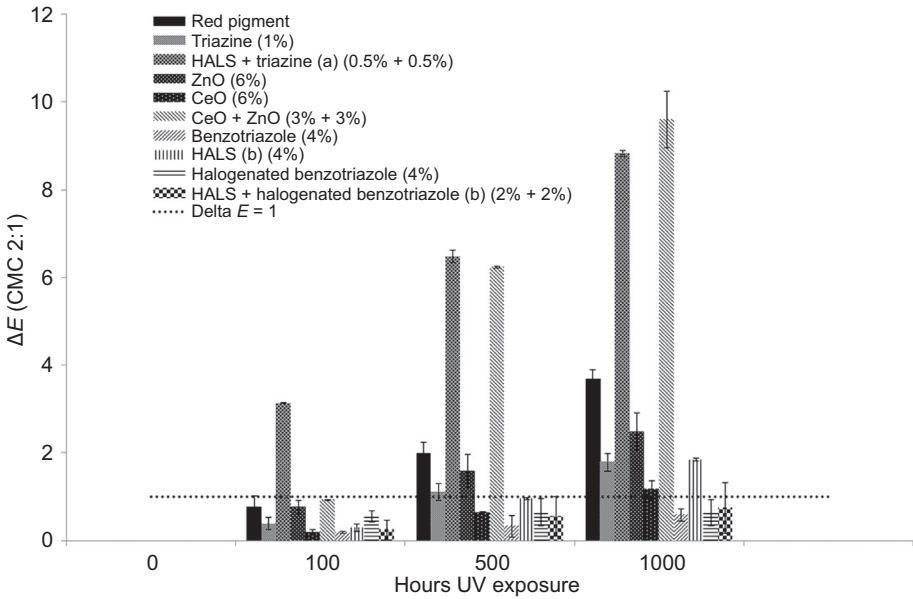


Figure 4.7 Effect of various UV-stabilising agents in a red-pigmented acrylic textile coating after UV exposure (according to EN 14836). Colour difference is expressed as ΔE according to ISO 105-J03 (1995), $\Delta E > 1$ (.....) is observable by the human eye. Concentrations are advised by the TDS of the respective manufacturer. (a) and (b) denote different producers.

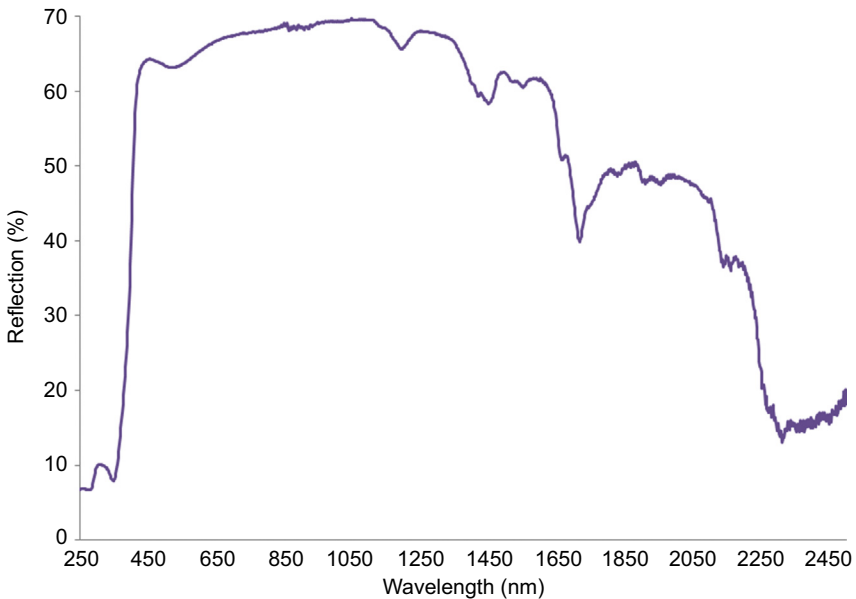


Figure 4.8 Solar reflectance by a double-layered PVC coating with 15 wt% mica pigments incorporated in the top layer.

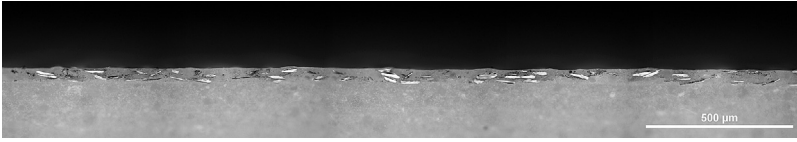


Figure 4.9 Microscopic image of IR-reflecting aluminium flakes incorporated into the top layer of a double-layered PVC coating: cross-section of the coating.

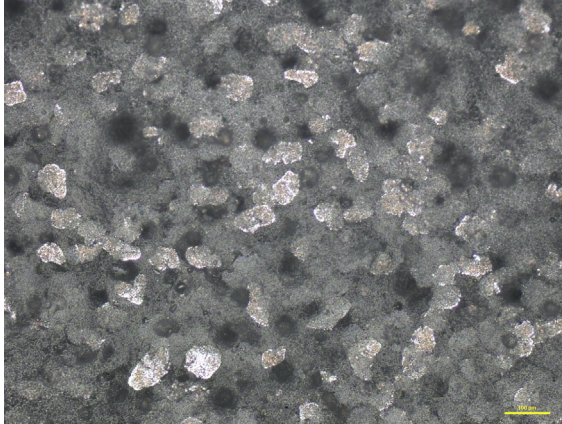


Figure 4.10 Microscopic image of IR-reflecting aluminium flakes incorporated into the top layer of a double-layered PVC coating: top view of the coating.

4.4 Applications of smart durable and self-healing textiles

4.4.1 *New generation of architectural fabrics*

Developments in the building industry have shown a clear evolution of traditional construction in buildings with sensible and adaptable envelopes equipped with sensors and able to interact with the surrounding environment on the basis of inputs such as temperature, humidity and solar radiation. For structures designed for extreme applications (eg, large-span structures prone to fluttering and ponding, industrial applications characterised by high working temperatures, biogas basins with corrosive gases), there is a need for continuous monitoring to highlight anomalies and avoid progressive propagation of the initial damage.

The progressive miniaturisation of the sensor and the innovative manufacturing techniques for technical fabrics and foils resulted in new prospects for a new generation of sensible technical fabrics equipped with sensors focussing on temperature monitoring, pressure monitoring, and chemical sensing of noxious gasses.

Temperature monitoring of tensile structures is of particular interest for PVC-coated fabrics. PVC-coated fabrics for tensile structures have a glass transition temperature

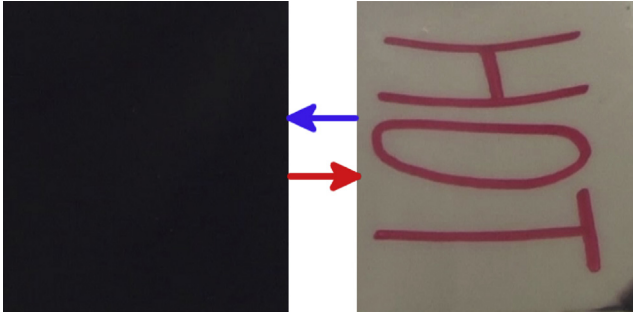


Figure 4.11 Textile coating with thermochromic pigments. The coating instantaneously becomes transparent at temperatures above 70°C (right) and becomes black when cooling down (left).

roughly between 70°C and 90°C (Sen, 2007; Wypych, 2008). At these temperatures, the polymer will become weaker and welded seams will slowly extend or even detach while under tension (Llorens, 2015). To signal a pending failure, temperature sensors can be mounted on the construction after erection. However, most exposed locations are often difficult to reach and attaching several sensors is laborious. In addition, the wiring compromises the aesthetics of the often admired organic shapes that can be achieved in textile architecture.

To overcome these issues, miniature temperature sensors are integrated into hybrid fabrics with integrated electric leads (Heyse et al., 2015). Electronic sensors are well known for their accuracy and ease of data acquisition, but for fabrics, connecting the monitor to the sensor fabric remains an issue of intense research (Chapman, 2012). Alternative to electronics, thermochromic pigments also respond to variations in temperature. Apart from liquid crystals, the temperature resolution of these materials is limited (Seeboth and Löttsch, 2013). However, integrated in a coating, the spatial resolution is considerably higher than the point-wise electronic sensors. In addition, a quick visual inspection will indicate hot spots in real time. Although such thermochromic coatings may not be suitable for larger structures, they can be advantageous for quality control during welding of the seams where high enough temperatures have to be reached to ensure proper connection of the fabric parts (Fig. 4.11).

Unfortunately, tensile structures are not always used for the purposes for which they are designed. In case of a defect, the user points to the manufacturer although misuse is sometimes the real cause of failure (Huntington, 2004; Seidel and Sturge, 2009). Common failure is caused by corrosive gases emitted by, for example, cattle or biological waste. For two of such gases, an irreversible indicator patch has been developed. Colour will change upon exposure to ammonia or hydrogen sulphide, indicating that the fabric properties can no longer be guaranteed (Fig. 4.12).

4.4.2 Protective clothing

Protective clothing is a comprehensive field because it contains garments for fire-fighters, fishermen, welders, divers, sports enthusiasts, motorcyclists, surgeons and

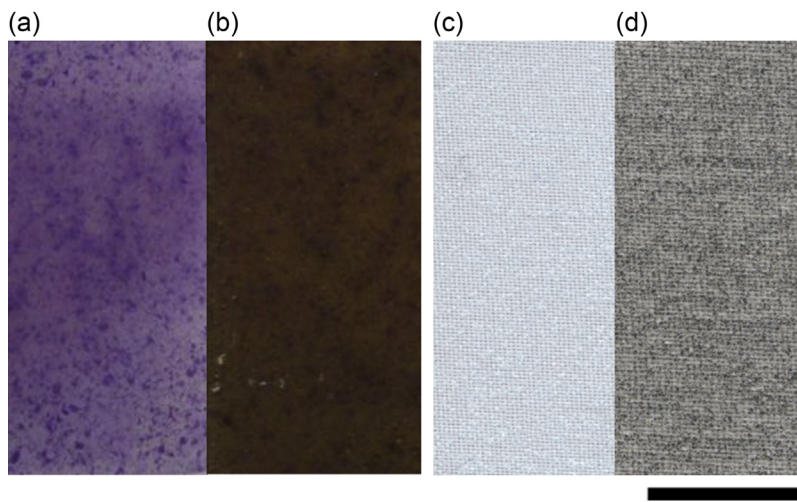


Figure 4.12 Fabrics responsive to corrosive or toxic gases. Left: ammonia sensitive ((a) no NH_3 ; (b) in the presence of NH_3). Right: hydrogen sulphide sensitive ((c) no H_2S ; (d) exposed to H_2S). Scale bar is 1 cm.

military personnel. Specific suits have been developed for environments with chemical and/or biological danger, extreme temperatures, and so on. Each garment has specific properties adapted to the intended use, but a common demand is longevity. Besides an economical advantage, a more durable coating will result in prolonged protection, and in certain cases it can save lives.

In most cases protective clothing consists of multiple layers. The outer layer of the laminate, often coated, is most prone to wear and tear. The durability and therefore the lifetime of protective clothing can be prolonged by the use of wear- and tear-resistant coatings. Hence, the outer layer can be functionalised to improve abrasion/scratch/rub resistance and UV stability by incorporating specific additives.

Frequently used high-performance fibres such as *p*-aramid (PA) and *m*-aramid have poor resistance to abrasion. Thus they can be combined with fibres that have superior abrasion-resistant properties, protected by a PU coating (Mao, 2014). The durability of such a protective coating can be improved with additives.

The following example of a functionalised PU coating in protective clothing demonstrates the possibilities. Fishermen in the North Atlantic currently use heavyweight PVC-coated garments. Within the FP7 project Safe@Sea (Anon, 2016a) a lightweight alternative was developed based on PU-coated PA (De Vilder et al., 2012). In changing from a PVC-coated textile to a PU-coated one, an improvement in abrasion resistance was already noticeable. By incorporating specific additives into the PU coating, resistance to abrasion could be even further increased. Besides improved comfort owing to the lighter weight, prolonged durability of the garment was achieved (ie, less weight loss was observed) (Table 4.6).

In many protective garments, the inner layer makes contact with the body of the person and is subjected to abrasion to a lesser extent. This fabric can be finished with

Table 4.6 Weight loss of coated textiles for fishermen (Martindale, EN 530-2, 10.000 cycles, F2 sandpaper)

Fabric	Weight	Weight loss coating after Martindale (F2)
PVC-coated CO	465 g/m ²	5.9 wt%
Polyurethane-coated PA	330 g/m ²	
Without additives		4.0 wt%
With additives		2.2 wt%

additives such as sol–gel (Brzeziński et al., 2011) or silicones to diminish the impact of the abrading action.

4.4.3 Securing cargo

Although securing cargo may sound self-evident, correct loading and securing of cargo is not a trivial task (Rosi et al., 2012). Proper knowledge of the cargo mass, shape, content and expected accelerations, and appropriate use of securing tools and aids are prerequisites for the safe transportation of goods around the globe. Unfortunately, it is estimated that up to 25% of all accidents in the EU in which trucks are involved result from inadequate securing of cargo (Copsey, 2010). Despite the lack of a fully harmonised standard and legislation in EU, the member states impose clear rules on cargo securing (Andersson et al., 2012). In addition, well-defined guidance documents are available for normal and exceptional transports explaining how and with what tools cargo should be secured safely (European Commission, 2007, 2014). One of the most recognised tools is the use of flat fabric webbing slings and lashes that have to comply with EN 12195 standards. Off-the-shelf lashes are compliant with these strict regulations, but how do such materials behave during use and at what point is safe practise no longer guaranteed? Periodic inspection is voluntary and is based on subjective, visual inspections focusing on (ASME, 2014):

- Acid or caustic burns
- Melting or charring
- Holes, tears, cuts or snags
- Broken or worn stitching in load-bearing splices
- Excessive abrasive wear
- Knots in any part of the sling
- Discolouration and brittle or stiff areas
- Fittings that are pitted, corroded, cracked, bent, twisted, gouged or broken
- Clear labels indicating lashing capacity

It is obvious that these observations can discriminate between reliable and potentially unsafe lashings but there is no clear threshold value, and if one is set, it is imposed arbitrarily. In addition, a given lashing may appear to be in good condition

but there are no means to check whether it has endured excessive charging beyond the loading capacity or has elongated beyond the EN 12195 threshold of 7% at loading capacity (for flat fabric lashings). For slings, an integrated overload sensor is available via SlingMax and their patented Check-Fast[®] slings.

4.4.3.1 *The road ahead for smart lashings*

In the framework of a transnational collective research project between small and medium size enterprise associations and research organisations (Rescotex), research is focussing on identifying thresholds for UV ageing, abrasion, and repeated tensioning of flat fabric lashings for cargo securing.

This section highlights the use of smart coatings to indicate excessive UV exposure of tie-down straps.

Although the lashings are UV stabilised according to the standard, there is no indication as to what extent this stabilisation should be. Moreover, a given belt will last longer if it is used in mild UV conditions (eg, indoor, sporadically) compared with severe UV conditions (eg, southern Europe, long-distance open transport). As a result, there is no general rule of thumb to assess the safety of a used belt with respect to UV ageing. To counteract this concern, a coating has been developed using a mixture of UV stabilisers to be printed on the belt. In case of UV damage, the print will discolour and indicate the level of UV damage endured by the belt so far. If the safety limit has been exceeded, a text urging the user to replace the belt becomes visible. Fig. 4.13 exemplifies such label printed on a 35-mm flat web lashing. At UV exposures above 1000 h (EN14836, QUV accelerated ageing test), the replace text is clearly visible and indicates that the belt has endured too much UV irradiation to be used safely.

4.5 Future trends

Because textiles are used in an increasing number of technical applications, durability is increasing in importance. Much research has been done so far and products and processes developed are commercially available. Still, new end applications are detected in which durability in various environments are a prerequisite. For instance, in the At~Sea Project (<http://www.atsea-project.eu/>), coated textiles were developed for use as a substrate for growing seaweed. For this application, a unique balance between antifouling properties and seaweed anchoring points is crucial.

The concept of self-healing coating is most developed in the field of automotives, aerospace, and building (concrete). A known example is the Scratch Shield clear coat developed by Nissan and already implemented in their cars and on iPhones (Anon, 2016b). To date, no examples of commercially available self-healing textiles are known. Research in this area is limited but the outcome is promising. In the future, self-healing coatings based on the microcapsule technology or an intrinsic approach can be expected. The self-healing coating will be able to repair at an early stage of damage, enhancing the durability and prolonging the lifetime of the coated textile.

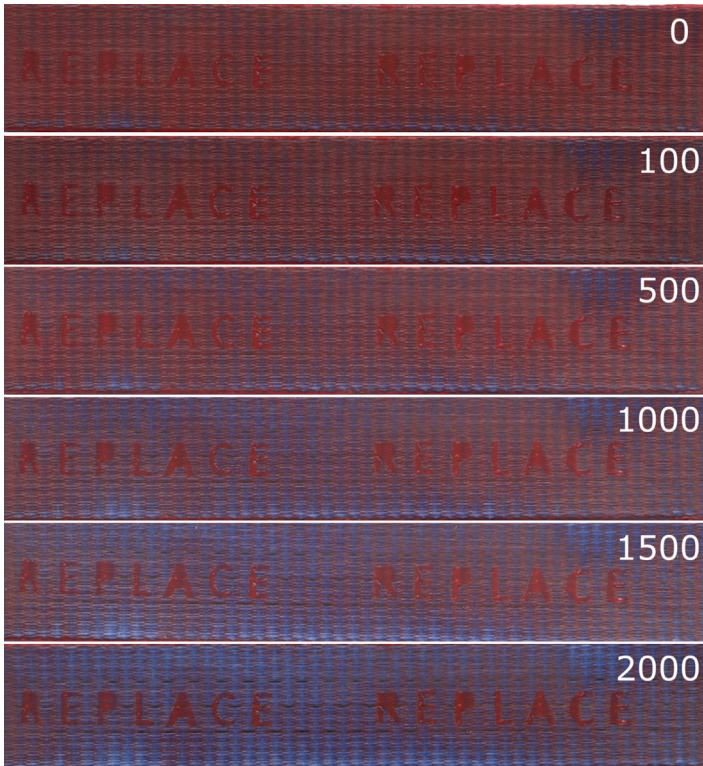


Figure 4.13 UV-exposed label printed on 35-mm flat fabric lashing. Numbers indicate the exposure level in hours according to EN14836 (QUV accelerated ageing test).

All textile areas will benefit from these developments (eg, protective clothing, architectural textile, cargo securing).

4.6 Conclusions

Coated textiles are being used in a wide range of end applications in which the textile is employed as a long-lasting solution. It is clear that the durability of textile coatings is an important property. In this chapter some smart technologies were presented enabling the enhancement of the durability of coated textiles, properties that can be realised with these technologies and some (future) applications in which these durable coated textiles can be implemented.

Sources of further information

Textile chemicals (Lacasse and Baumann, 2004)

Smart coatings (Aguilar and Román, 2014)

Acknowledgments

The authors are indebted to the Flemish Agency for Innovation by Science and Technology (IWT; grant 130372) and the European Union's Seventh Framework Programme (grant agreements nos. NMP2-SE-2009-229334, FP7-NMP-2001-SME-5-280860, FP7-SEC-2011-284931 and FP7-SME-2013-606411) for funding of their research.

References

- Aguilar, M.R., Román, J.S., 2014. *Smart Polymers and Their Applications*. Woodhead Publishing.
- Alen, N.S., Edge, M., 1993. *Fundamentals of Polymer Degradation and Stabilization*. Springer.
- Andersson, P., Sökjer-Petersen, S., Agelčák, J., 2012. Differences in Cargo Securing Regulations. How Could We Achieve Harmonization? International Symposium on Heavy Vehicle Transportation Technology (HVTT). International Forum for Road Transport Technology, Stockholm, Sweden.
- Andrady, A.L., Hamid, S.H., Hu, X., Torikai, A., 1998. Effects of increased solar ultraviolet radiation on materials. *Journal of Photochemistry and Photobiology B: Biology* 46, 96–103.
- Anon, 2016a. Final Report Summary – safe@sea (protective clothing for improved safety and performance in the fisheries) *CORDIS*. Available from: http://cordis.europa.eu/result/rcn/57672_en.html (accessed 08.01.2016.).
- Anon, 2016b. Scratch Shield. Available from: <http://www.nissan-global.com/EN/TECHNOLOGY/OVERVIEW/scratch.html> (accessed 08.01.2016.).
- ASME, 2014. Safety Standard for Cableways, Cranes, Derricks, Hoists, Hooks, Jacks, and Slings. The American Society of Mechanical Engineers, New York.
- BASF, 2016. Light Stabilizers. Available from: http://www.dispersions-pigments.basf.com/portal/basf/ien/dt.jsp?print=center&setCursor=1_556325 (accessed 08.01.2016.).
- Baumann, W., et al., 2000. Gathering and Review of Environmental Emission Scenarios for Biocid. Institute for Environmental Research, Dortmund.
- Bixler, G.D., Bhushan, B., 2012. Biofouling: lessons from nature. *Philosophical Transactions. Series A Mathematical, Physical and Engineering Sciences* 370, 2381–2417.
- Blaiszik, B.J., Kramer, S.L.B., Grady, M.E., Mcilroy, D.A., Moore, J.S., Sottos, N.R., White, S.R., 2012. Autonomic restoration of electrical conductivity. *Advanced Materials* 24, 398–401.
- Boryo, D.E.A., 2013. The effect of microbes on textile material: a review on the way-out so far. *The International Journal of Engineering and Science* 2, 09–13.
- Brzeziński, S., Kowalczyk, D., Borak, B., Jasiorski, M., Tracz, A., 2011. Nanocoat finishing of polyester/cotton fabrics by the sol-gel method to improve their wear resistance. *Fibres & Textiles in Eastern Europe* 19, 6.
- Burgess, R., 1954. Micro-organisms and textiles. *Journal of Applied Bacteriology* 17, 230–245.
- Chapman, R., 2012. *Smart Textiles for Protection*. Elsevier Science.
- Coleman, W.F., 2005. Antimicrobial agents used on textiles. *Journal of Chemical Education* 82, 171.
- Copsey, S., 2010. A Review of Accidents and Injuries to Road Transport Drivers. European Agency for Safety and Health at Work.
- Creemers, J.M., 2010. 12 – Textiles for insulation systems, control of solar gains and thermal losses and solar systems. In: Pohl, G. (Ed.), *Textiles, Polymers and Composites for Buildings*. Woodhead Publishing, pp. 351–374.

- Curtis White, W., Bellfield, R., Ellis, J., Vandendaele, I.P., 2010. Controlling the spread of infections in hospital wards by the use of antimicrobials on medical textiles and surfaces. In: Anand, S.C., Kennedy, J.F., Mirafitab, M., Rajendran, S. (Eds.), *Medical and Healthcare Textiles*. Woodhead Publishing, pp. 55–75.
- Dafforn, K.A., Lewis, J.A., Johnston, E.L., 2011. Antifouling strategies: history and regulation, ecological impacts and mitigation. *Marine Pollution Bulletin* 62, 453–465.
- Dastjerdi, R., Montazer, M., 2010. A review on the application of inorganic nano-structured materials in the modification of textiles: focus on anti-microbial properties. *Colloids and Surfaces B: Biointerfaces* 79, 5–18.
- De Smet, D., Leppchen-Fröhlich, K., Meyer, M., 2015a. Renewable antimicrobials for textile finishing. *Melliand International* 45–47.
- De Smet, D., Weydts, D., Myriam, V., 2015b. Environmental friendly fabric finishes. In: Blackburn, R.S. (Ed.), *Sustainable Apparel: Production, Processing and Recycling*. Woodhead Publishing.
- De Vilder, I., Vanneste, M., 2013. Self-healing coatings for textile. Ghent. In: *Fourth International Conference on Self-healing Materials – ICSHM2013 16/6/2013*, pp. 307–311.
- De Vilder, I., Vanneste, M., Peltonen, C., Varheenmaa, M., 2012. Safe@sea: protective clothing for improved safety and performance in the fisheries. Development of comfortable wear resistant and stain repellent coated materials. In: *5th ECPC and NOKOBETEF Congress: Future of Protective Clothing: Intelligent or Not?* Valencia.
- Dikić, T., Ming, W., Van Benthem, R.A.T.M., Esteves, A.C.C., De With, G., 2012. Self-replenishing surfaces. *Advanced Materials* 24, 3701–3704.
- Ding, X., Yang, C., Lim, T.P., Hsu, L.Y., Engler, A.C., Hedrick, J.L., Yang, Y.-Y., 2012. Antibacterial and antifouling catheter coatings using surface grafted peg-b-cationic polycarbonate diblock copolymers. *Biomaterials* 33, 6593–6603.
- European Commission, 2007. *European Best Practice Guidelines for Abnormal Road Transports*. European Commission, Directorate-General for Energy and Transport.
- European Commission, 2014. *European Best Practices Guidelines on Cargo Securing for Road Transport*. Publications Office of the European Union.
- Fang, V., Kennedy, J., Futter, J., Manning, J., 2013. A Review of Near Infrared Reflectance Properties of Metal Oxide Nanostructures.
- García, S.J., Fischer, H.R., 2014. 9-Self-healing polymer systems: properties, synthesis and applications. In: Aguilar, M.R., Román, J.S. (Eds.), *Smart Polymers and Their Applications*. Woodhead Publishing, pp. 271–298.
- García, S.J., Fischer, H.R., Van Der Zwaag, S., 2011. A critical appraisal of the potential of self healing polymeric coatings. *Progress in Organic Coatings* 72, 211–221.
- Genzer, J., Efimenko, K., 2006. Recent developments in superhydrophobic surfaces and their relevance to marine fouling: a review. *Biofouling* 22, 339–360.
- Ghosh, S.K., 2009. *Self-healing Materials: Fundamentals, Design Strategies, and Applications*. Wiley-VCH Verlag GmbH & Co. KGaA, pp. 1–28.
- Gouveia, I.C., 2010. Nanobiotechnology: a new strategy to develop non-toxic antimicrobial textiles. In: Mendez-Vilas, A. (Ed.), *Current Research, Technology and Education Topics in Applied Microbiology and Microbial Biotechnology*. Formatex Research Center, pp. 407–414.
- Huntington, C.G., 2004. *The Tensioned Fabric Roof*. ASCE Press.
- Harder, T., Yee, L.H., 2009. 5-Bacterial adhesion and marine fouling. In: Hellio, C., Yebra, D. (Eds.), *Advances in Marine Antifouling Coatings and Technologies*. Woodhead Publishing, pp. 113–131.

- Heyse, P., Buyle, G., Walendy, B., Beccarelli, P., Loriga, G., Zangani, D., Tempesti, A., 2015. Multitexco – high performance smart multifunctional technical textiles for the construction sector. *Procedia Engineering* 114, 11–17.
- Janssen, P.J.C.M., et al., 2000. Health risk assessment for organotins in textiles. Dutch National Institute for Public Health and the Environment.
- Joshi, M., et al., 2009. Ecofriendly antimicrobial finishing of textiles using bioactive agents based on natural products. *Indian Journal of Fibre & Textile Research* 34, 295–304.
- Joshi, M., et al., 2010. Antimicrobial textiles for health and hygiene applications based on eco-friendly natural products. In: Anand, S.C., Kennedy, J.F., MirafTAB, M., Rajendran, S. (Eds.), *Medical and Healthcare Textiles*. Woodhead Publishing, pp. 84–92.
- Kasza, G., 2013. Thermal, Antioxidative and Photochemical Stabilization of Polymers: Low Molecular Weight versus Macromolecular Stabilizers. Polyfriend. Polymer Institute of the Slovak Academy of Science, Bratislava.
- Klemm, P., Schembri, M.A., 2000. Bacterial adhesins: function and structure. *International Journal of Medical Microbiology* 290, 27–35.
- Lacasse, K., Baumann, W., 2004. *Textile Chemicals: Environmental Data and Facts*. Springer, Berlin.
- Lejars, M., Margailan, A., Bressy, C., 2012. Fouling release coatings: a nontoxic alternative to biocidal antifouling coatings. *Chemical Reviews* 112, 4347–4390.
- Lemire, J.A., Harrison, J.J., Turner, R.J., 2013. Antimicrobial activity of metals: mechanisms, molecular targets and applications. *Nature Reviews Microbiology* 11, 371–384.
- Leung, M., Chan, A.H.S., 2006. Control and management of hospital indoor air quality. *Medical Science Monitor* 12, 8.
- Llc, B., 2010. Testing for Antimicrobial Activity in Textiles – Quick Overview. Biovation, Boothbay, USA. Available from: <http://biovation.com/wp-content/uploads/AnOverviewofBiocideTestingsRevA11.pdf> (accessed 27.06.15.).
- Llorens, J., 2015. *Fabric Structures in Architecture*. Elsevier Science.
- Lorenz, C., Windler, L., Von Goetz, N., Lehmann, R.P., Schuppler, M., Hungerbühler, K., Heuberger, M., Nowack, B., 2012. Characterization of silver release from commercially available functional (nano)textiles. *Chemosphere* 89, 817–824.
- Mao, N., 2014. 3-High performance textiles for protective clothing. In: Lawrence, C.A. (Ed.), *High Performance Textiles and Their Applications*. Woodhead Publishing, pp. 91–143.
- Mauldin, T.C., Kessler, M.R., 2010. Self-healing polymers and composites. *International Materials Reviews* 55, 317–346.
- Mookhoek, S.D., Fischer, H.R., Van Der Zwaag, S., 2012. Alginate fibres containing discrete liquid filled vacuoles for controlled delivery of healing agents in fibre reinforced composites. *Composites Part A: Applied Science and Manufacturing* 43, 2176–2182.
- OEKO-TEX[®], 2015. Limit Values and Fastness. Available from: https://www.oeko-tex.com/en/manufacturers/test_criteria/limit_values/limit_values.html (accessed 29.07.15.).
- Patra, J.K., Gouda, S., 2013. Application of nanotechnology in textile engineering: an overview. *Journal of Engineering and Technology Research* 5, 104–111.
- Pasternack, G., May 2013. Main Factors Affecting the Coating's IR Reflectivity. *SpecialChem*.
- Patel, P., Choi, C.K., Meng, D.D., 2010. Superhydrophilic surfaces for antifogging and antifouling microfluidic devices. *Journal of the Association for Laboratory Automation* 15, 114–119.
- Piccinini, P., et al., 2007. European Survey on the Release of Formaldehyde from Textiles. Institute for Health and Consumer Protection.
- Pinho, E., Magalhães, L., Henriques, M., Oliveira, R., 2011. Antimicrobial activity assessment of textiles: standard methods comparison. *Annals of Microbiology* 61, 493–498.

- Qin, Z., Buehler, M.J., 2014. Molecular mechanics of mussel adhesion proteins. *Journal of the Mechanics and Physics of Solids* 62, 19–30.
- Rabek, J.F., 1996. *Photodegradation of Polymers*. Berlin Heidelberg, Springer-Verlag.
- Rosi, B., Cvahte, T., Bálint Čeh, J., Tojnko, M., Lerher, T., Jereb, B., 2012. Load fastening and securing. *JLST* 3, 53–57.
- Salminen, L., 2014. *The Influence of Solar Reflective Black Pigments on the Durability of Wood Coatings*. Helsinki Metropolia University of Applied Sciences.
- Scott, G., 1999. *Polymers and the Environment*. Royal Society of Chemistry.
- Seeboth, A., Löttsch, D., 2013. *Thermochromic and Thermotropic Materials*. Pan Stanford.
- Seidel, M., Sturge, D.S., 2009. *Tensile Surface Structures: A Practical Guide to Cable and Membrane Construction*. John Wiley & Sons.
- Sen, A.K., 2007. *Coated Textiles: Principles and Applications*, second ed. CRC Press.
- Shahidi, S., Wiener, J., 2012. Antibacterial agents in textile industry. In: Bobbarala, V. (Ed.), *Antimicrobial Agents*. InTech, pp. 387–406.
- Silver, S., 2003. *Bacterial Silver Resistance: Molecular Biology and Uses and Misuses of Silver Compounds*.
- Simoncic, B., Tomsic, B., 2010. Structures of novel antimicrobial agents for textiles – a review. *Textile Research Journal* 80, 1721–1737.
- Smith, E., et al., 2010. Comparison of antimicrobial textile treatments. In: Anand, S.C., Kennedy, J.F., Mirafitab, M., Rajendran, S. (Eds.), *Medical and Healthcare Textiles*. Woodhead Publishing, pp. 38–47.
- Toohey, K.S., Sottos, N.R., Lewis, J.A., Moore, J.S., White, S.R., 2007. Self-healing materials with microvascular networks. *Nature Materials* 6, 581–585.
- Treacle, A.M., Thom, K.A., Furuno, J.P., Strauss, S.M., Harris, A.D., Perencevich, E.N., 2009. Bacterial contamination of health care workers' white coats. *American Journal of Infection Control* 37, 101–105.
- Varesano, A., Vineis, C., Aluigi, A., Rombaldoni, F., 2011. Antimicrobial polymers for textile products. In: Mendez-Vilas, A. (Ed.), *Science against Microbial Pathogens: Communicating Current Research and Technological Advances*. Formatex Research Center, pp. 99–110.
- Vaun Mearthur, J., Tuckfield, R.C., Baker-Austin, C., 2012. Antimicrobial textiles. In: Coates, A.R.M. (Ed.), *Antibiotic Resistance*. Springer Berlin Heidelberg, Berlin Heidelberg, pp. 135–152.
- Wang, H., Zhou, H., Gestos, A., Fang, J., Lin, T., 2013. Robust, superamphiphobic fabric with multiple self-healing ability against both physical and chemical damages. *ACS Applied Materials & Interfaces* 5, 10221–10226.
- White, S.R., Sottos, N.R., Geubelle, P.H., Moore, J.S., Kessler, M.R., Sriram, S.R., Brown, E.N., Viswanathan, S., 2001. Autonomic healing of polymer composites. *Nature* 409, 794–797.
- Windler, L., Height, M., Nowack, B., 2013. Comparative evaluation of antimicrobials for textile applications. *Environment International* 53, 62–73.
- Wypych, G., 2008. *PVC Degradation & Stabilization*. ChemTec Publishing.
- Yuan, G., Cranston, R., 2008. Recent advances in antimicrobial treatments of textiles. *Textile Research Journal* 78, 60–72.
- Van Zoelen, W., Buss, H.G., Ellebracht, N.C., Lynd, N.A., Fischer, D.A., Finlay, J., Hill, S., Callow, M.E., Callow, J.A., Kramer, E.J., Zuckermann, R.N., Segalman, R.A., 2014. Sequence of hydrophobic and hydrophilic residues in amphiphilic polymer coatings affects surface structure and marine antifouling/fouling release properties. *ACS Macro Letters* 3, 364–368.

Smart breathable coatings for textiles

5

V.K. Midha, A. Mukhopadhyay

National Institute of Technology Jalandhar, Punjab, India

5.1 Introduction

Breathable coatings for textile fabrics usually maintain fabric permeability towards air and moisture in addition to other functionalities, depending on their end uses. Coating materials can be permeable, smart, waterproof, etc., which in turn are influenced by polymer and specialty chemicals, additives, process aids, and many other chemicals necessary to produce the specified customer properties of the quality standards and durability demanded. Before the details of smart breathable coatings are discussed, some important points must be considered. First, smart breathable coatings can be technically defined as smart or intelligent materials which can ‘respond to an external stimulus in a specific, controlled way’ to regulate water vapour permeation. Put another way, the materials should have a number of distinct states, with differing physical properties in these states, and should transition repeatedly between the states with a given external stimulus. Therefore, a smart coating might actually alter the size of its pores and thus occupy distinct high or low states for permeability or thermal insulation. The external stimulus might be humidity, temperature, wind and so on. Conventional materials based on either microporous or hydrophilic coatings cannot work on this principle. These breathable coating materials can be termed passive smart. On the other hand, breathable fabrics based on shape memory polymers (Ding et al., 2004; Hayashi et al., 1993; Hu et al., 2001; Russell et al., 1999) can be termed active smart. These fabrics restrict the loss of body warmth by stopping the transfer of vapour and heat at a low temperature, and transfer more heat and water vapour from inside to outside at high-temperature conditions (Mitsubishi and Hayashi, 1992). The classification of different kinds of coatings according to the perspective of breathability is shown in Fig. 5.1. Breathable coatings based on biomimetics and phase change materials (PCM) discussed later in the chapter are other classes of smart textiles, useful for making breathable fabrics (Anon, 2004, 2002; Chung and Cho, 2004; Li and Zhu, 2004; Ying et al., 2004; Choi et al., 2004; Ghali et al., 2004; Pause, 2003; Shim et al., 2001; Pause, 2001; Hasse, 2003). Although the role of PCMs is not directly to regulate the passage of water vapour through fabrics, their incorporation into the fabric leads to improved thermal and moisture management. Vapour-permeable, water-repellent fabrics treated with microcapsule-containing PCMs are more comfortable than water-repellent fabric (Chung and Cho, 2004).

Second, the term ‘breathable’ implies that the fabric is actively ventilated, but this is not the case. Waterproof, breathable fabrics passively allow the transmission of

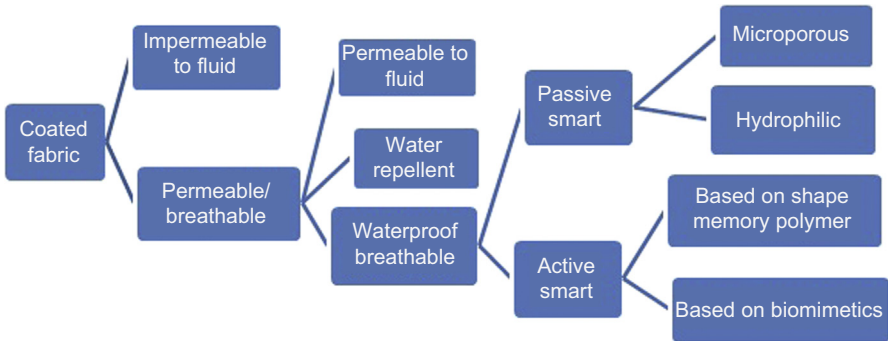


Figure 5.1 Classification of breathable fabrics.

moisture vapour by diffusion and therefore facilitate evaporative cooling. Regular polyurethane (PU), polyvinylchloride (PVC), or rubber-coated fabrics are waterproof but do not ‘breathe’ because they do not allow perspiration to pass through to enable body cooling. This perspiration condenses inside the garment, making the wearer wet from his or her own perspiration. The definition of breathability is often confused with wind penetration or the clothing’s ability to wick liquid water away from the skin; both of these processes are also referred to as breathability, but they depend on entirely different fabric properties (Tanner, 1979; Painter, 1996). Commonly, breathability is meaningless without a high standard of waterproofness, and an initial hydrostatic head of 500 cm of water (50 kPa) for high-quality products to 130 cm of water (13 kPa) for lower-grade products is required (Fung, 2002).

Third, waterproof or water-repellent coatings come under the specific category of coatings and are designed for use in garments to prevent the human body from external heat, wind, water and many harmful agents, and permit the effective transmission of moisture vapour from the inside to outside atmosphere. The applications may range from the well-known foul weather leisure clothing to specialised medical and military uses. Impermeable coated fabrics are waterproof but uncomfortable to wear. Water repellent-treated fabrics are comfortable to wear but cannot prevent the penetration of water for a long time.

Fourth, the development of waterproof breathable material in the form of films began in the early 1970s, when WL Gore introduced Gore-Tex material, which has a high standard of water resistance combined with a high level of breathability. Gore-Tex is a polytetrafluoroethylene (PTFE) film with nine billion tiny micropores in every square inch (6.45 cm²); these are 20,000 times smaller than a drop of liquid water but 700 times larger than a water molecule. Thus they are too small to allow liquid water to pass but large enough to allow the passage of molecules of water vapour. Because Gore-Tex is an expensive product, over the next decade there was intense activity by chemical material manufacturers to develop an alternative material with a similar high standard of performance but at a lower cost. This led to the development of many microporous coatings mainly made of PU (eg, Entrant, UCB products). A solid film-type product (Sympatex polyester film material) introduced by

Akzo, based on a completely different principle, became a commercial success in the late 1970s. The water molecules move through the film using hydrophilic groups in the molecular chain to reach the other side. The driving force for this action is the high relative humidity near the human body on the inner side of the garment and the lower humidity on the outer side. Waterproof and breathable membranes are used in many applications such as footwear, gloves and even socks. However, it is important to understand that membranes need to be laminated on the fabric or in some cases directly transferred onto the fabrics, and the lamination process increases the stiffness of fabrics in addition to significantly reducing breathability. Therefore, for optimum performance, breathable adhesives are being developed. Coated materials offer higher resistance to moisture flow and offer longer service life compared to membranes.

Fifth, coated textile materials can be made permeable or impermeable to moisture vapour, depending on their end use. For example, tarpaulin cloth does not demand a permeable structure whereas high-altitude clothing essentially requires vapour permeability. Impermeable coated fabrics function by blocking the pores of the textile material by a compact polymeric coating that forms a physical barrier to wind and water. In extreme cold climate, if the sensible perspiration cannot evaporate and the thermal insulation of the fabric remains high, the body is prevented from cooling and hypothermia can result. [Table 5.1](#) shows the consequences of wearing impermeable fabric ([Scott, 2000](#)). Although these fabrics are not breathable, they are comparatively inexpensive and are widely used for rainwear and foul weather clothing. Various materials are available for rainwear and offer different levels of protection, but generally single- or double-textured rubberised fabrics are used. A single-textured fabric consists of a coating material of natural or synthetic rubber coated on one side of a base fabric of cotton, viscose or nylon fabric. A typical fabric has a weight of 250 g/m^2 with a proofing content of 140 g/m^2 . A double-textured fabric has a rubber coating between two layers of cotton or viscose fabric. Such a fabric is heavy ($400\text{--}575 \text{ g/m}^2$) but gives excellent protection against rain ([Taylor, 1982](#); [Sen, 2001](#)). By providing proper ventilation in rainwear, it is possible to transfer condensed sweat outside, which minimises discomfort to the wearer. During wearing trials, breathable garments cause thermal strain equal to impermeable clothes in cold environments but lower strain in hot

Table 5.1 Effect of wearing impermeable clothing under different conditions

Conditions	Activity	Consequences
Cold/wet climate	Medium activity	Discomfort
Cold/wet climate in sweat-wetted clothing	High activity followed by low activity	Hypothermia (cold stress)
Hot/moist climate and wearing protective clothing	High activity	Hyperthermia (heat stress)

conditions. During hard work, moisture accumulation in breathable fabrics is lower but still large enough to cause discomfort. However, when worn for the whole day, with continually changing moisture production and climate, breathable garments dissipate moisture all the time, whereas impermeable garments only cause accumulation. For extended periods of wear, breathable fabrics give a more comfortable and dry feeling. Ventilation at appropriate places in the garment has been designed an alternative means to transport water vapour (COMA, 1986).

Sixth, breathable fabrics produced by coating or laminating are used for different applications, and the concept of breathability is used in a wider sense. In a cold storage-temperature house, where temperature ranges from -5 to -50°C , high resistivity of heat is required along with the breathable characteristics of fabric. On the other hand, in a firefighting operation, because the body perspires heavily, fabric should transmit a high level of water vapour while protecting the body from external heat. Breathable fabrics are used in clothing for outdoor occupations such as the farming and construction industries and for arduous pursuits (eg, cycling and mountaineering). Such fabrics are also used in protective clothing and for exposure to low temperatures and to wind, rain, and occasionally severe conditions of wind-driven rain. Breathable fabrics for medical applications are frequently characterised by synthetic blood penetration or viral penetration tests (ASTM F1670 and F1671, respectively).

Seventh, the construction of the breathable garment for different applications may consist of several layers in addition to a composite layer of breathable coated or laminated fabric. Additional layers may serve as insulating layers or contact layers with the human body to control the microclimate temperature and humidity. A fleece or membrane may be used in the middle layer for elasticity, insulation, wind protection, waterproofness and breathability. The breathable component may have a coating on the inner or outer side and the performance of each layer in the multilayer garment is influenced by the performance of other layers and its position. During physical activity that produces sensible perspiration, removal of an insulating layer such as a fleece garment should improve the comfort of the clothing system by increasing the temperature of the breathable layer, improving its vapour transport and reducing condensation. The use of a laminated fleece (presumably meaning the wind-resistant type) promotes the formation of condensation on the fleece and the waterproof breathable layer, owing to the restriction of ventilation within the clothing system. However, if the vapour permeability is restricted largely by using a waterproof breathable fabric, the overall performance of garment will be least affected by the other components. The concept of 'soft shell' breathable fabrics originated from the desire to scale down the 'overprotectiveness' in less challenging situations.

Eighth, the choice of a suitable coating material can be based on many other criteria apart from breathability, such as fabric tear, tensile and peel strength; flex and abrasion resistance; ability to be laundered; ability to be sealed by tape; thermophysiological comfort, etc., and to perform efficiently over the lifetime of the product. For illustration, soldiers' cloth must be as versatile as possible because they may not be able to change in the field, and during a particular operation the weather may change significantly. In addition to wind, rain, and cold, soldiers need protection against thorns, solar radiation, and heat stress. Therefore, all of these properties are important in such arduous situations in addition to the weight of the garments and the restrictions

they place on body movements. Furthermore, the rustling noise produced by garments made from coated and laminated fabric is a security issue in stealth operations (Fung, 2002). Outer layers are usually PU-, PVC- or neoprene-coated fabrics. PVC- and neoprene-coated fabrics have some limitations when used in extremely cold conditions. PVC-coated fabrics have poor low-temperature properties and are affected by solvents, whereas neoprene-coated fabrics are heavy. PU-coated nylon is the fabric of choice because of its lightweight, thin coating and excellent low-temperature flexibility (Lomax, 1984; Cooper, 1979). Some popular PU-coated nylon fabrics have weights ranging from 100 to 250 g/m² with a PU coating of 10–30 g/m². These fabrics are also used by military personnel for various items of cold-weather clothing such as jackets, trousers, caps and gaiters.

5.2 Working principles of smart breathable coatings

Different types of breathable components can be classified into the following groups based on the basic component used in multilayer construction (Sen, 2001; Gretton et al., 1998; Yadav et al., 2002; Holmes, 2000b; Save et al., 2002; White et al., 2004; Mukhopadhyay and Midha, 2008a,b; Jassal and Agarwal, 2010; Fung, 2002). A suitable substrate is essential for membranes and coatings, whereas other material such as a closely woven fabric can be used in isolation:

- Closely woven fabrics
- Microporous membranes and coatings
- Hydrophilic membranes and coatings
- A combination of microporous and hydrophilic membranes and coatings
- Use of retroreflective microbeads
- Smart breathable fabrics

In this chapter, only the principles underlying breathable coatings will be discussed. The working principles of membranes and coatings in specific groups such as microporous and hydrophilic ones are the same.

5.2.1 Microporous coatings

Generally, breathable coatings are made of hydrophobic microporous coatings and laminates with a pore size of 0.1–50 µm, which allows the passage of water vapour but resists liquid water. The micropores are much smaller (0.02–1 µm) than the smallest water drops (100 µm) (Mayer et al., 1989). Molecules of water vapour resulting from sweat are usually smaller than 40×10^{-6} µm and can easily penetrate the micropores and diffuse away using a capillary mechanism (Fig. 5.2(a)) (Gulbiniene et al., 2007). Fig. 5.3 is a schematic representation of moisture vapour regulation through microporous coatings and the surface of a typical coating showing the micropores. The rate of water vapour transmission (WVT) through a structure has been shown to be related to its porosity, thickness, and pore size. For a constant porosity and thickness, WVT through the surface increases as the pore size decreases. Furthermore, as the fabric thickness increases, the water vapour permeability decreases (Whelan et al., 1955). A typical

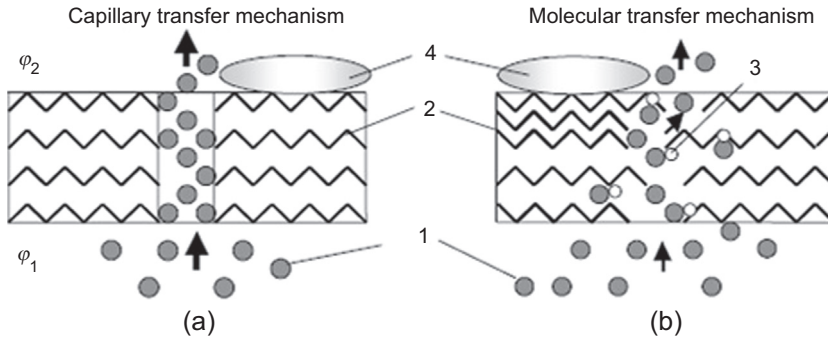


Figure 5.2 Water vapour transfer through microporous (a) and hydrophilic (b) membranes: 1, water vapour molecules; 2, polymer molecular chains; 3, active hydrophilic groups; 4, water droplet (ϕ_1 and ϕ_2 , relative humidity $\phi_1 < \phi_2$) (Gulbiniene et al., 2007).

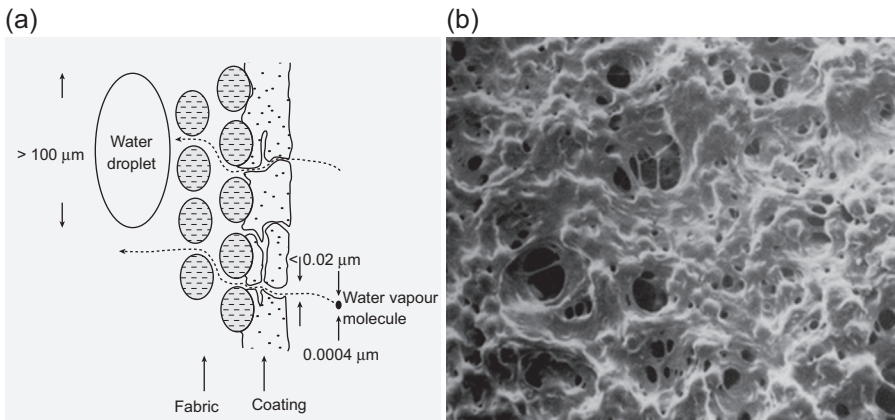


Figure 5.3 (a) Moisture vapour regulation through microporous coating; (b) surface of cyclone fabric (Ucecoat, 2000), a PU-coated nylon filament woven fabric showing the micropores (Lomax, 1985b).

membrane is only about 10 μm thick and therefore is laminated to a conventional textile fabric to provide the necessary mechanical strength. However, coatings are much thicker than membranes and their method of application is different.

5.2.2 Hydrophilic breathable coatings and their combination with microporous membranes and coatings

Hydrophilic films are totally solid with no pores, pinholes, microcracks or other defects. It is therefore physically impossible for droplets of liquid water to pass through. Fig. 5.4 shows a scanning electron microscopy image of a hydrophilic surface layer and a hydrophilic layer partly removed, showing a PTFE layer. The transmission of water vapour molecules occurs via osmotic potential by adsorbing and desorbing the vapour

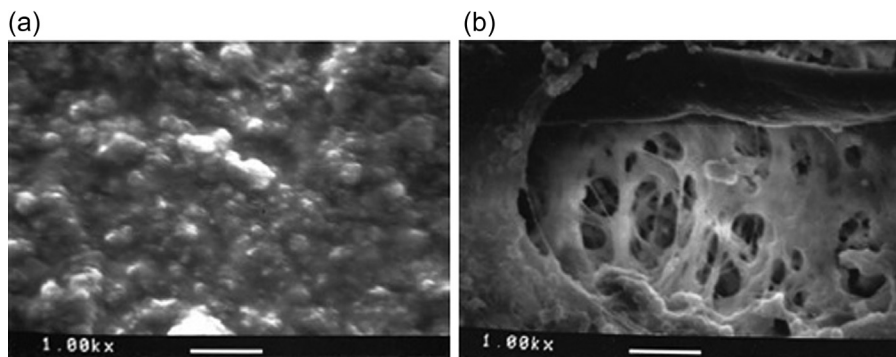


Figure 5.4 SEM of (a) hydrophilic surface layer, (b) hydrophilic layer partly removed showing PTFE layer.

molecules and then conveying them to the other side, much in the way that cells in the human body allow the diffusion of monomolecular and ionic species through their membrane walls (Fig. 5.2(b)). The driving force for WVT, however, is the difference in water vapour pressure between the two faces of the membrane or coating. The internal climate next to the skin is hot and humid because the body generates heat and moisture as it exercises. The external climate is usually much drier and cooler. Consequently, water vapour is driven from the inside of the garment to the outside. As the skin gets hotter during an activity, the film becomes more efficient in expelling moisture.

Breathability in hydrophilics is an adsorption—diffusion—desorption process accelerated by hydrogen bonds between water molecules and functional groups built into the molecular chains. The water vapour molecules first adsorb onto the surface with higher vapour concentration, occupy free volume between the polymer molecular chains and move across the membrane or coating without interacting chemically with the polymer. The amorphous regions (usually associated with the place of soft segment within the copolymeric structure) act like intermolecular pores, allowing water vapour molecules to pass but preventing the penetration of liquid water owing to the solid nature of the membrane or coating. In the case of active hydrophilic groups, vapour molecules not only fill the free volume but also interact with the active hydrophilic groups (Painter, 1996). They then diffuse across by dissolving in the polymer membrane or coating, which is known as activated diffusion. Upon arriving at the opposite surface of the membrane or coating, they are desorbed into the surrounding air space (Gulbinienė et al., 2007).

Solid-film hydrophilic films and coatings work more efficiently in the presence of condensation, whereas Microporous membranes and coatings function less effectively when the surface is covered with a layer of condensation. A detailed comparison of microporous and hydrophilic films is given in Table 5.2. Microporous and hydrophilic coatings are sometimes used in combination to overcome the tendency of blockage of pores of microporous coating by residues of detergents and sweat, and improve the strength and toughness of fabrics. Further, microporous and hydrophilic coatings, when combined reduce the noise effects in wet hydrophilic laminates. However, addition of bicomponent microporous films increases the cost and stiffness of the laminate and reduces the overall breathability of fabrics.

Table 5.2 Features of microporous and hydrophilic films/coatings [Johnson and Samms 1997; Mukhopadhyay and Midha, 2008a]

Hydrophilic	Microporous
Windproof	Windproof (arguments)
Waterproof and liquid proof	Waterproof and liquid resistance
Selective permeability	Non-selective permeability
High water entry pressure	Low water entry pressure
Good tearing strength	Low tearing strength
Insensitive to surfactants	Surfactants cause leakage
Variable swelling when wet, produce possible noise effects during rubbing	Little swelling when wet
Insensitive to contamination during use	Possibility of blockage due to contaminants during use
Tend to wet out in rain and give cold clammy handle	No chances of wetting, cold clammy handle
High water vapor transmission	High water vapor transmission

5.2.3 Use of retroreflective microbeads

Retroreflective fabrics are made by printing or coating the fabrics with a retroreflective ink or coating. In some fabrics, the ink coating contains microbeads hemispherically coated with aluminium. Each millimetre printing dot contains several hundred light-transmissive microbeads, which are typically sized in the range of 20–90 μm . During printing or coating, these microbeads are randomly aligned with only a proportion of them disposed to be capable of retroreflectivity. This kind of printing or coating is in effect ‘solid’, but leaves uncoated areas which enable the fabric to ‘breathe’ and/or allow moisture management, which is particularly important for firefighter or other protective clothing (White et al., 2004).

5.2.4 Temperature-responsive breathable coating

5.2.4.1 Shape memory polymers

Fabrics made of shape memory polymers (SMP) (Ding et al., 2004; Crowson, 1996) are termed smart breathable fabrics and act as a switch to control the transmission of water vapour. At lower temperatures, the coating substance on the fabric exists in a swollen state (by absorbing water from the surroundings), which results in the closure of microcracks. At a temperature higher than the transition temperature, the coating exists in a collapsed state (owing to the predominance of hydrophobic interactions), which results in opening of the microcracks. Another result is diffusion flux, which is governed by changes in both the diffusion coefficient and the diffusion path of water molecules through the swollen and collapsed coating.

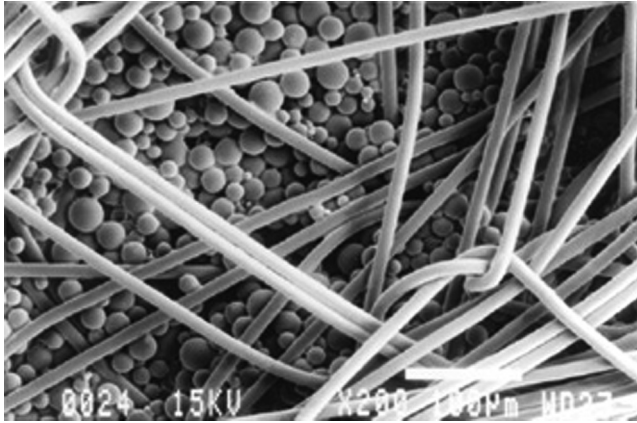


Figure 5.5 PCM microcapsules in a fabric (magnification $\times 200$; scale = 100 μm).
(© Outlast Technologies LLC.)

PCMs (Anon, 2004; Chung and Cho, 2004; Li and Zhu, 2004; Ying et al., 2004; Choi et al., 2004; Ghali et al., 2004; Pause, 2003, 2001; Anon, 2002; Shim et al., 2001; Hassee, 2003) are another class of smart textiles useful for making breathable fabrics. PCMs are enclosed in small plastic spheres with a diameter of only a few micrometres, known as PCM microcapsules (Fig. 5.5). They are permanently embedded in either the fibres or PU foams, or coated on the surface of a textile structure. PCMs absorb heat energy as they change from a solid to a liquid state and release heat as they return to a solid state (Fig. 5.6). By careful selection of the PCM, the fabric can act as a transient thermal barrier by protecting the wearer from the effect of a cold or hot environment within limited temperature conditions. When a sudden change in ambient conditions occurs, PCM fabrics delay the transient response and decrease body heat loss. Fibres, foams and fabrics with PCM microcapsule treatment are widely used today in garments such as ski suits, gloves, socks, sweaters, boots, protective garments and shoes to improve thermophysiological wear comfort in cold climate. These fabrics are also used in polar coveralls with a wind and waterproof lining. Poor thermophysiological wear comfort of protective clothing can be improved by using PCMs. PCMs act as a highly productive thermal storage medium which can be used to absorb excessive heat released by the human body under strenuous activities. Heat absorption by PCMs results in a delay in an increase in the microclimate temperature and hence a substantial decrease in a release of the skin's moisture (Pause, 2003). However, the magnitude of heating and cooling effect, and the time duration of the effect in garments depend on the number of garment layers, the orientation of the PCM layer to the body and the amount of body surface area covered with PCM garments (Shim et al., 2001).

5.2.4.2 *Fabrics based on biomimetics*

Biomimetics is the mimicking of biological mechanisms, with modification, to produce useful artificial products. There is potential to improve the vapour permeability

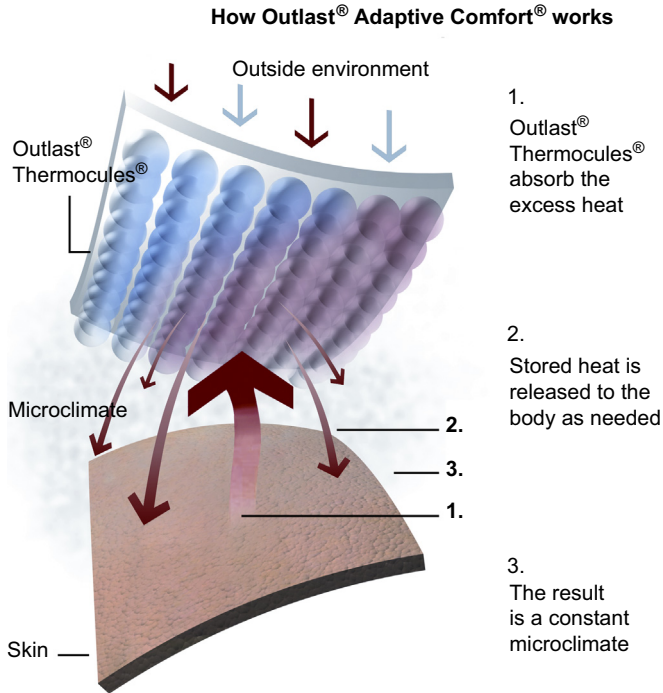


Figure 5.6 Functioning principle of PCM in a fabric.
(© Outlast Technologies LLC)

of fabric coatings by incorporating an analogue of the leaf stomata, which opens when the plant needs to increase moisture vapour transpiration and closes when it needs to reduce it. AkzoNobel is marketing the product under the trade name of Stomatex. This is a closed-foam insulating material made from neoprene incorporating a series of convex domes vented by a tiny aperture at the apex. These domes mimic the transpiration process that takes place within a leaf, supplying the controlled release of water vapour to provide comfortable wear characteristics (Fig. 5.7). Stomatex is claimed to respond to the level of activity by pumping faster as more heat is produced, returning to a more passive state when the wearer is at rest. Stomatex is used in conjunction with Sympatex, AkzoNobel's waterproof breathable membrane, to produce a breathable waterproof insulating barrier for use in clothing and footwear (Holmes, 2000a).

5.3 Materials for breathable coating

Regular PU, PVC and rubber coatings have been in use for some time to make fabrics waterproof, but they do not provide breathability. Rubber has been in use as a coating for fabrics since 1823, when Scotsman Macintosh patented the first raincoat by sandwiching a layer of rubber between two layers of cloth. PVC resins are available in diverse physical forms; they are low cost and have excellent physical properties,

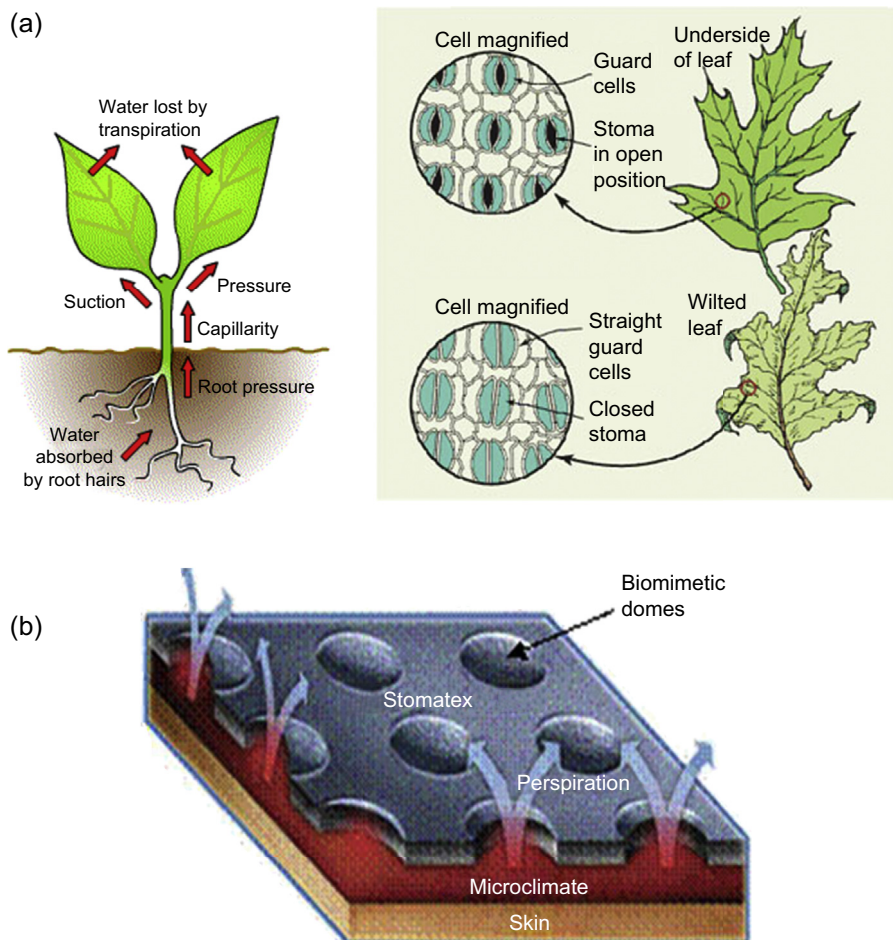


Figure 5.7 (a) Transpiration effect in plants, (b) AkzoNobel's Stomatex fabric based on transpiration effect.

and are useful and able to be processed by a wide variety of techniques. Materials used for breathable coatings are discussed next:

1. In the 1970s, WL Gore introduced Gore-Tex, material which had a high standard of water resistance combined with a high level of breathability. Gore-Tex[®] is a thin film of expanded PTFE polymer claimed to contain 1.4 billion tiny holes per square centimetre. PTFE polymer can also be used as a coating on textile substrate.
2. Polyurethane coatings are used in wide applications such as apparel, artificial leather, fuel and water storage tanks, inflatable rafts and so on, owing to several advantages over other polymeric coatings, such as low-temperature flexibility; softer handle and very high tensile, tear, and abrasion resistance. PU has been widely used to prepare microporous films and coatings (Jassal et al., 2004). There are various commercial PU-based breathable microporous films:
 - a. Entrant made by Toray Industries and Porelle by Porvair are microporous films and coatings made from PU (Lomax, 1985b).

5.4 Methods of generating hydrophilic and microporous coatings

A number of different methods have been used to apply hydrophilic and microporous coatings on fabrics. Hydrophilic coatings and microspheres containing PCMs dispersed in water solution are mainly applied using the knife coating technique, screen printing technology, pad dry cure and transfer/cast coating. Sometimes the coating is built up in several layers by a number of applications. To achieve thinner coatings and therefore more flexible fabric, and to apply coating to warp knitted, nonwoven, open weave and elastic fabric, transfer coating is used. In the transfer coating process, a film is also obtained by casting on a release paper, which is subsequently adhered to the fabric to make laminates. The coating is applied to the side of the fabric that becomes the inside of the garment. These regular coatings have good abrasion resistance and it is not necessary to protect the coated surface with fabric lining. PU is also applied by transfer coating to knitted fabrics to produce much softer and flexible coated fabric, but in this case, the coating is applied to the side which becomes the outside of the garment. Some commercial products using this process are Cyclone (Carrington), Entrant (Toray) and Keelatex (Sen, 2001; Woodruff, 1998). Methods of applying coatings onto different substrates are discussed separately in another chapter. For a given polymer coating weight, transfer-coated and laminated fabrics are more permeable than direct-coated fabrics of the same fibre type because of blocking of the interstices by coating material in the latter case (Lomax, 1985a).

A number of different methods have been used to produce hydrophilic and microporous coatings. Conventional coatings like PU, PVC or rubbers do not have polar groups required to activate hydrophilic mechanism for the transport of water. Hydrophilicity is generated by optimizing the hydrophilic-hydrophobic balance. This can be achieved by three ways (Lomax, 1985a; 1990; Scott, 1995):

1. Using polymer blends,
2. incorporating pendant hydrophilic groups such as $-O-$, $CO-$, $-OH$ or $-NH_2$ in a block copolymer
3. using segmented copolymers.

Two major hydrophilic coatings are based on hydrophilic polyurethanes and hydrophilic polyesters, which have been discussed in the previous section on the materials for coating. Methods for generating microporous coatings are discussed below (Sen, 2001; Holmes, 2000b; Scott, 1995; Kannekens, 1994):

- Mechanical fibrillation (only for membranes)
- Wet coagulation process
- Thermocoagulation (only for coatings)
- Foam coating (only for coatings)
- Solvent extraction
- Solubilising one component in the mixture (only for coatings)
- Radio frequency/ion/UV or E beam radiation
- Melt-blown/hot melt technology
- Point-bonding technology
- Nanofibres

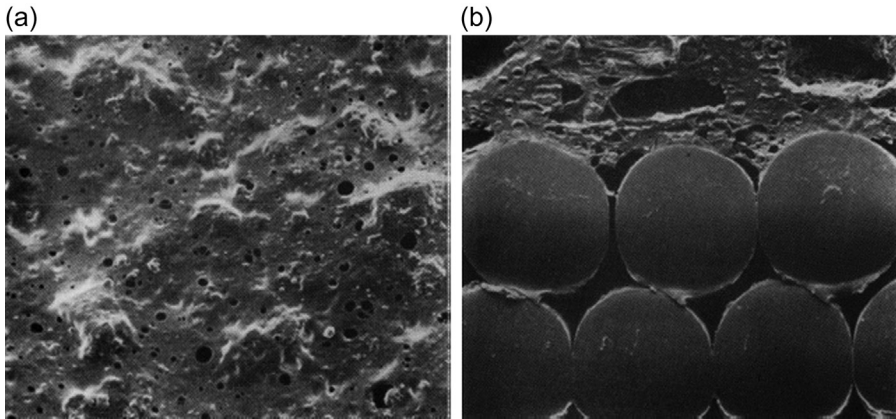


Figure 5.9 PU coated on filament nylon woven fabric Entrant, produced by wet coagulation method: (a) surface; (b) cross section (Lomax, 1985b).

5.4.1 Mechanical fibrillation

Certain polymer films can be stretched in both directions and annealed to impart microscopic rips and tears throughout the membrane, which imparts a suitable microporous structure. For example, Gore-Tex PTFE membranes are made from a solid PTFE sheet using this method (Bajaj, 2001a; Painter, 1996; Gore, 1976). The film is mechanically weak and therefore laminated to textile fabric with a nonflammable layer of silicone on one side to give bicomponent properties (Painter, 1996; Sen, 2001).

5.4.2 Wet coagulation process

A group of PU-based microporous films use the chemical ability of PU to coagulate into a fine interconnecting porous structure through a solvent exchange process with dimethyl formamide (DMF) and water (Painter, 1996; Krishnan, 1992). PU dissolved in DMF is used to produce a solution insoluble in water and is then coated onto the fabric. Coated fabric is passed through a conditioning chamber containing water vapour, in which DMF becomes diluted and PU precipitates. The process produces a very fine interconnecting microporous structure such as Entrant fabric, produced by Toray Industries (Fig. 5.9) (Lomax, 1985a; Roey, 1991).

Microporosity can also be created by leaching the salts upon treatment of the film with water. Products in this class are Porvair, Porelle and Permair (Lomax, 1985a; Scott, 1995). Addition of a water-repellent agent and nonionic surfactants in the coating solution imparts water repellency to the pores, resulting in better waterproofness of the coated fabrics (Naka and Kawakami, 1985). A much higher water vapour permeability and waterproofness can be achieved by incorporating about 1% nonporous inorganic filler, eg, silica (Aerosil) or magnesium oxide of particle size $<0.1 \mu\text{m}$ in the PU resin. The coating obtained on wet coagulation shows ultrafine pores of $<1 \mu\text{m}$ in addition to a honeycomb skin core structure of 1- to 20- μm pores (Sen, 2001).

A combination of polyamino acid (poly- γ -methyl-L-glutamate) and PU resin in the ratio 60:40 to 40:60 was used by Unitika Co., Japan, to produce the Exceltech brand of

microporous-coated fabric by wet coagulation process (Furuta and Yagihara, 1990). When bicomponent properties are required, a further layer of hydrophilic PU is added to one side (Painter, 1996).

5.4.3 Thermocoagulation

The coating polymer can also be applied to the fabric from a relatively volatile solvent mixed with a proportion of a higher boiling nonsolvent. The polymer coating precipitates out as a microporous layer when the true solvent evaporates faster than the nonsolvent during the two-stage drying operation. The process has an advantage over the wet coagulation process in that immersion and washing baths are not required. The Ucecoat 2000 system (Sen, 2001; Lomax, 1985a; Shekar et al., 2003), a PU-based coating technique, operates according to the thermocoagulation technique. In this process, PU is dissolved in a solvent mixture of methyl ethyl ketone, toluene and water, with 15–20% solids, and is coated on the fabric. The low-boiling solvent evaporates, leading to the precipitation of PU in the nonsolvent. As the concentration of the nonsolvent reaches a critical concentration level, the PU precipitates out in a highly porous form and the remainder of the solvent and the nonsolvent evaporates from the coating as the fabric passes through the oven.

5.4.4 Foam coating

In this process, a mixture of PU and PU–polyacrylic acid esters is dispersed in water and then foamed. The foam is stabilised with the help of additives and applied to one side of the fabric. The coated fabric is dried to form a microporous coating. The fabric is finally calendered under low pressure to compress the coatings. Because the foam cells are relatively large, a fluorocarbon (FC) polymer water-repellent finish is applied to improve the water-resistant properties (Mayer et al., 1989). Based on the study on foam coating techniques on breathable nylon fabrics, it was observed that the water vapour permeability of foam-coated fabrics was higher and their water resistance was lower than those of non-foam coated fabrics with the same coating weight.

5.4.5 Solvent extraction

Solvent extraction is a process in which the polymer dissolved in a water-miscible solvent is coated directly onto the fabric. The microporous structure of the coating is developed by passing the coated fabric through a coagulation bath in which the solvent is displaced by water. In an older process, finely divided, water-soluble salts are incorporated into the coating formulation. The salt particles are subsequently extracted from the dried and cured coating by passing the fabric through a water bath.

A process of making breathable fabric with a microporous polyethylene-tetrafluoroethylene (ETFE) layer was reported by Kafchinski et al. (Sen, 2001; Kafchinski et al., 1994). The process consists of making a dope containing a suspension of ETFE, about 0.5–1 μm , in an extractable polymeric binder. Subsequently the dope is cast onto a release paper and dried. The film is next calendered above the flow temperature of ETFE (about 300°C) and laminated to a fabric substrate using heated

calendar rolls. The binder is then extracted by a suitable solvent which is a nonsolvent for ETFE and does not damage the fabric. This leaves behind a microporous ETFE layer on the fabric. Polymeric binders such as polycarbonate, polymethylmethacrylate, and so forth, are preferred because they can be extracted by immersion in water. The fabrics made of polybenzimidazole, Kevlar, Nomex, etc., are preferred as the base material. The resultant laminated fabric is flame resistant as well as breathable. The microporous film can be bonded to the fabric by adhesive, as well.

5.4.6 Solubilising one component in the mixture

In this method of forming a moisture-permeable, waterproof coating on a fabric, the following steps are involved: applying to fabric a water-based coating containing a film-forming polymer which forms a water-insoluble polymeric layer upon being dried or heat treated and a water-soluble, enzyme-degradable polymer; drying or heat treating the fabric to form a layer on it; treating the fabric with an aqueous solution of an enzyme capable of selectively degrading the water-soluble polymer; and extracting the degraded water-soluble polymer from the layer, in which the layer on the fabric is rendered microporous.

5.4.7 Radio frequency/ion/UV or E beam radiation

The application of FC coatings to polyethylene terephthalate (PET) fabrics by ion beam sputtering of PTFE under different conditions is reported (Qi et al., 2002). In the process, various FC films were deposited by ion beam sputtering in the deposition chamber. A Teflon target was used and sputtering was performed by an Ar ion beam with energy in the range of 1.0–2.1 KeV at an ion current ranging from 20 to 35 Ma. Commercial PET fabrics with various weave structures were used as substrates over which the films grew at room temperature. When the Ar beam was emitted by the ion source, the PTFE target first broke down into CF_x or larger fragments by energetic ions and these fragments were then deposited onto the growing film surface (Hishmeh et al., 1996).

A rapid method of making microporous film was developed (Anon, 1989; Gregor et al., 1988) by Gelman Science, United States, and patented in 1984 as the sunbeam process. The polymer is based on acrylates. Monomers and oligomers are cross-linked under a radiation source, UV/E beam and cured in milliseconds. The pores are of the order of 0.2 μm and the film can be very thin, of the order of a few angstroms. These films are marketed as Repel and can be laminated on nonwovens to make disposable protective clothing for a variety of applications such as clean room garments, medical gowns and chemical splash suits.

5.4.8 Melt-blown/hot melt technology

Breathable fabric produced with melt-blown technology may be composed of at least one layer of coarse melt-spun thermoplastic filaments and at least one layer of fine melt-blown thermoplastic microfibres. The layers are thermally bonded together at intermittent points, and while being heated, are subjected to a force in at least one direction without tearing. The coarse filaments are elongated in the direction of force and the fine microfibres are straightened in the direction of force, in the absence of

drawing, to form a denser array of the microfibrils with a lesser thickness within the resulting fabric (Etzold, 1999).

5.4.9 Point-bonding technology

The Point-in-Point (PiP) patented technology (Krings et al., 2003) is complementary to the continually increasing hot melt applications in the bonding and laminating areas. In the PiP process, the adhesive points on two sides of a three-ply system are brought into alignment by means of electronic control. The lamination and bonding occurs in one production step. With this process, adhesive points on one side are congruent with the points on the second side of a film or textile. Advantages of PiP technology include the possibility of greater WVT because there is a higher amount of free surface between the adhesive points, leading to greater breathability (up to about 40%) and comfort for the wearer. However, the gap between the adhesive points is small for water particles. Application areas include climate membranes used for protective weather, medical and work garments. The technology is particularly advantageous in so-called soft shells and trilaminates and is usually used in sportswear, active wear, and leisurewear.

5.4.10 Nanofibres

Electrospinning of ultrathin membrane of extremely fine nanofibres with a very small pore size onto different substrate fabrics has been tried by various researchers to produce waterproof breathable fabrics. An improved and cheaper method of producing breathable waterproof film—nonwoven laminates by a combined film extrusion and lamination process was reported by Reifenhäuser. This method incorporates coating by an electrostatic process rather than by using mechanical pressure (Anon, 2001).

5.5 Testing and evaluation of different breathable coated fabrics

In many applications, breathable coated fabrics are expected to satisfy many functional characteristics other than breathability, such as fabric mechanical strength, tear and abrasion resistance, coating strength, ability to be laundered, ability to be sealed by tape, thermophysiological comfort and so on, and to perform efficiently over the lifetime of the product (Lomax, 1991; Shekhar et al., 2003; Sen, 2001; Krishnan, 1992; David, 2000; Weder, 1997; Keighley, 1985). Surface modification or stitching may also adversely affect the functionality of fabrics.

However, the performance evaluation of waterproof breathable fabrics is done mainly by measuring three properties (Holmes, 2000b):

- Resistance of penetration and absorption of liquid water
- Wind resistance
- Water vapour permeability

5.5.1 Resistance to penetration and absorption of water

The fabric's resistance to penetration and absorption of water can be measured by two different kinds of tests: simulated rain and penetration pressure.

5.5.1.1 Simulated rain tests

Spray test

American Association of Textiles Chemists and Colorists (AATCC) test method 22 measures the resistance of fabrics to wetting by water. This test method is suitable for testing the water repellency of fabrics but it cannot be used to predict probable rain penetration resistance for fabrics. A 180×180 -mm specimen is fastened in a 152.4-mm-diameter hoop and placed on an inclined plane at an angle of 45 degree. Then, 250 mL distilled water is allowed to spray onto the face of test specimen for 25–30 s from a height of 150 mm, as shown in Fig. 5.10. Upon completion of spraying, hoop is removed and tapped firmly against a solid object. The wet/spotted pattern is compared with the rating chart supplied with the apparatus.

Rain test

AATCC test method 35 provides the method of testing the penetration of water by impact. This method can be used to predict the rain penetration resistance of fabrics. A 20×20 -cm test specimen backed by 15.2×15.2 -cm blotter paper is mounted in a

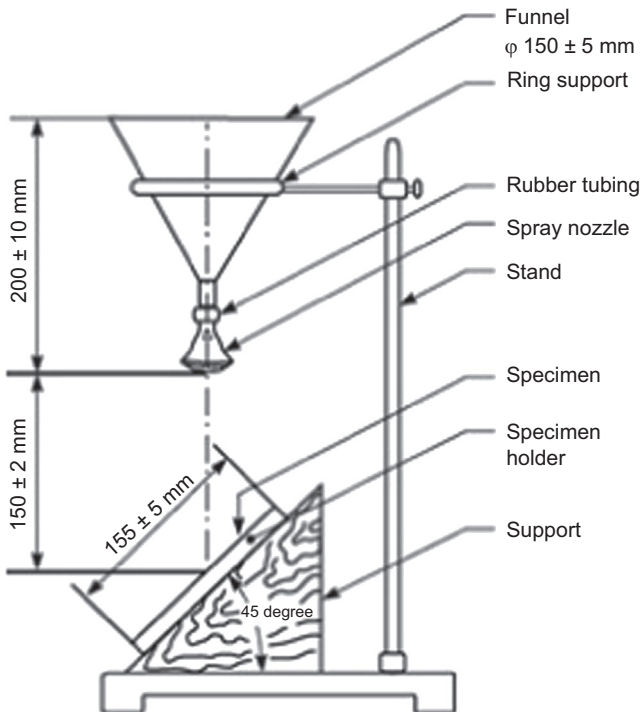


Figure 5.10 AATCC spray test.

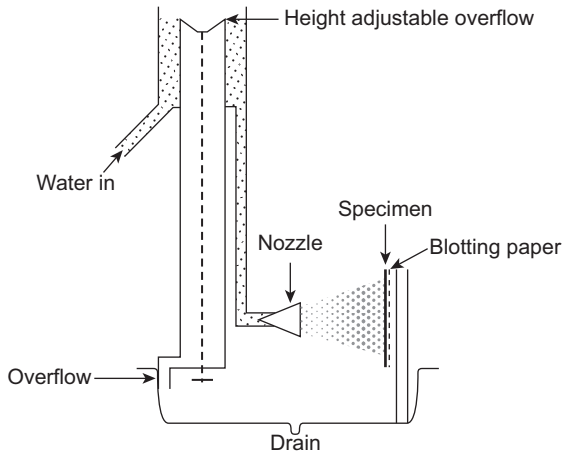


Figure 5.11 AATCC rain test apparatus.

vertical rigid support frame, as shown in Fig. 5.11. The specimen is exposed to a horizontal pressurised spray of water from a distance of 30.5 cm for 5 min. The change in the weight of blotter is used as a measure of water penetration resistance of the fabric. The test can be carried out at different impact intensities and a complete picture of the penetration resistance of the fabric or a combination of fabrics can be obtained by performing the test at different pressure heads. The pressure head should be varied by 300-mm increments to determine (1) the maximum head at which no penetration occurs, (2) the change in penetration by increasing the head, and (3) the minimum head required to cause breakdown or the penetration of more than 5 g of water.

Impact penetration

[AATCC test method 42](#) provides an impact penetration test to measure the resistance of fabrics to the penetration of water by impact. The apparatus is similar to the spray test apparatus but the impact penetration resistance of fabrics is estimated by measuring the change in weight of the blotter paper placed below the 178×330 -mm sample. Five hundred millilitres distilled water is poured into the funnel of the tester and allowed to spray onto the specimen from a height of 60 cm.

Bundesmann rain tester

The test consists of four specimen holders 100 mm in diameter placed over inclined cups with a rotating member rubbing the underside of specimens, as shown in Fig. 5.12. Specimens are subjected to simulated rain from a height of 150 cm using filtered water under pressure. Water penetrating through the fabrics is collected in the cups and is measured on a mass basis.

5.5.1.2 Penetration pressure tests

Hydrostatic pressure test

[AATCC-127](#) and [ISO 811](#) test methods measure the resistance of a fabric to the penetration of water under hydrostatic pressure. A test specimen mounted under the orifice of

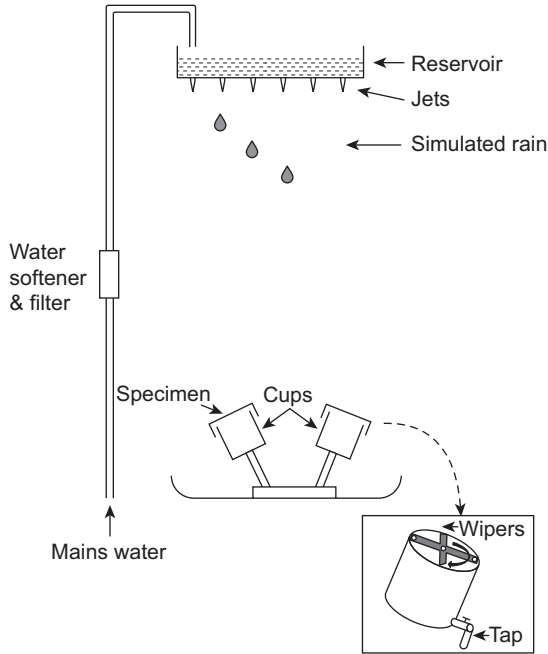


Figure 5.12 Bundemann simulated rain tester.

a conical well is subjected to water pressure constantly increasing at 10 ± 0.5 cm/min until three leakage points appear on its surface, as shown in Fig. 5.13 (Midha et al., 2012). The higher the column height that is achieved before the appearance of the third water droplet on the fabric surface, the greater is the water resistance of the specimen.

5.5.2 Wind resistance

Wind resistance is assessed by measuring the air permeability of the fabrics. [ASTM D737](#) determines the rate of air flow per unit area of the fabric at a standard pressure difference across the fabric faces. A specimen is mounted over a test head area of

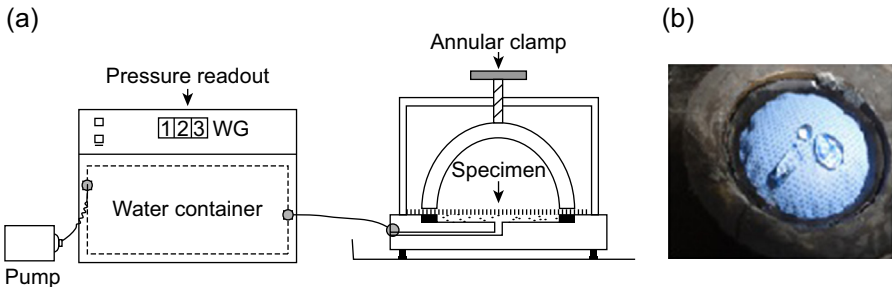


Figure 5.13 (a) Hydrostatic head apparatus; (b) appearance of three leakage points on breathable fabric.

38.3 cm², clamped at a force of 50 ± 5 N. Air velocity through the test area is measured when a pressure drop of 125 Pa across the specimen is observed. British standard measures the air flow at a pressure of 100 Pa for apparel fabrics and at 200 Pa for industrial fabrics.

5.5.3 Water vapour permeability

Hong et al. (1988) suggested two approaches to measure moisture vapour transfer:

- Dynamic methods, which measure moisture transfer before the samples reach equilibrium
- Equilibrium methods, which measure moisture transfer after samples reach equilibrium

Dynamic methods are important in fabrics where excessive swelling of fibres or yarns leads to reduction of pores in the fabrics.

From the water vapour permeability point of view, textile materials behave in two different ways: first, materials in which moisture vapour transfer takes place predominantly by diffusion through air spaces between yarns and fibres, following Fick's law. Measured water vapour permeability values are independent of the measuring conditions. Woven, nonwoven, and semipermeable membrane laminates fall into this category. Materials that contain a layer of hydrophilic membranes behave differently. In particular, the rate of diffusion through the hydrophilic membrane depends on test conditions such as the concentration of water vapour in the layer or relative humidity (Gibson, 1993; Keighley, 1985). Several methods are available to test the water vapour permeability of textiles. The most commonly used methods are discussed next.

5.5.3.1 Cup method

ASTM Standard E96, Standard Test Method for Water Vapour Transmission of Materials, provides a method to determine the WVT of materials such as paper, plastic films, other sheet materials, fibre boards, gypsum and plaster products, wood products and plastics. This method has been used for textiles for some time, although it does not simulate actual wearing conditions for clothing.

A circular sample 74 mm in diameter is sealed over the open mouth of a cup containing water and placed in standard atmospheric conditions. The evaporation of water through the fabric specimen is observed by successive weighing of the cup after the specimen has reached equilibrium. The cup is filled with 100 mL distilled water and an air gap of 19 mm is left between the water surface and the fabric. Air velocity over the specimen is maintained at 2.8 m/s, as shown in Fig. 5.14. After a suitable time (for example, overnight), the dishes are reweighed and the time is noted (Huang and Qian, 2008). The WVT is given by (Eq. [5.1]):

$$\text{WVT} = \frac{G \times 24}{t \times A} \quad [5.1]$$

where WVT = WVT rate (g/m² per day); G = weight change (g); t = time during which G occurred (h) and A = test area (m²).

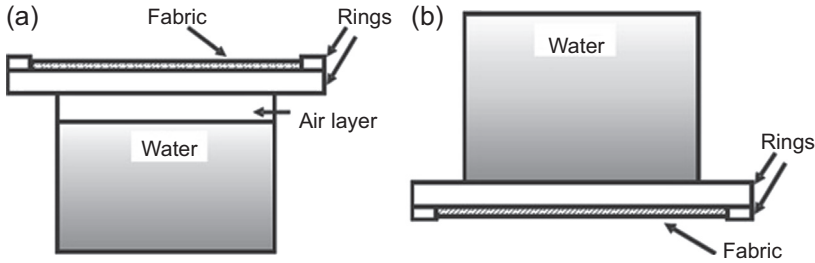


Figure 5.14 (a) Cup method; (b) inverted cup method for water vapour transmission.

The water vapour permeability index can also be calculated by expressing the WVT of the fabric as a percentage of the WVT of a reference fabric, which is tested alongside the test specimen. The main drawback of this method is that the still air layer inside the cup between the water surface and the fabric offers higher water vapour resistance than the fabric itself.

The experiment is sometimes carried out with the cup inverted so that the water is in contact with the inner surface of the fabric. This form of the test tends to give more favourable results for hydrophilic films.

5.5.3.2 Desiccant inverted cup method

ISO 15496 uses an inverted cup method to measure the water vapour permeability of textile fabrics. A cup filled with a desiccant (eg, potassium acetate) is sealed with a circular piece of waterproof and vapour-permeable membrane. A 180 mm circular specimen is fitted to the groove of the specimen holder and covered by another piece of waterproof and vapour-permeable membrane. The specimen holder is then inserted into the support frame, which is fitted with four vertically adjustable screws so that the specimen holder is immersed to a depth of 5 ± 2 mm in a water bath filled with distilled water at 23°C . The measuring cup is weighed at a precision of ± 1 mg, inverted and inserted into the specimen holder. After 15 min, the measuring cup is removed and reweighed. The WVT of the specimen is calculated as (Eq. [5.2]):

$$\text{WVT} = \frac{96 \times (a_1 - a_0)24}{A} \quad [5.2]$$

where WVT = water transmission vapour rate, g/m^2 per day; a_1 = mass of test body after test (g); a_0 = mass of test body before test (g) and A = test area (m^2).

5.5.3.3 Sweating guarded hot plate method

ISO 11092 provides the sweating guarded hot plate method for measuring the water vapour permeability of the fabric by simulating the actual cloth-wearing conditions in human beings. This method is similar to the guarded hot plate method for measuring the thermal transmission of fabrics. The instrument measures the power required by a

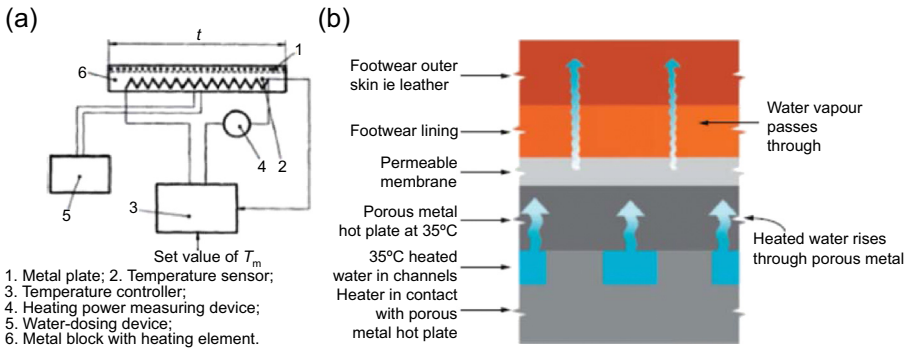


Figure 5.15 Sweating guarded hot plate; (a) side view, (b) in operation (Huang & Qian, 2008; Mckeown, SATRA Bulletin).

hot plate to maintain it at a constant temperature (Fig. 5.15). When covered with the sample, the power required to maintain it at a constant temperature can be related to the dry thermal resistance of the fabric. If the plate is saturated with water, the amount of power required to maintain it at a constant temperature is related to the rate at which water evaporates from the surface of the plate and diffuses through the fabric.

The $300 \times 300\text{-mm}^2$ fabric sample is mounted onto a square porous plate which is heated to a constant temperature that approximates body skin temperature (eg, 35°C). The plate temperature is measured by a sensor sandwiched directly underneath the plate surface. The whole apparatus is housed in a chamber so that the environmental conditions can be carefully controlled. Air speed above the specimen is regulated at 1 m/s. After steady-state conditions are reached, the total evaporative resistance of the fabric is calculated by (Huang and Qian, 2008) (Eq. [5.3]):

$$R_{\text{et}} = \frac{A(P_s - P_a)}{H - \Delta H_e} \quad [5.3]$$

where R_{et} = total evaporative resistance provided by the fabric and boundary air layer ($\text{m}^2 \cdot \text{Pa}/\text{W}$); A = test area (m^2); P_s = water vapour pressure at the plate surface; P_a = water vapour pressure of the air; H = heating power (W) and ΔH_e = correction term for heating power (W).

The intrinsic evaporative resistance of the fabric can be obtained by subtracting the evaporative resistance of the boundary air layer, measured by conducting a test on the bare plate without the fabric (Eq. [5.4]):

$$R_{\text{ef}} = R_{\text{et}} - R_{\text{eb}} \quad [5.4]$$

where R_{ef} = intrinsic evaporative resistance of the fabric ($\text{m}^2 \cdot \text{Pa}/\text{W}$); and R_{eb} = evaporative resistance provided by the boundary air layer ($\text{m}^2 \cdot \text{Pa}/\text{W}$).

Of the various methods used for water vapour permeability, only the sweating guarded hot plate method simulates actual clothing wearing conditions; results can

be related to the thermophysiological responses of human beings. The upright cup method provides the lowest WVT rates, followed by the inverted cup and desiccant inverted cup methods.

5.6 Applications

Breathable coated fabrics are of two-, three- or four-layered construction with one of the layers coated or laminated with the breathable membrane or coatings. The breathable membrane or coating may be applied with either

- the outer layer (inner or outer face)
- the middle layer
- the inner layer
- in some cases, it may be laminated with both the inner and the outer layer, as indicated in Fig. 5.16 (Mayer et al., 1989).

Depending on the application, the substrate on which the coating has to be applied is chosen, such as when it is:

- woven for garments and wound dressing
- nonwovens for wound dressing, inserts/lining and roofing membranes
- foams for upholstery

These multilayered breathable fabrics are then combined with other layers of the garment system to make the garment suitable for specific applications. The performance of each layer in a multilayer-component breathable fabric is influenced by the performance of other layers and their positioning. During physical activity that produces sensible perspiration, removal of an insulating layer such as a fleece garment

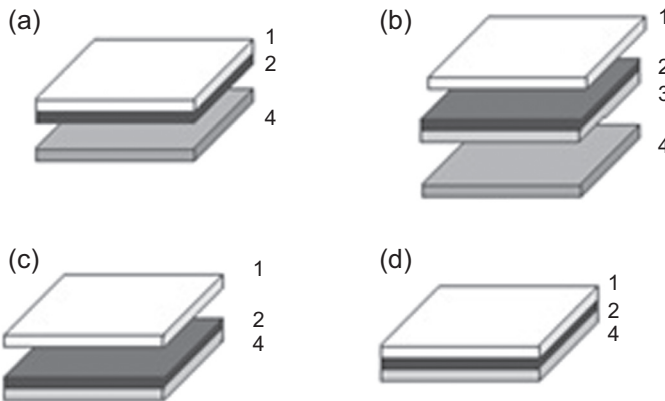


Figure 5.16 Breathable fabric constructions: (a) outer fabric laminate, (b) insert laminate, (c) lining laminate, (d) three-layer laminate, (1) outer fabric, (2) breathable film, (3) insert fabric, and (4) lining material.

should improve the comfort of the clothing system by increasing the temperature of the breathable layer, improving its vapour transport, and reducing condensation. The use of a laminated fleece (presumably meaning the wind-resistant type) promotes the formation of condensation on the fleece and the waterproof breathable layer owing to the restriction of ventilation within the clothing system. However, if vapour permeability is restricted largely by the use of waterproof breathable fabric, the overall performance of fabrics will be least affected by the other components. However, for extreme conditions, appropriate breathable fabrics are required for protection.

Examples of over 50 applications of smart breathable membrane and coated fabrics can be seen in [Table 5.3](#) (Shekar et al., 2003; Mondal, 2008).

In this section, a few specific applications of smart breathable coated fabrics are discussed.

- For similar applications there may be many choices of breathable fabrics. In active sportswear, breathable fabrics widely differing in material characteristics, such as Gore-Tex,

Table 5.3 Application of smart breathable membrane/coated fabrics

Microporous and hydrophilic breathable membrane/coatings and their combinations	<p>Foul weather clothing: survival suits, special military protective clothing, clean room garments, surgical garments, hospital drapes, mattress and seat covers, specialised tarpaulins, packaging, wound dressings, filtration</p> <p>Domestic and transport: nonallergic bedding, car covers, fire smoke curtains in ships, cargo wraps in aircraft</p> <p>Fashionable weather protection: rainwear, skiwear, golf suits, waling boot linings, panels and inserts, sports footwear linings, panels and inserts</p> <p>Heavy-duty, foul weather clothing: anoraks, cagoules, packs, overtrousers, hats, gloves, gaiters</p> <p>Defence: parkas, skiwear, expedition suits, cycling gear, gloves, gaiters, caps, overmitts, and jackets, military and civil emergency tents, sleeping bags</p>
Breathable fabrics based on biomimetics	Sports garments
PCM-based breathable coatings	<p>Space: spacesuits and gloves</p> <p>Active sportswear: snowboard gloves, active sportswear, ice climbing, cycling and running undergarments</p> <p>Bedding and accessories: quilts, pillows and mattress covers</p> <p>Medical and hygiene: surgical gauze, diapers and incontinence products</p> <p>Shoes and accessories: ski boots, race car drivers' boots, mountaineering boots</p> <p>Protective clothing: firefighter suits</p>

Sympatex, Microft, Ertrant G II and Isofix Super, are available (Kothari and Sanyal, 2003; Bajaj, 2001b; Toray, 1993; Teijin, 1993; Kanebo, 1994). Gore-Tex and Sympatex fabric possess breathability owing to microporous and hydrophilic membranes, respectively, laminated with fabric; whereas Microft fabric is composed of a polyester microfibre of 0.7 denier/filament. Ertrant G II and Isofix Super are coated fabrics.

- Toray developed a high-performance, waterproof, breathable fabric, Entrant G II. It consists of a three-layer PU coating membrane including two different microporous layers. The top layer is a foam layer with miniscule micropores which improve waterproofness and durability. The middle layer, which is regularly configured micropores, increases moisture permeability. In the bottom layer, pores in the resin surface enhance waterproofing and inhibit dew condensation (Toray, 1993).
- The Diaplex membrane, produced by Mitsubishi Heavy Industries Ltd., Japan, is a PU-based shape memory polymer fabric which intelligently responds to the wearer's metabolic heat output and changes its vapour permeation properties significantly (Parys, UNITEX).
- Mondal and Hu (2006) developed temperature-stimulating shape memory PU for smart breathable clothing. They reported that the permeability of SMP-coated or laminated fabrics changes as the wearer's environment and body temperature change. The fabrics offer lower water vapour permeability at lower temperature and keep body heat inside. When the body sweats, The higher WVP lets moisture escape and keeps the body cool. The use of composite film of SMP as an interlining provides the apparel system with variable tog values to protect against a variety of weather conditions.
- Hu et al. (2012) used SMP to design fabrics for wound dressing, scaffolding materials and orthodontics. As a wound dressing material, SMP fabric changes modulus and the pressure being applied on the wound may change in response to body temperature changes.
- Another class of coated fabrics using microencapsulation is thermochromic fabrics, which release perfume upon rupture of the microcapsules or change colours with temperature. An example of colour-changing fabric is Sway brand skiwear (Toray Industries, Hong Kong), which is a PU-coated nylon fabric that contains microcapsules containing heat-activated dyes.
- Isofix Super, developed by Kanebo, is the name applied to a coating which incorporates new processing and structural technologies by fusing an antisublimation/antimigration coating technique to a special ceramic with a countless number of pores. The fabric exhibits anticondensation property, a dry feel and a soft touch (Kanebo, 1994). Other waterproof breathable fabrics such as Thintech, H₂OFF, Staycool, Prematex and Prooface are gaining popularity in skiwear and other active sportswear (Sen, 2001).

5.7 Conclusions and future trends

The technology behind designing breathable fabrics is continuously evolving to achieve improved functionality in addition to cost-effective manufacturing processes for a variety of applications. This has led to the development of smart breathable fabrics, which technically should respond to an external stimulus in a specific, controlled way to regulate water vapour permeation. In a true sense, most advanced breathable textiles cannot be considered smart because they do not adapt their functionality to the environment. However, smart breathable coated fabrics based on biomimetics and shape memory polymers can be regarded as active smart, and those based on conventional microporous and hydrophilic coatings can be called passive smart.

Textile materials that can store heat when it is warm and release the heat again when it becomes cold (PCMs) react to a change in the environment and therefore possess the required level of context sensitivity but they have no active control. To date, it is not possible to regulate the temperature of clothing according to the user's needs. However, it may be a future requirement that needs to be addressed for better performance in health-care and wound care applications. This may necessitate an electronic system that processes sensor data and decides on the reaction. In this particular context, however, it is difficult to merge electronics and textiles which possess diverse properties.

References

- AATCC Test Method 127-2003, Water Resistance: Hydrostatic Pressure Test, 82: 2007, AATCC Technical Manual, North Carolina.
- AATCC Test Method 22-2005, Water Repellency: Spray Test, 82: 2007, AATCC Technical Manual, North Carolina.
- AATCC Test Method 35-1980, Water Resistance: Rain Test, 82: 2007, AATCC Technical Manual, North Carolina.
- AATCC Test Method 42-2000, Water Resistance: Impact Penetration Test, 82: 2007, AATCC Technical Manual, North Carolina.
- Anon, 2002. PCMs reduce humidity and sweat. *World Sports Activewear* 8 (2), 5.
- Anon, 2004/2005. Cool fabrics from the world's freezer. *Knitting International* 111 (1321), 38.
- Anon, 1989. Microporous fabrics for garments. *High Performance Textiles* 9 (11), 7.
- Anon, January 2001. Nonwoven backing gives new strength to breathable films. *British Plastics and Rubber* 20–21.
- ASTM D737, 2012. Standard Test Method for Air Permeability of Textile Fabrics, D737-04. American Society for Testing and Materials, Pennsylvania.
- ASTM E96, 2014. Standard Test Method for Water Vapor Transmission of Materials, E96/E96M. American Society for Testing and Materials, Pennsylvania.
- ASTM F1670, 2014. Standard Test Method for Resistance of Materials Used in Protective Clothing to Penetration by Synthetic Blood, F1670M-08. American Society for Testing and Materials, Pennsylvania.
- ASTM F1671, 2013. Standard Test Method for Resistance of Materials Used in Protective Clothing to Penetration by Blood Borne Pathogens Using Phi-x174 Bacteriophage Penetration as a Test System, F1671M-13. American Society for Testing and Materials, Pennsylvania.
- Bajaj, P., 2001a. Eco-friendly finishes for textiles. *Indian Journal of Fibre and Textile Research* 26 (1–2), 162–186.
- Bajaj, P., 2001b. Thermally sensitive materials. In: Tao, X. (Ed.), *Smart Fibres, Fabrics and Clothing*. The Textile Institute, Woodhead, pp. 63–64.
- Bhatkhande, P.S., 2011. Development of Thermo Regulating Fabric Using Phase Change Material (PCM) (M.S. thesis). Eastern Michigan University, Michigan.
- Bryant, Y.G., Colvin, D.P., July 12, 1988. Fiber with Reversible Enhanced Thermal Storage Properties and Fabrics Made Therefrom. USP 4756958.
- Choi, K., Cho, G., Kim, P., Cho, C., 2004. Thermal storage/release and mechanical properties of phase change materials on polyester fabrics. *Textile Research Journal* 74 (4), 292–296.

- Chung, H., Cho, G., 2004. Thermal properties and physiological responses of vapor-permeable water repellent fabrics treated with microcapsule containing PCMs. *Textile Research Journal* 74 (7), 571–575.
- Cooper, C., 1979. Textiles as protection against extreme winter weather. *Textiles* 8 (3), 72–83.
- Crowson, A., 1996. Smart materials based on polymeric systems, smart structures and materials. In: *Proc. SPIE 2716* (February 9, 1996), Smart Materials Technologies and Biomimetics, Bellingham, WA.
- COMA, 1986. Institute for Perception. TNO report no. IZ F 1986-26, October.
- David, I., 1995. Weather-proof membrane. *High Performance Textiles* 4, 10–11.
- David, A.H., 2000. Performance characteristics of waterproof breathable fabrics. *Journal of Industrial Textiles* 29 (4), 306–308.
- Desai, V.M., Athawale, V.D., 1995. Water resistant breathable hydrophilic polyurethane coatings. *Journal of Coated Fabrics* 25, 39–46.
- Ding, X.M., Hu, J.L., Tao, X.M., 2004. Effect of crystal melting on water vapor permeability of shape-memory polyurethane film. *Textile Research Journal* 74 (1), 39–43.
- Etzold, S., (EMDOCS.Corovin GmbH.), January 5, 1999. Waterproof, Multilayered Nonwoven Fabric of Reduced Weight Having Good Vapour Permeability and Method for its Production. USP 5855992.
- Fung, W., 2002. Products from coated and laminated fabrics. In: Fung, W. (Ed.), *Coated and Laminated Textiles*. The Textile Institute, Woodhead, Cambridge, pp. 149–249.
- Furuta, T., Yagihara, S., 1990. Exceltech: a polyamino acid derivative highly moisture permeable, waterproof material. *Journal of Coated Fabrics* 20 (1), 11–23.
- Ghali, K., Ghaddar, N., Harathani, J., Jones, B., 2004. Experimental and numerical investigation of the effect of phase change materials on clothing during periodic ventilation. *Textile Research Journal* 74 (3), 205–214.
- Gibson, P.W., 1993. Factors influencing steady state heat and water vapour transfer measurements for clothing materials. *Textile Research Journal* 63 (12), 749–764.
- Gore, R.W., April 27, 1976. Process for Producing Porous Products. USP 3953566.
- Gregor, E.C., Tanny, G.B., Shchori, E., Kenigsberg, Y., 1988. Sunbeam process microporous membranes: a high performance barrier for protective clothing. *Journal of Coated Fabrics* 18 (1), 26–37.
- Gretton, J.C., Brook, D.B., Dyson, H.M., Harlock, S.C., 1998. Moisture vapour transport through waterproof breathable fabric and clothing systems under a temperature gradient. *Textile Research Journal* 68 (12), 936–941.
- Gulbinienė, A., Jankauskaitė, V., Sacevičienė, V., Mickus, K.V., 2007. Investigation of water vapour sorption/desorption of textile laminates. *Materials Science* 13 (3), 255–261.
- Hale, D.V., Hoover, M.J., O'Neill, M., 1971. Phase Change Materials Handbook: NASA CR 61365. NASA Marshall Space Flight, Alabama.
- Hasse, J., 2003. Nonwovens for apparel. In: Albrecht, W., Fuchs, H., Kittelmann, W. (Eds.), *Nonwoven Fabrics: Raw Materials, Manufacture, Applications, Characteristics, Testing Processes*. Wiley, New Delhi, pp. 533–535.
- Hayashi, S., Ishikawa, N., Giordano, C., 1993. High moisture permeability polyurethane for textile application. *Journal of Coated Fabrics* 23 (7), 74–83.
- Hishmeh, G.A., Barr, T.L., Sklyarov, A., Hardcastle, S., 1996. Thin polymer films prepared by radio frequency plasma sputtering of polytetrafluoroethylene and polyetherimide targets. *Journal of Vacuum Science and Technology* 14 (3), 1330–1338.
- Hu, J., Meng, H., Li, G., Ibeke, S.I., 2012. A review of stimuli-responsive polymers for smart textile applications. *Smart Materials and Structures* 21, 1–23.
- Holme, I., 1990. Combating the worst of all weathers. *Textile Month* 5, 13–14.

- Holmes, D.A., 2000a. Textiles for survivals. In: Horrocks, A.R., Anand, S.C. (Eds.), *Handbook of Technical Textiles*. The Textile Institute, Woodhead, Cambridge, pp. 461–489.
- Holmes, D.A., 2000b. Waterproof breathable fabrics. In: Horrocks, A.R., Anand, S.C. (Eds.), *Handbook of Technical Textiles*. The Textile Institute, Woodhead, Cambridge, pp. 282–315.
- Hong, K., Hollies, N.R.S., Spivak, S.M., 1988. Dynamic moisture vapour transfer through textiles: part I: clothing hygrometry and the influence of fiber type. *Textile Research Journal* 58, 697.
- Hu, J., Ding, X., Tao, X., Yu, J., 2001. Shape memory polymers at work. *Textile Asia* 32 (12), 42–46.
- Huang, J., Qian, X., 2008. Comparison of test methods for measuring water vapour permeability of fabrics. *Textile Research Journal* 78 (4), 342–352.
- ISO 11092: 2014, 2014. Textiles-physiological Effects-Measurement of Thermal and Water-vapour Resistance under Steady State Conditions (Sweating Guarded-Hotplate Test). International Standards Organisation.
- ISO Test Method 15496: 2004(E), 2004. Textiles-measurement of Water Vapour Permeability of Textiles for the Purpose of Quality Control. International Standards Organisation.
- Jassal, M., Agrawal, A.K., 2010. Intelligent breathable coatings and laminates for textile applications technology. In: Smith, W.C. (Ed.), *Smart Textile Coatings and Laminates*. Woodhead, Cambridge, pp. 189–219.
- Jassal, M., Khungar, A., Bajaj, P., 2004. Waterproof breathable polymeric coatings based on polyurethanes. *Journal of Industrial Textiles* 33 (4), 269–280.
- Johnson, L., Samms, J., 1997. Thermoplastic Polyurethane Technologies for the Textile Industry. *Journal of Coated Textiles* 27 (1), 48–62.
- Kafchinski, E.R., Chung, T.S., Timmons, W., Gasman, J., October 25, 1994. Breathable Water Resistant Fabrics. USP 5358780.
- Kanebo Ltd, 1994. Isofix super. *Japan Textile News* 407, 36.
- Kannekens, A., 1994. Breathable coatings and laminates. *Journal of Coated Fabrics* 24 (1), 51–59.
- Keighley, J.H., 1985. Breathable fabrics and comfort in clothing. *Journal of Coated Fabrics* 15 (2), 89–104.
- Kim, K.S., Park, C.H., 2013. Thermal comfort and waterproof breathable performance of aluminum coated polyurethane nanowebs. *Textile Research Journal* 83 (17), 1808–1820.
- Kothari, V.K., Sanyal, P., 2003. Fibres and fabrics for active sportswear. *Asian Textile Journal* 12 (3), 55–61.
- Krings, W., Hansch, M., Krings, M., 2003. Lamination and bonding of three layer textile systems and breathable films. *Melliand International* 9 (2), 133–134.
- Krishnan, S., 1992. Technology of breathable coatings. *Journal of Coated Fabrics* 22, 71–74.
- Li, Y., Zhu, Q., 2004. A model of heat and moisture transfer in porous textiles with phase change materials. *Textile Research Journal* 74 (5), 447–457.
- Lomax, G.R., 1984. Recent developments in coated apparels. *Journal of Coated Fabrics* 14, 91–99.
- Lomax, G.R., 1985a. Design of waterproof, water vapour permeable fabrics. *Journal of Coated Fabrics* 15 (1), 40–66.
- Lomax, G.R., 1985b. Coated fabrics: part 1-lightweight breathable fabrics. *Journal of Coated Fabrics* 15, 115–126.
- Lomax, G.R., 1990. Hydrophilic polyurethane coatings. *Journal of Coated Fabrics* 20 (2), 88–107.
- Lomax, G.R., 1991. Breathable, waterproof fabrics explained. *Textiles* 20 (4), 12–16.

- Mckeown D. Evaluating comfort using the SATRA STM 511 sweating guarded hotplate. SATRA Bulletin.
- Mayer, W., Mohr, U., Schrierer, M., 1989. High-tech textiles: contribution made by finishing, in an example of functional sports and leisurewear. *International Textile Bulletin* 35 (2), 16–32.
- Mondal, S., Hu, J.L., 2006. Temperature stimulating shape memory polyurethane for smart clothing. *Indian Journal of Fibre and Textile Research* 31, 66–71.
- Mondal, S., 2008. Phase change materials for smart textiles- an overview. *Applied Thermal Engineering* 28, 1536–1550.
- Midha, V.K., Dakuri, A., Midha, V., 2012. Studies on the properties of nonwoven surgical gowns. *Journal of Industrial Textiles* 43 (2), 174–190.
- Mitsubishi, Hayashi, S., October 13, 1992. Makeup Material for Human Use. USP 5155199.
- Mukhopahdyay, A., Midha, V.K., 2008a. A review on designing the waterproof breathable fabrics part I: fundamental principles and designing aspects of breathable fabrics. *Journal of Industrial Textiles* 37 (3), 225–262.
- Mukhopahdyay, A., Midha, V.K., 2008b. A review on designing the waterproof breathable fabrics part II: construction and suitability of breathable fabrics for different uses. *Journal of Industrial Textiles* 38 (1), 17–41.
- Naka, Y., Kawakami, K., (Shirley Institute & Toray Industries Inc.), December 24, 1985. Moisture-Permeable Waterproof Coated Fabric. USP 4560611.
- Outlast Technologies LLC, Retrieved from <http://www.outlast.com/en/media-center/downloads/the-americas/> on 26.08.2015.
- Painter, C.J., 1996. Waterproof, breathable fabric laminates: a perspective from film to market Place. *Journal of Coated Fabrics* 26 (2), 107–130.
- Parys, M.V. Anticipating the Future- Assessing the Impact, *Technical Bulletin Part 4: Biomimetica and Smart Coatings*, 1–8.
- Pause, B., 2001. Textiles with improved thermal capabilities through the application of phase change material (PCM) microcapsules. *Melliand-Textilberichte* 81 (9), E179–E180.
- Pause, B., 2003. Nonwoven protective garments with thermo-regulating properties. *Journal of Industrial Textiles* 33 (2), 93–99.
- Pushaw, R.J., October 14, 1997. Coated Skived Foam and Fabric Article Containing Energy Absorbing Phase Change Material. USP 5677048.
- Qi, H., Sui, K., Ma, Z., Wang, D., Sun, X., Lu, J., 2002. Polymeric Fluorocarbon Coated Polyester Substrates for Waterproof Breathable Fabrics. *Textile Research Journal* 72 (2), 93–97.
- Roey, M.V., 1991. Water resistant breathable fabrics. *Journal of Coated Fabrics* 21 (1), 20–31.
- Russell, D.A., Hayashi, S., Yamada, T., 1999. The potential use of shape memory film in clothing. *Asian Textile Journal* 8 (11), 72–74.
- Save, N.S., Jassal, M., Agrawal, A.K., 2002. Polyacrylamide based breathable coating for cotton fabric. *Journal of Coated Fabrics* 32 (2), 119–138.
- Save, N.S., Jassal, M., Agarwal, A.K., 2005. Smart breathable fabric. *Journal of Industrial Textiles* 34 (3), 139–155.
- Scott, R.A., 1995. Coated and laminated fabrics. In: Carr, C.M. (Ed.), *Chemistry of the Text Ind*, Glasgow, New Zealand. Blackie Academic & Professional, Bishopbriggs, pp. 210–247.
- Scott, R.A., 2000. Textile in defence. In: Horrocks, A.R., Anand, S.C. (Eds.), *Handbook of Technical Textiles*. The Textile Institute, Wood head Publishing Ltd, Cambridge, England, pp. 425–460.
- Sen, A.K., 2001. *Coated Textiles: Principles & Applications*. Technomic Publishing Co. Inc., Lancaster, Basel, pp. 133–154.

- Shekar, R.I., Yadav, A.K., Kumar, K., Tripathi, V.S., 2003. Breathable apparel fabrics for defence applications. *Man-Made Textiles in India* 46 (12), 9–16.
- Shim, H., McCullough, E.A., Jones, B.W., 2001. Using phase change materials in clothing. *Textile Research Journal* 71 (6), 495–502.
- Silva, L.U., Sanchez, P., Rodriguez, J.F., 2011. Effective method of microcapsules production for smart fabrics. In: Bernardes, M.A.D.S. (Ed.), *Developments in Heat Transfer*. InTech, ISBN 978-953-307-569-3, pp. 649–666.
- Tanner, J.C., 1979. Breathability, comfort and gore-tex laminates. *Journal of Coated Fabrics* 8 (4), 312–322.
- Taylor, M.A., 1982. Fabrics and garments for rainwear. *Textiles* 11 (1), 24–28.
- Teijin Ltd, 1993. New Super Microft yarn. *Japan Breaking News* 459, 43.
- Toray Industries Inc., 1993. High performance waterproof/breathable fabric-Entrant G II. *Japan Breaking News* 459, 39.
- Weder, M., 1997. Performance of rainwear material with respect to protection, physiology, durability and ecology. *Journal of Coated Fabrics* 27 (2), 146–168.
- Whelan, M.E., MacTattie, L.E., Goodings, A.C., Turl, L.H., 1955. The diffusion of water vapour through laminae with particular reference to textile fabrics. *Textile Research Journal* 25 (3), 197–223.
- White, P.A., Sleeman, M.J., Smith, P.R., (Fixed Constructions, Mining), 2004. *Retroflective Fabrics and Method of Production*. EP 1402107.
- Woodruff, F.A., 1998. In: *Coating and Laminating Techniques*, Clemson University Presents – Industrial Textiles Conference. Clemson University, USA.
- Yadav, A.K., Kasturiya, N., Mathur, G.N., 2002. Breathability in polymeric coatings. *Man-Made Textiles in India* 45 (2), 56–60.
- Ying, B.A., Kwok, Y.L., Li, Y., Yeung, C.Y., Song, Q.W., 2004. Thermal regulating functional performance of PCM garments. *International Journal of Clothing Science and Technology* 16 (1–2), 84–96.

Conductive polymer coatings

6

A. Kaynak

Deakin University, Geelong, VIC, Australia

6.1 Introduction

Intrinsically conducting polymers (ICPs) such as polypyrrole (PPy), polyaniline, and polythiophene are conjugated polymers with alternating double and single bonds along their polymer chain that result in a wide range of electrical conductivity from 10^{-4} to 10^2 S/cm upon doping with counterions. Consequently, the ability of ICPs for electrical conduction originates from their electronic structure, as opposed to metal fiber or particle-filled conductive composites, which require significant concentrations of the filler to achieve a percolation threshold for conduction to happen; conductivity is not an intrinsic property of the polymer structure but the property of the material as a whole (Kaynak et al., 1996).

ICPs can be electrochemically or chemically polymerized with estimated electrical conductivity values by controlling the synthesis parameters. Furthermore, electrical properties of these polymers are sensitive to radiation and temperature. Unlike metals, their conductivity increases with temperature similar to amorphous semiconductors (Kaynak, 1998). Variable electrical conductivity, electroactive properties, and ability to produce these polymers at low cost have led to investigation of potential applications of these materials as electromagnetic (EMI) shields (Joo and Epstein, 1994), corrosion protection (Truong et al., 2000), radar absorbers (Wong et al., 1992; Makeiff and Huber, 2006), sensors (Partridge et al., 1996), and polymer actuators (Kaynak et al., 2011; Minato et al., 2007; Amiri Moghadam et al., 2015a,b,c, 2014). However, commercial applications of conducting polymers have been limited owing to the lack of processability, poor mechanical properties (Diaz and Hall, 1983), and decay of electrical properties (Kaynak, 2009; Chen et al., 1994; Kaynak et al., 2000). The limitations in mechanical property have been overcome by polymerizing on flexible substrates such as textiles, which offer flexible fiber assemblies with an infinite variety of geometry, texture, mechanical property, and chemical makeup.

6.2 Conductive polymers for textile coating

6.2.1 Methods of coating

6.2.1.1 Solution polymerization

ICP coatings can be achieved through chemical polymerization by immersing the substrate into the polymerization solution, which includes monomer, oxidant, and

an organic dopant counterion. Polymerization is initiated by oxidation of the monomer into radical cations, which in turn combine to form dimers, trimers, oligomers, and finally polymers in the bulk of the solution, which precipitate as insoluble polymer particles. While the bulk polymerization is taking place, some polymer deposition occurs directly on the substrate. Direct deposition on the substrate surface is desirable whereas bulk polymerization and subsequent precipitation are undesirable (Malinauskas, 2001). Increasing the reactant concentration and polymerization time increases the conductivity; however, prolonged polymerization times and/or high concentrations of the reactants lead to excessive bulk polymerization. These nodular bulk-polymerized polymer particles precipitate onto the fabric and find their way into the textile structure. Thorough washing becomes necessary to remove the loosely bound bulk-polymerized PPy particles. The resulting electrical resistivity of a conducting polymer-coated textile depends on the reactant concentrations, polymerization time, and temperature. These conditions were optimized by Kaynak and Beltran (2003) in a study on the effect of synthesis parameters on the electrical properties of PPy-coated polyester (PET) fabrics.

Fig. 6.1 shows an anthraquinone sulfonic acid (AQSA)-doped PPy coated on a white-colored PET fabric. Dark gray areas are PPy film whereas the small parts that appear white are regions of abrasion. The loosely bound bulk-polymerized dendritic polymer deposits can be seen on the fibers and diffused throughout the textile structure.

In general, the resistivity of the conducting polymer-coated fabrics is higher than that of freestanding polymer films. The thickness of the coating on textiles is limited to a few microns whereas the thickness of electrochemically synthesized PPy films can exceed 100 μm . The resistivity is influenced by various factors such as the concentration of the reactants, the thickness of the polymer coating, the nature of the substrate surface, the extent of penetration of the polymer into the textile structure, and the binding strength of the coating to the textile surface. The resistivity of the coating can be visually assessed as the color of an initially white fabric transforms to deeper

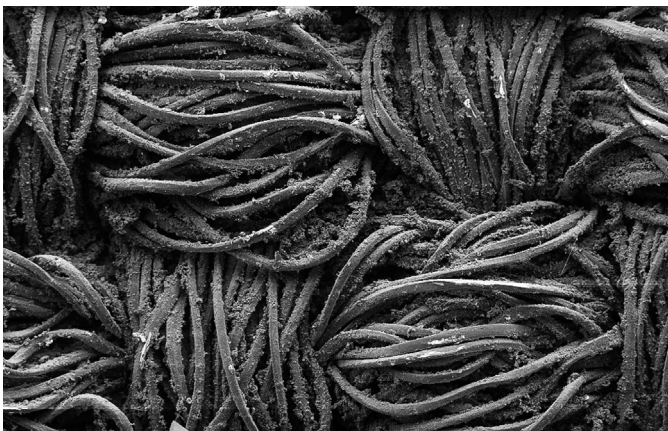


Figure 6.1 Polyester (PET) fabric coated by AQSA-doped PPy (A. Kaynak).

shades of gray as the polymerization reaction progresses, finally resulting in a deep black coating with high conductivity. Such a coating can be achieved by optimum values of reactant concentrations, polymerization times, and plasma pretreatment of the textile surfaces (Garg et al., 2007).

The conductivity of films and pellets in S/cm are measured by the four-probe method. However, the four-probe method cannot give an accurate measure of electrical property of conductive textiles because the coating is confined to the fabric surface and the bulk of the fabric is insulating. Thus the thickness required for the evaluation of volume conductivity cannot be clearly defined for a fibrous cross section, which is mostly insulating. Therefore the surface resistivity (sheet resistance, R_s) in ohms per square is measured by test method 76-1995 of the American Association of Textile Chemists and Colorists (AATCC) (Fig. 6.2). The surface resistivity R_s is given by:

$$R_s = R \left(\frac{l}{w} \right)$$

where R is the measured resistance of the fabric, l is the distance between the electrodes, and w is the width of each electrode. Not only the electrode size and separation but also the weight of the two-probe is standardized. This is important for consistent surface resistivity measurements because the pressure applied on the probe during measurement influences the resistance reading.

Fig. 6.2 shows the decrease in surface resistivity with increasing dopant concentration at certain polymerization times. Surface resistivity of the PPy-pTS-coated

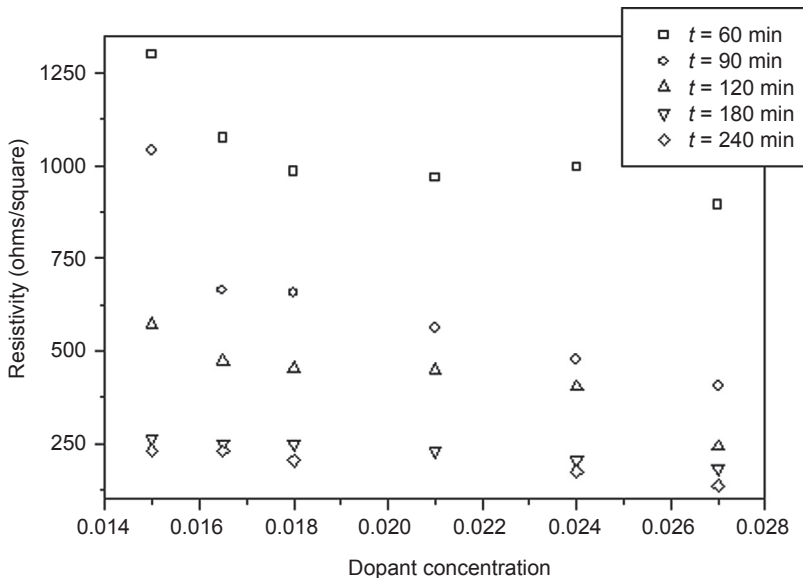


Figure 6.2 Surface resistivity change with dopant concentration (*para*-toluene-2-sulfonic acid) for different polymerization times of PPy-coated nylon-Lycra specimens (Hakansson, 2007).

nylon-Lycra samples ranged from 150 to 1300 Ω /square (Hakansson, 2007). Resistivity of samples coated for longer polymerization times was lower owing to more conducting polymer buildup both on surface and within the textile structure, resulting in better electrical contact. As the concentration of dopant was increased very slightly, from 0.015 to 0.018 mol/L, there was a large drop in surface resistivity that was more evident at shorter polymerization times. The rate of decrease in surface resistivity decreased with the increase in concentration of the dopant. The rate was further reduced at longer polymerization times because the polymerization yield decreased exponentially with time. When surface resistivity change at a wider concentration range of the dopant (*p*-toluene sulfonic acid (pTSA)), starting from no dopant, was considered, the conductive PPy-coated textile sample with no dopant had a resistance of around 1 k Ω , which rapidly dropped to less than 400 Ω with the addition of a small amount of dopant. The surface resistivity continued to drop with an increase in dopant concentration but at a much lower rate than at the initial drop. The electrical property studies on both electrochemically synthesized freestanding conducting polymer films and ICP-coated textiles showed that dopant anions have a dramatic effect on conductivity.

6.2.1.2 *Continuous vapor-phase polymerization to produce conductive yarns*

Conductive yarns can be incorporated into textile structures for intelligent textile applications. Depending on the application type, the resistance requirement may range from kilo-ohms down to metallic-level resistivity. The ICP-coated yarns in the kilo-ohm range are better suited to sensors or heating applications. Although the low conductivity of the conducting polymer-coated yarns limit their scope of applications, they are easier to incorporate into textile structures by conventional textile processes compared with metallic wires, because they can possess the same mechanical properties of the host yarn structures. Synthetic filaments can be extruded with conductive fillers incorporated into the yarn structure, but achieving a homogeneous dispersion with threshold conductivity is extremely challenging and at best limited to synthetic yarns and is likely to result in poor mechanical and electrical properties.

Attempts to coat the loosely wound yarns by conducting PPy in batch processes using solution or vapor-phase polymerization methods resulted in irregular, nonuniform coatings with poor electrical conductivity. This is because only the surface yarns exposed to the vapor or solution were coated. Neither the oxidant-monomer solution nor the monomer vapor could penetrate into the bulk of the yarn assembly. The uniform coating of yarns could be achieved only by continuously feeding the yarn to pass through oxidation and vapor-phase polymerization stages. The preoxidized yarn was coated uniformly during passage through the monomer vapor. The process could be repeated to reduce the resistance of the yarn. Using this method, both natural and synthetic yarns were coated to yield uniform coatings with low resistivity (Najar et al., 2007; Kaynak et al., 2008). The nature and structure of the yarn also had a role in the resistivity of the coated yarn. More open yarn structures and hydrophilic fibers resulted in yarns with lower resistance. In this work, the electrical property of yarns

was reported as the mass-specific resistance, R_s in $\Omega \text{ g/cm}^2$ (Morton and Hearle, 1993). For textile fiber or yarn, the mass-specific resistance, R_s was expressed in terms of fiber or yarn linear density as:

$$R_s \frac{R \cdot N \cdot T}{l \cdot 10^5}$$

where R is the resistance in ohms, l is the distance between the ends of the specimen in centimeters, N is the number of ends of yarn or fiber, and T is the linear density of yarn or fiber in tex (g/1000 m).

The mass-specific resistance of wool, cotton, and nylon66 yarns ranged from 1.5 to 6.5 $\Omega \text{ g/cm}^2$. In general wool yarns had higher mass-specific resistance compared with cotton and nylon yarns over a range of FeCl_3 concentrations (Najar et al., 2007). Cotton, which is a hydrophilic fiber, allowed polymerization to penetrate into the yarn structure owing to better take-up of the dilute solution of the oxidant. This can be visually appreciated in the scanning electron micrograph image in Fig. 6.3(a), which shows darkening in the core fibers of the cotton yarn resulting from deeper penetration of the pyrrole vapor into the core of the yarn structure. Fig. 6.3(b) shows the cross section of a PPy-coated wool yarn. The reduced penetration of the polymer into the yarn can be attributed to the increased level of twist. More open yarn structures allowed polymerization to penetrate the yarn interior, thus causing higher conductivity. These studies on the continuous vapor-phase polymerization showed that yarn hydrophilicity, surface morphology, yarn shape, twist, and linear density affected yarn conductivity through the thickness of the coating and penetration of the conducting polymer into the yarn interior.

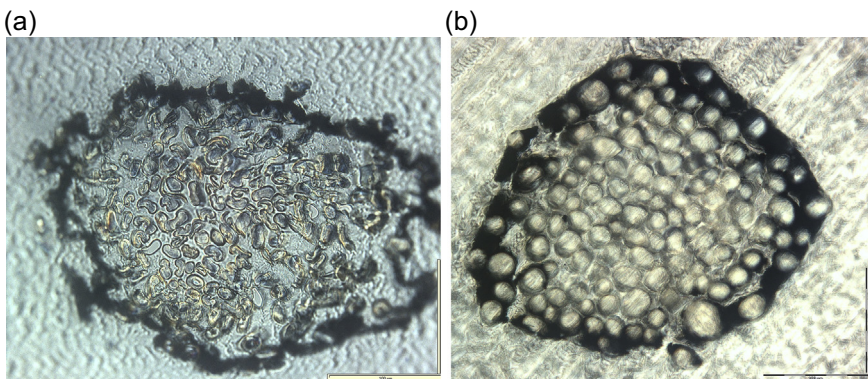


Figure 6.3 (a) Cross sections of PPy-coated cotton yarn using continuous vapor-phase method (rotor-spun yarn, yarn twist = 400 TPM; yarn count = 40 tex; magnification = 400 \times ; FeCl_3 concentration = 80 g/L; and yarn surface speed = 1 m/min). (b) Cross sections of PPy-coated wool yarn, 500 TPM, using continuous vapor-phase method (FeCl_3 concentration: 80 g/L; yarn surface speed: 1 m/min).

Unpublished images from A. Kaynak and S. Najar archives.

6.2.2 Soluble conducting poly(3-alkylpyrrole) polymers

Methods of coating textiles with conducting polymers by solution and vapor-phase polymerization and optimization of synthesis parameters have been published (Diaz and Hall, 1983; Lin et al., 2005; Kaynak, 1997). The reported methods of chemical polymerization are simple and effective, resulting in uniform coatings with low surface resistivity. However, the use of corrosive oxidants and dopants in the polymerization process has prevented the large-scale production of conducting polymer-coated textiles. The coating process also needed to be carried out under a ventilated setup. To circumvent these problems, a range of soluble conducting polymers could be produced and applied to any substrate surface by conventional printing techniques, avoiding controlled laboratory conditions and exposure of the equipment to corrosive agents. The soluble conducting polymers were derived from monomers formed by adding alkyl groups of various lengths to the three position of pyrrole. Various 3-alkylpyrroles have previously been chemically polymerized and found to be soluble in most organic solvents (Delabouglise et al., 1989; Ruehe et al., 1989a,b). A detailed investigation of the optimum synthesis conditions and application of soluble conductive polymers onto textiles was first reported by Foitzik et al. (2005, 2006a).

When alkyl chains of various lengths were attached to the pyrrole ring, the solubility of the resulting polymer increased with the length of the alkyl chain without considerably affecting the resistivity of the coating. The conductivity of the soluble conducting PPy films decreased with the increase in alkyl chain length (Fig. 6.4) and the optimum lengths of alkyl chains with regard to solubility and surface resistivity varied between 10 and 14 carbon atoms (Foitzik et al., 2005).

A similar trend was seen when the soluble poly(3-alkylpyrrole) polymers were applied to textiles; that is, considering the solubility and conductivity, optimum carbon

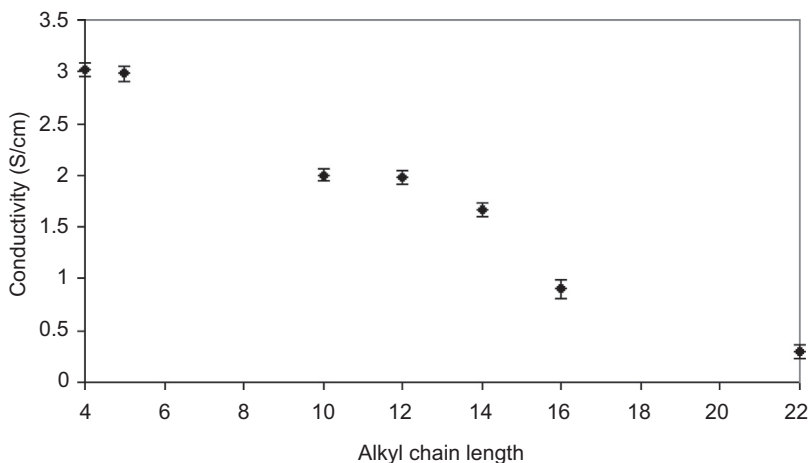


Fig. 6.4 Conductivity change with the alkyl chain length for poly(3-*n*-alkylpyrrole) pellets, measured by four-probe (Foitzik et al., 2005).

chain lengths were between $n = 10$ and $n = 14$, with no loss of flexibility and drape properties of the fabrics (Fig. 6.5) (Kaynak and Foitzik, 2010, 2011).

The increase in the resistance with the increase in the number of alkyl groups was attributed to twisting of the conjugated π system, thus causing an increase in resistivity (Diaz et al., 1995; Sato et al., 1987; Bryce et al., 1987; Bhattacharya and De, 1999).

Poly(3-alkylpyrrole) could be applied to textiles by solution and vapor-phase polymerization of 3-alkylpyrrole derivatives in the presence of an oxidant such as iron (III) chloride (FeCl_3), spraying of the monomer to a preoxidized surface, or by direct application of solutions of the polymer onto textiles. These polymer solutions could be packaged as paint and applied like spray-painting onto any surface (Foitzik et al., 2006b). However, the chemical polymerization of 3-alkylpyrroles by immersing the fabric into solution or by exposing the preoxidized fabric to monomer vapor or spray resulted in lower resistance than direct application of the soluble poly(3-alkylpyrrole) polymer solution onto a fabric. Nevertheless, the direct application method avoided the problems of using corrosive oxidizing agents and setting up a complex synthesis procedure for coating the substrate. Also, the polymer could be coated onto any substrate by conventional printing techniques.

Low resistivity in fabrics result from highly doped thicker conducting polymer coatings that penetrated well into the textile structure, thus enabling good electrical contact between fibers. The resistivity of the conductive textiles can show large fluctuations as a result of stretching as the electrical contact between fibers changes depending on the direction of the stretch.

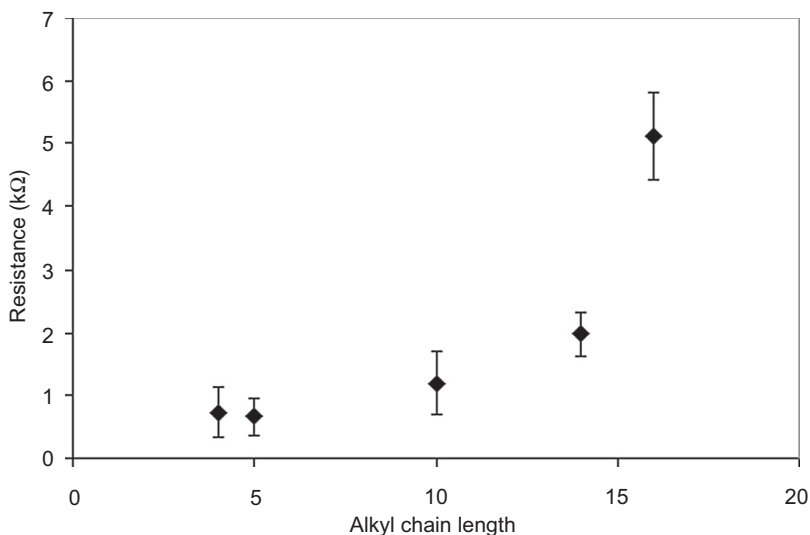


Figure 6.5 Surface resistance change with alkyl chain length of poly(3-alkylpyrrole) on wool fabric (Kaynak and Foitzik, 2011).

6.2.3 Effect of plasma treatment on conducting polymer coatings

Commercial applications of conducting polymers have been limited owing to inherent electrical aging and loss of conductivity caused by poor adhesion of the conducting polymer to the substrate surface. Plasma treatment not only changes the surface morphology of the substrate but also binds active sites to the surface, rendering the surface active for subsequent reactions (Hegemann et al., 2003). Thus, it may cause improved bonding between the substrate and any polymeric coating. Atmospheric pressure glow discharge (APGD) plasma treatment improves the physical interaction between the coating and the substrate by introducing reactive groups and free radicals. This system has a uniform, stable discharge that enables it to be used in a continuous process (d'Agostino et al., 2005). It has also been observed that plasma treatment significantly improved the dyeing ability of textile fabrics (Kan et al., 1998). In an initial plasma work, various gas mixtures were used in the APGD process to study their effect on the binding strength of PPy on PET and wool fabrics (Garg et al., 2007). PET fabrics were better than wool in terms of surface resistivity and fastness of the coating, resulting in deeper shades of coating that indicated lower surface resistivity. Conversely, as the coating was abraded from the fabric, the deep black conducting PPy coating reversed to lighter shades of gray as the white color of the fabric revealed itself, with a corresponding increase in surface resistivity. In this work, all of the relevant test methods such as contact angle, wettability, electrical resistivity, surface reflectance, abrasion, and optical and electron microscopy indicated that plasma treatment improved binding of the polymer to the fiber, and in particular, the helium–nitrogen gas combination resulted in the best abrasion resistance for both wool and PET fabrics (Garg et al., 2007).

Fig. 6.6 shows surface resistivity of PPy–PET samples after being subjected to 200 cycles in the Martindale abrasion tester. The untreated PPy–PET sample had a surface

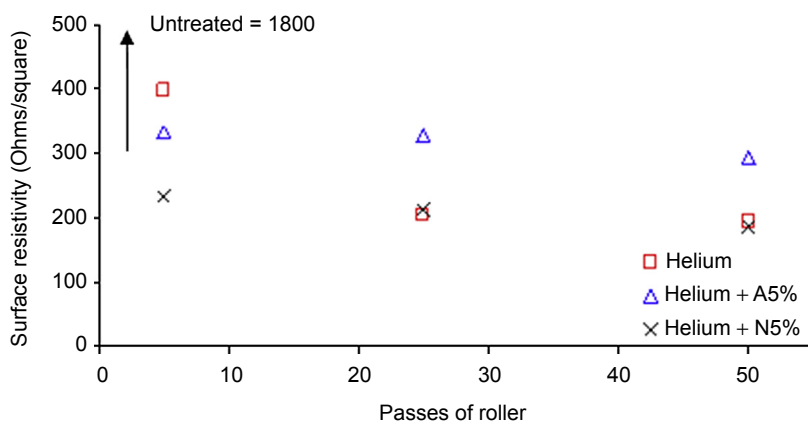


Figure 6.6 Surface resistivity of PPy-coated PET samples after 200 cycles in the Martindale abrasion tester (Garg et al., 2007).

resistivity of 1800 Ω /square after abrasion. This is considerably higher than that of abraded plasma-treated samples, which appeared to be much less affected by the abrasion, and also showed lower resistivity levels with an increase in the dosage of the plasma treatment. These initial investigations showed that APGD plasma-pretreated natural and synthetic fabrics showed significant improvement in binding strength of the PPy coating and surface resistivity. Although it was shown that plasma treatment improved the quality of the coating, the mechanism of bonding and variations in surface roughness were not considered.

In further studies to understand the nature of the conducting polymer-fabric bonding, argon, oxygen, and nitrogen plasma gases were used on PET films and fabrics before solution polymerization of pyrrole in a low-pressure plasma setup (Mehmood et al., 2012a; Kaynak et al., 2013). Results of X-ray photoelectron spectroscopy showed that plasma treatment improved bonding between the conducting polymer and fabric through fusion of COOH functional groups onto the PET surface (Mehmood et al., 2012a). Oxygen plasma in particular was found to introduce a high level of oxygen functional groups and to yield the strongest binding of the polymer to the fabric surface. Atomic force microscopy (AFM) studies showed an increase in surface roughness and contact angle measurements revealed an increase in surface wettability with an increase in the dosage of the plasma treatment. Plasma treatment also resulted in a significant reduction in the resistivity of the fabrics. To have an accurate characterization of the effect of the plasma treatment on the surface morphology, thin PET films were used as substrates. The untreated PET films had smooth surface morphology with an average surface roughness of 0.79 nm, whereas after being subjected to low-pressure oxygen plasma for 120 s the average roughness almost tripled (Mehmood et al., 2014). The progressive increase in the surface roughness of PET films with the increase in plasma exposure time can be seen in Fig. 6.7, which shows AFM images of an untreated PET film and plasma treated for 60 and 500 s, respectively (Mehmood et al., 2014).

Abrasion resistance of untreated and plasma-treated samples was compared using the Martindale abrasion test. These tests were conducted for all plasma gases and treatment times. Results from the oxygen plasma treatment are shown here for a visual appreciation of the effect of plasma on the abrasion resistance of the coating. Fig. 6.8 shows abrasive circular marks made on untreated (control) and oxygen plasma-treated PPy-pTS-coated PET fabric samples after being subjected to 5000 abrasive cycles in the Martindale abrasion tester. Fig. 6.8(a), which is a photograph of the untreated sample, clearly shows the most abrasion, followed by samples plasma treated for 15 s (Fig. 6.8(b)), 120 s (Fig. 6.8(c)), and 500 s (Fig. 6.8(d)), respectively. After being subjected to abrasion, the 500-s oxygen plasma-treated PPy-pTS-coated PET fabric sample (Fig. 6.8(d)) was still deep black, with the least abrasion of the PPy coatings. Clearly the untreated sample had the weakest PPy coating whereas the 500-s plasma-treated sample had the highest binding strength of the coatings. After the abrasion test the untreated sample lost most of its conductive coating; thus, it was not possible to obtain a resistance reading, whereas the sheet resistance of 500 s did not show a significant increase in resistance after the abrasion test.

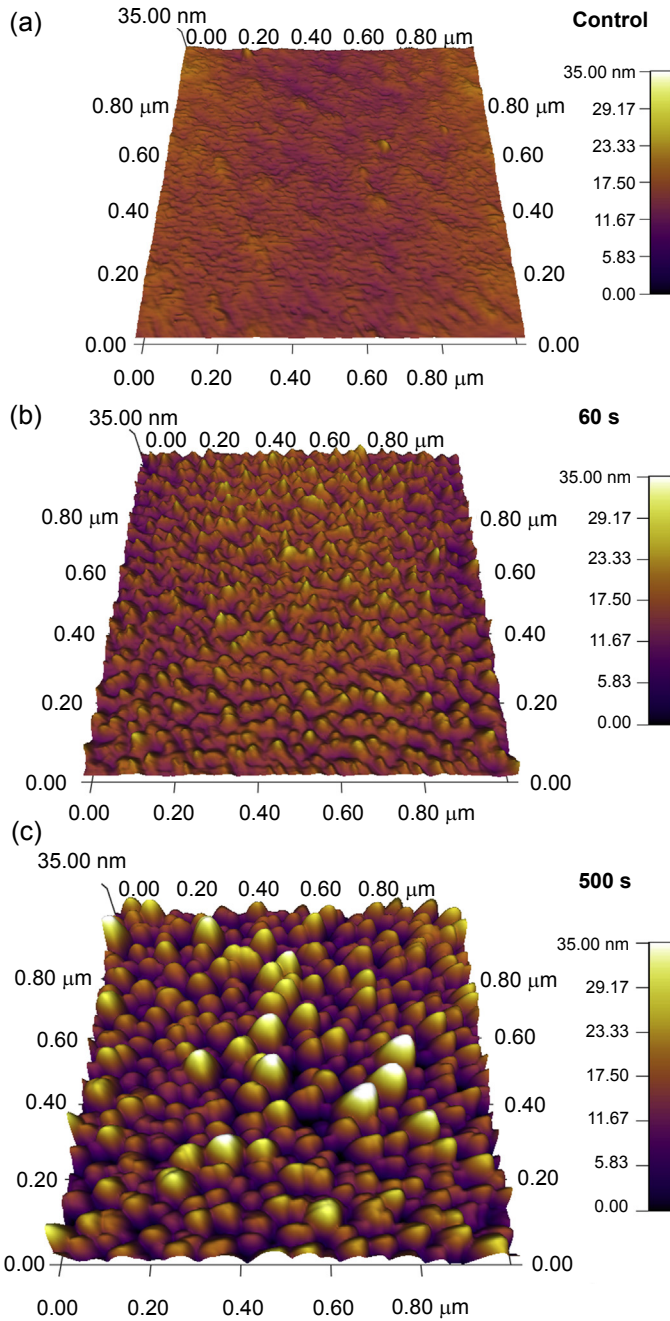


Figure 6.7 AFM scans of PET films (a) before and after plasma treatment at (b) 60 s and (c) 500 s, respectively (Mehmood et al., 2014).

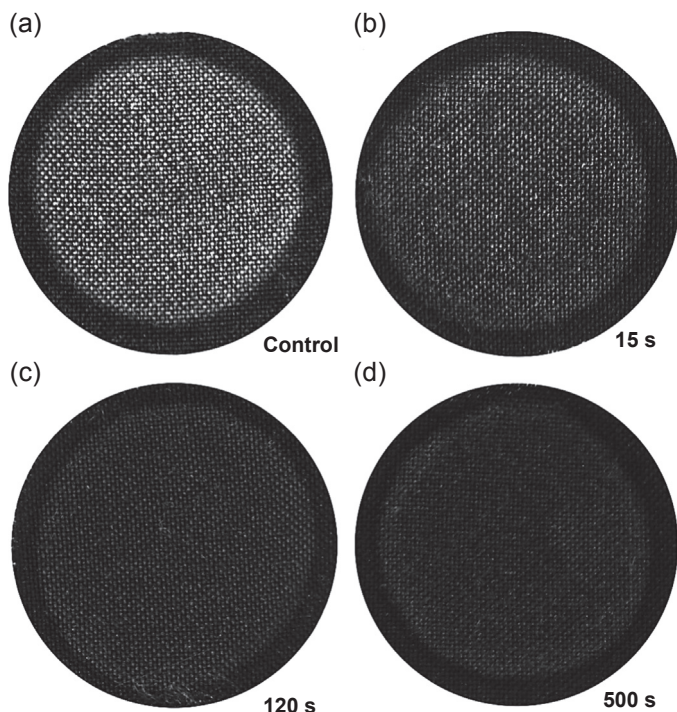


Figure 6.8 PPy–pTSA-coated PET fabric samples after being subjected to 5000 cycles of abrasion in the Martindale abrasion tester: (a) untreated; (b) oxygen plasma-treated, 15 s; (c) oxygen plasma-treated, 120 s; (d) oxygen plasma-treated, 500 s (Mehmood, 2014).

Systematic investigations into the effects of various plasma gases on the binding strength of PPy coatings on a range of natural and synthetic fabric surfaces have shown that plasma treatment significantly improved interfacial bonding. Further investigations into the effect of plasma treatment on the binding between PPy–pTS-coated polyester fabrics showed that plasma treatment resulted in the incorporation of functional groups to the PET surface and increased the surface roughness of the substrates. The combined effect of these resulted in better adhesion of the coating and manifested as improved electrical conductivity.

6.3 Properties and applications of conducting polymers

6.3.1 Microwave properties of conducting polymers

ICPs such as PPy, polyaniline, and polythiophene have potential applications as microwave-absorbing and shielding materials. Accessibility of a wide range of electrical properties results in a wide spectrum of microwave properties from highly

reflective shielding materials to highly absorptive composites of ICP-coated substrates or freestanding films.

Early research on the microwave properties of conducting polymers was carried out on electrochemically synthesized polymers by placing samples in the form of freestanding films or powders compressed into discs into coaxial transmission lines, waveguides, and TEM-t cells and evaluating their interaction with microwave radiation at a wide frequency range (Unsworth et al., 1993, 1992; Kaynak, 1996; Kaynak et al., 1994a). Microwave interactions of films and powders but also of composites of conducting polymers dispersed in rubber or epoxy matrices or chemically polymerized conductive films on insulating substrates were also studied (Olmedo et al., 1993). Results showed that conducting polymers displayed a wide range of reflection, transmission, and absorption and dielectric properties by controlling the parameters of the synthesis such as the dopant and monomer concentration, time and temperature (Unsworth et al., 1993, 1992; Kaynak, 1996; Kaynak et al., 1994a). Lightly doped samples exhibited high transmission, whereas heavily doped, higher conductivity films were reflective in the 2.45- to 10-GHz region. The ability to produce films with a wide range of electrical and microwave properties sparked interest in investigations into the microwave properties of conducting polymers. In one of the first sets of studies on the microwave properties of conducting polymers, complex dielectric constant measurements were carried out by compressing bulk-polymerized PPy particles into toroid-shaped samples and placing them inside coaxial transmission lines operating at a 2- to 10-GHz frequency range. Galvanostatically synthesized freestanding films with thicknesses of 20–100 μm with electrical conductivities from 0.01 to 50 S/cm were placed between waveguides operating at specific frequencies of 2.45 and 10 GHz in conjunction with a carefully calibrated HP Network Analyzer to measure the insertion and reflection losses (S-parameters) and the complex dielectric constant (d'Agostino et al., 2005; Kan et al., 1998; Mehmood et al., 2012a; Kaynak et al., 2013). In addition to using coaxial methods, complex dielectric constant measurements were made by TM_{012} cylindrical resonant cavity perturbation methods at specific resonant frequencies. This method required the conducting polymer sample to be compressed into a disc shape and placed in the center of the resonant cavity. Calculations of the real and imaginary parts of the complex dielectric constant were based on the perturbation of the resonant frequency peak (Unsworth et al., 1993, 1992; Kaynak, 1996; Kaynak et al., 1994a). Temperature dependence of the complex dielectric constant, ac, and dc components of the conductivity at a wide temperature range was also discussed (Unsworth et al., 1993). This study was followed by a detailed investigation of the EMI shielding effectiveness of freestanding conducting PPy films using a TEM-t cell, which is a rectangular coaxial line with rectangular inner and outer conductors that are separated by a gap where the sample is placed (Kaynak et al., 1994b). Electrochemically prepared highly doped conducting PPy films with dc conductivity values of around 50 S/cm exhibited high insertion losses exceeding 33 dB, indicating high reflectivity of the incident microwave radiation. All of these experiments were modeled using HP High-Frequency Structure Simulator software before physical measurements and results were found to be in good agreement with those predicted by the models. Highly doped electrochemically fabricated films had high

reflection-dominated interaction with microwaves. There was also a significant contribution from absorption. The shielding effectiveness increased with the increase in thickness of the film, owing to a thicker conductive barrier presented to the impinging radiation. The loss of reflection also increased as the conductivity of the film increased. These results demonstrated that electrochemically synthesized PPy films displayed a wide range of controllable microwave properties. However, the brittleness and the fact that PPy could only be produced as films or powders considerably limited their applications. This disadvantage could be bypassed by chemical polymerization on textiles, because textiles offered an unlimited variety of flexible substrate structures with excellent mechanical properties (Gregory et al., 1989; Kuhn et al., 1995). As a result, conducting polymers were chemically deposited on various textile substrates by solution and vapor-phase polymerization methods, and the effects of synthesis parameters such as the choice and concentration of the monomer, oxidant, dopant, polymerization time, and temperature on the surface resistivity of the conductive textiles were studied in detail (Kaynak and Beltran, 2003).

From conducting polymer films and powders, microwave work shifted to conductive textiles, and a series of detailed studies were carried out on the reflection, transmission, absorption behavior, effectiveness of EMI shielding, and dielectric properties of conducting polymer-coated textiles in the 1- to 18-GHz regime using a free-space transmission measurement technique for large sheet materials, which eliminated diffraction errors from the measurements (Hakansson et al., 2006, 2007a,b; Kaynak et al., 2009).

As in films, microwave results were influenced by the choice and concentration of the monomer, oxidant, and the dopant counterion. Moreover, the polymerization time, the temperature, and the structure of the fabric also affected the microwave interaction. The influence of polymerization time and dopant concentration on microwave transmission, reflection, and absorption of PPy-coated nylon-Lycra fabrics are shown in Figs. 6.7 and 6.8. Both reflection and absorption increased whereas transmission decreased sharply with the increase in polymerization time and/or dopant concentration. Surface resistivity decreased with the increase in reactant concentrations, reaching a plateau beyond which there were no further changes in microwave transmission, reflection, and absorption. In the case of conducting polymer-coated fabrics, the skin depth of the coating produced was not small enough to manifest as reflective, and therefore we see significant levels of transmission and absorption. Conversely, early experiments with electrochemically synthesized highly doped PPy films were more reflective (Unsworth et al., 1993, 1992; Kaynak, 1996; Kaynak et al., 1994a) than conductive textiles. This is because of the higher conductivity and larger thickness of the electrochemically synthesized films compared with those of conductive textiles coated with a much thinner layer of conducting polymer. Nevertheless, increasing the concentrations of monomer, dopant, and oxidant increased the microwave reflectivity of conductive textiles. Moreover, using thick, fibrous, felt-like substrates in which the polymerization solution could penetrate into the thick fabric, thus forming a thicker barrier to the microwave radiation, would be expected to result in higher reflection and absorption response. The uncoated fabric was totally transparent to microwaves; however, as the polymerization time increased, reflection increased whereas

transmission decreased, reaching a plateau around 180 min (Fig. 6.9) (Hakansson, 2007). Such prolonged reaction times caused excessive bulk-polymerized deposits on the fabrics and fractured PPy coatings. Absorption increased more rapidly than reflection with an increase in the polymerization time, reaching a plateau of 50%. The absorption levels were higher at lower frequencies of the 2- to 18-GHz frequency range.

Fig. 6.10 shows the effect of the dopant concentration on the microwave response of fabrics at a fixed polymerization time. When the polymerization resulted only from the oxidant ferric chloride but excluded the dopant pTSA, the result was high transmission and low reflection because the conductivity of the coating was low. As the dopant pTSA was added and its concentration increased, transmission rapidly dropped while the reflection and absorption increased.

There is also a frequency-dependent change in both reflection and absorption. As seen in the scans in the 2- to 18-GHz range, reflection increased steadily for all samples with increasing frequency; the longest polymerization time was the most reflective throughout the frequency range (Fig. 6.11) (Hakansson, 2007). Conversely, we see a steady decrease in transmission for all samples with increasing frequency; the shortest polymerization time was the most transmitting throughout the frequency range (Fig. 6.12) (Hakansson, 2007). For good conductors, skin depth is given by:

$$\delta = \sqrt{\frac{2}{\pi f \mu_0 \sigma}}$$

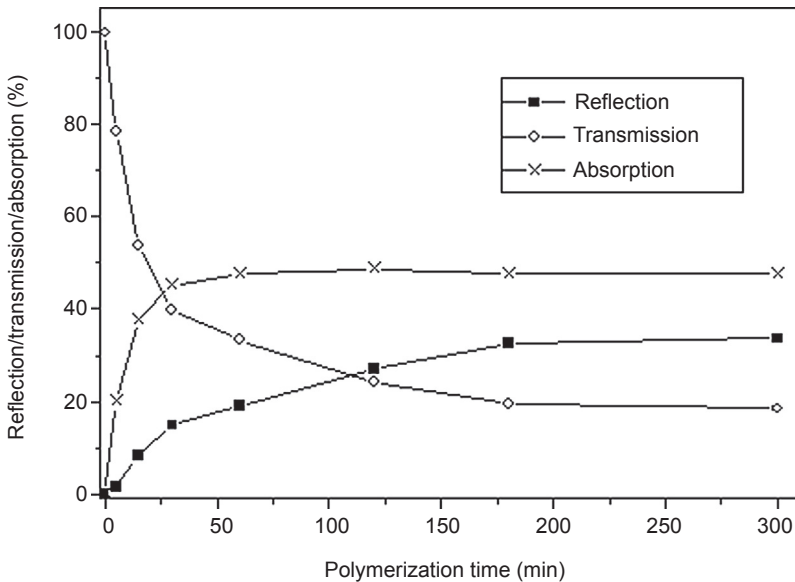


Figure 6.9 Variations in reflection, transmission, and absorption of PPy-pTSA-coated nylon-Lycra with polymerization time in the frequency range of 1–18 GHz (Hakansson, 2007).

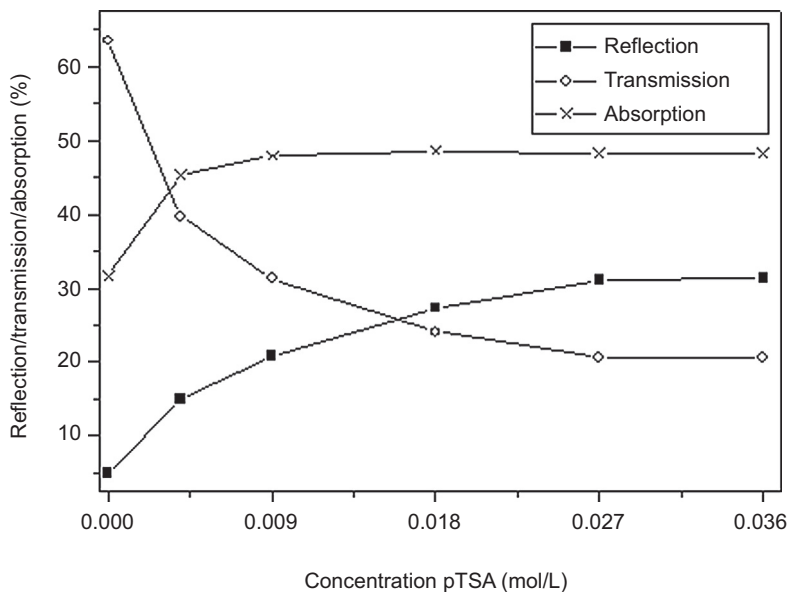


Figure 6.10 Variations in reflection, transmission, and absorption of PPy-pTSA-coated nylon-Lycra with dopant concentration (Kaynak and Hakansson, 2009).

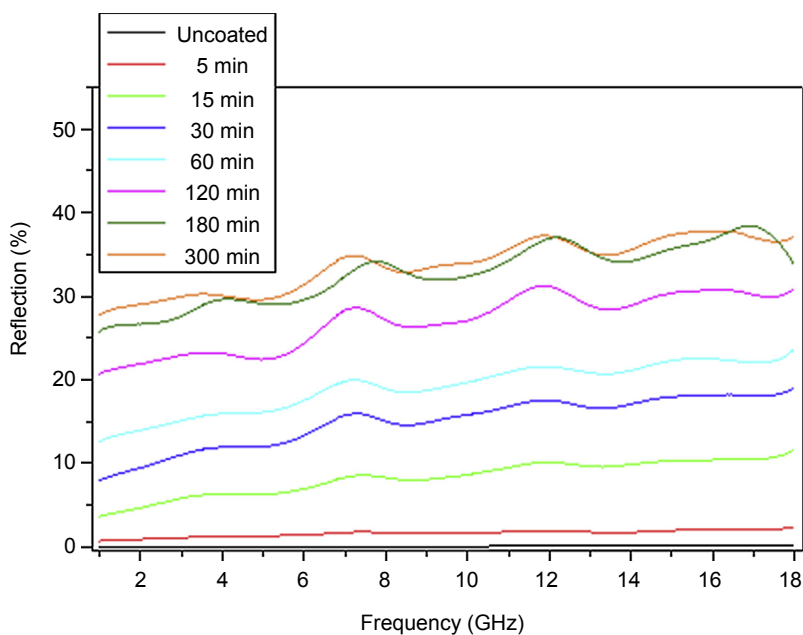


Figure 6.11 Percentage reflection for nylon-Lycra fabrics coated with PPy at different polymerization times including an uncoated sample. Dopant: 0.018 mol/L pTSA. The sample with the longest polymerization time is the most reflective throughout the frequency range. Conversely the sample with the shortest polymerization time is the least reflective throughout the frequency range (Hakansson, 2007).

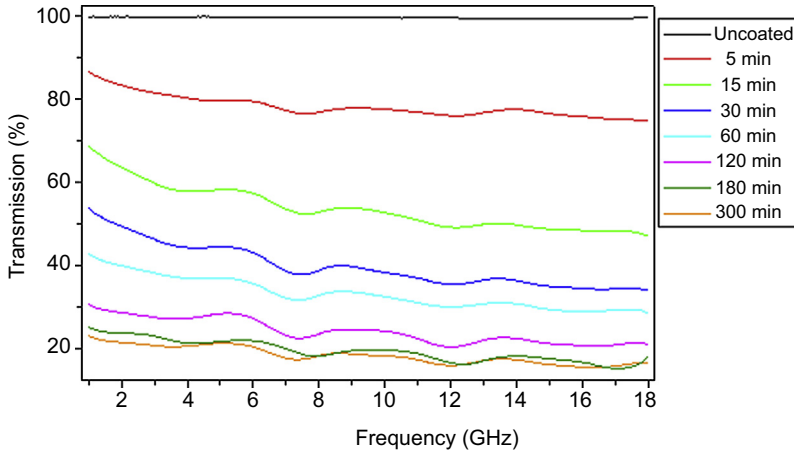


Figure 6.12 Percentage transmission for nylon-Lycra fabrics coated with PPy at different polymerization times including an uncoated sample. Dopant: 0.018 mol/L pTSA. The uncoated sample is totally transparent to radiation and the sample with the lowest polymerization time is the most highly transmitting among the coated samples throughout the frequency range. Conversely, the sample with the longest polymerization time has the lowest transmission throughout the frequency range (Hakansson, 2007).

which shows that the depth of penetration of EMI radiation to a conductor is inversely proportional to the frequency of radiation and the conductivity of the sample.

These studies show that conductive textiles are not highly effective as EMI shielding materials owing to their medium-level conductivity and therefore large skin depth. Combined with the fact that coatings are naturally thin, they cannot act as effective reflective barriers to EMI radiation. However, because they are highly absorptive in the microwave region, microwave-absorbing composite materials can be designed in conjunction with conductive textiles.

6.3.2 Heated fabrics

Conducting polymer-coated textiles offer the possibility of heating without placing wiring across the fabric. The moderate to high resistance values of conductive fabrics are ideally suited for heating applications. Heat-generating in fabrics with conducting PPy doped with three different counterions were investigated (Kaynak and Hakansson, 2005; Hakansson et al., 2004). Among the dopants used, AQSA showed the best temperature profile and power density per unit area, followed by naphthalene sulfonic acid (NSA), pTSA, and sodium perchlorate (NaClO_4), respectively (Hakansson et al., 2004). Polymerizations were carried out for 3 h, which resulted in PPy-coated fabrics with surface resistivity ranging between 700 and 1500 Ω /square, depending on the polymerization time, type of the dopant, and concentrations used. The PPy coatings were deep black, demonstrating a coating with low surface resistivity. Biaxial stretching of the fabric during polymerization resulted in further lowering of resistivity owing

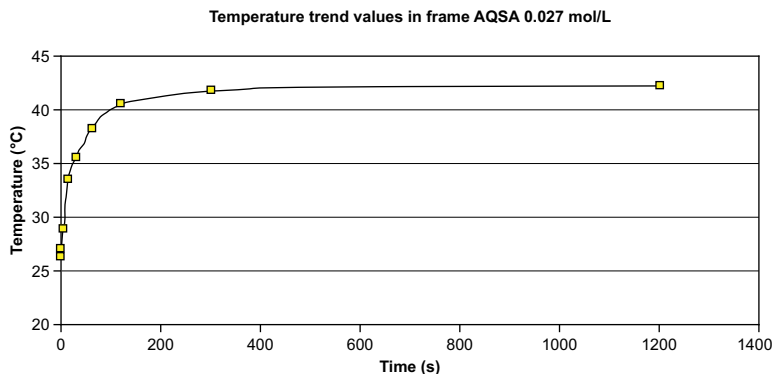


Figure 6.13 Change in temperature with time of heated PPy–AQSA-coated PET fabrics (Kaynak and Hakansson, 2005).

to better penetration of the conducting polymer, thus enabling improved electrical contact between fibers in their relaxed state. However, the long polymerization times resulted in a significant amount of bulk polymerization, which deposited onto the fabric as black dendritic polymer particles. These loosely bound polymer particles had to be removed from the fabric by thorough washing. A dc power supply was used to generate voltage across the fabric and produce heating. The temperature change was recorded as a function of time (Fig. 6.13), which showed an initial sharp rise followed by a plateau (Hakansson et al., 2006). When a constant potential of 24 V was used, current decreased whereas the surface resistance increased with time. This was attributed to prolonged heating of the fabric, which led to degradation of the polymer through damage inflicted onto the conjugated structure of the polymer backbone. A thermal camera was used to observe the temperature change and the pattern of heating. Fig. 6.14 shows a sequence of thermal images from 1 to 30 s (Kaynak and Hakansson, 2005; Hakansson et al., 2004).

Some current challenges in the heating applications of conductive textiles are the choice of battery to be used and integration of the battery to the textile structure. Although traditional batteries are more effective, better integration with the textile may require exploration of substitute power sources such as solar power or flexible batteries that may be incorporated into the fabric without causing discomfort to the user. Incorporation of an outer protective layer would reduce heat loss to the surroundings, thus reducing input power requirements. However, the main challenge in using conducting polymer-coated textiles in heat generation is to reduce the degradation of electrical properties, especially as the rate of degradation accelerates at elevated temperatures.

6.3.3 Conducting polymer actuators

Applications such as EMI shielding, microwave absorption, heated fabrics, antistatic clothing, and soluble conducting polymers have used the variable electrical properties

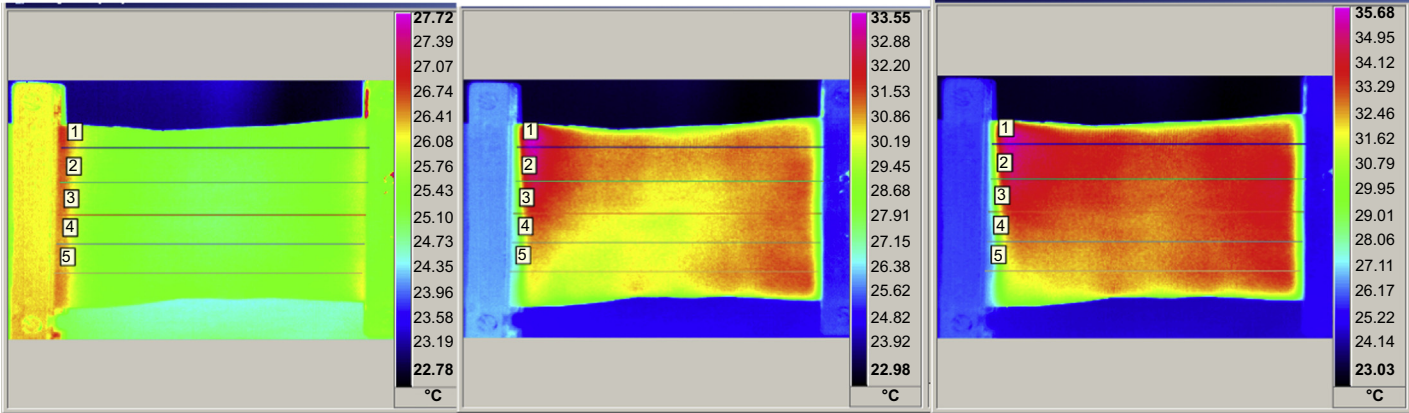


Figure 6.14 Sequential thermal images of PPy-AQSA-coated PET fabrics, starting from 1 to 30 s after power is turned on (Kaynak and Hakansson, 2005).

of conducting polymers, whereas the property of electroactivity of conducting polymers has been exploited in the development of conducting polymer actuators. Reversibility of the oxidation and reduction process enabled design of conducting polymer actuators that could exhibit bending motion with significant force. Conducting polymer actuators convert electrical impulse input into physical movement. Layered structures of doped conducting polymers can be fabricated through electrochemical processes that enable transport of dopant anions through a porous boundary upon application of a potential difference across the layers. The mass transport across the porous membrane results in the bending motion of the trilayer actuators. Fig. 6.15 (Amiri Moghadam et al., 2015a) depicts the bending motion of the actuator and identifies the layers within a trilayer conducting PPy actuator. A lightly gold-coated porous polyvinylidene fluoride (PVDF) forms the core of the actuator. The outer layers are electrochemically deposited PPy films. The volumetric strain of the actuator results from a redox reaction that causes the PPy layer on the anode side to expand upon oxidation and contract on the cathode side. The volume difference is responsible for the bending motion (Amiri Moghadam et al., 2015a; 2014; Kaynak et al., 2011). Fig. 6.16 is a stacked image of a conducting PPy actuator during motion, showing the actuator at horizontal and negative bending moment positions.

There have been various studies on the fabrication, characterization, and mathematical modeling of polymer actuators (Amiri Moghadam et al., 2015a,b, 2014, 2011; Kaynak et al., 2010). A novel application of conducting polymer actuators was published (Amiri Moghadam et al., 2015c) that presented a novel soft parallel robot for biomicromanipulation devices. The actuator assembly consisted of two active polymer actuator-based links connected to two rigid links through flexible joints. The assembly was mathematically modeled to link the input voltage to the end position of the of the robot arm, which had two degrees of freedom to enable planar micromanipulation. These flexible, elastic, slow-moving, controllable devices have considerable potential

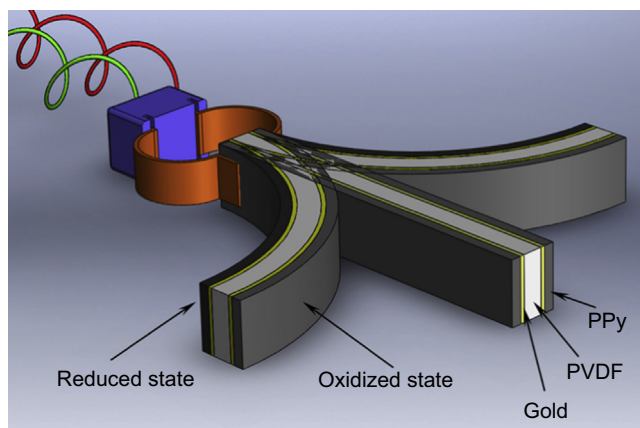


Figure 6.15 Diagram of the trilayer PPy actuator showing the layered structure and the bending motion (Amiri Moghadam et al., 2015a).

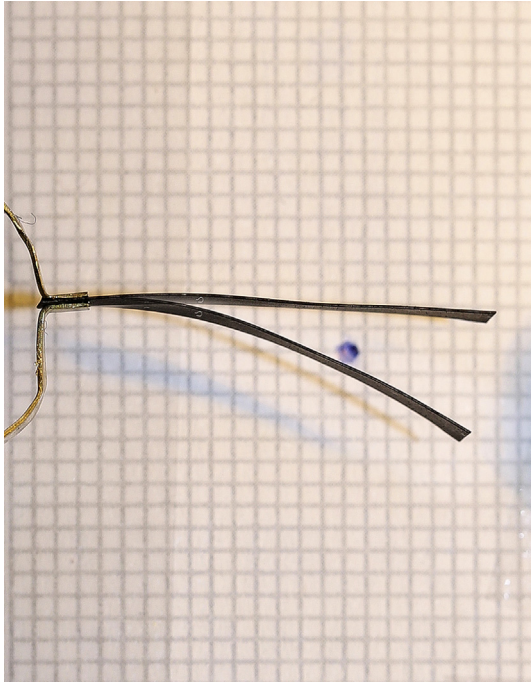


Figure 6.16 Stacked image of the PC/PF6 actuator in motion, showing the bending deformation during motion.

in biological applications and require interdisciplinary research. There have been significant developments in the design and mechanical modeling of conducting polymer actuators; however, the major challenge in actuator research is the stability of the actuating properties.

6.4 Conclusion

6.4.1 *Electrical degradation of conductive textiles and future trends*

Degradation is a major drawback of conducting polymers that needs to be characterized before considering these materials for potential applications. Electrical aging should be taken into account and incorporated into the projected use of the material. The aging of electrical conductivity of pTSA-doped conducting PPy films were studied at room temperature and elevated temperatures in an effort to understand the mechanism of aging and predict the long-term performance of these organic conductive films (Kaynak, 2009). Aging experiments showed that the overall aging trend of PPy films deviated from first-order kinetics at elevated temperatures. From kinetic

studies, electrical decay at room temperature over a period of 1 year was estimated to be $\sigma = 0.013\sigma_0$, where σ and σ_0 are conductivities at time t and at the beginning of aging, respectively. This estimate was found to agree approximately with the aging data taken from a lightly pTSA (0.005 M)-doped PPy (0.05 M) that started with 3×10^{-2} S/cm and reduced about one order of magnitude in 1 year. There have been reports on the effect of the type of dopant on the electrical degradation (Briet et al., 1997) but it was found that not only the type of dopant but also its concentration influenced the rate of degradation. Highly doped PPy–pTSA films were more stable than lightly doped films. The pTSA dopant appeared to have a preserving effect on the electrical properties of PPy films (Kaynak and Hakansson, 2005).

Study of Fourier transform infrared spectra of aged PPy films has shown an increase in intensity of an α,β -unsaturated conjugated carbonyl peak that may be linked to a loss of conductivity (Kaynak et al., 2000) but cannot be the only factor because the aging features appeared to obey a multiorder kinetics behavior, because the rate of electrical decay was influenced by several factors such as temperature, the type and concentration of the dopant, and the aging time, all of which signify a complex mechanism of degradation of conductivity.

In the case of textiles, PPy-coated PET fabrics gained less than one order of magnitude when aged for 18 months at room temperature. Again, the stabilizing effect of the pTSA against degradation was validated. As in the case of electrochemically synthesized freestanding PPy films, PPy-coated PET fabrics without the dopant pTSA increased in resistance approximately two orders of magnitude, reaching a resistance of 40 k Ω , whereas pTSA-doped, PPy-coated fabrics reached a resistance of less than 2 k Ω at the same temperature within the same time frame (Mehmood et al., 2012b). However, the aging behavior of conducting polymer systems may vary and each should be investigated separately.

When a set of PPy–pTSA-coated PET samples with initial resistance values less than 100 Ω were kept at different elevated temperatures for 2 h and normalized sheet resistance was displayed as a function of time, in all samples there was an initial decrease in resistance followed by an increase with time (Fig. 6.17) (Mehmood, 2014). The initial drop in resistance is attributed to a characteristic of conducting polymers, which is an increase of conductivity with temperature similar to that seen in amorphous semiconductors. This is due to the thermal excitation of the charge carriers to the conduction band. However, in a thermal aging experiment this behavior is not persistent; the degradation manifests as an increase in resistance for the rest of the experiment. The 120°C curve shows a higher rate of aging than fabrics aged at lower temperatures, because the aging has been observed to accelerate rapidly beyond 100°C (Kaynak, 2009a). Long-term aging at room temperature for 18 months resulted in a 2.5 times increase in surface resistivity for a highly pTSA-doped PET fabric, showing better stability than undoped or lightly doped PPy coatings. This is in agreement with previous studies conducted on electrochemically synthesized freestanding PPy films with a wide range of pTSA concentrations, with the highly pTSA doped films showing more resistance to degradation (Kaynak, 2009a).

Because they are electroactive and have a wide range of electrical properties, conducting polymers have potential in many applications such as functional and

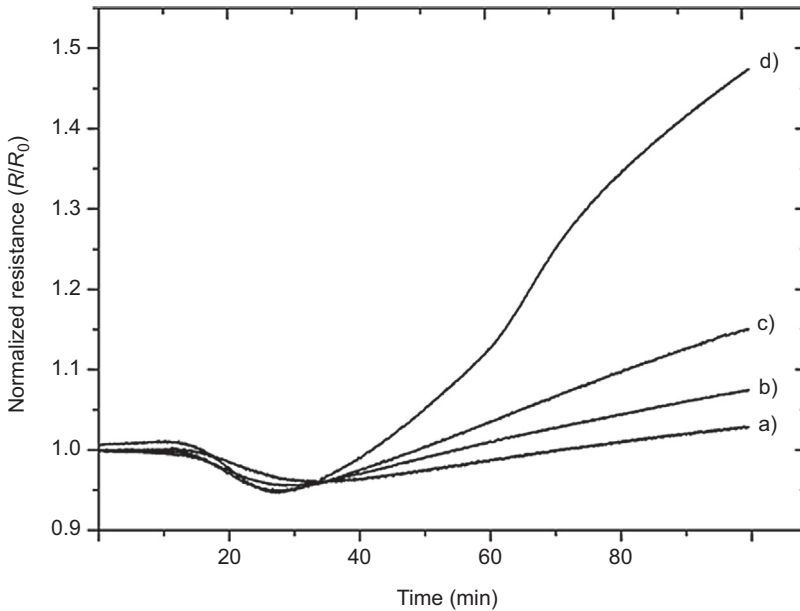


Fig. 6.17 Normalized resistance (R/R_0) versus time (first 100 min) of pTSA-doped PPy-coated fabric aged at (a) 60, (b) 80, (c) 100, and (d) 120°C (Mehmood et al., 2012b).

intelligent textiles, electroactive polymer actuators, microwave absorbers and textile-based antennas, heated fabrics, electrostatic materials, and chemical and thermal sensors. However, there are challenges in the area of electrical stability and mechanical properties that need to be addressed in a multidisciplinary approach.

References

- Amiri Moghadam, Amir A., Moavenian, M., Torabi, K., Tahani, M., 2011. *Journal of Intelligent Material Systems and Structures* 24 (4), 484–498.
- Amiri Moghadam, Amir A., Hong, W., Kouzani, A., Kaynak, A., Zamani, R., Montazami, R., 2014. *Sensors and Actuators A: Physical* 217, 168–182.
- Amiri Moghadam, Amir A., Kouzani, A., Zemani, R., Magniez, K., Kaynak, A., 2015. *Smart Structures and Systems* 15 (6).
- Amiri Moghadam, Amir A., Alizaded, V., Tahani, M., Kouzani, A., Kaynak, A., 2015. *Polymers for Advanced Technologies* 26 (4), 385–391.
- Amiri Moghadam, Amir A., Kouzani, A., Torabi, K., Kaynak, A., Shahinpoor, M., 2015. *Smart Materials and Structures* 24 (3), 035017.
- Bryce, M.R., Chissel, A., Kathirgamanathan, P., Parker, D., Smith, N.R.M., 1987. *Journal of the Chemical Society, Chemical Communications* 6, 466–467.
- Bhattacharya, A., De, A., 1999. *Journal of Macromolecular Science, Reviews in Macromolecular Chemistry and Physics* C39 (1), 17–56.
- Brie, M., Turcu, R., Mihut, A., 1997. *Materials Chemistry and Physics* 49, 174.

- Chen, X.B., Devaux, J., Issi, J.P., Billaud, D., 1994. *European Polymer Journal* 30, 809.
- Diaz, A.F., Hall, B., 1983. *IBM Journal of Research and Development* 27 (4), 342–347.
- Delabouglise, D., Roncali, J., Lemaire, M., Garnier, F., 1989. *Journal of the Chemical Society, Chemical Communications* 8, 475–477.
- Diaz, A.F., Nguyen, M.T., Leclerc, M., 1995. *Physical Electrochemistry* 555–583.
- d'Agostino, R., Favia, P., Oehr, C., Wertheimer, M.R., 2005. *Plasma Processes and Polymers* 2, 7.
- Foitzik, R.C., Kaynak, A., Beckmann, J., Pfeffer, F.M., 2005. *Synthetic Metals* 155, 185–190.
- Foitzik, R.C., Kaynak, A., Pfeffer, F.M., Beckman, J., 2006. *Synthetic Metals* 156, 1333–1340.
- Foitzik, R.C., Kaynak, A., Pfeffer, F.M., 2006. *Synthetic Metals* 156, 637–642.
- Garg, S., Hurren, C., Kaynak, A., 2007. *Synthetic Metals* 157, 41–47.
- Gregory, R.V., Kimbrell, W.C., Kuhn, H.H., 1989. *Synthetic Metals* 28, C823.
- Eva Hakansson, 2007. (Ph.D. thesis), Characteristics of Conducting Textiles in the Microwave Frequency Range. Deakin University.
- Hegemann, D., Brunner, H., Oehr, C., 2003. *Nuclear Instruments and Methods in Physics Research Section B: Beam Interactions with Materials and Atoms* 208, 281–286.
- Hakansson, E., Amiet, A., Kaynak, A., 2006. *Synthetic Metals* 156, 917–925.
- Hakansson, E., Amiet, A., Kaynak, A., 2007. *Synthetic Metals* 157, 1054–1063.
- Hakansson, E., Amiet, A., Nahavandi, S., Kaynak, A., 2007. *European Polymer Journal* 43, 205–213.
- Hakansson, E., Kaynak, A., Lin, T., Nahavandi, S., Jones, T., Hu, E., 2004. *Synthetic Metals* 144, 21–28.
- Joo, J., Epstein, A.J., 1994. *Applied Physics Letters* 65, 2278.
- Kaynak, A., Polat, A., Yilmazer, U., 1996. *Materials Research Bulletin* 31 (10), 1195–1206.
- Kaynak, A., 1998. *Materials Research Bulletin* 33 (1), 81.
- Kaynak, A., Yang, C., Lim, Y.C., Kouzani, A., 2011. *Materials Chemistry and Physics* 125, 113–117.
- Kaynak, A., 2009a. *Fibers Polymers* 10 (5), 590–593.
- Kaynak, A., Rintoul, L., George, G.A., 2000. *Materials Research Bulletin* 35 (6), 813–824.
- Kaynak, A., Beltran, R., 2003. *Polymer International* 52, 1021–1026.
- Kaynak, A., Najar, S.S., Foitzik, R.C., 2008. *Synthetic Metals* 158, 1–5.
- Kaynak, A., 1997. *Materials Research Bulletin* 32 (3), 271–285.
- Kaynak, A., Foitzik, R.C., 2010. *RJTA* 14 (2).
- Kaynak, A., Foitzik, R.C., 2011. *RJTA* 15 (2).
- Kan, C.W., Chan, K., Yuen, C.W.M., Miao, M.H., 1998. *Journal of Materials Processing Technology* 82, 122.
- Kaynak, A., Mehmood, T., Dai, Xiujuan J., Magniez, K., Kouzani, A., 2013. *Materials* 6, 3482–3493.
- Kaynak, A., 1996. *Materials Research Bulletin* 31 (7), 845–860.
- Kaynak, A., Unsworth, J., Clout, R., Mohan, A.S., Beard, G.E., 1994. *Journal of Applied Polymer Science* 54 (3), 269–278.
- Kaynak, A., Mohan, A.S., Unsworth, J., Clout, R., 1994. *Journal of Materials Science Letters* 13 (15), 1121–1123.
- Kuhn, H.H., Child, A.D., Kimbrell, W.C., 1995. *Synthetic Metals* 71, 2139.
- Kaynak, A., Hakansson, E., Amiet, A., 2009. *Synthetic Metals* 159, 1373–1380.
- Kaynak, A., Hakansson, E., 2009. *International Journal of Clothing Science and Technology* 21 (2/3), 117–126.
- Kaynak, A., Hakansson, E., 2005. *Advances in Polymer Technology* 24 (3), 194–207.
- Kaynak, A., Yang, C., Kouzani, A., 2010. *Materials Forum* 654, 2467–2470.
- Lin, T., Wang, L., Wang, X., Kaynak, A., 2005. *Thin Solid Films* 479 (1–2), 77–82.

- Makeiff, D.A., Huber, T., 2006. *Synthetic Metals* 156 (7–8), 497.
- Minato, R., Alici, G., McGovern, S., Spinks, G., 2007. In: *Proc. SPIE 6524, Electroactive Polymer Actuators and Devices (EAPAD)*, p. 65241J.
- Malinauskas, A., 2001. *Polymer* 42 (9), 3957–3972.
- Morton, W.E., Hearle, J.W.S., 1993. *Physical Properties of Textile Fibers*, third ed. Textile Institute, London.
- Mehmood, T., Dai, Xiujuan J., Kaynak, A., Kouzani, A., 2012. *Plasma Processes and Polymers* 9, 1006–1014.
- Mehmood, T., Kaynak, A., Dai, Xiujuan J., Kouzani, A., Magniez, K., de Celis, D.R., Hurren, C.J., du Plessis, J., 2014. *Materials Chemistry and Physics* 143 (2), 668–675.
- Mehmood, T., 2014. (Ph.D. thesis), *Improvement of Polypyrrole Coating Adhesion by Radio Frequency Plasma*. Deakin University.
- Mehmood, T., Kaynak, A., Mahmood, A., Kouzani, A., 2012. *Fibers Polymers* 13 (2), 153–158.
- Najar, S.S., Kaynak, A., Foitzik, R.C., 2007. *Synthetic Metals* 157, 1–4.
- Olmedo, L., Hourquebie, P., Jousse, F., 1993. *Advanced Materials* 5 (5), 373–377.
- Partridge, A.C., Harris, P., Andrews, M.K., 1996. *Analyst* 121, 1349.
- Ruehe, J., Ezquerro, T.A., Wegner, G., 1989. New conducting polymers from 3-alkylpyrroles. *Synthetic Metals* 28 (1–2), C177–C181.
- Ruehe, J., Ezquerro, T., Wegner, G., 1989. *Makromolekulare Chemie, Rapid Communications* 10 (2), 103–108.
- Sato, M., Tanaka, S., Kaeriyama, K., 1987. *Synthetic Metals* 18 (1–3), 229–232.
- Truong, V.T., Lai, P.K., Moore, B.T., Muscat, R.F., Russo, M.S., 2000. *Synthetic Metals* 110, 7–15.
- Unsworth, J., Kaynak, A., Lunn, B.A., Beard, G.E., 1993. *Journal of Materials Science* 28, 3307–3312.
- Unsworth, J., Lunn, B.A., Innis, P.C., Jin, Z., Kaynak, A., Booth, N.G., 1992. *Journal of Intelligent Material Systems and Structures* 3 (3), 380–395.
- Wong, P.T.C., Chambers, B., Anderson, A.P., Wright, P.V., 1992. *Electronics Letters* 28 (17).

Natural photonic materials for textile coatings

7

H. Fan¹, N. Lin¹, X.Y. Liu^{1,2}

¹Research Institute for Biomimetics and Soft Matter, Fujian Provincial Key Lab for Soft Functional Materials Research, Xiamen University, Xiamen, China; ²Department of Physics, FOS, National University of Singapore, Singapore

7.1 Introduction

7.1.1 Typical optical process of photonic materials

Multifunctional structural color reflection is one of the most crucial innovations in more than 400 million years of biological evolution. In this chapter, we first introduce the typical optical process of some natural photonic materials exploiting photonic structures to produce shining structural coloration, ie, the colorful wings of butterflies, the blazing feathers of many birds (ie, peacocks), and the elytra of many insects (Kinoshita et al., 2008).

Different from pigment coloration, structural colors originate from the complex interaction between light and sophisticated nanostructures generated in the natural world. Those unique micro- and nanostructures in creatures are called photonic crystals, with highly ordered materials containing regularly repeating regions of high and low dielectric constants with the period on the scale of visible light wavelengths about 380–750 nm (Anderson and Richards, 1942).

In principle, their mechanism results from a photonic band gap (PBG), a band of frequencies that do not propagate light in the photonic crystals (Toader and John, 2001). Generally structural colors are mainly based on several elementary optical processes including thin-layer interference, diffraction grating, light scattering, and photonic crystals (Liu, 2012). However, in nature these processes mixed together to produce complex optical phenomena.

In general structural colors can be divided into two classes: iridescent and noniridescent. Iridescent color is normally generated by reflection or scattering of light from an ordered array of scatters (Berthier, 2007) whereas noniridescent color from the feathers of many birds is produced by the quasioordered array of air vacuoles in the medullary keratin (Noh et al., 2010). The investigation of the color-mixing mechanisms of these biologically photonic nanostructures may offer a convenient way to fabricate optical devices based on biomimicry (Kinoshita et al., 2008).

7.1.2 Fabrication of photonic crystals based on colloidal crystals

Colloidal template technique is a facile, flexible experimental method used to fabricate micro/nanostructured arrays with the advantage of simple operation and low cost. Using colloidal nanospheres as templates or masks, different periodic micro/nanostructured arrays including nanoparticle arrays and air-filled cavities, a nanonetwork can easily be fabricated by chemical and physical processes (Li et al., 2013). On the other hand, when monodisperse colloidal crystals (ie, polystyrene (PS), SiO₂) are adopted as the opal structure model, the color of the inverse opal photonic crystals fabricated would be more abundant and satiating because of the ultrafine crystal structure and high refractive index difference.

The direct use and reengineering of biological materials into technological material platforms is already under way in many laboratories and offers a path forward for a green reinterpretation of materials (Tao et al., 2012). We will focus specifically on opportunities offered by silk proteins as a promising biopolymer platform for high-technology applications. What particularly distinguishes silk fibroin from other biopolymers for high-technology applications are the robust mechanical properties, the facile control of material properties through the control of water content during processing, the programmable and controllable degradation lifetime, and the unique optical and electronic properties of the material (Tao et al., 2012). Furthermore, the ambient environment during silk processing allows for the incorporation of labile biological components without loss of function and with retention of bioactivity over extended time frames.

The procedure for fabricating silk fibroin inverse opal structures (Aguirre et al., 2010; Seelig et al, 2003) is illustrated in Fig. 7.1. First, colloidal crystals with the FCC (face-centered cubic) structure are grown from monodispersed PS colloidal spheres with a proper size to create templates to produce silk fibroin inverse opals. Second, the regenerated silk fibroin solution (1–4% w/v) prepared by raw silk fibers (Sah and Pramanik, 2010) are cast into the PS colloidal crystals (Swinerd et al., 2007). The process of filling the voids of colloidal crystals is one of the rate-determining steps to acquire silk fibroin inverse opal films, which is achieved through an evaporation-induced self-assembly process (Bogomolov et al., 1997). Third, after

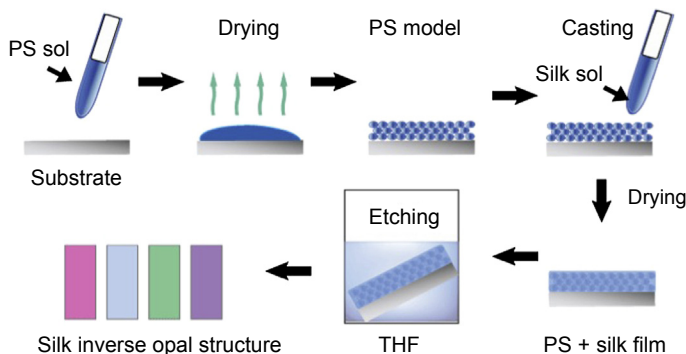


Figure 7.1 Fabrication steps for silk inverse opal structures.

natural drying, the colloidal templates are removed by chemical etching to obtain silk fibroin inverse opal films.

Changing the size of colloidal spheres as the lattice constant changed can alter the main reflection peaks of the silk fibroin inverse opal structure. For a ready-made silk fibroin inverse opal, tuning the reflection peaks is an important issue for all kinds of sensors.

7.1.3 Characterization of textile coatings

To date, traditional textile developments have had significant limitations in color, design, and function (Qian, 1985). Textile coating technology has become clearly highlighted and has gradually formed a new product line in the field of textiles. Textile coating technology and its product development has become one of the most important signs of practical technology progress in the world today.

This kind of product not only upgrades clothes, decoration, and other consumer goods, it gives new vitality to the construction, traffic, transportation, military, and aerospace industries.

Textile coating can be divided into three categories: electrostatic flocking coating, direct polymer coating, and pasting and indirect polymer film coating (Qian, 1985). In terms of the coating process, it belongs to a kind of new surface-modified textiles. With this simple technique, the useful function of textiles could be enhanced and underlying weaknesses could be masked, such as whitewashing the surface of textiles.

As a cross-discipline in the textile and chemical industries, coating technology is an important field for new textile materials, and will see a vital change after the advent of chemical fibers (Qian, 1985); this will require our attention to new trends in technological development.

7.2 Types and classifications of natural photonic materials (Zi et al., 2012)

7.2.1 Thin-film interference

The most basic method of structural coloration is thin-film interference (Born and Wolf, 1999), as shown schematically in Fig. 7.2(a). The n_0 , n , n_1 is the refractive index of the air medium, the single-layer thin film, and the other materials that are upside-down, respectively. When a light beam from air medium (n_0) hits the single-layer thin film (n), it will be reflected and transmitted at the upper surface (n) simultaneously (Zi et al., 2012).

The transmitted light beam at the upper surface (n) will go on and once again be reflected and transmitted (into n_1) when reaching the lower surface. The reflected beam at the lower surface will go on and also be reflected and transmitted (into n_0) at the upper surface. When the two reflected light beams at the upper surface (n_0) recombine, they interfere and form a pattern that depends on the difference between

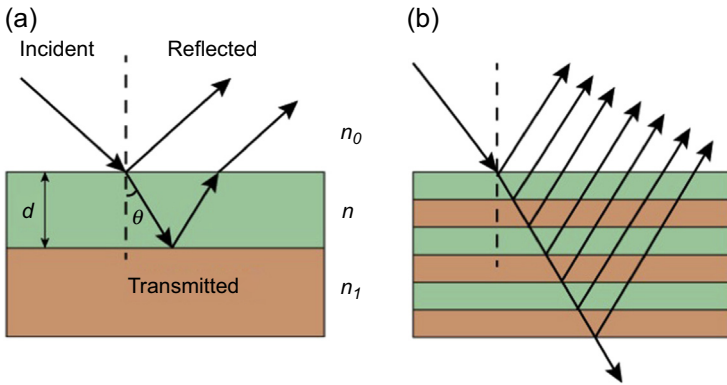


Figure 7.2 (a) Thin-film interference. A thin film with thickness d and refractive index n is sandwiched between an upper medium with refractive index n_0 and a lower medium with refractive index n_1 . The refracted angle with respect to the surface normal in the thin film is denoted by θ . (b) Interference in multilayer.

the distances they traveled. The optical path difference depends on the refracted angle (α) and the thickness (d) and refractive index of the film (n), given by the second $\cos \theta$.

In calculating the optical path difference, an extra contribution $\lambda/2$ should be considered when the light beam is reflected from a low-refractive index medium to a high-refractive index medium.

In traditional optical methods, constructive interference occurs when the optical path difference is an integral number of wavelengths, and destructive interference happens for a half-integral number of wavelengths. The possible phase change upon reflection caused by the condition for constructive interference should be readjusted, as shown in Table 7.1.

For a thin film, structural coloration occurs when the peak wavelength of reflected light beams meet the constructive interference condition. Iridescence results from reflection peaks undergoing a wavelength shift with changing the incident angle. Similar to that in thin films, in a multilayer successively reflected light from each interface could interfere with each other, as shown in Fig. 7.2(b).

Table 7.1 Condition for constructive interference readjusted by the refractive index indifference

Constructive interference	$n_0 < n < n_1$ $n_0 > n > n_1$	Second $\cos \theta = m\lambda$ Eq. [7.1]
	$n_0 < n > n_1$ $n_0 > n < n_1$	Second $\cos \theta = (m - 1/2)\lambda$ Eq. [7.2]

The wings of most insects are mainly composed of two integument layers apposed closely to form a thin membrane. In small Hymenoptera and Diptera, the transparent wings can produce structural colors via thin-film interference (Shevtsova et al., 2011), as shown in Fig. 7.3. The visibility of this reflected structural color pattern is affected dramatically by a changing background. In a light reflecting white background, because of the good transparency of the wings, the reflected structural color pattern is too weak or may even be ignored completely. In contrast, the structural coloration pattern can clearly be distinguished against a light-absorbing black background. For typical thin-film interference, the thickness of wing membranes varies in different wing positions in the range of several hundred nanometers. Wings in different position can produce different reflective colors, resulting in specific structural color patterns. The visibility of these color patterns strongly depends on the way the insects display their wings against backgrounds.

7.2.2 Multilayer interference

Multilayer interference is multilayer thin-film interference with a coloration mechanism similar to that of thin-film interference (Liu et al., 2009), given in Fig. 7.2(b). In general, multilayer interference is the most common form of structural coloration in the biological world, ie, butterfly, insects, fishes, and some plants (Berthier, 2007).

In a single thin-film structure, if the refractive index is independent of wavelength; thin-film interference will produce a series of successive reflection peaks with equal intensity and frequency intervals. However, the intensity of the reflection peaks is low enough to barely attract human eyes. For example, for a thin film with a refractive index of 1.5, its maximal reflectance is less than 20% at normal incidence. In contrast,

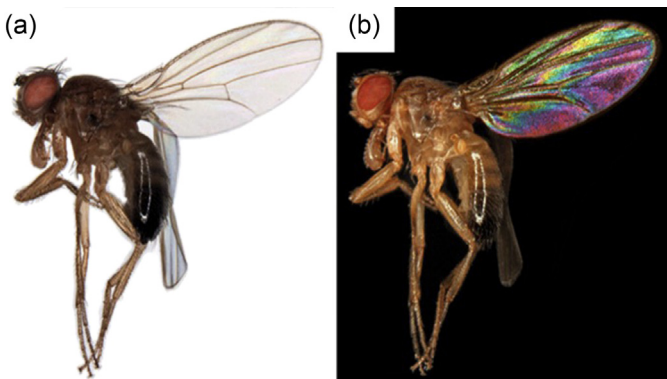


Figure 7.3 Photos of small Hymenoptera and Diptera against different backgrounds. The left side wing displays a nearly transparent pattern against the white background whereas the right side wing displays a structural reflection against the black background.

Reproduced from an article by Shevtsova, E., Hansson, C., Janzen, D., Kjærandsen, J., 2011. Stable structural color patterns displayed on transparent insect wings. *Proceedings of the National Academy of Sciences of the United States of America* 108, 668–673.

a multilayer thin film can achieve a high reflective peak, ideally as high as 100% in principle (Zi et al., 2012).

The elytra of some beetles, eg, *Tmesisternus isabellae*, display brilliant, metallic structural coloration caused by a multilayer in the cuticle, as shown in Fig. 7.4. Furthermore, the original golden-colored region of the elytra in the dry state turns red in some minutes when dropped into water. In the reflection spectrum of the colored region, a broad peak is positioned at about 600 nm, showing that the golden color in the dry state shifts to 662 nm, corresponding to the red color when wet, as shown in Fig. 7.4(c).

As seen in both scanning electron microscopy (SEM) and transmission electron microscopy (TEM) images, the microstructures of the colored region in the dry state are composed of two alternating layers: the homogeneous layer (dark layers in TEM images, about 105 nm) and the inhomogeneous layer (brighter layers in TEM images,

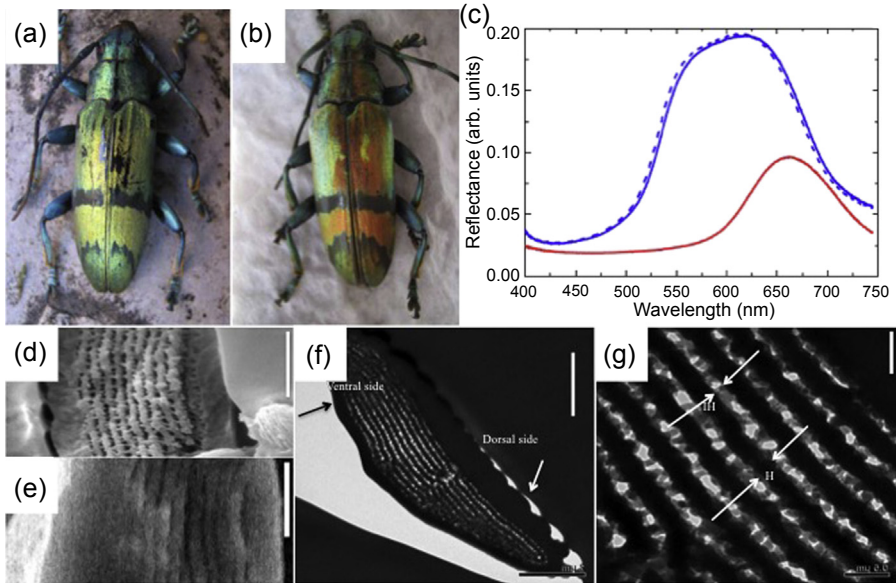


Figure 7.4 Optical images of beetle *Tmesisternus isabellae* in the (a) dry and (b) wet states. The iridescent golden color in the dry state changes to red when fully wet. (c) Measured reflection spectra of the colored region in the dry state (solid blue line) and in the wet state (solid red line). The spectrum for the redried beetle is shown as a dashed blue line. The iridescent golden color in the dry state changes to red when fully wet. It will change color reversibly by adjusting the humidity. (d) SEM images of transverse cross section of elytra in a dry state. The multilayer structure in the interior can be seen. (e) ESEM images of transverse cross section of elytra when fully wet. TEM images of (f) the left one indicates ventral side, and the right one indicates dorsal side of the multilayer structure and (g) close-up view of the multilayer structure. H and IH label a homogeneous layer (dark regions) and an inhomogeneous layer (gray and bright regions). Scale bars: (d, e) 1 μm ; (f) 2 μm ; and (g) 0.5 μm .

Reproduced from an article by Liu, F., Dong, B., Liu, X., Zheng, Y., Zi, J., 2009. Structural color change in longhorn beetles *Tmesisternus isabellae*. Optics Express 17, 16183–16191.

about 70 nm). The inhomogeneous layer consists of nanoparticles (gray areas in TEM images) and air voids (bright areas in TEM images).

The microstructural change in the wet state is characterized by environmental SEM. The existed multilayer swells from about 175 nm in the dry state to about 190 nm after water absorption. The increase in spacing of the multilayer causes a color change from golden in the dry state to red in the wet state. Furthermore, the refractive index difference is reduced after the air voids in the inhomogeneous layer are filled with water in the fully wet state, which causes the intensity of reflection in the wet state to be lower than that in the dry state.

7.2.3 Biological photonic crystals

The plumage of the male peacock impresses every visitor because of its magnificent and diversified coloration and mysterious eye-shaped patterns. Peacock feathers serve as a representative example for investigating structural colors in avian feathers. In the eye pattern of a feather of a male green peacock, *Pavo muticus* (Zi et al., 2003), blue, green, yellow, and brown patterns are visible to the naked eye, as shown in Fig. 7.5.

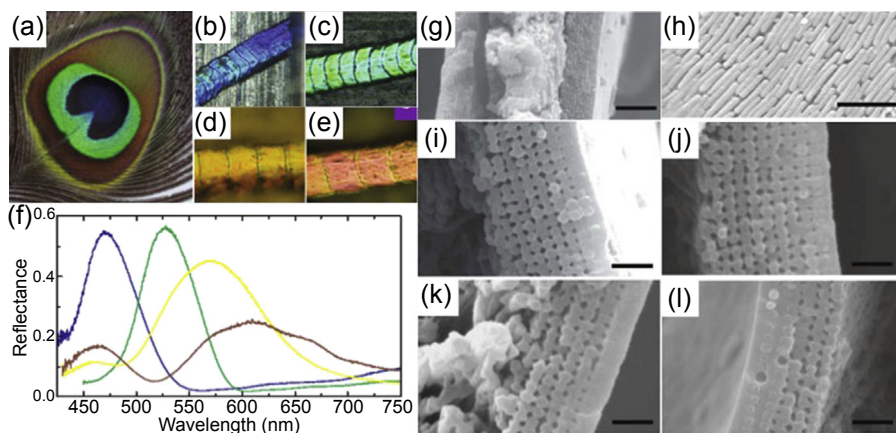


Figure 7.5 (a) Eye pattern of a tail feather of a male green peacock, *Pavo muticus*. The blue, green, yellow, and brown color patterns can be observed. (b–e) Optical microscopic images of blue (b), green (c), yellow (d), and brown (e) barbules. (f) Measured reflection spectrum of different-colored barbules of the male *P. muticus* at a normal incidence. Blue, green, yellow, and brown lines indicate results for blue, green, yellow, and brown barbules, respectively. SEM images of barbule structures. (g) Transverse cross section of a green barbule. The outer cortex layer contains a periodic structure. (h) Longitudinal cross section of a green barbule under higher magnification with the surface keratin layer removed. Melanin rods can be clearly seen. (i–l) Transverse cross-sectional images of the cortex for the blue (i), green (j), yellow (k), and brown (l) barbules. Scale bars: (g) 2 μm ; (h) 1 μm ; and (i–l) 500 nm. Reproduced from an article by Zi, J., Yu, X., Li, Y., Hu, X., Xu, C., Wang, X., Liu, X., Fu, R., 2003. Coloration strategies in peacock feathers. *Proceedings of the National Academy of Sciences of the United States of America* 100, 12576–12578. Copyright (2003) National Academy of Sciences, USA.

Barbs are orderly arrayed on the sides of a central stem in the peacock tail feather, as illustrated in Fig. 7.5(g). In fact, the barbs are colorless when observed using an optical microscope. On each side of a barb, the arrays have flat barbules and each barbule has round indentations typically of 20–30 μm . This barbule pattern produces incident light, providing clues as to the origin of coloration.

In transverse cross section, the round indentations have a smoothly curved, crescent-like profile. A barbule consists of a medullary core of about 3 μm enclosed by a regular structural cortex layer. The medulla consists of randomly dispersed keratin and melanin. The cortex layer consists of a thin outer surface of keratin and two-dimensional (2D) photonic-crystal structure patterns made of an array of melanin rods connected by keratin, as shown in Fig. 7.5(i)–(l). Photonic-crystal structures in differently colored barbules are similar, which means a similar coloration mechanism. In blue, green, and yellow barbules, the lattice structures are all of a square lattice whereas in the brown barbule it is a rectangular lattice. The only differences are the lattice constant (rod spacing) and the number of periods (melanin rod layers) along the direction normal to the cortex surface. The lattice constant for the blue, green, and yellow barbules is about 140, 150, and 165 nm, respectively. In the brown barbule, the lattice constant is about 150 and 185 nm along the directions parallel and perpendicular to the cortex surface, respectively. The number of periods is about 9–12 for the blue and green barbules, about 6 for the yellow barbules, and about 4 for the brown barbules. These differences in the lattice constant and the number of periods in differently colored barbules result in diversified coloration.

Measured reflection spectra for differently colored barbules under normal incidence are shown in Fig. 7.5(f). The blue and green barbules display a single reflection peak located in blue and green wavelengths, respectively, whereas the yellow and brown barbules have two reflection peaks, which indicates that mixed coloration exists. For the yellow barbule, the main peak located in green to orange wavelengths occupies a dominant position for ignorable contributions from the secondary peak at blue. For the brown barbule, coloration results from mixed coloration of the peaks at blue, green, yellow, and orange to red wavelengths.

7.2.4 Noniridescent colorations

Light scattering is another source of structural color, which is completely different from thin-film interference, multilayer interference, and the classical photonic-crystal type, because it has a vital origin in the irregularity of the microstructure and depends on the light wavelength (Kinoshita et al., 2008). Light scattering can be classified into incoherent or coherent scattering. Whether light scattering is coherent or incoherent depends on the coherent length of illumination light and the scatter arrangement. If the separation of scatter is smaller than the coherent length, light scattering is coherent because scattered light may interfere with each other. In contrast, if the separation of scatter is larger than the coherent length, it is considered incoherent scattering. For natural light such as sunlight, the coherent length is about a few microns.

Generally speaking, light is scattered when encountering irregularities (scatters), eg, particles. Particle or molecule sizes much smaller than light wavelengths belong to

Rayleigh scattering (Rayleigh, 1871): for example, the blue sky resulting from light scattering by atmospheric molecules. In Rayleigh scattering, the intensity of scattered light varies inversely as the fourth power of wavelength and has a strong angle dependence as factor $(1 + \cos^2 \theta)$, where θ is the scattering angle. Particles comparable to light wavelengths belong to Tyndall scattering (Tyndall, 1869), which is much more intense than Rayleigh scattering. There are no simple mathematic formulas for Tyndall scattering. For spherical particles, however, light scattering can be mathematically treated by the Mie theory (Hulst, 1981). In all, Rayleigh scattering and Tyndall scattering are typical incoherent scattering by single particles.

The noniridescent blue color of a feather of a common kingfisher, *Alcedo atthis*, is widely believed to be structural coloration resulting from Rayleigh scattering (Dyck, 1971a; Dyck, 1971b), as shown in Fig. 7.6. Irregular spongy medullary keratin

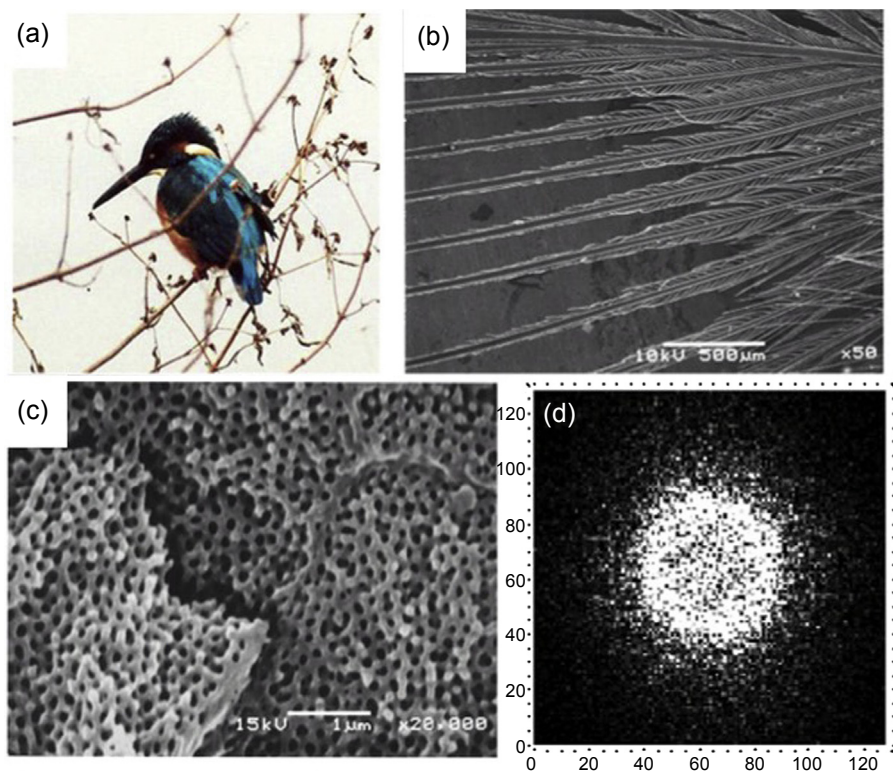


Figure 7.6 (a) Common kingfisher (body length = 150 mm), *Alcedo atthis* (photographed by Matsumiya) and (b) its feather barbs observed under SEM. (c) SEM image of cross section of the spongy medullary matrix and (d) 2D Fourier transformation of the TEM image. Bars: (b) 500 μm and (c) 1 mm.

Reproduced from an article by Kinoshita, S., Yoshioka, S., 2005. Cover picture: structural colors in nature: the role of regularity and irregularity in the structure (ChemPhysChem 8/2005). ChemPhysChem 6, 1429.

matrices are found after magnifying the barb of the bird feathers. To gain insight into the coloration mechanism of the irregular structure, Prum et al. (1998, 1999) illustrated a clear ring structure in the momentum space by a spatial Fourier transformation image of the electron microscopic image, as shown in Fig. 7.6(c). The ring structure means that the characteristic size of the matrix is uniform and is modeled by angularly distributed, broken multilayers whose layer thickness coincides with the widths of the air hole and keratin bridge. Prum et al. (2003) pointed out that there are other, similar structures in avian skins of various species, which appear as quasicrystalline arrays of parallel collagen fibers, a similar spatial order. The seemingly random structure of the spongy matrix actually has a uniform characteristic size that changes incoherent light scattering into coherent scattering, enforcing reflection to a large extent.

7.2.5 Structural color mixing

For thin films, multilayers, and diffraction gratings, their coloration can be understood simply as interference or diffraction. In the biological world, there exist many nontrivial photonic structures, eg, 2D and 3D periodic photonic structures. Their structural coloration cannot simply be interpreted as interference, diffraction, or scattering alone. Instead, it results from the combination of interference, diffraction, and scattering.

In butterflies, some respective structures also exist that result in structural colors. For example, the butterflies *Papilio ulysses* and *Papilio blumei* display bright blue and green color, respectively (Diao and Liu, 2011), as shown in Fig. 7.7. The reflectance spectra of *P. ulysses* illustrate the two distinct spectral peaks and have apparent

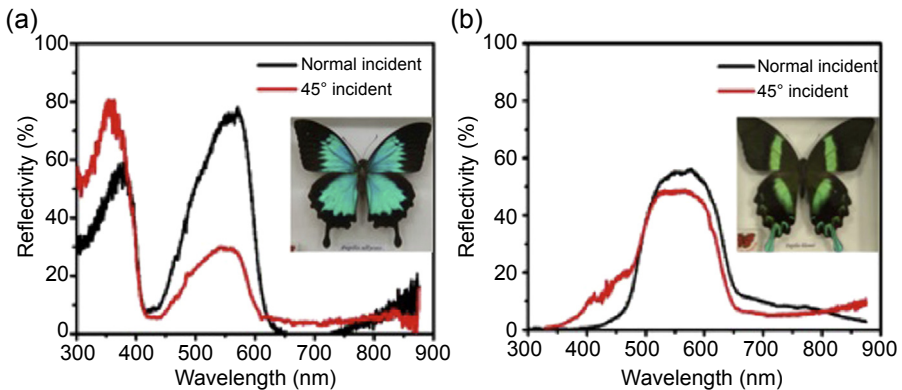


Figure 7.7 Measured reflectance spectra for (a) *Papilio Ulysses* and (b) *Papilio blumei* butterflies; black lines indicate spectra for normal incident light whereas red lines are spectra for 45 degrees incident light; the inset images are photograph of (a) *P. ulysses* and (b) *P. blumei* butterflies showing their blue and green colors, respectively.

Reproduced from an article by Diao, Y., Liu, X. 2011. Mysterious coloring: structural origin of color mixing for two breeds of *Papilio* butterflies. Optics Express 19, 9232–9241.

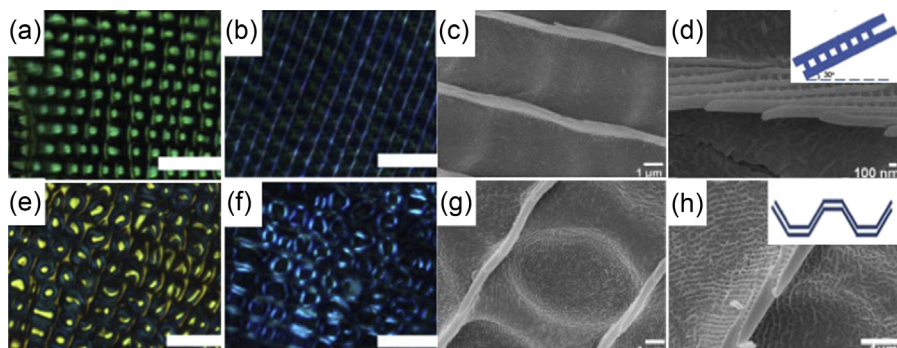


Figure 7.8 Optical microscopy and SEM images of butterflies. (a) Bright-field image and (b) taken under crossed polarizers for *Papilio ulysses*. (c) Bright-field image and (d) taken under crossed polarized light for *Papilio blumei*. Scale bar: 20 μm . SEM images of concavities (e) and ridges (f) for *P. ulysses*. SEM images of concavities (g) and ridges (h) structures for *P. blumei*. Inset images schematically illustrate concavities for (a) *P. ulysses* and (b) *P. blumei* butterflies.

Reproduced from an article by Diao, Y., Liu, X. 2011. Mysterious coloring: structural origin of color mixing for two breeds of *Papilio* butterflies. *Optics Express* 19, 9232–9241.

shifts of spectral peaks under different illumination conditions (normal and 45 degrees incident light), which indicates that the blue coloration in *P. ulysses* possibly originates from a color-mixing mechanism. In contrast, the reflectance spectra of *P. blumei* remain the same at different incident angles.

The optical microscopy images under normal incident light and linear polarized light and SEM images of the two breeds of butterflies illustrate their different principles caused by different microstructures, as shown in Fig. 7.8. The blue color seen in *P. ulysses* is mixed by green and deep purple colors reflected by concavities and ridges, respectively. The green color from *P. blumei* is mixed by yellow and blue colors reflected by the flat portions and inclined sides of concavities. The differences in their coloration mixing mechanisms and optical performances result from variations in their nanostructures.

7.3 Photonic structures brought to textile coating

We next introduce some applications of photonic-crystal structures successfully brought to textile coating by mimicking those natural structures. Compared with traditional fabrication methods, we turn our attention to simpler and less expensive self-assembled materials based on silk fibroin constructed on the surface of silk fabrics. To fabricate silk-coating photonic crystals with an opal structure on the surface of silk fabrics (Liu and Diao, 2013), a PS colloidal suspension was loaded onto the surface of silk fabric. The colloidal crystal was then self-assembled on the silk fabric surface.

Table 7.2 Calculated and measured reflections wavelength of silk inverse opal structures template by self-assembled PS spheres with different diameters

Sample	Lattice constant (a)	Calculated midgap wavelength		Measured reflection peaks
		$\lambda_1 = 1.43a$	$\lambda_2 = 0.69a$	
350 nm	415 nm	592 nm	284 nm	590 and 285 nm
450 nm	560 nm	810 nm	383 nm	800 and 380 nm
500 nm	620 nm	885 nm	424 nm	870 and 430 nm
700 nm	900 nm	1285 nm	616 nm	620 nm

Reproduced from one patent by Liu, X., Diao, Y., National university of Singapore, 2013. Inverse Opal Structures and Methods for Their Preparation and Use. US patent application 20130329281 A1. 2013–Dec-12.

Afterward, silk fibroin solution was loaded to fix the colloidal crystals to the surface of silk fabric. The procedure for fabricating silk fibroin inverse opal structures is illustrated in [Section 7.1.2](#).

In some reported experiments, the structural-color reflection offered by inverse opal structure could be adjusted by the positions of the two reflection peaks (λ_1 , λ_2) and wavelength difference ($\Delta\lambda$) can be adjusted by changing (1) the lattice constant because the midgap frequencies are inversely proportional to the lattice constant; (2) the difference in refractive indices between the constituent materials and filler in the voids; and (3) the illumination angle for some angle-dependent structures.

The simplest way to adjust the coloration of silk inverse opal structure is to fabricate a different polymer model with an opal structure: for example, monodispersed PS latex spheres with different diameters (350, 450, 500, and 700 nm) ([Liu and Diao, 2013](#)). Then the silk fibroin solution is introduced into the voids of colloidal crystals. After the silk fibroin solution is dry, the PS should be etched to provide silk inverse opal structures with lattice constants of about 410, 560, 620, and 900 nm, giving diversified structural coloration ([Table 7.2](#)). The red and golden-colored silk fabrics are fabricated using 270- and 240-nm monodisperse PS colloidal crystals, respectively, as shown in [Fig. 7.9](#).

Reflection peaks in ultraviolet (UV) and near-infrared (IR) wavelength range indicate the potential applications of structural-colored textile materials in ecodying engineering, UV protection, and IR radiation shielding. For example, adjusting the main reflection peaks into the UV range could technically produce UV protective textiles materials. Similarly, thermal-insulating textiles can be achieved by adjusting the main reflection peaks into the IR range, which could create an autocooling effect in the hot summer or provide insulation in the cold winter when the structure is coated on the outer or inner layer of textiles, respectively.

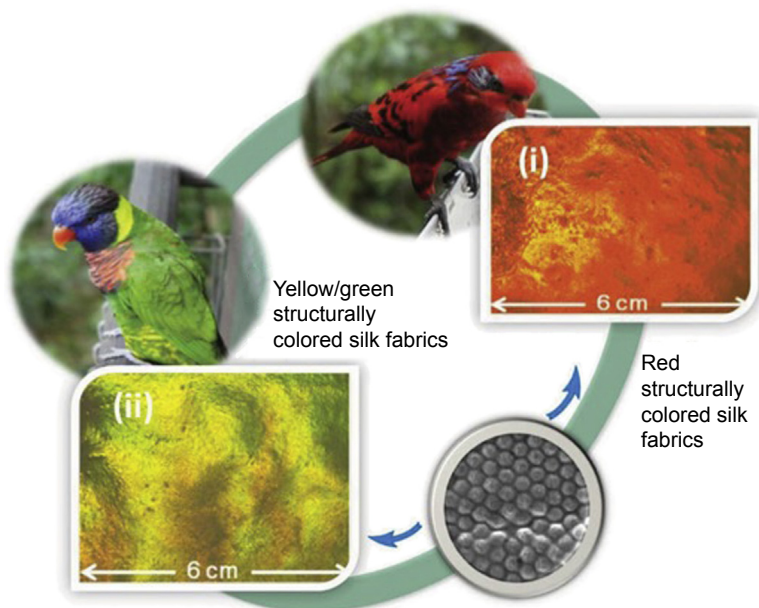


Figure 7.9 Creation of structural color for silk fabrics. Silk fabrics with structural color were created in which colloidal crystals were fixed onto the surface of silk fabrics by silk fibroin solution. Two examples of silk fabrics with structural red (i) and golden (ii) colors were fabricated using 240- and 270-nm self-assembled colloidal crystals, respectively. Reproduced from an article by Diao, Y., Liu, X., Toh, G., Shi, L., Zi, J., 2013. Multiple structural coloring of silk-fibroin photonic crystals and humidity-responsive color sensing. *Advanced Functional Materials* 23, 5373–5380.

7.4 Structural-colored sensors by external stimuli

7.4.1 Solvents

Silk fibroin has emerged as a highly promising biomaterial in various applications not only because of its excellent mechanical and optical properties but because of some special properties, ie, humidity induces cyclic contraction. By taking advantage of its special properties, tunable structural color reflection can be achieved by external stimuli.

By decreasing the refractive index contrast, wavelengths corresponding to the peak reflected light are redshifted. To illustrate this concept, [Kim et al. \(2012\)](#) exposed silk fibroin inverse opal structures to acetone, which has a low enough surface tension to infiltrate the nanostructured lattice. Acetone ($n \approx 1.36$) is volatile enough not to cause swelling in the protein matrix, and results in a decrease in index contrast from the original 0.54–0.18, causing a shift of the PBG to a lower frequency, as described in [Fig. 7.10](#).

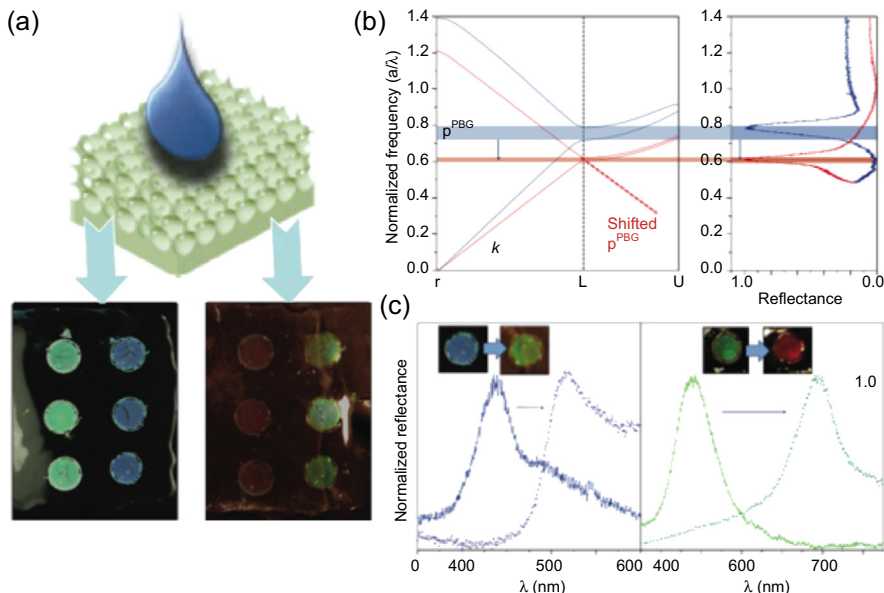


Figure 7.10 Before and after immersing silk fibroin inverse opal structures into acetone. (a) Photograph under visible light in dry air (left) and acetone (right), indicating remarkable changes in structural color. (b) Calculated photonic band structures of the silk fibroin inverse opal structures in dry air (blue) and acetone (red) by the plane-wave expansion method. (c) Reflectance spectra of silk fibroin inverse opal structures with lattice constant of about 300 nm, showing two clearly visible reflectance peaks. Reproduced from an article by Kim, S., Mitropoulos, A., Spitzberg, J., Tao, H., Kaplan, D., Omenetto, F., 2012. Silk inverse opals. *Nature Photonics* 6, 818–823.

7.4.2 Humidity

Diao et al. (2013) reported that the humidity-induced cyclic expanding and contraction of silk fibroin structures could be used to control the optical property of silk fibroin inverse opal structures precisely, as shown in Fig. 7.11. At a high humidity level, the decrease in tensile stress would induce the swelling of silk fibroin structures, leading to the expansion of silk fibroin structures in the inverse opal. In addition, water infiltration would change the refractive indices of the silk fibroin structures and air spheres. Therefore, the redshift of the visible reflection peak of the 350-nm silk fibroin inverse opal results from the water infiltration induced by the swelling of silk fibroin structures and the changes in refractive indices. On the contrary, the reflection peak of the silk fibroin inverse opal structures exhibits a blueshift when the humidity level is lowered, allowing for precise tuning of the reflection peak of a silk fibroin inverse opal structures within a certain range. During the cyclic process, the shift in the reflection peak is also reversible; Agnarsson et al. (2009) found powerful cyclic contractions of silk to act as a high-performance mimic of biological muscles actuated by changes in humidity.

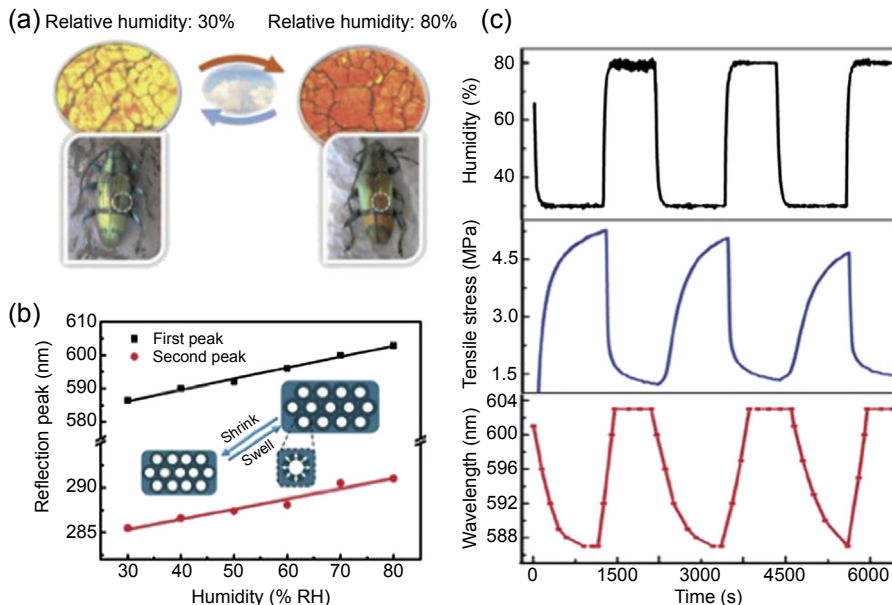


Figure 7.11 Control of reflection peaks of silk fibroin inverse opal structures by humidity. (a) Color of silk fibroin inverse opals structures under optical microscopy changes from orange at 80% humidity level to yellow at 30% humidity level, illustrating the humidity responsive structural color of a beetle. (b) Linear relationship between reflection peaks and humidity levels. (c) Cyclic tensile stress of silk fibroin structures in response to humidity change (*blue curve*) and measured reflection peaks for 350-nm silk fibroin inverse opal structures with changes in humidity levels (*red curve*).

Reproduced from an article by Diao, Y., Liu, X., Toh, G., Shi, L., Zi, J., 2013. Multiple structural coloring of silk-fibroin photonic crystals and humidity-responsive color sensing. *Advanced Functional Materials* 23, 5373–5380.

7.4.3 Temperature

Saito et al. (2003) reported the design and synthesis of a novel porous gel sensitive to both potassium ions and temperature, obtained using the template method. The porous hydrogel responded to changes in temperature, and at constant temperature the material also changed color with varying potassium ion concentrations. Fig. 7.12 shows photos of the NIPA-VBC6 porous gel at different temperatures from about 20°C to 40°C in pure water. The change in the structural color of the gel can be observed when the water temperature is changed. As the water temperature increased, this gel decreased in volume and the main peaks of the reflection spectrum were obviously blueshifted.

7.4.4 Stress

Viel et al. (2007) introduced a kind of elastomeric opal film production. Using extrusion and melt-flow techniques, complex elastomeric core–interlayer–shell beads were

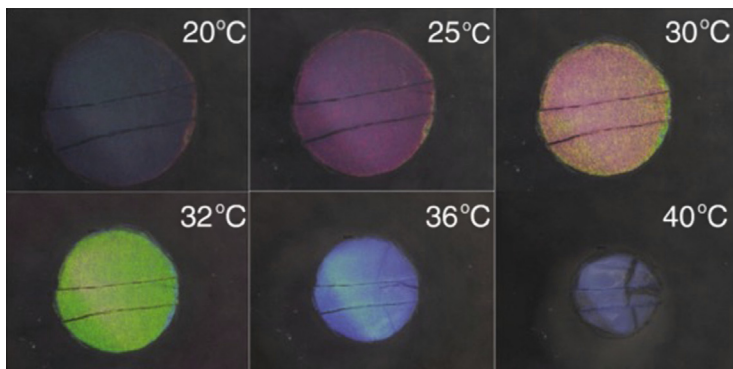


Figure 7.12 Porous poly(NIPA-*co*-VBC6) gel at various temperatures from about 20°C to 40°C in pure water. Adjusting the water temperature change may change the structural color of the gel.

Reproduced from an article by Saito, H., Takeoka, Y., Watanabe, M., 2003. Simple and precision design of porous gel as a visible indicator for ionic species and concentration. *Chemical Communications* 17, 2126–2127.

self-assembled into orderly opal structure films with the FCC lattice. In one example, beads consisted of a PS core with a thin interlayer of poly(methyl methacrylate) and a soft, deformable, outer shell of polyethylacrylate. After extrusion, the colloidal mass was self-assembled into a film over large areas when placed between the plates of a press and then stabilized by photo-cross-linking, characterized as an elastic and deformable reversibly sheet. When placed on a hard, curved mold, it displayed a range of different colors owing to different extents of deformation, as shown in Fig. 7.13.

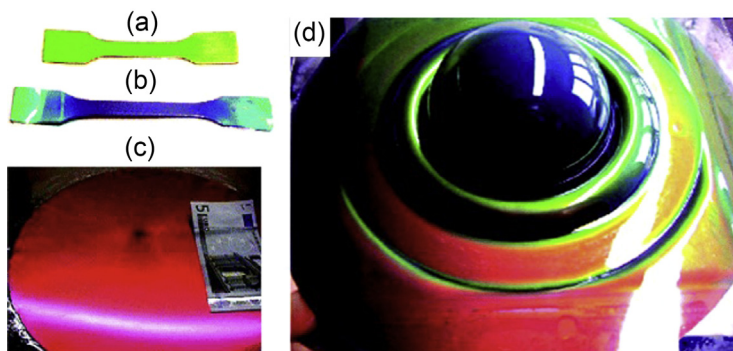


Figure 7.13 Elastomeric opal films: (a, b) test bars: (a) original; (b) strained to $\epsilon = 200\%$ and then released (residual deformation $\Delta\epsilon_\infty = 95\%$); (c, d) disk prepared by compression molding: (c) original and (d) deformed to a cup by deep drawing.

Reproduced an article by Viel, B., Ruhl, T., Hellmann, G., 2007. Reversible deformation of opal elastomers. *Chemistry of Materials* 19, 5673–5679.

Furthermore, the color intensity was significantly enhanced by adding carbon nanoparticles into the polymer mixtures (Pursiainen et al., 2007).

7.4.5 pH

Hydrogels capable of sensing ionic species generally can detect changes in pH value. Weak cationic polyelectrolyte can exhibit fast and substantial swelling under acidic conditions as a result of protonation of the pyridine group (Aguirre et al., 2010). Li and Lotsch (2012) reported a versatile photonic crystal pH sensor based on a 2D inverse opal monolayer of polyelectrolyte gel, as shown in Fig. 7.14. The stimuli-responsive 2D polyelectrolyte photonic crystals showed a prompt response to pH and the difference in pH conditions was readily seen from the transmission dip shift in the 2D polyelectrolyte photonic crystals. In addition, the swollen 2D polyelectrolyte photonic crystals entirely recovered the original color by washing with pure water and the reversible color response could be cycled more than 10 times without degradation.

7.4.6 Light

As previously mentioned, photonic crystals can benefit from organic molecules that are able to change their geometry reversibly upon exposure to UV or visible light. Matsubara et al. (2007) fabricated a bilayer porous gel composed of upper SiO₂ particles 280 nm in diameter and lower SiO₂ particles 220 nm in diameter. Storing the porous gel in darkness for a certain time and then exposing them to UV light through a photomask with some particular patterns causes the irradiated portion to increase in volume and results in a change in color, as shown in Fig. 7.15.

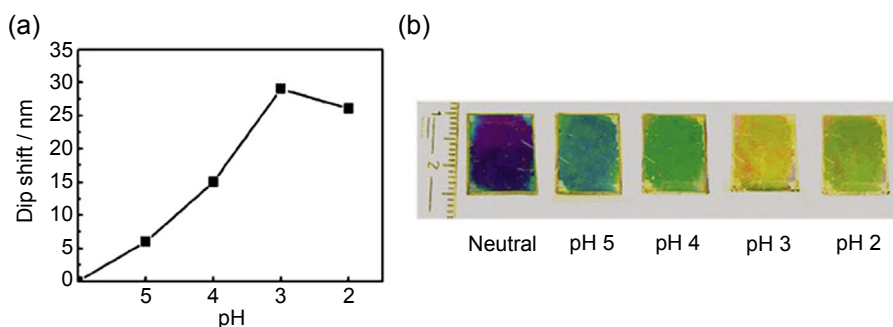


Figure 7.14 Transmission dip shift (a) and interference colors (b) of 2DPC-PGs in response to different pH conditions. The 2DPC-PGs were prepared with 470-nm opal monolayers and a spin-coating speed of 2000 rpm on glass (a) and silicon wafer (c).

Reproduced an article by Li, C., Lotsch, B., 2012. Stimuli-responsive 2D polyelectrolyte photonic crystals for optically encoded pH sensing. *Chemical Communications* 48, 6169–6171.

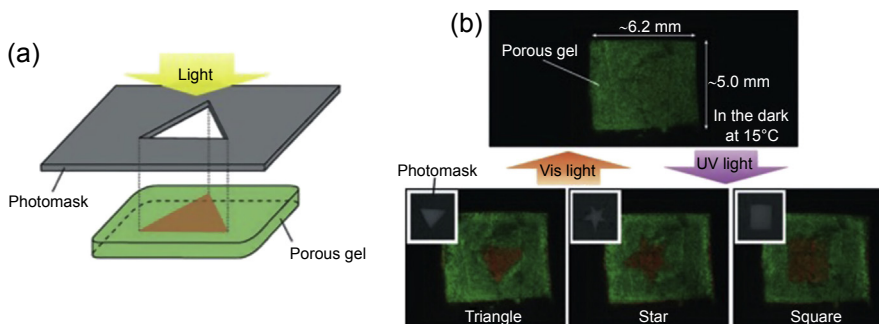


Figure 7.15 Multicolor photochromic behavior of the bilayer porous gel. (a) Schematic view of structural-color patterning of the porous gel by irradiation with UV light through a photomask. (b) Photos of the porous poly(NIPA-co-AAB) gel marked with a triangle, a star, and a square. These images result from the structural color change caused by irradiation with UV light through the corresponding photomasks.

Reproduced from an article by Matsubara, K., Watanabe, M., Takeoka, Y., 2007. A thermally adjustable multicolor photochromic hydrogel. *Angewandte Chemie International Edition* 46, 1688–1692.

7.5 Summary and outlook

We have reviewed structural coloration in natural photonic materials, the way to use photonic structures in textile coating and some products inspired by natural photonic crystals. Clearly, the evolution of coloration stems from regular structures but also from irregularity in order in the light wavelength, which produces optical phenomena by physical means such as interference, diffraction, scattering, and their mixed effects.

Silkworm silk has been adopted as a textile material for more than 7000 years. Silk photonic crystals offer a new function at the interface of photonics and biological applications by taking advantage of the inspiring characterization of silk.

By coating silk photonic crystals onto the surface of fabrics, we can produce multifunctional fabrics with vivid structural colors, which may revolutionize the eco-dyeing industry. The adjustable UV and visible and near-IR reflection peaks indicate the potential applications of structural colors in eco-dyeing engineering, UV protection, and IR radiation shielding. Furthermore, structural colors are bright and highly saturated and will not fade provided that the associated photonic structures remain unchanged.

Opal and inverse opal structures based on colloidal crystals have long been used to adjust their light and response to external stimuli such as solvents, temperature, stress, pH, and light. Through appropriate use or structural modification, each of these structure types could be designed to respond rapidly to external stimuli. The results point to a promising path for multiple applications, including display, sensing technologies, and drug delivery.

Acknowledgement

This study is financially supported by “111” Project (B16029), National Nature Science Foundation of China (No. U1405226), Fujian Provincial Department of Science & Technology (2014H6022) and the 1000 Talents Program from Xiamen University.

References

- Agnarsson, I., Dhinojwala, A., Sahni, V., 2009. Spider silk as a novel high performance bio-mimetic muscle driven by humidity. *Journal of Experimental Biology* 212, 1990–1994.
- Aguirre, C., Reguera, E., Stein, A., 2010. Tunable colors in opals and inverse opal photonic crystals. *Advanced Functional Materials* 20, 2565–2578.
- Anderson, T., Richards, G., 1942. An electron microscope study of some structural colors of insects. *Journal of Applied Physics* 13, 748–758.
- Berthier, S., 2007. *Iridescences: The Physical Colors of Insects*. Springer, New York.
- Bogomolov, V., Gaponenko, S., Germanenko, I., Kapitonov, A., Petrov, E., Gaponenko, N., Prokofiev, A., Ponyavina, A., Silvanovich, N., Samoilovich, S., 1997. Photonic band gap phenomenon and optical properties of artificial opals. *Physical Review E* 55, 7619–7625.
- Born, M., Wolf, E., 1999. *Principles of Optics*. Cambridge University, Cambridge.
- Diao, Y., Liu, X., 2011. Mysterious coloring: structural origin of color mixing for two breeds of *Papilio* butterflies. *Optics Express* 19, 9232–9241.
- Diao, Y., Liu, X., Toh, G., Shi, L., Zi, J., 2013. Multiple structural coloring of silk-fibroin photonic crystals and humidity-responsive color sensing. *Advanced Functional Materials* 23, 5373–5380.
- Dyck, J., 1971a. Structure and colour-production of the blue barbs of *Agapornis roseicollis* and *Cotinga maynana*. *Zeitschrift für Zellforschung und Mikroskopische Anatomie* 115, 17–29.
- Dyck, J., 1971b. Structure and spectral reflectance of green and blue feathers of the Lovebird (*Agapornis roseicollis*). *Biol Skrift* 18, 1–67.
- Hulst, V., 1981. *Light Scattering by Small Particles*. Dover, New York.
- Kim, S., Mitropoulos, A., Spitzberg, J., Tao, H., Kaplan, D., Omenetto, F., 2012. Silk inverse opals. *Nature Photonics* 6, 818–823.
- Kinoshita, S., Yoshioka, S., Miyazaki, J., 2008. Physics of structural colors. *Reports on Progress in Physics* 71, 175–180.
- Kinoshita, S., Yoshioka, S., 2005. Cover picture: structural colors in nature: the role of regularity and irregularity in the structure (ChemPhysChem 8/2005). *ChemPhysChem* 6, 1429.
- Li, C., Lotsch, B., 2012. Stimuli-responsive 2D polyelectrolyte photonic crystals for optically encoded pH sensing. *Chemical Communications* 48, 6169–6171.
- Li, Y., Duan, G., Liu, G., Cai, W., 2013. Physical processes-aided periodic micro/nanostructured arrays by colloidal template technique: fabrication and applications. *Chemical Society Reviews* 42, 3614–3627.
- Liu, F., Dong, B., Liu, X., Zheng, Y., Zi, J., 2009. Structural color change in longhorn beetles *Tmesisternus isabellae*. *Optics Express* 17, 16183–16191.
- Liu, X., 2012. *Bioinspiration: From Nano to Micro Scales*. Springer, New York.
- Liu, X., Diao, Y., National university of Singapore, 2013. Inverse Opal Structures and Methods for Their Preparation and Use. US patent application 20130329281 A1. 2013–Dec-12.

- Matsubara, K., Watanabe, M., Takeoka, Y., 2007. A thermally adjustable multicolor photochromic hydrogel. *Angewandte Chemie International Edition* 46, 1688–1692.
- Noh, H., Liew, S., Saranathan, V., Mochrie, S., Prum, R., Dufresne, E., Cao, H., 2010. How noniridescent colors are generated by quasi-ordered structures of bird feathers. *Advanced Materials* 22, 2871–2880.
- Prum, R., Torres, R., 2003. Structural colouration of avian skin: convergent evolution of coherently scattering dermal collagen arrays. *Journal of Experimental Biology* 206, 2409–2429.
- Prum, R., Torres, R., Kovach, C., Williamson, S., Goodman, S., 1999. Coherent light scattering by nanostructured collagen arrays in the caruncles of the malagasy asities (Eurylaimidae: aves). *Journal of Experimental Biology* 202, 3507–3522.
- Prum, R., Torres, R., Williamson, S., Dyck, J., 1998. Coherent light scattering by blue feather barb. *Nature* 396, 28–29.
- Pursiainen, O., Baumberg, J., Winkler, H., Viel, B., Spahn, P., Ruhi, T., 2007. Nanoparticle-tuned structural color from polymer opals. *Optics Express* 15, 9553–9561.
- Qian, Y., 1985. Textile coating technology and its equipment. *Journal of Beijing Textile* 4, 1–9.
- Rayleigh, L., 1871. On the light from the sky, its polarization and colour. *Philosophical Magazine* 41, 107.
- Sah, M., Pramanik, K., 2010. Regenerated silk fibroin from *B. mori* silk cocoon for tissue engineering applications. *International Journal of Environmental Science and Development* 1, 404–408.
- Saito, H., Takeoka, Y., Watanabe, M., 2003. Simple and precision design of porous gel as a visible indicator for ionic species and concentration. *Chemical Communications* 17, 2126–2127.
- Seelig, E., Tang, B., Yamilov, A., Cao, H., Chang, R., 2003. Self-assembled 3D photonic crystals from ZnO colloidal spheres. *Materials Chemistry and Physics* 80, 257–263.
- Shevtsova, E., Hansson, C., Janzen, D., Kjærandsen, J., 2011. Stable structural color patterns displayed on transparent insect wings. *Proceedings of the National Academy of Sciences of the United States of America* 108, 668–673.
- Swinerd, V., Collins, A., Skaer, N., Gheysens, T., Mann, S., 2007. Silk inverse opals from template-directed β -sheet transformation of regenerated silk fibroin. *Soft Matter* 11, 1377–1380.
- Tao, H., Kaplan, D., Omenetto, F., 2012. Silk materials—a road to sustainable high technology. *Advanced Materials* 24, 2824–2837.
- Toader, O., John, S., 2001. Proposed square spiral microfabrication architecture for large three-dimensional photonic band gap crystals. *Science* 292, 1133–1135.
- Tyndall, J., 1869. On cometary theory. *Philosophical Magazine* 37, 384.
- Viel, B., Ruhl, T., Hellmann, G., 2007. Reversible deformation of opal elastomers. *Chemistry of Materials* 19, 5673–5679.
- Zi, J., Dong, B., Zhan, T., Liu, X., 2012. Photonic structures for coloration in the biological world. In: Liu, X. (Ed.), *Bioinspiration: From Nano to Micro Scales*. Springer, New York, pp. 275–329.
- Zi, J., Yu, X., Li, Y., Hu, X., Xu, C., Wang, X., Liu, X., Fu, R., 2003. Coloration strategies in peacock feathers. *Proceedings of the National Academy of Sciences of the United States of America* 100, 12576–12578.

Coating processes and techniques for smart textiles

8

R.E. Meirowitz

RnD Technical Solutions Inc., San Diego, CA, United States

8.1 Introduction

Any discussion of why and how we modify textile materials must start with an understanding of why we use textiles at all. Probably the most basic textile function, for the individual, is separation or protection from the environment: for example, protection from thermal conditions (hot or cold), radiation (ultraviolet), environmental chemical hazards (plants and animals), environmental mechanical hazards (cuts and scrapes), and strength improvements. Textiles also provide many of these same benefits for technical applications including agriculture, construction, medical, military, and packaging. In addition to these physical characteristics, textiles are used for fashion, signaling, identification, and rituals.

In the textile industry there has always been an ongoing thrust to improve the performance of textile materials. Properties of interest range from the quantifiable, such as water resistance/repellency, fire resistance, and adhesion performance to the subjective, such as comfort. Two distinct pathways for improved performance have historically been followed: development of new fibers and surface modification of existing fibers and/or fabrics. Development of new fibers is costly and often requires relearning how to manufacture the product or retooling for different materials. Surface modification is an attempt to obtain the desired properties while effecting minimum changes and adding minimum cost to the process. Textile materials are often subjected to coating and lamination processes to improve their performance. This was nicely captured by William Smith in “Coating and laminating are textile finishing processes designed to add or improve function and to add value to a material and/or to create a material with specific properties” (Smith, 2000). We will look at surface modification of fabrics, specifically coating. Coating is defined as “the application of a semi liquid material such as a rubber, polyvinyl chloride, or polyurethane to one or both sides of a textile material. Once the coating has been dried (and cured, if necessary), it forms a bond with the fabric” (Kosa, 1999).

Over time we have improved textiles by enhancing and blending material properties. Now we are at the point where we have not only improved the primary properties of textiles but are also engineering textiles that interact with and respond to their environment. These are smart textiles.

8.2 Substrate and coating interactions

In most cases when coating a fabric two factors related to the coating/fabric interactions are of critical importance. These factors are wetting of the fabric (which also affects wicking) by the coating material and adhesion of the coating to the fabric.

The need for adhesion is clear. Without good adhesion the coating will not stay attached to the fabric during use. Adhesion arises from intermolecular forces between two materials. These forces can be from actual bonds (ionic or covalent) or from weaker intermolecular forces (hydrogen bonding, dipole–dipole or induced dipole–dipole interactions, or dispersive forces) (Mittal, 1976, p. 31; Garbassi, Marco, & Occhiello, 1994, p. 3). In most textile coating processes these forces are polar or dispersive forces that arise between the two materials (although covalent and ionic bonds can be achieved). For our purposes adhesion occurs when the surfaces are in contact and do not when they are separated. On a flat smooth geometric surface having intimate contact with the adhesive these forces can be compared for various substrates and adhesives.

One of the more common test methods for testing adhesion is the 180 degree or 90 degree (Fig. 8.1(a) and (b)) peel test of a material from a substrate. The force required to remove a set width of material (usually 1 inch) from a surface is measured. Common units for this test are pounds per inch or Newtons per millimeter. It is apparent from this test that the greater the width of the coverage the higher the force is required to effect peel. There are two important notes related to adhesion. First, if coverage is not intimate across the surface, adhesion will be lower (Fig. 8.2); second, if we mechanically increase the surface area (sanding) we increase the area possible for coverage and therefore for adhesion.

To understand the fabric–coating interaction we must define the physical system. Fabric coating is usually performed in air. Therefore the physical materials are fabric (solid (S)), coating (liquid (L)), and air (gas or vapor (V)). When these three phases come into contact with each other, they result in interfaces. When the coating is applied to the fabric, three interfaces are formed: a solid–liquid interface (γ_{SL}), a solid–vapor interface (γ_{SV}), and a liquid–vapor interface (γ_{LV}). The γ refers to the surface tension

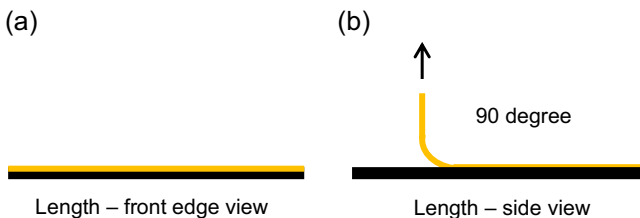


Figure 8.1 (a, b) Adhesion testing.



Figure 8.2 Incomplete or inconsistent coverage.

of the interface. Physicist Thomas Young reasoned that because the energy of a system must be at a minimum at thermodynamic equilibrium, the only mobile (flexible) interface in this system is the liquid–vapor interface (γ_{LV}). Taking this postulate as the starting point, the geometry of the system can be described by an equation (the Young equation) (Fig. 8.3).

We have started with the postulate that the only mobile interface is the liquid–vapor interface (γ_{LV}). From our starting point it is axiomatic that the shape of the droplet formed by the liquid will be variable (depending on the specific liquid, solid, and vapor). At equilibrium the liquid–vapor interface can be described by a line anchored at the three-phase line and tangent to the surface of the droplet at that point. The angle formed between this line and the solid–liquid interface is defined as the equilibrium contact angle and is given the Greek letter theta (θ) as its symbol. The contact angle (θ) measures a material’s wettability by the wetting media. As the material–liquid becomes less wettable the contact angle becomes larger. Conversely as the material–liquid combination becomes more wettable the contact angle becomes smaller (Fig. 8.3) (Garbassi, Marco, & Occhiello, 1994; Good, 1979; Schwartz, 1985). If the material is tipped at an angle, an advancing (leading edge) and receding (trailing edge) contact angle (θ_a and θ_r , respectively) develop. These angles arise owing to hysteresis, but for this discussion the equilibrium contact angle (θ) is sufficient. What is important for our purposes is that liquids with contact angles less than 90 degree on the surface to be coated will spread (to some degree) whereas liquids with contact angles greater than 90 degree will not spread on that surface. The lower the contact angle, the greater the wetting.

It was stated earlier that by increasing the surface of a material we can increase the amount of coverage and therefore the adhesion. That assumes that the surface is wetted by the coating material. Fig. 8.4(a) and (b) represents a fabric and a coating liquid.

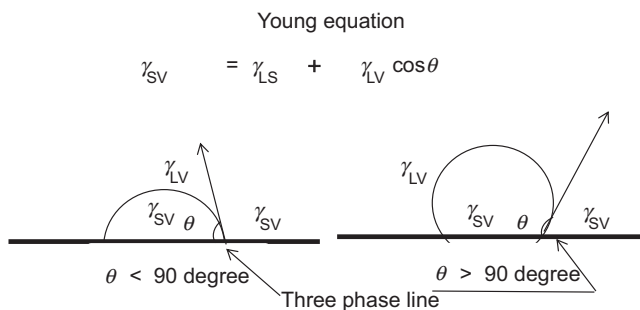


Figure 8.3 Contact angle and wetting.

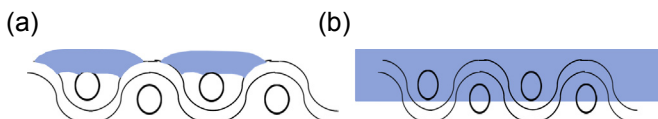


Figure 8.4 (a, b) Liquid (coating)/fabric coverage.

Fabrics have a large and irregular surface. Fig. 8.4(a) shows what happens when a poorly wetting liquid is applied to the surface of the fabric. The coverage is spotty and does not penetrate, leading to poor overall adhesion. However, as the liquid wets the surface better (the contact angle approaches 0 degree), the coverage and therefore the adhesion becomes greater. In fact, at some point the coating may wrap around the individual fibers and fill in the interstitial spaces such that the cohesive strength of the coating must be overcome (in addition to the liquid–surface adhesion) to remove the coating. The desired goal for the coated product must be kept in mind because there are tradeoffs to be considered. In the case of the example shown in Fig. 8.4(b) the adhesion of the coating to the substrate will be maximized for that system; however, the breathability, noise, hand, etc. will be dramatically affected.

Because the surface of the fabric's material and the contaminants on the surface will have an impact on the contact angle of the coating (and therefore adhesion), the fabric as received for coating may need to be prepared or pretreated for optimized fabric–coating interactions. Residual spin finishes or dirt, oil, grease, and stains may render the as-received fabric unwettable by the coating material, or with spots which are variably wettable. This preparation (if necessary) could be as simple as an aqueous or solvent scour to remove residual spin finishes, a caustic etch, or plasma ablation to improve wettability, or application of a bond (tie) coat to improve adhesion of the coating to the substrate.

8.3 Overview of coating

The goal of textile coating is to impart material improvements and or add value to a textile without detracting (or minimally doing so) from positive fabric properties inherent to the starting material.

When discussing coating processes often parameters are not included that should be considered. These factors may need to be accommodated (changed) for running coated versus uncoated fabrics. These include batching of fabrics, tension control (machine and cross-machine directions), and cleanliness (specifically particulates). Batch sizes must be thought through, especially if the coating formulation has a short pot life. Usually the largest batch size is the goal so that the process can be more cost-efficient. Machine direction tension is normally controlled; however, the treatment may affect the strength, elongation, tendency to crease, degree of edge curl, or friction of the fabric (Fung, 2002). These potential variations from normal fabric behavior may require changes to normal run conditions for the fabric. The same holds true for cross-machine direction via Stentor. There is the additional caveat that dust and particulates can be created when clipping or pinning the fabric or if there is interaction with the coating and the clips or pins. This dust or particulate can cause streaks and imperfections in the coating. If the resin in the reservoir is not controlled sufficiently dried or cured bits may get into the application head and wind up under the blade, which also can cause streaks and imperfections in the coating. Both the machine and cross-direction machine tensions must be controlled so that the coating thickness profile across the width of the fabric is as desired. This is most often uniform in thickness

across the fabric width as opposed to thicker in the middle and tapering off at the sides (Fung, 2002; Shim, 2010).

In the broadest possible sense, all coating operations can be described in four sections: (1) substrate preparation (if necessary), (2) coating formulation preparation, (3) application/metering, and (4) postprocessing (if necessary). Substrate preparation would involve any pretreatment that modifies the substrate to accept the coating (discussed in the section on surface and coating interaction). This step is where things such as caustic etching for wettability or application of a bonding coat (tie coat) would be performed. Preparation of the coating formulation could be as simple as using a single 100% solid coating or as complex as mixing a multicomponent reactive mixture in a solvent or as an emulsion. The agitation and stabilizing additives required to keep the coating formulation stable over its entire use time will need to be determined for each formulation. Application and metering of the coating onto the substrate are the focus of this section and will be discussed subsequently. Finally, the coating may or may not require postprocessing. This includes curing (or cross-linking) of the polymer by energy: for example, gas or infrared oven or ultraviolet light (Benkreira, 1993; Shim, 2010).

8.4 Traditional processes for textile coating

In classical textile coating, the overall objective of the application and metering portion of the coating process is to deposit a specific quantity (weight or thickness) of a polymer uniformly (unless discrete patches or gradients are desired) onto the surface of a fabric. In this chapter we will examine only continuous processing techniques (as opposed to batch). There are many different coating techniques, which is unsurprising considering the variations in substrates, coating materials, and desired end results. Given the plethora of techniques, we will look at some of these as a function of three categories: free withdrawal (free meniscus) coating, metered (roll or nonroll), and constrained flow and die or exact coating. Some examples of each will be given.

In free withdrawal, the fabric is run through a bath of the coating formulation. The line speed, rheology of the liquid, and the interaction with the fabric determine the weight and thickness add-on of the coating. The effect of contact angle can be seen in a padding (dip/squeeze) application (Fig. 8.5). If the weight add-on of the coating to the fabric cannot be sufficiently lowered by line speed and other variables, the fabric can be subjected to postimmersion squeezing or scraping.

Metered or constrained flow can be achieved using rolls or other devices to achieve metering. Metering (setting the coating thickness) can be done before, during, or after the point of application. The two most common metering techniques are roll and knife (or blade) coating.

There are many roll-coating techniques. The simplest roll one is the use of a single roll to bring the coating material up from a reservoir and lightly touch the fabric with the liquid (hence, the name “kiss roll”—Fig. 8.6(a)). The amount of liquid is controlled by the liquid rheology, line speed, and fabric geometry. The coating thickness can be

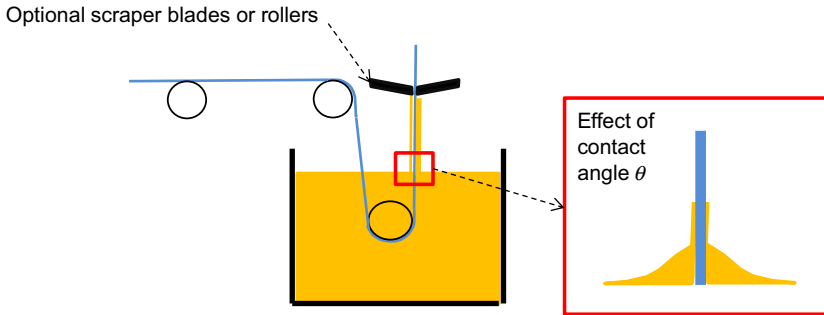


Figure 8.5 Free withdrawal coating (padding, dip/squeeze).

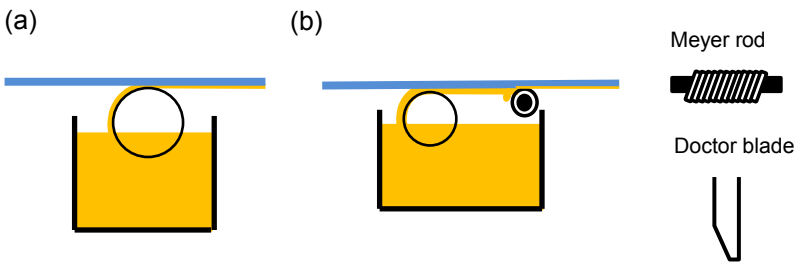


Figure 8.6 Kiss roll coating (single roll coating). (a) Free Kiss roll; (b) kiss and scrap.

decreased using a Meyer rod or knife after the application to scrape the some of the coating off (Fig. 8.6(b)).

Another roll-coating procedure includes reverse roll coating, in which the coating thickness is controlled by the gap between the metering roll and the application roll (Fig. 8.7). The metering roll usually has excess coating material removed (scraped)

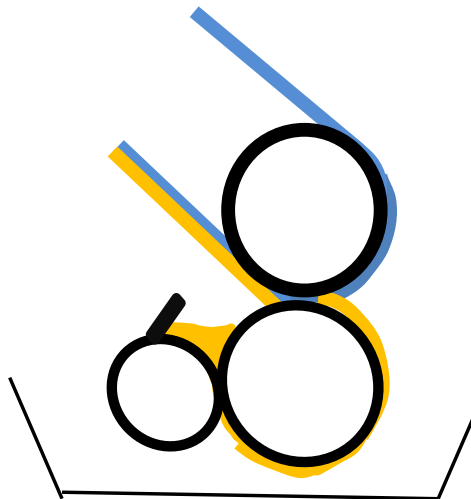


Figure 8.7 Metered roll coating (nip roll coating).

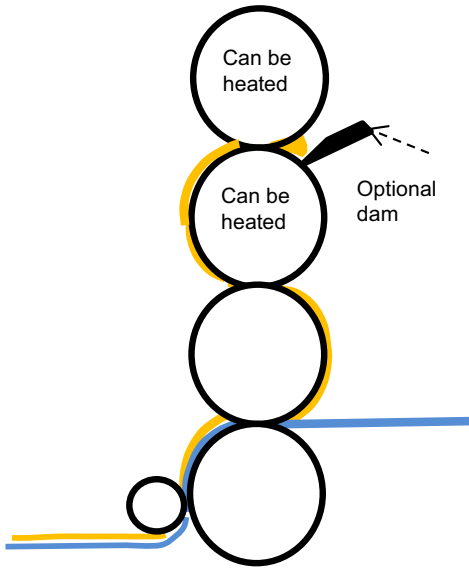


Figure 8.8 Calendar roll coating.

by a doctor blade. In addition, thick (very high-viscosity) coatings can be applied by calendar coating. In this technique, a highly viscous (or semisolid) polymer coating can be formed into a film using high-pressure calendar rolls (Fig. 8.8). The rolls can be heated or chilled as needed to keep the coating malleable or release the coating, respectively.

Metered or constrained flow can also be achieved using elements other than rolls. The most common metering element (other than a roll) is a knife (doctor blade or air knife) (Figs. 8.9–8.11). The blade can be placed in various positions relative to the fabric and other table elements. Two popular configurations are shown. In knife over air (sometimes called a floating knife) (Fig. 8.9), the knife is positioned on the

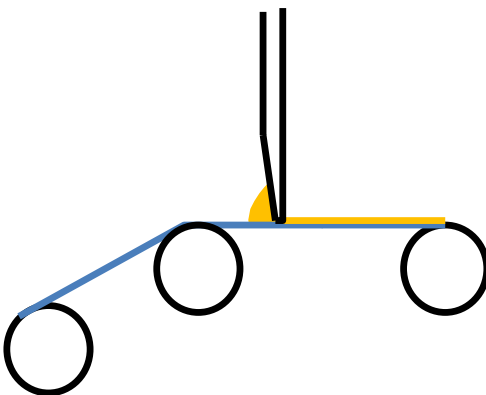
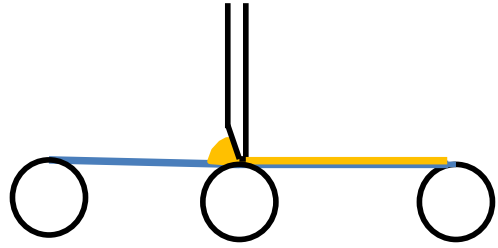
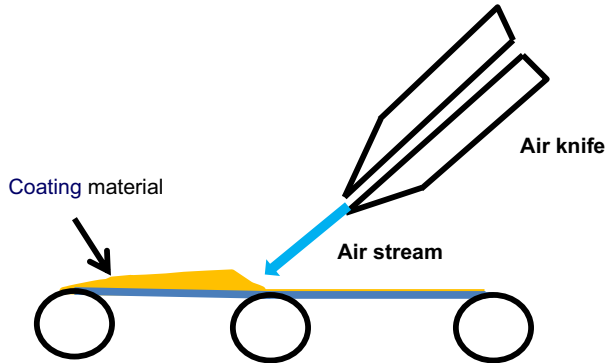
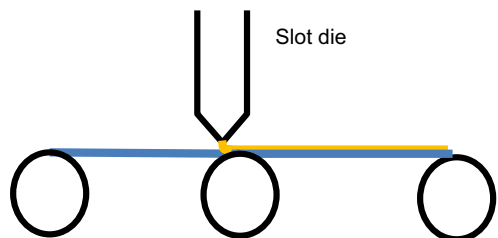


Figure 8.9 Knife over air coating.

Figure 8.10 Knife over roll coating.**Figure 8.11** Air knife coating.

fabric with no supporting surface below the knife. Deflection of the fabric caused by the movement of the coating material beneath the knife determines the thickness. Mechanical tension from increasing the knife's penetration into the fabric or line speed can be used to control the thickness of the coating. Alternatively, in knife over roll coating, the knife is positioned over the fabric with a roll behind the fabric (Fig. 8.10). A gap can be left between the knife and the fabric to control the thickness of the coating. Air knife coating is essentially the same as coating with a doctor blade but a jet or curtain of air is used to control the coating thickness (Fig. 8.11).

Die or exact coating is when the exact amount of coating is applied directly onto the fabric. Two examples of this are die coating and transfer coating. For die coating, the exact amount of polymer coating is extruded through a slot die directly onto the fabric across the width of the fabric to be coated (Fig. 8.12). For transfer coating, a specific

Figure 8.12 Die coating (exact coating).

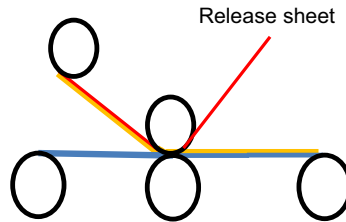


Figure 8.13 Transfer coating.

thickness of coating material is preformed onto a release sheet that is then brought into contact with the fabric; the coating transfers to the fabric and the release sheet is removed (Fig. 8.13). Additional, in-depth information on traditional coating can be found in Benkreira (1993, p. 49), Shim (2010, p. 10), Fung (2002), Kovacevic, Ujevic, and Brnada (2010, p. 241), and Singha (2012).

8.5 Coating for smart textiles

There are many definitions of “smart textiles”; to add the confusion, the term has become a buzz word and is often used to describe materials other than those in the popular definition. The materials referred to in this chapter will adhere to this definition:

Smart materials and structures can be defined as the materials and structures that sense and react to environmental conditions or stimuli, such as those from mechanical, thermal, chemical, electrical, magnetic or other sources.

Tao (2001, pp. 2, 3)

Further smart textiles are often broken down into groups. These include:

passive smart materials which can only sense the environmental conditions or stimuli; active smart materials which will sense and react to the conditions or stimuli and very smart materials which can sense, react and adapt themselves accordingly.

Tao (2001, p. 3)

The materials referred to in this chapter will not differentiate between the types of smart textile but will address the overall category.

These materials are prepared by many old techniques and some newer ones. Most of the published literature discusses technologies and their uses (eg, nanotechnology or microencapsulation). In addition, quite a few publications describe the benefits or performance characteristics of the materials but not the method used to apply the technology to the substrate. There is interest in using various application techniques to generate smart textile materials. The terminology used is often inconsistent and may not actually reflect what the author wishes it to reflect. To attempt to clarify terminology and techniques, the basic principles of some of these techniques, the names by which they are sometimes called and the applications for which they are being applied

will be discussed. The most basic commonality for all of these techniques is that they all take a chemical moiety and fix it to the surface of another material (textile). The different techniques result from the differences in the modifying material, the material to be modified (substrate), the type of modification required, etc.

Vapor deposition can be broken into two major groups: physical vapor deposition (PVD) and chemical vapor deposition (CVD). In the most general sense, PVD is a vapor coating (processing) in which a solid target material is converted and has atoms or molecules removed from it on an atomic or molecular scale. A vapor is first created and then deposited and condensed on the surface to be modified. The first step in PVD process (Fig. 8.14) occurs with vaporization (evaporation) of the target material (Regenstein, 1996; Wei, Xu, & Wang, 2009, p. 58). PVD uses purely physical processes (as opposed to chemical) to achieve vaporization of the target material. This physical vaporization can be achieved in multiple ways, including vacuum evaporation, laser bombardment, and sputtering. The commonality in all of these techniques is that energy is put into the target material until some of the atoms (or molecules) are removed from the target material. The target material is hotter than the substrate material, so the evaporated molecules can condense onto substrate surface. The apparatus is in a vacuum chamber, so as the molecules travel from the target to the substrate they do not collide with other superfluous molecules. The difference between these vaporization techniques is primarily how the energy is put into the target material. Vacuum evaporation heats the target material under high vacuum. Heating can be achieved electrically. When the target material evaporates, it moves to the substrate material and

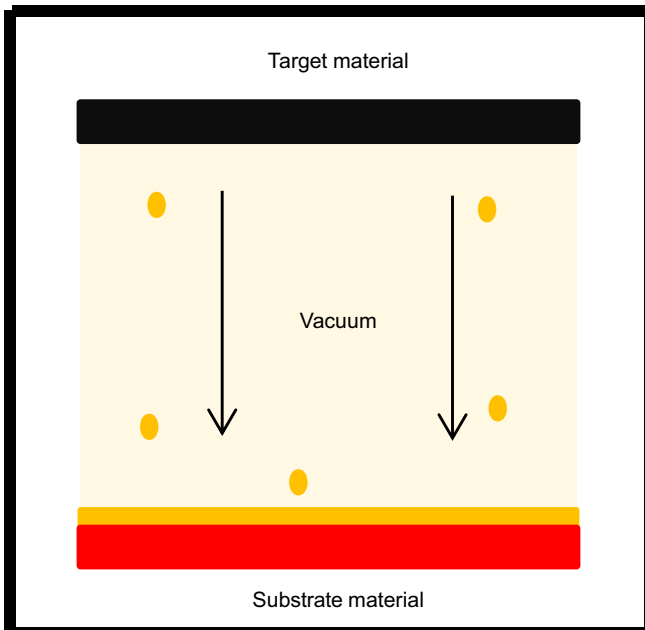


Figure 8.14 Schematic for physical vapor deposition (PVD).

condenses. In laser bombardment, an electron beam strikes the surface of the target material, which is then ablated by the laser. The target molecules that are ejected (vaporized) from the surface of target material can then deposit onto the substrate material. Sputtering is a technique in which plasma (usually from an inert or nonreactive gas) is generated near the surface of the target material. The plasma ejects some molecules from the target material, which deposits onto the substrate surface. If a reactive gas is used instead of an inert gas (eg, oxygen or nitrogen), the target vapor particle reacts with the gas and then is deposited onto the surface of the substrate-forming oxides, nitrides, and carbides, respectively. This technique has seen much use in the metallization of films and fabrics to give conductive materials that can be used for electromagnetic interference shielding. PVD is usually used for gold sputter coating of samples for scanning electron microscopy. Because of the nature of the techniques, the target material vapor must follow a straight-line path, so the technique is useful for line-of-sight applications (Fig. 8.14).

In its simplest form, CVD (Creighton & Ho, 2001; Wilson, 2009, p. 126) is a vapor coating process in which a reactive gas or gases are introduced into a chamber by forced flow. The chamber contains one or more heated objects to be coated (Fig. 8.15). The reactive gas or gases chemically change (react) on or near the heated surface of the materials to be coated and then diffuse onto the surface and chemically attach. Unwanted chemical by-products of the reaction and unreacted precursor gases are evacuated from the chamber. One advantage of CVD is that it is not a line-of-site technique and will allow for conformal coating on all exposed surfaces of the substrate. CVD does not usually require the same high vacuum as PVD; however, because the reactive material must be volatilized to a gas stream, the substrate must be hotter than the gas stream and therefore it is often desirable to have precursors that are volatile near room temperature.

To expand the selection of useful precursors and control the degree to which the reaction goes to completion, there are many variations of CVD based on temperature control. Each variation has advantages and disadvantages. For instance, reactor

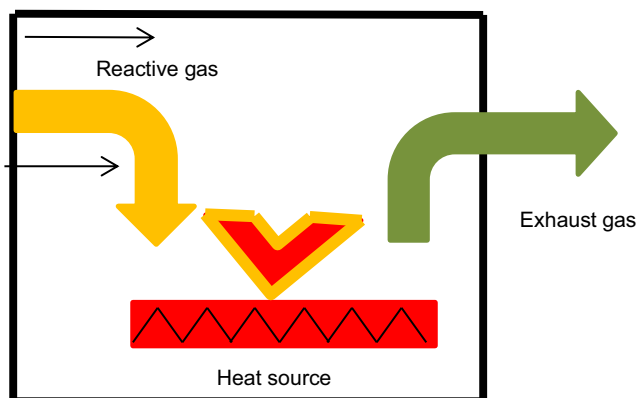


Figure 8.15 Schematic for chemical vapor deposition (CVD).

chambers can have walls which may or may not be heated. Hot wall reactors can often be run at lower pressures and are often designated as low-pressure CVD. Although this can be a distinct advantage, the hot walls also provide surfaces on which the precursor gases can react and which therefore must be cleaned. In the case of a precursor material which requires very high volatilization temperatures, the reactive gas stream may have additional energy supplied in the form of plasma, resulting in plasma-enhanced or plasma-assisted CVD. This broadens the window of precursors but it makes the process more complex. The specific technique and variation are chosen so as to be optimal for the system being run. CVD has been used to produce uniform conformal conductive coatings using polypyrrole (Wilson, 2009, p. 126). It has also been used to prepare wear-resistant, corrosion-resistant, and superhydrophobic coated surfaces. A technique related to CVD that gives subnanometer control is atomic layer epitaxy (Creighton & Ho, 2001), also referred to as atomic layer deposition (ALD) (Greer, Fraser, Coburn, & Graves, 2002; Puurunen, 2014). Epitaxy is a process in which the formation of a crystalline overlayer occurs on a crystalline substrate. The ALD technique uses two reactive chemical precursors. These precursors are pulsed into the chamber sequentially with the purge of an inert gas between and after the pulses. This sequential deposition allows for the creation of a multilayer film.

Both CVD and PVD can be used to produce conductive or metallized textiles and fibers. Electroplating and electroless plating are two additional methods which can be used to produce conductive textiles. Electroplating, also referred to as electrodeposition, is used on textiles that are conductive at the start of the process. They are modified to have the desired properties (eg, electrical conductivity, reflectivity, barrier) by the deposition of a layer of metal particles. The process is driven by an external electric current (Holland, 2013, p. 8; Paunovic, Schlesinger, & Snyder, 2010, p. 1; Wang, Wang, & Lin, 2010, p. 155). Electroplating is a process performed in an electrolytic cell in which a reduction–oxidation reaction occurs when electrical energy is applied (Fig. 8.16). The anode (positive charge) is the plating material and the cathode (negative charge) is the material to be coated (which must be conductive). They are connected through a power source which removes electrons from the anode (oxidation) and deposits them at the cathode (reduction). The two materials are immersed in an electrolyte (salt bath) which allows the oxidized metal (in this case, silver) to traverse the bath be reduced and deposited at the cathode.

Electroless plating (Guo & Jiang, 2009; Wang et al., 2010, p. 155), also called chemical or autocatalytic plating, is a similar process, except that the electrons for the redox reaction are not supplied from an external power source but rather from a reducing agent in the reaction mix. An advantage of this process is that it can be used to coat nonconductive materials. As an example, the silver coating achieved in the process described previously needed to be done on a material that was already conductive (electrons must be able to flow from the anode (coating material) to the cathode (material to be coated)). Silver coating can be performed by electroless plating on a nonconductive material. The reagent (Tollen's reagent) is short-lived and must be prepared fresh for each use. Preparation of the reagent will not be described. The reaction occurs when the diamminesilver (I) complex $[\text{Ag}(\text{NH}_3)_2]^+$ (Eq. [8.1]) oxidizes the aldehyde RCHO to form carboxylate ion (RCO_2^-) and in doing so is

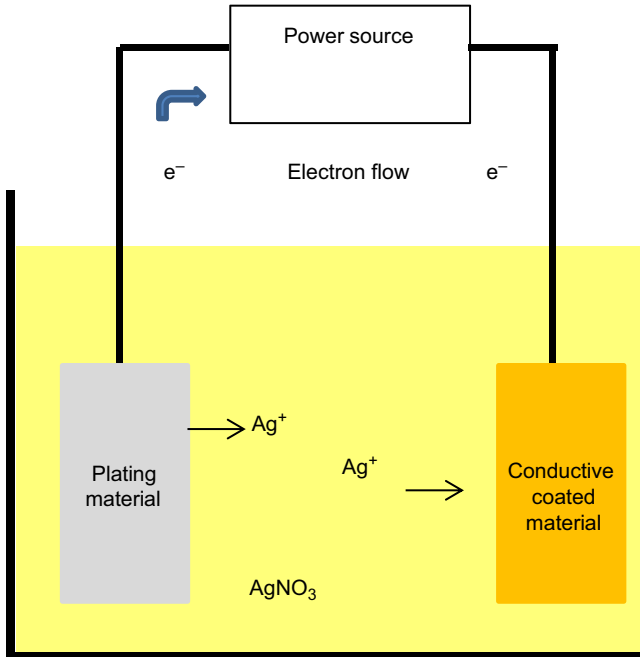


Figure 8.16 Schematic for electroplating deposition of silver.

reduced to elemental silver (Ag). The elemental silver then deposits onto the surface of the material to be coated (Antonello et al., 2012):



Wet methods can be used in addition to the vapor deposition and plating methods to create smart textile coatings. For instance, in many cases phase-change materials, microcapsules, and nanomaterials can be incorporated into textile substrates using a number of traditional methods such as padding and knife coating (Singha, 2012, pp. 39–49; Vigneshwaran, 2009, pp. 164–184; Zhang, 2001). A description of some of the more innovative, less traditional methods follows.

Sol–gel application is a wet method well-suited for the application of thin layers of inorganic or inorganic–organic hybrid materials, and particularly nanoparticles. At the heart of the sol–gel process is the sol–gel synthesis of metal oxide nanoparticles. Application of these nanoparticles to the substrate often uses a conventional process such as dip squeeze or padding. For example, a self-cleaning textile was prepared using the sol–gel process (Qi, 2008; Qi & Xin, 2010). Titanium dioxide (TiO_2) sols were prepared by hydrolysis and concentration using titanium tetra-isopropoxide ($Ti\{OCH(CH_3)_2\}_4$) as the precursor with nitric acid and the combined catalysts of nitric acid and acetic acid, respectively (Qi, 2008). The as-prepared sols were used to assemble TiO_2 films on substrates by a dip–pad–neutralize process. The resultant

textile exhibited photocatalytic self-cleaning and had the ability to decompose a colorant (Mazeyar, Farbod, Song, & Amir, 2012).

Surface modification which attaches chemical moieties to the surface of a material is also well-known. There are essentially three different ways a moiety may be attached to modify a surface. The first type of attachment is when the modifier is bound covalently to the surface of the substrate material (Allcock & Lampe, 1990; Odian, 1991). The second type of surface modification involves association or entrapment of the modifying molecule (or part of the molecule) with the substrate material (Hansen, 1967a,b; Hansen, 1969; Hansen & Skaarup, 1967; Meirowitz, 1992a,b; Meirowitz, 1993a,b). This commingling of modifier molecules and substrate uses molecular attractions such as Van der Waals forces, dipole–dipole interactions, and hydrogen bonding as well as steric factors to hold the modifier in or on the surface of the substrate. The third type of modification involves retention of the modifier by the substrate with only adhesive and cohesive forces between the modifier to the substrate and the modifier to itself, respectively (Mittal, 1976).

Grafting is a technique for providing covalent surface modification. At the heart of all grafting are some common steps:

1. Create active sites on the substrate.
2. Bring the reactive species into intimate contact.
3. Covalently graft (bond) the modifier onto the polymer backbone of the substrate.

In textile chemistry, one usually creates active sites with free radicals and the material to be grafted usually contains a vinyl moiety ($R-CH=CH_2$) which reacts with the free radical site. The names of the various grafting techniques usually refer to the ways in which the active sites are generated. Creation of the free radical sites can be performed by chemical means (chemical grafting). For instance, a mixture of perfluorooctyl-2 ethanol acrylate ($C_8F_{17}-C_2H_4-O-CO-CH=CH_2$) and stearyl methacrylate ($CH_3(CH_2)_{17}-O-CO-(CH_3)C=CH_2$) was grafted onto poly(ethylene terephthalate) to impart water repellency using benzoyl peroxide $C_6H_5CO_2\cdot$ as the initiator (Shaihi, El-Achari, Abdellah, & Caze, 2002). The benzoyl peroxide generates free radical sites on the surface of the substrate to which the acrylate portion of the modifying material attaches.

Radiation-induced grafting uses high-energy radiation (eg, gamma radiation from cobalt 60) to generate the active sites. In plasma-induced grafting, a high-energy system of ions, radicals, and metastable molecules (plasma) is used to create the active sites on the substrate. Plasmas can be generated in various gases including O_2 , N_2 , and Ar. Light-induced grafting uses materials which can be activated by ultraviolet light.

An example of a wet chemical process which uses electrostatic charge to attach the materials to the surface, instead of covalently grafting, is layer-by-layer (LbL) deposition. LbL is a self-assembly method that is useful for multilayer depositions (Decher, 2012). It can be thought of as applying layers of materials with alternating charges and using electrostatic forces to keep the layers together. Cotton fibers were prepared by LbL coating (Hyde, Rusa, & Hinstroza, 2005) with anionic poly(styrene-sulfonate) (PSS) and cationic poly(allylamine) (PAH). The cotton fibers were pretreated with

2,3-epoxypropyltrimethylammonium chloride to yield a positively charged surface. This would then receive and hold the anionic PSS. Cationic PAH was then applied to the resulting negatively charged surface. The LbL technique is useful for incorporating many different building blocks into the multilayer film and thereby holds promise for preparing versatile materials.

8.6 Future trends

When one looks at the body of research that has been and is being done in the preparation of smart textiles, a few general areas come to the forefront. These include materials development (molecules for modifying textiles), improving and optimizing existing methods of application, combining multiple areas of technology, and improving environmental and economic impacts. Many research papers have been published in these areas and quite a few bridge two or more areas. A small sample of the published references is included by way of examples. In an effort to curb redundancy, each paper is used to represent a research area even if it is applicable to more than one area.

New modified materials for application to textiles are an area in which much active research is ongoing. The use of hybrid organic–inorganic coatings using sol–gel technology has been reported (Scolan, Monnier, Voirin, Pasche, & Pugin, 2009). Graphene–MnO₂ nanostructured textiles for use as electrochemical capacitors have been prepared using a simple dip-and-dry process (Yu et al., 2011). A range of 3-alkylpyrrole monomers have been synthesized and then polymerized to form soluble conducting polymers. These were applied to the fabric by a solution polymerization method in which the monomer was polymerized on the fabric or the polymer was applied directly to the surface of the fabric as soluble polymers (Kaynak & Foitzik, 2011). Organically modified silica was applied to textile fabrics using a sol–gel process that yielded photostability and superior thermal and mechanical properties (Parhizkar, Zhao, Wang, & Lin, 2014).

Unsurprisingly, improvement and/or optimization of existing methods of application is an area of much active research. Being able to use existing techniques directly or scale them up has dramatic implications for organizations which have existing equipment to coat or modify textiles. Currently electroless plating is a popular technique for metallizing textile surfaces. The electroless plating process was optimized for silver coating of optical and plasmonic applications (Antonello et al., 2012). Work done using the LbL technique has implications which are important for textile applications. In this research, the LbL technique was applied on flat surfaces. Variations of this technique using spray-and-spin applications in addition to dip coating were performed. Implications regarding the amount of material used and ease of coverage were discussed (Decher, 2012). Stain repellency and self-cleaning properties were imparted to textiles using a sonochemical process. Sonochemical coating involves the creation, growth, and collapse of a bubble that is formed in the liquid coating material (Samal, Jeyaraman, & Vishwakarma, 2010).

The combination of multiple technologies is an area recognized by many researchers. Part of the conclusion reached in one of these studies (Gulrajani & Gupta, 2011)

was that “the future of research in textile finishing is undoubtedly based on assimilation of different sciences such as nanotechnology, physics, biotechnology and biology.” Another study (Vihodceva & Kukle, 2012) using sol–gel technology stated, “For this reason, the use of nanotechnology in the field of textiles has attracted considerable interest in recent years.” Nanoscale manipulation and composition result in improved properties and new functionalities for all kinds of textiles, such as self-cleaning, sensing, healing, decorating, actuating, and communication. Nanocomposite coating for functionalizing textiles was also presented as a topic of interest (Gashti, 2014).

Economic impact has always been a driving force in developing or improving processing techniques; increasingly, environmental impact has become a driving force. This includes using less water, lower thermal requirements, and avoiding the use of solvents with high volatile organic compounds. Plasma technology often has the drawback of requiring a high-vacuum condition. Low-pressure air plasma was examined as a way to clean cotton surfaces before vacuum evaporation and the deposition of copper on cotton (Vihodceva & Kukle, 2013). Plasma treatment had a significant effect on cotton morphology but negatively affected copper adhesion to cotton. The authors noted that one reason for looking at low-pressure plasma cleaning is that the technology “offers many advantages over wet techniques including the absence of harmful chemicals, wet processes, wastewater” Finally, a case was made for dramatic water reduction using spray and inkjet systems to deposit nano- or picodrops (Craamer, 2008; Jovic, 2008).

References

- Allcock, H., & Lampe, F. (1990). *Contemporary polymer chemistry* (2nd ed.). Englewood Cliffs, New Jersey: Prentice Hall.
- Antonello, A., Jia, B., He, Z., Buso, D., Perotto, G., Brigo, L., et al. (2012). Optimized electroless silver coating for optical and plasmonic applications. *Plasmonics*, 7(4), 633–639.
- Benkreira, H. (1993). Classification of coating flows. In H. Benkreira (Ed.), *Thin film coating* (pp. 49–57). Cambridge: The Royal Society of Chemistry.
- Craamer, J. (2008). *Textile processes for the future*. <http://www.craamer.com/TextileProcesses.pdf>.
- Creighton, J., & Ho, P. (2001). *Introduction to chemical vapor deposition (CVD)*. Materials Park, Ohio, USA: ASM International. www.asminternational.com.
- Decher, G. (2012). Layer-by-layer assembly (putting molecules to work). In G. Decher, & J. Schlenoff (Eds.), *Multilayer thin films: Sequential assembly of nanocomposite materials* (2nd ed., pp. 1–19). Wiley-VCH Verlag GmbH & Co. KGaA.
- Fung, W. (2002). *Coated and laminated textiles*. Woodhead Publishing in Association with the Textile Institute, Oxford, Cambridge, New Delhi and CRC Press, Boca Raton, Boston, New York, Washington, DC.
- Garbassi, G., Marco, M., & Occhiello, E. (1994). *Polymer surfaces: From physics to technology* (pp. 3–48). Chichester, New York, Brisbane, Toronto, Singapore: John Wiley & Sons.
- Gashti, M. (2014). Nanocomposite coatings: state of the art approach in textile finishing. *Journal of Textile Science and Engineering*, 4(2).

- Good, R. (1979). Contact angles and the surface free energy of solids. In R. Good, & R. Stromberg (Eds.), *Experimental methods: Vol. 11. Surface and colloid science* (pp. 1–25). New York and London: Plenum Press.
- Greer, F., Fraser, D., Coburn, J., & Graves, D. (2002). *Fundamental vacuum beam studies of Radical Enhanced Atomic Layer Chemical Vapor Deposition (REAL-CVD) of TiN*. http://www.avusergroups.org/tfug_pdfs/TFUG_12_2002_Greer.pdf.
- Gulrajani, M., & Gupta, D. (2011). Emerging techniques for functional finishing of textiles. *Indian Journal of Fibre and Textile Research*, 36, 388–397.
- Guo, R., & Jiang, S. (2009). Modification of textile surfaces using electroless deposition. Publishing in textiles: Number 97. In Q. Wei (Ed.), *Surface modification of textiles* (pp. 126–138). Boca Raton, Boston, New York, Washington, DC: Woodhead Publishing in Association with the Textile Institute, Cambridge and CRC Press.
- Hansen, C. (1967a). The three dimensional solubility parameter – key to paint component affinities II. – Dyes, emulsifiers, mutual solubility and compatibility, and pigments. *Journal of Paint Technology*, 39(511), 505–510.
- Hansen, C. (1967b). The three dimensional solubility parameter – key to paint component affinities I. – Solvents, plasticizers, polymers, and resins. *Journal of Paint Technology*, 39(505), 104–117.
- Hansen, C. (1969). The universality of the solubility parameter. *Industrial and Engineering Chemistry Product Research and Development*, 8(1), 2–11.
- Hansen, C., & Skaarup, K. (1967). The three dimensional solubility parameter – key to paint component affinities III. – Independent calculation of the parameter components. *Journal of Paint Technology*, 39(511), 511–514.
- Holland, S. A. (2013). *Conductive textiles and their use in combat wound detection, sensing, and localization applications* (Master's thesis) (pp. 8–10). University of Tennessee http://trace.tennessee.edu/utk_gradthes/1627.
- Hyde, K., Rusa, M., & Hinesroza, J. (2005). Layer-by-layer deposition of polyelectrolyte nanolayers on natural fibres: cotton. *Nanotechnology*, 16(7), S422. <http://iopscience.iop.org/0957-4484/>.
- Jocic, D. (2008). Smart textile materials by surface modification with biopolymeric systems. *Research Journal of Textile and Apparel*, 12(2), 58–65.
- Kaynak, A., & Foitzik, R. (2011). Methods of coating textiles with soluble conducting polymers. *Research Journal of Textile and Apparel*, 15(2), 107–113.
- Kosa. (1999). *Dictionary of fiber & textile technology* (p. 36).
- Kovacevic, S., Ujevic, D., & Brnada, S. (2010). Coated textile materials. In P. Dubrovski (Ed.), *Woven fabric engineering* (pp. 241–254). <http://www.intechopen.com/books/woven-fabric-engineering/coated-textile-materials>.
- Mazeyar, P., Farbod, A., Song, G., & Amir, G. (2012). Characterization of nanocomposite coatings on textiles : a brief review on microscopic technology. In A. Méndez-Vilas (Ed.), *Microscopy book series number 5: Vol. 1. Current microscopy contribution to advances in science and technology* (pp. 1424–1437). Badajoz, Spain: Formatex Research Center.
- Meirowitz, R. (1992a). *Method of making polyester article with a hydrophilic surface*. US Patent 5130073.
- Meirowitz, R. (1992b). *Polyester articles*. US Patent 5175050.
- Meirowitz, R. (1993a). *Method of making polyolefin articles*. US Patent 5200130.
- Meirowitz, R. (1993b). *Polyolefin articles*. US Patent 5258221.
- Mittal, K. L. (1976). Electrocomponent science and technology. In *Adhesion measurements of thin films* (Vol. 3, pp. 21–42).

- Odian, G. (1991). *Principles of polymerization* (3rd ed.). New York, Chichester, Brisbane, Toronto, Singapore: John Wiley & Sons, Inc.
- Parhizkar, M., Zhao, Y., Wang, X., & Lin, T. (2014). Photostability and durability properties of photochromic organosilica coating on fabric. *Journal of Engineered Fibers and Fabrics*, 9(3).
- Paunovic, M., Schlesinger, M., & Snyder, D. (2010). Fundamental considerations. In M. Schlesinger, & M. Paunovic (Eds.), *Modern electroplating* (5th ed., pp. 1–31). Hoboken, New Jersey: John Wiley & Sons Inc.
- Puurunen, R. (2014). A short history of atomic layer deposition: Tuomo Suntola's atomic layer epitaxy. *Chemical Vapor Deposition*, 20, 332–344.
- Qi, K. (2008). *Study of photocatalytic activities of nanoscaled metal oxides on textiles*. The Hong Kong Polytechnic University. Available from Pau Yue-kong Library (2008).
- Qi, K., & Xin, J. H. (2010). Room-temperature synthesis of single-phase anatase TiO₂ by Aging and its self-cleaning properties. *Applied Material and Interfaces*, 2(12), 3479–3485.
- Regenstein, L. (1996). *Pollution prevention for the metals finishing industry – a manual for pollution prevention technical assistance providers*. Agency NEWMOA. <http://www.p2pays.org/ref/03/02454.htm>.
- Samal, S., Jeyaraman, P., & Vishwakarma, V. (2010). Sonochemical coating of Ag-TiO₂ nanoparticles on textile fabrics for stain repellency and self-cleaning-the Indian scenario: a review. *Journal of Minerals and Materials Characterization and Engineering*, 9(6), 519–525.
- Schwartz, A. (1985). Surface tension and surface energy. In P. K. Chatterjee (Ed.), *Textile science and technology, absorbency* (Vol. 7, pp. 85–120). Amsterdam, Oxford, New York, Tokyo: Elsevier.
- Scolan, E., Monnier, V., Voirin, G., Pasche, S., & Pugin, R. (2009). *Advanced sol-gel coatings for smart textiles* (p. 65). CSEM Scientific and Technical Report.
- Shaihi, D., El-Achari, A., Abdellah, G., & Caze, C. (2002). Graft copolymerization of a mixture of perfluorooctyl-2 ethanol acrylic and stearyl methacrylate onto polyester fibers using benzoyl peroxide as initiator. *Polymer Testing*, 21(5), 607–612.
- Shim, E. (2010). Coating and laminating processes and techniques for textiles. Publishing in textiles: Number 90. In W. Smith (Ed.), *Smart textiles coatings and laminates* (pp. 10–40). Boca Raton, Boston, New York, Washington, DC: Woodhead Publishing in Association with the Textile Institute, Cambridge and CRC Press.
- Singha, K. (2012). A review on coating & lamination in textiles: processes and applications. *American Journal of Polymer Science*, 2(3), 39–49.
- Smith, W. (2000). *Coated and laminated fabrics, putting the industry in prospective*. <http://www.intexa.com/downloads/coated.pdf>.
- Tao, X. (2001). *Smart fibres, fabrics and clothing*. Boca Raton, Boston, New York, Washington, DC: Woodhead Publishing in association with the Textile Institute, Cambridge and CRC Press.
- Vihodceva, S., & Kukle, S. (2012). Cotton fabric surface modification by sol-gel deposition of ZnO thin films. *Materials Science and Engineering*, 38, 1–5.
- Vihodceva, S., & Kukle, S. (2013). Low-pressure air plasma influence on cotton textile surface morphology and evaporated Cooper coating adhesion. *American Journal of Materials Science and Technology*, 2, 1–9.
- Vigneshwaran, N. (2009). Modification of textile surfaces using nanoparticles. Publishing in textiles: Number 97. In Q. Wei (Ed.), *Surface modification of textiles* (pp. 164–184). Boca Raton, Boston, New York, Washington, DC: Woodhead Publishing in Association with the Textile Institute, Cambridge and CRC Press.

- Wang, L., Wang, X., & Lin, T. (2010). Conductive coatings for textiles. Publishing in textiles: Number 90. In W. Smith (Ed.), *Smart textiles coatings and laminates* (pp. 155–188). Boca Raton, Boston, New York, Washington, DC: Woodhead Publishing in Association with the Textile Institute, Cambridge and CRC Press.
- Wei, Q., Xu, Y., & Wang, Y. (2009). Textile surface functionalization by physical vapor deposition (PVD). Publishing in textiles: Number 97. In Q. Wei (Ed.), *Surface modification of textiles* (pp. 58–90). Boca Raton, Boston, New York, Washington, DC: Woodhead Publishing in Association with the Textile Institute, Cambridge and CRC Press.
- Wilson, J. (2009). Textile surface functionalization by chemical vapour deposition (CVD). Publishing in textiles: Number 97. In Q. Wei (Ed.), *Surface modification of textiles* (pp. 126–138). Boca Raton, Boston, New York, Washington, DC: Woodhead Publishing in Association with the Textile Institute, Cambridge and CRC Press.
- Yu, G., Hu, L., Vosgueritchian, M., Wang, H., Xie, X., McDonough, J., et al. (2011). Solution-processed graphene/MnO₂ nanostructured textiles for high-performance electrochemical capacitors. *Nano Letters*, *11*(7), 2905–2911.
- Zhang, X. (2001). Heat-storage and thermo-regulated textiles and clothing. In X. Tao (Ed.), *Smart fibres, fabrics and clothing* (pp. 34–57). Boca Raton, Boston, New York, Washington, DC: Woodhead Publishing in Association with the Textile Institute, Cambridge and CRC Press.

Microencapsulation technology for smart textile coatings

9

F. Salaün

University of Lille Nord de France, Lille, France; ENSAIT, GEMTEX, Roubaix, France

9.1 Introduction

The term ‘microencapsulation’ derives from the Greek *mikros*, meaning ‘small’, and from the Latin *en* and *capsula*, meaning ‘in’ and ‘little box’, respectively. Thus this technology refers to the formation of polymeric particles with a range of diameters from nanometres to millimetres, enclosing an active substance whatever its physical state, ie, solid, liquid or gaseous form; and that exhibits several kinds of morphologies. Microencapsulation is a growing field that has found application in many technological disciplines. However, the principle of encapsulation is old; if we consider that biochemistry to be a main founding principle of life, it is because of the presence of membranes that allow the confinement of vital molecules within the cells. Nature is filled with examples of encapsulation, ranging from macroscale to nanoscale, that protect material from the surrounding environment, such as a seed in a coat, birds’ eggs and cells in membranes (Viladot et al., 2014; Ghosh, 2006). Therefore, the development of microencapsulation processes is just an imitation of nature to gain innovating structures to immobilise, structure, release or structure active principles. Because encapsulation is used in various industrial fields; there are many definitions according to the needs of a specific field. Nevertheless, one possible generic definition may be the entrapment of a compound or system in a dispersed material to its immobilisation, its protection, its control of transfer, its structure and its functionalisation (Poncelet et al., 2007). Microparticles range in size between 1 and 1000 μm ; if they are greater than 1 mm they can be termed macroparticles, whereas if they are smaller than 1 μm they are qualified to be nanoparticles. Furthermore, particles with a mean diameter of 100 to 1000 μm are sometimes defined as milliparticles.

9.1.1 Historical background

The development of microencapsulation technology is closely related to the progress of many contemporary technologies to realise an innovative component for a particular application or industry field, and thus to create a new product application. The field of microencapsulation combines various technologies from other unrelated industrial fields, which are merged to create a new product for a specific application. Furthermore, the development of microencapsulation technology has been accompanied by a reduction in the size of particles, whereas the first applications had macroscale

ranges, which were progressively reduced to the microscale range. Thus, currently nanosized particles can be found on the market (Ripoll et al., 2012a).

The first technologies of microencapsulation via mechanical processes were developed at the end of the 19th century (Thies, 1999), and more specifically from pan coating and spray drying (Sobel et al., 2014). Nevertheless, the first attempts at microencapsulation by phase coacervation were realised in 1931 by Bungenburg de Jong and Kass (1931). Several years later, B. Green, a research chemist at the National Cash Register Company in Dayton, began investigating how the concept of microencapsulation might have potential application in copying documents. He used the concept of Bungenburg de Jong and Kass of phase coacervation and prepared the first gelatine microcapsules (Fanger, 1974). Development of this technology from the laboratory scale to industrial ones took 9 long years. In 1954, NCR introduced the first successful carbonless paper in the business world, and Green received a patent for microencapsulation on 5 July 1955.

At the end of the 1950s, microencapsulation was introduced in the pharmaceutical and chemical fields. Since then, microencapsulation processes and technologies have been constantly improved and modified as well as adapted for various purposes and uses. Thus, the development of new methods and an increasing range of new polymeric materials suitable for different entrapment techniques allowed the creation of new products and applications according to customer supply and demand or sometimes from merged projects. As described by Boh and Kardos (2003), the development of microencapsulation technology is characterised by the rapid growth of patent applications and scientific articles, reflecting industrial and university research interest in this topic. Therefore, microencapsulation has a host of potential applications in a wide range of industrial sectors, such as cosmetics, pharmaceutical and medical, electronics, waste treatment, printing, food, agriculture, biotechnology, chemical and textiles (Finch and Bodmeier, 2000; Madene et al., 2006; Vandamme et al., 2007). The microencapsulation market, mainly located in North America and Europe in 2013, is expected to growth at a compound annual growth rate of 9.7% during the forecast period from 2014 to 2020, owing to rising consumer awareness regarding the benefits of this technology and to growing awareness about health and well-being (Research, 2014).

9.1.2 Definition: generalities

Microencapsulation is a process by which individual particles of an active agent can be stored within a shell, surrounded or coated with a continuous film of polymeric material to produce particles in the micrometre to millimetre range, for protection and/or later release. Particles obtained by this process are called microparticles, microcapsules and microspheres according their morphologies and internal structure. For particles with a size range below 1 μm , the terms ‘nanoparticles’, ‘nanocapsules’ and ‘nanospheres’ are used, respectively. Furthermore, particles larger than 1000 μm are designed as macrocapsules (Thies, 2002). The nomenclature used to define different parts of the encapsulated product includes terms for the shell, ie, ‘wall’, ‘coating’, ‘membrane material’; and for the core material, ie, ‘active agent’, ‘payload’, ‘internal

phase', respectively. Different kinds of compounds such as dye, protein, fragrance, monomers, catalyst and so on can be encapsulated with different types of wall materials such as natural polymer (gelatine, cellulose, chitosan, etc.), artificial polymers (cellulosic derivatives, etc.) and synthetic polymers (polyamide, polyester, etc.), with a loading content between 5% and 90% of the microparticles in weight.

Microcapsules can exhibit a wide range of geometries and structures. Their morphologies depend mainly on the physicochemical characteristics of the core material and the deposition process or formation of the membrane around it. Thus microparticles may have regular or irregular shapes, and on the basis their morphology several classifications may be done as mononuclear or core/shell structure, multinuclear or polynuclear particles and matrix particle or microsphere. Microspheres consist of a polymeric network structure in which an active substance is distributed homogeneously, whereas microcapsules or core/shell structures exhibit a reservoir structure, ie, the core substance is surrounded by a distinct polymeric layer (Ghosh, 2006; Thies, 1996). Furthermore, the layer and the core numbers are not limited to a single one: double-layered microcapsules shell, multilayer microcapsules or dual-core particle are found in the literature; and the microparticles can also be obtained from clusters of microcapsules (Salaün et al., 2009c; Vinogradova, 2004) (Fig. 9.1). These different characteristics as well as the functional properties are dictated by the process choice and the formulation used. Gander et al. (1996) showed that the morphology of the microparticles depended mainly on the polymer solvent system.

9.1.3 Functional coating and microencapsulation

On the one hand, a functional coating as described by Wulf et al. (2002) is a system possessing the classical properties of a coating (ie, decoration and protection) and an additional functionality which may be brought, for example, by thermal insulation, moisture management, soil release, softening, self-cleaning, insect-repellent, antimicrobial or flame-retardant properties if we consider only the textile aspect (Paul, 2015). Thus, a functional coating can be sensitive to environmental changes and

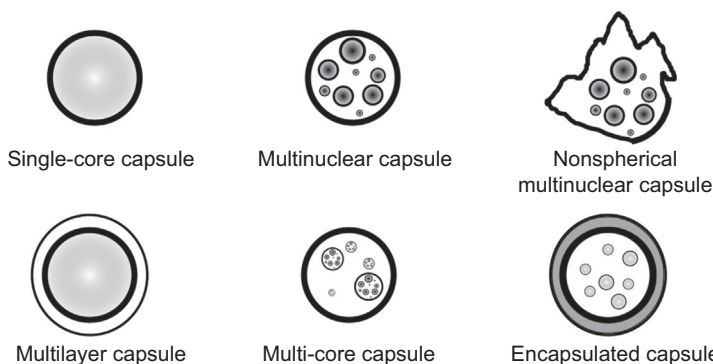


Figure 9.1 Schematic diagrams of possible particle structures according to A. Kondo (Kondo, 1979).

can permanently respond to a stimulus. On the other hand, according to [Baghdachi \(2009\)](#), a smart coating corresponds to a coating's being able to sense its environment and make an appropriate response to that stimulus in changing its physical or chemical properties, and preferably in a reversible way. Therefore, functional or smart coating can be classified as different type depending on its functional characteristics, ie, with optical, thermal, physicochemical, structural and mechanical, electrical or magnetic and hygienic properties ([Ghosh, 2006](#)). According to the property desired, the action of the functional coating can occur at the film–substrate interface, in the bulk of the coating or at the air–coating interfaces.

For the past two decades, the number of applications of capsules combined with coatings has grown to create new functional properties of the substrate, which would not be possible with any other existing technology. The coating film can act not only to promote adhesion between all components and therefore their durability, to modify the properties in the bulk such as opacity, colour, diffusion, etc., but also to improve mechanical resistance and surface state at the top surface. Therefore, according the location of the microparticles in the coating layer and their purposes, they can be completely embedded or remain partially at the surface.

9.1.4 Objective of the chapter

The textile field has significantly evolved over the past 30 years. First, textile products were based mainly on conventional technologies in the 1980s, when the product had to meet basic specifications such as a protective barrier for the body of the wearer or simply to hide it. From the 1990s onwards, with the emergence of new materials and fibres, the traditional textile was moved towards technical textiles with higher added value. Since then, textile products have become increasingly functional or multifunctional with the development of the intelligent textile or smart textiles, taking into account ecological criteria. Therefore, textile industries have grown rapidly with versatile products for a wide range of applications developed through modifying textile surfaces. In this context, the actors of the textile industry have been relatively slow to introduce microencapsulation technology in their field ([Nelson, 1991, 2001](#)), although this technology has been exploited since the 1950s in the chemical, paper and pharmaceutical industries. Currently, microcapsules can be found in various textile fields such as technical, medical and paramedical, cosmeo-textiles for various functional properties such as aesthetic effects, protection, comfort and skin care. In the highly competitive textile market, this functional coating providing additional benefits for users without modifying the basic required structure and characteristics of the product ([Erkan and Sariiski, 2004](#)).

This chapter is divided into five key areas: (1) benefits of microencapsulation for textiles; (2) microencapsulation technologies; (3) application procedures of microcapsules on textile substrate; (4) smart end uses of textile substrates containing microcapsules and (5) trends and future developments. The aim of this chapter is to provide an overview of specific encapsulation techniques used in textile applications and in other fields to show potential applications of microencapsulation in functional coatings.

9.2 Benefits of microencapsulation for textiles

According to the end use, various characteristics of microcapsules may be desired to design the final product. The size and the shape of the particles, the physicochemical properties of the shell, compatibility and permeability are some of the main parameters to consider in the choice of compounds and their associated processes. Microcapsules with porous, semiporous or impermeable shells are used for different applications.

9.2.1 Protection and shelf life enhancement

Some of the active substances used are chemically fragile, volatile when stored or unstable (chemically, thermally or physically), and cannot be used directly without being contained in a capsule. Thus, one of the main advantages of using microencapsulation technology is its ability to protect not only active substances from the surrounding environment (oxidisation, heat, acidity, alkalinity, moisture, etc.) to increase the shelf life of the product and its activity, especially for fragrance or cosmetic applications in textiles but also to prevent interaction with other compounds in the system or other components. The capsules can also prevent the evaporation of volatile substances. Furthermore, the microcapsules protect both workers and end users from exposure to toxic or hazardous substances, and therefore the active substances are handled more safely in this form before processing. This allows a soluble compound to be transformed in a temporarily insoluble form or to a complex mixture of various components to be placed in a single capsule for a specific application, such as an intumescent formulation or thermochromic solution from leuco dye. This process also allows an odour or unpleasant fragrance from active compounds to be masked during manufacture and end use.

9.2.2 Controlled release

The use of microencapsulation for controlled release is one of the best ways to increase efficiency and minimise environmental damage. This technology delays the release of an active substance until a stimulus is encountered at a specific rate, time or situation, ie, heat, moisture, mechanical pressure, etc. Thus, the shell acts as a protective barrier and can prevent diffusion and mass loss of the active substance, which allows the core compounds (fragrance, dye, drugs, enzymes, cosmetics, etc.) to be maintained intact during textile functionalisation. For these kinds of active substances, the microcapsules are expected to release the core contents to the wearer (or during the dyeing process for the dye) under a variety of controlled conditions, which depend mainly on the selection of wall materials, the microencapsulation process used and their specific end uses.

9.2.3 Compatibility

The ability to transform a liquid into a pseudosolid or powder not only prevents clumping but improves mixing of incompatible compounds. Furthermore, for a textile application, the efficiency of a binder to link microcapsules on a textile surface depends on

the compatibility of the different interfaces of the products involved in the coating process, and it closely relates to the chemical nature of each component (Salaün et al., 2009a).

9.3 Microencapsulation technologies

Although more than 200 microencapsulation methods are described in the scientific literature and patents, most include three basic steps: enclosure of core components, formation of microparticles and hardening. These methods are generally divided or classified into three main groups based on formation of the microparticles' mechanisms, such as mechanical, chemical and physicochemical processes. The choice of one method over another is based on the cost of processing and the use of organic solvents for health and environmental considerations. Polymer–solvent interactions occurring in the microencapsulation process probably have the stronger effect on the morphology and properties of the resulting particles. Thus each encapsulation step is affected by the solvency of the oil phase, and therefore, to form a distinct membrane or shell, the solvent used should favour the precipitation of the polymer at the early stage of the reaction and allow continuing diffusion of the monomers through the existing membrane to allow it to grow. Nevertheless, the microencapsulation processes used in the textile industry generally focus on chemical and physicochemical methods because mechanical processes lead to the formation of particles with a mean diameter too high for a textile application. Even if microparticles with a mean size distribution in the range of 20–40 μm are useful for textile applications (Nelson, 2001), very small microparticles (mean diameter ranging from 1 to 10 μm) are preferably incorporated within textile fibres (Cox, 1998; Bryant, 1999), but according to Colvin (2000), particles with a mean diameter less than 1 μm are suitable for fibre spinning, and larger microcapsules (mean diameter up to 100 μm) should be used for foams or coated formulations (Colvin and Bryant, 1996; Pushaw, 1997). For all that, the mean diameter of these capsules should range from several hundred nanometres to 40 μm , which is the upper limit to avoid breakage during the finishing step on textile substrates.

Therefore, the most suitable methods include interfacial, in situ and suspension polymerisation methods for chemical processes and simple or complex phase coacervation for physicochemical processes; spray drying for the mechanical processes can also be used for specific applications or to obtain dried powder (Fig. 9.2). In all cases, the microencapsulation process includes two main steps: emulsification, which determines the size and size distribution of the microcapsules; and formation of the capsules. The emulsification step may be influenced at once by physical parameters such as the apparatus configuration, stirring rate and volume ratio of the two phases, and by physicochemical properties such as interfacial tension, viscosities, densities and the chemical compositions of the two phases. The formation of microcapsules is greatly affected by the surfactant, which influences not only the mean diameter but also the stability of the dispersion. The surfactants used in the system have two roles. The first is to reduce interfacial tension between oil and aqueous phases,

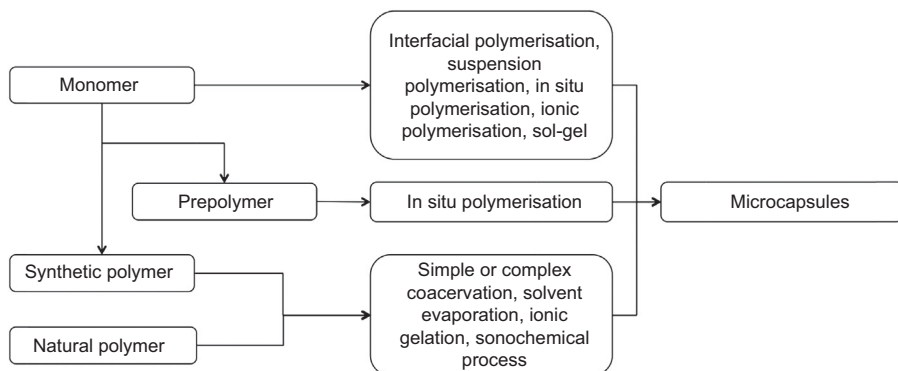


Figure 9.2 Methods to prepare microcapsules from raw shell materials.

allowing the formation of smaller microcapsules. The second is to prevent coalescence by adsorption on the oil–water interface, therefore forming a layer around the oil droplets (or around the aqueous dispersed phase). The second step, or the synthesis of a core/shell particle or other possible morphologies, is mainly governed by kinetic factors, ie, the ability of the monomers, prepolymer or polymer to react or to crosslink, and thermodynamic factors, ie, the minimum total free energy exchange in the system. The spreading coefficient should be used to predict the engulfment of the active substance within polymer in a continuous immiscible phase (Torza and Mason, 1970; Sundberg and Sundberg, 1993; Loxley and Vincent, 1998; Sánchez et al., 2007; Salaün et al., 2008). Furthermore, the choice of the polymer for the shell synthesis of the microcapsules depends on the considered application as well as the required material processes. For a textile application, these shell polymers should have sufficient thermomechanical properties to resist the thermal and mechanical request during the implementation process and daily use by the consumer.

9.3.1 Chemical processes

9.3.1.1 Interfacial polymerisation

Interfacial polymerisation, including polycondensation, polyaddition, in situ polymerisation and other heterophase polymerisation processes, is defined by the formation of the capsule shell at or on a droplet or particles by the polymerisation of reactive monomers. This technology allows a wide range of core materials to be encapsulated, such as aqueous solutions, water-immiscible liquids and solid particles. In all cases, the phase containing the core substance is dispersed until it reaches the desired droplet size in a continuous phase. A key feature of the encapsulation is the diffusion of reagents to the interface to react; during wall formation, the polymeric species create a barrier to diffusion and begin to limit the rate of the interfacial polymerisation reaction (Salaün, 2013). The interfacial polymerisation method is a widely used microencapsulation method characterised by the fact that the obtained microparticles have high

strength and stability, and membrane permeability can be adjusted or modified by selecting appropriate combinations of monomers or cross-linking agents. The use of this method is usually done so as to obtain particles with a mean diameter of 1 and 30 μm , to enhance the structural antipermeability to enable strong protection and improve the thermal stability of these particles. This process cannot easily produce microcapsules with high active loading content concentration. The polymeric shell represents only 5–15% in weight of the capsule, and it is possible to adjust the porosity and then the functionality of the shell, to control the permeation properties. The emulsification step of this process yields usually a broad size distribution influenced by the type of impeller used, the agitation rate and the concentration of emulsifier, temperature, etc. (Poncelet De Smet et al., 1989). Furthermore, the chemical nature of the active substance is an important factor to design the microencapsulation process; although most of the syntheses concern non-water-soluble active substances, the latter does not have some labile hydrogens to avoid reaction with the monomers. It seems that surfactant selection is a key parameter to limit the formation of an aggregated or agglomerated structure. A strategy described in the patent literature is to use the salt of partial ester of styrene–maleic anhydride copolymer as surfactant to encapsulate a liquid or solid with a low-melting point active substance (Lo, 1997).

The microencapsulation of an active substance by interfacial polymerisation involves the dispersion of the liposoluble phase in an aqueous continuous phase, or a hydrosoluble phase in an organic medium, depending on the solubility of the active substance, and also to induce the precipitation of the polymeric materials at the droplet interface. Each phase contains a dissolved specific monomer suitable to react with the other present in the other phase. The dispersed phase acts as a good solvent for the monomers but also serves as a nonsolvent for the formed polymer. Therefore during polymerisation, the system is composed of three mutually immiscible phases. Once, the various monomers are added to the system, the reactions occur at the interface, resulting in the formation of insoluble oligomers in the droplet with the tendency to precipitate at the interface to form a primary shell around the droplets. During growth, the polymer formed is not soluble in the dispersed phase and in the continuous phase, and precipitates at the interface. Formation of the membrane around the droplets is governed by the swelling power of both phases; a porous structure may be obtained when the solvency of the medium for the polymer is low (Arshady, 1989). Further cross-linking reactions lead to the formation of a growing shell by the diffusion of monomers. When multifunctional monomers are used, a three-dimensional cross-linked system is obtained. Nevertheless, the growing rate of the shell is relatively slow owing to the restricted diffusion of the starting monomers inducing changes in the layer morphology. The porosity of the capsules increases with the precipitation of the polymer at the interface and solvent molecule diffusion through the wall.

The main drawbacks of this technique are its complexity, the slowness of the reaction, the existence of parasite or secondary reactions that could disturb the system and create some unwanted reactive sides, the use of an organic solvent and, in some cases, nonbiocompatible carrier materials.

The morphology of the microparticles is mainly determined by the solubility of the polycondensate molecules or oligomers formed in the dispersed phase. Indeed, highly

insoluble oligomers lead to the formation of a microcapsule because they deposit themselves around the droplets to form a primary shell, where they are entrapped and can grow inside the particles to form microcapsules or microspheres if they are soluble in the dispersed droplets (Arshady, 1989). A high rate of polymer precipitation promotes the formation of a less uniform and more porous membrane. Using the interfacial polycondensation method, active core compounds are mostly encapsulated by polyurea, polyurethane (PU) and poly(urea-urethane) wall polymers for a textile application (Table 9.1). Most reported methods employ oil-in-water or water-in-oil systems, but oil-in-oil systems may also be used to prepare microcapsules, especially for PU and polyurea microcapsules.

9.3.1.2 *In situ* polymerisation

Encapsulation carried out by an *in situ* polymerisation is based on the presence of monomer or prepolymer in a single phase, either in a continuous medium or in a dispersed one. According to the monomer, prepolymer and resulting polymer solubilities in the continuous medium, Arshady and George denoted three distinct types of polymerisation: (1) suspension polycondensation, when the starting monomer was insoluble in the polymerisation medium; (2) precipitation polycondensation if the

Table 9.1 Examples of shell and core materials used in interfacial polymerisation for textile applications

Interfacial polymerisation		
Polymer	Active substance	References
Poly(urea urethane)	Dye	Chang et al. (2003)
Poly(urea urethane)	Cooling agent	Salaün et al. (2011b)
Poly(urea urethane)	Fragrance	Teixeira et al. (2012) and Rodrigues et al. (2008)
Polyurea	Dye	Yi et al. (2005)
Polyurea	Fragrance	Tekin et al. (2013)
Polyurea	Flame retardant	Giraud et al. (2001), Giraud et al. (2002), Giraud et al. (2005), and Vroman et al. (2010)
Polyurethane/polyurea	Antimicrobial agent	Salaün and Vroman (2008)
Polyurethane/chitosan	Thermochromic	Fan et al. (2015)
Polyurethane	Cosmetic agent	Azizi et al. (2014)
Cellulose derivative/PU	PCM	Salaün et al. (2010)

continuous phase was a solvent and a precipitant for the monomer and polymer, respectively and (3) dispersion polycondensation for a system when the polymerisation medium is a good and poor solvent for the monomer and polymer, respectively (Arshady and George, 1993). The microcapsules walls can be formed from starting monomers or precondensates present only in the discontinuous phase or in the continuous phase.

Among various shell materials that are presumably impermeable, amino resins, especially melamine–formaldehyde and urea–formaldehyde resins, have a main role in the encapsulation of active substance for textile applications (Table 9.2). This process was used to produce microcapsules for various applications such as fragrance or essential oils, insect repellents, flame retardants, dyes and phase change materials (PCMs). Polymerisation in situ allows the formation of microcapsules containing water-immiscible dispersed phase, with improved mechanical properties and thermal stability. The use of melamine–formaldehyde resin has attracted many researchers to improve the thermal stability of the microencapsulated core compound. Furthermore, melamine–formaldehyde prepolymers offer some advantages for the synthesis of microcapsules because of their high reactivity and therefore short reaction time and a controlled amount of polymer is required to form the shell with a high loading content, with good thermal and storage stabilities. Furthermore, other main advantages for using this microencapsulation method, which remains a popular and

Table 9.2 Examples of shell and core materials used in in situ polymerisation for textile applications

In situ polymerisation		
Polymer	Active substance	References
Melamine–formaldehyde resin	Fragrance	Hong and Park (1999), Golja et al. (2013), and Monllor et al. (2009)
Melamine–formaldehyde resin	Dye	Jun-Ling et al. (2007), Yan and Shuilin (2003), and Yan et al. (2011)
Melamine–formaldehyde resin	Fragrance, PCM	Boh and Knez (2006)
Melamine–formaldehyde resin	PCM	Shin et al. (2005) and Salaün et al. (2009b)
Melamine–formaldehyde resin	Flame retardant	Salaün et al. (2011d), Salaün et al. (2013b), and Vroman et al. (2010)
Urea–formaldehyde	PCM	Karthikeyan et al. (2014)
Polyurea–formaldehyde	PCM	Sarier and Onder (2007)
Melamine–formaldehyde	Antifungal	Erkan et al. (2010)

convenient industrial process for producing encapsulated formulations, are effective microencapsulation process, adjustable mean diameter and size distribution, and good transferability to large-scale industrial production (Boh and Sumigan, 2013).

Properties of the membrane depend not only on its chemical structure but also on all the synthesis conditions. Polycondensation of the amino resin occurs in the continuous phase, and the phase separation is linked to the pH and the formaldehyde–melamine molar ratio (Dietrich et al., 1989, 1990; Lee et al., 2002; Salaün et al., 2009b).

The first step of in situ polymerisation is to disperse a water-immiscible liquid or solid core materials in an aqueous phase containing monomers (ie, melamine and formaldehyde; urea and formaldehyde; urea, melamine and formaldehyde), or commercial prepolymers (ie, partially methylated trimethylolmelamine, dimethylolmelamine, hexamethoxy-methylolmelamine condensates), surfactant and water at an acidic pH. This dispersion is the determining step to establish the size distribution of the final particles with the desired physical properties. The acidic pH value helps to reduce surface tension of the continuous phase, because the intermolecular distance between surfactant molecules is decreased, leading to an enhanced emulsification (Salaün et al., 2009b), and to create electrostatic attraction between the resin and a polyelectrolyte (Fei et al., 2015), such as styrene–maleic acid anhydride copolymers, polyacrylic acid, or acrylamido-propylsulfonate and methacrylic acid–acrylic acid copolymers (Sliwka, 1983, 1990).

Furthermore, the phase volume ratio was established to obtain narrow size distribution and a mean diameter within the range of 1–10 μm in most studies. In the second step of the synthesis, the amino prepolymers, which are initially soluble in the continuous phase, are activated under acidic catalyst action and undergo etherification reactions. This results in an amino prepolymer of relatively low molecular weight in the continuous phase. In the third step, the reduction of hydroxyl content corresponding to a decrease in the water solubility of the amino resin can promote the phase separation from the continuous phase as a liquid solution relatively rich in active prepolymer. Thus, this phase can deposit itself as a continuous primary shell on the core material droplet by hydrogen bonds or electrostatic attraction to form a highly concentrated resin layer as the prepolymer molecular weight increases. Finally, in the fourth step, owing to enhanced resin concentration in the boundary layer, the polycondensation reaction occurs to form a cross-linked shell by ether or methylene linkages. Because the polycondensation occurs entirely on the aqueous phase side of the interface, the reactive agent does not have to be dissolved in the core material, and thus capsular morphology is obtained. To meet the technical standards, the free formaldehyde content can be reduced by adding formaldehyde scavengers in the last synthesis step, such as a primary, secondary or tertiary amine, ammonia (Frank et al., 2001) or glycine, urea, melamine, ethylene urea, sodium bisulphite acetoacetamide, etc. (Bône et al., 2011), by adjusting process parameters (temperature, pH, etc.).

9.3.1.3 Suspension polymerisation

The suspension polymerisation technique leads to the formation of particles with an average diameter between 10 μm and 2 mm, close to the initial droplet. Most of the

time, this process refers as bead polymerisation or pearl polymerisation. The dispersed phase suspended as droplet in the aqueous medium contains a water-insoluble monomer and active agent. The initiator may be solubilised in the monomer or introduced in the continuous phase. Stabilisation of these droplets in the continuous medium is ensured by the use of vigorous agitation and hydrophilic polymeric stabilisers such as poly(vinyl alcohol) (PVA), cellulosic derivative or polyvinylpyrrolidone. The aqueous phase may also contain, fillers, buffers or electrolytes. A washing step is needed after the process is completed to recover the particles. Advantages of this method, mainly used for styrene, methyl methacrylate monomers (Table 9.3), are the heat of polymerisation absorption by the continuous phase, the formation of spherical beads uniform in size and their release characteristics (Sánchez et al., 2007, 2008; Sánchez-Silva et al., 2010; Laus et al., 1996). Nevertheless, the coalescence of particles during the polymerisation process is a main drawback.

Sanchez et al. reported the development of a microencapsulation process based on the suspension polymerisation technique to entrap organic PCM by a polystyrene shell (Sánchez et al., 2007). They observed that the loading content and particle size distribution vary with the kind and nature of the core materials used. Furthermore, the method was more suitable for an active substance with a hydrophobic nature than with a hydrophilic one. They also noted that the reaction temperature affects the particle morphology, and it should be adjusted to between 98°C and 113°C to obtain spherical morphology. The particle size is closely related to the stirring rate. From the investigation of the paraffin/polymer mass ratio, they observed that encapsulation was difficult for a ratio higher than 2 (Sánchez et al., 2008). Furthermore, this encapsulation process was mainly governed by multiple simultaneous mechanisms, ie, coalescence, breakup, nucleation and diffusion of the monomer to the interface, which confers the size, structure, and surface properties of the particles. To improve these properties, they also copolymerised methyl methacrylate with styrene, which led to

Table 9.3 Examples of shell and core materials used in suspension polymerisation for textile applications

Suspension polymerisation		
Polymer	Active substance	References
PMMA	Thermochromic	Ju et al. (2002)
Poly(<i>n</i> -butyl acrylate)	PCM	Alay et al. (2011)
Polystyrene	PCM	Sánchez et al. (2010) and Sánchez-Silva et al. (2011)
Methyl methacrylate–styrene copolymer	Fragrance	Panisello et al. (2013)
poly(methyl methacrylate- <i>co</i> -acrylic acid)	PCM	Alkan et al. (2015)

a decrease in the reaction time and particle size. They also observed that the use of methyl methacrylate improved the loading content because of its higher reactivity and solubility in water.

9.3.2 Physicochemical processes

9.3.2.1 Phase coacervation

Phase coacervation is one of the oldest and most widely used techniques of microencapsulation and can be divided into two groups: simple coacervation, which implies the use of one colloidal solute such as gelatine, chitosan, etc. (Table 9.4); and complex coacervation (Table 9.5), in which the aqueous polymeric solution is prepared from the interaction of two oppositely charged colloids, such as gelatine (gum arabic or silk fibroin chitosan) (Deveci and Basal, 2009). Coacervation can be defined as the separation of a macromolecular solution into two immiscible liquid phases: a dense coacervate phase and a dilute equilibrium one. The general outline of this method consists of four consecutive steps carried out under stirring: (1) dispersion of the active substance into a solution of a surface-active hydrocolloid; (2) precipitation of the hydrocolloid onto the dispersed droplets by lowering the

Table 9.4 Examples of shell and core materials used in simple coacervation for textile applications

Simple coacervation			
Polymer	Coacervation agent	Active substance	References
Bovin serum albumin	Ethanol	Antibacterial agent	Sumithra and Vasugi Raaja (2012)
Chitosan	NaOH	Essential Oil	Souza et al. (2014)
Chitosan	Sodium dodecyl sulphate	Linseed Oil	Chatterjee et al. (2014a,b,c, 2012)
Chitosan	Sodium tripolyphosphate	Fragrance	Hu et al. (2011a)
Ethylcellulose	Water	Fragrance	Badulescu et al. (2008)
Carnauba wax/polyethylene or polystyrene	Ethanol/petroleum ether	Dye	Salaün et al. (2009c)
Gelatin	—	Acaricidal agent	Kim and Sharma (2011)
Gelatin	Acetone	Vitamin C	Cheng et al. (2009)

Table 9.5 Examples of shell and core materials used in complex coacervation for textile applications

Complex coacervation			
Polymer 1	Polymer 2	Active substance	References
Gum arabic	Gelatin	PCM	Onder et al. (2008)
Gum arabic	Gelatin	Insect repellent	Specos et al. (2010)
Gum arabic	Gelatin	Fragrance	Specos et al. (2010) and Miró Specos et al. (2010)
Gum arabic	Gelatin	Drug	Ma et al. (2009)
Gum arabic	Gelatin	Antibacterial agent	Li et al. (2013)
Gum arabic	Gelatin	Antimicrobial agent	Özyildiz et al. (2013)
Gum arabic	Chitosan	Dye	Butstraen and Salaün (2014)
Chitosan	Silk fibroin	PCM	Deveci and Basal (2009)
Chitosan	Gelatin	Antibacterial compound	Liu et al. (2013)

solubility of the hydrocolloid (nonsolvent, pH change, temperature or electrolyte); (3) addition of a second hydrocolloid to induce the polymer–polymer complex in the case of complex coacervation; and (4) stabilisation and hardening of the microcapsules by adding a cross-linking agent such as formaldehyde, glutaraldehyde or transglutaminase.

9.3.2.2 Solvent evaporation

The use of solvent evaporation or a solvent extraction method to prepare microcapsules has been widely used and investigated in the pharmaceutical field, and little studied for textile applications, except for the encapsulation of fragrance by polylactic acid (PLA) or thermochromic compound by ethyl cellulose ([Table 9.6](#)). This technical

Table 9.6 Examples of shell and core materials used in solvent evaporation for textile applications

Solvent evaporation			
Polymer	Solvent	Active substance	References
PLA	Dichloromethane	Fragrance	Hong and Park (2000)
PLA	—	Antibacterial agent	Goetzendorf-Grabowka et al. (2015)
Ethyl cellulose	Dichloromethane	Thermochromic compound	Feczko et al. (2012)

involves the use of emulsification of a solution containing coating polymers and an active substance previously dissolved in a volatile solvent in a continuous medium in which they are immiscible. The gradual removal of the solvent from the dispersed phase by heating the system allows the core substance to be coated by the polymer. The general outline of this method consists of four consecutive steps carried out under stirring: (1) dissolution or dispersion of the active substance in an organic solvent containing the coating material; (2) emulsification of this organic phase in a second continuous immiscible phase; (3) extraction of the solvent from the dispersed phase by the continuous phase by heating and (4) harvesting and drying of the microcapsules. The properties of the microcapsules depend mainly on the formulation and process parameters, such as the solubility parameters of the compounds, the type and the concentration of the dispersing agent, the selected polymer/active substance ratio, and the stirring rate and the temperature (Freitas et al., 2005).

9.3.3 Other microencapsulation methods

A variety of alternative microencapsulation techniques can also be used in textiles (Table 9.7). Among them, the use of cyclodextrins or their derivatives has gained increasing attention, especially for finishing and dyeing processes (Voncina and Vivod, 2013). Most applications revolve around the controlled release of fragrances,

Table 9.7 Miscellaneous microencapsulation process

Other methods			
Methods	Polymer	Application	References
Sonochemical	Bovine serum albumin, L-cysteine	Antibacterial	Gouveia (2012)
Ionic polymerisation	Polybutyl-cyanoacrylate	Fragrance	Hu et al. (2011a)
Ionic gelation	Alginate	Insect repellent	Anitha et al. (2011)
Sol-gel	Silica	PCM, FR, insect repellent	Liu and Lou (2015), Hu et al. (2011c), Salaün (2013b), and Chan et al. (2009)
Inclusion	β -Cyclodextrin	Insect repellent, insecticide, drug, antibacterial compounds, dye	İnceboz et al. (2015), Hebeish et al. (2014), Blanchemain et al. (2012), Ibrahim et al. (2013), and Voncina and Vivod (2013)
Coagulation	PVA/glutaraldehyde	FR	Lin et al. (2006)

insecticides and drug and antibacterial compounds, but they can also be used to capture unpleasant smells from perspiration. Processes based on sol–gel have also attracted much attention and can be considered an alternative to using melamine–formaldehyde resin even they do not offer the same guarantees.

9.4 Application procedures of microcapsules on textile substrate

The steps of encapsulation allow textiles containing microcapsules to be manufactured in various ways to fix the microcapsules within the fibre structure permanently, embed them into a binder, mix them into foam or graft them according to the expected end use. To produce these textiles, microcapsules should follow some criteria: uniformity of particle size; a ratio of core to shell with a core content as high as possible; stability to mechanical action and good thermal and chemical properties and good compatibility or affinity with the textile substrate and the binder used.

It is important to select the appropriate process of application to achieve the desired efficacy and durability of the functional coating containing microcapsules. This depends on the textile substrate (chemical nature, fibre type and construction), performance requirements (durability of the microcapsules with regard to their effectiveness), availability of the machinery, cost to benefit ratio, environmental considerations and legislation, as well as compatibility with other finishes.

Most microcapsules except silica can be applied by conventional finishing techniques or during the rinse cycle of a washing machine (Michael, 1990; DeNome et al., 2008) on any kind of fabric (woven, nonwoven, knitted or garments) regardless of their nature (natural or synthetic). Nevertheless, a main challenge in the textile field is the durability of functional properties with repeated use. In some applications such as comfort or well-being, microcapsules should not be damaged during washing cycles (at least 20 washing cycles), ironing or tumble drying.

Microcapsules can be applied to fabrics by conventional finishes treatments such as impregnation, bath exhaustion or padding, which is the most used in industrial applications, by coating or foaming and by grafting. Most of these methods require the use of a binder (acrylic, PU or silicone) to allow microcapsules to be linked to the fabric's fibres. Therefore, according to the selected functionalisation process, the adhesion of microcapsules on textiles can be achieved physically or chemically.

9.4.1 Conventional finishing treatment

Because of the lack of affinity between the microcapsules and the textile substrate, a mechanical process such as impregnation is a more appropriate method according to Monllor et al. (2007). Microcapsules can be introduced into the textile material using a dispersant to promote their diffusion through the textile material, followed by the addition of a cross-linking agent to fix them to the substrate.

In an exhaust process, the fabrics or garments are introduced in a dyeing apparatus with water. A formulation containing the microcapsule dispersion, binder, auxiliaries

and acids/bases for pH adjustment are then introduced in the apparatus at defined times, speeds, temperature and pH to allow fixation onto the textiles.

In a padding process, the fabric runs through the finishing bath containing the microcapsules, a softener, wetting agents and a binder. After emerging from the bath, the fabric is squeezed by a pair of mangles or rubber rolls at a constant pressure to reach a determined wet pickup level. The presence of the rolls is necessary to have contact between the microcapsules and the fibres. Thermal treatment with hot air in an oven is applied to remove water and to cure the resin or binder, and therefore to induce microcapsule adhesion onto the fibre surface. Monllor et al. showed that the formulation of the bath should contain 10 or 20 g/L of resin for 30 or 60 g/L of microcapsules (Monllor et al., 2009, 2007); Rodrigues et al. used 50 g/L of microcapsules and 50 g/L of binder (Rodrigues et al., 2009). The amount of binders should be sufficient to ensure good fixation without influencing the effectiveness of the microcapsules. Thus capsules completely embedded in the binder may be harder to break or the binder layer may disturb the release if the capsules are broken. Furthermore, the chemical nature of the binder used affects fixation of the capsules and therefore resistance to washing, rubbing and ironing (Salaün et al., 2009a; Sánchez et al., 2010). Furthermore, this process often leads to excessive weight add-on and poor durability and mechanical strength, with loss of feel and drape, and therefore affects the comfort of the fabrics.

Ionic bonding is another solution to fix charged capsules, such as chitosan, silica or gelatine, onto the fibre (Chatterjee et al., 2014). This method is based on the fact that the fibres have surface potential, such as polyamide in acid conditions. The capsules are synthesised so as to have cationic or anionic functional groups on the external surface of the membrane to impart affinity and strong ionic bonds between microcapsules and fibres during bath exhaustion treatment without a binder. In this case as well, one advantage is that the method may be carried out in a simple manner. A major drawback is low resistance to wetting, because after a few washes the capsules disappear from the surface of the fibres.

9.4.2 Chemical grafting

The use of a binder creates a three-dimensionally linked network, and in some cases may hinder release of the active substance. Furthermore, the lack of strong chemical bonding between the capsules and textiles results in poor washing durability and poor air permeability. Even if padding is a simple way to functionalise textiles, the applied pressure may break the microcapsules. To overcome these drawbacks, microcapsules can be covalently linked onto textiles by using polyfunctional cross-linking reagents.

Badulescu et al. used 1,2,3,4-butanetetracarboxylic acid, which can react with hydroxyl groups of cellulose to form ester bonds, to graft ethylcellulose capsules onto cotton fibres (Badulescu et al., 2008). Dimethyloldihydroxyethylene urea was used by Liu et al. as a cross-linker to form covalent bonds between hydroxyl groups of chitosan particles and cellulose, to improve washing durability (Liu et al., 2013). Citric acid was also used to graft chitosan microcapsules (Yang et al., 2014; Fan et al., 2015).

Grafting methods from particle surface modification have also been studied. The introduction of chemical reactive groups such as α -bromo-acrylic acid, adipic acid, 2,4,6-trichlorotriazine and dichloroquinoxaline, can be used to react with the microcapsule shells for further grafting reactions onto natural, synthetic or artificial fibres. Thus, [Frere et al. \(2009\)](#) and [Cuevas et al. \(2014\)](#) functionalised polyamide capsules and silica microspheres with 2,4,6-trichlorotriazine, respectively, for cotton fibres. [Hamaide et al.](#) used a click chemistry reaction for a sustainable functionalisation of cellulosic fibre to obtain a thermostable and nonhydrolysable covalent binding. From this technical, the obtained technical textiles are more resistant to washing and keep their function when worn ([Hamaide et al., 2010](#)). [N.R. Gomes et al.](#) reported successful bonding of the microcapsules to fibres by chemical grafting followed by thermal fixation ([Naylor et al., 2006](#)). Microcapsules were dispersed in water and glycidyl methacrylate monomer and potassium persulfate were added to initiate the formation of an outer shell of poly(glycidyl methacrylate). Then the microcapsules were applied by exhaustion in alkali medium to jersey cotton knitwear with a liquor ratio of 1:10 at 75°C for 30 min. After rinsing, the sample was dried at 120°C. The functional groups of the poly(glycidyl methacrylate) on the outer surface of the microcapsules directly bound to functional groups of the fibres, which also conveyed durability of the PCM microcapsule-incorporated fabric even when subjected to physical processes involving frictional forces, or chemical processes such as domestic and industrial washing, or dry cleaning.

Nevertheless, the curing time and temperature can alter the particle shell. [Salaün et al.](#) suggested the possibility of directly synthesising polyamide microcapsules onto cellulosic substrate with a high encapsulation yield around 80% ([Salaün et al., 2012](#)). [Gouveia](#) used a sonication method to produce and simultaneously bind the microspheres onto textile materials ([Gouveia, 2012](#)).

9.4.3 Coating and laminating

9.4.3.1 Coating

The use of a coating method to apply microcapsules onto the textile surface is convenient and practical. Most of these processes focus on the use of microcapsules containing PCM or flame retardant (FR). Microcapsules are dispersed in water containing a surfactant, a dispersant, an antifoam agent and a polymeric binder mixture, as described by [Zuckerman et al. \(2003\)](#). Various traditional coating methods are available, such as knife-over-roll ([Kim and Cho, 2002](#); [Pause, 1995](#)), knife-over-air, pad-dry-cure, gravure, dip coating ([Bryant and Colvin, 1996](#); [Choi et al., 2004](#)), transfer coating or screen printing ([Sutter and Lottenbach, 2002](#)) and pad-dry-cure ([Shin et al., 2005](#)). Furthermore, the use of polymeric binders has some drawbacks because the amount incorporated should be enough to obtain permanent linkage, which can alter the fabric's properties adversely, such as drape, air permeability, breathability, thermal resistance, softness, tactile comfort properties and tensile strength, as the percentage of binder add-on increases. [Salaün et al. \(2009a\)](#) proposed a thermodynamic method based on a comparison of the surface energy component to select the most suitable polymeric binder for melamine–formaldehyde

microcapsules. The polymer binder may be in the form of a solution, dispersion or emulsion in water or in an organic solvent. For most garment applications, an elastomeric polymer with a glass transition temperature varying from about -30°C to about $+12^{\circ}\text{C}$ was reported by [Sarier and Onder \(2012\)](#). However, the fabric and articles became stiff and moisture-impermeable, thereby reduced the fabric softness, flexibility, breathability and moisture transport properties.

9.4.3.2 Laminating

Microcapsules can also be incorporated into a thin polymer film and applied to a side of a fabric system by lamination. Two kinds of applications can be envisaged. The first is for glue formation, in which the microcapsules are broken to release their content. Thus, microcapsules containing a cross-linking agent can be used to preserve reactivity until the laminating process. The core content in the microcapsules may be released by heat activation or by pressure, and cross-linking of the polymer is thus achieved. The adhesive layer passes by a liquid state to allow wetting of the substrate and under the effect of the cross-linking becomes thermosetting to provide final adhesion with high quality ([Grosheins and Paire, 1994](#)). The second concerns the use of microencapsulated PCMs to improve thermophysiological wear comfort of a protective garment, as described by [Shim et al. \(2001\)](#). Shim et al. constructed one- and two-layer body suits with a fabric laminated with PU foam including 60% of mPCMs (microcapsules of PCMs) of *n*-octadecane or *n*-hexadecane, and investigated the effects of mPCMs on heat and moisture transfer in clothing. The method for manufacturing foam containing mPCMs (between 20 and 60 wt%) was first described by [Bryant and Colvin \(1996\)](#). This foam is useful in heat-insulating applications because it may be used as a lining for gloves, shoes or outerwear, when it has been integrated into the textile's complex by glue, fusion or lamination. Advantages of this technology are the use of a greater amount of mPCMs and also the possibility of incorporating various PCM formulations to cover a broad range of regulation temperatures. Furthermore, passive insulation should be increased with the formation of a honeycomb structure which can entrap a considerable amount of air ([Sarier and Onder, 2007](#)). Nevertheless, interactions between the chemical structure of the microcapsules and the polymeric material used to form the foam may lead to a defoaming process at high loading content, as observed by [You et al. \(2008\)](#).

9.4.4 Miscellaneous applications

9.4.4.1 Atmospheric plasma treatment

Surface modification of textiles by plasma treatment allows their functional performance to be modified, ie, roughens the fibre surface and therefore increases the specific surface area, polar functional groups of fabrics and wetting ability. Plasma treatments are usually employed to modify the surface of textile materials to adapt them for specific application without affecting bulk properties. These modifications also enhance the uptake of microcapsules on textiles and their adhesion, especially for hydrophobic

textile materials. Plasma posttreatment may also be used to enhance the durability of microcapsules adhered to textile, in adjusting the binder fixation. Plasma treatment can be considered a new way to promote the functional performance of textile products finished with microcapsules and achieve more durable properties, and to contribute to the sustainability of innovative textiles.

Dielectric barrier discharge plasma treatment was applied to a wool fabric by Oliveira et al. (2013) who noted a good microcapsule fixation on the surface fibre even after several wash cycles. Yuen et al. (2013) also used atmospheric pressure plasma for both pre- and posttreatments with chitosan or gelatine microcapsules. The pretreatment enhanced adhesion between the microcapsules and the surface of the fabric and therefore grafted them, whereas the posttreatment was used for thermal fixation after padding, exhaustion or printing. From results of scanning electron microscopy, they demonstrated that the cosmetic textiles could achieve satisfactory and acceptable performance at least for 10 washing cycles without causing damage to the attached microcapsules. The same observations were realised by Chatterjee et al., who used plasma treatment to enhance chitosan microcapsules to polyethylene terephthalate fibres (Chatterjee et al., 2014).

9.4.4.2 *Ultraviolet curing*

Conventional fixation processes include thermal treatment between 130°C and 170°C for 1–10 min to make the components of the binder cross-link together and then fixing the capsules onto the fabric. However, when fragrances are encapsulated, this process may lead to degradation and loss of the core compound, which reduces the amount of fragrance on the fabric and decreases durability. To overcome this problem, Li et al. investigated the effects of UV curing at low temperatures for encapsulated aroma finishing on cotton. Aroma function was prolonged to 50 washing cycles whereas the traditional curing method could withstand only 25 washing cycles. When a cotton fabric was finished with the selected aroma capsule and UV resin and cured under optimal conditions, the aroma function could withstand 50 washing cycles (Li et al., 2005).

9.4.4.3 *Electrostatic interactions*

Most of the fixation processes of microcapsules described previously induce the creation of covalent bonds with the fibres or a coating around the fibres, which entails modification to the physical or chemical structure of the fibre, which can lead to degradation and/or breakage of the textile material. Ionic bonds between the microcapsules and the fibres may overcome this problem. The binding is caused by electrostatic interaction between the negative charges of the fibres of the textile materials and the microcapsules, which were previously cationised. Principal advantages of this type of binding or link over previous types are that it is not limited to one type of active ingredient and that this type of binding to the fibres or textile materials is not detrimental to the mechanical properties of the textile material. In addition, and unlike previous types of binding of microcapsules containing active ingredients to textile materials, there is

the possibility of the final consumer himself reloading the textile material with microencapsulated active ingredients.

The process described in Patent EP 2 550 391 B1 resolves the problem of the loss of active ingredient in the fibres and/or textile materials after being washed (Viladot et al., 2014). The microencapsulated active ingredient has a cationic polymer before linking or binding the particles by exhaustion bath or foulard. The percentage of active substance present in the textile materials after five washes varied from 27% to 66% with regard to the percentage initially linked and according to the selected fabric (cotton or polyester) and the process used.

Adsorption and desorption from polyamide fibres of amino-functionalised poly(methyl methacrylate) particles, a cationic latex, was studied by Ripoll et al. (2012b,c) to determine the driving parameters governing such processes. The observed behaviour was related to the effect of ionic strength and to the reduction of cationic charges on the particle surfaces induced by increasing pH. Adsorption was mainly governed by electrostatic interactions, as evidence by the effect of salinity and pH. The adsorption process was favoured by increasing the pH of the medium, because the difference between particle and fibre zeta potentials was greater. Desorption experiments showed strong interactions between particles and fibres, with only 20% of the initially fixed particles desorbing after 10 washing cycles. They concluded that the functionalisation of washing-resistant cosmeo-textiles based on electrostatic interactions is a new functionalisation route for the preparation of active textiles.

9.4.4.4 *Double-layered shell*

For microcapsules with a double-layered shell in which the outer one is made of a thermoplastic polymer such as polystyrene (Da Rocha Gomes and Lima, 2012), polyethylene (Salaün et al., 2009c) can also be used to be fixed directly onto the textile substrate. The outer walls of the microcapsules are melted into the textile fibres through heat treatment to the softening temperature or up to the melting temperature of the thermoplastic wall. The outer shell can be synthesised either during the microencapsulation process or after it by dispersion of the synthesised capsules in a medium containing the monomer, to induce suspension polymerisation.

9.5 Smart end uses of textile substrates containing microcapsules

Fabrics containing microcapsules can be considered the latest generation of smart textiles, because new properties are brought to bear as well as added value. A smart textile is one that can provide a specific function to the wearer through the direct contact of a textile material to transfer active substances to the human body or skin. It has its own function depending on the kind of microcapsules embedded inside the fabric or fibres. Microencapsulated materials are commercially available from many companies (Van Parys, 2006) for various areas of application to offer potential for use in smart textiles.

Applications include the use of (1) PCMs and cooling agents for comfort; (2) delivery systems for cosme-to-textiles (including fragrance release, aromatherapy agents, skin moisturising or skin cooling agents, controlled release of vitamins or other agents absorbed through the skin, etc.), antimicrobials, biocides and insect repellent and resist treatments; (3) fire-retardant compounds; (4) dyes and pigments, thermochromic, or photochromic agents for dyeing and printing; (5) sizing and bonding agents; (6) blowing and expanding agents and (7) additives for washing textiles (detergents, fabric softeners, enzymes, bleaching agents and so on) (Boh and Knez, 2006). In addition, microcapsules can be used as biosensors and anticounterfeiting agents.

9.5.1 Thermal comfort (phase change material) and cooling effects

9.5.1.1 Historical background

The microencapsulation of PCMs has been widely investigated since the late 1970s to provide significantly enhanced thermal management for various application fields. Thus, preliminary work on microencapsulating PCMs began at General Electric under the sponsorship of the US Department of Energy. This was the first such attempt and was directed towards developing a two-component heat transfer fluid for use in solar systems for residential applications (Colvin and Mulligan, 1986). The microencapsulation of PCMs provides some beneficial effects for heat storage because the shape of the storage material is arbitrary, temperature gradient is more favourable and PCM lifetime increases. Furthermore, the product is always in a dried state because the phase change occurs within the coating material. The microcapsules' embedment in heat storage is relatively simple and the various PCM formulations with different melting temperatures should be used to obtain the desired temperature in which the phase change occurs. The use of microcapsules increases the specific exchange area, which is provided for effective heat transfer; and thus large quantities of thermal energy can be stored and released at a relatively constant temperature without significant volume change, because the size remains constant in the particles and sufficient space or free volume exists. Finally, the encapsulation step allows reduction or problems such as supercooling and phase separation to be avoided. Therefore, to maintain the reversibility of PCM functionality, they are encapsulated within impermeable microcapsule walls for the whole product life. Furthermore, the microcapsules need to be resistant to mechanical and thermal stresses. PCMs with a phase change temperature between -10°C and 80°C can be used for encapsulation. Furthermore, according to Lane, over 200 PCMs with a melting point from 10°C to 90°C are suitable for encapsulation (Lane, 1980).

Since 1983, Colvin and co-workers have begun investigations at Triangle Research and Development Corporation (TRDC) to demonstrate the possibility of microencapsulated paraffinic PCM. After demonstrating the possibility of manufacturing textiles containing mPCMS for the air force (Bryant and Colvin, 1988), TRDC participated from 1987 onwards in developing the encapsulation of paraffin for NASA for the use in astronaut gloves during extravehicular activities. The patent was issued in 1988 for the incorporation of mPCMs within a fibre mixture of polyester, nylon,

acrylics and modacrylics. Then, [Bryant and Colvin \(1994\)](#) demonstrated the feasibility of incorporating PCMs, ie, *n*-eicosane, 2,2-dimethyl-1,3-propanediol and 2-hydroxymethyl-2-methyl-1,3-propanediol, within textile fibres, patented in 1994. In 1991, Gateway Technologies (Outlast Technologies after 1997) acquired the exclusive patent rights for incorporating phase change technology in commercial fibres and fabrics from TRDC. Since the 1990s, Outlast Technologies has developed and patented several processes to apply microcapsules into textile structures to enhance wearer comfort and provide temperature control for consumers in bedding, medical supplies, sportswear, protective clothing, etc. Furthermore, the microencapsulation of PCMs and the manufacture of smart textile containing these microcapsules has drawn increasing interest for researchers from universities, as shown by the amount of published studies on the manufacture and thermal comfort characterisation of these materials ([Bendrowska, 2006](#); [Sarier and Onder, 2012](#)).

9.5.1.2 *Performance in textiles*

When mPCMs are applied to a textile substrate, they can absorb heat energy from the body or from the environment, to go from a solid to a liquid state, and then create a temporary cooling effect in the clothing layer until the completed melting of the core material. The reversibility of this effect can be obtained when the smart textile is worn in an environment, where the temperature is below the crystallisation point of the PCM formulation. Thus, the temperature of the smart fabrics falls below the crystallisation point, and when the liquid PCMs change back to a solid state, the heat energy is released to the surrounding medium, which gives to the wearer a temporary warming effect. From these two effects, a thermoregulating effect should be reached to keep the temperature of the surrounding medium nearly constant. Therefore, this kind of textiles can react as an active thermal barrier effect to regulate heat flux through the structure and adapt the heat flux to thermal needs according to the activity level or ambient temperature changes ([Pause, 2001](#)).

Because the sensation of thermal comfort refers to the state of mind that expresses satisfaction with the thermal environment, this feeling is influenced by various parameters in which the garment design has an important role. Thus, the use of mPCMs in clothing should act in addition to the passive thermal insulation effect of the garment system. To design a specific clothing layer, the quantity of mPCMs should be adjusted with regard to the activity level and duration of the garment worn, bearing in mind maintaining sufficient breathability, flexibility and mechanical stability of the structure. Thus, to obtain the desired effect, the manufacturer should pay attention to selecting an appropriate PCMs formulation to determine the sufficient quantity of the PCMs, choosing the appropriate fibrous substrate and designing the product ([Bendrowska, 2006](#)). The magnitude and duration of thermal effect depend on design textile factors.

9.5.1.3 *Examples of commercial applications of phase change materials*

One advantage of microencapsulated PCMs is their use for fabricating any kind of active smart textiles which sense and react to the conditions or stimulus, for a

wide and diversified market. mPCMs can be applied in various ways to the textile substrate, and thus they are permanently incorporated in the fibre to obtain thermo-regulated fibres, embedded in a coating compound during the finishing process or mixed into a foam before the lamination process to obtain a layer. mPCMs can be used for apparel (outwear underwear, gloves, military uniform, etc.), bedding (duvets, pillows, mattresses, bed linen, blankets, etc.), footwear (shoes, socks, insoles, etc.), seating (car seats, wheelchair, furniture covering, etc.) and medical applications. To date, 150 textile companies or brands such as Reebok and Timberland use mPCMs licenced by Outlast technology. Thus Outlast controls the production of mPCMs for incorporating into textiles and licences other companies to produce and sell the microcapsules. Amongst them, BASF produce Lurapret PCMs for textile applications. Microsized particles containing PCMs for interlining and gloves are sold by Outlast under Thermasorb, a trademark. The interlinings are incorporated in footwear and clothing, but they can also be used in automotive applications. Ciba Encapsulence PC410, provided by Ciba Speciality Chemicals, can be applied to fibre or coatings for automotives, clothing, buildings and floor coverings. Mikro-tek Laboratories, Inc. proposes a variety of mPCM products with a particle size between 15 and 25 μm for thermoregulation and macroparticles (3–5 mm) to regulate body temperature in a hot environment with application in cooling vests and undergarments.

9.5.1.4 *Microcapsules for a cooling effect*

Most studies on microcapsules of PCMs in clothing have been reported to provide a small temporal heating/cooling effect, for a short period of time. Other strategies can be used to obtain a cooling effect based on either physiological cooling via the stimulation of skin receptors such as Skintex Supercool (Cognis) or on physical cooling in which the cooling sensation is imparted by a decrease in the outside temperature (Maret et al., 2010). The second action concerns the use of reversible chemical reaction heat storage, which is less popular in the thermal comfort area, whereas thermo-chemical heat storage has numerous advantages, ie, high energy density, high discharge power owing to high reaction enthalpy, wide reaction temperature range, high heat and mass transfer rates, fast reaction kinetics, low material prices, nontoxic material. A wide variety of substances may result in a temperature change when in contact with an aqueous solution, eg, crystalline polyols or sugar alcohol, salt hydrates, anhydrous salts.

The core substance used in this study is xylitol, which has a cooling effect as a result of its negative heat of solution at 35°C (–36.5 kcal/kg) supported by humidity absorption, which contributes to a fresh sensation when it dissolves. A semiporous polyurea–urethane shell to improve its thermal performances has been used to encapsulate this compound (Salaün et al., 2011a,b). The microcapsules have been chemically grafted to a textile substrate to design a self-refreshing textile in which the diffusion of the sweat of the wearer through the shell induces an endothermic reaction.

9.5.2 Protection: flame retardant

9.5.2.1 Microencapsulation of flame retardant

The microencapsulation of IFR (intumescent flame retardant) has been few investigated since the late 1990s to provide the significantly enhanced thermoprotection properties and flammability of polyolefins for various application fields. Preliminary work on the microencapsulation of FRs and mainly for paint applications began in the 1970s. The aim was to improve the flame retardancy of materials by the use of flame-retardant additives, but the addition of these additives had a detrimental effect on the properties of the substrate. Thus microencapsulation has been suggested as a means to overcome most of these problems, ie, encapsulating a flame-retardant compound within a substantially impermeable shell should prevent the migration and/or volatilisation of the active substance and reduce potential toxicity.

The choice of shell materials has been widely investigated by several researchers to enhance structural antipermeability or create solid protection and to improve the thermal stability of these particles (Salaün et al., 2013c). Selection of the microencapsulation process is governed mainly by the choice of the chemical nature of shell materials and by the desired mean diameter. Thus in situ polymerisation is suitable for melamine derivatives; interfacial polymerisation is used to obtain polyurea and PU walls, whereas acrylates are obtained from dispersion polymerisation reactions, respectively. In addition, microencapsulation of IFR is essentially restricted to phosphate derivatives, which are moisture- or water-sensitive materials, whereas the process technology allows a polymeric shell to be obtained that is sufficiently tightened to prevent the diffusion of small water molecules.

9.5.2.2 Coating with microencapsulated flame retardant

For a coating process, the wetted microencapsulated flame retardants are dispersed throughout a polymeric binder, a surfactant, a dispersant, an antifoam agent and a thickener. All of the common coating processes, such as knife-over-roll, screen printing, pad-dry-cure, knife-over-air and gravure and dip coating should be used. The method for the composition of manufacturing a coating containing microcapsules has been widely described in the patent literature; nevertheless few articles published in the literature have given an account of the formulation of coating, finishing of fabrics and therefore the evaluation of their characteristics, especially the thermal and durability properties. From the 2000s onwards, Giraud et al. demonstrated the FR effect of ammonium phosphate microcapsules on cotton fabric coated with PU and polyurea binders (Giraud et al., 2001, 2002, 2005). From the cone calorimeter evaluation at 35 kW m^{-2} , they found that the microcapsules containing DAHP (diammonium hydrogen phosphate) had better performance than the raw DAHP compound. Vroman et al. evaluated the flame-retardant properties of polypropylene fabrics with three types of microcapsules containing DAHP and with various polymeric shells: ie, polyvinyl alcohol–urethane–urea, melamine–formaldehyde and melamine–poly(*n*-hexyl methacrylate)-formaldehyde (Vroman et al., 2010). Polypropylene fabric was treated

by laboratory pad-dry process in which the padding solution containing a commercial PU and microcapsules in a ratio of 1:2. The main degradation of the padded fabrics was slightly affected by the presence of microcapsules, and all the samples had a residue at 800°C under nitrogen gas. From the cone calorimeter tests, it was expected that despite a decrease in ignition time, the DAHP-containing fabrics would have decreased flame intensity with regard to the fabric. The best results were obtained for melamine–formaldehyde capsules even though they had the lowest loading content in DAHP.

9.5.3 Printing and dyeing

Microencapsulated dyes have attracted interest in the textile area for their ability to release their content upon rupturing by physical pressure or shell degradation (Lacasse and Baumann, 2004). They are also interesting because they overcome the degradation of dye able to volatilise at temperature lower than required processing in textiles; limit the environmental impact of dyeing (Jun-Ling et al., 2007); and protect sensitive dye against the environment, such as fluorescent compounds and in colour-change technology. Encapsulation methods using liposomes, molecular complexation such as cyclodextrin and interfacial and in situ polymerisations can be used to entrap the dye. For smart coating applications, the last two are mainly used.

9.5.3.1 Colour change technology

This technology deals with colour changing, which has been around for a number of years. Substances with the ability to exhibit the phenomenon of chromism (a term used for the reversible change of colour) are known as chromic materials. The reversible change results from an alteration in the electronic state involving either π - or d-electrons, and a physical change in the substance or rearrangement of molecules in a matrix, initiated by external stimuli. Depending on the stimuli involved, chromism may be classified as thermochromism (colour change owing to a change in temperature), photochromism (UV light-induced colour change), electrochromism (colour change owing to electric current flow), ionochromism (colour change related to pH variation), piezochromic (pressure-induced colour change), solvatochromism or hydrochromism (in response to the polarity of a solvent) or carsochromism (electron beam–induced colour change). The first four phenomena have been most extensively studied for textile applications as passive smart materials (Christie, 2013).

9.5.3.2 Textile application of thermochromism

The two types of thermochromic systems (Bamfield and Hutchings, 2010), ie, liquid crystalline and leuco dye, including the interaction of a colour former (leuco dye), a developer (proton donor) and a low melting solvent, may be applied to textile substrates in their microencapsulated form to protect them against undesirable influences

from surroundings. Thermochromic systems are encapsulated by complex coacervation, in situ or interfacial polymerisation (White and LeBlanc, 1999). Because of their lack of affinity and water insolubility, they are applied as pigments with binders on the fabric surface (Chowdhury et al., 2014). To obtain good colour strength, they are used at 15–30% by weight in the coating (Aitken et al., 1996), which affects the feel and handle of the textile. One drawback of these textile products is their poor wash fastness, which limits applications.

Thermochromic systems can be used on textiles for aesthetic effects (lingerie, sportswear and promotional T-shirts), apparel (T-shirts marketed by the Global Hypercolor brand since 1991), heat-sensitive labels, textile sensors and industrial clothing such as safety and protective clothes. Visualisation of changes in children's body temperature was also patented by Ebejer (2010), Babyglow has developed a pyjama indicating temperature increases such as fever to assist with baby care. The Thermochromic system was used by Carvalho et al. to stimulate the indigo-fade effect of jeans (Carvalho et al., 2010).

Thermochromic technology has been associated with electronics to develop new range of products. Chen and Huang developed thermochromic home textiles which can change colours and patterns by integrating thermochromic pigments and electrically conductive yarns into textile structures (Chen and Huang, 2015). Warning Signs, created by Nien Lam and Sue Ngo, is a textile that changes colour and patterns to indicate higher levels of carbon monoxide in the atmosphere to warn the wearer and those around.

9.5.3.3 Textile applications of photochromism

Photochromic materials are uncoloured systems which do not absorb light and may be activated only by energetically rich photons of nearby UV. For a textile application, organic compounds such as spiropyrans, spirooxanines and fulgides are mainly used to act as a sensor (Billah et al., 2008). The last category has found application in garments, toys and logos on T-shirts. Microencapsulation is used to improve the fatigue resistance of the compounds as a result of deterioration after numerous repetitive cycles of irradiation and is affected by environmental factors (Fan and Wang, 2014; Zhou et al., 2013).

Photochromism is used in textiles to provide new functional smart fabrics such as garments capable of blocking UV radiation and sensing environmental changes (Cheng et al., 2008), and also for aesthetics or functional effects such as camouflage, security printing, brand protection (Billah et al., 2008) and anticounterfeiting. Microencapsulated photochromic compounds can be applied by screen printing or by grating onto a textile surface (Feczko et al., 2013).

Di Credico et al. worked on a microencapsulation process to entrap a photochromic UV-sensitive dye dissolved in sunflower oil as a core material. After optimising the UV screening properties of the microcapsule shell by tuning the chemical composition of the core material, they demonstrated the use of such UV screening microcapsules in

functional coatings for the nondestructive in situ visual detection of mechanical damage by colour change (Di Credico et al., 2013).

9.5.4 Well-being

According to the Bureau de Normalisation des Industries Textiles et de l' Habillement, a cosmeto-textile is a textile containing a substance or preparation intended to be released permanently on different parts of the epidermis and that claims one or several special property(ies) such as cleaning, fragrance, change in appearance, protection and upkeep or correction of body odours. The integration of cosmetic ingredients started to appear in the late 1980s in Japan. The first perfumed men's handkerchiefs containing such capsules were put on the market in Europe in 1995. More and more efforts have been put into developing this technique in the textile industry, and it can be considered a French innovation, with the presence of Euracli. In 1999, Dim was the first company to launch fabrics with microcapsules containing a moisturising agent grafted on textile fibres. Multinational companies such as Cognis in 2001 and Invista in 2003 launched their brand solutions for cosmeto-textiles: in 2003, it was the creation of Lytess (France), supplier for L'Oréal since 2009 with Mixa (2010), Mennen Garnier (2011), Biotherm, and then Nivea (2014). This company is exclusively dedicated to the development and commercialisation of cosmeto-textiles and has become a European market leader as a textile brand in this area. Cosmeto-textiles represent a small niche market estimated at 500 million Euros in 2013, in which the slimming branch represents at least 10% of the slimming market. France is the first producer and consumer of these textiles, with 64% of the market in 2012. The development of new applications will provide new market opportunities for textile and apparel firms. Cosmeto-textiles can be divided into two categories: (1) dermocosmetics (skin care) and (2) aromatherapy (release of essential oil). Microcapsules containing fragrance or cosmetic agents can be applied by grafting, padding, coating, spraying or screen printing (Theberge et al., 2010) onto a textile. Nevertheless, the exhaust method requiring the control of temperature and pH is most suitable to treat knits and woven garments (Van Parys, 2006).

9.5.4.1 Dermocosmetics

Most people in the world are careful about their health and beauty, especially in an efficient and convenient way, no matter how much they have to pay for cosmetic products such as facial masks and antiageing creams. The release mechanism of a cosmetic ingredient from microcapsules is based on diffusion, molecular trigger, dissolution, thermal or biodegradation, or mechanical rupture. Major interest in microencapsulation is currently in the application of vitamins, essential oils, slimming agents, skin-moisturising agents, or compounds for energising, perfuming, refreshing, relaxing and UV protection, and also to improve the firmness and elasticity of skin.

9.5.4.2 Aromatherapy

Aromatherapy can be considered a form of alternative medicine that uses volatile compounds such as essential oils. Fragrance from the capsule is released only during the

application of pressure onto the fabric and acts as a healing substance. This type of healing with the help of fragrances using essential oils has been found to have an effect on feelings, moods and emotions. To make aromatherapy easier, textiles can be chosen as a medium. The end-use product includes ribbons, handkerchiefs, curtains and furnishings. To ensure a pharmaceutical effect, the microcapsules should contain fragrance compounds and essential oils without omitting ingredients. Furthermore, to avoid degradation during manufacturing, a low-temperature binder is required to fix the perfumed microcapsules to the textile's surface. Durability in laundering and a soft handle should be also carefully considered (Nelson, 2001). There are a myriad of essential oils with many applications, such as peppermint, which may provide clear thinking, or lavender, which is used to help people relax, as well as valerian or amber oil (Wang and Chen, 2005).

To respond to consumer demand, research and development are mainly focused on opportunities and limits for cosmetic and wellness applications of textiles, on possible ways of incorporating active substances in a functional manner with increased durability, on the characterisation model for assessing cosmetic textiles for safety and on biological safety and benefits to human skin (Cheng et al., 2009).

9.5.5 *Insect repellent*

Insect repellent compounds used in textile finishes are either synthetic chemicals such as DEET (*N,N*-diethyl-3-methylbenzamide), picaridin (1-piperidinecarboxylic acid 2-[2-hydroxyethyl]-1-methylpropylester) or permethrin, or natural products (essential oils) such as citronella, neem, lemon and eucalyptus. Insect repellent agents have been investigated but only a few have been applied to textile materials (İnceboz et al., 2015). Application of these compounds without being entrapped by the impregnation method leads to poor wash fastness. Thus most of them have been microencapsulated by sodium alginate (Anitha et al., 2011), melamine–formaldehyde (Boh and Knez, 2006) and silica (Chan et al., 2009), before being applied by pad-dry-cure to improve longevity and controlled release of the core substance.

Thus, N'Guessan et al. showed that the microencapsulation of DEET inhibits blood feeding and kills mosquitoes for at least 6 months under laboratory conditions. This formulation can find application in nets against pyrethroid-resistant mosquitoes or on clothing or bedding materials distributed in disasters, emergencies or refugee camp situations (N'Guessan et al., 2008). Textiles treated with microcapsules containing citronella developed by Miro Specos et al. have higher and longer-lasting protection from insects compared with fabrics sprayed with an ethanol solution of citronella oil, and ensure a repellent effect higher than 90% for 3 weeks. The repellent textiles were developed by padding cotton fabrics with microcapsule slurries using the conventional pad-dry method (Specos et al., 2010).

Microencapsulated lemongrass oil extract was studied by Anitha et al. for its repellence abilities and compared with extract-finished fabrics. Their results showed 92% repellence activity for polyester fabric finished with lemongrass aqueous extract microcapsules. Polyester fabric exhibited only 80% mosquito-repellent activity when it was finished with methanolic microcapsules of lemongrass leaves. Lemongrass oil

is capable of repelling mosquitoes on fabric to a greater extent. This study concluded that lemongrass oil extract exhibits significant irritant and repellent properties and deserves further investigation for possible use as active ingredients in topical skin and indoor dispersed repellent systems (Anitha et al., 2011).

The use of microencapsulated insect repellents such as sesquiterpenes, diethyltoluamide, ethyl butylacetylaminopropionate, hydroxyethyl isobutyl piperidine carboxylate, pyrethroids and their mixtures for a textile application was patented by Cognis IP Man GmbH (Mathis and Sladek, 2007). Results showed that inventive textiles finished after 25 machine washes contained more than 80% of the originally applied insect repellent whereas the content of unencapsulated insect repellent under the same conditions fell to below 40%. The use of foulard to incorporate melamine–formaldehyde microcapsules containing permethrin or toluamide is described in the US Patent 20100183690 (Paya et al., 2010). In this invention, the active ingredient may be released by skin pressure and friction. The patent filed by Syngenta Ltd. concerns a treated textile fabric with a microencapsulated insecticide and a polymeric binder (Barnett and Silverthorne Lesley, 2007). The coated or partially coated fabric maintains a sufficient amount of microencapsulated insecticide on the fabric surface to kill or repel insects, particularly mosquitoes, even after repeated washings. The fabric can be made into a net or a garment for protection against insect-transmitted diseases such as malaria.

9.5.6 Antimicrobials

Antimicrobial finishing of textiles can protect users from pathogenic or odour-generating microorganisms which can cause medical and hygienic problems, and protects textiles from undesirable aesthetic changes or damage caused by rotting, which can result in reduced functionality. As a consequence, the demand for antimicrobial finishes has become important not only because of the attitude of consumers towards hygiene and lifestyle but also in the production of protective garments and in the health care sector and home furnishings. The development of odour on areas worn close to the skin and of infections in the case of pathogen organisms is related to the development of microorganisms (bacteria, fungi, virus, etc.) under appropriate temperature, dirt and humidity conditions (Klemenčič et al., 2010; Ramachandran et al., 2004). Most antimicrobial agents applied by conventional exhaust and pad-dry-cure processes use a controlled release or leaching mechanism (Nayak and Padhye, 2015).

Chemical compounds such as quaternary ammonium compounds, triclosan, polybiguanides, metallic compounds and N-halamines are relatively toxic and their contact with the human body at high concentrations may be harmful. Thus encapsulation is one of the best methods to overcome this problem and control release, substantially diminishing toxicity. Microencapsulation also allows the use of antibacterial agents that are highly water-soluble, and that would otherwise leach out quickly from fabric during washing and sweating (Özyildiz et al., 2013).

Hassan and Sunderland (2015) microencapsulated four antibacterial agents including triclosan, dodecyltrimethylammonium chloride, PDPAC (poly(N,N-dimethyl-2-hydroxypropylammonium chloride)) and chlorhexidine gluconate and applied them to wool fabrics. Microencapsulated PDPAC had the best overall

antibacterial performance after 10 cycles of ISO 7A washing and after ageing. The encapsulated clothing had the best insect-resistant performance at a level of 50 parts per million and passed Wools of New Zealand Test Method 25 even after 10 cycles of washing. The washed fabric showed 85% mortality and mean mass loss was only 4.6 mg. The encapsulated permethrin and imidacloprid performed equally well. The handle properties were only slightly affected by the treatments.

Sánchez-Navarro et al. (2013) proposed various strategies to use microencapsulated antimicrobial compounds in footwear applications. The release of antimicrobial oil in gelatine microcapsules was proposed by shell rupture by rubbing during footwear in contact with the foot. Because controlled-release systems for long-lasting natural antimicrobial oils are employed, the use of melamine–formaldehyde microcapsules were proposed. In this case, antimicrobial oil release occurs via diffusion through the polymeric shell favoured by the temperature, humidity and sweat conditions in the shoe, which affect shell microcapsule permeability. Boh and Knez (2007) used essential oils of lavender, rosemary and sage were microencapsulated into melamine–aldehyde resin pressure-sensitive microcapsules and impregnated onto nonwoven textiles. The main goal of microencapsulating essential oils with antimicrobial properties for textile shoe insoles was to achieve targeted release during walking and no release when the shoes were not worn.

The microencapsulation of an herbal mixture by a natural encapsulation technique using yeast was developed by Saraswathi et al. (2010). The treated fabric has shown effective antimicrobial activity against *Staphylococcus*, *Escherichia coli* and *Pseudomonas*.

In Ozyildiz's article, the preparation of ozonated red pepper seed oil (ORPSO) containing microcapsules by complex coacervation and their application to nonwoven fabrics to prepare functional textiles was tested (Özyildiz et al., 2013). ORPSO has considerable antimicrobial activity against test microorganisms with antibiotic resistance. ORPSO can be readily encapsulated using complex coacervation to produce microcapsules. It was possible to obtain functional textiles by applying ORPSO-loaded microcapsules to nonwoven fabrics.

Melamine–formaldehyde polymer wall microcapsules with a triclosan core were applied to a cotton fabric by screen printing (Ocepek et al., 2012). Printed samples were dried and cured. The fabric hand properties of washed and unwashed samples were tested and antibacterial activity against *Staphylococcus aureus* and *E. coli* was evaluated. The quantity of free formaldehyde on the printed and washed samples was monitored for 2 months. Results showed that microcapsules with triclosan can be successfully applied to a cotton fabric by printing, and they provide good antibacterial protection without substantially changing the fabric properties. The quantity of formaldehyde on the unwashed samples is high and changes with time; however, it significantly decreases with washing.

9.6 Conclusions

Microencapsulation as an area for research has great potential for development, particularly in environmentally friendly formulations according to the choice of the active

ingredients to be coated, the structure of polymer membrane, method of textile finishing for fixing the particles and the functionalisation of the supports. As noted by Gordon Nelson in 2001, the ultimate achievements for most textile applications using an microencapsulation formulation are to be easily applicable, not to alter the properties of the fabric and to have having sufficient durability to the garment to simplify maintenance of the fabrics. Moreover, if the potential applications of microencapsulation in the textile field are as important as the imagination of researchers and the industry, the fact remains that the major issues are the evolution of legislation in terms of the toxicity of the products used, the biocompatibility of the raw materials of textile finishing systems in response to environmental stimuli (smart membranes), the extension of encapsulation methods for water-soluble active coating and the integration of these functional coatings (microcapsule textiles) in other application areas. Thus, future work will focus not only on microcapsules but also on the textile processes. Therefore, exploiting the potential of microencapsulation through research, process control, and the combination and adaptation of different technologies, research in textile industry must continue to open up other sectors to develop the textiles of the future desired by consumers.

References

- Aitken, D., Burkinshaw, S.M., Griffiths, J., Towns, A.D., 1996. Textile applications of thenochromic systems. *Review of Progress in Coloration and Related Topics* 26 (1), 1–8.
- Alay, S., Göde, F., Alkan, C., 2011. Synthesis and thermak properties of poly(n-butyl acrylate)/n-hexadecane microcapsules usinf different cross-linkers and their application to textile fabrics. *Journal of Applied Polymer Science* 120 (5), 2821–2829.
- Alkan, C., Aksoy, S.A., Anayurt, R.A., 2015. Synthesis of poy(methyl methacrylate-co-acrylic acid)/n-eicosane microcapsules for thermal comfort in textiles. *Textile Research Journal* 85 (19), 2051–2058.
- Anitha, R., Ramachandran, T., Rajendran, R., Mahalakshmi, M., 2011. Microencapsulation of lemon grass oil for mosquito repellent finishes in polyester textiles. *Elixir Bio Physics* 40, 5196–5200.
- Arshady, R., 1989. Preparation of microspheres and microcapsules by interfacial polycondensation techniques. *Journal of Microencapsulation* 6 (1), 13–28.
- Arshady, R., George, M.H., 1993. Suspension, dispersion, and interfacial polycondensation : a methodological survey. *Polymer Engineering and Science* 33 (14), 865–876.
- Azizi, N., Chevalier, Y., Majdoub, M., 2014. Isosorbide-based microcapsules for cosmeto-textiles. *Industrial Crops and Products* 52 (0), 150–157.
- Badulescu, R., Vivod, V., Jausovec, D., Voncina, B., 2008. Grafting of ethylcellulose microcapsules onto cotton fibers. *Carbohydrate Polymers* 71 (1), 85–91.
- Baghdachi, J., 2009. Smart coatings. In: *Smart Coatings II*. American Chemical Society, pp. 3–24.
- Bamfield, P., Hutchings, M.G., 2010. Chapter 1 phenomena involving a stimulated colour change. In: *Chromic Phenomena: Technological Applications of Colour Chemistry* (2). The Royal Society of Chemistry, pp. 9–140.
- Barnett, D., Silverthorne Lesley, A., 2007. Insecticidal Textile Material. WO 2007036710 A2.

- Bendrowska, W., 2006. Intelligent textiles with PCMs. In: Mattila, I. (Ed.), *Intelligent Textiles and Clothing*. Woodhead Publishing in Textiles, Cambridge, England, pp. 34–62.
- Billah, S.M., Christie, R., Morgan, M., 2008. Direct coloration of textiles with photochromic dyes. Part 2: the effect of solvents on the colour change of photochromic textiles. *Coloration Technology* 124, 229–233.
- Blanchemain, N., Karrou, Y., Tabary, N., Bria, M., NEUT, C., Hildebrand, H.F., Siepmann, J., Martel, B., 2012. Comparative study of vascular protheses coated with polycyclodextrines for controlled ciprofloxacin release. *Carbohydrate Polymers* 90 (4), 1695–1703.
- Boh, B., Kardos, D., 2003. Microcapsule patents and products: innovation and trend analysis. In: Arshady, R., Boh, B. (Eds.), *Microspheres, Microcapsules and Liposomes*. Citus Books, London, pp. 47–83.
- Boh, B., Knez, E., 2006. Microencapsulation of essential and phase change material for applications in textile products. *Indian Journal of Fibre & Textile Research* 31, 72–82.
- Boh, B., Knez, E., 2007. Microencapsulated antimicrobials on non-woven textiles for shoe insoles. In: XVth International Workshop on Bioencapsulation, Vienna, September 6–8.
- Boh, B., Sumigan, B., March 2013. In Situ Polymerisation Microcapsules. *Bioencapsulation Innovations*, pp. 4–6.
- Bône, S., Vautrin, C., Barbesant, V., Truchan, S., Harrison, I., Geffroy, C., 2011. Microencapsulated fragrances in melamine formaldehyde resins. *CHIMIA* 65 (3), 177–181.
- Bryant, Y.G., Colvin, D.P., 1988. Fiber with Reversible Enhanced Thermal Storage Properties and Fabrics Made Therefrom. US 4756958 A.
- Bryant, Y.G., Colvin, D.P., 1994. Fabric with Reversible Enhanced Thermal Properties. US 5366801 A.
- Bryant, Y.G., Colvin, D.P., 1996. Moldable Foam Insole with Reversible Enhanced Thermal Storage Properties. US 5499460 A.
- Bryant, Y.G., 1999. Melt spun fibres containing microencapsulated phase change material. *Advances in Heat and Mass Transfer in Biotechnology* HTD- vol. 363/BED-vol. 44, 225–234.
- Bungenburg de Jong, H.G., Kaas, A.J., 1931. Zur kenntnis der komplex-koazervation, v. Mitteilung: Relative verschiebumer im elektrischen gleichstromfelde von flüssigkeits-einschließungen in komplex-koazervat-tropfehen. *Biochem Z* 232, 338–345.
- Butstraen, C., Salaün, F., 2014. Preparation of microcapsules by complex coacervation of gum arabic and chitosan. *Carbohydrate Polymers* 99 (0), 608–616.
- Carvalho, A., Neves, J., Heriberto, J., Neves, M., 2010. Contribution of thermochromic pigments for nanocoatings on jeanswear. In: 41st International Symposium on Novelties in Textiles, Ljubljana, Slovenia.
- Chan, A.S.C., del Valle, J., Lao, K., Malapit, C., Chua, M., So, R.C., 2009. Evaluation of silica sol-gel microcapsule for the controlled release of insect repellent, *n,n*-diethyl-2-methoxybenzamide, on cotton. *Philippine Journal of Science* 138 (1), 13–21.
- Chang, C.P., Yamamoto, T., Kimura, M., Sato, T., Ichikawa, K., Dobashi, T., 2003. Release characteristics of an azo dye from poly(ureaurethane) microcapsules. *Journal of Controlled Release* 86 (2-3), 207–211.
- Chatterjee, S., Salaün, F., Campagne, C., Vaupre, S., Beirão, A., 2012. Preparation of microcapsules with multi-layers structure stabilized by chitosan and sodium dodecyl sulfate. *Carbohydrate Polymers* 90 (2), 967–975.
- Chatterjee, S., Salaün, F., Campagne, C., 2014a. Development of multilayer microcapsules by a phase coacervation method based on ionic interactions for textile applications. *Pharmaceutics* 6 (2), 281–297.

- Chatterjee, S., Salaün, F., Campagne, C., 2014b. The influence of 1-butanol and trisodium citrate ion on morphology and chemical properties of chitosan-based microcapsules during rigidification by alkali treatment. *Marine Drugs* 12 (12), 5801–5816.
- Chatterjee, S., Salaün, F., Campagne, C., Vaupre, S., Beirão, A., El-Achari, A., 2014c. Synthesis and characterization of chitosan droplet particles by ionic gelation and phase coacervation. *Polymer Bulletin* 71 (4), 1001–1013.
- Chen, H.-J., Huang, L.-H., 2015. An investigation of the design potential of thermochromic home textiles used with electric heating techniques. *Mathematical Problems in Engineering* 2015, 5.
- Cheng, S.Y., Yuen, M.C., Kan, C.W., Cheuk, K.K., Chui, C.H., Lam, K.H., 2009. Cosmetic textiles with biological benefits: gelatin microcapsules containing vitamin c. *International Journal of Molecular Medicine* 24, 411–419.
- Cheng, T., Lin, T., Brady, R., Wang, X., 2008. Photochromic fabrics with improved durability and photochromic performance. *Fibers and Polymers* 9 (5), 521–526.
- Choi, K., Cho, G., Kim, P., Cho, C., 2004. Thermal storage/release and mechanical properties of phase change materials on polyester fabrics. *Textile Research Journal* 74 (4), 292–296.
- Chowdhury, M.A., Joshi, M., Butola, B.S., 2014. Photochromic and thermochromic colorants in textile applications. *Journal of Engineered Fibers and Fabrics* 9 (1), 107–123.
- Christie, R.M., 2013. 1-chromic materials for technical textile applications. In: Gulrajani, M.L. (Ed.), *Advances in the Dyeing and Finishing of Technical Textiles*. Woodhead Publishing, pp. 3–36.
- Colvin, D.P., Mulligan, J.C., 1986. *Spacecraft Heat Rejection Methods: Active and Passive Heat Transfer for Electronic Systems – Phase 1. Final report for period September 1985–July 1986*.
- Colvin, D.P., Bryant, Y.G., 1996. Thermally Enhanced Foam Insulation.
- Colvin, D.P., 2000. Encapsulated phase change materials. In: *The 2nd International Conference on Safety & Protective Fabrics*, Winston-Salem, North Carolina, 28–30 April 2000.
- Cox, R., 1998. Synopsis of the new thermal regulation fiber outlast. *Chemical Fibers International* 48 (6), 475–479.
- Cuevas, J.M., Gonzalo, B., Rodríguez, C., Domínguez, A., Galán, D., Loscertales, I.G., 2014. Grafting electrosprayed silica microspheres on cellulosic textile via cyanuric chloride reactive groups. *Journal of Experimental Nanoscience* 10 (11), 868–879.
- Di Credico, B., Griffini, G., Levi, M., Turri, S., 2013. Microencapsulation of a uv-responsive photochromic dye by means of novel uv-screening polyurea-based shells for smart coating applications. *ACS Applied Materials & Interfaces* 5 (14), 6628–6634.
- Da Rocha Gomes, J.I.N., Lima, C.J.E., 2012. Double Walled Microcapsules with an Outer Thermoplastic Wall and Application Process Thereof. US 8329223 B2.
- DeNome, F., Berges-Cabrera, T., Wahl, E., Brown, J., Fossum, R., Catalfamo, V., Gizaw, Y., Boekley, L., 2008. Functionalized Substrates Comprising Perfume Microcapsules. US20080014393 A1.
- Deveci, S., Basal, G., 2009. Preparation of PCM microcapsules by complex coacervation of silk fibroin and chitosan. *Colloid and Polymer Science* 287 (12), 1455–1467.
- Dietrich, K., Bonatz, E., Geistlinger, H., Herma, H., Nastke, R., Purz, H.-J., Schlawne, M., Teige, W., 1989. Amino resin microcapsules. II. Preparation and morphology. *Acta Polymerica* 40 (5), 325–331.
- Dietrich, K., Bonatz, E., Nastke, R., Herma, H., Walter, M., Teige, W., 1990. Amino resin microcapsules. IV. Surface tension of the resins and mechanism of capsule formation. *Acta Polymerica* 41 (2), 91–95.

- Ebejer, C., 2010. Baby Clothing Comprising a Thermochromic Material. US 20100313325 A1.
- Erkan, G., Sariiski, M., 2004. Microencapsulation in textile. *Colourage* 51, 61–64.
- Erkan, G., Sarişik, M., Pazarlioğlu, N.K., 2010. The microencapsulation of terbinafine via in situ polymerization of melamine-formaldehyde and their application to cotton fabric. *Journal of Applied Polymer Science* 118 (6), 3707–3714.
- Fan, F., Wang, C., 2014. UV–VIS irradiation fatigue resistance improvement of azo photochromic compound using polyurethane-chitosan double shell encapsulation. *Journal of Applied Polymer Science* 131 (20) n/a–n/a.
- Fan, F., Zhang, W., Wang, C., 2015. Covalent bonding and photochromic properties of double-shell polyurethane-chitosan microcapsules crosslinked onto cotton fabric. *Cellulose* 22 (2), 1427–1438.
- Fanger, G.O., 1974. Microencapsulation: a brief history and introduction. In: Vandergaer, J.E. (Ed.), *Microencapsulation: Processes and Application*. Plenum Press, New York and London, pp. 1–20.
- Feczko, T., Samu, K., Wenzel, K., Neral, B., Voncina, B., 2012. Textiles screen-printed with photochromic ethyl cellulose-spirooxazine composite nanoparticles. *Coloration Technology* 129, 18–23.
- Feczko, T., Samu, K., Wenzel, K., Neral, B., Voncina, B., 2013. Textiles screen-printed with photochromic ethyl cellulose-spirooxazine composite nanoparticles. *Coloration Technology* 129 (1), 18–23.
- Fei, X., Zhao, H., Zhang, B., Cao, L., Yu, M., Zhou, J., Yu, L., 2015. Microencapsulation mechanism and size control of fragrance microcapsules with melamine resin shell. *Colloids and Surfaces A: Physicochemical and Engineering Aspects* 469 (0), 300–306.
- Finch, C.A., Bodmeier, R., 2000. Microencapsulation. In: *Ullmann's Encyclopedia of Industrial Chemistry*. Wiley-VCH Verlag GmbH & Co. KGaA.
- Frank, G., Biastoch, R., Kummer, M., 2001. Microcapsules of Low-formaldehyde Melamine/formaldehyde Resins. US 6261483.
- Freitas, S., Merkle, H.P., Gander, B., 2005. Microencapsulation by solvent extraction/evaporation: reviewing the state of the art of microsphere preparation process technology. *Journal of Controlled Release* 102 (2), 313–332.
- Frere, Y., Danicher, L., Merji, M., 2009. Capsules with a Modified Surface for Grafting onto Fibres. US 8586143 B2.
- Gander, B., Johansen, P., Nam-Trân, H., Merkle, H.P., 1996. Thermodynamic approach to protein microencapsulation into poly(d,l-lactide) by spray drying. *International Journal of Pharmaceutics* 129 (1–2), 51–61.
- Ghosh, S.K., 2006. Functional coatings and microencapsulation: a general perspective. In: Ghosh, S.K. (Ed.), *Functional Coatings by Polymer Microencapsulation*. WILEY-VCH Verlag GmbH & Co. KGaA, Weinheim.
- Giraud, S., Bourbigot, S., Rochery, M., Vroman, I., Tighzert, L., Delobel, R., 2001. Flame behavior of cotton coated with polyurethane containing microencapsulated flame retardant agent. *Journal of Industrial Textiles* 31 (1), 11–26.
- Giraud, S., Bourbigot, S., Rochery, M., Vroman, I., Tighzert, L., Delobel, R., 2002. Microencapsulation of phosphate: application to flame retarded coated cotton. *Polymer Degradation and Stability* 77 (2), 285–297.
- Giraud, S., Bourbigot, S., Rochery, M., Vroman, I., Tighzert, L., Delobel, R., Poutch, F., 2005. Flame retarded polyurea with microencapsulated ammonium phosphate for textile coating. *Polymer Degradation and Stability* 88 (1), 106–113.

- Goetzendork-Grabowka, B., Polus, Z., Kiwala, M., Karaszewka, A., Kaminska, I., Maczka, I., 2015. Antibacterial air filter nonwovens modified by poly(lactide) microspheres containing triclosan. *Fibres & textiles in Eastern Europe* 23 (1(109)), 114–119.
- Golja, B., Šumiga, B., Forte Tavčer, P., 2013. Fragrant finishing of cotton with microcapsules: Comparison between printing and impregnation. *Coloration Technology* 129 (5), 338–346.
- Gouveia, I.C., 2012. Synthesis and characterization of a microsphere-based coating for textiles with potential as an in situ bioactive delivery system. *Polymers for Advanced Technologies* 23 (3), 350–356.
- Groshens, P., Paire, C., 1994. Thermally Adhesive Textile Item Comprising a Micro-encapsulated Crosslinking Agent. EP 0326444 B1.
- Hamaide, T., Fleury, E., Bertholon, I., Drockenmuller, E., Tillement, O., Roux, S., Boulon, G., 2010. Fibres de polysaccharides sur lesquelles des nanoparticules sont greffées par click chemistry. FR 10 53849.
- Hassan, M.M., Sunderland, M., 2015. Antimicrobial and insect-resist wool fabrics by coating with microencapsulated antimicrobial and insect-resist agents. *Progress in Organic Coatings* 85 (0), 221–229.
- Hebeish, A., El-Sawy, S.M., Ragaei, M., Hamdy, I.A., El-Bisi, M.K., Abdel-Mohdy, F.A., 2014. New textiles of biocidal activity by introduce insecticide in cotton-poly(GMA) copolymer containing β -cd. *Carbohydrate Polymers* 99 (0), 208–217.
- Hong, K., Park, S., 2000. Preparation of poly(l-lactide) microcapsules for fragrant fiber and their characteristics. *Polymer* 41 (12), 4567–4572.
- Hu, J., Xiao, Z.B., Zhou, R.-J., Ma, S.-S., Li, Z., Wang, M.-X., 2011a. Comparison of compounded fragrance and chitosan nanoparticles loaded with fragrance applied in cotton fabrics. *Textile Research Journal* 81 (19), 2056–2064.
- Hu, J., Xiao, Z., Li, Z., Wang, M., Ma, S., 2011b. Synthesis and characterization of poly-butylcyanoacrylate-encapsulated rose fragrance nanocapsules. *Flavour and Fragrance Journal* 26, 162–173.
- Hu, J., Xiao, Z., Zhou, R., Ma, S., Wang, M., Li, Z., 2011c. Properties of aroma sustained-release cotton fabric with rose fragrance nanocapsules. *Chinese Journal of Chemical Engineering* 19 (3), 523–528.
- Ibrahim, N.A., Eid, B.M., Youssef, M.A., Ibrahim, H.M., Ameen, H.A., Salah, A.M., 2013. Multifunctional finishing of cellulosic/polyester blended fabrics. *Carbohydrate Polymers* 97 (2), 783–793.
- İnceboz, T., Erkan, G., Türkoğlu, G.C., Saruşık, A.M., Bakırcı, S., Üner, S., Üner, A., 2015. In-vivo and in-vitro tick repellent properties of cotton fabric. *Textile Research Journal* 85 (19), 2071–2082.
- Ju, H.K., Kim, J.W., Han, S.H., Chang, I.S., Kim, H.K., Kang, H.H., Lee, O.S., Suh, K.D., 2002. Thermotropic liquid-crystal/polymer microcapsules prepared by in situ suspension polymerization. *Colloid and Polymer Science* 280 (10), 879–885.
- Jun-Ling, J., Shui-Lin, C., Xu-Jie, Y., Lu-De, L., Xin, W., Li-Min, Y., 2007. The dyeing of nylon with a microencapsulated disperse dye. *Coloration Technology* 123 (5), 333–338.
- Karthikeyan, M., Ramachandran, T., Sundaram, O.S., 2014. Nanoencapsulated phase change materials based on polyethylene glycol for creating thermoregulating cotton. *Journal of Industrial Textiles* 44 (1), 130–146.
- Kim, J., Cho, G., 2002. Thermal storage/release, durability, and temperature sensing properties of thermostatic fabrics treated with octadecane-containing microcapsules. *Textile Research Journal* 72 (12), 1093–1098.

- Kim, J.R., Sharma, S., 2011. Acaricidal activities of clove bud oil and red thyme oil using microencapsulation against hdms. *Journal of microencapsulation* 28 (1), 82–91.
- Klemenčič, D., Simončič, B., Tomšič, B., Orel, B., 2010. Biodegradation of silver functionalised cellulose fibres. *Carbohydrate Polymers* 80 (2), 426–435.
- Kondo, A., 1979. *Microcapsule processing and technology*. Marcel Dekker, New York.
- Li, S., Boyter, H., Qian, L., 2005. Uv curing for encapsulated aroma finish on cotton. *The Journal of The Textile Institute* 96 (6), 407–411.
- Lin, M., Yang, Y., Xi, P., Chen, S.L., 2006. Microencapsulation of water-soluble flame retardant containing organophosphorus and its application on fabric. *Journal of Applied Polymer Science* 102 (5), 4915–4920.
- Liu, X., Lou, Y., 2015. Preparation of microencapsulated phase change materials by the sol-gel process and its application on textiles. *Fibres & Textiles in Eastern Europe* 23 (2(110)), 63–67.
- Lo, C.-C., 1997. *Microcapsule Suspension and a Process for Its Preparation*. EP19920811017 19921222.
- Lacasse, K., Baumann, W., 2004. *Textile Chemicals — Environmental Data and Facts*. Springer-Verlag, Berlin.
- Lane, G.A., 1980. Low temperature heat storage with phase change materials. *International Journal of Ambient Energy* 1 (3), 155–168.
- Laus, M., Dinnella, C., Lanzarini, G., Casagrande, A., 1996. Core-shell functional microspheres by dispersion polymerization: 2. Synthesis and characterization. *Polymer* 37 (2), 343–347.
- Lee, H.-Y., Lee, S.-J., Cheong, W., Kim, J.-H., 2002. Microencapsulation of fragrant oil via in situ polymerisation: effects of ph and melamine-formaldehyde molar ratio. *Journal of Microencapsulation* 19 (5), 559–569.
- Li, L., Au, W., Hua, T., Zhao, D., Wong, K., 2013. Improvement in antibacterial activity of moxa oil containing gelatin-arabic gum microcapsules. *Textile Research Journal* 83 (12), 1236–1241.
- Liu, J., Liu, C., Liu, Y., Chen, M., Hu, Y., Yang, Z., 2013. Study on the grafting of chitosan–gelatin microcapsules onto cotton fabrics and its antibacterial effect. *Colloids and Surfaces B: Biointerfaces* 109 (0), 103–108.
- Loxley, A., Vincent, B., 1998. Preparation of poly(methylmethacrylate) microcapsules with liquid cores. *Journal of Colloid and Interface Science* 208 (1), 49–62.
- Ma, Z.-H., Yu, D.-G., Branford-White, C.J., Nie, H.-L., Fan, Z.-X., Zhu, L.-M., 2009. Microencapsulation of tamoxifen: Application to cotton fabric. *Colloids and Surfaces B: Biointerfaces* 69 (1), 85–90.
- Madene, A., Jacquot, M., Scher, J., Desobry, S., 2006. Flavour encapsulation and controlled release — a review. *International Journal of Food Science & Technology* 41 (1), 1–21.
- Maret, O., Tillmann, B., Bedek, G., Salaun, F., Devaux, E., Dupont, D., Deranton, D., 2010. Microcapsules for Self-refreshing Textile. EP 2218498 A2.
- Mathis, R., Sladek, H.J., 2007. *Fibres and Textile Sheet Prepared for Repelling Insects*. EP 1845186 A1.
- Michael, D.W., 1990. *Microcapsules Containing Hydrophobic Liquid Core*. EP0385535 A1.
- Monllor, P., Bonet, M.A., Cases, F., 2007. Characterization of the behaviour of flavour microcapsules in cotton fabrics. *European Polymer Journal* 43 (6), 2481–2490.
- Monllor, P., Sánchez, L., Cases, F., Bonet, M.A., 2009. Thermal behavior of microencapsulated fragrances on cotton fabrics. *Textile Research Journal* 79 (4), 365–380.
- N'Guessan, R., Knols, B.G.J., Pennetier, C., Rowland, M., 2008. Deet microencapsulation: a slow-release formulation enhancing the residual efficacy of bed nets against malaria vectors. *Transactions of the Royal Society of Tropical Medicine and Hygiene* 102 (3), 259–262.

- Nayak, R., Padhye, R., 2015. 12-antimicrobial finishes for textiles. In: Roshan, P. (Ed.), *Functional Finishes for Textiles*. Woodhead Publishing, pp. 361–385.
- Naylor, R.G.J.L., Magalhaes, V.V.R.M., Pinto, C.B.S., 2006. Microcapsules with Functional Reactive Groups for Binding to Fibres and Process of Application and Fixation. WO 2006117702 A2.
- Nelson, G., 1991. Microencapsulates in textile coloration and finishing. *Review of Progress in Coloration and Related Topics* 21 (1), 72–85.
- Nelson, G., 2001. Microencapsulation in textile finishing. *Review of Progress in Coloration and Related Topics* 31 (1), 57–64.
- Ocepek, B., Boh, B., Šumiga, B., Tavčer, P.F., 2012. Printing of antimicrobial microcapsules on textiles. *Coloration Technology* 128 (2), 95–102.
- Oliveira, F.R., Fernandes, M., Carneiro, N., Pedro Souto, A., 2013. Functionalization of wool fabric with phase-change materials microcapsules after plasma surface modification. *Journal of Applied Polymer Science* 128 (5), 2638–2647.
- Onder, E., Sarier, N., Cimen, E., 2008. Encapsulation of phase change materials by complex coacervation to improve thermal performances of woven fabrics. *Thermochimica Acta* 467 (1-2), 63–72.
- Özyildiz, F., Karagönlü, S., Basal, G., Uzel, A., Bayraktar, O., 2013. Micro-encapsulation of ozonated red pepper seed oil with antimicrobial activity and application to nonwoven fabric. *Letters in Applied Microbiology* 56 (3), 168–179.
- Panisello, C., Peña, B., Gilabert Oriol, G., Constantantí, M., Gumí, T., Garcia-Valls, R., 2013. Polysulfone/vanillin microcapsules for antibacterial and aromatic finishing of fabrics. *Industrial and Engineering Chemistry Research* 52 (29), 9995–10003.
- Paul, R., 2015. 1-functional finishes for textiles: an overview. In: Paul, R. (Ed.), *Functional Finishes for Textiles*. Woodhead Publishing, pp. 1–14.
- Pause, B., 1995. Development of heat and cold insulating membrane structures with phase change material. *Journal of Industrial Textiles* 25 (1), 59–68.
- Pause, B.H., 2001. Interactive Thermal Insulating System Having a Layer Treated with a Coating of Energy Absorbing Phase Change Material Adjacent a Layer of Fibers Containing Energy Absorbing Phase Change Material. US Patent 6217993.
- Paya, J.G., Aracil, M.A.B., Aboy, P.M.R., Perez, P.M., 2010. Insect Repellent Textile. US 20100183690 A1.
- Poncelet, D., Dreffier, C., Subra-Paternault, P., Vandamme, T., 2007. Introduction aux techniques de microencapsulation. In: Vandamme, T., Poncelet, D., Subra-Paternault, P. (Eds.), *Microencapsulation: Des Sciences Aux Technologies*. Editions TEC & DOC, Paris.
- Poncelet De Smet, B., Poncelet, D., Neufeld, R.J., 1989. Control of mean diameter and size distribution during formulation of microcapsules with cellulose nitrate membranes. *Enzyme and Microbial Technology* 11 (1), 29–37.
- Pushaw, R.J., 1997. Coated Skived Foam and Fabric Article Containing Energy Absorbing Phase Change Material.
- Ramachandran, T., Rajendrakumar, K., Rajendran, R., 2004. Antimicrobial textiles—an overview. *Journal of the Institution of Engineers (India), Part TX: Textile Engineering Division* 84 (2), 42–47.
- Research, G.V., 2014. *Microencapsulation Market for Pharmaceuticals Household Products Agrochemicals Food Additives and Other Applications Global Industry Analysis Size Share Growth Trends and Forecast 2014 2020*. Grand View Research, Inc.
- Ripoll, L., Bordes, C., Fessi, H., Elaissari, A., Faure, P., Etheve, S., 2012a. Cationic Micro-particles and Use in the Field of Cosmetotextiles. WO/2012/107694.

- Ripoll, L., Bordes, C., Marote, P., Etheve, S., Elaissari, A., Fessi, H., 2012b. Polymer particle adsorption at textile/liquid interfaces: a simple approach for a new functionalization route. *Polymer International* 61 (7), 1127–1135.
- Ripoll, L., Bordes, C., Marote, P., Etheve, S., Elaissari, A., Fessi, H., 2012c. Electrokinetic properties of bare or nanoparticle-functionalized textile fabrics. *Colloids and Surfaces A: Physicochemical and Engineering Aspects* 397 (0), 24–32.
- Rodrigues, S.N., Martins, I.M., Fernandes, I.P., Gomes, P.B., Mata, V.G., Barreiro, M.F., Rodrigues, A.E., 2009. Scentfashion®: microencapsulated perfumes for textile application. *Chemical Engineering Journal* 149 (1–3), 463–472.
- Rodrigues, S.N., Fernandes, I., Martins, I.M., Mata, V.G., Barreiro, F., Rodrigues, A.E., 2008. Microencapsulation of limonene for textile application. *Industrial & Engineering Chemistry Research* 47 (12), 4142–4147.
- Salaün, F., Devaux, E., Bourbigot, S., Rumeau, P., 2008. Preparation of multinuclear micro-particles using a polymerization in emulsion process. *Journal of Applied Polymer Science* 107 (4), 2444–2452.
- Salaün, F., Vroman, I., 2008. Nanoencapsulation of curcumin prior their incorporation on textile substrate to improve antibacterian property. In: 8th Autex World Textile Conference, Biella, Italia, 24–26 June.
- Salaün, F., Devaux, E., Bourbigot, S., Rumeau, P., 2009a. Application of contact angle measurement to the manufacture of textiles containing microcapsules. *Textile Research Journal* 79 (13), 1202–1212.
- Salaün, F., Devaux, E., Bourbigot, S., Rumeau, P., 2009b. Influence of process parameters on microcapsules loaded with n-hexadecane prepared by in situ polymerization. *Chemical Engineering Journal* 155 (1–2), 457–465.
- Salaün, F., Vroman, I., Aubry, C., 2009c. Preparation of double layered shell microparticles containing an acid dye by a melt dispersion-coacervation technique. *Powder Technology* 192 (3), 375–383.
- Salaün, F., Devaux, E., Bourbigot, S., Rumeau, P., 2010. Influence of the solvent on the microencapsulation of an hydrated salt. *Carbohydrate Polymers* 79 (4), 964–974.
- Salaün, F., Bedek, G., Devaux, E., Dupont, D., 2011a. Influence of the washings on the thermal properties of polyurea-urethane microcapsules containing xylitol to provide a cooling effect. *Materials Letters* 65 (2), 381–384.
- Salaün, F., Bedek, G., Devaux, E., Dupont, D., Gengembre, L., 2011b. Microencapsulation of a cooling agent by interfacial polymerization: influence of the parameters of encapsulation on poly(urethane-urea) microparticles characteristics. *Journal of Membrane Science* 370 (1–2), 23–33.
- Salaün, F., Lewandowski, M., Vroman, I., Bedek, G., Bourbigot, S., 2011d. Development and characterisation of flame-retardant fibres from isotactic polypropylene melt-compounded with melamine-formaldehyde microcapsules. *Polymer Degradation and Stability* 96 (1), 131–143.
- Salaün, F., Vroman, I., Elmajid, I., 2012. A novel approach to synthesize and to fix microparticles on cotton fabric. *Chemical Engineering Journal* 213 (0), 78–87.
- Salaün, F., 2013. Microencapsulation by interfacial polymerization. In: Mittal, V. (Ed.), *Encapsulation Nanotechnologies*. John Wiley & Sons, Inc, Hoboken, NJ, USA, pp. 137–173.
- Salaün, F., Creach, G., Rault, F., Almeras, X., 2013a. Thermo-physical properties of polypropylene fibers containing a microencapsulated flame retardant. *Polymer for Advanced Technologies* 24 (2), 236–248.

- Salaün, F., Creach, G., Rault, F., Giraud, S., 2013b. Microencapsulation of bisphenol-A bis(diphenyl phosphate) and influence of particle loading on thermal and fire properties of polypropylene and polyethylene terephthalate. *Polymer Degradation and Stability* 98 (12), 2663–2671.
- Salaün, F., Giraud, S., Vroman, I., Rault, F., 2013c. A review of microencapsulation of flame retardant formulations suitable for application in polypropylene textile substrates. In: Siva, L.P., Barbosa, E.F. (Eds.), *Polypropylene: Synthesis, Applications and Environmental Concerns*. NOVA Publishers, pp. 195–222.
- Sánchez-Navarro, M.M., Pérez-Limiñana, M.A., Cuesta-Garrote, N., Maestre-López, M.I., Bertazzo, M., Martínez-Sánchez, M.A., Orgilés-Barceló, C., Arán-Aís, F., 2013. Latest developments in antimicrobial functional materials for footwear. In: Méndez-Vilas, A. (Ed.), *Microbial Pathogens and Strategies for Combating Them: Science, Technology and Education*. Formatex.
- Sánchez-Silva, L., Rodríguez, J.F., Romero, A., Borreguero, A.M., Carmona, M., Sánchez, P., 2010. Microencapsulation of PCMs with a styrene-methyl methacrylate copolymer shell by suspension-like polymerisation. *Chemical Engineering Journal* 157 (1), 216–222.
- Sánchez-Silva, L., Rodríguez, J.F., Carmona, M., Romero, A., Sánchez, P., 2011. Thermal and morphological stability of polystyrene microcapsules containing phase-change materials. *Journal of Applied Polymer Science* 120 (1), 291–297.
- Sánchez, L., Sánchez, P., de Lucas, A., Carmona, M., Rodríguez, J., 2007. Microencapsulation of PCMs with a polystyrene shell. *Colloid & Polymer Science* 285 (12), 1377–1385.
- Sánchez, L., Sánchez, P., Carmona, M., de Lucas, A., Rodríguez, J., 2008. Influence of operation conditions on the microencapsulation of PCMs by means of suspension-like polymerization. *Colloid & Polymer Science* 286 (8), 1019–1027.
- Saraswathi, R., Krishnan, P.N., Dilip, C., 2010. Antimicrobial activity of cotton and silk fabric with herbal extract by micro encapsulation. *Asian Pacific Journal of Tropical Medicine* 3 (2), 128–132.
- Sarier, N., Onder, E., 2007. The manufacture of microencapsulated phase change materials suitable for the design of thermally enhanced fabrics. *Thermochim Acta* 452 (2), 149–160.
- Sarier, N., Onder, E., 2012. Organic phase change materials and their textile applications: an overview. *Thermochim Acta* 540 (0), 7–60.
- Shim, H., McCullough, E.A., Jones, B.W., 2001. Using phase change materials in clothing. *Textile Research Journal* 71 (6), 495–502.
- Shin, Y., Yoo, D.-I., Son, K., 2005. Development of thermoregulating textile materials with microencapsulated phase change materials (PCM). II. Preparation and application of PCM microcapsules. *Journal of Applied Polymer Science* 96 (6), 2005–2010.
- Sliwka, W., 1983. Process for the Preparation of Microcapsules, and the Microcapsules Obtained Thereby. US 4406816.
- Sliwka, W., 1990. Continuous Preparation of Microcapsules with Melamine-formaldehyde Condensate Walls in Aqueous Dispersion. US 4898696.
- Sobel, R., Versic, R., Gaonkar, A.G., 2014. Chapter 1-introduction to microencapsulation and controlled delivery in foods. In: Gaonkar, A.G., Vasisht, N., Khare, A.R., Sobel, R. (Eds.), *Microencapsulation in the Food Industry*. Academic Press, San Diego, pp. 3–12.
- Souza, J.M., Caldas, A.L., Tohidi, S.D., Molina, J., Souto, A.P., Fangueiro, R., Zillz, A., 2014. Properties and controlled release of chitosan microencapsulated limonene oil. *Revista Brasileira de Farmacognosia* 24 (6), 691–698.

- Specos, M.M., Garcia, J.J., Tornesello, J., Marino, P., Vecchia, M.D., Tesoriero, M.V., Hermida, L.G., 2010. Microencapsulated citronella oil for mosquito repellent finishing of cotton textiles. *Transactions of the Royal Society of Tropical Medicine and Hygiene* 104 (10), 653–658.
- Sumithra, M., Vasugi Raaja, N., 2012. Micro-encapsulation and nano-encapsulation of denim fabrics with herbal extracts. *Indian Journal of Fibre and Textile Research* 37 (4), 321–325.
- Sundberg, E.J., Sundberg, D.C., 1993. Morphology development for three-component emulsion polymers: Theory and experiments. *Journal of Applied Polymer Science* 47 (7), 1277–1294.
- Sutter, S., Lottenbach, R., 2002. Method for Producing Temperature-regulating Surfaces with Phase Change Material. WO 2002095314 A1.
- Teixeira, M.A., Rodríguez, O., Rodrigues, S., Martins, I., Rodrigues, A.E., 2012. A case study of product engineering: Performance of microencapsulated perfumes on textile applications. *AIChE Journal* 58 (6), 1939–1950.
- Tekin, R., Bac, N., Erdogmus, H., 2013. Microencapsulation of fragrance and natural volatile oils for application in cosmetics, and household cleaning products. *Macromolecular Symposia* 333 (1), 35–40.
- Theberge, K., Goudreault, I., Quirion, F., Perron, G., 2010. Articles of Manufacture Releasing an Active Ingredient. US 20100226947 A1.
- Thies, C., 1996. A survey of microencapsulation processes. In: Benita, S. (Ed.), *Microencapsulation Methods and Industrial Applications*. Marcel Dekker, Inc, New York, USA, pp. 1–19.
- Thies, C., 1999. A short history of microencapsulation technology, microspheres, microcapsules and liposomes. In: Arshady, R. (Ed.), *Preparation & Chemical Applications*. Citus Books, London.
- Thies, C., 2002. Microencapsulation. In: *Encyclopedia of Polymer Science and Technology*. John Wiley & Sons, Inc.
- Torza, S., Mason, S.G., 1970. Three-phase interactions in shear and electrical fields. *Journal of Colloid and Interface Science* 33 (1), 67–83.
- Vandamme, T., Poncelet, D., Subra-Paternault, P., 2007. *Microencapsulation: Des Sciences Aux Technologies*. TEC & DOC, Paris.
- Viladot, P.J.L.L., Delgado, G.R., Fernandez, B.A., 2014. Process of Treatment of Fibers And/or Textile Materials. EP 2550391 B1.
- Van Parys, M., 2006. Smart textiles using microencapsulation technology. In: Ghosh, S.K. (Ed.), *Functional Coatings*. Wiley-VCH Verlag GmbH & Co. KGaA, pp. 221–258.
- Vinogradova, O.I., 2004. Mechanical properties of polyelectrolyte multilayer microcapsules. *Journal of Physics: Condensed Matter* 16 (32), R1105.
- Voncina, B., Vivod, V., 2013. Cyclodextrins in textile finishing. In: Gunay, M. (Ed.), *Eco-friendly Textile Dyeing and Finishing*. InTech.
- Vroman, I., Giraud, S., Salaün, F., Bourbigot, S., 2010. Polypropylene fabrics padded with microencapsulated ammonium phosphate: effect of the shell structure on the thermal stability and fire performance. *Polymer Degradation and Stability* 95 (9), 1716–1720.
- Wang, C.X., Chen, S.L., 2005. Aromachology and its application in the textile field. *Fibres & Textiles in Eastern Europe* 13 (6), 41–44.
- White, M.A., LeBlanc, M., 1999. Thermochromism in commercial products. *Journal of Chemical Education* 76 (9), 1201.
- Wulf, M., Wehling, A., Reis, O., 2002. Coatings with self-cleaning properties. *Macromolecular Symposia* 187 (1), 459–468.

- Yan, L., Shuilin, C., 2003. Preparation and properties of disperse dye microcapsules. *Coloration Technology* 119 (1), 37–40.
- Yan, L., Yi, Z., Ben, Z., Juan, D., Shuilin, C., 2011. Effect of microencapsulation on dyeing behaviors of disperse dyes without auxiliary solubilization. *Journal of Applied Polymer Science* 120 (1), 484–491.
- Yi, Z., Jihong, F., Shuilin, C., 2005. Dyeing of polyester using micro-encapsulated disperse dyes in the absence of auxiliaries. *Coloration Technology* 121 (2), 76–80.
- Yang, Z., Zeng, Z., Xiao, Z., Ji, H., 2014. Preparation and controllable release of chitosan/vanillin microcapsules and their application to cotton fabric. *Flavour and Fragrance Journal* 29 (2), 114–120.
- You, M., Zhang, X.X., Li, W., Wang, X.C., 2008. Effects of microPCMs on the fabrication of microPCMs/polyurethane composite foams. *Thermochim Acta* 472 (1–2), 20–24.
- Yuen, M.C.W., Yip, J.Y.W., Cheuk, K., Kan, C.W., Cheng, S.Y., 2013. Item of Clothing for Daily Pharmacological Treatment of a Fungal Infection. US 20130052248 A1.
- Zhou, Y., Yan, Y., Du, Y., Chen, J., Hou, X., Meng, J., 2013. Preparation and application of melamine-formaldehyde photochromic microcapsules. *Sensors and Actuators B: Chemical* 188 (0), 502–512.
- Zuckerman, J.L., Pushaw, R.J., Perry, B.T., Wyner, D.M., 2003. Fabric Coating Containing Energy Absorbing Phase Change Material and Method of Manufacturing Same. US 6514362 B1.

Plasma surface treatments for smart textiles

10

C.-W. Kan

The Hong Kong Polytechnic University, Kowloon, Hong Kong

10.1 Introduction

The concept of plasma was introduced by [Tonks and Langmuir \(1929a,b,c\)](#). Plasma in general refers to the excited gaseous state consisting of atoms, molecules, ions and metastables and electrons such that the concentration of positively and negatively charged species is nearly the same. Physical and chemical properties of the ionised gas system are significantly different from neutral condition. Theoretically plasma is referred to as a ‘fourth state of matter’ and is characterised in terms of the average electron temperature and the charge density within the system ([Clark et al., 1978](#); [Chan, 1994](#)).

The physical phenomena called plasma can be divided into hot plasma (equilibrium) and cold plasma (low temperature, nonequilibrium). Low-temperature plasma is commonly used in material modification. In low-temperature plasma, electron temperature is 10 to 100 times higher than the gas temperature ([Luo and van Ooij, 2002](#)). However, because of the very low density and very low heat capacity of the electrons, the very high temperature of electrons does not imply that the plasma is hot. This means that although the electron temperature rises over several tens of thousands Kelvin, the gas temperature remains at 100 K. This explains why plasma is termed a low-temperature plasma (thereafter called plasma) and is used to modify polymer surfaces.

Depending on the gas pressure, two different forms of electrical discharge in gases are known, often referred to as plasma treatment ([Rakowski, 1997](#)):

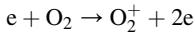
1. Corona discharge: This is generated at gas pressure equal to or near atmospheric pressure with an electromagnetic field at high voltage (>15 kV) and frequency in the 20- to 40-kHz range for most practical applications.
2. Glow discharge: This is generated at gas pressure in the 0.1- to 10-MPa range with an electromagnetic field in a lower voltage range (0.4–8.0 kV) and a very broad frequency range (0–2.45 GHz).

‘Smart textile’ or intelligent textile applications range from medical care to response to environmental stimuli and rehabilitation of athletes ([Cherenack et al., 2010](#)). Basically, smart textiles refer to textiles with added value and properties desired for specific end use. With the merits of low waste, single-step treatment and low pollution, the process does not affect bulk properties; therefore, plasma technique is popular for textile surface modification. With advanced and matured technology, a great variety of smart applications have been identified for plasma-modified textiles.

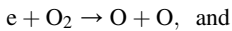
10.2 Principles of plasma creation

Oxygen gas is used as an example to show the production of plasma species (Manos and Flamm, 1989):

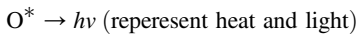
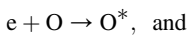
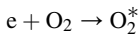
1. Ion and electron formation



2. Atom and radical formation



3. Generation of heat and light

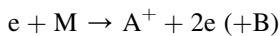


where O_2^* and O^* are excited states of O_2 and O ; h is Planck's constant; and ν is frequency of electromagnetic radiation.

Each step in the process of formation of the plasma balances various loss processes. The equilibrium between formation and loss determines the concentration of species in a discharge. These formation and loss processes may be grouped into a few categories.

10.2.1 Ionisation and detachment

Ionisation reactions are the main source of ions and electrons. The general form of these reactions is:



where M is either a molecule (AB) or an atom. If the molecule dissociates in this process to yield the neutral fragment B , it is called dissociative ionisation. When the species M is a negative ion, the process is called detachment because the negatively charged electron is said to be attached when a negative ion is formed in the first place. The detachment process, $e + A^- \rightarrow A + 2e$, is no less an ionisation and similarly creates a free electron. Less frequently, another process called Penning ionisation can make an important contribution. In Penning ionisation, an excited metastable state is formed by electron impact, $e + C \rightarrow C^* + e$, and the excitation energy of the metastable state is enough to ionise a second species via $C^* + M \rightarrow C + M^+ + e$, or

(where again $M = AB$), $C^* + AB \rightarrow C + A^+ + B + e$ or $C^* + M \rightarrow CM^+ + e$. Penning ionisation has been found to be significant in mixtures where C is a rare gas, eg, neon, with a metastable state excited energy that is just above the ionisation energy for M (Penning, 1927; Kan and Yuen, 2007).

10.2.2 Recombination, detachment and diffusion

A series of loss processes balances the formation steps outlined earlier. Some of the most important mechanisms are electron–ion recombination, $e + M^+ \rightarrow A + B$, attachment, $e + M \rightarrow A^- + B$, and diffusion of ions and electrons to the walls of the reaction vessels. These reactions take place in a variety of ways, depending on the species involved. In the case of oxygen plasma, the dissociative recombination is the most rapid ion–electron recombination process, $e + O_2^+ \rightarrow O + O$, whereas in a pure argon discharge only simple electron–ion recombination is possible, $e + A^+ \rightarrow A$ (Kan and Yuen, 2007).

In highly exothermic reactions, channels that form two or more product fragments with comparable mass are generally favoured because they make it easier to conserve both energy and momentum.

Reactive species (positive and negative ions, atoms, neutrals, metastables and free radicals) are generated in the plasma by ionisation, fragmentation and excitation. These species lead to chemical and physical interactions between plasma and the substrate surface depending on plasma conditions such as gas, power, pressure, frequency and exposure time. The depth of interaction and modification, however, is independent of gas type and is limited to 5 mm (Rakowski, 1997).

10.3 Plasma–substrate interactions

Because plasma is a gaseous mixture consisting of electrons, equally charged ions, molecules and atoms, many reactions occur simultaneously in a plasma system. There are two major processes with opposite effects: (1) polymer formation leading to the deposition of materials, called plasma polymerisation; and (2) ablation leading to the removal of materials. Besides the conditions of discharge, such as energy density, the plasma gas mainly determines which of the two processes is dominant (Luo and van Ooij, 2002). If the plasma gas has high proportions of carbon and hydrogen atoms, such as methane, ethylene and ethanol, it results in plasma polymerisation. The plasma polymer films are typically pinhole-free, highly cross-linked and insoluble. It is easy to obtain very thin films (Rakowski, 1997). Ablation of materials by plasma can occur by means of two principal processes, physical sputtering and chemical etching. The sputtering of materials by chemically nonreactive plasma, such as argon gas plasma, is a typical example of physical sputtering. Chemical etching occurs in chemically reactive types of plasma gas, including inorganic and organic molecular gases, such as O_2 , N_2 and CF_4 , which are chemically reactive but do not deposit polymers in the pure gas plasma. Plasma ablation competes with polymer formation in almost all cases when plasma is used to treat the surface of solid materials (Luo and van Ooij, 2002).

A scheme of interaction between a solid phase and a plasma phase is depicted in Fig. 10.1 (Luo and van Ooij, 2002).

After plasma treatment, a large number of free radicals remain on the treated fibre surface. These free radicals have an important role in forming functional groups and bonds between the fibre and the matrix. They are extinguished when exposed to atmosphere, especially oxygen, thereby decreasing the extent of bonding between the fibre and the matrix. Hence, the time lapse between plasma treatment and composite fabrication should be as short as possible.

10.3.1 Polymerisation

Plasma polymerisation is a unique technique for modifying polymer and other material surfaces by depositing a thin polymer film (d'Agostino et al., 1983; Wertheimer and Schreiber, 1981; Moshonov and Avny, 1980; Inagaki et al., 1982, 1983; Chen et al., 1982; Cho and Yasuda, 1988; Ho and Yasuda, 1990; Ho and Yasuda, 1988; Ertel et al., 1990; Yeh et al., 1988; Iriyama and Yasuda, 1988). Plasma-deposited films have many special advantages:

1. A thin conformal film a few hundred angstroms to 1 μm thick can be easily prepared.
2. Films can be prepared with unique physical and chemical properties. Such films, highly cross-linked and pinhole-free, can be used as very effective barriers.
3. Films can be formed on practically any kind of substrate including polymers, metal, glass and ceramics. Generally speaking, good adhesion between the film and substrate can be easily achieved.

Plasma polymerisation is a very complex process. The structure of plasma-deposited films is highly complex and depends on many factors, including reactor design (Chan et al., 1996), power level (Chan et al., 1996), substrate temperature (Ohkubo and

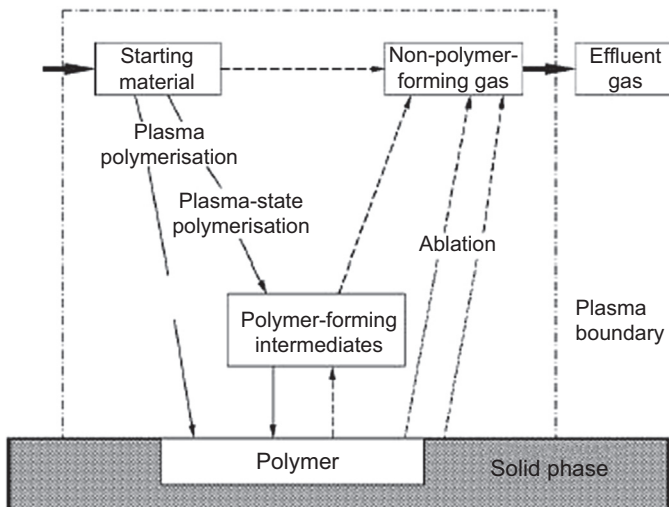


Figure 10.1 Polymerisation—ablation competition of plasma treatment (Luo and van Ooij, 2002).

Inagaki, 1990), frequency (Charlson et al., 1984), monomer structure, monomer pressure (Donohoe and Wydeven, 1979) and monomer flow rate (Yasuda and Hirotsu, 1977a,b). Two types of polymerisation reactions can occur simultaneously: plasma-induced and polymer-state. In the former case, the plasma initiates polymerisation at the surface of liquid or solid monomers (Bradley and Czuhra, 1975; Epailard et al., 1989; Simionescu et al., 1981). For this to occur, monomers must contain polymerisable structures such as double bonds, triple bonds or cyclic structures. In the latter case, polymerisation occurs in plasma in which electrons and other reactive species have enough energy to break any bond. Any organic compound and even those without a polymerisable structure, needed for the conventional type of polymerisation, can be used in plasma-state polymerisation. The rates at which monomers polymerise are relatively similar regardless of the structure of the monomer (Chan et al., 1996).

10.3.2 Plasma ablation (physical sputtering and chemical etching)

In the case of glow discharge, plasma with different magnitudes of ionisation can be produced. The active plasma species carry high kinetic energy (1 eV to several electronvolts) which can initiate reactions of saturated as well as unsaturated organic compounds. Although the kinetic energy is high, the temperature of the plasma is relatively low. The active species in plasma lose the energy once they interact with the polymer material. As a result, penetration of the plasma into the polymer material is shallow (beyond 1000) (Yan and Guo, 1989) and the interior of the material is only slightly affected. Hence, plasma treatment can be considered to be a surface treatment: ie, (1) sputtering, (2) chemical etching, (3) ion-enhanced energetic etching and (4) ion-enhanced protective etching (Manos and Flamm, 1989). The plasma species, carrying high kinetic energy, bombard the polymer, causing a sputtering or etching effect on the surface (Manos and Flamm, 1989). This bombardment therefore alters the surface characteristics of the polymeric material.

10.3.2.1 Sputtering

In sputtering, ions across the sheath potential bombard the surface with high energy. The sudden energy impulse can immediately eject surface atoms outward, or by a billiard ball-like collision cascade can even stimulate ejection of subsurface species. If there is to be net material removal, however, molecules sputtered from the surface must not return. This requires a low gas pressure, or equivalently, a mean free path comparable to the vessel dimensions. If the mean free path is too short, collision in the gas phase reflects and redeposits the sputtered species. Sputtering requires plasma conditions and ions with high energy. These conditions exist in low pressure (<50 mTorr) where mean free paths are also long. As a mechanical process, sputtering lacks selectivity. It is sensitive to the magnitude of bonding forces and the structure of a surface rather than its chemical nature; quite different materials can also sputter at similar rates. In a way this is symptomatic of using ion bombardment with energy far higher than the surface binding energy (Manos and Flamm, 1989; Lieberman and Lichtenber, 1994).

10.3.2.2 Chemical etching

In chemical etching, gas phase species merely react with a surface according to elementary chemistry. Fluorine atom etching of silicon is a good example of this mechanism. The important and really the only requirement for this kind of process is that a volatile reaction can form a product. In silicon/F-atom etching, spontaneous reactions between F-atoms and the substrate form SF_4 , a gas. The only purpose of the plasma in chemical etching is to make the reactive etchant species, eg, F-atoms. The etchant species are formed through collisions between energetic free electrons and gas molecules, which stimulate dissociation and reaction of the feed gas, ie, plasma feeds such as F_2 , NF_3 and CF_4/O_2 , all of which make F-atoms. Chemical etching is the most selective kind of process because it is inherently sensitive to differences in bonds and the chemical consistency of a substrate. However, the process is usually isotropic or nondirectional, which is sometimes a disadvantage. With isotropic etching, both vertical and horizontal material removal proceed at the same rate, which makes it impossible to form the fine lines (less than about $3\ \mu\text{m}$ in the usual approximately $1\text{-}\mu\text{m}$ -thick films) (Manos and Flamm, 1989; Lieberman and Lichtenber, 1994).

10.3.2.3 Ion-enhanced energetic etching

In ion-enhanced energetic etching, a directional etching mechanism, the impinging ions damage the surface and increase its reactivity. For example, an undoped single crystal silicon surface is not etched by Cl_2 or Cl atoms at room temperature. When the surface is simultaneously exposed to a high energy ion flux, the result is a rapid reaction that forms silicon chlorides and removes material much faster than the physical sputtering rate (Bogaerts et al., 2002). The word ‘damage’ in this case refers to part dissociation of the surface compound. Whatever the microscopic details (which undoubtedly can vary greatly from one surface/etchant system to another), the generic mechanism is one in which ions impart energy to the surface, modify it and render the impact zone as well as its environment more reactive (Rossnagel et al., 1990).

10.3.2.4 Ion-enhanced protective etching

This kind of etching mechanism can be classified as inhibitor ion-enhanced etching requiring two conceptually different species, ie, etchants and inhibitors. The substrates and etchants in this mechanism react spontaneously and etch isotropically, if it were not for the inhibitor species. The inhibitors form a very thin film on the surface that causes little or no ion bombardment. The film acts as a barrier to etchant and prevents the attack of the feature sidewalls, thereby making the process anisotropic (Shul and Pearton, 2000).

10.3.3 Functionalisation

Plasma functionalisation is a chemical modification of the surface achieved by some functions. After the plasma species interacts with the samples, it forms a thin film at

the surface of the material if the product is not volatile (Cardinaud et al., 2002; Chattopadhyay, 2015). Specially, the plasma species and the material surface preferably should be covalently bonded rather than just be like a physically adsorbed coating (Brétagnot et al., 2006). In some cases, the addition of functionality and surface roughening occurs simultaneously (Chattopadhyay, 2015). Deposition of hydrophobic particulates on the material surface can also occur (Lee et al., 2011). This particulate formation is known to occur at relatively high density of reactive radicals and ions in the plasma (Mikikian et al., 2010).

10.4 Applications of plasma surface treatments in smart textiles

Shishoo (2007), Morent et al. (2008) and Rauscher et al. (2010) conducted comprehensive review of plasma surface treatment of textile substrates. In addition to their work, other textile applications are reviewed in the following sections.

10.4.1 Hydrophilicity and oleophobicity

Surfaces that can display hydrophilicity and oleophobicity simultaneously, based on a favourable interaction with polar liquids and an unfavourable interaction with nonpolar liquids, are of great interest for different technological applications such as oil–water separation membranes (Yang et al., 2012; Howarter and Youngblood, 2009; Wen et al., 2013) or self-cleaning surfaces (Howarter and Youngblood, 2007, 2008). The design of hydrophilic–oleophobic surfaces is often based on the realisation of stimuli-responsive materials combining moieties of largely different surface tension, such as fluoroalkylated oligomeric silanes containing hydrophilic monomers (Sawada et al., 1996) or segmented polyurethanes (PUs) containing an assembly of polyoxyethylene, polydimethylsiloxane and perfluoropolyether. These soft polymer blocks can switch to oleophobic, hydrophobic or hydrophilic surface behaviours in response to the changing polarity of the contact liquid (Vaidya and Chaudhury, 2002). Stimuli-responsive surfaces can also be obtained by complexation of cationic fluorinated surfactants on negatively charged films obtained by means of plasma-assisted polymerisation of acrylic acid (Hutton et al., 2000) or maleic anhydride (Lampitt et al., 2000). Different methods are usually employed to promote plasma polymerisation of a monomer on a solid substrate. The common method involves introducing the monomer with a carrier gas in the plasma reactor and polymerisation takes place as a result of the free radicals generated during plasma treatment. Plasma-polymerised acrylic acid films have been obtained at low (Gilbert Carlsson and Johansson, 1993) and atmospheric pressure plasmas (Ward et al., 2003; Nisol et al., 2013). In addition, at atmospheric pressure, plasma-assisted polymerisation can be obtained with aerosol or atomised liquid droplets of monomer inside a carrier gas (Tatoulian et al., 2007; Mix et al., 2012). The use of atmospheric pressure dielectric barrier discharge plasma to initiate the polymerisation of a monomer

solution is an interesting novel procedure that promotes the deposition of polymer films onto different solid substrates (Molina et al., 2013). Discharges into and in contact with liquids generate ultraviolet (UV) radiation, shock waves, very active molecules or atoms (OH, O and H₂O₂) and free radicals that can promote polymerisation, oxidation and degradation processes of pollutants. However, under mild experimental conditions, polymerisation of monomers prevails over oxidation and degradation processes and the properties of the final polymer coating resemble those obtained by conventional polymerisation methods.

Molina et al. (2014) studied the deposition of functional polymer films onto cellulosic substrates (bleached cotton and filter paper) by means of plasma-initiated polymerisation in liquid phase. In this way, the initial study of plasma-assisted polymerisation of acrylic acid solutions over glass was carried out to study polymerisation processes in liquid phase and properties of the obtained films. Subsequently, plasma polymerisation of acrylic acid solutions at different concentrations was carried out on cellulosic substrates. Hydrophilic–oleophobic behaviour can be obtained after cationic fluorosurfactant complexation on the plasma-polymerised acrylic acid films over cellulosic substrates.

Wetting properties of polymerised acrylic acid surfactant functionalised samples on liquids with different natures and characteristics were studied (Molina et al., 2014). To confirm hydrophilic–oleophobic behaviour, the contact angle was measured for water and hexadecane for both paper and bleached cotton polymerised acrylic acid surfactant functionalised samples. Fig. 10.2 shows contact angle values as a function of time for hexadecane and water over bleached cotton and filter paper after acrylic acid (20%) plasma-assisted polymerisation and fluorosurfactant complexation. The water contact angle on functionalised cotton changes from 126 degree to 53 degree in 50 s and water absorption time is estimated at about 60 s. This value is significantly higher than the water absorption time corresponding to bleached cotton (<5 s) and constitutes evidence of the presence of the hydrophobic groups on a bleached cotton surface. Hexadecane contact angle on functionalised cotton changed from 76 degree to 29 degree in 80 s and hexadecane absorption time is 100 s, whereas in bleached cotton hexadecane absorption time is very low (<5 s).

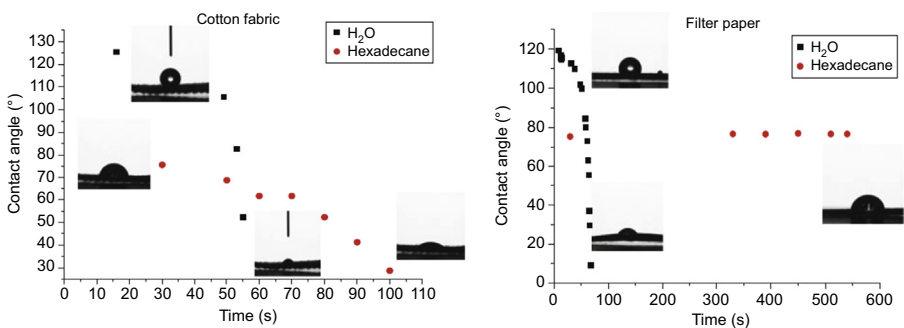


Figure 10.2 Contact angle as a function of time for hexadecane and water over (left) bleached cotton and (right) filter paper after acrylic acid (Molina et al., 2014).

Therefore, hexadecane absorption time is greater than water absorption time, indicating a moderate oleophobic–hydrophilic behaviour of the cotton functionalised substrates. The water contact angle on functionalised filter paper changes from 119 degree to 0 degree in 70 s (absorption time of 70 s) whereas the hexadecane contact angle value remains constant at 76 degree for more than 10 min. This result shows the hydrophilic–hydrophobic behaviour of the filter paper functionalised surface. It is suggested that the different wetting behaviours of filter paper and cotton functionalised surfaces can be attributed to the different degrees of surface roughness present on both substrates and film homogeneity (Molina et al., 2014).

10.4.2 Environmentally responsive or stimuli-responsive materials

There is a significant interest in developing environmentally responsive or stimuli-responsive smart materials. One application is to deliver therapeutic drug molecules selectively based on environmental changes such as temperature or pH value. Researchers have focused on developing smart interfaces that develop better thermal and molecular exchange with the environment as well as developing surfaces for better diffusion of medical products.

10.4.2.1 pH responsive

pH-sensitive polymers synthesised with either acidic or basic components demonstrate reversible swelling and deswelling under an acidic or basic medium (Lee and Shim, 2001). Polymeric membranes with permselective property act as chemical valves. Mechanochemical contractile forces exerting within the membrane enlarge and contract the pores reversibly, resulting in controlled water permeability and improved performance in the separation of macromolecular solutes (Osada et al., 1986). Isoporous films help control drug release and analysis of biomolecules and other valuable solutes by responding to changes in pH or small concentrations of analytes, acting as chemical gates (Nunes et al., 2011).

Osada et al. (1986) investigated composite membranes consisting of a porous substrate on which poly(methacrylic acid) (PMAA) was grafted using plasma treatment. The results showed that water permeability reacted sensitively to changes in pH. The mechanochemically induced conformational changes of PMAA chains resulted in enhanced permeation of water through PMAA-grafted membranes. The conformational changes tended to increase the apparent micropore size of the membrane. Water permeability was increased by adding poly(ethylene glycol), albumin, or γ -globulin because of polymer–polymer or protein–polymer complexation. Ito et al. (1992) synthesised a straight-pored membrane, which controls the rate of water permeation according to pH and ionic strength. The membrane was prepared by surface-graft polymerisation of vinyl monomers with a carboxylic acid substituent. By altering the density and length of graft chains, the pH response of water permeation was controlled. The rate of water permeation could be changed reversibly, depending on the pH variation of an aqueous solution.

10.4.2.2 Temperature responsive

Temperature-sensitive polymers demonstrate lower critical solution temperatures (LCST), which provide reversible low swelling at high temperatures and high swelling at low temperatures (Lee and Shim, 2001). When passing up the LCST, the polymer chains collapse and display intramolecular hydrophobic interactions. Intermolecular hydrophobic interactions of partly collapsed polymer chains enhance phase separation (Dubovik et al., 2005). Collapse of the macromolecules involves a large decrease or increase in permeability of the material, depending on its mode of preparation (Crespy and Rossi, 2007).

Poly(*N*-isopropyl acrylamide) (PNIPAM) is a well-known type of thermoresponsive polymer with an LCST in the physiological range (20–25°C) because its aqueous solution of PNIPSM has an LCST around 32°C (Crespy and Rossi, 2007). Plasma polymerisation of NIPAM on synthetic materials such as polyethylene and polypropylene membranes were investigated (Chu et al., 2003; Hunag et al., 2003; Liang et al., 2000). Temperature-sensitive membranes were prepared by grafting PNIPAM and its copolymers onto a porous poly(vinylidene fluoride) membrane (Iwata et al., 1991). Iwata et al. (1991) suggested that the grafted chains acted as a temperature sensor and as a valve to regulate filtration characteristics. The temperature sensitivity was reversible and reproducible, and the size of membranes remained constant. The temperature region where the filtration rate changed could be shifted to higher or lower temperature by copolymerising IPAAm with a hydrophilic monomer such as acrylamide or a hydrophobic monomer such as *n*-butyl methacrylate, respectively. Liang et al. (2000) reported that the microfiltration membrane with pores was filled with PNIPAM. The pores open at a temperature above the LCST of PNIPAM in the presence of water.

10.4.3 Textiles for biomedical application

Textiles for biomedical use are one of the fast growing sectors within plasma-treated textiles. Biomedical textiles are designed according to the desired properties. For instance, preparation of PET surfaces with poly(acrylic acid) (PAA) grafts by plasma processing may be used for coupling of precise amounts of collagen promoting smooth muscle cell growth in vitro (Gupta et al., 2002).

Plasma treatment is applied on a textile surface to cultivate an environment for maximised cell growth. Adhesive proteins are considered to be molecules that function as a sort of bridge between substrate and cells (Lamba, 1998). Substrates with excellent surface hydrophobicity usually show maximum cell attachment (Sigal, 1998). The combination of wet treatment and plasma techniques leads to biomaterials that optimise cell growth. Sipehia (1993) applied ammonia plasma treatment to artificial corneas fabricated from poly(hydroxyethyl methacrylate) to enhance corneal epithelial cell growth and enhancement. Vohrer (2007) pointed out that the increase in cell growth can be explained by the increase in wettability and the introduction of oxygen-containing functional groups after plasma treatment. Fig. 10.3 shows scanning electron micrographs (SEM) of stem cells attaching to a plasma-treated polyester

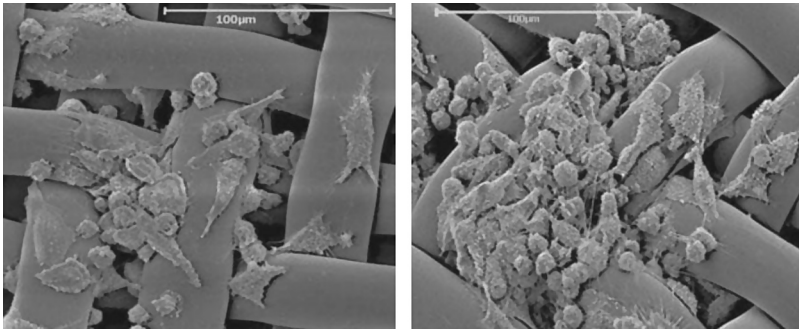


Figure 10.3 SEM micrographs of stem cells attaching on to plasma-modified fabric (Vohrer, 2007).

fabric. Fig. 10.4 shows the growth of cornea cells and keratinocytes on technical textiles with and without oxygen plasma treatment. The enhancement in hydrophilicity (introduction of oxygen functional group) promotes cell growth (Vohrer, 2007).

10.4.4 Antimicrobial textiles

Apart from the purpose of decoration, metallisation introduces antimicrobial properties to textile products. Different amounts of Ag ions released by the fabric (substrate) can inhibit the growth of different microorganisms (Schierholz et al., 1998). To meet broad

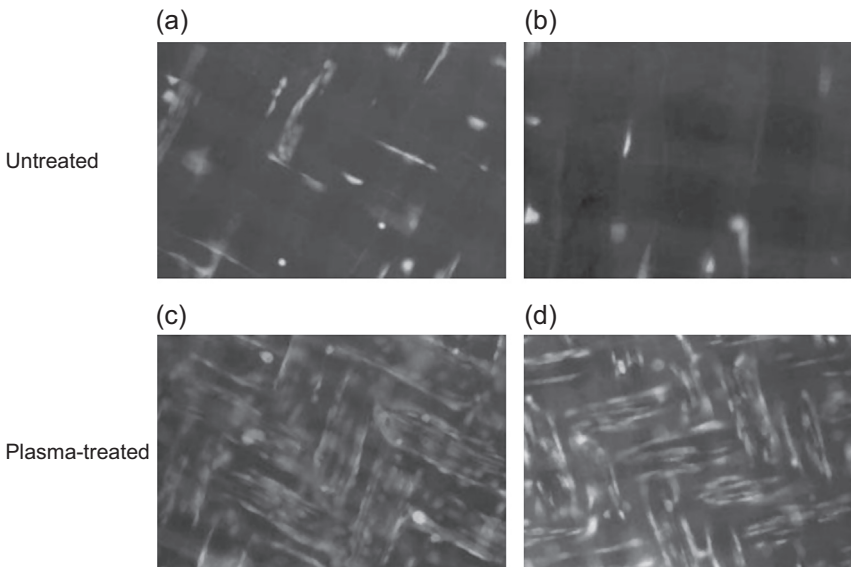


Figure 10.4 Growth of keratinocytes and cornea cells on technical fabric: (a) keratinocytes on untreated fabric; (b) cornea cells on untreated fabric; (c) keratinocytes on plasma-treated fabric and (d) cornea cells on plasma-treated fabric (Vohrer, 2007).

the range of antimicrobial functionalities, the release of Ag ions should result in the parts per million range (for example, $\mu\text{g/mL}$) (Gilchrist et al., 1991). Hegemann et al. (2009) deposited silver (Ag) onto polyester fibres by means of plasma sputtering. Electrical conductivity and antimicrobial properties were achieved. A small amount of Ag is deposited to impart a metallic appearance to textiles. Antimicrobial properties of plasma-treated fibres were tested by immersing the fabric in distilled water and recording the amount of Ag ions released. The cumulative Ag ions released over 14 days of use meets the range required for medical applications. Sciarratta (2003) applied pulsed or low-power plasma treatment to polymerise PAA on substrates, followed by wet treatment with silver nitrate, which produces silver carboxylated coatings. An antimicrobial is formed because of the release of Ag ions.

Chitosan is another agent able to promote antimicrobial properties on textiles. If carboxyl groups are generated, chitosan can be grafted onto a plasma-functionalised polymer surface (Vohrer, 2007). Huh et al. (2001) grafted chitosan onto PET by oxygen glow discharge plasma and subsequent wet treatment with acrylic acid.

Zhou and Kan (2014, 2015) used plasma treatment to enhance coating on cotton to obtain an *N*-halamine structure with antimicrobial function. When the chlorine from domestic bleaching solution was introduced into the nitrogen-containing groups in the coated fabric, the fabric had an antimicrobial effect and the effect was rechargeable.

10.4.5 Immobilisation of growth factor for therapeutics in tissue regeneration

To fabricate the desired biocompatibility on a textile surface, plasma acts as a subordinate tool in the process of fabrication. For instance, the growth factor can facilitate cellular behaviours. Immobilisation of the growth factor ensures cellular behaviours. Plasma treatment can be used to introduce amino groups which aid immobilisation of the growth factor.

A variety of cellular behaviours such as cell proliferation, migration, differentiation and protein expression can be regulated by polypeptide growth factors. These molecules are regarded as important therapeutics in tissue regeneration, eg, in closing bone defects and in healing chronic ulcers in the skin (Vohrer, 2007). Kuhl (1996) demonstrated the ability of immobilised growth factors (IGFs) which remain biologically active. The system involved epidermal growth factor conjugated on synthetic polymer surfaces. The result shows that the ability to immobilise is capable of directing hepatocytes to maintain liver-specific morphology and function.

Collaborating with the German Competence Centre for Biomaterials and Artificial Organs, Vohrer (2007) used IGF-1 to investigate a wound-healing pad mainly made up of PU nonwoven textile. The IGF-1 supports wound healing (Ulcer). Biotin–streptavidin was applied as the biolinker system to immobilise the growth factor. To attach biotin, the presence of free primary amino groups is essential and amino groups can be generated on a substrate surface by means of plasma treatment with ammonia. Müller and Oehr (1999) obtained more defined functionalisation by using diaminocyclohexane (DACH) with optimised plasma parameters. Fig. 10.5 shows the processes of immobilisation of bioactive species (Vohrer, 2007). Amino-functional groups are

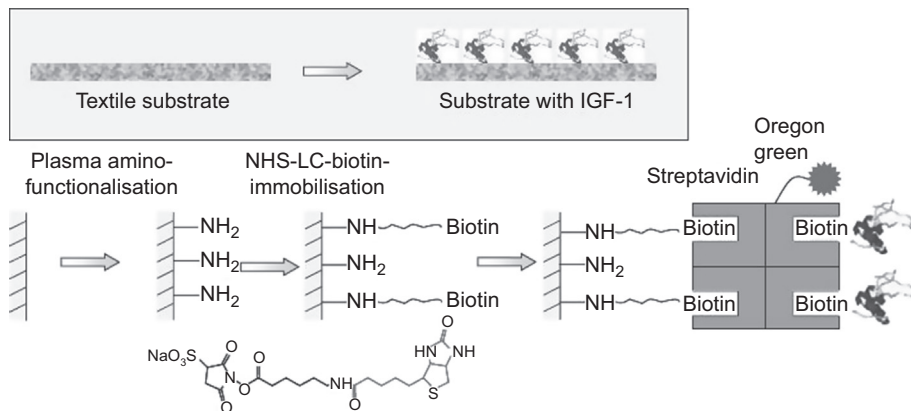


Figure 10.5 Processes of introducing immobilisation of bioactive species (Vohrer, 2007).

attached on the PU nonwoven pad by DACH plasma treatment. When followed by attaching NHS-LC-biotin and streptavidin, the PU surface is ready to immobilise growth factors such as IGF-1.

10.4.6 Antibiofouling

Biofouling is often referred to as bacterial adhesion. For instance, this phenomenon results in blocked catheters and tooth plaque. The undesirable result of bacteria attaching to a substrate surface is results from proteins in the extracellular matrix (Vohrer, 2007). To decrease the absorption of proteins and adhesion of cells, an amphoteric substance such as polyethylene glycol (PEG) or (also known as polyethylene oxide (PEO)) is applied.

A PEG-like surface was formed using plasma deposition of short-chained oligomers. The surface resists protein adsorption and cell adhesion (Mar et al., 1999; Shen et al., 2003). Gombotz et al. (1991) demonstrated a significant reduction in the adsorption of albumin and fibrinogen by depositing PEO despite incomplete surface coverage. Amine groups were introduced onto a poly(ethylene terephthalate) surface using allylamine plasma glow discharge. The surface was subsequently treated with amine-terminated PEO using cyanuric chloride chemistry. Fig. 10.6 shows the minimisation of unspecified protein adsorption (immunoglobulin G (IgG)) after different surface treatments. Oxygen, nitrogen and argon plasma treatment was applied and the results were investigated. Sample was fixed with PEO-PPO-PEO after dip coating and with subsequent plasma treatment (Vohrer, 2007).

10.4.7 Enhancing dyeability

Consciousness about the need for wildlife protection has risen globally. Genuine leather is being replaced by artificial leather. Microfibres are similar to genuine leather in terms of their outward appearance and the characteristics of touch and feel.

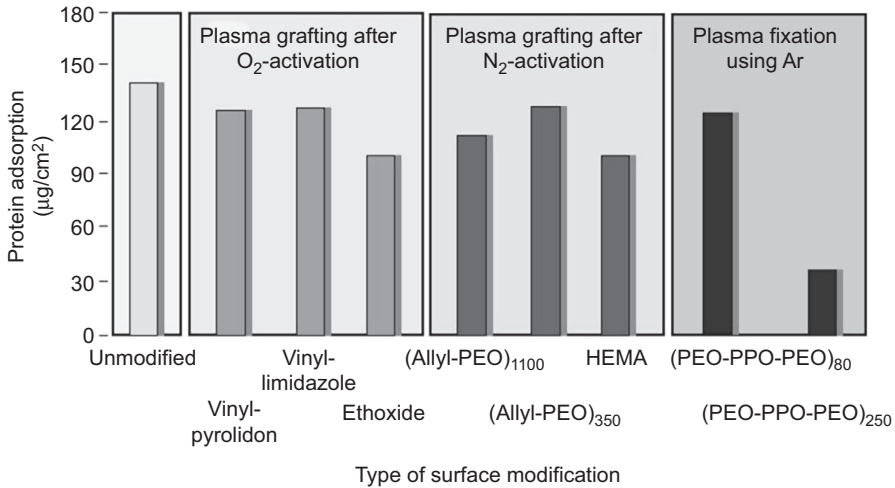


Figure 10.6 Minimisation of unspecified protein adsorption (IgG) after different surface modifications (Vohrer, 2007).

However, they have the problem of colour depth and fastness in the dyeing processes (Burkinshaw and Allafan, 2004; Zhu et al., 2007; Hocker, 2002). Surface modification has an important role in many applications involving various fields. Many methods have been considered and developed to alter the interactions of materials with their environments. In addition to keeping warm, microfibre has the advantage of softness and a shining surface. However, microfibres must use large amounts of dye because the fibre does not take up dye well and fades easily (Choi et al., 2003; Son et al., 2005). The thinness of microfibre increased significantly, ie, the number of fibres per unit of surface area has increased significantly. Accordingly, compared with common textile fibres, the adhesion of dye has become worse for thin textile fibres. Surface modification treatments are often used to solve these problems by plasma (Kan, 2015). Plasma-deposited film has many advantages, including good adhesion to most substrates, excellent uniformity, easy control of thickness, easy preparation, low porosity and no pinhole formation, and it provides some free radicals and peroxide groups. Free radicals formed on the surface of polymers and other solid materials exposed to plasma can be used to initiate graft polymerization in a manner similar to preirradiated grafting. Although the surface properties (wettability, electricity or photo-reactivity) of polymers can be improved after plasma treatment owing to formation of the induced polar groups and free radicals, this activated surface is not stable because free radicals on the surface readily react with oxygen atoms in the air. Whether the textiles are hydrophilic or hydrophobic before modification, surface treatment by plasma improves adhesion of dye and repellency properties (Choi et al., 2003; Son et al., 2005; Chen et al., 2006; Fan et al., 2004; Mukherjee and Jabrain, 1995; Tyczkowski et al., 2003). Compared with other treatment processes, surface treatment by plasma does not damage the products and it is not restricted by surface chemistry and topography of the modified material. Liao et al. (2013) modified nylon microfibre artificial

leather by cold plasma deposition which formed peroxides on surface, and then graft polymerization using various concentrations of acrylamide solution by UV light. Their results revealed that the acrylamide plasma-treated artificial leather achieved significant improvement in dye uptake with good dye density over the dyed surface.

10.5 Future trends

Because of technological advancements, plasma applications in different areas of textiles are expected to expand significantly, for these reasons:

1. **Economics:** Plasma treatment is a surface modification process that allows modification of surface properties without changing bulk properties of the substrate. The low power needed to maintain plasma gas activation in the chamber saves large quantities of electrical energy. In addition, from an economic point of view, the small consumption of chemicals makes the process superior for the textile industry.
2. **Environment:** Plasma treatment does not employ harmful chemical solutions, does not generate contaminated water, and does not create mechanical hazards for treated fabrics. The technology significantly reduces pollution caused by residual chemicals. In addition, plasma is able to modify the substrate surface properties such as microroughness and induces chemically active functional groups without affecting bulk properties.
3. **Social accountability:** Environmental problems associated with the textile industry are typically related to water pollution and the emission of volatile compounds which affect the daily lives of people. For this reason, plasma treatment may replace the conventional wet treatment while providing the same or even better treatment effects.

10.6 Conclusion

Compared with traditional finishing processes, plasma treatment has a crucial advantage in that it reduces the use of chemicals, water and energy. It also offers the possibility of achieving a wide range of functional effects on textiles. In this chapter, some developments are discussed which may be considered a starting point for this interesting topic.

Sources of further information

- Shishoo, R. (Eds.), 2007. *Plasma Technologies of Textiles*. Woodhead Publishing Limited, Cambridge.
- Rausher, H., Perucca, M., Buyle, G. (Eds.), 2010. *Plasma Technology for Hyperfunctional Surfaces: Food, Biomedical, and Textile Applications*. Wiley-VCH, Darmstadt.
- Pan, N., Sun, G. (Eds.), 2011. *Functional Textiles for Improved Performance, Protection and Health*. Woodhead Publishing Limited, Cambridge.
- Chapman, R.A. (Eds.), 2013. *Smart Textiles for Protection*. Woodhead Publishing Limited, Cambridge.

Kan, C.W., 2015. A Novel Green Treatment for Textiles: Plasma Treatment as a Sustainable Technology. CRC Press, Boca Raton.

Nema, S.K., Jhala, P.B. (Eds.), 2015. Plasma Technologies for Textile and Apparel. Woodhead Publishing India Pvt. Limited, New Delhi.

References

- d'Agostino, R., Cramarossa, F., Colaprico, V., d'Ettore, R., 1983. Mechanisms of etching and polymerization in radiofrequency discharges of CF_4-H_2 , $CF_4-C_2F_4$, C_2F_6 and $C_3F_8-H_2$. *Journal of Applied Physics* 54, 1284–1288.
- Bogaerts, A., Neyts, E., Gijbels, R., van der Mullen, J., 2002. Gas discharge plasmas and their applications. *Spectrochimica Acta Part B* 57, 609–658.
- Bradley, A., Czuha Jr., M., 1975. Analytical methods for surface grafts. *Analytical Chemistry* 47, 1838–1840.
- Brétagne, F., Valsesia, A., Ceccone, G., Colpo, P., Gilliland, D., Ceriotti, L., Hasiwa, M., Rossi, F., 2006. Surface functionalization and patterning techniques to design interfaces for biomedical and biosensor applications. *Plasma Processes and Polymers* 3, 443–455.
- Burkinshaw, S.M., Allafan, B.B., 2004. The development of a metal-free, tannic acid-based after treatment for nylon 6,6 dyed with acid dyes. Part 4: tannic acid. *Dyes and Pigments* 62, 159–172.
- Cardinaud, C., Peignon, M.C., Tessier, P.Y., 2002. Plasma etching: principles, mechanisms, application to micro- and nano-technologies. *Applied Surface Science* 164, 72–83.
- Chan, C.M., 1994. *Polymer Surface Modification and Characterization*. Hanser Publisher, New York.
- Chan, C.M., Ko, T.M., Hiraoka, H., 1996. Polymer surface modification by plasmas and photons. *Surface Science Reports* 24, 1–54.
- Charlson, E.J., Charlson, E.M., Sharma, A.K., Yasuda, H.K., 1984. Electrical properties of glow-discharge polymers, parylenes, and composite films. *Journal of Applied Polymer Science: Applied Polymer Symposium* 38, 137–148.
- Chattopadhyay, S., 2015. *Biomimetic Architectures by Plasma Processing: Fabrication and Applications*. Stanford Publishing Pte. Ltd, Singapore.
- Chen, K.S., Inagaki, N., Katsuura, K., 1982. Preliminary experiment of surface hardening of polymers by glow discharge polymerization. *Journal of Applied Polymer Science* 27, 4655–4660.
- Chen, K.S., Li, M.S., Wu, H.M., Yang, M.R., Tian, J.Y., Huang, F.Y., Hung, H.T., 2006. Surface organic modification of inorganic substrates by plasma deposition of tin oxide organic-like thin films and grafting polymerization. *Surface and Coatings Technology* 200, 3270–3277.
- Cherenack, K., Zysset, C., Kinkeldei, T., Münzenrieder, N., Tröster, G., 2010. Woven electronic fibers with sensing and display functions for smart textiles. *Advanced Materials* 22, 5178–5182.
- Cho, D.L., Yasuda, H., 1988. Tribological application of plasma polymers. *Journal of Applied Polymer Science: Applied Polymer Symposium* 42, 139–156.
- Choi, J.H., Lee, E.S., Baik, H.K., Lee, S.J., Song, K.M., Hwang, M.K., Huh, C.S., 2003. Surface modification of natural leather using low-pressure parallel plate plasma. *Surface and Coatings Technology* 171, 257–263.

- Chu, L.Y., Niitsuma, T., Yamaguchi, T., Nakao, S.I., 2003. Thermoresponsive transport through porous membranes with grafted PNIPAM Gates. *AIChE Journal* 49, 896–909.
- Clark, D.T., Dilks, A., Shuttleworth, D., 1978. *Polymer Surface*. John Wiley and Sons Inc., New York.
- Crespy, D., Rossi, R.M., 2007. Mini-review temperature-responsive polymers with LCST in the physiological range and their application in textiles. *Polymer International* 56, 1461–1468.
- Donohoe, K.G., Wydeven, T., 1979. Plasma polymerization of ethylene in an atmospheric pressure-pulsed discharge. *Journal of Applied Polymer Science* 23, 2591–2601.
- Dubovik, A.S., Makhava, E.E., Grinberg, V.Y., Khokhlov, A.R., 2005. Energetics of cooperative transitions of *N*-vinylcaprolactam polymers in aqueous solutions. *Macromolecular Chemistry and Physics* 206, 915–928.
- Epaillard, F., Broose, J.C., Legeary, G., 1989. Plasma-induced polymerization. *Journal of Applied Polymer Science* 38, 887–898.
- Ertel, S.I., Ratner, B.D., Horbett, T.A., 1990. Radiofrequency plasma deposition of oxygen-containing films on polystyrene and poly(ethylene terephthalate) substrates improves endothelial cell growth. *Journal of Biomedical Materials Research* 24, 1637–1659.
- Fan, Q., Hoskote, S., Hou, Y., 2004. Reduction of colorants in nylon flock dyeing effluent. *Journal of Hazardous Materials* 112, 123–131.
- Gilbert Carlsson, C.M., Johansson, K.S., 1993. Surface modification of plastics by plasma treatment and plasma polymerization and its effect on adhesion. *Surface and Interface Analysis* 20, 441–448.
- Gilchrist, T., Healy, D.M., Drake, C., 1991. Controlled silver-releasing polymers and their potential for urinary-tract infection control. *Biomaterials* 12, 76–78.
- Gombotz, W.R., Wang, G.H., Horbett, T.A., Hoffmann, A.S., 1991. Protein adsorption to poly(ethylene oxide) surfaces. *Journal of Biomedical Materials Research* 25, 1547–1562.
- Gupta, B., Plummer, C., Bisson, I., Frey, P., Hilborn, J., 2002. Plasma-induced graft polymerization of acrylic acid onto poly(ethylene terephthalate) films: characterization and human smooth muscle cell growth on grafted films. *Biomaterials* 23, 863–871.
- Hegemann, D., Amberg, M., Ritta, A., Heuberger, M., 2009. Recent developments in Ag metalised textiles using plasma sputtering. *Materials Technology* 24, 41–45.
- Ho, C.P., Yasuda, H., 1988. Ultrathin coating of plasma polymer of methane applied on the surface of silicone contact lenses. *Journal of Biomedical Materials Research* 22, 919–937.
- Ho, C.P., Yasuda, H., 1990. Coatings and surface modification by methane plasma polymerization. *Journal of Applied Polymer Science* 39, 1541–1552.
- Hocker, H., 2002. Plasma treatment of textile fibers. *Pure and Applied Chemistry* 74 (3), 423–427.
- Howarter, J.A., Youngblood, J.P., 2009. Amphiphile grafted membranes for the separation of oil-in-water dispersions. *Journal of Colloid and Interfacial Science* 329, 127–132.
- Howarter, J.A., Youngblood, J.P., 2007. Self-cleaning and anti-fog surfaces via stimuli-responsive polymer brushes. *Advanced Materials* 19, 3838–3843.
- Howarter, J.A., Youngblood, J.P., 2008. Self-cleaning and next generation anti-fog surfaces coatings. *Macromolecular Rapid Communications* 29, 455–466.
- Huang, J., Wang, X., Chen, X., Yu, X., 2003. Temperature-sensitive membranes prepared by the plasma-induced graft polymerization of *N*-isopropylacrylamide into porous polyethylene membranes. *Journal of Applied Polymer Science* 89, 3180–3187.
- Huh, M.W., Kang, I.K., Lee, D.H., Kim, W.S., Lee, D.H., Park, L.S., Min, K.E., Seo, K.H., 2001. Surface characterization and antibacterial activity of chitosan-graft poly(ethylene terephthalate) prepared by plasma glow discharge. *Journal of Applied Polymer Science* 81, 2769–2778.

- Hutton, S.J., Crowther, J.M., Badyal, J.P.S., 2000. Complexation of fluorosurfactants to functionalized solid surfaces: smart behavior. *Chemistry of Materials* 12, 2282–2286.
- Inagaki, N., Itami, M., Katsuura, K., 1982. Adhesion between polymer substrates and plasma films from tetramethylsilane and tetramethyltin by glow discharge polymerization. *International Journal of Adhesion and Adhesives* 2 (3), 169–174.
- Inagaki, N., Ohnishi, Y., Chen, K.S., 1983. Glow discharge polymerization of tetramethylsilane by capacitive coupling of 20 kHz frequency and surface hardening of polyethylene sheet. *Journal of Applied Polymer Science* 28, 3629–3640.
- Iriyama, Y., Yasuda, H., 1988. Plasma treatment and plasma polymerization for surface modification of flexible poly(vinyl chloride). *Journal of Applied Polymer Science: Applied Polymer Symposium* 42, 97–124.
- Ito, Y., Inaba, M., Chung, D.J., Imanishi, Y., 1992. Control of water permeation by pH and ionic strength through a porous membrane having poly(carboxylic acid) surface grafted. *Macromolecules* 25, 7313–7316.
- Iwata, H., Oodate, M., Uyama, Y., Amemiya, H., Ikada, Y., 1991. Preparation of temperature-sensitive membranes by graft polymerization onto a porous membrane. *Journal of Membrane Science* 55, 119–130.
- Kan, C.W., Yuen, C.W.M., 2007. Plasma technology in wool. *Textile Progress* 39 (3), 121–187.
- Kan, C.W., 2015. *A Novel Green Treatment for Textiles – Plasma Treatment as a Sustainable Technology*. CRC Press, Boca Raton.
- Kuhl, P.R., Griffith-Cima, L.G., 1996. Tethered epidermal growth factor as a paradigm for growth factor-induced stimulation from the solid phase. *Nature Medicine* 2, 1022–1027.
- Lamba, N.M.K., Baumgartner, J.A., Cooper, S.L., 1998. Cell-synthetic surfaces interactions. In: Patrick Jr., A.G., Mikos, L.V., McIntire, L.V. (Eds.), *Frontiers in Tissue Engineering*. Pergamon, New York, pp. 121–132.
- Lampitt, R.A., Crowther, J.M., Badyal, J.P.S., 2000. Switching liquid repellent surfaces. *Journal of Physical Chemistry B* 104, 10329–10331.
- Lee, S.H., Dilworth, Z.R., Hsiao, E., Barnette, A.L., Marion, M., Kim, J.H., Kang, J.G., Jung, T.H., Kim, S.H., 2011. One-step production of superhydrophobic coatings on flat substrates via atmospheric RF plasma process using non-fluorinated hydrocarbons. *ACS Applied Material and Interface* 3, 476–481.
- Lee, Y.M., Shim, J.K., 2001. Permeation control through stimuli-responsive polymer membrane prepared by plasma and radiation grafting techniques. In: Tao, X.M. (Ed.), *Smart Fibers, Fabrics and Clothing*. Woodhead Publishing Limited, Cambridge, pp. 109–112.
- Liang, L., Shi, M., Viswanathan, V.V., Peurrung, L.M., Young, J.S., 2000. Temperature-sensitive polypropylene membranes prepared by plasma polymerization. *Journal of Membrane Science* 177, 97–108.
- Liao, S.C., Chen, K.S., Che, W.Y., Chou, C.Y., Kan, C.W., 2013. Surface graft polymerization of acrylamide onto plasma activated nylon microfiber artificial leather for improving dyeing properties. *International Journal of Chemical Engineering and Applications* 4 (2), 78–81.
- Lieberman, M.A., Lichtenber, A.J., 1994. *Principles of Plasma Discharges and Materials Processing*. John Wiley & Sons, Inc., New York.
- Luo, S., van Ooij, W.J., 2002. Surface modification of textile fibers for improvement of adhesion to polymeric matrices: a review. *Journal of Adhesion Science and Technology* 16 (13), 1715–1735.
- Manos, D.M., Flamm, D.L., 1989. *Plasma Etching: An Introduction*. Academic Press, London.
- Mar, M.N., Ratner, B.D., Yee, S.S., 1999. An intrinsically protein-resistant surface plasma on resonance biosensor based upon a RF-plasma-deposited thin film. *Sensors and Actuators B* 54, 125–131.

- Mikikian, M., Couédel, L., Cavarroc, M., Tessier, Y., Boufendi, L., 2010. Dusty plasmas: synthesis, structure and dynamics of a dust cloud in a plasma. *The European Physical Journal – Applied Physics* 49, 13106.
- Mix, R., Friedrich, J.F., Inagakin, B., 2012. Modification of branched polyethylene by aerosol-assisted dielectric barrier discharge. *Plasma Processes and Polymers* 9, 406–416.
- Molina, R., Ligeró, C., Jovancic, P., Bertran, E., 2013. In situ polymerization of aqueous solutions of NIPAAm initiated by atmospheric plasma treatment. *Plasma Processes and Polymers* 10, 506–516.
- Molina, R., Gómez, M., Kan, C.W., Bertran, E., 2014. Hydrophilic-oleophobic coatings on cellulosic materials by plasma assisted polymerization in liquid phase and fluorosurfactant complexation. *Cellulose* 21, 729–739.
- Morent, R., De Geyter, N., Verschuren, J., De Clerck, K., Kiekens, P., Leys, C., 2008. Non-thermal plasma treatment of textiles. *Surface and Coatings Technology* 202, 3427–3429.
- Moshonov, A., Avny, Y., 1980. The use of acetylene glow discharge for improving adhesive bonding of polymeric films. *Journal of Applied Polymer Science* 25, 771–781.
- Müller, M., Oehr, C., 1999. Plasma aminofunctionalisation of PVDF microfiltration membranes: comparison of the in plasma modifications with a grafting method using ESCA and an amino-selective fluorescent probe. *Surface and Coatings Technology* 116–119, 802–807.
- Mukherjee, H.S., Jabrain, S.A., 1995. Aging characteristics of oriented poly(ethylene terephthalate). *Polymer Engineering and Science* 35, 1145–1154.
- Nisol, B., Batan, A., Dabeux, F., Kakaroglou, A., De Graeve, I., Van Assche, G., Van Mele, B., Terryn, H., Reniers, F., 2013. Surface characterization of atmospheric pressure plasma-deposited allyl methacrylate and acrylic acid based coatings. *Plasma Processes and Polymers* 10, 564–571.
- Nunes, S.P., Behzad, A.R., Hooghan, B., Sougrat, R., Karunakaran, M., Pradeep, N., Vainio, U., Peinemann, K., 2011. Switchable pH-responsive polymeric membranes prepared via block copolymer micelle assembly. *ACS Nano* 5, 3516–3522.
- Ohkubo, J., Inagaki, N., 1990. Influences of the system pressure and the substrate temperature on plasma polymers. *Journal of Applied Polymer Science* 41, 349–359.
- Osada, Y., Honda, K., Ohta, M., 1986. Control of water permeability by mechanochemical contraction of poly(methacrylic acid)-grafted membranes. *Journal of Membrane Science* 27, 327–338.
- Penning, F.M., 1927. Über ionization durch metastabile Atome. *Naturwissenschaften* 15 (40), 818.
- Rakowski, W., 1997. Plasma treatment of wool today, Part I – fiber properties, spinning and shrinkproofing. *Journal of Society of Dyers and Colourists* 113, 250–255.
- Rauscher, H., Perucca, M., Buyle, G., 2010. *Plasma Technology for Hyperfunctional Surfaces: Food Biomedical, and Textile Applications*. Wiley-VCH, Darmstadt.
- Rosnagel, S.M., Cuomo, J.J., Westwood, W.D., 1990. *Handbook of Plasma Processing Technology*. Noyes Publishing, New York.
- Sawada, H., Ikematsu, Y., Kawase, T., Hayakawa, Y., 1996. Synthesis and surface properties of novel fluoroalkylated flipflop-type silane coupling agents. *Langmuir* 15, 3529–3530.
- Schierholz, J.M., Lucas, L.J., Rump, A., Pulverer, G., 1998. Efficacy of silver-coated medical devices. *Journal of Hospital Infection* 40, 257–262.
- Sciarratta, V., Vohrer, U., Hegemann, D., Müller, M., Oehr, C., 2003. Plasma functionalization of polypropylene with acrylic acid. *Surface and Coatings Technology* 174–175, 805–810.

- Shen, M., Wagner, M.S., Castner, D.G., Ratner, B.D., Horbett, T.A., 2003. Multivariate surface analysis of plasma-deposited tetraglyme for reduction of protein adsorption and monocyte adhesion. *Langmuir* 19 (5), 1692–1699.
- Shishoo, R., 2007. *Plasma Technologies for Textiles*. Woodhead Publishing Limited, Cambridge.
- Shul, R.J., Pearson, S.J., 2000. *Handbook of Advanced Plasma Processing Techniques*. Springer, Heidelberg.
- Sigal, G.B., Mrksich, M., Whitesides, G.M., 1998. Effect of surface wettability on the adsorption of proteins and detergents. *Journal of American Chemical Society* 120, 3464–3473.
- Simionescu, B.C., Leanca, M., Loan, S., Simionescu, C.I., 1981. Plasma-induced polymerization 4. Low conversion bulk polymerization of styrene. *Polymer Bulletin* 4, 415–419.
- Sipehia, R., 1993. X-ray photoelectron spectroscopy studies, surface tension measurements, immobilization of human serum albumin, human fibrinogen and human fibronectin onto ammonia plasma treated surfaces of biomaterials useful for cardiovascular implants and artificial cornea implants. *Biomaterials, Artificial Cells and Immobilization Biotechnology* 21, 647–658.
- Son, Y.A., Hong, J.P., Lim, H.T., Kim, T.K., 2005. A study of heterobifunctional reactive dyes on nylon fibers: dyeing properties, dye moiety analysis and wash fastness. *Dyes and Pigments* 66, 231–239.
- Tatoulian, M., Arefi-Khonsari, F., Borra, J.P., 2007. Deposition of organic coatings at atmospheric pressure from liquid precursors. *Plasma Processes and Polymers* 4, 360–369.
- Tonks, L., Langmuir, L., 1929a. Oscillations in ionized gases. *Physics Review* 33, 195–210.
- Tonks, L., Langmuir, L., 1929b. The interaction of electron and positive ion space charges in cathode sheaths. *Physics Review* 33, 954–989.
- Tonks, L., Langmuir, L., 1929c. A general theory of the plasma of an arc. *Physics Review* 34, 876–922.
- Tyczkowski, J., Krawczyk, I., Woźniak, B., 2003. Modification of styrene–butadiene rubber surfaces by plasma chlorination. *Surface and Coatings Technology* 174–175, 849–853.
- Vaidya, A., Chaudhury, M.K., 2002. Synthesis and surface properties of environmentally responsive segmented polyurethanes. *Journal of Colloid and Interfacial Science* 249, 235–245.
- Vohrer, L., 2007. Interfacial engineering of functional textiles for biomedical applications. In: Shishoo, R. (Ed.), *Plasma Technologies for Textiles*. Woodhead Publishing Limited, Cambridge, pp. 202–222.
- Ward, L.J., Schofield, W.C.E., Badyal, J.P.S., Goodwin, A.J., Merlin, P.J., 2003. Atmospheric pressure plasma deposition of structurally well-defined polyacrylic acid films. *Chemistry of Materials* 15, 1466–1469.
- Wen, Q., Jiancheng, D., Jiang, L., Yu, J., Xua, R., 2013. Zeolite-coated mesh film for efficient oil–water separation. *Chemical Science* 4, 591–595.
- Wertheimer, M.R., Schreiber, H.P., 1981. Surface property modification of aromatic polyamides by microwave plasmas. *Journal of Applied Polymer Science* 26, 2087–2096.
- Yan, H.J., Guo, W.Y., 1989. A study on change of fiber structure caused by plasma action. In: *Proceedings of the Fourth Annual International Conference of Plasma Chemistry and Technology*, pp. 181–188.
- Yang, J., Zhang, Z., Xu, X., Zhu, X., Men, X., Zhou, X., 2012. Superhydrophilic-superoleophobic coatings. *Journal of Materials Chemistry* 22, 2834–2837.

- Yasuda, H., Hirotsu, T., 1977a. Polymerization of organic compounds in an electrodeless glow discharge IX – flow-rate dependence of properties of plasma polymers of acetylene and acrylonitrile. *Journal of Applied Polymer Science* 21, 3167–3177.
- Yasuda, H., Hirotsu, T., 1977b. Polymerization of organic compounds in an electrodeless glow discharge VIII – dependence of plasma polymerization of acrylonitrile on glow characteristic. *Journal of Applied Polymer Science* 21, 3139–3145.
- Yeh, Y.S., Iriyama, Y., Matsuzawa, Y., Hanson, S.R., Yasuda, H., 1988. Blood compatibility of surfaces modified by plasma polymerization. *Journal of Biomedical Materials Research* 22, 795–818.
- Zhou, C.E., Kan, C.W., 2014. Plasma-assisted regenerable chitosan antimicrobial finishing for cotton. *Cellulose* 21, 2951–2962.
- Zhou, C.E., Kan, C.W., 2015. Plasma-enhanced regenerable 5,5-dimethylhydantoin (DMH) antibacterial finishing for cotton fabric. *Applied Surface Science* 328, 410–417.
- Zhu, L., Wang, C., Qiu, Y., 2007. Influence of the amount of absorbed moisture in nylon fiberson atmospheric pressure plasma processing. *Surface & Coatings Technology* 201, 7453–7461.

Nanotechnology-based coating techniques for smart textiles

11

*M. Parvinzadeh Gashti*¹, *E. Pakdel*², *F. Alimohammadi*^{3,4}

¹Young Researchers and Elites Club, Yadegar-e-Imam Khomeini (RAH) Branch, Islamic Azad University, Tehran, Iran; ²Deakin University, Geelong, VIC, Australia; ³Clarkson University, Potsdam, NY, USA; ⁴Young Researchers and Elites Club, Islamic Azad University, South Tehran Branch, Tehran, Iran

11.1 Introduction

Nanotechnology-based coatings are widely considered to be a new insight into finishing procedures for textiles. Nanoparticles and nanostructured materials are introduced for the purposes of surface modification and smart functionalisation of textiles. The success of nanoparticles is related to their size-related properties and high surface area-to-volume ratio, which result in their enhanced characteristics compared with macrometre-sized particles. Their use in the textile industry is rapidly growing in the world and covers a wide range of applications such as industrial, apparel and technical textiles. These procedures include in situ synthesis, immobilisation and cross-linking of nanoparticles and nanostructures on textile surfaces. The main aims of researchers are to produce multiple functionalities through nanoparticles such as antibacterial, superhydrophobic, fire retardant, self-cleaning, superhydrophilic, moth-proofing, electromagnetic shielding and electrical conductivity.

Because of the intensive efforts in textile nanocoatings, several methods have been developed, including spraying, transfer printing, immersion, rolling, padding and simultaneous exhaust dyeing. Among all of these, rinsing and pad-dry-cure methods are the most commonly used procedures for textile nanocoatings. However, some important issues concern the application of nanoparticles, including their size uniformity, nanoparticle shape and purity, dispersibility in colloids and health and safety, as well as their durability in textiles.

Size uniformity can be achieved through size-selection procedures, which are time-consuming. In this regard, repeated centrifuging, rinsing and dispersing of nanoparticles are necessary to narrow the size distribution of nanoparticles.

On the other hand, nanoparticles have a variety of shapes including nanospheres, nanocubes, nanopyramids, nanorods, nanowires, nanobars, nanoprisms and nanostars. Such morphologies are obtained by changing different factors in synthesis procedures

including temperature, the concentration of the precursor, the pH of the solution, the application of reducing or oxidising agents and the type of method used. The physical and chemical properties of nanoparticles strongly depend on the nanoparticle shapes.

An important issue concerning the application of nanoparticles on textiles is their dispersion in colloids before coating. Generally, nanoparticles tend to aggregate into microclusters owing to van der Waals and electrostatic double-layer forces. Stable dispersions can be produced by adding dispersing agents such as surfactants, effective grinding and covalent surface functionalisation of nanoparticles by organic compounds and monomers.

The durability of nanoparticles on textiles is a major problem addressed by researchers through different methods. It is well known that nanoparticles have no attraction to textile fibres owing to the lack of surface functional groups. To enhance the binding ability between them and thus ensure the long-term durability of achieved effects, the surface functionalisation of fibres or nanoparticles through physical and chemical methods is proposed. On the other hand, nanoparticles can be embedded in polymer matrices on the textile surfaces to produce inorganic–organic hybrid nanocomposite coatings.

The main aim of this chapter is thus to introduce nanotechnology-based textile coating methods. Moreover, different types of nanoparticles or nanostructures which are produced on textiles and their applications on textiles are described.

11.2 Types and classifications of nanotechnology-based coating techniques

11.2.1 *Sol–gel method*

One of the most important approaches to coating fabrics is the sol–gel method. In brief, the sol–gel process involves synthesising metal oxide nanoparticles such as SiO_2 and TiO_2 from the molecules of precursors. The fabricated colloidal sols are able to produce a continuous network of nanoparticles creating a thin film on polymeric substrates. Metal alkoxides such as titanium tetraisopropoxide (TTIP), tetrabutyl titanate and tetraethyl orthosilicate (TEOS) among others have mainly been used to synthesise titanium and silicon oxide nanoparticles. Using the sol–gel method to synthesise nanoparticles results in the homogeneous colloids of nanoparticles. Main mechanisms associated in this method are hydrolysis and the polycondensation of precursors under controlled pH, time and temperature. All of these factors contribute to the ultimate characteristics and stability of the synthesised sols. Therefore the rheological properties of prepared sols can affect the final applications of sols such as fibre spinning, dip-coating and impregnation. In the main, the mechanism and chemistry of synthesising the metal oxide nanoparticles through the sol–gel method consist of three steps: hydrolysis, water-producing condensation and alcohol-producing condensation (Doughty Daniel et al., 1989). Fig. 11.1 illustrates the main stages for a silicate sol–gel system. In the first step, hydrolysis reactions occur where the precursor

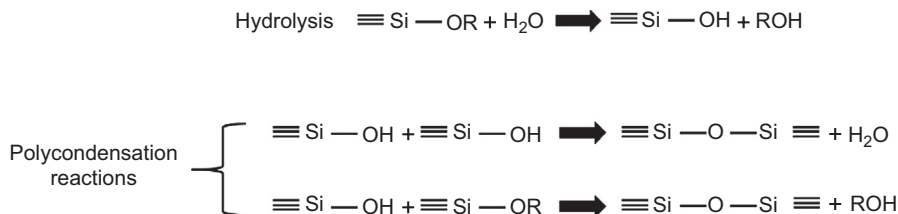


Figure 11.1 Main mechanisms of sol–gel in silicate system (Doughty Daniel et al., 1989; Pakdel et al., 2014c).

molecules react with water molecules, producing alcohol-based products such as silanol (Doughty Daniel et al., 1989). This is considered an important by-product because it can prolong the stability and miscibility of synthesised sols. Then, during polycondensation, silanol groups can react either with each other or with other available alkoxy groups to produce siloxane linkages (Doughty Daniel et al., 1989).

The concept of surface functionalisation of textiles through the sol–gel method has attracted a great deal of scientific attention (Pakdel et al., 2014c). Surface coating of textiles through the sol–gel method has inspired much research on introducing novel functionalities such as ultraviolet (UV) protection, antimicrobial activity, fire retardance, and self-cleaning, among others, to textiles (Montazer and Pakdel, 2011a). The application of TiO₂ nanoparticles in this pursuit has widely been hailed by researchers owing mostly to its availability, nontoxicity and physiochemical stability (Fujishima et al., 2000; Hashimoto et al., 2005). There are many publications regarding the application of metal oxide nanoparticles such as TiO₂ synthesised through the sol–gel method to the fabric's surface (Mahltig et al., 2005; Pakdel et al., 2014c). In a series of publications, Xin and Daoud investigated the applicability of TiO₂ nanoparticles to the cotton fabric's surface (Daoud et al., 2005; Daoud and Xin, 2004b, 2005). They synthesised TiO₂ nanosols through a low-temperature sol–gel method from the precursor of TTIP in the presence of ethanol, acetic acid and nitric acid (HNO₃). The coating process of fabrics was conducted based on the conventional method of dip-pad-dry-cure. In their publications, they characterised the synthesised TiO₂ nanoparticles and assessed the UV protection and antimicrobial properties of fabrics (Daoud et al., 2005; Daoud and Xin, 2004a,b; Xin et al., 2004). UV protection was assessed according to the UV protection factor of coated fabrics (Xin et al., 2004). The obtained results demonstrated that the presence of TiO₂ nanoparticles on the surface of cotton results in an excellent UV protection factor (+50) on cotton fabrics (Xin et al., 2004). Moreover, an efficient antimicrobial property was observed against *Staphylococcus aureus*, a gram-positive bacteria (Daoud et al., 2005). The applied coating layers to cotton fabrics showed a good washing fastness until 55 cycles of wash (Xin et al., 2004). The great stability of nanoparticles on the surface of cellulosic substrates stems from the existence of stable bonds between the nanoparticles and hydroxyl groups on the fibre's surface, established during the curing process.

Qi et al. (2006) treated cotton samples with TiO₂ colloid and produced a self-cleaning property in samples. The coated fabrics were able to decompose red wine and concentrate coffee stains within 20 h of illumination under simulated

sunlight (Qi et al., 2006). The photocatalytic efficiency of coated samples was quantitatively demonstrated by monitoring UV-induced dye solution decomposition in the presence of coated fabrics (Qi et al., 2006). The researchers analysed the impact of sol preparation temperature on the obtained results. The novel feature of fabrics was ascribed to the photocatalytic property of TiO₂ nanoparticles. In the presence of UV, the TiO₂ nanoparticles are excited and electrons of the valence band absorb the UV energy and excite to the conduction band, producing negative electrons and positive holes (Ochiai and Fujishima, 2012). The electrons and holes in turn react with oxygen and water molecules, producing superoxide anions and hydroxyl radicals, respectively (Ochiai and Fujishima, 2012). These two products have a main role in decomposing organic stains absorbed on the fabrics (Qi et al., 2006). In the main, the photocatalytic aspects of TiO₂ nanoparticles are triggered by UV light whose energy is greater than the semiconductor band gap (3.2 eV for anatase TiO₂).

Daoud et al. (2008) fabricated the self-cleaning wool fabrics through a low-temperature sol–gel method. Considering the lack of efficient functional groups on the surface of wool fibres, surface modification is more challenging and pretreatment is necessary before the coating process (Daoud et al., 2008). Daoud and coworkers used succinic acid solution in dimethylformamide (DMF) to introduce further reaction sites on fibres to stabilise the TiO₂ nanoparticles on the fabric's surface. Put simply, the main purpose of surface pretreatment is to introduce additional hydroxyl groups on the fibre's surface, thereby increasing the affinity of TiO₂ nanoparticles to the substrate and anchoring to the fabric's surface (Daoud et al., 2008). The surface acylation of the wool surface had a tangible bearing on the self-cleaning property of fabrics over 20 h of exposure to simulated sunlight. The fabrics that underwent an acylation process are able to absorb a greater amount of nanoparticles and hence higher photocatalytic activity. The mechanism associated with anchoring the TiO₂ nanoparticles on the acylated wool surface is been proposed in Fig. 11.2.

Tung and Daoud optimised diverse parameters of the sol preparation process for the surface functionalisation of wool fabrics (Tung and Daoud, 2009, 2010; Tung et al., 2009). They assessed the impact of some influential parameters such as acid type, sol preparation duration, and concentration of precursor and posttreatment conditions on photocatalytic activity, UV protection, and the mechanical properties of fabrics (Tung and Daoud, 2011). The impact of two types of acids including hydrochloric acid (HCl) and nitric acid (HNO₃) used in sol synthesis on the photocatalytic activity of nanoparticles was assessed (Tung and Daoud, 2009). The presence of nitric acid in the sols escalated the pace of photoyellowing on wool samples. Based on the SEM images, the sol–gel method resulted in a uniform and continuous coating layer of nanoparticles on the surface of fibres. However, in the mentioned series of publications, no pretreatment was used to stabilise the TiO₂ nanoparticles on the fibre's surface. The photocatalytic activity of TiO₂ nanoparticles was assessed based on the colour fading of concentrated coffee and red wine stains (Tung and Daoud, 2009). Also, the photodegradation of methylene blue dye under UV was employed to understand the photoefficiency of coated textiles quantitatively. In that research, the surface of wool and cotton fabrics was coated with TiO₂ colloids synthesised through the low-temperature sol–gel method. The coated wool fabrics successfully decomposed

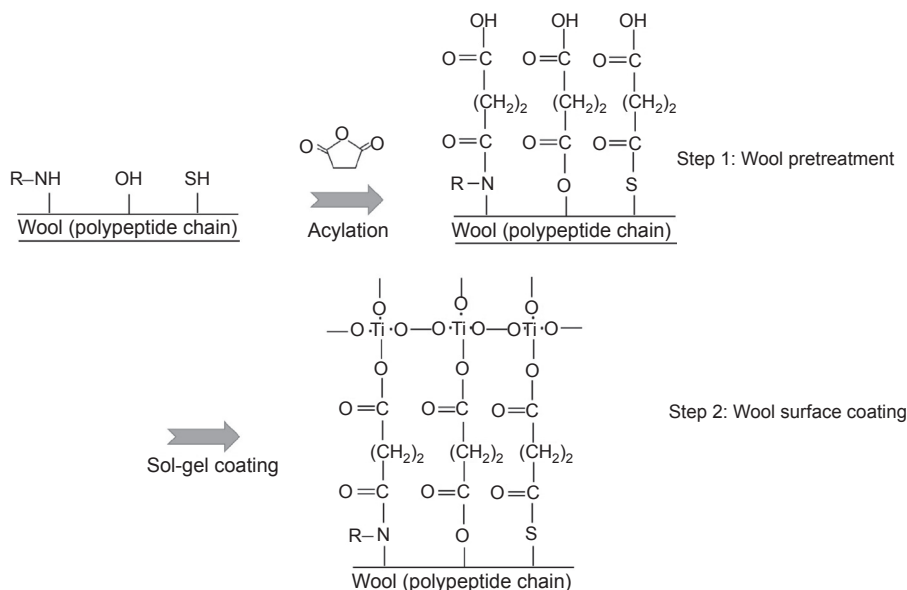


Figure 11.2 Surface coating of wool fabric with TiO_2 colloid (Daoud et al., 2008).

red wine and coffee stains within 20 h of exposure to simulated sunlight. Abidi et al. applied TiO_2 sols to cotton fabrics and investigated UV protection and the self-cleaning property of fabrics (Abidi et al., 2009). They analysed the impact of acid concentration on the ultimate quality of the fabrics' features.

Researchers have been trying to improve the synthesis process and functionality of TiO_2 nanoparticles through different methods. Of these approaches, blending with other metal oxides, doping with metals and nonmetals, and dye sensitisation are noteworthy (Pakdel et al., 2014c). Qi et al. synthesised the core-shell structure of TiO_2 anatase-silica through the sol-gel method and applied it to the cotton surface. Based on the obtained results, cotton fabrics coated with composite sols had greater photocatalytic performance in decomposing the Neolan Blue 2G dye (Qi et al., 2007). Pakdel et al. demonstrated that by integrating an optimised amount of SiO_2 into the TiO_2 sol, the photocatalytic activity of wool and cotton fabrics could improve (Pakdel et al., 2013; Pakdel and Daoud, 2013). Based on their research, TiO_2-SiO_2 in the proportion 30/70 was the most efficient composition to degrade coffee stains on wool and cotton fabrics (Pakdel and Daoud, 2013; Pakdel et al., 2013). This result is helpful for shortening the duration of UV exposure to fabrics and minimising the destructive impact of UV on fabrics. TTIP and TEOS were employed as the precursors of TiO_2 and SiO_2 colloids, respectively. Also, the presence of silica can have a role as a protective barrier against UV-induced free radicals generated from photocatalysts (Veronovski et al., 2010). Zhang et al. demonstrated that the application of $ZnO-SiO_2$ to wool fabrics resulted in better protection against UV-induced photoyellowing compared with pure ZnO (Zhang et al., 2014).

The surface coating of fabrics with TiO_2 colloids modified with noble metals (Ag, Au and Pt) was also carried out and diverse aspects of functionalised fabrics were brought to light (Pakdel et al., 2014a,b, 2015). The impact of noble metals and silica concentration on some characteristics of coated fabrics such as self-cleaning, UV protection, photostability, antimicrobial activity and the mechanical properties of fabrics were investigated and discussed. By incorporating an optimised amount of noble metals (Ag, Au and Pt) into the synthesis process of TiO_2 sol, the photocatalytic activity of coated wool and cotton increased (Pakdel et al., 2014a,b). However, an inverse relation was established between the photocatalytic activity and photostability of wool fabrics coated with Au- and Pt-modified sols (Pakdel et al., 2015). Based on SEM images, coating the fabric's surface with the sol–gel method results in an even and continuous coating layer of composite nanoparticles on fibres (Pakdel et al., 2014a). Fig. 11.3 illustrates the surface of wool fibres coated with TiO_2 nanoparticles synthesised through the sol–gel method.

Afzal et al. (2012) reported that using a meso-tetra(4-carboxyphenyl) porphyrin– TiO_2 composite system can increase visible light–induced photocatalytic activities on cotton fabrics. Their synthesised coating layer successfully decomposed coffee and red wine stains under an illuminated visible light source. The main mechanism associated with increasing the efficacy of TiO_2 nanoparticles is the excitement of porphyrin dye molecules under visible light and injection of the electrons into the conduction band of TiO_2 nanoparticles. This in turn results in the generation of active species of superoxide anions which have a main role in decomposing adsorbed stain molecules and breaking them down. Although porphyrin enhances the visible light activity of coated fabrics, it had poor photostability. However, this problem was tackled by using three metals, Fe(III), Co(II) and Zn(II), in the coating layer on cotton fabrics (Afzal et al., 2013a,b).

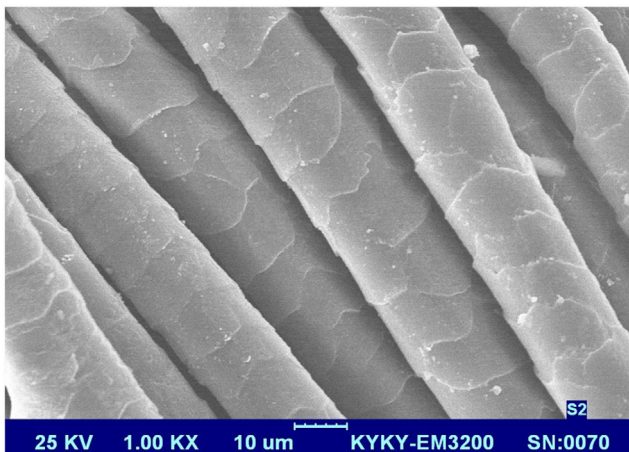


Figure 11.3 Wool fibres coated with TiO_2 nanoparticles.

11.2.2 Cross-linking method

Stabilising the applied nanoparticles on the surface of textiles is considered to be one of the most challenging hurdles in integrating novel finishing methods in the textile industry (Harifi and Montazer, 2012). Stabilising nanoparticles on fabrics is of prominent importance mostly because of potential health and environmental concerns. This has led to attempts at different methods of fabric surface treatments. Besides the sol–gel process, some researchers have tried other methods to anchor commercially produced TiO₂ nanoparticles such as Degussa-P25 on the surface of fabrics (Harifi and Montazer, 2012). The applied nanoparticles were stabilised on the fabric surface using some chemical spacers and cross-linking agents. Meilert et al. (2005) attached TiO₂ nanoparticles on the cotton fabric surface by using some carboxylic acids as the linking spacers. They used succinic acid, 1,2,3-propanetricarboxylic acid and 1,2,3,4-butanetetracarboxylic acid (BTCA) and established stable linkage between the particles and substrate. The coating process consisted of two main steps including fabrics pretreatment with the chemical spacers and coating with TiO₂ nanoparticles (Meilert et al., 2005). The fabrics were treated with the aqueous solution of spacers in the presence of NaH₂PO₂ for 1 h followed by a curing step. In the next step, the pretreated samples were soaked in the finishing bath containing 5 g/L TiO₂ (P25) nanoparticles and dried at 100°C for 1 h. The samples were then washed to remove the loosely attached nanoparticles. Furthermore, other techniques such as radiofrequency plasma, microwave plasma, and vacuum-UV light irradiation were introduced as effective pretreatments by Bozzi et al. (Bozzi et al., 2005a,b; Yuranova et al., 2003). They introduced some negatively charged groups such as $-\text{COO}^-$ and $-\text{O}-\text{O}^-$, among others, on the fabric surface to augment the tendency of positively charged TiO₂ nanoparticles towards the fabric surface. This research team assessed the efficiency of these pretreatments on the stability of TiO₂ nanoparticles on some substrates such as cotton, wool–polyamide and polyester fibre by analysing the photocatalytic activity of coated fabrics (Bozzi et al., 2005a,b). The photoefficiency of coated fabrics was assessed based on the decomposition of coffee stains and the CO₂ gas rate released during the mineralisation of adsorbed stains after exposure to a light source. It was revealed that the fabrics that had undergone a pretreatment process generated a higher amount of CO₂, indicating better photocatalytic activity on fabrics owing to the greater adsorption of nanoparticles. Yuranova et al. (2003) used the pretreatment method to activate the surface of polyester–polyamide fabrics before coating with a silver antibacterial agent. These methods of pretreatment are crucial to stabilise nanoparticles on the fabric's surface, notably synthetic ones.

Stabilising TiO₂ nanoparticles on proteinases fibres is more challenging owing to the lack of efficient functional groups on the surface of fibres. Montazer and Pakdel in a series of publications examined different characteristics of wool fabrics coated with TiO₂ (P25) nanoparticles (Montazer and Pakdel, 2010, 2011b; Montazer et al., 2011c). They used BTCA and citric acid (CA) as two cross-linking agents in the presence of sodium hypophosphite (SHP) to anchor the TiO₂ nanoparticles onto the wool surface. In addition, surface oxidation of wool fabrics by potassium permanganate

solution (pH 3) was employed as a pretreatment to increase the uptake of nanoparticles on the fabric's surface. The coating process of wool fabrics through this method immersed the scored wool fabrics into an ultrasonic bath containing polycarboxylic acids, SHP and TiO_2 (P25) followed by drying and curing at 120°C . The reaction between cross-linking agents and the wool was related to the established bonds between the carboxyl groups of linking agents with functional groups of wool such as $-\text{NH}_2$, $-\text{SH}$ and $-\text{OH}$ during the curing step. The coated fabrics had features such as self-cleaning, photostability and being shrink proof. Antimicrobial activity test demonstrated 70% and 0% efficiency against *Escherichia coli* and *S. aureus* bacteria, respectively. However, no data are available regarding the wash fastness and the impact of the coating process on the mechanical properties of fabrics. Inorganic–organic hybrid coating has been used to stabilise different types of nanoparticles such as TiO_2 , $\text{TiO}_2\text{-Ag}$, Ag and carbon nanotubes (CNTs) (Montazer et al., 2011a,b). The impact of three influential parameters such as the role of the duration of finishing, the concentration of TiO_2 and cross-linking agents on the obtained features was assessed statistically using the respond surface methodology (Montazer et al., 2010). The proposed mechanism of cross-linking process is shown in Fig. 11.4. More aggregations were observed among nanoparticles applied to fabrics through the impregnation method compared with sol–gel.

The cross-linking method was also employed by Parvinzadeh Gashti et al. (2012a) to apply hydrophobic silica nanoparticles on the cotton fabric surface. They used different concentrations of commercial SiO_2 nanoparticles along with BTCA as the cross-linking agent and SHP as the catalyst to coat the fabrics. The fabrics were treated in an ultrasonic bath containing silica, BTCA and SHP at 40°C for

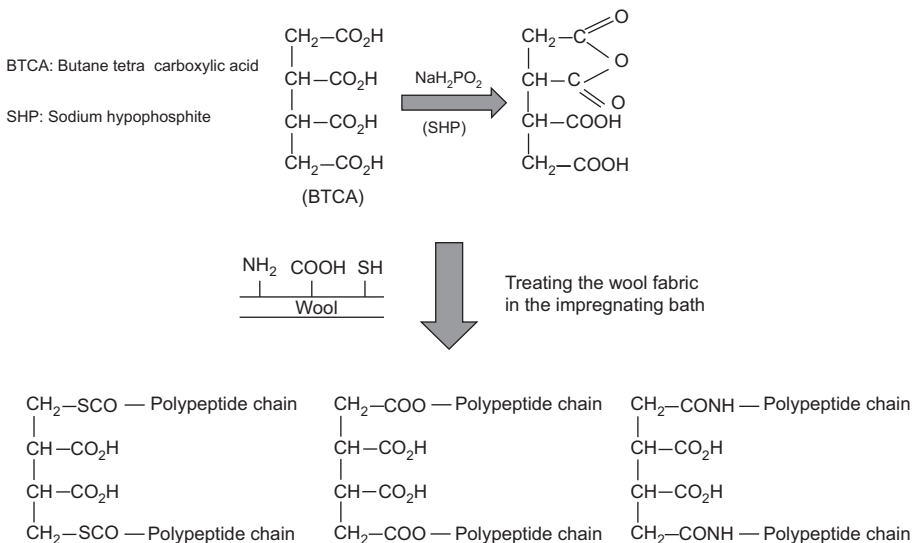


Figure 11.4 Reaction of BTCA cross-linking agent with wool (Montazer & Pakdel, 2011a).

20 min followed by a curing process. They demonstrated the existence of linkages between the BTCA and hydroxyl and carbonyl groups of cotton using Fourier transform infrared spectra. Furthermore, the presence of silica nanoparticles on the fabric surface resulted in some flame retardancy features on cotton (Gashti et al., 2012). The degradation temperature of cotton fabrics increased from 323°C for untreated samples to 358°C for treated samples. The higher the amount of silica was on the surface, the greater the resistance was against the decomposition for cotton samples. The water contact angle (WCA) for cotton samples coated with 40 g/L silica nanoparticles was around 132 degree. The increase in WCA is ascribed to the low surface energy of silica nanoparticles (Gashti et al., 2012). The same research group conducted further research on surface-functionalising cotton and wool substrates using CNTs (Alimohammadi et al., 2013, 2012; Parvinzadeh Gashti and Almasian, 2013a), ZrO₂ (Parvinzadeh Gashti and Almasian, 2013b, Parvinzadeh Gashti et al., 2012b) and silica–kaolinite (Parvinzadeh Gashti et al., 2013c) through the same method. They reported that the surface coating of wool fabrics with nanozirconia imparts some novel features such as flame retardancy and electromagnetic reflection wool. The wool fabrics were treated with different concentrations of ZrO₂ nanoparticles in an ultrasonic bath containing CA and SHP followed by padding and UV illumination. Cross-links between the nanoparticles and substrate were established during the UV illumination process (Parvinzadeh Gashti et al., 2015; Parvinzadeh Gashti and Eslami, 2015). Fig. 11.5 shows the SEM images of wool fibres coated with ZrO₂ nanoparticles stabilised by cross-linking agents.

11.2.3 Thin-film deposition technique

11.2.3.1 Physical vapour deposition

One method to produce a thin film on textile substrates is vapour deposition, which in turn is categorised as two main groups: physical vapour deposition (PVD) and chemical vapour deposition (CVD) methods. Some parameters such as substrate type, precursor, the thickness of the film and uniformity determine the selection of the method (Esen et al., 2014). In brief, PVD is a process in which a thin layer of coating is deposited on the substrate through a vapourisation process (Wei, 2009). A solid material is used as the source of vapour and then transformed into the vapour phase and then transferred to the surface of substrate, forming a uniform coating layer (Wei, 2009). Put simply, through the PVD method, the vapour atoms or molecules generated from a solid material are placed next to each other on the substrate. PVD in turn is subdivided into three main streams: vacuum evaporation, ion implantation and sputter coating. These methods are different in the energy of their depositing materials. In other words, the coating materials in vacuum evaporation, sputter coating and ion implantation techniques have low (a few tenths of electronvolts), moderate (tens to hundreds of electronvolts) and high energy, respectively (Bunshah, 1982). The applied energy is influential in interactions of coatings materials and substrates and the growth of the film (Bunshah, 1982).

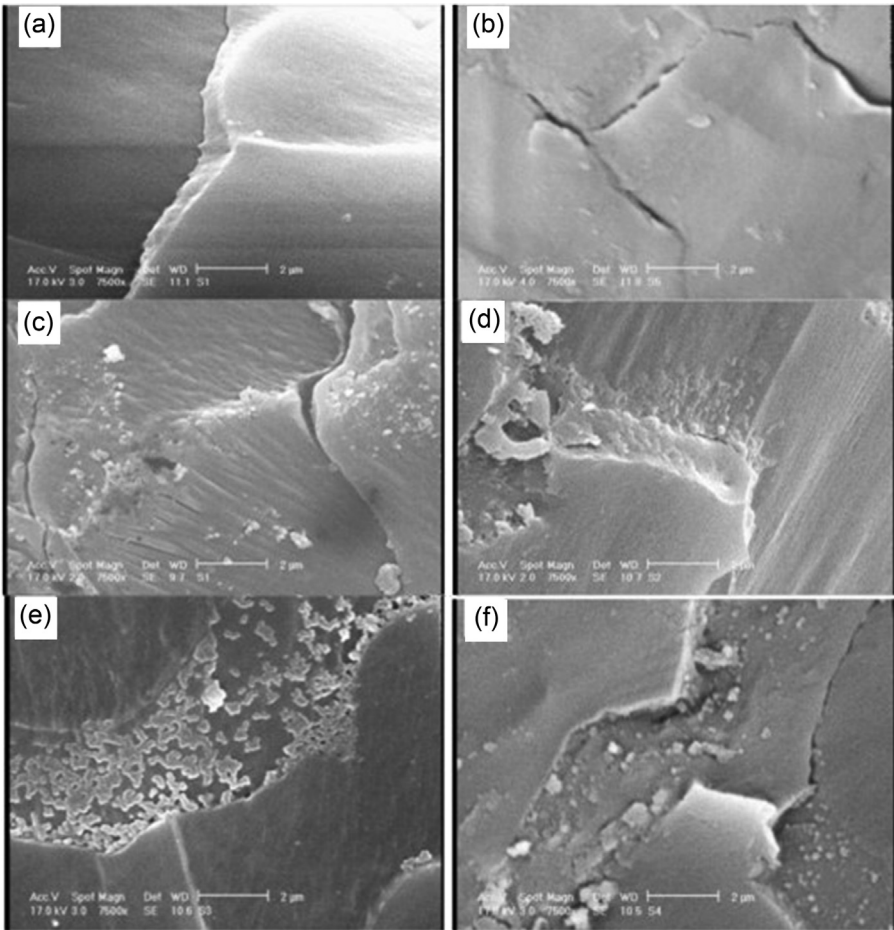


Figure 11.5 SEM images of (a) untreated wool fibre at 2 μm , (b) wool fibre cross-linked with CA under UV light at 2 μm , (c) wool fibre cross-linked with CA–1% ZrO_2 nanocomposite under UV light at 2 μm , (d) wool fibre cross-linked with CA–3% ZrO_2 nanocomposite under UV light at 2 μm , (e) wool fibre cross-linked with CA–6% ZrO_2 nanocomposite under UV light at 2 μm and (f) wool fibre cross-linked with CA–9% ZrO_2 nanocomposite under UV light at 2 μm . Reprinted from reference Parvinzadeh Gashti, M., Almasian, A., 2013. Citric acid/ ZrO_2 nanocomposite inducing thermal barrier and self-cleaning properties on protein fibers. *Composites Part B: Engineering* 52, 340–349. with permission from Elsevier.

11.2.3.2 Vacuum evaporation

In vacuum evaporation, the evaporation and deposition of film on substrate is carried out in the vacuum condition. This allows vapour molecules to condense directly on the substrate surface, creating a solid film, and prevents a reaction with the free space. This technique has been used to impart electromagnetic interference (EMI) shielding to protect textiles by depositing metal nanoparticles on textile materials (Hong et al., 2001;

Lee et al., 2002; Lacerda Silva et al., 2013). Lai et al. (2007) investigated EMI shielding efficiency of polyethylene terephthalate (PET) film coated with metals. They examined the functionality of four types of metals including silver, copper, aluminium and titanium applied to substrate using the vacuum evaporation deposition technique. Next, the coated PET films were cut into filaments 0.254 mm wide and then woven into fabrics. Results demonstrated that the PET substrates coated with silver and titanium showed the best and worst EMI shielding efficiencies, respectively (Lai et al., 2007). The impacts of other influential factors such as aperture ratio and filaments alignment on ultimate efficiency were discussed as well (Lai et al., 2007). It has been reported that using intrinsically conductive polymers (ICPs) such as polypyrrole (PPy) can be helpful to impart EMI shielding efficiency to the substrates. In the same line, using the complexes of metal–ICPs results in a higher level of efficiency on textiles (Lee et al., 2002). Hong et al. (2001) coated the surface of PET woven fabric using PPy–naphthalene sulfonic acid and then PPy doped anthraquinone-2-sulfonic acid. In the next step, they deposited a layer of silver (Ag) on the prepared complex through a thermal evaporation vacuum method. EMI shielding efficiency was measured based on the absorption–reflection and transmittance of the *S* (scattering)-parameter analysis over 50 MHz to 1.5 GHz (Hong et al., 2001). The presence of Ag increased the EMI shielding efficiency (Hong et al., 2001). Although applying metallic coating layers to textiles has been promising to impart novel characteristics to substrates, the lack of coating stability is considered to be one of the main drawbacks of this method notably on synthetic fibres (Bula et al., 2006). Therefore, the surface activation of fibres using plasma was suggested as a pretreatment before applying metallic coating through the vacuum evaporation method (Bula et al., 2006).

11.2.3.3 Sputter coating

The sputter-coating method can be used to deposit a thin layer of nanoparticles on a fabric surface. The main mechanism of this approach is to create plasma from a low-pressure inert gas such as argon in a vacuum condition (0.001–0.1 torr) (Sen, 2007; Wei, 2009). The surface of solid materials is hit by the created plasma, which consists of electrons and highly energetic ions. This results in the ejection of atoms from the solid material of the coating layer and bonding to the substrate owing to their high energy (Sen, 2007). The target material and substrate are located on the cathode and anode of the coater equipment, respectively. The electrical potential between two electrodes results in the movement of electrons from cathode to anode, creating a glow discharge. The argon gas present in the chamber is ionised by electrons and accelerated, hitting the target coating material on the cathode (Sen, 2007). Bombarding the target material can lead to producing the secondary electrons whose generation rate depends mostly on the kinetic energy of ionised argon gas (Sen, 2007). The energy of striking ions determines the rate of atoms being ejected from the target material. On the whole, the number of ejected atoms by incident ions is considered to be the sputtering yield (Sen, 2007). In magnetron sputter coating, there has been an attempt to keep the secondary electrons in close vicinity to the material via a magnetic field. This technique can result in some advantages such as producing more uniform,

compact and durable coating layers on substrates. This technique is considered to be expensive but environmentally friendly (Yip et al., 2009).

The surface functionalisation of textiles through magnetron sputter coating has been widely reported (Jiang et al., 2010). This approach is employed to coat textile substrates with a very thin layer of metal nanoparticles to impart novel features to substrates. The surface of PET fibres was coated with silver nanoparticles through a sputtering method. The coating process of PET fibres through this method resulted in some new properties such as UV protection, hydrophobicity and antimicrobial activity on fabrics. The obtained SEM images showed a uniform coating layer of silver nanoparticles with the approximate grain size of 50 nm on fibres (Jiang et al., 2010).

In a research study conducted by Wang et al. (2007), polypropylene nonwovens were functionalised by a silver coating layer and some novel features such as antibacterial activity and conductivity were characterised. A direct relation between the thickness of Ag films on nonwovens and antimicrobial activity against *E. coli* was established. The more silver that was deposited on the substrate, the more efficient was the antimicrobial property. The duration of coating through the sputtering method had a bearing on the silver grain size grown on nonwovens. Larger grains, rougher surfaces and more compact coating layers were observed on nonwovens after increasing the coating duration (Wang et al., 2007). The researchers reported an optimum coating layer of 2 nm to achieve an efficient antibacterial activity on substrates. Scholz et al. conducted a comparative laboratory-scale investigation on antimicrobial and antifungal activities of silica fibres coated with silver, copper, platinum, platinum–rhodium and gold through a magnetron sputter deposition method (Scholz et al., 2005).

11.2.3.4 Ion implantation

Another approach to PVD used to modify textile surfaces is the ion implantation technique (Öktem et al., 2006). The main principle of this environmentally friendly technique is to bombard the surface of a solid material with known metallic ions to implant them into the near surface of substrates such as textiles, polymers and ceramics, among others, to modify the surface characteristics (Öktem et al., 2006). Three main compartments of an ion implanting system are ion source, accelerator and substrate. Oktem et al. investigated the impacts of Cu ion implantation on electrostatic features of PET fabrics as well as C, Ti and Cr implantation on mechanical properties of membrane fabrics (PET fabric coated with a PET membrane). The ions were produced by a vapour vacuum arc (MEVVA) implanter. The substrate surface located in the vacuum chamber was bombarded with produced ions at the rate of 1×10^{14} to 1×10^{17} ions/cm². The surface modification of PET fabrics with Cu ions via MEVVA produced antistatic features on fabrics in such a way that the surface resistance of fabrics decreased from 10^{13} to $10^9 \Omega \text{ cm}$. As for the PET membrane, after surface modification with C, Ti and Cr ions, some parameters such as friction coefficient and wear loss of fabrics decreased, whereas the employed ions and dose were effective on findings (Öktem et al., 2006). In the ion implantation method the coating material is ionised, energised in an accelerating step and then shot towards the substrate. This results in the implantation of ions into the shallow depth near the surface area of the substrate, producing a thin film (Bunshah, 1982).

11.3 Nanofibre coating via electrospinning

Electrospray and electrospinning have the same principles. If a polymer solution with a sufficient viscosity is applied in the electrospinning, the initial jet does not break into drops and fibres form (Fig. 11.6). Electrospun fibre can be achieved from a solvent solution and melt form. Many parameters affect the transformation of polymer solutions into nanofibres, including the solution properties, the governing variables and the ambient parameters (Deitzel et al., 2001; Bhardwaj and Kundu, 2010; Huang et al., 2003).

Electrospinning is a flexible technique and enable the uniform coating of nanofibres onto different substrate. It is a process in which high voltage is introduced to the nozzle and a substrate to achieve an interconnected membrane-like web of fibres (mat). The diameter of fibres in this technique is variable and can be between 10 and 500 nm. A wide range of polymers including nylon, polyurethane (PU), polyacrylonitrile, polyvinyl alcohol and polylactic acid was applied to produce ultrathin fibres with different properties (Deitzel et al., 2001; Bhardwaj and Kundu, 2010; Huang et al., 2003).

11.3.1 Electrospun nanofibre coating application

11.3.1.1 Solid-phase microextraction

Analytical approaches involve extensive sample preparation such as solvent and liquid–liquid extractions. Solid-phase microextraction (SPME) is an alternative approach; it appeared as a sample preparation method in the early 1990s and involved a thin-film coating on the fibre to extract analytes of interest from a sample matrix. SPME has been established as an extraction approach across a diverse array of

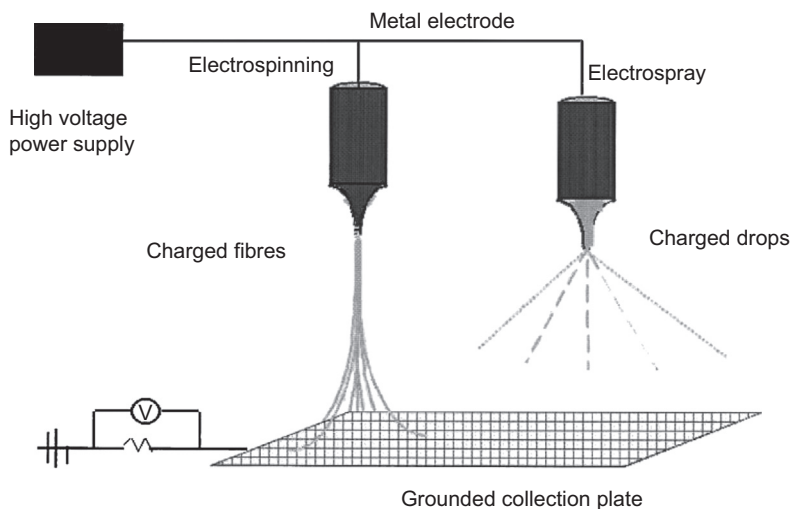


Figure 11.6 Schematic diagram of setup of electrospinning and electrospay apparatus. Adapted from Deitzel, J.M., Kleinmeyer, J., Harris, D., Beck Tan, N.C., 2001. The effect of processing variables on the morphology of electrospun nanofibers and textiles. *Polymer* 42, 261–272.

analytical approaches such as organic solvents in water, explosives, flavours and pesticides. It has been shown that SPME is a convenient and efficient extraction method (Pawliszyn, 1999; Spietelun et al., 2010). Electrospun nanofibres are used as coatings on thin stainless-steel wires for SPME application (Bagheri and Roostaie, 2014; Bagheri et al., 2012; Bagheri and Aghakhani, 2011).

SPME has four sections, as shown in Fig. 11.7; they are connected to a rotor and allow rotation and movement of the SPME syringe. For electrospinning coating, the plunger is pulled down and the 1-cm end of internal needle (part D) appears and is used to coat the nanofibres. Polyamide (nylon 6) is used for this purpose. SEM images of nanofibres coated on stainless steel are presented in Fig. 11.8. The higher surface area, porous structure and functional groups (amide groups) make this coating a good candidate for the extraction of polar compound (Bagheri and Roostaie, 2014).

Coating SPME by the electrospun method and polyamide is a good method for extracting trace amounts of phenols dissolved in aqueous solutions. This coating provides an easy, simple and inexpensive SPME method for extracting phenols with good sensitivity and reproducibility (Bagheri et al., 2012).

In another study, four different polymers, PU, polycarbonate, polyamide and polyvinyl chloride (PVC) were coated on the stainless-steel needle, and headspace-SPME of some chlorophenols from aqueous samples was applied. The extraction efficiencies of these polymers were investigated by gas chromatography–mass spectrometry analysis. PU is a prominent candidate for extraction because it is able to generate

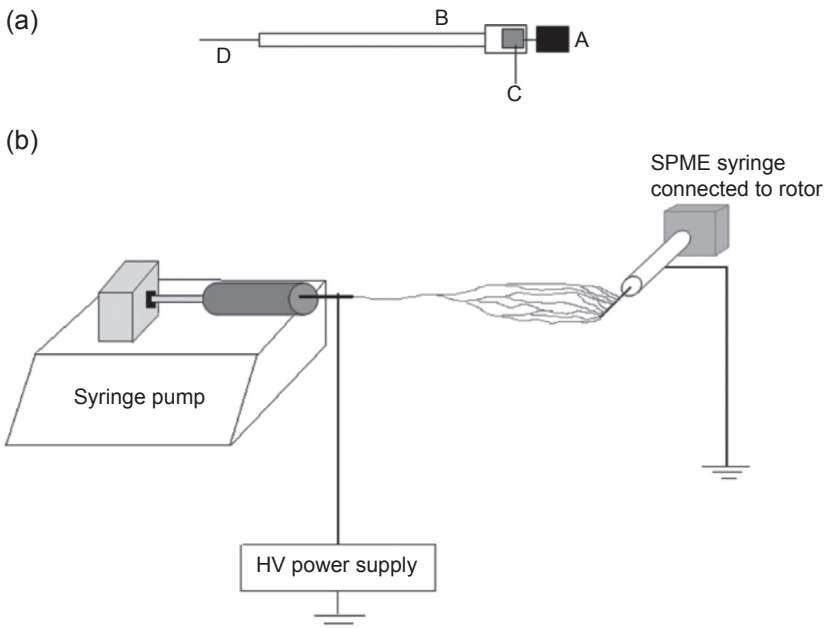


Figure 11.7 Scheme of homemade SPME syringe: (a) internal needle, (b) external needle, (c) sealing materials and (d) 1-cm end of internal needle (Bagheri and Roostaie, 2014).

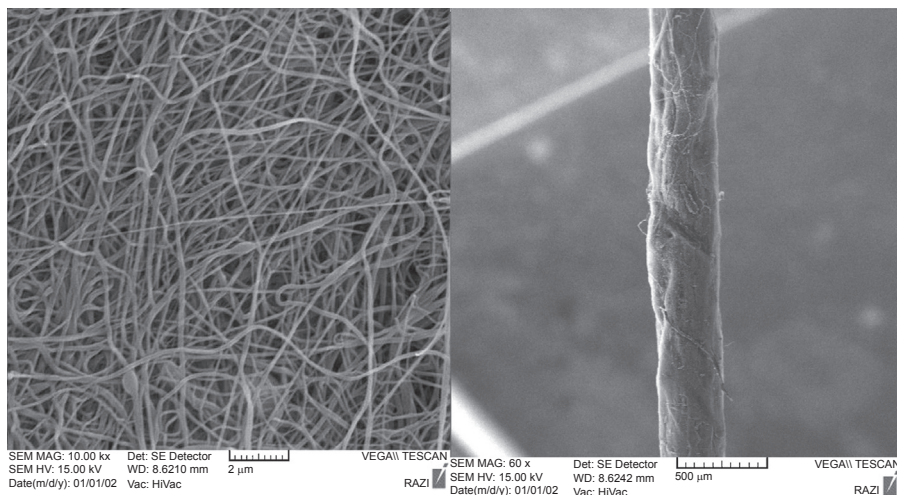


Figure 11.8 SEM images of SPME needle coated by polyamide nanofibres at different magnifications (Bagheri and Roostaie, 2014).

the π – π interactions with analytes owing to excess functional groups in the polymer nanofibre (Bagheri and Aghakhani, 2011).

11.3.1.2 Corrosion inhibitor

Coating a thin layer of polymer on metal surfaces is a pivotal technique to avoid corrosion. Electrospun coating has been used as a corrosion inhibitor for aluminium, steel and brass in chloride solutions. The electrospun polymer nanofibre coating of PVC exhibited good functionality in decreasing the corrosion rates and higher polarisation resistance to aluminium, steel and brass (Es-Saheb et al., 2012).

In another study, self-healing transparent core–shell nanofibre was coated on steel for anticorrosive protection. In this procedure, dual-emulsion electrospinning was required, presented in Fig. 11.9. Dimethylvinyl-terminated dimethylsiloxane was applied as the core material using n-hexane as a solvent. Dimethyl methyl hydrogen siloxane was used as a liquid curing agent with no solvent. Then, PAN was used as a shell and dissolved in DMF. In the next step, the core solution was added and dispersed in the PAN solution. Finally, the two emulsions were used to electrospin the matrix from a different single nozzle to prepare a dual-nanofibre mat on the steel surface. This mat contained the polydimethylsiloxane (PDMS) or curing agent as cores and PAN as the shell. This mat was placed in PDMS polymer, which solidified and formed an outer matrix of nanofibres. The thickness of the formed PDMS matrix was around 28.6 mm (Lee et al., 2014).

The diameter of these nanofibres was around 440 nm and was highly transparent to visible light. Results showed that the thinnest coatings supplied complete anticorrosive protection to a steel substrate. As a result, the resin and the curing agent were rapidly

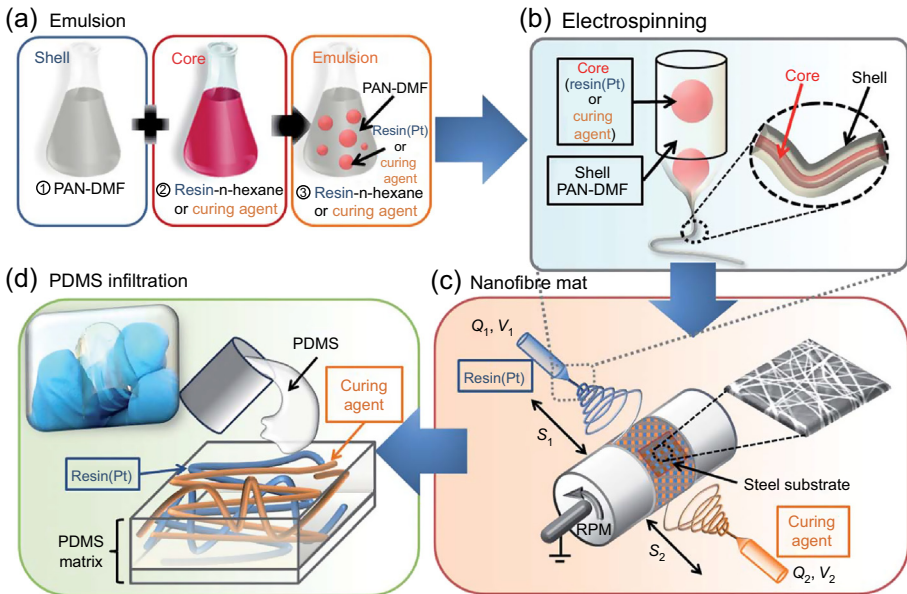


Figure 11.9 Schematic of core–shell nanofiber preparation. (a) The shell polymer solution and two emulsions (DMF resin and curing agent). (b) Electrospinning of core–shell nanofiber. (c) Formation of dual-nanofiber mat. (d) PDMS matrix infiltration.

Adapted from Lee, M.W., An, S., Lee, C., Liou, M., Yarin, A.L., Yoon, S.S., 2014. Self-healing transparent core-shell nanofiber coatings for anti-corrosive protection. *Journal of Materials Chemistry A* 2, 7045–7053.

released from the damaged fibres and the polymerisation reaction was fast enough to cover the damaged space with the restored PDMS (Lee et al., 2014).

11.3.1.3 Sensors

Polymeric coatings on the sensor surface can increase sensor response sensitivity. Electrospinning can control the porous structure, thickness and permeability of the sensor by coating. Coating nanofibres by electrospinning was first used to promote electrodes with a large ratio of surface area to volume. Glucose biosensor (a miniature coil-type implantable biosensor) was prepared by an inner electrode (metal), a middle enzyme layer (glucose oxidase) and electrospun PU membrane (Fig. 11.10). Both static and dynamic collector systems cover the sensor surface, but it has been illustrated that the dynamic collector allowed uniform fibroporous PU coating. Fig. 11.10(c)–(g) shows SEM images of PU-spun coating using a dynamic collector, which in turn shows the uniform covering and porosity of the miniature coil-type sensor. The thickness of coating can be controlled by electrospinning time, and increasing the thickness of coating led to an insignificant decrease in sensor sensitivity (Wang et al., 2013).

In another study, an electrospun nanofiber membrane was applied to cove quartz crystal microbalance (QCM) to achieve a gas sensor for NH_3 detection. QCMs are

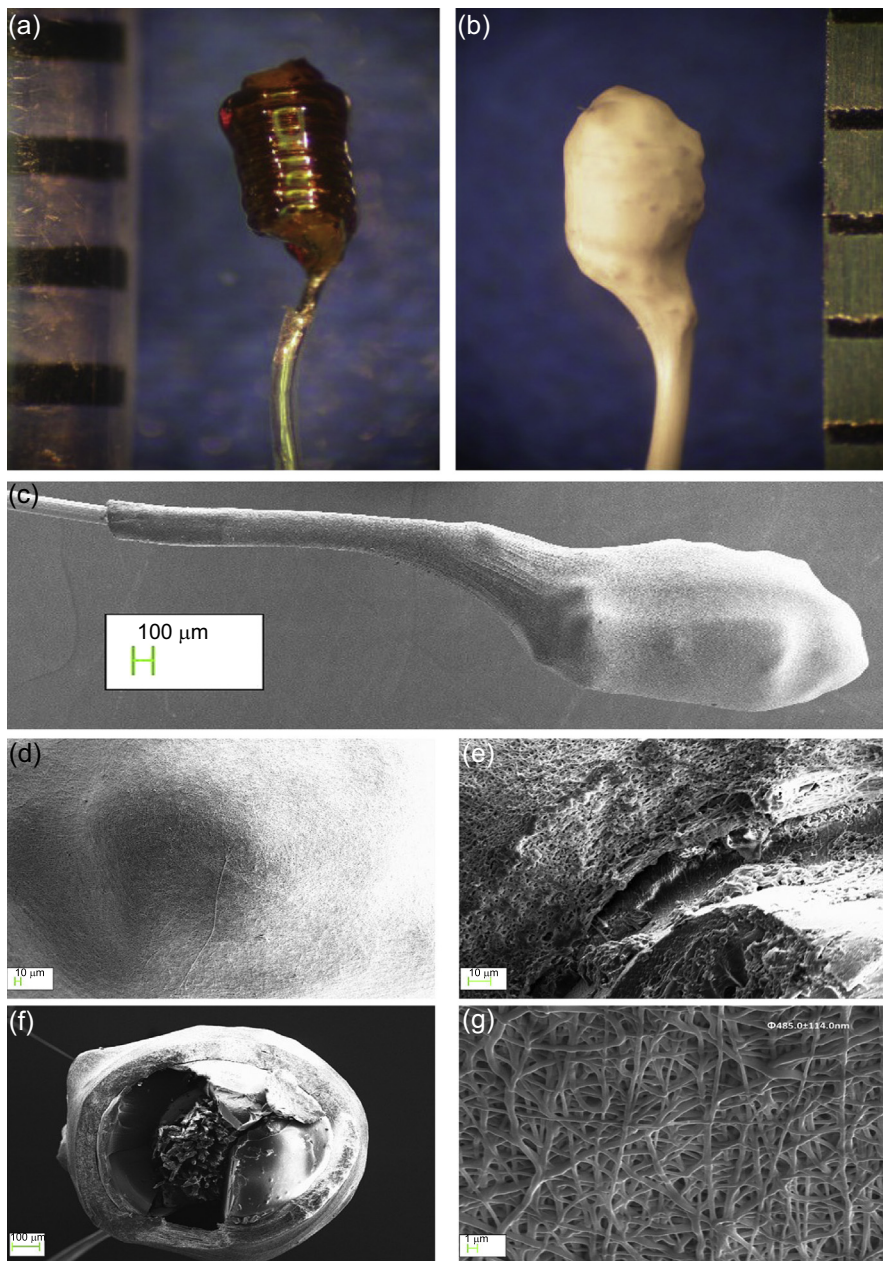


Figure 11.10 Optical microscope (a and b). Scale in millimetres and SEM (c–g) images showing the morphology of a coil-type biosensor without (a) and with (b–g) electrospun PU coating spun using a dynamic collector.

Adapted from Wang, N., Burugapalli, K., Song, W., Halls, J., Moussy, F., Ray, A., Zheng, Y., 2013. Electrospun fibro-porous polyurethane coatings for implantable glucose biosensors. *Biomaterials* 34, 888–901.

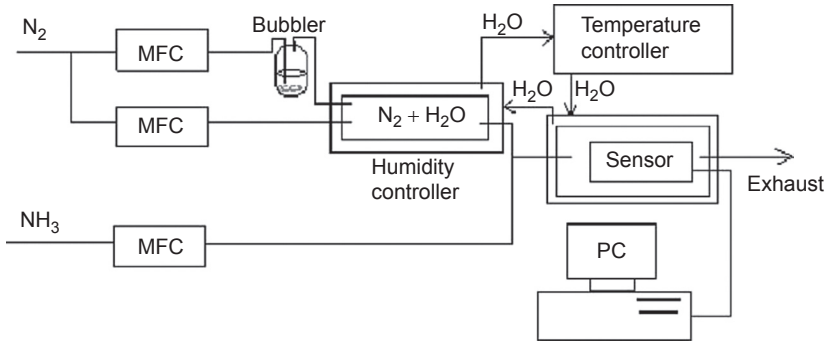


Figure 11.11 Schematic of a gas sensor for NH₃ detection.

Adapted from Ding, B., Kim, J., Miyazaki, Y., Shiratori, S., 2004. Electrospun nanofibrous membranes coated quartz crystal microbalance as gas sensor for NH₃ detection. *Sensors and Actuators B: Chemical* 101, 373–380.

an acoustic wave techniques for detecting a small mass. The experimental setup for sensing NH₃ is presented in Fig. 11.11 (Ding et al., 2004).

There is irreversible absorption process and a strong interaction between NH₃ molecules and carbonyl groups of poly(acrylic acid) (PAA), so it influences the sensing properties of QCCM and causes frequency shifts. Cross-linkable PAA and poly(vinyl alcohol) were used as a blend solution to prepare nanofibrous membranes. The increment in average diameter and rigidity of nanofibres were achieved by increasing the viscosity and conductivity of the blend solutions and the content of PAA component. The sensing properties of the sensor were significantly influenced by relative humidity and the concentration of NH₃ and PAA content in the blend (Ding et al., 2004).

11.3.1.4 Membrane coatings

Electrospun nanofibres have high porosity and a small pore size, so these properties are desirable for membranes. A conventional filtration system (ultra or nano) is based on porous membranes for water treatment. Therefore electrospun nanofibre coatings are a promising candidate for preparing composite membranes (Yoon et al., 2006). Also, electrospun nanofibre-supported thin-film composite membranes were used for pressure-retarded osmosis (Bui and McCutcheon, 2014).

Porous membranes were prepared based on electrospun nanofibres, which produce exceptionally lightweight multifunctional substrates for protective clothing applications. They exhibit high breathability, elasticity and filtration efficiency. The electrospun nanofibres were applied directly to open-cell PU foam. Results showed that the flow resistance of the electrospun fibres is higher than for normal clothing materials, whereas the high resistance to air flow does not impede the diffusion of water vapour through the porous structure. Also, the electrospun fibre coating was extremely efficient at trapping aerosol particles (Gibson et al., 2001).

Electrospun nanofibres were coated on separator membranes for lithium-ion rechargeable batteries. The separator is electrochemically inert and is the critical

component in the lithium-ion batteries. The separator is placed between the positive and negative electrodes to prevent electrical short circuits, while acting as the electrolyte reservoir to enable ionic transport. Single-nozzle and nozzle-less electrospinning methods have been applied to coat nanofibres on the microporous separator membrane. The nozzle-less electrospinning method provided nanofibres with smaller diameters and better adhesion to the membrane substrate (Huang and Hitt, 2013; Alcoutlabi et al., 2013).

Lee et al. (2013) used polyvinylidene fluoride-co-chlorotrifluoroethylene (PVDF-co-CTFE) and PVDF-co-CTFE–polyvinylidene fluoride-co-hexafluoropropylene (PVDF-co-HFP) to prepare nanofibre-coated composites, and a nozzle-less electrospinning method was used to coat nanofibres onto Celgard microporous battery separator membranes. The electrolyte absorption of the separator and the separator adhesion was improved by using the PVDF-based electrospun fibre. They demonstrated that both PVDF-co-CTFE and PVDF-co-CTFE–PVDF-HFP coatings had desirable adhesion to the membrane substrate and possessed higher electrolyte uptake capacity compared with the uncoated membranes.

11.3.1.5 Textile coatings

The electrospun technique was also applied to coat textile fabrics, which in turn reduced abrasion resistance. In this context, hybrid yarns were prepared by twisting nanofibre-coated filaments. Electrospun nanofibres were coated onto the monofilaments, and the coated nanofilaments were then twisted into yarn (Fig. 11.12). Coating of monofilaments via electrospinning and subsequent twisting improved abrasion resistance as a result of the cohesion phenomenon (Zhou et al., 2010).

Electrospun nanofibres were also coated onto textile surfaces for filtration. According to results, electrospun fibres improved the filtration efficiency of textile substrates even with a low amount of nanofibres (0.02 g/m^2). The efficiency of uncoated samples was less than 10% for $1\text{-}\mu\text{m}$ particles and depended on the particle size, whereas the highest coating weight (0.50 g/m^2) eliminated approximately 90% of all aerosol particles (Heikkilä et al., 2007).

11.4 Future trends

Optimising and using these coating methods from laboratory-scale experiments to supply chain platforms is an important issue for textile manufacturers. Some of these methods, such as thin-film deposition and electrospinning coating techniques, are still challenging for industrial scale production. Thus, intensive studies are necessary for a wide range of commercial applications. In this regard, Nanotex (founded in 1998), a subsidiary of the United States-based Burlington Industries, is known as a leading nanotechnology-based textile coatings company for commercialised products in clothing and household applications. Controlling nanocoating procedures and quality inspection of output products may not be as simple as for macroscale coating products. Implementing advanced pretreatment machines for nanomaterials and textiles such as

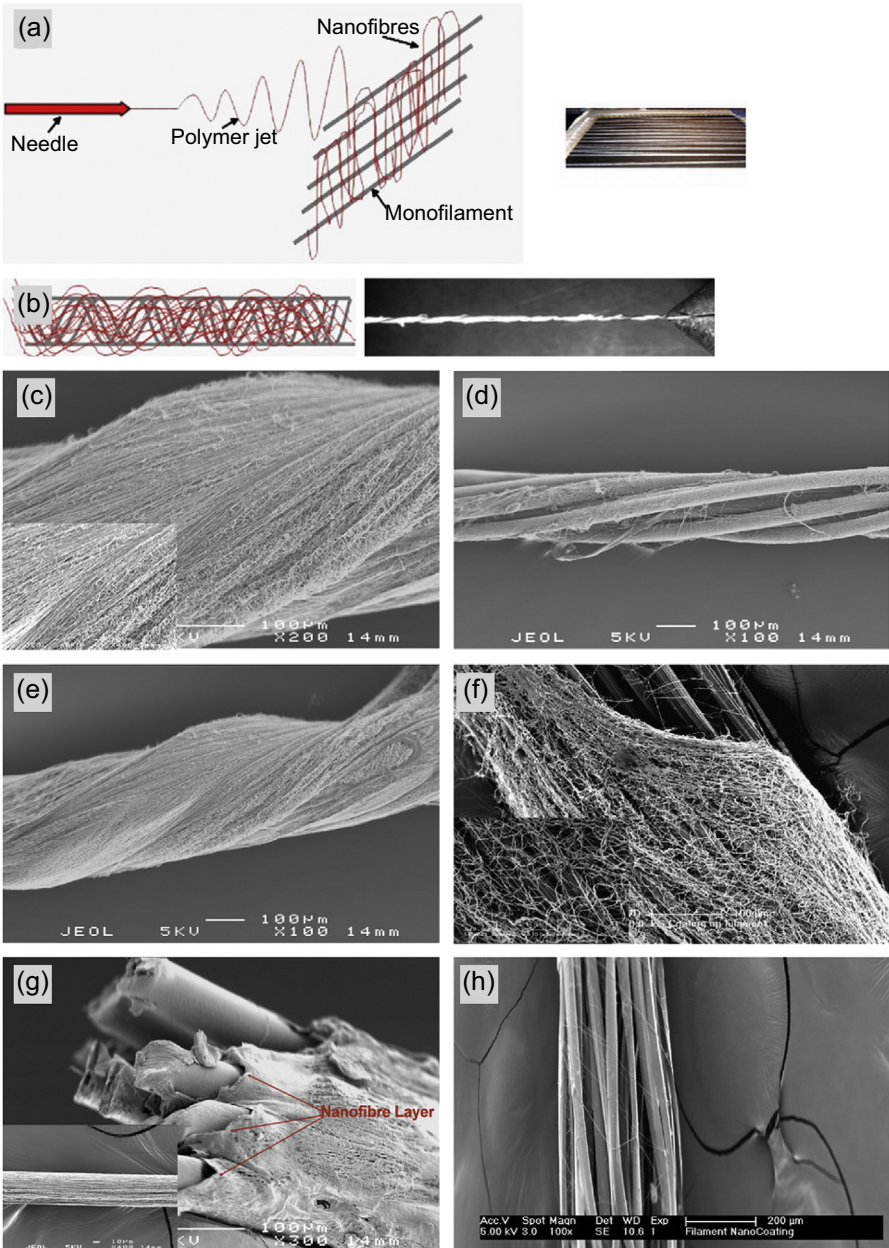


Figure 11.12 Formation of electrospun fibres on hybrid yarn: (a and b) schematic of the electrospinning process; (c–h) morphology and porosity of the coated yarn.

Adapted from Zhou, F.-L., Gong, R.-H., Porat, I., 2010. Nano-coated hybrid yarns using electrospinning. *Surface and Coatings Technology* 204, 3459–3463.

ball mills, sol–gel equipment and continuous plasma chambers must be established in the industrial sectors. The labour workplace should be safe and wastewater treatment should be provided at the production line.

Another important issue for the application of nanoparticles and nanostructures on textiles is the environment and human health effects that could result from their unintended release from textile products. Use of CNTs, ZnO, TiO₂, SiO₂, Al₂O₃ and Ag in textile nanocoatings is commercialised in developed countries (Parvinzadeh Gashti et al., 2012a; Gashti, 2014). Effects of these nanoparticles on biological aspects of life is extensively assessed by researchers covering some areas as acute toxicity, chronic toxicity, impairment of DNA, crossing and damaging tissue barriers, damage to the central nervous system, and the effects on skin, the gastrointestinal tract and the respiratory tract. Exposure of healthy skin to different types of nanoparticles has not shown short-term effects, whereas the lungs are the most important part of the body where free nanoparticles may enter. Application of the electrospinning method to produce nanowebs will be more intensive in the near future to coat technical textiles, biosensors and metal surfaces.

11.5 Conclusion

Studies on nanotechnology-based coatings for textiles have mostly focused on the generation of multifunctionality by simplified techniques. The sol–gel method, cross-linking method, thin-film deposition technique, and electrospinning-based coatings can impart smart properties to different textile- and non-textile-based materials, improving their effectiveness while decreasing the maintenance time of products. Novel coating techniques such as thin-film deposition and nanofibre coating via electrospinning have been introduced but their durability on textiles as well as commercialisation are still questionable.

Therefore progress in nanotechnology-based coating methods in the textile sectors and optimisation of coating procedures may reveal new insights into the application of smart textiles.

References

- Abidi, N., Cabrales, L., Hequet, E., 2009. Functionalization of a cotton fabric surface with titania nanosols: applications for self-cleaning and UV-protection properties. *ACS Applied Materials and Interfaces* 1, 2141–2146.
- Afzal, S., Daoud, W.A., Langford, S.J., 2013a. Photostable self-cleaning cotton by a copper (II) porphyrin/TiO₂ visible-light photocatalytic system. *ACS Applied Materials and Interfaces* 5, 4753–4759.
- Afzal, S., Daoud, W.A., Langford, S.J., 2013b. Visible-light self-cleaning cotton by metalloporphyrin-sensitized photocatalysis. *Applied Surface Science* 275, 36–42.
- Alcoutlabi, M., Lee, H., Watson, J., Zhang, X., 2013. Preparation and properties of nanofiber-coated composite membranes as battery separators via electrospinning. *Journal of Materials Science* 48, 2690–2700.

- Alimohammadi, F., Gashti, M.P., Shamei, A., 2012. A novel method for coating of carbon nanotube on cellulose fiber using 1,2,3,4-butanetetracarboxylic acid as a cross-linking agent. *Progress in Organic Coatings* 74, 470–478.
- Alimohammadi, F., Parvinzadeh Gashti, M., Shamei, A., 2013. Functional cellulose fibers via polycarboxylic acid/carbon nanotube composite coating. *Journal of Coatings Technology and Research* 10, 123–132.
- Afzal, S., Daoud, W.A., Langford, S.J., 2012. Self-cleaning cotton by porphyrin-sensitized visible-light photocatalysis. *Journal of Materials Chemistry* 22, 4083–4088.
- Bagheri, H., Aghakhani, A., 2011. Novel nanofiber coatings prepared by electrospinning technique for headspace solid-phase microextraction of chlorobenzenes from environmental samples. *Analytical Methods* 3, 1284–1289.
- Bagheri, H., Aghakhani, A., Baghernejad, M., Akbarinejad, A., 2012. Novel polyamide-based nanofibers prepared by electrospinning technique for headspace solid-phase microextraction of phenol and chlorophenols from environmental samples. *Analytica Chimica Acta* 716, 34–39.
- Bagheri, H., Roostaie, A., 2014. Electrospun modified silica-polyamide nanocomposite as a novel fiber coating. *Journal of Chromatography A* 1324, 11–20.
- Bhardwaj, N., Kundu, S.C., 2010. Electrospinning: a fascinating fiber fabrication technique. *Biotechnology Advances* 28, 325–347.
- Bozzi, A., Yuranova, T., Guasaquillo, I., Laub, D., Kiwi, J., 2005a. Self-cleaning of modified cotton textiles by TiO₂ at low temperatures under daylight irradiation. *Journal of Photochemistry and Photobiology A: Chemistry* 174, 156–164.
- Bozzi, A., Yuranova, T., Kiwi, J., 2005b. Self-cleaning of wool-polyamide and polyester textiles by TiO₂-rutile modification under daylight irradiation at ambient temperature. *Journal of Photochemistry and Photobiology A: Chemistry* 172, 27–34.
- Bui, N.-N., Mccutcheon, J.R., 2014. Nanofiber supported thin-film composite membrane for pressure-retarded osmosis. *Environmental Science and Technology* 48, 4129–4136.
- Bula, K., Koprowska, J., Janukiewicz, J., 2006. Application of cathode sputtering for obtaining ultra-thin metallic coatings on textile products. *Fibre Textile Eastern Europe* 59, 75–79.
- Bunshah, R.F., 1982. Deposition technologies: an overview. *Deposition Technologies for Films and Coatings, Developments and Applications*, 200–250.
- Daoud, W.A., Leung, S.K., Tung, W.S., Xin, J.H., Cheuk, K., Qi, K., 2008. Self-cleaning keratins. *Chemistry of Materials* 20, 1242–1244.
- Daoud, W.A., Xin, J.H., 2004a. Low temperature sol-gel processed photocatalytic titania coating. *Journal of Sol-Gel Science and Technology* 29, 25–29.
- Daoud, W.A., Xin, J.H., 2004b. Nucleation and growth of anatase crystallites on cotton fabrics at low temperatures. *Journal of the American Ceramic Society* 87, 953–955.
- Daoud, W.A., Xin, J.H., 2005. Synthesis of single-phase anatase nanocrystallites at near room temperatures. *Chemical Communications* 2110–2112.
- Daoud, W.A., Xin, J.H., Zhang, Y.-H., 2005. Surface functionalization of cellulose fibers with titanium dioxide nanoparticles and their combined bactericidal activities. *Surface Science* 599, 69–75.
- Deitzel, J.M., Kleinmeyer, J., Harris, D., Beck Tan, N.C., 2001. The effect of processing variables on the morphology of electrospun nanofibers and textiles. *Polymer* 42, 261–272.
- Ding, B., Kim, J., Miyazaki, Y., Shiratori, S., 2004. Electrospun nanofibrous membranes coated quartz crystal microbalance as gas sensor for NH₃ detection. *Sensors and Actuators B: Chemical* 101, 373–380.

- Doughty Daniel, H., Assink Roger, A., Kay Bruce, D., 1989. Hydrolysis and Condensation Kinetics of Dimeric Sol-Gel Species by Si NMR Spectroscopy. American Chemical Society, Washington DC.
- Es-Saheb, M., Elzatahry, A.A., Sherif, E.-S.M., Alkaraki, A.S., Kenawy, E.-R., 2012. A novel electrospinning application for polyvinyl chloride nanofiber coating deposition as a corrosion inhibitor for aluminum, steel, and brass in chloride solutions. *International Journal of Electrochemical Science* 7, 5962–5976.
- Esen, M., Ilhan, I., Karaaslan, M., Unal, E., Dincer, F., Sabah, C., 2014. Electromagnetic absorbance properties of a textile material coated using filtered arc-physical vapor deposition method. *Journal of Industrial Textiles*.
- Fujishima, A., Rao, T.N., Tryk, D.A., 2000. Titanium dioxide photocatalysis. *Journal of Photochemistry and Photobiology C: Photochemistry Reviews* 1, 1–21.
- Gashti, M.P., 2014. Nanocomposite coatings: state of the art approach in textile finishing. *Journal of Textile Science and Engineering* 4, e120. <http://dx.doi.org/10.4172/2165-8064.1000e120>.
- Gashti, M.P., Alimohammadi, F., Shamei, A., 2012. Preparation of water-repellent cellulose fibers using a polycarboxylic acid/hydrophobic silica nanocomposite coating. *Surface and Coatings Technology* 206, 3208–3215.
- Gibson, P., Schreuder-Gibson, H., Rivin, D., 2001. Transport properties of porous membranes based on electrospun nanofibers. *Colloids and Surfaces A: Physicochemical and Engineering Aspects* 187–188, 469–481.
- Harifi, T., Montazer, M., 2012. Past, present and future prospects of cotton cross-linking: new insight into nanoparticles. *Carbohydrate Polymers* 88, 1125–1140.
- Hashimoto, K., Irie, H., Fujishima, A., 2005. TiO₂ photocatalysis: a historical overview and future prospects. *Japanese Journal of Applied Physics* 44, 8269–8285.
- Heikkilä, P., Sipilä, A., Peltola, M., Harlin, A., Taipale, A., 2007. Electrospun PA-66 coating on textile surfaces. *Textile Research Journal* 77, 864–870.
- Hong, Y.K., Lee, C.Y., Jeong, C.K., Sim, J.H., Kim, K., Joo, J., Kim, M.S., Lee, J.Y., Jeong, S.H., Byun, S.W., 2001. Electromagnetic interference shielding characteristics of fabric complexes coated with conductive polypyrrole and thermally evaporated Ag. *Current Applied Physics* 1, 439–442.
- Huang, X., Hitt, J., 2013. Lithium ion battery separators: development and performance characterization of a composite membrane. *Journal of Membrane Science* 425–426, 163–168.
- Huang, Z.-M., Zhang, Y.Z., Kotaki, M., Ramakrishna, S., 2003. A review on polymer nanofibers by electrospinning and their applications in nanocomposites. *Composites Science and Technology* 63, 2223–2253.
- Jiang, S.X., Qin, W.F., Guo, R.H., Zhang, L., 2010. Surface functionalization of nanostructured silver-coated polyester fabric by magnetron sputtering. *Surface and Coatings Technology* 204, 3662–3667.
- Lacerda Silva, N., Gonçalves, L.M., Carvalho, H., 2013. Deposition of conductive materials on textile and polymeric flexible substrates. *Journal of Materials Science: Materials in Electronics* 24, 635–643.
- Lai, K., Sun, R.-J., Chen, M.-Y., Hui, W.U., Zha, A.-X., 2007. Electromagnetic shielding effectiveness of fabrics with metallized polyester filaments. *Textile Research Journal* 77, 242–246.
- Lee, C.Y., Lee, D.E., Jeong, C.K., Hong, Y.K., Shim, J.H., Joo, J., Kim, M.S., Lee, J.Y., Jeong, S.H., Byun, S.W., Zang, D.S., Yang, H.G., 2002. Electromagnetic interference shielding by using conductive polypyrrole and metal compound coated on fabrics. *Polymers for Advanced Technologies* 13, 577–583.

- Lee, H., Alcoutlabi, M., Watson, J.V., Zhang, X., 2013. Electrospun nanofiber-coated separator membranes for lithium-ion rechargeable batteries. *Journal of Applied Polymer Science* 129, 1939–1951.
- Lee, M.W., An, S., Lee, C., Liou, M., Yarin, A.L., Yoon, S.S., 2014. Self-healing transparent core-shell nanofiber coatings for anti-corrosive protection. *Journal of Materials Chemistry A* 2, 7045–7053.
- Mahltig, B., Haufe, H., Böttcher, H., 2005. Functionalisation of textiles by inorganic sol-gel coatings. *Journal of Materials Chemistry* 15, 4385–4398.
- Meilert, K.T., Laub, D., Kiwi, J., 2005. Photocatalytic self-cleaning of modified cotton textiles by TiO₂ clusters attached by chemical spacers. *Journal of Molecular Catalysis A: Chemical* 237, 101–108.
- Montazer, M., Behzadnia, A., Pakdel, E., Rahimi, M.K., Moghadam, M.B., 2011a. Photo induced silver on nano titanium dioxide as an enhanced antimicrobial agent for wool. *Journal of Photochemistry and Photobiology B: Biology* 103, 207–214.
- Montazer, M., Ghayem Asghari, M.S., Pakdel, E., 2011b. Electrical conductivity of single walled and multiwalled carbon nanotube containing wool fibers. *Journal of Applied Polymer Science* 121, 3353–3358.
- Montazer, M., Pakdel, E., 2010. Reducing photoyellowing of wool using nano TiO₂. *Photochemistry and Photobiology* 86, 255–260.
- Montazer, M., Pakdel, E., 2011a. Functionality of nano titanium dioxide on textiles with future aspects: focus on wool. *Journal of Photochemistry and Photobiology C: Photochemistry Reviews* 12, 293–303.
- Montazer, M., Pakdel, E., 2011b. Self-cleaning and color reduction in wool fabric by nano titanium dioxide. *Journal of the Textile Institute* 102, 343–352.
- Montazer, M., Pakdel, E., Behzadnia, A., 2011c. Novel feature of nano-titanium dioxide on textiles: antifelting and antibacterial wool. *Journal of Applied Polymer Science* 121, 3407–3413.
- Montazer, M., Pakdel, E., Moghadam, M., 2010. Nano titanium dioxide on wool keratin as UV absorber stabilized by butane tetra carboxylic acid (BTCA): a statistical prospect. *Fibers and Polymers* 11, 967–975.
- Ochiai, T., Fujishima, A., 2012. Photoelectrochemical properties of TiO₂ photocatalyst and its applications for environmental purification. *Journal of Photochemistry and Photobiology C: Photochemistry Reviews* 13, 247–262.
- Öktem, T., Özdoğan, E., Namligöz, S.E., Öztarhan, A., Tek, Z., Tarakçıoğlu, I., Karaaslan, A., 2006. Investigating the applicability of metal ion implantation technique (MEVVA) to textile surfaces. *Textile Research Journal* 76, 32–40.
- Pakdel, E., Daoud, W., 2013. Self-cleaning cotton functionalized with TiO₂/SiO₂: focus on the role of silica. *Journal of Colloid and Interface Science* 401, 1–7.
- Pakdel, E., Daoud, W.A., Afrin, T., Sun, L., Wang, X., 2014a. Self-cleaning wool: effect of noble metals and silica on visible-light-induced functionalities of nano TiO₂ colloid. *The Journal of the Textile Institute* 106, 1348–1361.
- Pakdel, E., Daoud, W.A., Sun, L., Wang, X., 2014b. Visible and UV functionality of TiO₂ ternary nanocomposites on cotton. *Applied Surface Science* 321, 447–456.
- Pakdel, E., Daoud, W.A., Wang, X., 2014c. Assimilating the photo-induced functions of TiO₂-based compounds in textiles: emphasis on the sol-gel process. *Textile Research Journal* 85, 1404–1428.
- Pakdel, E., Daoud, W.A., Sun, L., Wang, X., 2015. Photostability of wool fabrics coated with pure and modified TiO₂ colloids. *Journal of Colloid and Interface Science* 440, 299–309.

- Pakdel, E., Daoud, W.A., Wang, X., 2013. Self-cleaning and superhydrophilic wool by TiO₂/SiO₂ nanocomposite. *Applied Surface Science* 275, 397–402.
- Parvinzadeh Gashti, M., Alimohammadi, F., Song, G., Kiumarsi, A., 2012a. Characterization of nanocomposite coatings on textiles: a brief review on microscopic technology. In: Mendez-Vilas, A. (Ed.), *Current Microscopy Contributions to Advances in Science and Technology*. Formatex, Spain.
- Parvinzadeh Gashti, M., Almasian, A., Parvinzadeh Gashti, M., 2012b. Preparation of electromagnetic reflective wool using nano-ZrO₂/citric acid as inorganic/organic hybrid coating. *Sensors and Actuators A: Physical* 187, 1–9.
- Parvinzadeh Gashti, M., Almasian, A., 2013a. UV radiation induced flame retardant cellulose fiber by using polyvinylphosphonic acid/carbon nanotube composite coating. *Composites Part B: Engineering* 45, 282–289.
- Parvinzadeh Gashti, M., Almasian, A., 2013b. Citric acid/ZrO₂ nanocomposite inducing thermal barrier and self-cleaning properties on protein fibers. *Composites Part B: Engineering* 52, 340–349.
- Parvinzadeh Gashti, M., Elahi, A., Parvinzadeh Gashti, M., 2013c. UV radiation inducing succinic acid/silica–kaolinite network on cellulose fiber to improve the functionality. *Composites Part B: Engineering* 48, 158–166.
- Parvinzadeh Gashti, M., Eslami, S., 2015. A robust method for producing electromagnetic shielding cellulose via iron oxide pillared clay coating under ultraviolet irradiation. *Functional Materials Letters* 08, 1550073, 4. <http://dx.doi.org/10.1142/S179360471500733>.
- Parvinzadeh Gashti, M., Ghehi, S.T., Arekhloo, S.V., Mirsmaeeli, A., Kiumarsi, A., 2015. Electromagnetic shielding response of UV-induced polypyrrole/silver coated wool. *Fibers and Polymers* 16, 585–592.
- Pawliszyn, J., 1999. *Applications of Solid Phase Microextraction*. Royal Society of Chemistry.
- Qi, K., Chen, X., Liu, Y., Xin, J.H., Mak, C.L., Daoud, W.A., 2007. Facile preparation of anatase/SiO₂ spherical nanocomposites and their application in self-cleaning textiles. *Journal of Materials Chemistry* 17, 3504–3508.
- Qi, K., Daoud, W.A., Xin, J.H., Mak, C.L., Tang, W., Cheung, W.P., 2006. Self-cleaning cotton. *Journal of Materials Chemistry* 16, 4567–4574.
- Scholz, J., Nocke, G., Hollstein, F., Weissbach, A., 2005. Investigations on fabrics coated with precious metals using the magnetron sputter technique with regard to their anti-microbial properties. *Surface and Coatings Technology* 192, 252–256.
- Sen, A.K., 2007. *Coated Textiles: Principles and Applications*. CRC Press.
- Spietelun, A., Pilarczyk, M., Kloskowski, A., Namieśnik, J., 2010. Current trends in solid-phase microextraction (SPME) fibre coatings. *Chemical Society Reviews* 39, 4524–4537.
- Tung, W.S., Daoud, W.A., 2009. Photocatalytic self-cleaning keratins: a feasibility study. *Acta Biomaterialia* 5, 50–56.
- Tung, W.S., Daoud, W.A., 2010. Self-cleaning surface functionalisation of keratins: effect of heat treatment and formulation preparation time on photocatalysis and fibres mechanical properties. *Surface Engineering* 26, 525–531.
- Tung, W.S., Daoud, W.A., 2011. Self-cleaning fibers via nanotechnology: a virtual reality. *Journal of Materials Chemistry* 21, 7858–7869.
- Tung, W.S., Daoud, W.A., Leung, S.K., 2009. Understanding photocatalytic behavior on biomaterials: insights from TiO₂ concentration. *Journal of Colloid and Interface Science* 339, 424–433.
- Veronovski, N., Sfiligoj-Smole, M., Viota, J.L., 2010. Characterization of TiO₂/TiO₂-SiO₂ coated cellulose textiles. *Textile Research Journal* 80, 55–62.

- Wang, H., Wang, J., Hong, J., Wei, Q., Gao, W., Zhu, Z., 2007. Preparation and characterization of silver nanocomposite textile. *Journal of Coatings Technology and Research* 4, 101–106.
- Wang, N., Burugapalli, K., Song, W., Halls, J., Moussy, F., Ray, A., Zheng, Y., 2013. Electrospun fibro-porous polyurethane coatings for implantable glucose biosensors. *Biomaterials* 34, 888–901.
- Wei, Q., 2009. *Surface Modification of Textiles*. Elsevier.
- Xin, J.H., Daoud, W.A., Kong, Y.Y., 2004. A new approach to UV-blocking treatment for cotton fabrics. *Textile Research Journal* 74, 97–100.
- Yip, J., Jiang, S., Wong, C., 2009. Characterization of metallic textiles deposited by magnetron sputtering and traditional metallic treatments. *Surface and Coatings Technology* 204, 380–385.
- Yoon, K., Kim, K., Wang, X., Fang, D., Hsiao, B.S., Chu, B., 2006. High flux ultrafiltration membranes based on electrospun nanofibrous PAN scaffolds and chitosan coating. *Polymer* 47, 2434–2441.
- Yuranova, T., Rincon, A.G., Bozzi, A., Parra, S., Pulgarin, C., Albers, P., Kiwi, J., 2003. Antibacterial textiles prepared by RF-plasma and vacuum-UV mediated deposition of silver. *Journal of Photochemistry and Photobiology A: Chemistry* 161, 27–34.
- Zhang, M., Tang, B., Sun, L., Wang, X., 2014. Reducing photoyellowing of wool fabrics with silica coated ZnO nanoparticles. *Textile Research Journal* 84, 1840–1848.
- Zhou, F.-L., Gong, R.-H., Porat, I., 2010. Nano-coated hybrid yarns using electrospinning. *Surface and Coatings Technology* 204, 3459–3463.

Biomimetic nanocoatings for structural coloration of textiles

12

J. Shao, G. Liu, L. Zhou

Zhejiang Sci-Tech University, Hangzhou, China

12.1 Introduction

Color is a visual perception in humans and is described as red, blue, yellow, etc. In fact, it can be defined as the sensation of a particular composition of light perceived by the eye and brain (Dong et al., 2007). Light and color are closely related, so visible light of a certain wavelength can produce specific color vision.

In view of the interaction of light with objects, colors can basically be divided into two main categories: pigmentary and structural. Pigmentary color, also known as chemical color, is the most common way to produce colors. Chemical colorants can produce colors because they selectively absorb certain wavelengths of visible light (Nassau, 2001; Zhang et al., 2011). Structural color, also known as physical color, requires no chemical colorants and is a visual perception of selectively reflected light by a specific physical structure interacting with incident light, such as dispersion, scattering, interference, and diffraction (Kinoshita et al., 2008). Many living creatures in nature, such as butterfly wings, peacock feathers, and beetles, exhibit bright colors, which have been referred to as structural colors. It is thought that the color properties of pigmentary color and structural color are significantly different from each other. Generally, structural color exhibits high brightness, high saturation, less discoloration, and an iridescent effect, which are difficult to achieve with conventional pigmentary colors (Berthier et al., 2007; Land, 1972; McPhedran et al., 2003; Zhang et al., 2001).

Structural colors in nature are based mainly on the following five fundamental optical processes and their combinations: thin-film interference, multilayer interference, the diffraction grating effect, photonic crystals, and light scattering. Biomimetic structural coloration has been attracting increasing attention in a wide variety of research fields. Regarding the textile field, biomimetic structural colors originate from thin-film interference and photonic crystals have been mostly focused upon. There are various techniques for obtaining biomimetic structural colors, such as vapor deposition, sputtering, spin coating, dipping-adsorption, electrostatic self-assembly, colloidal self-assembly, and ink jet printing. Among them, electrostatic self-assembly and colloidal self-assembly have become the most promising methods for nanocoatings on textile substrates to generate bright, vivid, and tunable structural colors, owing to the simplicity and universality of the methods with high-quality nanocoatings.

Compared with the traditional coloration of textiles using chemical colorants, biomimetic structural coloration with nano-coatings is an eco-coloration technology.

Furthermore, the combination of pigmentary and structural coloration is anticipated to broaden textile coloration technology and develop more charming and added-value textile products.

12.2 Characterization of biomimetic structural coloration

Generally, the property of pigmentary color can be measured and characterized by spectrophotometric color measurement instruments. However, because of the special iridescent phenomenon of biomimetic structural color, it cannot be directly characterized by conventional measurement methods of pigmentary colors. Therefore, a new testing technique has been developed to characterize the iridescence of structural colors using a multiangle spectrophotometer. In our study, the iridescence of structural colors was recorded using a digital camera (EOS600D, Canon, Japan) in qualitative analysis and a multiangle spectrophotometer (MA98, X-Rite, USA) with a colorimetric illuminant of D65 and a colorimetric standard observer of 10 degree in quantitative analysis. The MA98 multiangle spectrophotometer is an intelligent handheld tool based on reflection measurements, and it can provide images, L^* a^* b^* values, and reflectance spectra of samples under various viewing directions. The measurement geometries (Fig. 12.1) are as follows: The sample is directionally illuminated at 45 degree from normal and aspecular viewing angles in plane are at -15 , 15 , 25 , 45 , 75 , and 110 degree; secondary illumination is at 15 degree from normal and aspecular viewing angles in plane are at -15 degree and 15 degree. The intensity of

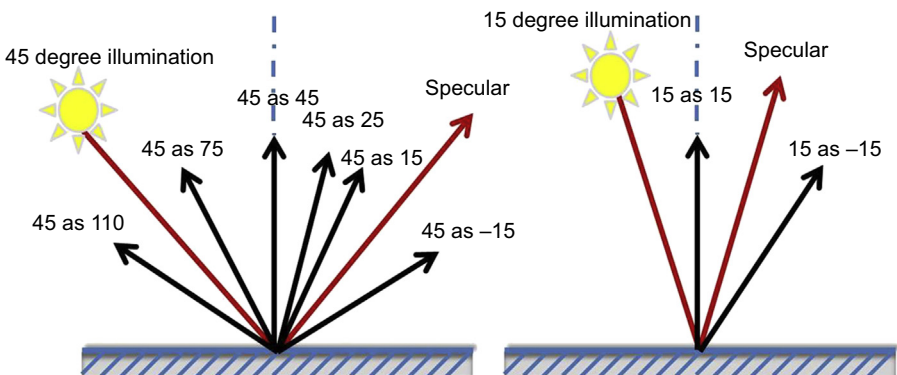


Figure 12.1 Eight different viewing angles of multiangle spectrophotometer at two illumination angles. Left: six viewing angles of 45 as -15 , 45 as 15 , 45 as 25 , 45 as 45 , 45 as 75 , and 45 as 110 at 45 degree illumination. Right: Two viewing angles of 15 as -15 and 15 as 15 at 15 degree illumination. Note: The angle “45 as -15 ” means the sample was directionally illuminated at 45 degree from normal, and the aspecular viewing angles in plane was at -15 degree.

reflectance spectra measured by this multiangle spectrophotometer are in the range 0–400% and reflectance data reported are in agreement with ASTM E2539-08.

12.3 Structural colors of thin-film interference on textiles with electrostatic self-assembly

12.3.1 Principle of thin-film interference

Thin-film interference is a dominant approach to produce structural colors in nature; it can be divided into single thin-film and multilayer thin-film interference.

Let a plane wave of light be incident on a thin film of thickness d and refractive index n with the angles of incidence and refraction as θ_1 and θ_2 (Fig. 12.2). Light reflected at the two surfaces interferes with each other (Parker and Martini, 2006).

Constructive interference equation (Eq. [12.1]):

$$p = 2nd \cos \theta_2 = (2m + 1) \frac{\lambda}{2} \quad [12.1]$$

Destructive interference equation (Eq. [12.2]):

$$p = 2nd \cos \theta_2 = 2m \frac{\lambda}{2} \quad [12.2]$$

where n is the refractive index of thin film; d is the thickness of thin film; θ_2 is the angle of refraction; m is a nonzero integer; and λ is the reflected light wavelength.

Under the irradiation of unidirectional polychromatic light, the optical path difference (p) and the wavelength of constructive interference (λ) varied with the variation of thickness of thin film (d). The optical path difference is also closely related to the refractive index (n) of thin film. Only when the product of the refractive index (n) and thickness (d) are a certain amount, can the thin film be a vivid structural color. Single-layer reflectors are commonly found in nature, such as in a soap bubble in the sunshine, in the wings of dragonflies and flies, and so on.

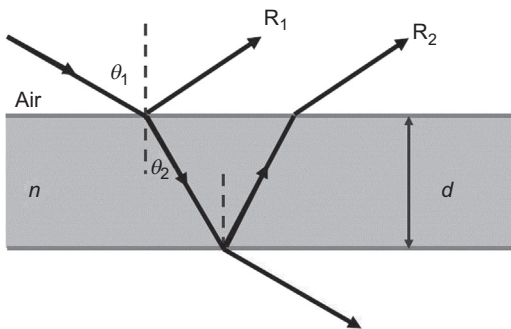
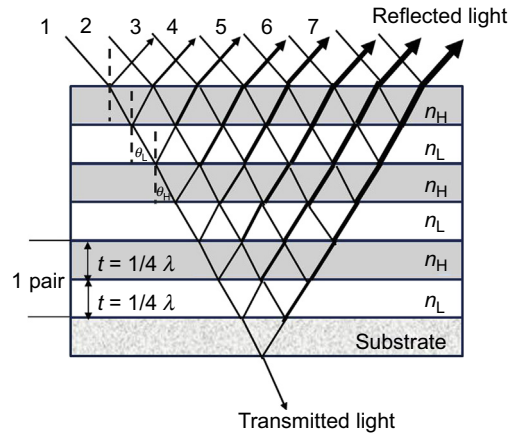


Figure 12.2 Schematic diagram of single thin-film interference.

Figure 12.3 Schematic diagram of multilayer interference.



12.3.1.1 Multilayer interference

A typical principle diagram of multilayer interference is shown in Fig. 12.3. Multilayer films are usually made of two thin films with different refractive indexes alternately; the relation of the reflection wavelength (λ) and the two kinds of thin-film refractive indexes (high refractive index n_H and low refractive n_L) and the thickness (d_H and d_L) of thin film is shown as Eq. [12.3] (Tilley, 2001). The relation of reflection intensity (R) to the refractive index of substrate (n_S), the ratio of two kinds of thin-film index (n_L/n_H), and the number of pairs (N) is shown in Eq. [12.4] (Land, 1966). The hue of structural color is determined by the reflected wavelength (λ) and the brightness of structural color is influenced by the reflection intensity (R).

$$m\lambda = 2(n_H d_H \cos \theta_H + n_L d_L \cos \theta_L) \quad [12.3]$$

$$R = \left[\frac{\left(n_S - \left(\frac{n_L}{n_H} \right)^{2N} \right)}{\left(n_S + \left(\frac{n_L}{n_H} \right)^{2N} \right)} \right]^2 \quad [12.4]$$

Multilayer interference is also commonly found in nature, such as *Paracheirodon innesi*, paradise whiptail, blue damselfish, tortoise beetle, Hercules beetle, and so on. Generally, the structural colors vary with the viewing angles regardless of thin-film interference or multilayer interference.

12.3.2 Basics of electrostatic self-assembly

There are various methods to construct thin films, such as chemical deposition (Mitra et al., 1998), gravitational sedimentation (Davis et al., 1989; Miguez et al., 1997), spin coating (Chen et al., 2013), and electrostatic self-assembly (Chen et al., 2009; Fu and Kobayashi, 2010; Li et al., 2010). Electrostatic interaction has a longer

range than hydrophobic or hydrogen-bonding interaction (Krupp, 1967; Maboudian and Howe, 1997), and the electrostatic force controls the amount of particles involved in each self-assembly step. It is the most convenient way to prepare charged microstructures and avoid sophisticated chemical reactions. Thus, electrostatic self-assembly has become an effective technique to fabricate composite films with multilayered structures. However, to date, little study has been reported on electrostatic self-assembly in textiles for fabricating thin films with structural colors.

12.3.3 Structural colors of silica–polyethylenimine-coated surfaces

In our research, thin films with structural color were fabricated on various textile surfaces and substrates by electrostatic self-assembly, and the factors affecting structural colors were investigated. The mechanism generating structural colors and the assembly process of silica (SiO_2)–polyethylenimine (PEI) thin film with structural color were studied.

12.3.3.1 Optical properties of silica–polyethylenimine-coated surfaces

As shown in Figs. 12.4–12.8, the structural colors of the nano-coated fabrics are affected by SiO_2 size, the number of assembly cycles, and the viewing angle. The coated fabrics have various structural colors with changes in SiO_2 particles sizes and number of assembly cycles. The same sample shows different structural colors at various viewing angles (Jia et al., 2014).

As represented in Figs. 12.9 and 12.10, bright and uniform structural colors and optical properties of as-prepared $(\text{SiO}_2/\text{PEI})_n$ films covered on polyester fabric surfaces are achieved under illumination of natural light. It can be seen from Fig. 12.9(a1–d1) that polyester fabrics assembled with 100-nm SiO_2 nanoparticles in various cycles ($n = 0, 8, 9$, and 11, respectively) display various structural colors viewed at the same viewing angle. In addition, a distinguished phenomenon shown in Fig. 12.9(a2–d2)

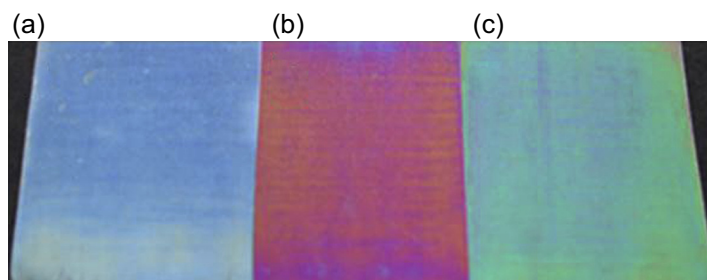


Figure 12.4 Structural colors of 20-cycle SiO_2/PEI films with various sizes of SiO_2 particles: (a) 50 nm, (b) 100 nm, and (c) 165 nm.

From Jia, Y.R., Zhang, Y., Shao, J.Z., 2014. Structural colors of the SiO_2 /Polyethylenimine thin films on poly(ethylene terephthalate) substrates. *Thin Solid Films* 569, 10–16.

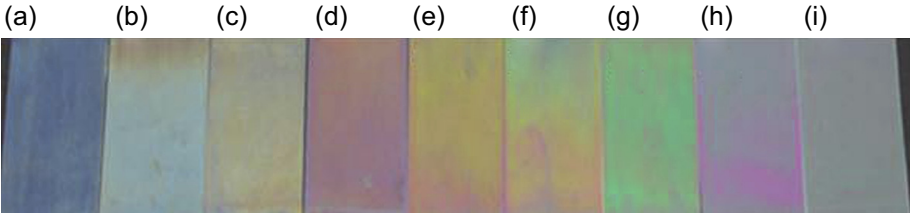


Figure 12.5 Structural colors of SiO₂/PEI films with various cycles: (a) 5, (b) 10, (c) 15, (d) 20, (e) 25, (f) 30, (g) 40, (h) 50, and (i) 60.

From Jia, Y.R., Zhang, Y., Shao, J.Z., 2014. Structural colors of the SiO₂/Polyethyleneimine thin films on poly(ethylene terephthalate) substrates. *Thin Solid Films* 569, 10–16.

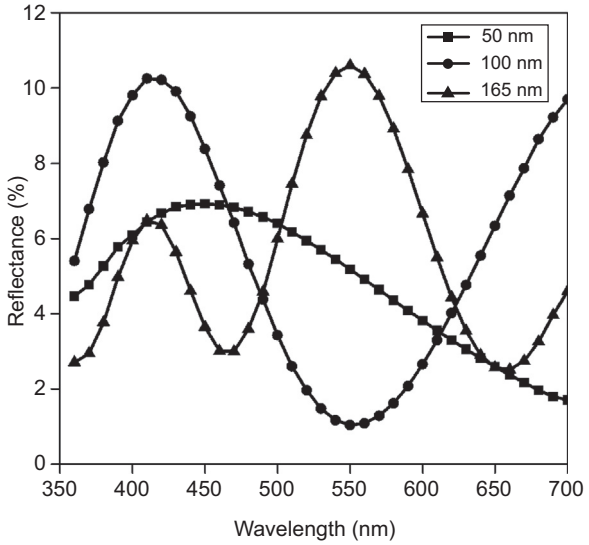


Figure 12.6 Reflectance of 20-cycle SiO₂/PEI film with various sizes of SiO₂ particles.

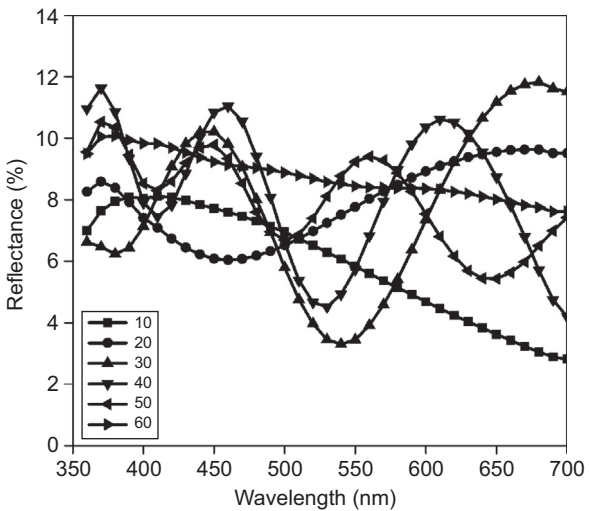


Figure 12.7 Reflectance of SiO₂/PEI films with various cycles.

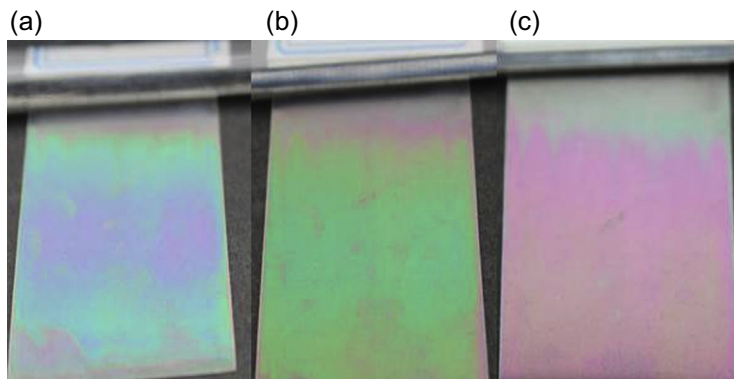


Figure 12.8 Structural colors of 40-cycle SiO_2/PEI film observed at three various viewing angles (a–c: increasing angles).

From Jia, Y.R., Zhang, Y., Shao, J.Z., 2014. Structural colors of the $\text{SiO}_2/\text{Polyethyleneimine}$ thin films on poly(ethylene terephthalate) substrates. *Thin Solid Films* 569, 10–16.

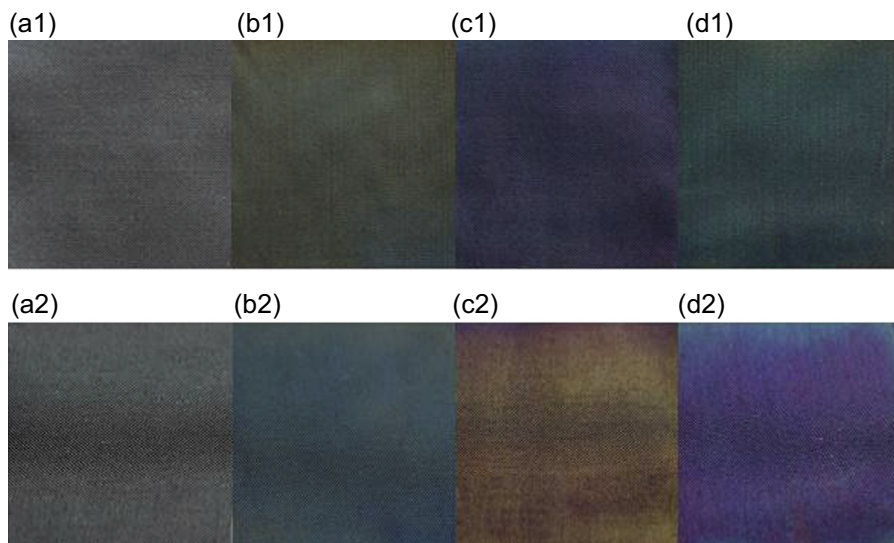


Figure 12.9 Photos of various structural colors of polyester fabric samples self-assembled with 100-nm SiO_2 nanoparticles in n assembly cycles ($n = 0, 8, 9,$ and 11) from left to right in the same row and photos taken at two different viewing angles for the same sample presented in the same column.

From Zhang, Y., Zhuang, G.Q., Jia, Y.R., 2015. Structural coloration of polyester fabrics with electrostatic self-assembly of $(\text{SiO}_2/\text{PEI})_n$. *Textile Research Journal* 85, 785–794.

is that the structural color of the same sample varies from different viewing angles. This suggests that the structural color of polyester fabric can be controlled by controlling the assembly cycles, and its variable color effect shown at various viewing angles is distinctly different from that displayed by traditionally colored fabrics using dyes or pigments. Fig. 12.10 shows the reflectance spectra of $(\text{SiO}_2/\text{PEI})_n$ films coated on polyester fabric with various cycles and viewing angles (Zhang et al., 2015).

To further investigate the variable color effect of $(\text{SiO}_2/\text{PEI})_n$ film coated on polyester fabric at various viewing angles, polyester fabric specimens with $(\text{SiO}_2/\text{PEI})_n$ film ($n = 8, 9, \text{ and } 11$) were measured with a multiangle spectrophotometer; the results are shown in Fig. 12.11. The noticeable hue and lightness variation are observed with the viewing angle varying from “45 as -15° ” to “45 as 110° ,” and “15 as -15° ” to “15 as 15° .”

The $L^* a^* b^*$ values listed in Table 12.1 show the detail structural color changes of $(\text{SiO}_2/\text{PEI})_9$ film with eight diversified angles measured by a multiangle spectrophotometer. The L^* values are attributed to the lightness, whereas the a^* axis points from red (positive) to green (negative) and b^* axis points from yellow (positive) to blue (negative) (Lee et al., 2012; Schanda, 2007). Based on the CIE 1976 $L^*a^*b^*$ system, the color difference (ΔE^*) of the sample at different angles can be quantified by the following formula (McLaren, 1976):

$$\Delta E^* = \left[(\Delta L^*)^2 + (\Delta a^*)^2 + (\Delta b^*)^2 \right]^{1/2} \quad [12.5]$$

where ΔE^* (color difference) is the differences in lightness and color opponents between two viewing conditions; ΔL^* , Δa^* , and Δb^* are the differences in L^* , a^* , and b^* values respectively, between two viewing angles of one sample. The ΔE^* values in Table 12.2 show the color difference at each pair of viewing angles. For instance, ΔE^* of polyester fabric with $(\text{SiO}_2/\text{PEI})_9$ film between the viewing angles of “45 as -15° ” and “45 as 45° ” is 24.67, which indicates that there is a significant color difference between them. These results directly confirm that the variation in structural colors generated from the $(\text{SiO}_2/\text{PEI})_n$ film coated on polyester fabrics significantly depended on the assembly cycles and the viewing angles.

Based on this analysis, the bright structural colors coated with $(\text{SiO}_2/\text{PEI})_n$ films vary with the various assembly cycles and the nanoparticle sizes under the same assembly condition. The same sample displays various structural colors (hue, brilliance, and brightness) at different viewing angles, which shows an obvious rainbow effect.

12.3.3.2 Generating mechanism of structural colors from silica–polyethylenimine-coated surface

Electrostatic self-assembly is a widely used, versatile process in which the patterned layer-by-layer (LBL) films can be readily prepared. LBL films, such as many kinds of functional films, are usually referred to as multilayer films. Figs. 12.12 and 12.13 show the surface morphology of single-cycle films with various sizes and assembly

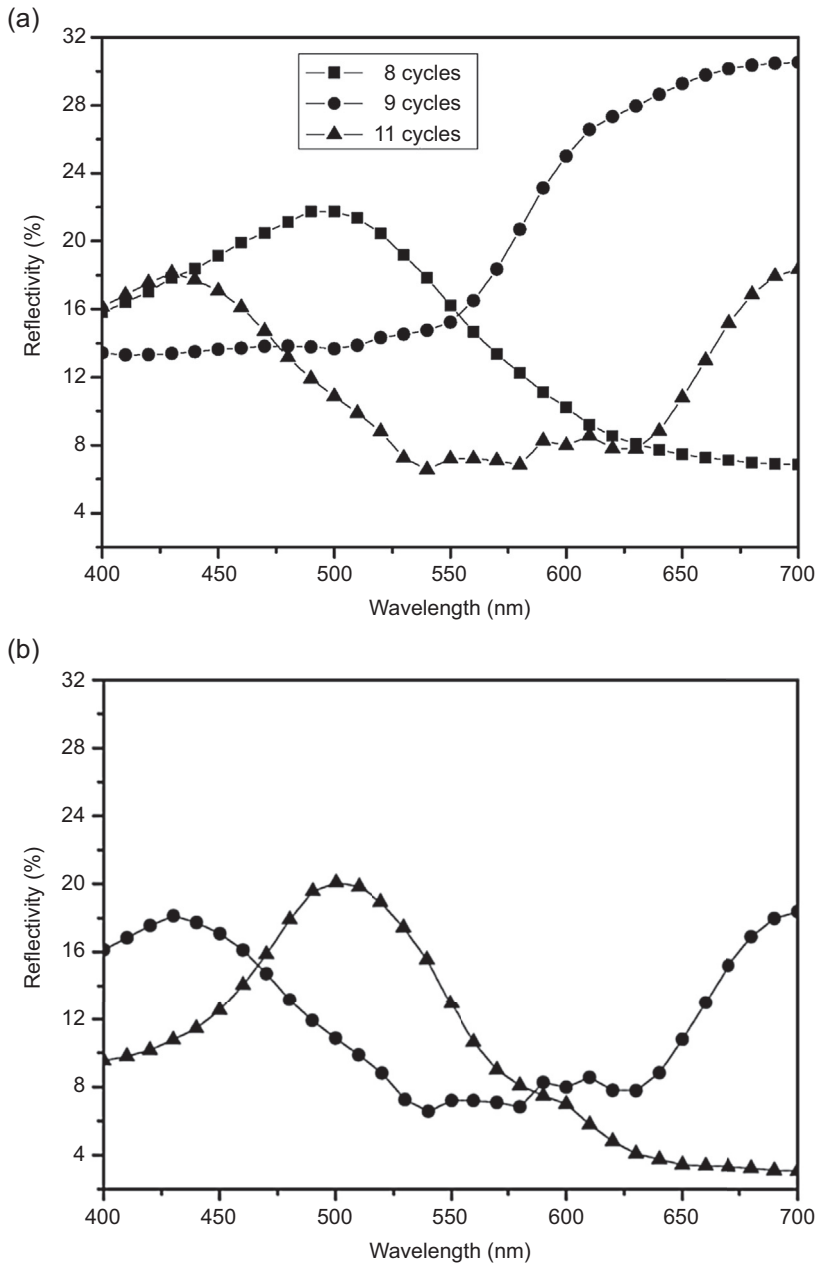


Figure 12.10 Reflectance spectra of $(\text{SiO}_2/\text{PEI})_n$ films on polyester fabrics in (a) n assembly cycles ($n = 8, 9,$ and 11) at a same viewing angle and (b) 11 cycles at two different viewing angles.

From Zhang, Y., Zhuang, G.Q., Jia, Y.R., 2015. Structural coloration of polyester fabrics with electrostatic self-assembly of $(\text{SiO}_2/\text{PEI})_n$. *Textile Research Journal* 85, 785–794.

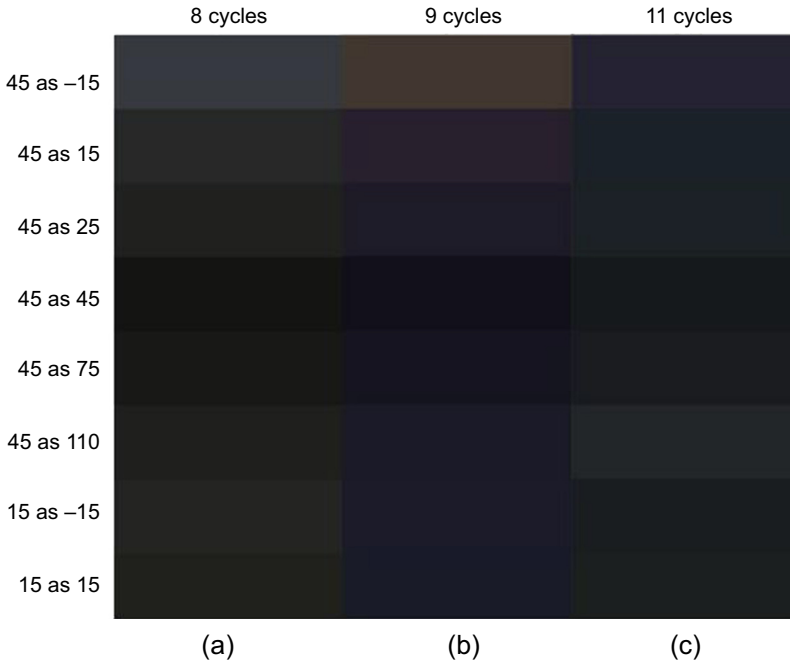


Figure 12.11 Various structural colors of polyester fabrics coated with $(\text{SiO}_2/\text{PEI})_n$ film ($n = 8, 9,$ and 11) at eight different viewing angles: (a) 50 nm, (b) 100 nm, and (c) 165 nm. From Zhang, Y., Zhuang, G. Q., Jia, Y. R., 2015. Structural coloration of polyester fabrics with electrostatic self-assembly of $(\text{SiO}_2/\text{PEI})_n$. Textile Research Journal 85, 785–794.

Table 12.1 The L^* a^* b^* values of polyester fabric with $(\text{SiO}_2/\text{PEI})_9$ film at various viewing angles

Viewing angle	L^*	a^*	b^*
45 as -15	32.26	5.269	7.186
45 as 15	22.41	6.630	-6.571
45 as 25	19.22	6.159	-7.962
45 as 45	13.25	2.880	-8.360
45 as 75	15.81	1.593	-7.607
45 as 110	18.85	1.712	-8.478
15 as -15	18.99	1.300	-9.503
15 as 15	19.14	-0.6704	-9.829

Note: The angle “45 as -15” means the sample was directionally illuminated at 45 degree from normal and the aspecular viewing angles in plane was at -15 degree.

From Zhang, Y., Zhuang, G. Q., Jia, Y.R., 2015. Structural coloration of polyester fabrics with electrostatic self-assembly of $(\text{SiO}_2/\text{PEI})_n$. Textile Research Journal 85, 785–794.

Table 12.2 Comparison between gravitational sedimentation and vertical deposition methods on polyester fabrics

Content	Gravitational sedimentation	Vertical deposition
Structural color	Vivid and monochromatic	Vivid and monochromatic
Main driving force	Gravity	Capillary force
Coloration effect	Single-sided	Double-sided
Thickness of photonic crystals	Thick	Thin
Clarity of texture	General	Distinct

From Liu, G., Zhou, L., Wu, Y., 2015b. The fabrication of full color P(St-MAA) photonic crystal structure on polyester fabrics by vertical deposition self-assembly. *Journal of Applied Polymer Science* 132. <http://dx.doi.org/10.1002/app.41750>.

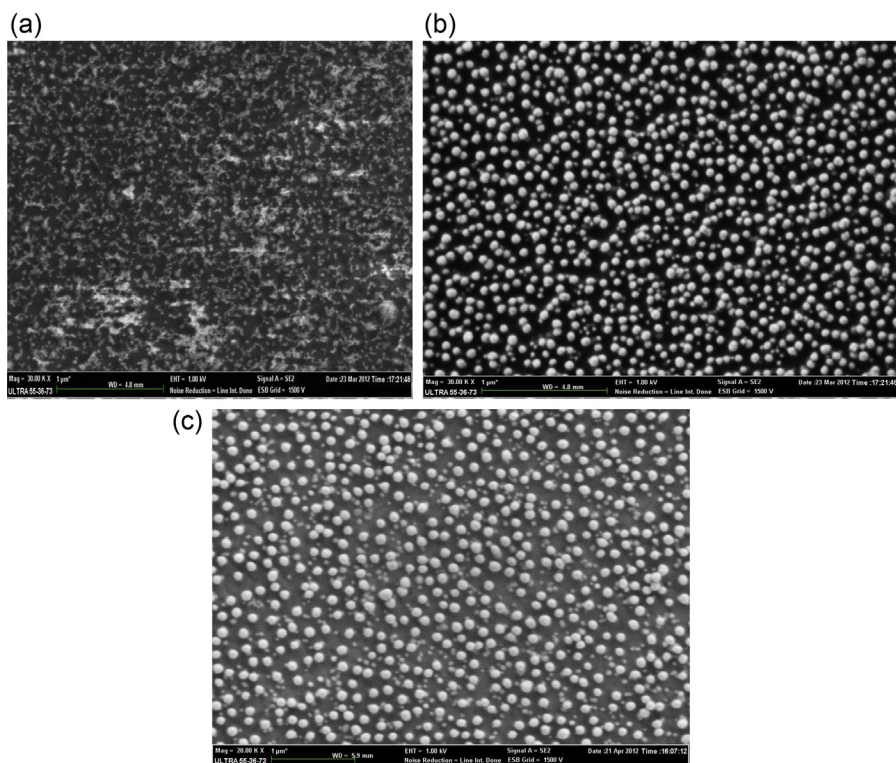


Figure 12.12 SEM images of single-cycle SiO_2/PEI films with various sizes of SiO_2 particles: (a) 50 nm, (b) 100 nm, and (c) 165 nm.

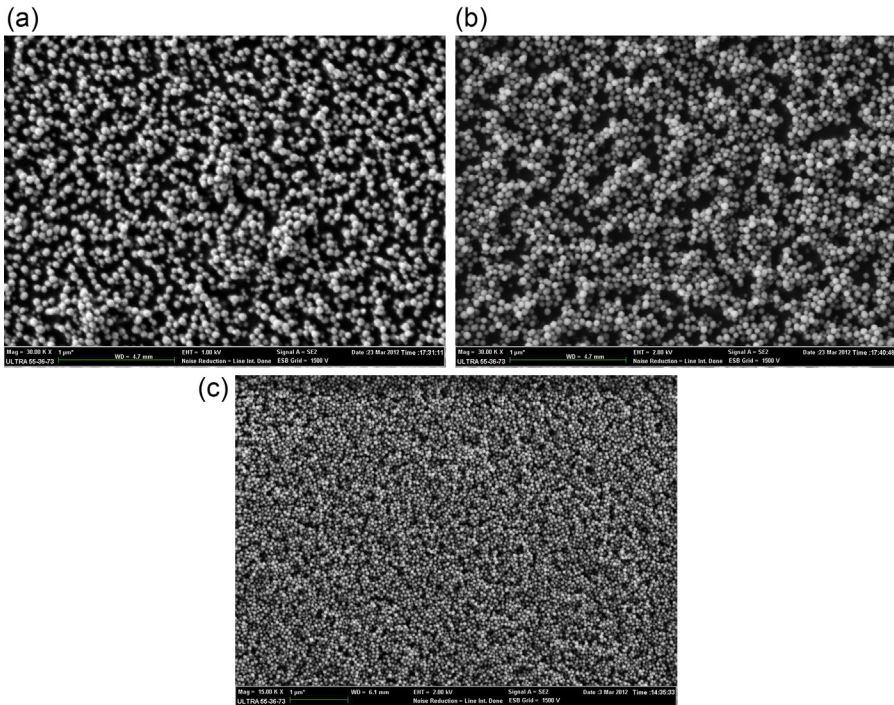


Figure 12.13 SEM images of SiO_2/PEI film with various cycles: (a) 2-cycle, (b) 4-cycle, and (c) 20-cycle.

cycles of SiO_2 colloidal particles on polyethylene terephthalate substrates. The results of this study indicate that the SiO_2/PEI film may be considered a single thin film of a homogeneous inorganic–organic SiO_2/PEI composite material with a uniform refractive index. The thickness of the thin film is much less than the expected value calculated from the SiO_2 diameter multiplied by the number of cycles, which suggests that a theoretical 1-cycle assembly does not produce an actual one-thickness layer.

Results obtained on the basis of the scanning electron microscopy (SEM) analysis confirm that the $(\text{SiO}_2/\text{PEI})_n$ film is a homogeneous porous composite monolayer with structural colors originated from single thin-film interference.

Based on this analysis, the optical behaviors of $(\text{SiO}_2/\text{PEI})_n$ film are well satisfied with the theory of single thin-film interference (Fig. 12.14). When the refractive index of the substrate is greater than the refractive index of the thin film and air, the conditions for constructive interference are given by Eq. [12.6] (Gao et al., 1994; Kinoshita, 2008):

$$2nd \cos \theta_1 = m\lambda \quad [12.6]$$

where n is the refractive index of thin film; d is the thickness of thin film; θ_1 is the light incidence angle; m is the integer; and λ is the largest reflected light wavelength.

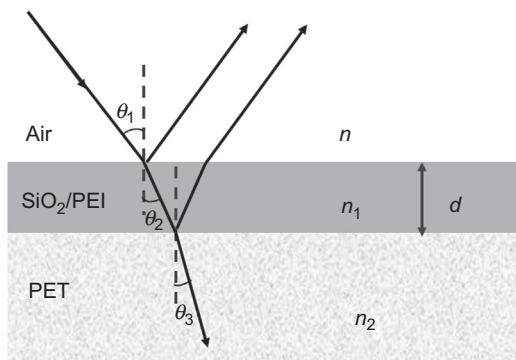


Figure 12.14 Diagram of light on single thin film of refractive index n_1 and thickness d .

According to Eq. [12.6], λ varies with the thickness of the thin film and viewing angle, and the thickness of the thin film is influenced by the assembly cycles and particle size.

From another perspective, if the SiO₂/PEI film is a multilayer film, constructive interference with angles of refraction in high (H) and low (L) refractive index layers of equation is applicable (Kinoshita, 2008; Kinoshita et al., 2008) (Eq. [12.7]):

$$2(n_H d_H \cos \theta_H + n_L d_L \cos \theta_L) = m\lambda \quad [12.7]$$

where n_H and n_L are the refractive index of the two different transparent layers of the films, and d_H and d_L are the thickness of the H and L layers.

Because the thickness of the absorbed PEI monomolecular layer is much smaller than that of the SiO₂ particle layer, the optical path difference through the PEI layer may be negligible. Thus the optical properties of the presumed multilayer film may approximate that of a single thin film to achieve the corresponding optical performance.

All of the results obtained in this study indicate that the SiO₂/PEI film may be considered a single thin film of a homogeneous inorganic–organic SiO₂/PEI composite material with a uniform refractive index. The effective refractive index can be calculated approximately from Eq. [12.8] (Fudouzi, 2004):

$$n^2 = n_p^2 V_p + n_m^2 V_m \quad [12.8]$$

where n is the effective refractive index of the SiO₂/PEI film, n_p is the refractive index of the common dense silica film, about 1.46, and the surrounding medium in the air, namely the n_m , is 1. V_p and V_m are the volume fractions of the particulate SiO₂ and surrounding medium, respectively.

12.3.3.3 Self-assembly process of (silica–polyethylenimine)_n film coated on polyester fabric surface

To investigate the process of formation of (SiO₂/PEI)_n films with electrostatic self-assembly, the morphological structure of (SiO₂/PEI)_n films ($n = 1, 2, 3, \text{ and } 4$)

was examined. The assembly process of an $(\text{SiO}_2/\text{PEI})_n$ film using the electrostatic self-assembly approach is illustrated in Fig. 12.15.

In the assembly system, long-range electrostatic forces in electrostatic self-assembly of films are obvious compared with short-range interactions such as van der Waals forces or hydrogen, which are considered to be weaker and negligible (Aizenberg et al., 2000; Ostrander et al., 2001). SiO_2 nanoparticles are adsorbed on the substrate surface owing to the electrostatic attraction between positively charged PEI and negatively charged SiO_2 nanoparticles as one cycle is completed; SiO_2 nanoparticles in $(\text{SiO}_2/\text{PEI})_1$ film are uniformly and randomly distributed, and most SiO_2 nanoparticles from cycle 2 occupy the gaps between the SiO_2 nanoparticles in $(\text{SiO}_2/\text{PEI})_1$ film because the residual negative charge of SiO_2 nanoparticles in the $(\text{SiO}_2/\text{PEI})_1$ film is shielded by the PEI absorbed in cycle 2, resulting in decreased porosity of the film. However, the electrostatic repulsion between the absorbed SiO_2 nanoparticles in film and the unabsorbed SiO_2 nanoparticles in the colloidal solution cannot be thoroughly eliminated because of the additional negative charges introduced into the film by SiO_2 nanoparticles from cycle 2. Thus, there are still some pores in $(\text{SiO}_2/\text{PEI})_2$ film unoccupied by the SiO_2 nanoparticles. There are, of course, some particles superimposed onto the previous particles in the $(\text{SiO}_2/\text{PEI})_1$ film. In the $(\text{SiO}_2/\text{PEI})_3$ film, part of the particles are superimposed onto previous particles in the $(\text{SiO}_2/\text{PEI})_2$ film, whereas some occupy gaps left in previous cycles, so that the porosity of the $(\text{SiO}_2/\text{PEI})_3$ film apparently decreases. Similarly, particles from cycle 4 are assembled, indicating that the distribution of particles is mainly along with the direction of the growth in thickness of the film as the cycle increases.

The $(\text{SiO}_2/\text{PEI})_n$ films are fabricated using the electrostatic self-assembly approach by overcompensating for the surface charge when PEI and SiO_2 nanoparticles are adsorbed at the solid–liquid interface. Actually, the growth of the $(\text{SiO}_2/\text{PEI})_n$ film can be considered a process of dynamic equilibrium of electrostatic attraction and repulsion. SiO_2 nanoparticles pack in the $(\text{SiO}_2/\text{PEI})_n$ film owing to electrostatic forces. Also, some particle clusters exist in the $(\text{SiO}_2/\text{PEI})_n$ film; thus, the lateral

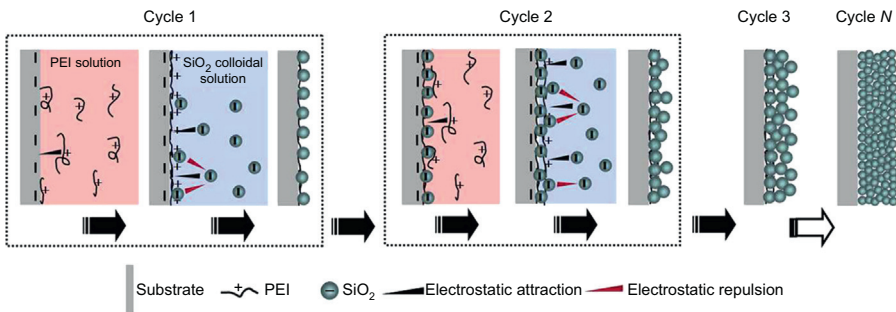


Figure 12.15 Schematic presentation of assembly process of $(\text{SiO}_2/\text{PEI})_n$ film by electrostatic self-assembly with PEI and SiO_2 nanoparticles (simplified pictures of positively charged PEI molecule and negatively charged SiO_2 nanoparticles in cycle 3 and cycle N).

From Zhang, Y., Zhuang, G.Q., Jia, Y.R., 2015. Structural coloration of polyester fabrics with electrostatic self-assembly of $(\text{SiO}_2/\text{PEI})_n$. *Textile Research Journal* 85, 785–794.

capillary forces that originated from the transition of film from the wet to the dry state should be taken into account to arrange the adsorbed particles further. The particles in the region affected by lateral capillary attraction can get close to each other whereas those outside it cannot. Hence, the self-assembly process of an $(\text{SiO}_2/\text{PEI})_n$ film on a polyester fabric is driven by multiple forces, with the dominant force of equilibrium of electrostatic attraction and repulsion.

12.3.3.4 Property evaluation of $(\text{silica-polyethylenimine})_n$ -coated polyester fabrics

As shown in Fig. 12.16(b), the texture of polyester fabric coated with $(\text{SiO}_2/\text{PEI})_9$ film can be clearly observed, with no blockage between interstices of yarns and no obvious differences between the polyester fabrics with or without $(\text{SiO}_2/\text{PEI})_9$ film coated at low magnification (Fig. 12.16(a) and (b)). Fig. 12.16(c) shows that the fibers were uniformly covered by $(\text{SiO}_2/\text{PEI})_9$ film and the fiber surface shape can still be seen clearly. Furthermore, the $(\text{SiO}_2/\text{PEI})_9$ film, which has been confirmed to be submicron (about 500 nm), is thin compared with conventional coating films. Owing to the existence of the electrostatic attraction force and the feature of a very thin film coating, the polyester

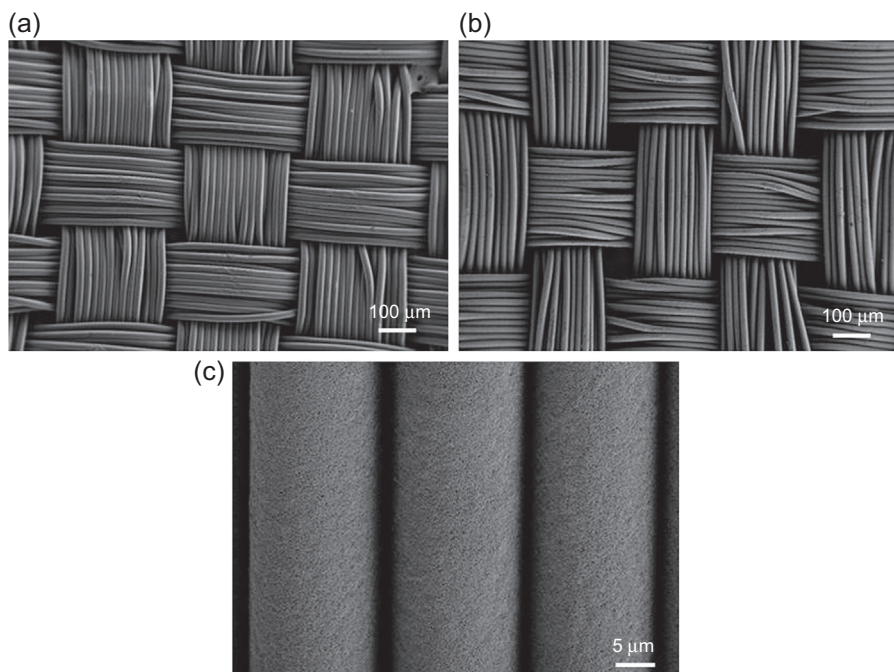


Figure 12.16 SEM images of (a) raw polyester fabric, (b) polyester fabric coated with $(\text{SiO}_2/\text{PEI})_9$ film, and (c) high magnification of (b).

From Zhang, Y., Zhuang, G.Q., Jia, Y.R., 2015. Structural coloration of polyester fabrics with electrostatic self-assembly of $(\text{SiO}_2/\text{PEI})_n$. *Textile Research Journal* 85, 785–794.

fabrics dyed with $(\text{SiO}_2/\text{PEI})_n$ show a good bending resistance, a pleasantly soft handle, and satisfactory colorfastness to rubbing according to our preliminarily subjective observation.

12.4 Structural colors of photonic crystals on textiles

12.4.1 *The concept of photonic crystals*

Photonic crystals (PCs) are highly ordered materials that possess a periodically modulated dielectric constant, with the properties of confining and controlling the propagation of light owing to the existence of photonic band gap, a band of frequencies in which light propagation in the photonic crystal is forbidden (Freyman et al., 2013; Lee et al., 2013; Koenderink and Vos, 2005). Therefore, photonic crystals are also known as photonic band gap materials. Photonic crystals have been the subject of numerous investigations since the original work of Yablonovitch (1987) and John (1987). Because of their unique characteristics, the potential applications of photonic crystals are highly prospective, ranging from gas sensing to optical filters, photonic papers, inkless printing, and reflective flat displays.

According to variations in the refractive index and period in space, there are one-dimensional (1D), two-dimensional (2D), and three-dimensional (3D) photonic crystals. In particular, 3D photonic crystals have permittivity modulation along all three directions. If the 3D PCs possess a sufficiently high refractive index ratio, suitable periodicity, and a dielectric filling ratio, a full band gap might be formed. Thus, light with a specific frequency will be forbidden within three directions of photonic crystals, which facilitates control of the spontaneous emission and propagation of light. Thus 3D photonic crystals are considered to be one of the most potential materials.

12.4.2 *Fabrication of photonic crystals*

In nature, there are many natural photonic crystals such as butterfly wings, sea mouse hair, and natural opal. Electron microscopy revealed that these natural photonic crystals are composed of some periodic microstructures which can make lights with different frequencies scatter and transmit in different directions; therefore, brilliant colors can be presented. However, most photonic crystals are fabricated by manual methods. The emergence of the photonic band gap is always related to the structure of photonic crystals, the connectivity of the medium, the dielectric constant or refractive index contrast, and the filling ratio. In general, the larger the contrast of the dielectric constant, the greater is the possibility of obtaining a photonic band gap. In 1991, Yablonovitch first prepared 3D photonic crystals with a complete band gap in the laboratory. Subsequently, the fabrication of photonic crystals expanded and the photonic band gap gradually advanced from the microwave band to the far-infrared, infrared, near-infrared, and even visible light wave bands. Overall, precision machining and colloidal self-assembly are the main methods of fabricating artificial photonic crystals, in which the precision machining is suitable for fabricating photonic crystals with large

periodicity, such as microwave and far-infrared bands; however, colloidal self-assembly has a key role in fabricating photonic crystals with a photonic band gap in the visible and near-infrared region.

To fabricate photonic crystals with a band gap within the visible band on textile fabrics, colloidal self-assembly is believed to be a simple and inexpensive approach. There are a variety of methods to assemble spherical colloids into crystalline lattices; notable examples include gravitational sedimentation (Comoretto et al., 2003), vertical deposition (Jiang et al., 1999; Zhong et al., 2002), centrifugal sedimentation (Johnson et al., 2001), electrophoretic deposition (Liu et al., 2013), and the microfluidic cell method (Park and Xia, 1999), among which gravity sedimentation and vertical deposition possess relatively mature technology, require simple equipment, and can obtain a high-quality crystal structure.

12.4.3 Structural color principles of photonic crystals

Structural color is an important property of photonic crystals. Clearly, photonic crystals can produce structural colors owing to the existence of a photonic band gap. If the photonic band gap falls into the visible light range between 380 and 780 nm, the visible light of specific wavelengths is not allowed to propagate in the photonic crystal structure, and thus is selectively reflected. The structural colors are then produced on the surface of periodic photonic crystals (Liu et al., 2015a,b). Bragg diffraction is the theoretical basis of structural color produced by photonic crystals. Fig. 12.17 shows a schematic of the Bragg diffraction law followed by a 3D photonic crystal structure. Specifically, Bragg's equation with Snell's law is presented as (Eq. [12.9]):

$$\lambda = 2d(n_{\text{eff}}^2 - \cos^2 \theta)^{1/2} \quad [12.9]$$

where λ_{max} is the wavelength of the reflectance peak maximum (ie, the position of the photonic band gap), d_{hkl} is the interplanar spacing between hkl planes, n_{eff} is the effective refractive index of the photonic structure, and θ is the angle between the

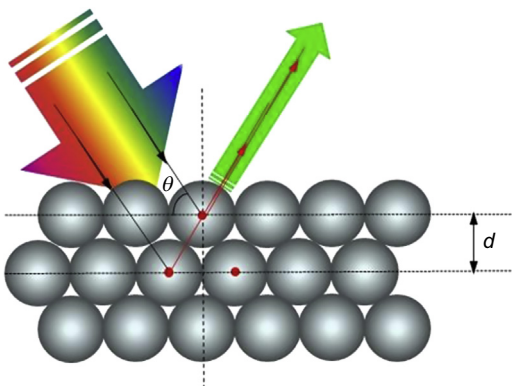


Figure 12.17 Schematic of Bragg's diffraction law followed by 3D photonic crystals with structural color.

incident light and the surface normal of the sample (the same as the viewing angle) (Richel et al., 2000; Romanov et al., 2001). Therefore, on the basis of Bragg's equation with Snell's law, the structural colors of photonic crystals are related to a number of factors including the diffracting plane spacing, the Bragg glancing angle, and the refractive index of the photonic crystal array. In other words, the photonic band gap can be adjusted by changing the diffracting plane spacing, the Bragg glancing angle, and the refractive index of the photonic crystal array.

12.4.4 Application of photonic crystals on textile fabrics

The fabrication of 3D photonic crystals on textile materials has aroused interest owing to its potential to initiate a new coloring mode in dyeing and the finishing process. Fortunately, in prior related domestic and international work, the group of Zhang (2010) of Suzhou University and Liu Xiangyang (Diao and Liu, 2012) of the National University of Singapore fabricated photonic crystals on fibers and silk fabric with structural colors, respectively. It was thought that they performed valuable preliminary explorations into applying coloration to photonic crystals on soft textiles; however, the relevant experimental methods, mechanisms, control measures, and many other, deeper relationships among photonic crystals, structural colors, and flexible textile substrates should be further studied. In our study, colloidal self-assembly technology was used to produce 3D photonic crystals on textile fabrics, and the related mechanisms and structural coloration characteristics were investigated in depth. The main research progress and results are summarized as follows.

12.4.4.1 Preparation and characterization of monodisperse colloidal microspheres

On the basis of Bragg's equation, the diameter of colloidal microspheres is a main factor in determining the structural colors of the photonic crystals. Colloidal microspheres with different diameters in the range 200–400 nm can be used to fabricate photonic crystals with variable structural colors in the visible light range. Moreover, the monodispersity of colloidal microspheres is an important parameter to fabricate an orderly photonic crystal structure which can directly affect the saturation and brightness of structural colors on textiles. Thus the dispersion index of colloidal microspheres used to construct orderly photonic crystals should be less than 0.08 (Jiang et al., 1999).

In our study, SiO₂ and polystyrene colloidal microspheres such as polystyrene (PSt), poly(styrene-methacrylic acid) (P(St-MAA)), and poly(styrene-methyl methacrylate-acrylic acid) (P(St-MMA-AA)) with a controlled particle size and good monodispersity prepared by Stöber method and soap-free emulsion copolymerization, respectively, were used in the colloidal self-assembly process to fabricate related photonic crystals with structural colors on textile fabrics. Specifically, the diameters and monodispersity of these microspheres could be adjusted by controlling some synthesis conditions including the amount of the reactants, and reaction times and temperatures. The prepared colloidal microspheres with different diameters had good sphericity and monodispersity (Figs. 12.18 and 12.19).

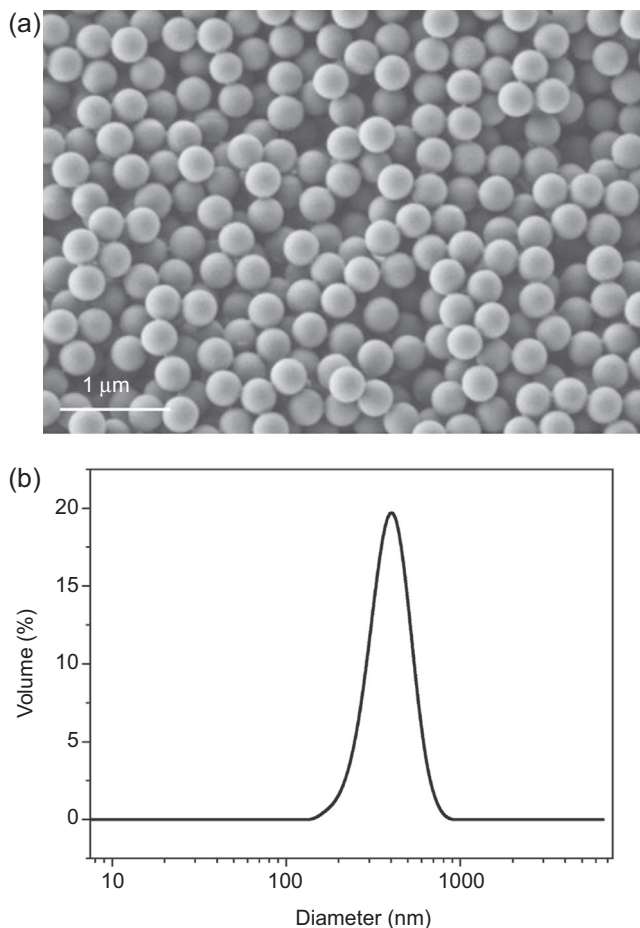


Figure 12.18 Surface morphology (a) and particle size distribution (b) of prepared PSt microspheres.

12.4.4.2 Self-assembly of colloidal microspheres on textile fabrics

After preparing colloidal microspheres with a controlled particle size and good monodispersity, gravitational sedimentation and vertical deposition were applied to fabricate photonic crystals on different kinds of textile fabrics such as polyester and silk (Fig. 12.20).

Fig. 12.21 shows an SEM image of the original silk and polyester woven fabrics. The warp yarns and filling yarns in the fabrics are arranged in an orderly fashion and the fibers in the same direction are less overlapped; moreover, there are a lot of gaps at the junction of warp yarns and filling yarns, which are in the typical structure characteristic of textile fabrics.

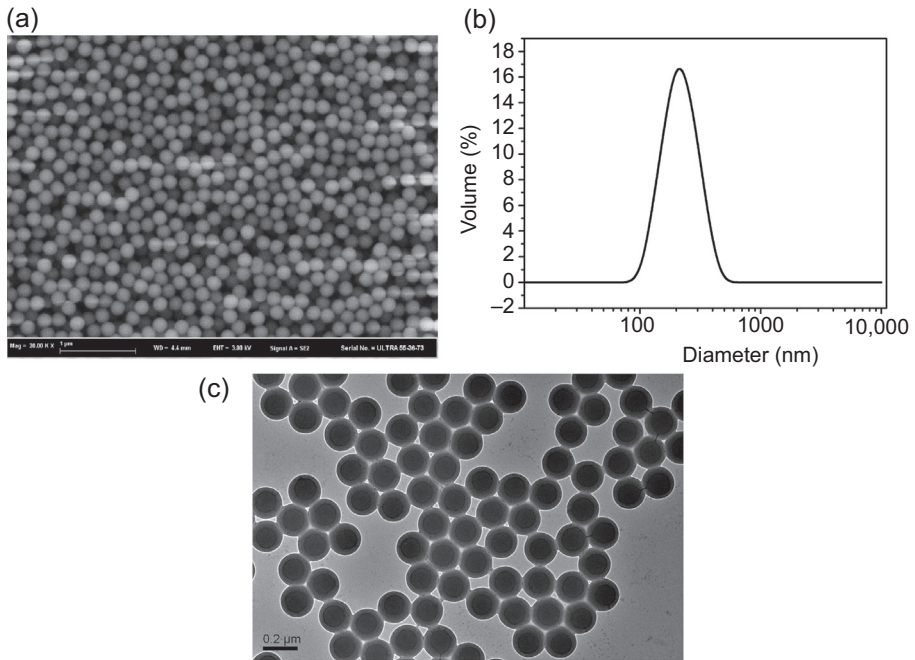


Figure 12.19 Surface morphology and particle size distribution of prepared (PSt-MAA) microspheres in which (a) is SEM image, (b) is particle size distribution, and (c) is transmission electron microscopy image.

Fig. 12.19(b) and (c): Liu, G., Zhou, L., Wu, Y., 2015a. Optical properties of three-dimensional P(St-MAA) photonic crystals on polyester fabrics. *Optical Materials* 42, 72–79. <http://dx.doi.org/10.1016/j.optmat.2014.12.022>.

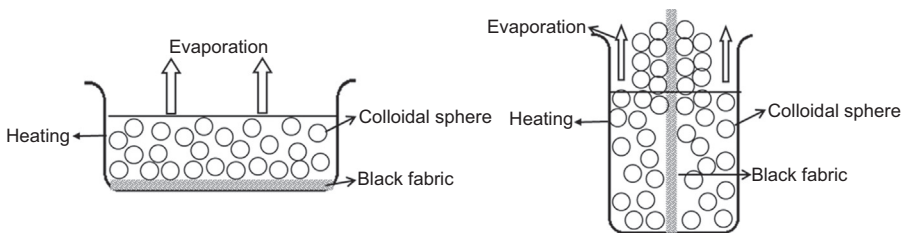


Figure 12.20 Schematic diagrams of gravitational sedimentation self-assembly (left) and the vertical deposition self-assembly (right) for colloidal microspheres on textile fabrics.

After gravitational sedimentation and vertical deposition, the highly disordered colloidal microspheres can form an ordered periodic array structure on the fabric surface. Figs. 12.22 and 12.23 show PSt and P(St-MAA) photonic crystal structures on silk and polyester fabrics, respectively, by gravity sedimentation. The top-view images show that the surfaces of textile fabrics are fully covered with the photonic crystals and the colloidal microspheres are closely packed, with each microsphere neighboring six

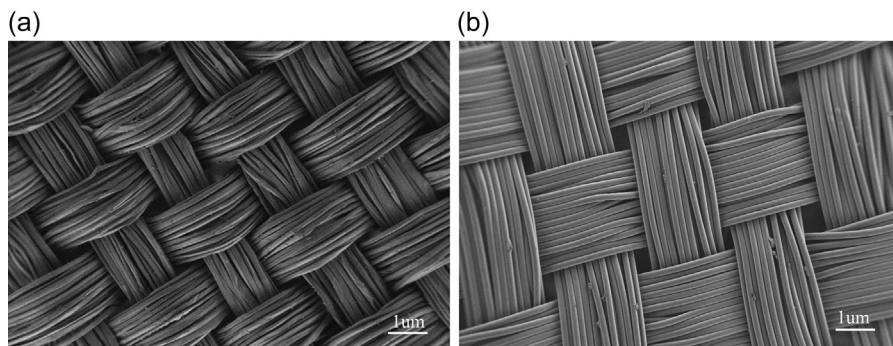


Figure 12.21 Surface morphology images of silk (a) and polyester (b) woven plain fabrics.

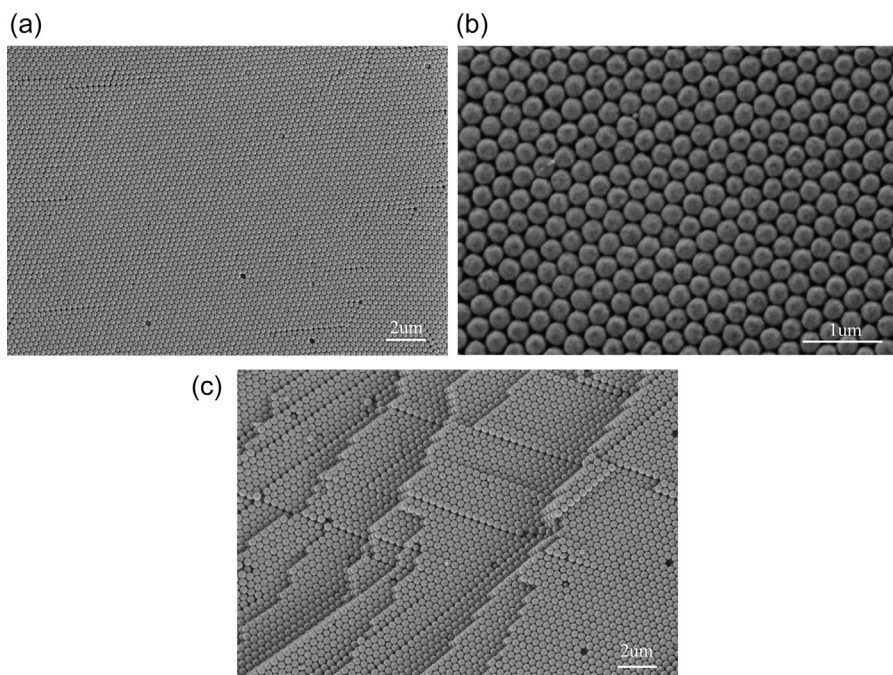


Figure 12.22 SEM images of PST photonic crystal structure on silk fabrics by gravitational sedimentation self-assembly, in which (a) is a typical top-view image, (b) is a magnified image of (a), and (c) is a typical cross-sectional image.

others in a layer. The square and hexagon arrangements of the microspheres are shown in the cross-sectional images, which suggest that the resulting close-packed structure of the microspheres is compatible with the 3D face-centered cubic (fcc) packing. Actually, a square arrangement corresponds to a $\{100\}$ -type plane fcc structure whereas a hexagonal arrangement corresponds to a $\{111\}$ -type plane fcc structure. Likewise, the similar photonic crystals of fcc structure on textile fabrics can be fabricated by vertical deposition self-assembly.

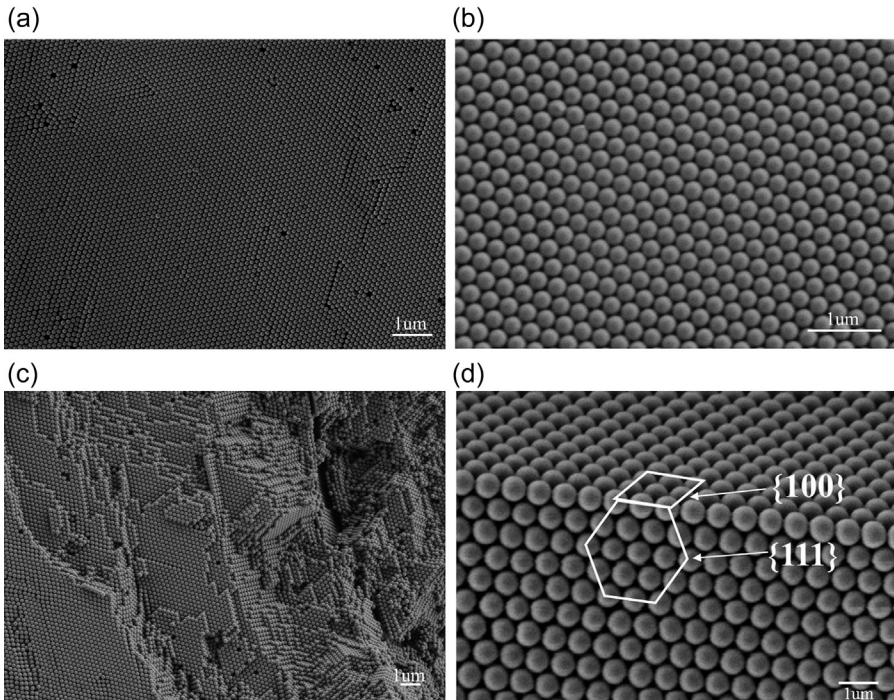


Figure 12.23 SEM images of P(St-MAA) photonic crystal structure on polyester fabrics by gravitational sedimentation self-assembly, in which (a) is a typical top-view image, (b) is a magnified image of (a), (c) is a typical cross-sectional image, and (d) is a local amplification of (c).

12.4.4.3 Color properties of textile fabrics with photonic crystals

To investigate the structural color properties of photonic crystals on textile fabrics, such as brightness, saturation, and iridescence, some characterization techniques including use of a digital camera, 3D video microscope, ultraviolet–visible light (UV–Vis) spectrometer, and multiangle spectrophotometer were used in our experiments. Taking P(St-MAA) microspheres as an example, Figs. 12.24 and 12.25 present digital camera photos, 3D video microscope images, and reflectance curves of the as-prepared structural colors on the polyester fabrics after gravitational sedimentation and vertical deposition, respectively (Liu et al., 2015a,b).

From those digital camera photos and 3D video microscope images, it can be seen that the surfaces of original polyester fabrics are covered with P(St-MAA) photonic crystals and have bright and uniform structural colors after gravitational sedimentation and vertical deposition. Moreover, the structural colors vary with the different microsphere sizes; that is, the full colors of photonic crystals can be produced by adjusting the sizes of the P(St-MAA) colloidal microspheres. From the 3D video microscope images, we can clearly distinguish the warp yarns and filling yarns in

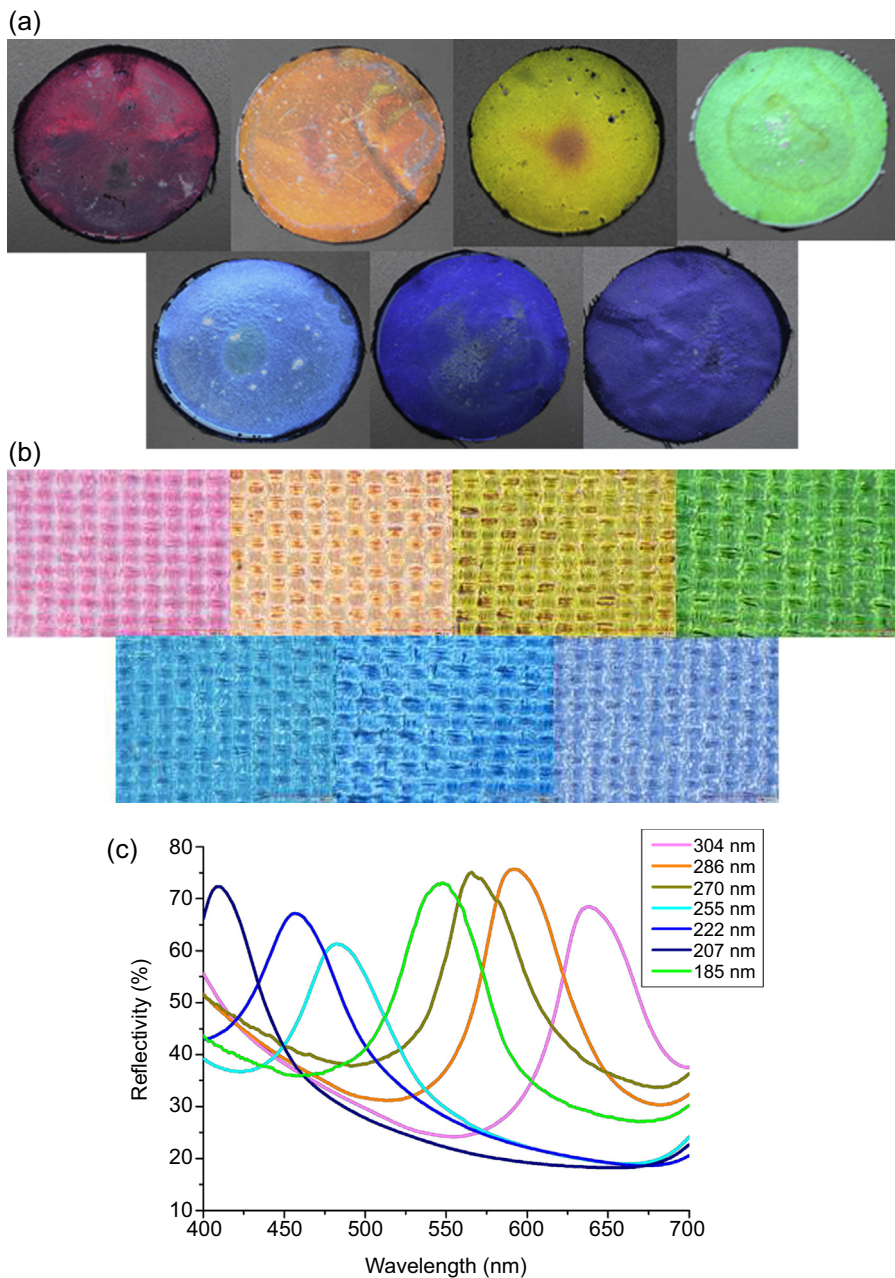


Figure 12.24 (a) Digital camera photos, (b) 3D video microscope images, and (c) reflectance curves of structural colors of P(St-MAA) photonic crystals on polyester fabrics by gravitational sedimentation self-assembly with different sizes of P(St-MAA) microspheres, in which from long to short wavelength, the diameters of microspheres are 304, 286, 270, 255, 222, 207, and 185 nm, respectively. The size of the fabric samples was about $\pi \times 3.5 \times 3.5 \text{ cm}^2$.

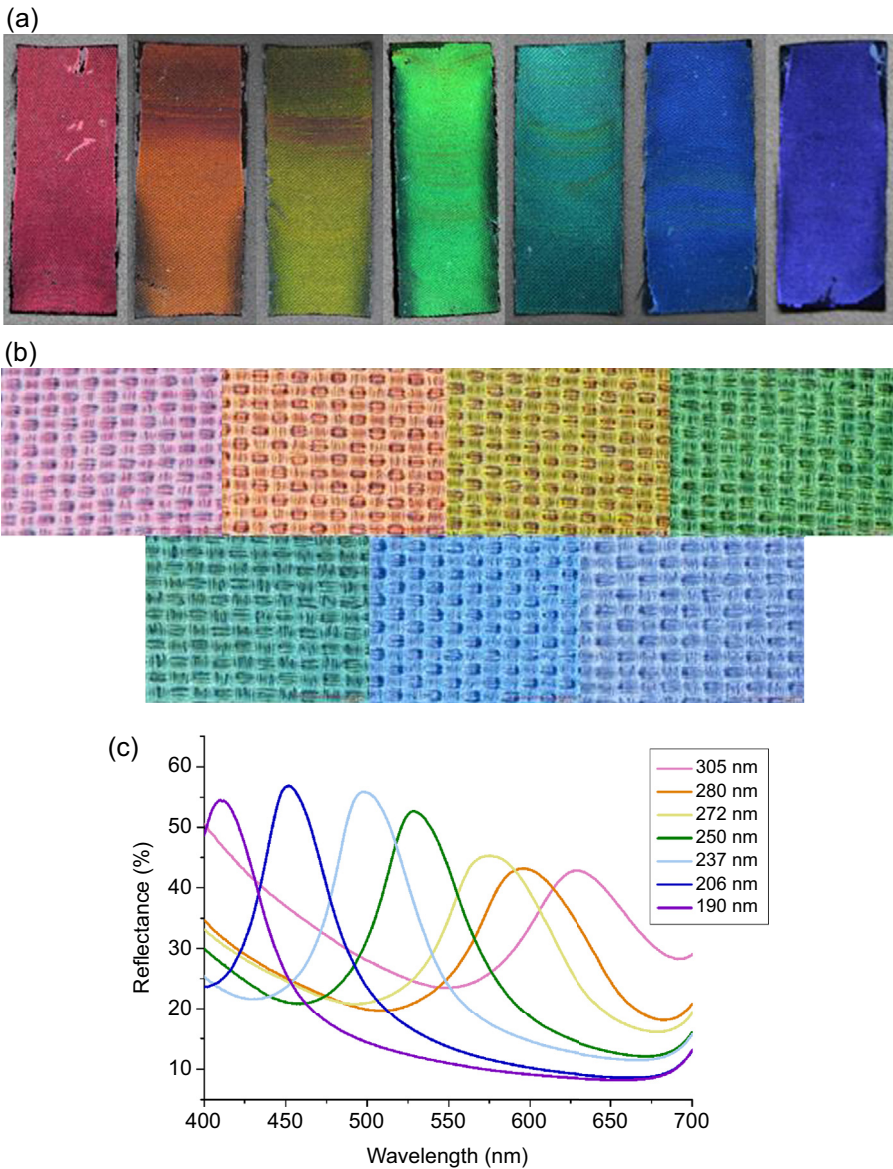


Figure 12.25 (a) Digital camera photos, (b) 3D video microscope images, and (c) reflectance curves of structural colors of P(St-MAA) photonic crystals on polyester fabrics by vertical deposition self-assembly with different sizes of P(St-MAA) microspheres, in which, from long to short wavelength, the diameters of microspheres are 305, 280, 272, 250, 237, 206, and 190 nm, respectively. The size of the fabric samples was about $5 \times 1 \text{ cm}^2$. From Liu, G., Zhou, L., Wu, Y., 2015b. The fabrication of full color P(St-MAA) photonic crystal structure on polyester fabrics by vertical deposition self-assembly. *Journal of Applied Polymer Science* 132. <http://dx.doi.org/10.1002/app.41750>.

the colored polyester fabrics, which implies that the thickness of P(St-MAA) photonic crystals on polyester fabrics in our study is suitable and acceptable as textile products.

In Figs. 12.24(c) and 12.25(c), the sharp reflection spectrum indicates the good quality of the photonic crystal structure formed by the P(St-MAA) colloidal microspheres. In addition, as the particle size increases, the reflection peak position of the photonic crystals shifts to a longer wavelength, which suggests that the photonic band gap position is red-shifted. In other words, the photonic band gap could be shifted to the blue side of the visible spectrum as well reduce the particle size, which could be easily explained by Bragg's law.

In addition to changing the particle sizes, varying the viewing angles is thought to be a simple way to change the structural color of photonic crystals on textile fabrics in view of Bragg's law. Specifically, the phenomenon of color changes with the viewing angles is commonly known as the iridescent effect. Figs. 12.26 and 12.27 show iridescent effects of as-prepared structural colors of P(St-MAA) photonic crystals on polyester fabrics using a digital camera and a multiangle spectrophotometer, respectively (Liu et al., 2015a,b).

As shown in Fig. 12.26, with the variation in viewing angles from 0 degree to 90 degree, the iridescence effects of different four structural colors—orange, golden yellow, emerald green, and green—are displayed for the same assembled polyester sample, which abides by Bragg's law: that is, the photonic band gap positions of P(St-MAA) photonic crystals on polyester fabric are blue-shifted simply by increasing the viewing angles. To understand the relationships among the exact viewing angles, the structural colors and their reflection spectra in depth, a novel multiangle spectrophotometer was applied in our research. Fig. 12.27(a) shows eight structural colors of the same P(St-MAA) photonic crystals on polyester fabrics at different aspecular viewing angles with the incident light source at 45 degree and 15 degree. Fig. 12.27(b) and (c) presents the relevant reflectance spectra of the structural colors

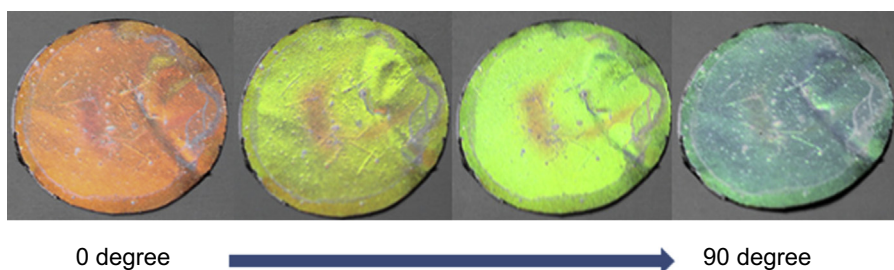


Figure 12.26 Photographs of various structural colors from P(St-MAA) photonic crystals on polyester fabrics fabricated by colloidal microspheres with the same diameter of 286 nm. Photographs were taken at different viewing angles from 0 degree (leftmost) to 90 degree (rightmost) along the direction of the arrow.

From Liu, G., Zhou, L., Wu, Y., 2015a. Optical properties of three-dimensional P(St-MAA) photonic crystals on polyester fabrics. *Optical Materials* 42, 72–79. <http://dx.doi.org/10.1016/j.optmat.2014.12.022>.

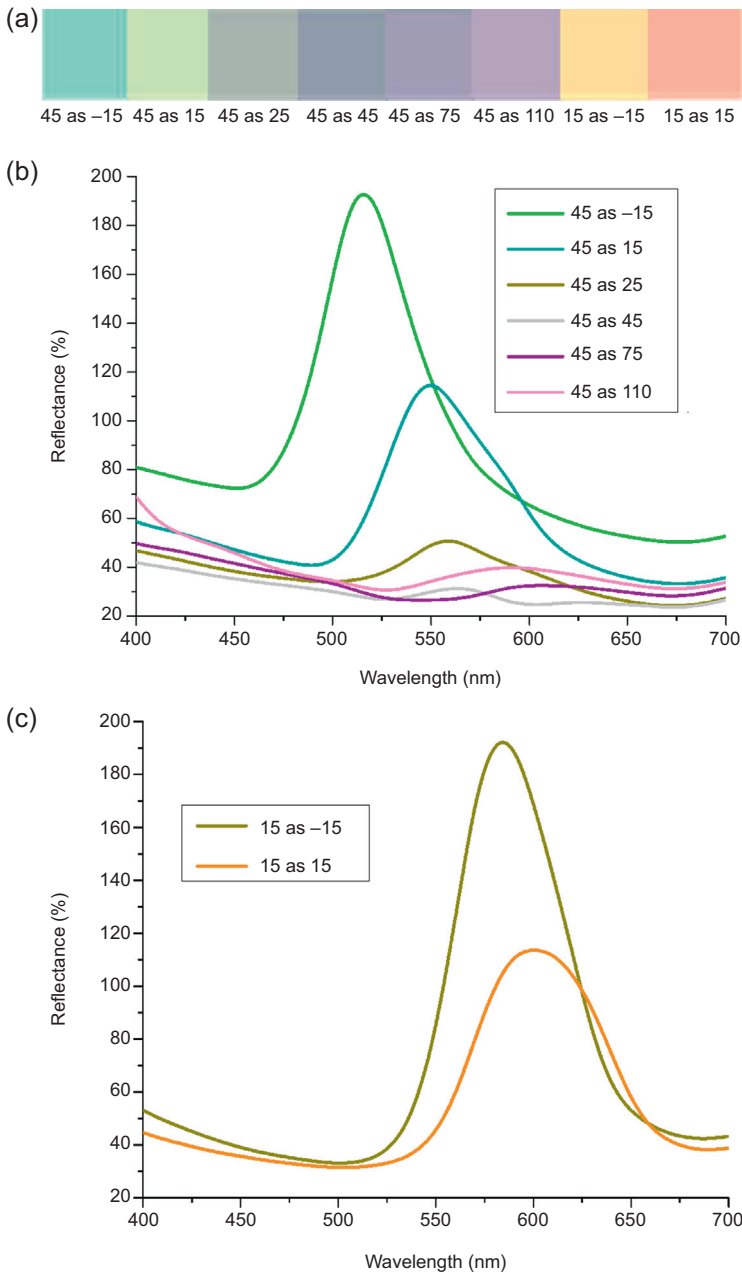


Figure 12.27 Photographs and reflectance spectra of structural colors on polyester fabrics characterized by a multiangle spectrophotometer: (a) Structural color photographs at different viewing angles; (b) reflectance spectra at a testing light source of 45 degree; and (c) reflectance spectra at a testing light source of 15 degree. The P(St-MAA) colloidal microspheres have the same diameter of 286 nm, the angle “45 as -15” means the sample is directionally illuminated at 45 degree from normal, and the aspecular viewing angle in plane is at -15 degree; others follow by analogy.

Fig. 12.27(a): Liu, G., Zhou, L., Wu, Y., 2015a. Optical properties of three-dimensional P(St-MAA) photonic crystals on polyester fabrics. *Optical Materials* 42, 72–79. <http://dx.doi.org/10.1016/j.optmat.2014.12.022>.

shown in Fig. 12.27(a). There are distinct positions and intensities of reflection peaks for the same sample at different viewing angles. In particular, under the same testing light source, the peak wavelengths of reflectance spectra varied with the different testing angles, in line with the structural color changes in Fig. 12.27(a), which implies that the photonic band gap of the prepared photonic crystals can vary with the viewing angles. Moreover, some reflectance intensity data in Fig. 12.27(b) and (c) are more than 100% higher in some viewing angles than the conventional reflectance obtained from a UV–Vis spectrometer. In our opinion, it might be explained via interference theory (Born and Wolf, 1999). If two beams of reflected lights from periodic photonic crystals form constructive interference, and the two beams are of equal intensity of I_0 , light intensity (I) can be calculated from the equation (Eq. [12.10]):

$$I = 4I_0 \cos^2 \frac{\delta}{2} \quad [12.10]$$

in which δ means the phase difference. This equation indicates that the maximum of light intensity is four times as bright as the individual beam, which is thought to account for some reflectance data and intensity data larger than 100% in Fig. 12.27.

In summary, the structural colors of photonic crystals on textile fabrics can vary with the microsphere size and viewing angles, in line with Bragg's law.

In our study, although both gravitational sedimentation self-assembly and vertical deposition self-assembly can produce well-ordered photonic crystals on textile fabrics displaying vivid and variable structural colors, vertical deposition can exhibit some interesting characteristics different from gravitational sedimentation, as shown in Table 12.2. Gravitational sedimentation is thought to be the easiest assembly method driven by gravity of colloidal microspheres, and involves the coupling of complex processes such as gravitational settling, translational diffusion (or Brownian motion), and crystallization (nucleation and growth). Nevertheless, vertical deposition is driven by capillary force, which can transfer colloidal microspheres to the substrates during the evaporation of microsphere emulsion; that is, microsphere emulsion evaporation causes a convective microsphere flux from the bulk of the colloidal suspension toward the drying microsphere layer. The balance between capillary force and convective microsphere flux during the evaporation process is essential for the formation of 3D colloidal crystals. Because of the different mechanisms and processes of gravitational sedimentation and vertical deposition, different coloration effects are inevitably generated on textile fabrics. Vertical deposition is able to achieve a double-sided coloration effect on textile fabrics owing to its particular assembly mode, which is different from the single-sided coloration effect of gravitational sedimentation. As shown in Fig. 12.28, the front and back sides of polyester fabrics have identical structural colors, similar to the color effect in traditional dyeing processes. Also, the warp yarns and filling yarns on the fabric sample fabricated by vertical deposition can easily be seen with the naked eye, which is different from that of gravitational sedimentation. Thus it is supposed that the thickness of the photonic crystal structure fabricated by vertical deposition on textile fabrics is thinner than that by gravitational sedimentation, which is favorable to keeping a soft fabric handle (Liu et al., 2015b).

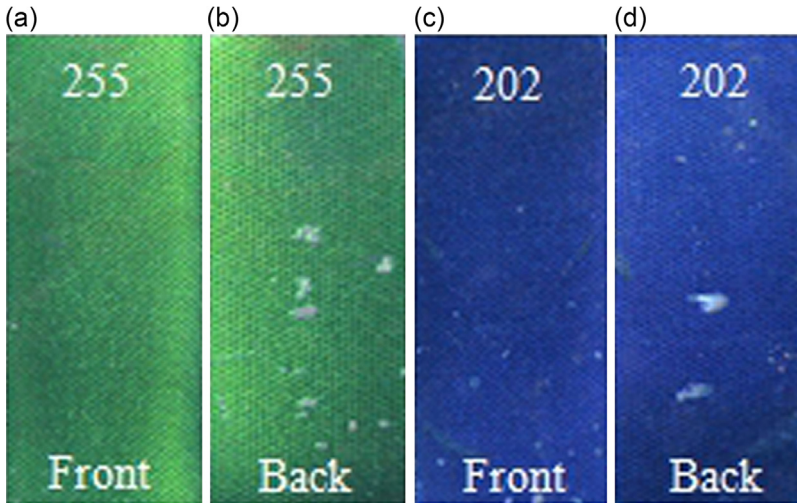


Figure 12.28 Double-sided coloration of photonic crystal structure on polyester fabrics with the incident light normal ([111] direction) to the polyester woven fabric substrate. Photonic crystals with P(St-MAA) microspheres of different diameters: (a, b) 255 nm; (c, d) 202 nm. From Liu, G., Zhou, L., Wu, Y., 2015b. The fabrication of full color P(St-MAA) photonic crystal structure on polyester fabrics by vertical deposition self-assembly. *Journal of Applied Polymer Science* 132. <http://dx.doi.org/10.1002/app.41750>.

12.5 Conclusions and future trends

Structural colors originating from thin-film interference and photonic crystals can be prepared by electrostatic self-assembly and colloidal self-assembly, respectively, and the structural colors feature bright, vivid, and variable color effects. When generating a tunable structural color in a specific location of a textile product, such as in the eyes of a tiger pattern, or the stamen of a flower pattern, the textile product is able to show a special magical lifelike effect; when combining pigmentary coloration with structural coloration, it further broadens the textile coloration technology and produces more colorful and charming textile products; when using digital printing to achieve locally selective nano-coating of textiles, it enables more controllable, high-quality textile products with tunable structural colors. Compared with traditional textile coloration, structural coloration is a novel eco-coloration technology that does not use chemical colorants and has the potential to reduce the pollution existing in current textile dyeing and printing industries.

In addition to structural colors, based on those nano-coatings, the development of functional and intelligent textiles such as humidity-sensitive, pressure-responsive, and radiation-resistant textile-based flexible materials is expected.

The biomimetic structural coloration of textiles using nano-coatings may be a new approach to textile coloration, but it is still in its infancy and it has many mysteries and challenges.

Acknowledgments

We are sincerely grateful for financial support from the National Natural Science Foundation of China (Grant Nos. 51073142 and 51403188), the Zhejiang Provincial Natural Science Foundation of China (Grant No. LY13E030004), and the Research Fund for the Doctoral Program of Higher Education of China (Grant No. 20123318120005).

References

- Aizenberg, J., Braun, P.V., Wiltzius, P., 2000. Patterned colloidal deposition controlled by electrostatic and capillary forces. *Physical Review Letters* 84, 2997–3000.
- Berthier, S., Boulenguez, J., Bálint, Z., 2007. Multiscaled polarization effects in *Suneve coronata* (Lepidoptera) and other insects: application to anti-counterfeiting of banknotes. *Applied Physics A* 86, 123–130.
- Born, M., Wolf, E., 1999. *Principles of Optics: Electromagnetic Theory of Propagation, Interference and Diffraction of Light*. Cambridge University Press, Cambridge.
- Chen, J., Dong, P., Di, D., 2013. Controllable fabrication of 2D colloidal-crystal films with polystyrene nanospheres of various diameters by spin-coating. *Applied Surface Science* 270, 6–15.
- Chen, X., Zhang, X., Yang, W., 2009. Biopolymer-manganese oxide nanoflake nanocomposite films fabricated by electrostatic layer-by-layer assembly. *Materials Science and Engineering: C* 29, 284–287.
- Comoretto, D., Grassi, R., Marabelli, F., 2003. Growth and optical studies of opal films as three-dimensional photonic crystals. *Materials Science and Engineering: C* 23, 61–65.
- Dong, Z.L., Zheng, B.H., Hu, G.F., Liu, J.Y., 2007. *Color Measurement and Computer Color Matching*. Chinese Textile Press, Beijing.
- Davis, K.E., Russel, W.B., Glantschnig, W.J., 1989. Disorder-to-order transition in settling suspensions of colloidal silica: X-ray measurements. *Science* 245, 507–510.
- Diao, Y.Y., Liu, X.Y., 2012. Bring structural color to silk fabrics. *Advanced Materials Research* 441, 183–186.
- Fu, H., Kobayashi, T., 2010. Multilayer composite surfaces prepared by electrostatic self-assembled technique for desalination. *Desalination* 264, 115–122.
- Fudouzi, H., 2004. Fabricating high-quality opal films with uniform structure over a large area. *Journal of Colloid and Interface Science* 275, 277–283.
- Freymann, G.V., Kitaev, V., Lotsch, B.V., 2013. Bottom-up assembly of photonic crystals. *Chemical Society Reviews* 42, 2528–2554.
- Gao, M., Gao, M., Zhang, X., 1994. Constructing PbI_2 nanoparticles into a multilayer structure using the molecular deposition (MD) method. *Journal of the Chemical Society, Chemical Communications* 24, 2777–2778.
- Jia, Y.R., Zhang, Y., Shao, J.Z., 2014. Structural colors of the SiO_2 /polyethyleneimine thin films on poly(ethylene terephthalate) substrates. *Thin Solid Films* 569, 10–16.
- John, S., 1987. Strong localization of photons in certain disordered dielectric superlattices. *Physical Review Letters* 58, 2486–2489.
- Jiang, P., Bertone, J.F., Hwang, K.S., 1999. Single-crystal colloidal multilayers of controlled thickness. *Chemistry of Materials* 11, 2132–2140.
- Johnson, N.P., McComb, D.W., Richel, A., 2001. Synthesis and optical properties of opal and inverse opal photonic crystals. *Synthetic Metals* 116, 469–473.

- Kinoshita, S., 2008. *Structural Colors in the Realm of Nature*. World Scientific, Singapore.
- Kinoshita, S., Yoshioka, S., Miyazaki, J., 2008. Physics of structural colors. *Reports on Progress in Physics* 71, 076401.
- Koenderink, A.F., Vos, W.L., 2005. Optical properties of real photonic crystals: anomalous diffuse transmission. *Journal of the Optical Society of America B: Optical Physics* 22, 1075–1084.
- Krupp, H., 1967. Particle adhesion, theory and experiment. *Advances in Colloid and Interface Science* 1, 111–239.
- Land, M.F., 1972. The physics and biology of animal reflectors. *Progress in Biophysics and Molecular Biology* 24, 75–106.
- Land, M.F., 1966. A multilayer interference reflector in the eye of the scallop, *Pecten maximus*. *Journal of Experimental Biology* 45, 433–447.
- Lee, J.H., Jang, G.E., Jun, Y.H., 2012. Investigation and evaluation of structural color of TiO₂ coating on stainless steel. *Ceramics International* 38, 661–664.
- Lee, H.S., Shim, T.S., Hwang, H., 2013. Colloidal photonic crystals toward structural color palettes for security materials. *Chemistry of Materials* 25, 2684–2690.
- Li, Z.P., Wang, J.Q., Liu, X.H., 2010. Electrostatic layer-by-layer self-assembly multilayer films based on graphene and manganese dioxide sheets as novel electrode materials for supercapacitors. *Journal of Materials Chemistry* 21, 3397–3403.
- Liu, Z., Zhang, Q., Wang, H., 2013. Structurally colored carbon fibers with controlled optical properties prepared by a fast and continuous electrophoretic deposition method. *Nanoscale* 5, 6917–6922.
- Liu, G., Zhou, L., Wu, Y., 2015a. Optical properties of three-dimensional P(St-MAA) photonic crystals on polyester fabrics. *Optical Materials* 42, 72–79. <http://dx.doi.org/10.1016/j.optmat.2014.12.022>.
- Liu, G., Zhou, L., Wu, Y., 2015b. The fabrication of full color P(St-MAA) photonic crystal structure on polyester fabrics by vertical deposition self-assembly. *Journal of Applied Polymer Science* 132, 4385–4393. <http://dx.doi.org/10.1002/app.41750>.
- McPhedran, R.C., Nicorovici, N.A., McKenzie, D.R., 2003. Structural colours through photonic crystals. *Physica B* 338, 182–185.
- Mitra, P., Chatterjee, A.P., Maiti, H.S., 1998. Chemical deposition of ZnO films for gas sensors. *Journal of Materials Science: Materials in Electronics* 9, 441–445.
- Miguez, H., Meseguer, F., Lopez, C., 1997. Evidence of FCC crystallization of SiO₂ nanospheres. *Langmuir* 13, 6009–6011.
- Maboudian, R., Howe, R.T., 1997. Critical review: adhesion in surface micromechanical structures. *Journal of Vacuum Science & Technology*, B 15, 1–20.
- McLaren, K., 1976. XIII—the development of the CIE 1976 ($L^* a^* b^*$) uniform colour space and colour difference formula. *Journal of the Society of Dyers and Colourists* 92, 338–341.
- Nassau, K., 2001. *The Physics and Chemistry of Color*. John Wiley & Sons Inc., New York.
- Ostrander, J.W., Mamedov, A.A., Kotov, N.A., 2001. Two modes of linear layer-by-layer growth of nanoparticle/polyelectrolyte multilayers and different interactions in the layer-by-layer deposition. *Journal of the American Chemical Society* 123, 1101–1110.
- Parker, A.R., Martini, N., 2006. Structural color in animals—simple to complex optics. *Optics and Laser Technology* 38, 315–322.
- Park, S.H., Xia, Y., 1999. Assembly of mesoscale particles over large areas and its application in fabricating tunable optical filters. *Langmuir* 15, 266–273.
- Richel, A., Johnson, N.P., McComb, D.W., 2000. Observation of Bragg reflection in photonic crystals synthesized from air spheres in a titania matrix. *Applied Physics Letters* 76, 1816–1818.

- Romanov, S.G., Maka, T., Torres, C.M.S., 2001. Diffraction of light from thin-film polymethylmethacrylate opaline photonic crystals. *Physical Review E* 63, 1–5.
- Schanda, J., 2007. *Colorimetry: Understanding the CIE System*. John Wiley and Sons & Inc., Hoboken, NJ, pp. 61–63.
- Tilley, R., 2001. *Color and the Optical Properties of Materials*. John Wiley & Sons Inc., New York.
- Yablonovitch, E., 1987. Inhibited spontaneous emission in solid-state physics and electronics. *Physical Review Letters* 58, 2059–2062.
- Zhang, K.Q., Yuan, W., Zhang, A., 2011. The structural colors of photonic crystals. *Functional Materials Information* 7, 39–44.
- Zhang, Q., Wang, J., Wu, G., 2001. Interference coating by hydrophobic aerogel-like SiO₂ thin films. *Materials Chemistry and Physics* 72, 56–59.
- Zhang, Y., Zhuang, G.Q., Jia, Y.R., 2015. Structural coloration of polyester fabrics with electrostatic self-assembly of (SiO₂/PEI)_n. *Textile Research Journal* 85, 785–794.
- Zhong, Z.G., Akira, F., Osamu, S., 2002. Fabrication of high-quality opal films with controllable thickness. *Chemistry of Materials* 14, 760–765.
- Zhang, K.Q., 2010. Structural colored fibers based on photonic crystal structures by colloidal assembly. *JFBI* 2, 222–226.

Functional modification of fiber surface via sol–gel technology

13

C. Wang, Y. Yin
Jiangnan University, Wuxi, China

13.1 Introduction

The sol–gel process is a versatile solution process for making functional or smart materials. The process involves the transition of a system from a liquid sol into a solid gel (Botcher, 2001). Because of its vast applicability, extensive catalogs of molecules have been developed throughout the years. It is possible to fabricate functional or smart materials in a wide variety of forms: thin-film coatings (Perez-Anguiano et al., 2015), ultrafine or spherical-shaped powders (Toledo-Fernandez et al., 2008), special ceramic fibers (Colomban and Gouadec, 2005; Si et al., 2015), microporous inorganic membranes, special glasses, intelligent or smart materials, and extremely porous aerogel materials through the sol–gel process (Koper, 2007).

Functional coatings on substrates are significant applications for functional sols (Textor et al., 1999). Their inorganic nature makes sol–gel layers strong so that one may obtain important effects with strength, thin, and flexible layers (Ma and Zhang, 2014; Pavlidou and Paspaspyrides, 2008; Rojaee et al., 2014). The reaction mechanism is a hydrolysis reaction which induces the substitution of OR groups linked to silicon by silanol Si–OH groups (Viert et al., 1997; Yang et al., 2010). These chemical species may react to form Si–O–Si (siloxane) bonds which lead to silica network formation, and this phase establishes a three-dimensional (3D) network. Available coating substrates are glass, wafer, metal, paper, fabric, and other materials.

Fiber surface is 3D surface and the fabric is a typical sheet material after weaving. It is now a common practice in the world to use fabric to import new characteristic properties by surface modification. Via modification, fabrics include various requirements such as water repellency, antibacterial effects, anti-ultraviolet (UV) behavior, and color properties. There will be important applications of sol–gel technology in the textile industry. How can sol–gel technology be used to modify textiles?

First, the thin and transparent gel film can be formed on the fabric surface by a coating process (Yin et al., 2011), and the coating can effectively improve the properties of the substrate. Second, various precursors based on silicon, titanium, aluminum, and zirconium have been used in the sol–gel process to synthesize inorganic parts, and the functions are abundant (Andersson et al., 2005; Villiers et al., 2010; Wedin et al., 2006). Third, the film formed on the fabric surface is soft, which is consistent with the characteristic of fabric. Also, sol–gel-derived materials can provide a variety of functional properties by embedding active species on fabric substrates. Once the hybrid sol was treated on fabric by dipping, spin-coating (Fong et al., 2015), layer-by-layer (LBL)

electrostatic self-assembly (Wang et al., 2015), and other processes, one or several characteristic properties, such as fixation properties (Yin et al., 2008), antibacterial properties (Wang et al., 2010; Yin and Wang, 2011), anti-UV behavior (Yin and Wang, 2011; Yin et al., 2012), and water- and oil-repellent properties (Yin and Wang, 2013) were presented. Because the functional properties show up in clothing and home textiles, consumers currently seek not only fashion but also ergonomics, especially for comfort and health.

13.2 Hydrophobic and oleophobic modifications

Hydrophobic and water-repellent modifications have been investigated because of their high commercial and industrial importance (Luo et al., 2011; Vilcnik et al., 2009). As a significant property, wettability has an important role in many natural and technological processes. The wettability of liquid to a fiber surface is governed by the chemical properties of the fiber surface and its surface morphology (Yin and Wang, 2013). The sol–gel method is a simple and effective technique for depositing water-repellent coatings onto substrates (Faustini et al., 2010). Moreover, it has advantages such as large deposition areas, uniform deposits on objects with desired shapes, and short processing times (Dhere et al., 2010; Li et al., 2008). Chemical and physical modifications jointly offer assistance to improve water and oil repellency.

To make the silica coating hydrophobic, some organic materials are applied to the inorganic sol matrix so that the surface behaves as a repellent toward water; ie, the water droplets tend to contract and form nearly spherical pearls on the modified silica surface (Yin and Wang, 2013). The treatment of textiles with inorganic–organic sols opens up numerous new possibilities for the improvement of their applicative properties and the functional properties of the fiber surface. Silane coupling agents have been widely used as structural units to construct a variety of silica-based hybrid materials. After it is doped into the matrix sol, the functional properties of the silica coupling agent are presented on the surface of sol–gel hybrid coating (Nistor et al., 2011; Yin et al., 2011).

13.2.1 Hydrophobic silane coupling agent hybrid sol modification

Functional hybrid sols doped with silane coupling agents containing hydrophobic chain are used for fabric hydrophobic modification. The process of preparing the functional hybrid is universal. Hybrid sols containing triethoxysilane (HTEOS) and γ -chloropropyltriethoxysilane (CPTS) were prepared via acidic hydrolysis of tetraethoxysilane (TEOS) solved in a mixture of ethanol and distilled water (Yin and Wang, 2013). Hydrolysis was performed by stirring a mixture of TEOS and ethanol. CPTS was added into the solution. Then the hydrophobic additive HTEOS was added to the sol. The pH value was adjusted with HCl and the sol was obtained after stirred. Other silane coupling agents are methyltriethoxysilane (MTEOS) (Zhang et al., 2014), octyltriethoxysilane (OTEOS) (Fang et al., 2011), and fluoroalkylsilane (FAS) (Tadanaga et al., 2000).

Original cellulose fiber is hydrophilic for massive hydroxyl groups on the surface of fibers, and a water droplet placed on the surface of cellulose fabric sinks completely into the fabric in 3 s, as shown in Fig. 13.1(a). The fabric was submerged into the hybrid sol and padded. Then the fabric was dried and baked. The surface of a treated cellulose fabric nearly supports the formation of spherical water droplets (Fig. 13.1(b)) (Yin and Wang, 2013), which indicates that the cellulose fabric is hydrophobic. The changes in wetting property are related to the chemical component of the fiber surface. Via dehydration and condensation reactions, the Si–O–Si chains are deposited onto the surface of cellulose fabric and many hydroxyl groups on the surfaces of cellulose fabric are enclosed by the silica coating.

The wettability of surfaces is affected not only by the chemical composition but also by the surface texture of the fiber (Li et al., 2011; Mahltig et al., 2010; Yin and Wang, 2013). The surface texture of cellulose fiber has a groove structure and natural distortion, whereas the roughness is not drastic; it has a slight effect on water repellency (Vince et al., 2006). The microsurface coated with hybrid sol is relatively scraggy and some weak peaks are displayed. The fiber in the fabric has a rough surface, according to the Wenzel model. When a substance surface is hydrophobic, and $90 \text{ degree} < \theta_e < 180 \text{ degree}$, so $\cos\theta^* < \cos\theta_e$, then $\theta^* > \theta_e$, which indicates that a larger roughness of a fabric surface can improve the hydrophobicity on a hydrophobic fabric surface (Dorrer and Ruhe, 2008; Yin et al., 2011).

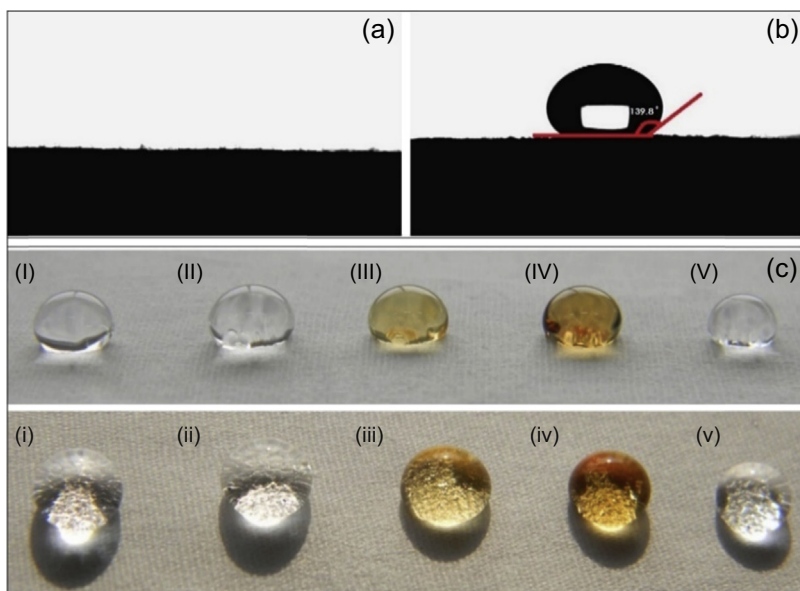


Figure 13.1 Contact angles of water (20 μm) on the original cellulose fabric (a) and treated fabrics with hybrid sol (b), and photos of liquid droplets on fabric coated with hybrid sol (front and top views, respectively): (I) and (i) deionized water; (II) and (ii) rainwater; (III) and (iii) tea; (IV) and (iv) cola; and (V) and (v) liquid soap (c) (Yin and Wang, 2013).

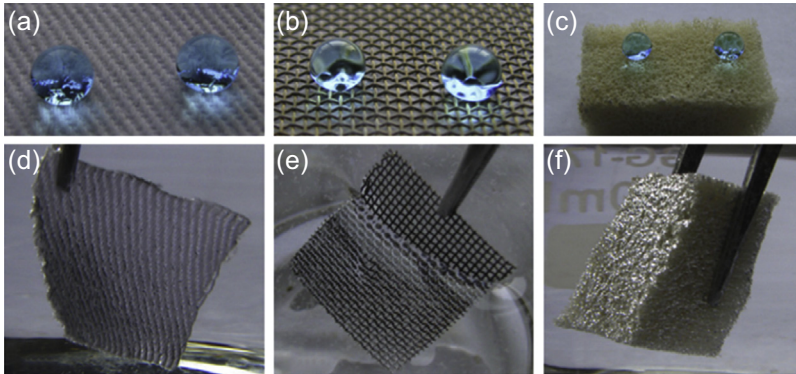


Figure 13.2 Water droplets (dyed with methylene blue) exhibiting a spherical shape on the resulting superhydrophobic materials (a–c); a mirror-like phenomenon can be observed on the resulting superhydrophobic materials submerged in water (d–f) (Zhu et al., 2014).

Some kinds of liquid droplets (Fig. 13.1(c)) (the surface tensions are H_2O : 72.01 N/m; rainwater: 71.36 N/m; tea water: 70.43 N/m; cola: 66.16 N/m; liquid soap: 29.35 N/m) were doped onto fabric coated with hybrid sol (Yin and Wang, 2013). In Fig. 13.1(c), all of the contact angles of liquid droplets are larger than 90 degree, which indicates that the water repellency of the fabric sample is universal.

Zhu et al. reported an interesting material that can be used for oil–water separation in an efficient and cost-effective process that is highly desirable yet still challenging. Three smart materials used for oil–water separation are readily produced by a dip-coating process. The fabric materials show excellent hydrophobic properties in Fig. 13.2(a)–(c). The modified superhydrophobic materials were immersed in water and a plastron (air pockets) that indicated a robust Cassie–Baxter state was formed. The submerged material surfaces acted like a silver mirror when viewed at a glancing angle, as shown in Fig. 13.2(d)–(f) owing to the total reflectance of light at the air layer trapped on the surface. This trapped air can effectively prevent wetting on the material surfaces underwater (Zhu et al., 2014).

13.2.2 Oleophobic modifications with silane coupling agent hybrid sol

It is difficult to realize oleophobic properties because of the low surface tension of water. To achieve oil repellency, the surface free energy of a substrate lower than 20 mN/m is necessary because typical surface tensions of oils are 20–40 mN/m. A one-step approach that significantly improves oil repellency as well as durability is rarely discussed in the literature. The oil-repellent characteristic usually can be realized by modifying a hybrid sol with fluorinated compounds.

A coating film on substrate was prepared by the sol–gel process using alkoxide solutions containing perfluoroalkylsilane and tetraethoxysilane, and the contact angles of the coating film for water and CH_2I_2 were extremely high, at 118.0 degree and 97.0 degree, respectively (Castelvetto et al., 2001).

Table 13.1 Water and CH₂I₂ contact angles of cotton fabric samples (Yu et al., 2007)

	Sample I	Sample II	Sample III	Sample IV	Sample V	Sample VI (treated with PFSC)
Water (°)	134	137	134	145	137	133
CH ₂ I ₂ (°)	125	125	119	131	125	125

PFSC, perfluorooctylated quaternary ammonium silane coupling agent.

Yu et al. reported a complex coating for cotton fabrics based on silica particles and prepared a perfluorooctylated quaternary ammonium silane coupling agent. The contact angle of the CH₂I₂ droplet on the fabric surface reached 131.0 degree (Table 13.1) (Yu et al., 2007). The oil repellent was evaluated according to AATCC-118-2007 and the oil uptake of the textile under full contact with water was determined. In this case, an oil drop is dripped onto a textile sample (20 × 20 cm) and allowed to rest for 30 s. The largest grade indicated by the tested oil when it does not wet the fabric in 30 s is the oil-repellent level. Table 13.2 shows that the cotton fabric treated with silica sol without a silica coupling agent did not show oil-repellent behavior. The fabric sample treated with hybrid silica sol doped with FAS (F-silica sol, FAS 4%) had a weak oil-repellent property (one grade). Fabric samples treated with the hybrid silica sol containing MTEOS, OTEOS, or HTMOS do not display evident oil repellency until the concentration of HTMOS is improved to 20% and the concentrations of MTEOS or OTEOS are improved to 24% (Yin and Wang, 2012a).

The capacity of oil repellency is unchanged at the beginning and keeps at one grade with an increase in FAS concentration. While the concentration continues to increase, the oil-repellent property is enhanced significantly. Oil repellency increases to five

Table 13.2 Oil-repellent ability of cotton fabric coated with hybrid silica sols (Yin and Wang, 2012a)

Concentration (wt%)	Oil repellency (grade)			
	MTEOS	OTEOS	HTMOS	FAS
0	0	0	0	0
4	0	0	0	1
8	0	0	0	1
12	0	0	0	2
16	0	0	0	3
20	0	0	1	5
24	1	1	1	5

grades and the additive is saturated when the concentration increases. The oil-repellent property mainly results from the special construction of the FAS silica coupling agent. With an increase in the silica coupling agent, alkyl chains containing fluorine are arranged on the surfaces of fibers. For extremely low surface tensions with the order $-\text{CF}_3 < -\text{CF}_2 < -\text{CH}_3 < -\text{CH}_2$, massive $-\text{CF}_3$ and $-\text{CF}_2$ effectively decrease the surface tension of the fabric.

The repelling properties were evaluated using contact angles of capsicum oil on different fabrics including cotton, silk, and wool treated with F-silica sol (Yin and Wang, 2012a). Fig. 13.3(a) shows that the surface tension of capsicum oil is 37.7 mN/m and is lower than that of H_2O . On the fabrics, the contact angle of capsicum oil on cotton fabric is 98.5 degree (Fig. 13.3(b)), on silk fabric is 111.59 degree (Fig. 13.3(c)), and on wool fabric is 122.15 degree (Fig. 13.3(d)) when treated with F-silica sol. The surface properties of the fabrics can affect the contact angle of the liquid drop. According to the principle of surface chemistry, if liquids (water, oil, etc.) do not wet a solid surface, the critical surface tension of the solid is lower than the surface tension of liquid and the contact angle of the liquid on the solid surface is larger than 90 degree. The surface free energies of the original cotton, silk, and wool fabrics are different. Although the surface free energy of cotton fiber is usually about 52.1 mN/m and is smaller than the surface tension of H_2O , the fabric surface is irregular, so most liquids can wet original cotton fiber easily.

Also for the same reason, most liquids can wet silk and wool fabrics, although the surface free energy of silk and wool is lower than that of cotton. The surface tension of pure FAS is about 18.6 mN/m; the surface tension of F-silica sol is about 31.0 mN/m after being doped with silica sol, mainly contributed by fluoric group (-F),

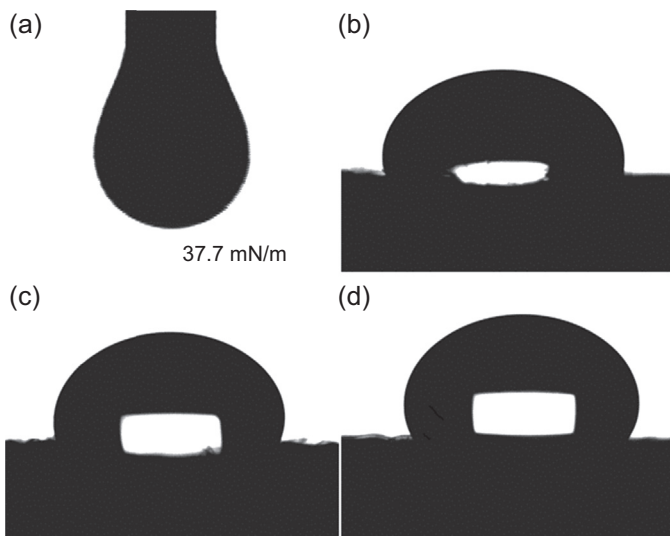


Figure 13.3 Surface tension of capsicum oil and its contact angles on cotton (98.5 degree), silk (111.6 degree), and wool (122.2 degree) fabrics (Yin and Wang, 2012a).

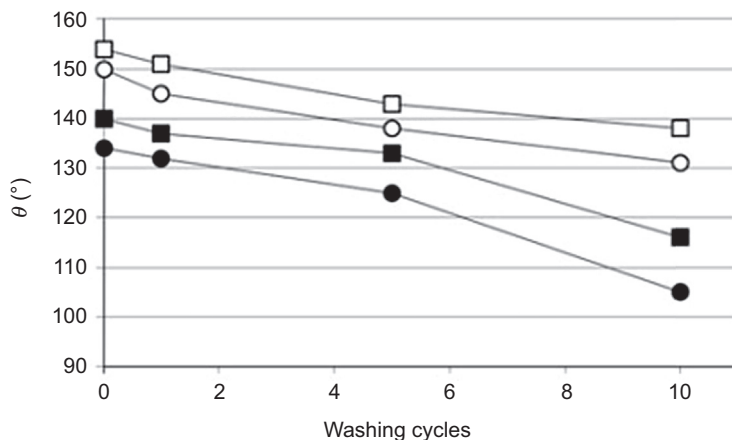


Figure 13.4 Contact angles of water and *n*-hexadecane obtained on the surface of cotton samples coated by FAS coating before (0) and after repetitive (1, 5, and 10) washings. (*Open squares*) water on CO(PT)-FAS, (*open circles*) water on CO(UN)-FAS, (*filled squares*) *n*-hexadecane on CO(PT)-FAS, (*filled circles*) *n*-hexadecane on CO(UN)-FAS (Vasiljevic et al., 2013).

ethyl alcohol, and H₂O. During gelation, the ethyl alcohol and H₂O are volatilized, so the surface tension is mainly determined by the coating, including the SiO₂ and the residue of fluoric additives (Abo-Shosha et al., 2005). For the -F, the surface tension of the coating is low, even smaller than the surface tension of capsicum oil (37.7 mN/m), which leads to a large contact angle.

Vasiljevic et al. performed surface modification of cellulose fibers with low-pressure water vapor plasma followed by the application of a pad–dry–cure sol–gel coating with the water- and oil-repellent organic–inorganic hybrid precursor FAS, with the aim of creating the lotus effect on the cotton fabric surface. Repetitive washing gradually decreased the hydrophobicity and oleophobicity of the FAS coating on both the CO(UN)-FAS and CO(PT)-FAS samples. The water sliding angle measured on the CO(PT)-FAS sample after the first washing cycle increased (to higher than 10 degree), indicating that the self-cleaning effect had been abolished (Fig. 13.4) (Vasiljevic et al., 2013).

13.3 Anti-ultraviolet property using titanium dioxide hybrid sol

Cellulose, the most abundant biopolymer in nature, organizes into microfibrils in plant cell walls, providing strength and flexibility to cotton fibers (Kim et al., 2011). The wide use of cellulose fibers in diversified outdoor and indoor applications, along with its traditional textile products, is mainly attributed to its economical, eco-friendly, biodegradable, and hydrophilic nature (Ibrahim et al., 2010). However,

cellulose fibers also provide a convenient medium for growing microorganisms because of their large surface areas and the ability to retain moisture along with other basic requirements such as nutrients, oxygen, and appropriate temperature. In addition, cotton fibers lack special chemical groups or elements to block harmful UV radiation, especially UVB in the wavelength region of 280–320 nm, which can result in severe skin damage. Accordingly, enhancing the smart properties of cellulose fibers such as anti-UV characteristics has attracted much attention to cope with the growing concerns about health and hygiene (Ibrahim et al., 2010; Mihailovic et al., 2011).

Many approaches, such as coating with titanium dioxide (TiO_2) particles, have been investigated to improve the UV protection function of cellulose textiles. However, nearly all of them have the critical shortcoming of poor rubbing resistance or washing fastness (El Shafei and Abou-Okeil, 2011). TiO_2 has many excellent properties such as nontoxicity, chemical durability, and high efficient photocatalysis. TiO_2 particles can nearly screen all parts of terrestrial UV radiation effectively, including UVA (320–400 nm), UVB (290–320 nm), and even the shortest wavelength, UVC (200–290 nm), which has been weakened by the ozone while transmitting the atmosphere. Different substrates treated with TiO_2 particles have an excellent anti-ultraviolet performance. Abidi et al. (2007) suggested that cellulose substrate was modified by the sol–gel process from the active ingredients tetraethyl orthotitanate and tetraethyl orthosilicate to impart a high UV radiation scattering property to the cellulose substrate surface.

13.3.1 Properties of hybrid sols and anti-ultraviolet property analysis

Hybrid sols containing TiO_2 , usually have excellent anti-UV properties. A novel cationic SiO_2 – TiO_2 sol with anti-UV performance was prepared. Tetraethoxysilane and tetrabutyl titanate were added as precursors and the ethylene-*bis*(octadecyl dimethyl ammonium chloride) (EBODAC) was used as an additive. Cationic SiO_2 – TiO_2 films were coated on the cellulose matrix by the pad–dry–cure process with the cationic SiO_2 – TiO_2 sol. Particle size distribution was displayed by the Zetasizer and the morphology of the sol particles was observed from the transmission electron microscopy (TEM) photograph under $\times 20,000$ magnification. Particle sizes were measured and the mean particle size was calculated (Fig. 13.5) (Yin and Wang, 2011).

From the TEM photograph in Fig. 13.5(b), the shape of sol particle distribution was elliptical, so there were two kinds of particle sizes: minor axis and macro axis. The mean particle size of the minor axis was 13.6 nm and the mean particle size of the macro axis was 52.6 nm.

The UV radiation transmittance (URT) of the cellulose substrate coated with the cationic SiO_2 – TiO_2 sol was lower than that of the original cellulose substrate in the whole UV radiation wave band (Yin and Wang, 2011). During the UVB (280 to 320 nm) and UVC (200 to 280 nm) wave bands, the lowest URT of the original cellulose substrate without washing was higher than 7.0% but the URT of the coated cellulose substrate was almost smaller than 5.0%, and after washing 30 times the URT

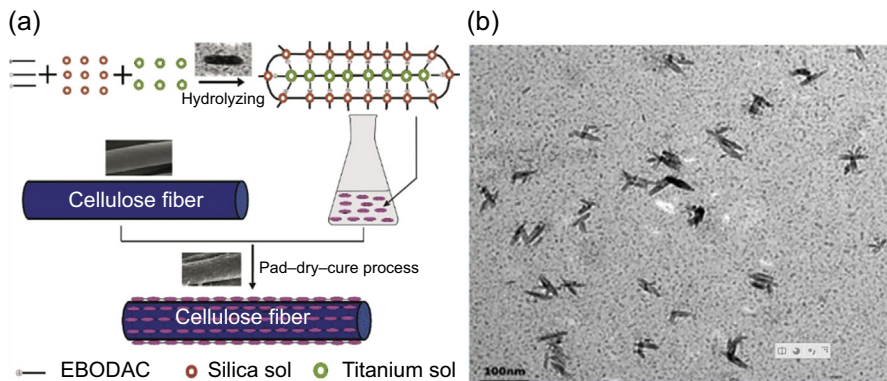


Figure 13.5 Schematic illustration of the process (a) and TEM photograph of the cationic $\text{SiO}_2\text{-TiO}_2$ sol (b) (Yin and Wang, 2011).

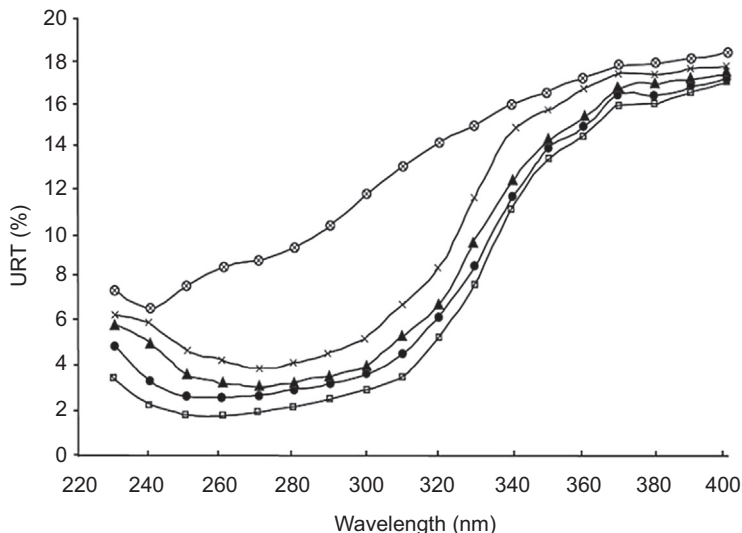


Figure 13.6 Anti-UV properties of cellulose substrates: (a) ● (closed circles) original cellulose substrate; □ (open squares) cellulose substrate coated with the cationic $\text{SiO}_2\text{-TiO}_2$ sol; ⊗ (crossed circles) cellulose substrate coated after washing 10 times; ▲ (closed triangles) cellulose substrate coated after washing 20 times; and × (crossed x) cellulose substrate coated after washing 30 times (Yin and Wang, 2011).

was lower than 6.0% (Fig. 13.6(a)). The URT of UV radiation during the wavelengths 305–310 nm, which was maximally dangerous to skin, changed to 3.2–3.8% from 12.5–13.3% of the original cellulose substrate. The improved screening effect was attributed to the many TiO_2 particles embedded in the film and deposited on the fiber surface. The electron structure of the TiO_2 particle was composed of the valence band and the conduction band. The valence band was low-energy and completely filled

with electrons, whereas the conduction band was high-energy and formed by the empty orbit without electrons. The band gap of the TiO_2 was subsistent and the band gap energy of the particles was estimated to be below 3.2 eV according to the Burs equation, which equaled the luminous energy of wavelength 387.5 nm. When TiO_2 was irradiated by light, the short wave light (the wavelength was shorter than 387.5 nm) was with a higher energy than the band gap energy and the electrons in the valence band were aroused and translated into the conduction band (e^-), leaving a hole (h^+) in the valence band. The TiO_2 particles could shift nearly all terrestrial UV radiation effectively: UVA 320–400 nm, UVB 290–320 nm, and UVC 200–290 nm.

13.3.2 Layer-by-layer self-assembly deposition on fiber and anti-ultraviolet property

Self-assembly can form a superstructure film, and it mainly occurs through noncovalent interactions such as van der Waals, hydrogen bonding, hydrophilic–hydrophobic, and electrostatic (Hou et al., 2009). LBL deposition, which may be combined with self-assembly, offers some distinctive advantages as a surface modification technique for fibers. When the fiber substrates are alternately dipped into different solutions containing opposite charges, multilayers can be spontaneously deposited on the fiber surface through electrostatic forces. Some studies have aimed at functional modification via LBL self-assembled process on fibers (Joshi et al., 2011). Ali et al. evaluated the effect of different processing parameters on the amount of polyelectrolyte adsorbed on a cotton textile substrate via sequential adsorption of negatively charged poly(styrene sulfonate) (PSS) and positively charged poly(allylamine hydrochloride) using the LBL self-assembly coating process. Dubas et al. (2007) reported using the LBL deposition method to immobilize silver particles on nylon and silk fibers and to improve the color fastness of silk against washing and rubbing.

Three hybrid sols, alkaline silica sol (sol a), tetrabutyl titanate (sol b), and cationic silica sol (sol c), were prepared and used on the fabric by self-assembly. The cellulose fabric samples were first dipped in the EBODAC solution and then dried. The process sequence is showed in Fig. 13.7(a).

The LBL self-assembled modified fabric could have a lower URT than that of the control cellulose fiber in the whole UV radiation wave band. The average URT of the control sample is 10.6% and the average URT of coated sample with sol a is 4.4%. The average URT decreases to 1.5%; when coated again with sol c after treatment with sol b, the average URT is reduced to 1.3% (Yin et al., 2012). Generally, the screening property of UVB radiation (280–320 nm), in which the UV radiation causes the greatest harm to the skin, is the key indicator for determining the effectiveness of a UV-shield agent (Fig. 13.7(b)). Within this wave band, the URT of the UVB is reduced to 0.4–0.7% after coating with sol c from the original URT value of 8.3–13.3%, which indicates that the coating process in this study can provide exceptional protection against UV radiation (Yang et al., 2004).

There were two main mechanisms regarding the anti-UV property of TiO_2 . One explanation is that when TiO_2 is irradiated by UV light, the electrons in the valence

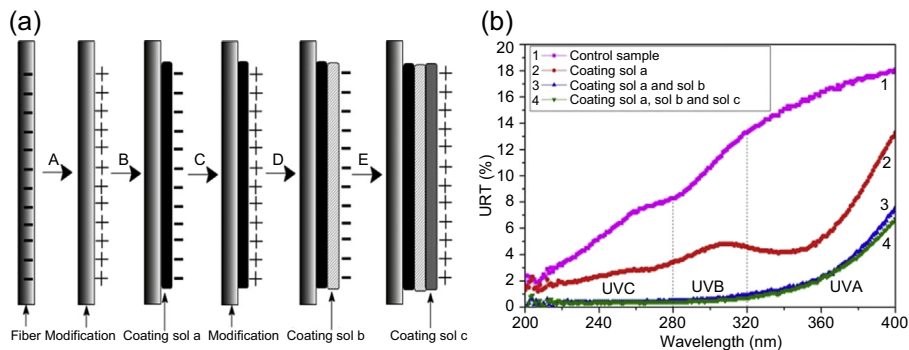


Figure 13.7 Schematic of LBL self-assembled process on cellulose fiber: (A) Cellulose fiber modified by EBODAC; (B) cellulose fiber coated by sol a; (C) cellulose fiber modified by EBODAC; (D) cellulose fiber coated by sol b; (E) cellulose fiber coated by sol c (a) and the anti-UV property of the cellulose fabrics (b) (Yin et al., 2012).

band are aroused and translated into the conduction band (e^-), leaving a hole (h^+) in the valence band so the energy of the UV ray is transferred (Castellote and Bengtsson, 2011; Fujishima et al., 2000). Another mechanism for TiO_2 to provide UV protection is by reflecting and/or scattering most of the UV rays owing to its high refractive index.

Liu et al. used LBL self-assembly technology to functionalize wool fabrics and endow them with anti-UV and antiaging properties. The electrostatic self-assembly deposition process was used to deposit nanolayers of poly(sodium 4-styrene-sulfonate) (PSSS) and TiO_2 sols alternately on the wool fabric. The UV transmittance and alkali solubility of the wool decreased along with the increasing assembled layer (Fig. 13.8), which confirmed the better anti-UV properties of wool fabric after TiO_2 sol treatment via LBL electrostatic self-assembly deposition (Liu et al., 2012).

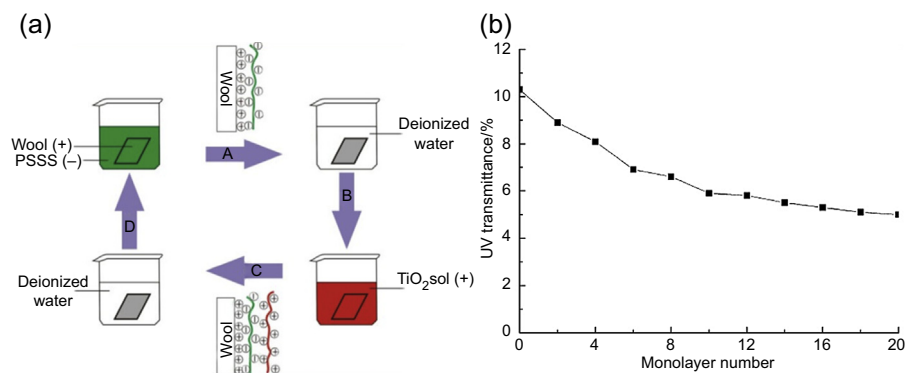


Figure 13.8 Schematic of the film deposition process (a) and (b) UV transmittance of wool fabric with different monolayer numbers at 368 nm (Liu et al., 2012).

13.4 Antibacterial finishing using cationic or titanium dioxide hybrid sol

Providing antibacterial property for textiles is an effective way to prevent disease transmission, with applications in the consumer, military, and health care markets. Many textiles are treated to afford protection against bacteria, fungi, and other related microorganisms for esthetic, hygienic, and medical purposes using various finishing techniques. Various antimicrobial agents, both organic and inorganic, have been applied to textiles (Balamurugan et al., 2008; Dastjerdi and Montazer, 2010). Antibacterial properties on cellulose substrates seem to be of practical interest for protecting the human body, especially skin, from microorganisms by coating antibacteria composite materials on cellulose substrates. Cellulose substrates are always considered conformable to offer a protective property for its massive hydroxyl groups (Li et al., 2009; Sayilkan et al., 2009).

Gemini quaternary ammonium salt usually consists of two hydrophobic chains and two polar head groups covalently linked with a spacer group. This special structure aroused a series of original properties, eg, efficient bacter-inertness, novel double-positive charge, and strong hydrophobic microdomain. The antibacterial research of gemini quaternary ammonium salt has become global research hot spot. It is available to suppress bacteria by interacting with the cell wall and cell membrane or by destroying the DNA molecules of bacteria to limit their replicate ability (Ao et al., 2008). Investigation into cationic hybrid sols is significant (Łuczynski et al., 2013).

13.4.1 Antibacterial cationic hybrid sol

The combination of surface modification with antibacterial properties seems to be particularly important for practical applications because cationic surfactants possess excellent antibacterial properties, eg, cetyltrimethylammonium bromide (CTAB), which is a quaternary ammonium salt with a positively charged nitrogen ion (Bagherzadeh et al., 2007). It binds strongly to electron donor groups on biological molecules containing sulfur, oxygen, phosphorus, or nitrogen atoms. These atoms are present in organisms as thio, amino, carboxyl, and phosphato groups (Bagherzadeh et al., 2007). CTAB interacts with bacterial cell membrane proteins, which induce protein inactivation. It also affects the DNA molecules of bacteria and causes a loss in their ability to replicate (Klueh et al., 2000).

CTAB was stirred into ethanol with a magnetic stirring apparatus until the CTAB completely dissolved. Then GPTMS, TEOS, and H₂O were subsequently added under stirring to prepare a smart hybrid sol. The fabric samples were immersed and modification in the sols. The inhibitory rates increased with the concentration of CTAB. The inhibitory rates for both *Staphylococcus aureus* and *Escherichia coli* were more than 95% when the concentration was at 0.10 mol, which can result from the high antibacterial activity of CTAB (Fig. 13.9). They were active moieties against microorganisms by interacting with the cell membrane, which induced protein inactivation. CTAB also affected the DNA molecules of bacteria and caused a loss in their ability to replicate

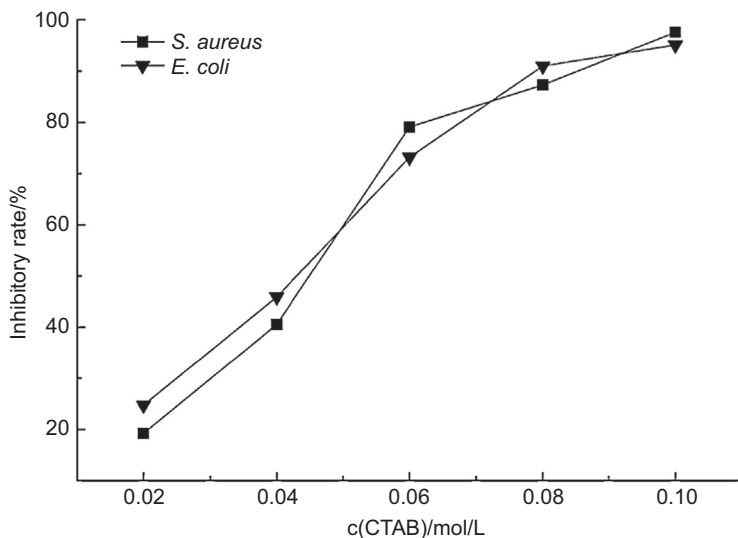


Figure 13.9 Inhibitory rate of samples treated by modified SiO_2 sols with different concentrations of CTAB (Wang et al., 2010).

and transfer (Wang et al., 2010). The sample with no treatment and the sample treated by sol without CTAB were tested as controls. As expected, no reduction in the bacteria *S. aureus* and *E. coli* was found on controls.

Smart sols contain quaternary ammonium salts via a sol–gel process. CTAB, octadecyl dimethyl benzyl ammonium chloride, and ethylene-*bis*(octadecyl trimethyl ammonium chloride) (E-Bis(OTAC)) were added to the sols and applied to cotton samples. The antibacterial activities of the samples were assessed against both *E. coli* and *S. aureus* bacteria. The samples treated by E-Bis(OTAC) sol exhibited satisfactory antibacterial activity that resulted from the better microorganism adsorption and hydrophobicity. The antibacterial activities were still excellent after 10 washings compared with the control samples (Table 13.3) (Wang and Wang, 2009).

13.4.2 Antibacterial activity of metallic oxide hybrid sol

Fabric finished with cationic SiO_2 – TiO_2 sol has excellent antibacterial properties. Antibacterial activity was estimated from gram-negative bacteria *E. coli* (ATCC 25922) and gram-positive bacteria *S. aureus* (ATCC 6538) according to the AATCC 100–2004 standard method. Reduction of the coated cellulose substrate with cationic SiO_2 – TiO_2 sol to gram-negative bacteria *E. coli* and gram-positive bacteria *S. aureus* without washing was 90.9% and 95.2%, respectively (Fig. 13.10) (Yin and Wang, 2011).

The presence of EBODAC endowed excellent anti-microbial property for special molecular structures. The antimicrobial effect of the EBODAC cationic component was mainly thought to involve interaction of the cationic group and anionic phospholipids in the bacterial cell walls, increasing the permeability of the cell walls. In

Table 13.3 Antibacterial activity against *Escherichia coli* and *Staphylococcus aureus* of control and treated samples after washing (Wang and Wang, 2009)

R (%)	<i>Escherichia coli</i>					<i>Staphylococcus aureus</i>				
	0 ^a	2	4	6	10	0	2	4	6	10
Control	91.3	46.5	0	0	0	91	43.3	0	0	0
1	91.3	73.9	61.1	61.1	59.8	91	75.8	70.3	63.4	57.7
2	96.7	79.9	67.5	67.5	60.0	97.5	78.9	70.1	64.9	62.5
3	100	85.5	68.7	68.7	65.0	100	87.3	72.6	66.2	61.1

^aNumber of washing cycles before testing.

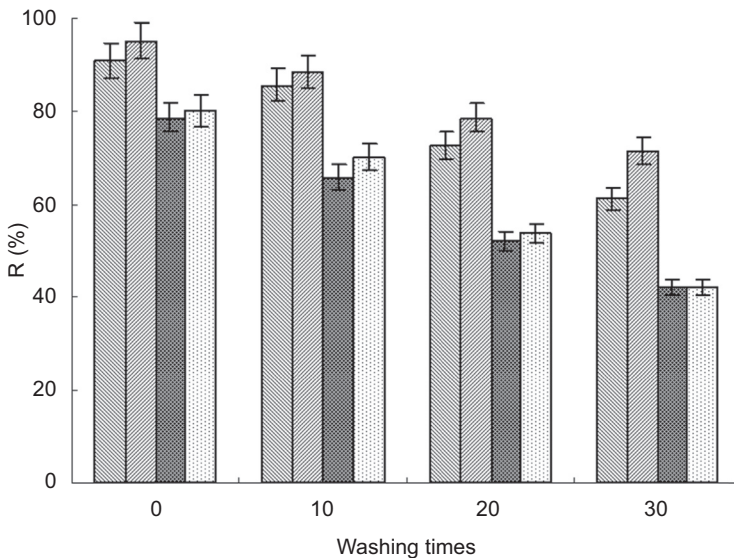


Figure 13.10 Antibacterial activity of cellulose substrates: coated with the cationic $\text{SiO}_2\text{-TiO}_2$ sol-resisted gram-negative bacteria *Escherichia coli*; coated with the cationic $\text{SiO}_2\text{-TiO}_2$ sol-resisted gram-positive bacteria *Staphylococcus aureus*; coated with EBODAC-resisted gram-negative bacteria *E. coli*; coated with EBODAC-resisted gram-positive bacteria *S. aureus* (Yin and Wang, 2011).

addition, the EBODAC might affect the DNA molecules of bacteria and limit their replication and transfer. The other reason for the antibacterial effect might be TiO_2 particles, which offer a photocatalytic reaction and photocatalytic crystalline phase of anatase. This validated that the antibacterial activity of the cellulose substrate coated with cationic $\text{SiO}_2\text{-TiO}_2$ sol increased by 8.3% and 10.9% compared with the antibacterial capability when coated only with EBODAC, respectively.

Cotton fabric deposited with sol a, sol b, and sol c showed antibacterial activity (Yin et al., 2012). Antibacterial activity was also estimated by the reduction rates (R) of the gram-negative bacteria *E. coli* (ATCC 25922) and the gram-positive bacteria *S. aureus* (ATCC 6538) according to the AATCC 100–2004 standard method.

Antibacterial activity is 61.6% for the gram-negative bacteria *E. coli* and 64.2% for the gram-positive bacteria *S. aureus*, respectively, after coating with sol a (Yin et al., 2012). When coated with sol b, the antibacterial activities increase significantly to 88.2% for the gram-negative bacteria *E. coli* and 89.7% for the gram-positive bacteria *S. aureus*, respectively. TiO₂ particles are generated after gelation from sol b, and the TiO₂ particles can improve antibacterial activity and offer a photocatalytic reaction and photocatalytic crystalline phase of anatase. When coated with sol c, the antibacterial component EBODAC in sol c further enhances antibacterial capability (Table 13.4).

Poli et al. studied the possibility of realizing a transparent sol by zinc-based precursors in a neutral medium without an acidic or alkaline catalyst, and zinc-based coatings for antibacterial capability was finished on cotton fabric. Sol–gel-synthesized cotton finishes based on nano-Zn acetate without and with GPTMS showed larger bactericidal and bacteriostatic activities (Fig. 13.11) (Poli et al., 2015).

El-Shafei et al. focused on an antibacterial finishing agent for cellulosic fabrics using TiO₂ nanoparticles and chitosan phosphate. The application of nano-TiO₂ onto cellulosic fabrics (cotton 100%) was achieved in the presence of polycarboxylic acid (1,2,3,4-butane tetracarboxylic acid (BTCA)) with sodium hypophosphite (SHP) as the catalyst and chitosan phosphate through a conventional pad–dry–cure method, and all treated fabrics possessed good antimicrobial activity under optimal finishing conditions (Fig. 13.12) (El-Shafei et al., 2015).

Farouk et al. reported eco-friendly multifunctional cationized cotton fabrics using nanomaterials based on TiO₂ nanoparticles. Cotton fabric was cationized with two durable cationizing agents, 3-chloro-2-hydroxypropyl trimethyl ammonium chloride (Quat 188) and diallyl dimethyl ammonium chloride using the pad–batch method. The application of TiO₂ nanomaterials on 100% cotton fabrics was achieved using BTCA as a polycarboxylic acid cross-linker with SHP as the catalyst through a

Table 13.4 Antibacterial activity of cellulose fabrics (Yin et al., 2012)

Coating	R (%)	
	<i>Escherichia coli</i>	<i>Staphylococcus aureus</i>
Control sample	0	0
Coating sol a	61.6	64.2
Coating sol a and sol b	88.2	89.7
Coating sol a, sol b, and sol c	95.3	96.1

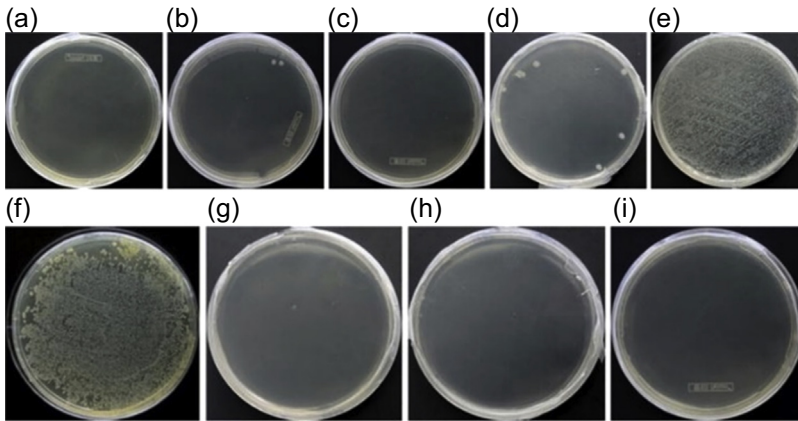


Figure 13.11 Photographs of incubated *Escherichia coli* agar plates demonstrating the effect of antibacterial finishing of cotton by zinc acetate on the number of colony-forming units after 24 h: (a) unwashed; (b) after 1 washing cycle; (c) after 5 washing cycles; (d) after 10 washing cycles; (e) after 20 washings cycles; (f) untreated; (g) 0.5% Zn acetate; (h) 1.5% Zn acetate; (i) 3% Zn acetate (Poli et al., 2015).

conventional pad–dry–cure method (Farouk et al., 2013). The cationization process along with BTCA–TiO₂ nanoparticles or BTCA–TiO₂–SiO₂ nanomaterials posttreated to a wet pickup of 100% is accompanied by a remarkable improvement in fabric antibacterial smart properties (Table 13.5).

13.5 Color fixation using smart silane coupling agent hybrid sol

Color fastness is the main problem in fabric dyeing; it restricts applicability, comfort, and appearance. Direct dyes are important dyes used straight on cellulose fiber and can be applied in the same dye bath with other dyes (Yin et al., 2008). Moreover, the price is much lower than that of other dyes. However, several problems often occur in dyed fabric with direct dyes, such as bad washing and rubbing fastness. Some direct dyes perform poorly with respect to washing and rubbing fastness. They are mainly caused by the water-soluble groups, sulfonic and/or carboxyl groups. Without appropriate treatment, direct dyes bleed slightly with each washing, lose their color from fabric, and endanger other clothes washed in the same bath. These are the same fastness problems of the pigment, reactive dye.

Currently, copper salt-fixing reagents and cationic fixing reagents are widely used in the textile industry to improve fastness by cross-linking reactions between metal ions or formaldehyde and other molecules. However, metal ions in fixing reagents such as cupric cation aggravate the difficulty of waste processing. Also, some reagents and intermediates used in diazotization or cross-linking reactions such as formaldehyde

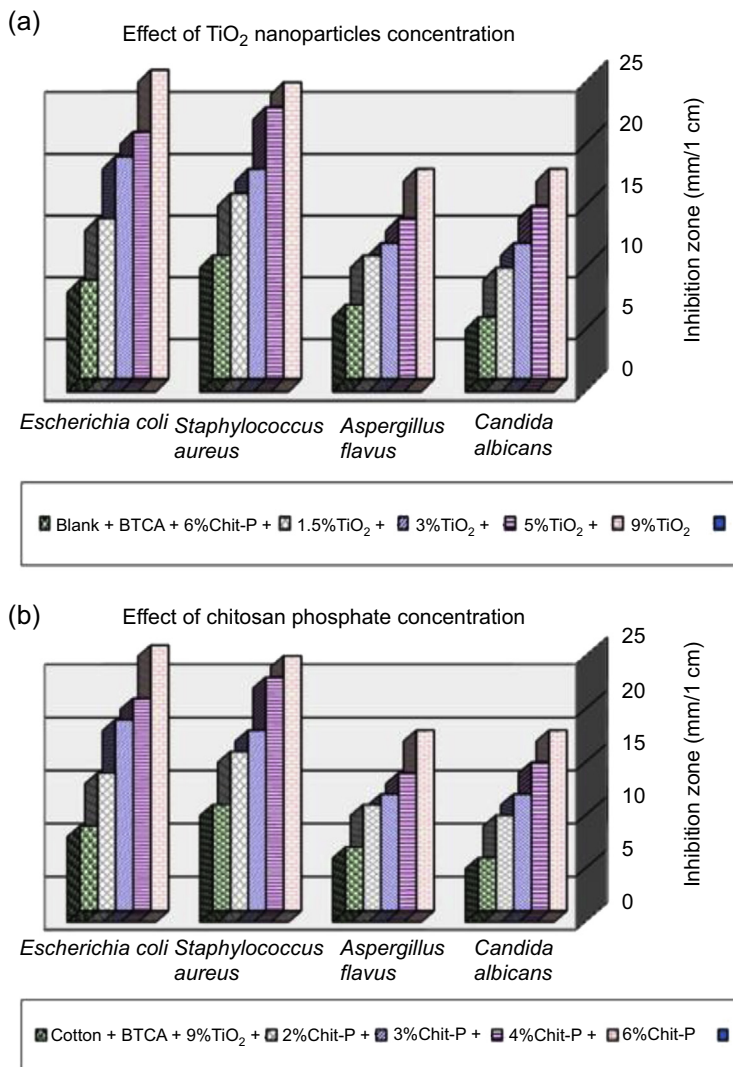


Figure 13.12 (a) Effect of TiO_2 particles concentration on antibacterial properties of treated cotton; (b) effect of chitosan phosphate concentration on antibacterial properties of the treated cotton (El-Shafei et al., 2015).

and nitroaniline seriously affect human health and the environment. Moreover, vividness after copper salt or diazotization finishing usually fades, so that the application scope of direct dyes has been seriously limited in the textile industry. Sol–gel technology has been applied in diverse sectors for decades. Its inorganic nature makes sol–gel layers strong so that one may obtain important effects with nanometer-thick layers (Pavlidou and Papaspyrides, 2008).

Table 13.5 Effect of cationization or nanoparticle treatment on antibacterial properties of cotton fabrics (Farouk et al., 2013)

Sample	Inhibition zone (mm)/1 cm sample			
	(G + ve)		(G - ve)	
	<i>Staphylococcus aureus</i>	<i>Bacillus subtilis</i>	<i>Pseudomonas aeruginosa</i>	<i>Escherichia coli</i>
Cotton treated with 0.5% TiO ₂	–ve	–ve	–ve	–ve
Cationized cotton treated with 1% TiO ₂	12	13	11	12
Cationized cotton treated with 1.5% TiO ₂	15	15	13	14
Cationized cotton treated with 1.5% TiO ₂ :0.5% SiO ₂	16	16	14	15

13.5.1 Sol–gel silica doped with dyes and fixation property

Sol–gel silica doped with direct dyes was prepared by mixing ethanol, TEOS, H₂O, and GPTMS in a rotating Erlenmeyer flask. The mixture was stirred with a magnetic stirring apparatus. The direct dye solution was added to the mixture. The dyeing solution was then stirred at 300–450 rpm at room temperature for 24 h. Fabric was dipped into the silica dyeing solution for 10 min at room temperature. The dyeing solution was heated to 90°C for 15 min during the dyeing process, and the fabric was dyed. NaCl was added to this dyeing solution when the fabric was dyed for 30 min. Then the fabric was predried and baked.

Fabrics were dyed with direct blue dye and fixed with MMF-1 (commercial name of a dye-fixing agent). Table 13.6 compares the fixative properties using the silica dyeing solution.

Table 13.6 Comparison of K/S value and fastness (Yin et al., 2008)

Method	K/S value	Rubbing fastness (grade)		Washing fastness (grade)	
		Dry	Wet	Change	Staining
Dyeing with silica dyeing solution	11.5	3	2–3	3–4	2–3
Dyeing fixed with MMF-1	9.3	3	2	3	2–3

Table 13.6 shows the results of the K/S value and fastness of fabrics treated with silica dyeing solution and MMF-1, respectively. It is evident that the K/S value of the fabric dyed with the silica dyeing solution is larger than that of the fabric fixed with MMF-1 by about 23.7%. This may be because some dye molecules dissolve into the fixing bath for absorption–resolution balance when the fabric is fixed with MMF-1. Besides absorption of the dyes to the cotton fiber, absorption of the sol–gel film to the dyes caused by van der Waals forces and hydrogen bonds in the silica dyeing solution enhances the K/S value. Color-fixing performance is better than that of the fixing reagent MMF-1. The wet rubbing fastness and washing change fastness are half a grade higher than those fixed with MMF-1. These results indicate favorable application performance using a silica dyeing solution (Yin et al., 2008).

Mahlting et al. embedded dyes in sol–gel coatings to improve fastness properties on textiles (Fig. 13.13). The fastness properties of once-colored textiles could be improved by sol–gel coatings or an uncolored sol–gel-treated fabric could be dyed afterward with higher fastness properties. Modified silica sols and dye molecules were applied together on textiles. The investigations were performed with the two triphenylmethane dyes, malachite green (MG) and guinea green (GG). The application, together with the silica sol or the after-treatment of dyed textile with a silica sol, led to significant improvement in leaching fastness. The low bleaching fastness of the triphenylmethane dyes can also be enhanced significantly (Mahlting and Textor, 2006).

Mahlting et al. incorporated triarylmethane dyes into sol–gel layers formed by modified silica to coat textile materials. The light and washing fastness of the positively charged triarylmethane dye MG on textiles could be improved by incorporating the dye in silica coatings prepared by the sol–gel process. Additional enhancement of fastness properties was reached by adding small amounts of epoxysilane to the silica sol. Washing fastness of the negatively charged GG and the uncharged dye reflex blue (RB) could be enhanced by incorporating a silica coating (Table 13.7). Because of the improved washing fastness obtainable by the sol–gel technique, the use of those classes of dyestuffs for textile materials may become possible (Mahlting et al., 2004).

13.5.2 Color fixation analysis of self-assembled deposition and after finishing

The reactive dye was doped in the hybrid sol and then deposited within self-assembly (Yin et al., 2012). Fig. 13.14 shows that the color strengths of the modified fabrics are higher than those of the control fabric. These results are attributed to the cationic modification of the fibers. Besides covalent bonding, some reactive dye molecules are absorbed into the fiber via electric adsorption. Although part of the dye may be desorbed when the fabric is submerged in solutions, such as the EBODAC solution, sol a, sol b, and sol c, owing to Brownian motion, even after being hydrolyzed or without chemical bonding with the fiber, some reactive dye molecules are protected by the silica network. The 3D network reduces the tendency for outside forces to extract the dye molecules as the dyes are fixed in the coating.

The maximum absorption wavelengths for the coated samples remain unchanged from the maximum absorption wavelength of the control sample (670 nm). This means

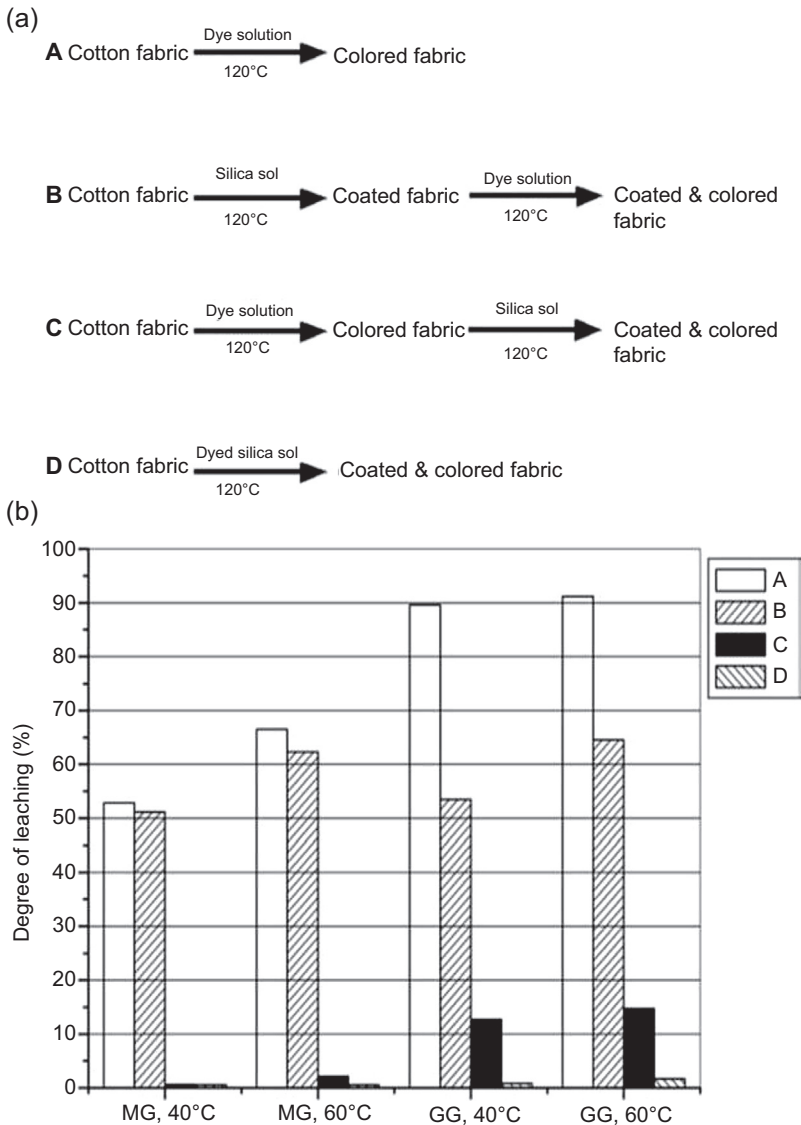


Figure 13.13 Schematic drawing of different procedures of sample preparation (a) and degree of leaching after washing procedure at 40 and 60°C (b) (Mahlting and Textor, 2006).

that the chromophore groups of the reactive blue 14 dye are not damaged and the conjugated systems are unaffected by the coating process so that the color hue coincides with that of the control sample. In addition, that within the wavelength range of 500–750 nm, the widths of the peaks of the coated samples are smaller than those of the control sample, which makes the color more vivid.

Table 13.7 Color fastness of finished fabric (Mahltig et al., 2004)

Dye	Textile	Without silica coating		With silica coating		Without silica coating		With silica coating	
		Leach (%) 40°C	Leach (%) 40°C	Leach (%) 40°C	Leach (%) 40°C	Bleach (%) 20 h	Bleach (%) 120 h	Bleach (%) 20 h	Bleach (%) 120 h
MG	PET	62	56	6	13	75	91	12	35
MG	PA	41	76	5	11	25	59	7	43
MG	CO	15	35	1	13	8	40	3	34
GG	PET	100	100	10	12	—	—	—	—
GG	PA	89	99	5	16	—	—	—	—
GG	CO	83	97	11	37	26	48	17	35
RB	PET	20	47	5	33	—	—	—	—
RB	PA	51	88	14	48	—	—	—	—
RB	CO	22	38	0	29	36	56	13	47

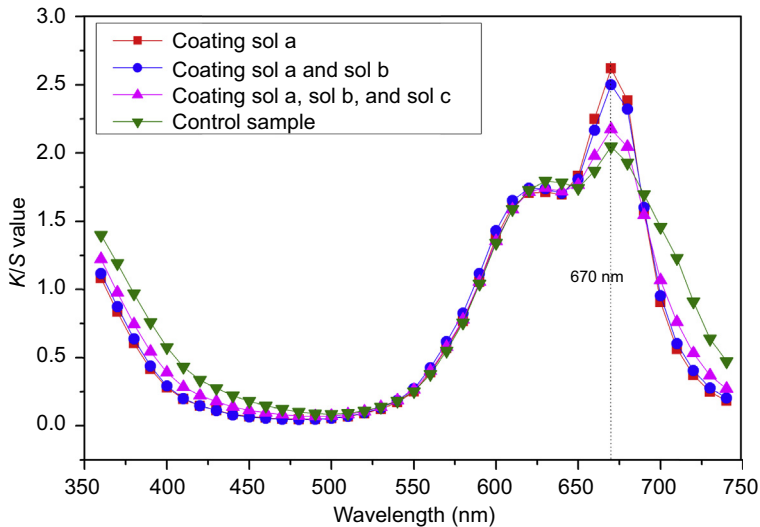


Figure 13.14 Color properties of coated cellulose samples (Yin et al., 2012).

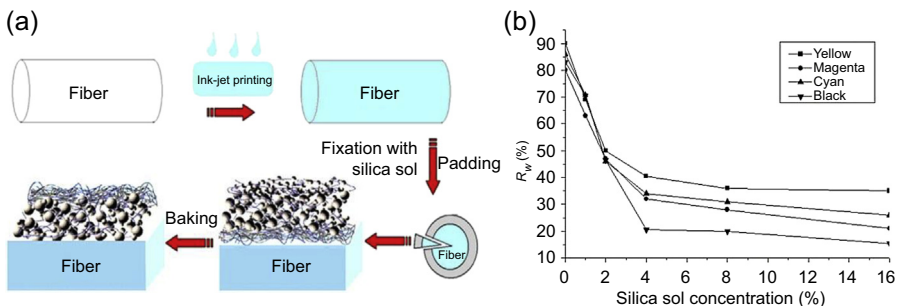


Figure 13.15 Process of fiber treatment with silica sol and effects of silica sol concentration on fading during washing (Yin and Wang, 2012b).

Silica hybrid coating to treat cellulose knitted fabrics printed with pigment-based ink could improve fixation properties (Fig. 13.15(a)). The color fastness of knitted fabrics treated with the silica sol improved significantly. The silica sol concentration between 4% and 8% was beneficial to washing fastness, and the fade rate of washing improved more than 50% (Fig. 13.15(b)). Dry and wet rubbing fastness were all enhanced one grade or more (Yin and Wang, 2012b).

13.6 Conclusion

Contemporary textiles are required to offer high efficiency and multifunctionality in terms of protection and comfort. Multifunctional textiles with improved or completely new combinations of properties that are not present in traditional textiles have scientific,

technological, and potentially economic significance. In the field of textile technology, the sol–gel process offers great opportunities and the possibility of achieving novel modifications by combining various inorganic and organic materials which can result in brand new multifunctional or intelligent properties of textiles (Mahltig et al., 2005; Nord-West, 2009). The general approach allows one not only to functionalize textile materials with conventional application technologies under moderate conditions but also to combine various functionalities in a single material. Many of these papers or reports mention only the modification of textiles to explain additional fields of application and do not describe the textile experience (Skoc et al., 2011).

Hybrid sol was prepared by doped smart or functional agent in silica sol, and was applied to fabric modification. Because of the different types of modifications to fabric gained by hybrid sols, there is a high number of potential applications. After the hybrid sol was treated on fabric, the color and fastness properties of fabric improved. Fabric treated by the functional silane coupling agent had good hydrophobic and oil-repellent properties (Yin et al., 2014; Yin and Wang, 2012a, 2013), antibacterial property (Wang et al., 2010; Yin and Wang, 2011), anti-UV behavior (Yin and Wang, 2011; Yin et al., 2012), and color fixation (Yin and Wang, 2012b; Yin et al., 2008). This method could shorten the treatment process, reduce pollution and energy, and provide a novel dyeing and printing method.

Future sol–gel research will unquestionably discover many new applications for sol–gel-derived coatings for finishing textile materials. Numerous properties will most probably become available in combination with textiles that we cannot foresee today (Skoc et al., 2011). The multifunctional fabric materials are potentially applicable in high-added-value applications such as dynamically wetting intelligent fabric materials (Mao et al., 2015; Yin et al., 2013), smart coatings for corrosion protection and abrasion resistance (Brzezinski et al., 2011; Cakir et al., 2014; Dalmoro et al., 2015), pervaporation and gas separation (Moein et al., 2015), artificial membranes for ultrafiltration and nanofiltration (Skoc et al., 2014), catalysts and nanoscopic reactors (Mahmoud et al., 2002; Tizjang et al., 2015), biomaterials for osteoreconstructive surgery (Catauro et al., 2015), and magnetic properties for telecommunications or information displays (Catauro et al., 2015; Nord-West, 2009). Further investigations are necessary to ensure that smart or functional coatings on fabric have high long-term and wash stability in industrial production (Periolatto and Ferrero, 2015).

Acknowledgments

The authors are grateful for the financial support of the National Natural Science Foundation of China (No. 21174055).

References

- Abidi, N., Hequet, E., Tarimala, S., Dai, L.L., 2007. Cotton fabric surface modification for improved UV radiation protection using sol-gel process. *Journal of Applied Polymer Science* 104 (1), 111–117.

- Abo-Shosha, M.H., El-Sayed, Z.M., Fahmy, H.M., Ibrahim, N.A., 2005. Synthesis of PEG/TDI/F6 adducts and utilization as water/oil repellents and oily stain release finishes for cotton fabric. *Polymer-Plastics Technology and Engineering* 44 (6), 1189–1201.
- Ali, S.W., Rajendran, S., Joshi, M., 2010. Effect of process parameters on layer-by-layer self-assembly of polyelectrolytes on cotton substrate. *Polymers & Polymer Composites* 18 (5), 175–187.
- Andersson, N., Alberius, P., Ortegren, J., Lindgren, M., Bergstrom, L., 2005. Photochromic mesostructured silica pigments dispersed in latex films. *Journal of Materials Chemistry* 15 (34), 3507–3513.
- Ao, M., Xu, G., Zhu, Y., Bai, Y., 2008. Synthesis and properties of ionic liquid-type Gemini imidazolium surfactants. *Journal of Colloid and Interface Science* 326 (2), 490–495.
- Bagherzadeh, R., Montazer, M., Latifi, M., Sheikhzadeh, M., Sattari, M., 2007. Evaluation of comfort properties of polyester knitted spacer fabrics finished with water repellent and antimicrobial agents. *Fibers and Polymers* 8 (4), 386–392.
- Balamurugan, A., Balossier, G., Laurent-Maquin, D., Pina, S., Rebelo, A., Faure, J., Ferreira, J., 2008. An in vitro biological and anti-bacterial study on a sol-gel derived silver-incorporated bioglass system. *Dental Materials* 24 (10), 1343–1351.
- Botcher, H., 2001. Functional coatings on basis of inorganic nanosols. *Materialwissenschaft und Werkstofftechnik* 32 (10), 759–766.
- Brzezinski, S., Kowalczyk, D., Borak, B., Jasiorski, M., Tracz, A., 2011. Nanocoat finishing of polyester/cotton fabrics by the sol-gel method to improve their wear resistance. *Fibres & Textiles in Eastern Europe* 19 (6), 83–88.
- Cakir, M., Kartal, I., Yildiz, Z., 2014. The preparation of UV-cured superhydrophobic cotton fabric surfaces by electrospinning method. *Textile Research Journal* 84 (14), 1528–1538.
- Castellote, M., Bengtsson, N., 2011. Principles of TiO₂ Photocatalysis Applications of Titanium Dioxide Photocatalysis to Construction Materials. Springer, pp. 5–10.
- Castelvetto, V., Francini, G., Ciardelli, G., Ceccato, M., 2001. Evaluating fluorinated acrylic latices as textile water and oil repellent finishes. *Textile Research Journal* 71 (5), 399–406.
- Catauro, M., Papale, F., Bollino, F., 2015. Characterization and biological properties of TiO₂/PCL hybrid layers prepared via sol-gel dip coating for surface modification of titanium implants. *Journal of Non-Crystalline Solids* 415, 9–15.
- Colomban, P., Gouadec, G., 2005. The ideal ceramic-fibre/oxide-matrix composite: how to reconcile antagonist physical and chemical requirements? *Annales de Chimie-Science des Materiaux* 30 (6), 673–688.
- Dalmoro, V., dos Santos, J.H.Z., Baibich, L.M., Butler, I.S., Armelin, E., Aleman, C., Azambuja, D.S., 2015. Improving the corrosion performance of hybrid sol-gel matrix by modification with phosphonic acid. *Progress in Organic Coatings* 80, 49–58.
- Dastjerdi, R., Montazer, M., 2010. A review on the application of inorganic nano-structured materials in the modification of textiles: focus on anti-microbial properties. *Colloids and Surfaces B: Biointerfaces* 79 (1), 5–18.
- Dhere, S.L., Lathe, S.S., Kappenstein, C., Pajonk, G., Ganesan, V., Rao, A.V., Wagh, P.B., Gupta, S.C., 2010. Transparent water repellent silica films by sol-gel process. *Applied Surface Science* 256 (11), 3624–3629.
- Dorrer, C., Ruhe, J., 2008. Drops on microstructured surfaces coated with hydrophilic polymers: Wenzel's model and beyond. *Langmuir* 24 (5), 1959–1964.

- Dubas, S.T., Chutchawatkulchai, E., Egkasit, S., Lamsamai, C., Potiyaraj, P., 2007. Deposition of polyelectrolyte multilayers to improve the color fastness of silk. *Textile Research Journal* 77 (6), 437–441.
- El Shafei, A., Abou-Okeil, A., 2011. ZnO/carboxymethyl chitosan bionano-composite to impart antibacterial and UV protection for cotton fabric. *Carbohydrate Polymers* 83 (2), 920–925.
- El-Shafei, A., ElShemy, M., Abou-Okeil, A., 2015. Eco-friendly finishing agent for cotton fabrics to improve flame retardant and antibacterial properties. *Carbohydrate Polymers* 118, 83–90.
- Fang, G., Koral, N., Zhu, C., Yi, Y., Glaser, M.A., MacLennan, J.E., Clark, N.A., Korblova, E.D., Walba, D.M., 2011. Effect of concentration on the photo-orientation and relaxation dynamics of self-assembled monolayers of mixtures of an azobenzene-based triethoxysilane with octyltriethoxysilane. *Langmuir* 27 (7), 3336–3342.
- Farouk, A., Sharaf, S., El-Hady, M.A., 2013. Preparation of multifunctional cationized cotton fabric based on TiO₂ nanomaterials. *International Journal of Biological Macromolecules* 61, 230–237.
- Faustini, M., Nicole, L., Boissiere, C., Innocenzi, P., Sanchez, C., Grosso, D., 2010. Hydrophobic, antireflective, self-cleaning, and antifogging sol-gel coatings: an example of multifunctional nanostructured materials for photovoltaic cells. *Chemistry of Materials* 22 (15), 4406–4413.
- Fong, C.Y., Ng, S.S., Yam, F.K., Abu Hassan, H., Hassan, Z., 2015. An investigation of sol-gel spin coating growth of wurtzite GaN thin film on 6H–SiC substrate. *Journal of Crystal Growth* 413, 1–4.
- Fujishima, A., Rao, T.N., Tryk, D.A., 2000. Titanium dioxide photocatalysis. *Journal of Photochemistry and Photobiology C: Photochemistry Reviews* 1 (1), 1–21.
- Hou, A.Q., Si, C., Zhou, Y.X., 2009. Self-assembly of the polysiloxane modified with cationic and perfluorocarbon groups on the polyester surface and its effect on the color shade of the dyed polyester. *Journal of Polymer Research* 16 (6), 687–692.
- Ibrahim, N.A., El-Gamal, A.R., Gouda, M., Mahrous, F., 2010. A new approach for natural dyeing and functional finishing of cotton cellulose. *Carbohydrate Polymers* 82 (4), 1205–1211.
- Joshi, M., Khanna, R., Shekhar, R., Jha, K., 2011. Chitosan nanocoating on cotton textile substrate using layer-by-layer self-assembly technique. *Journal of Applied Polymer Science* 119 (5), 2793–2799.
- Kim, H.J., Murai, N., Fang, D.D., Triplett, B.A., 2011. Functional analysis of *Gossypium hirsutum* cellulose synthase catalytic subunit 4 promoter in transgenic *Arabidopsis* and cotton tissues. *Plant Science* 180 (2), 323–332.
- Klueh, U., Wagner, V., Kelly, S., Johnson, A., Bryers, J.D., 2000. Efficacy of silver-coated fabric to prevent bacterial colonization and subsequent device-based biofilm formation. *Journal of Biomedical Materials Research* 53 (6), 621–631.
- Koper, G.J.M., 2007. *An Introduction to Interfacial Engineering*. VSSD.
- Li, S., Zhang, S., Wang, X., 2008. Fabrication of superhydrophobic cellulose-based materials through a solution-immersion process. *Langmuir* 24 (10), 5585–5590.
- Li, X., Xiong, R., Wei, G., 2009. Preparation and photocatalytic activity of nanoglued Sn-doped TiO₂. *Journal of Hazardous Materials* 164 (2), 587–591.
- Li, Y., Liu, H., Song, J., Rojas, O.J., Hinestroza, J.P., 2011. Adsorption and association of a symmetric PEO-PPO-PEO triblock copolymer on polypropylene, polyethylene, and cellulose surfaces. *ACS Applied Materials and Interfaces* 3 (7), 2349–2357.

- Liu, J., Wang, Q., Fan, X., 2012. Layer-by-layer self-assembly of TiO₂ sol on wool to improve its anti-ultraviolet and anti-ageing properties. *Journal of Sol-Gel Science and Technology* 62 (3), 338–343.
- Łucznyński, J., Frąckowiak, R., Włoch, A., Kleszczyńska, H., Witek, S., 2013. Gemini ester quat surfactants and their biological activity. *Cellular and Molecular Biology Letters* 18 (1), 89–101.
- Luo, J., Wu, Q., Huang, H.-c., Chen, J.-j., 2011. Studies of fluorinated methylacrylate copolymer on the surface of cotton fabrics. *Textile Research Journal* 81 (16), 1702–1712.
- Ma, H.Y., Zhang, M., 2014. Superhydrophilic titania wall coating in microchannels by in situ sol-gel modification. *Journal of Materials Science* 49 (23), 8123–8126.
- Mahltig, B., Arnold, M., Loethman, P., 2010. Surface properties of sol-gel treated thermally modified wood. *Journal of Sol-Gel Science and Technology* 55 (2), 221–227.
- Mahltig, B., Haufe, H., Böttcher, H., 2005. Functionalisation of textiles by inorganic sol-gel coatings. *Journal of Materials Chemistry* 15 (41), 4385–4398.
- Mahltig, B., Knittel, D., Schollmeyer, E., Böttcher, H., 2004. Incorporation of triarylmethane dyes into sol-gel matrices deposited on textiles. *Journal of Sol-Gel Science and Technology* 31 (1–3), 293–297.
- Mahltig, B., Textor, T., 2006. Combination of silica sol and dyes on textiles. *Journal of Sol-Gel Science and Technology* 39 (2), 111–118.
- Mahmoud, S., Hammoudeh, A., Gharaibeh, S., Melsheimer, J., 2002. Hydrogenation of cinnamaldehyde over sol-gel Pd/SiO₂ catalysts: kinetic aspects and modification of catalytic properties by Sn, Ir and Cu additives. *Journal of Molecular Catalysis A-Chemical* 178 (1–2), 161–167.
- Mao, H., Qiu, Z.S., Shen, Z.H., Huang, W.A., 2015. Hydrophobic associated polymer based silica nanoparticles composite with core-shell structure as a filtrate reducer for drilling fluid at ultra-high temperature. *Journal of Petroleum Science and Engineering* 129, 1–14.
- Mihailovic, D., Saponjic, Z., Radoicic, M., Lazovic, S., Baily, C.J., Jovancic, P., Nedeljkovic, J., Radetic, M., 2011. Functionalization of cotton fabrics with corona/air RF plasma and colloidal TiO₂ nanoparticles. *Cellulose* 18 (3), 811–825.
- Moein, M.M., Javanbakht, M., Karimi, M., Akbari-Adergani, B., Abdel-Rehim, M., 2015. A new strategy for surface modification of polysulfone membrane by in situ imprinted sol-gel method for the selective separation and screening of L-Tyrosine as a lung cancer biomarker. *Analyst* 140 (6), 1939–1946.
- Nistor, C.L., Donescu, D., Ianchis, R., Spataru, C., Raditoiu, V., Petcu, C., Ghiurea, M., Deleanu, C., 2011. Encapsulation of three different hydrophobic dyes in functionalized silica particles. *Journal of Sol-Gel Science and Technology* 59 (1), 48–56.
- Nord-West, T.T.D.T., 2009. Modification of Textile Surfaces Using the Sol-Gel Technique.
- Pavlidou, S., Papaspyrides, C.D., 2008. A review on polymer-layered silicate nanocomposites. *Progress in Polymer Science* 33 (12), 1119–1198.
- Perez-Anguiano, O., Wenger, B., Pugin, R., Hofmann, H., Socolan, E., 2015. Controlling mesopore size and processability of transparent enzyme-loaded silica films for biosensing applications. *ACS Applied Materials & Interfaces* 7 (4), 2960–2971.
- Periolatto, M., Ferrero, F., 2015. Cotton and polyester surface modification by methacrylic silane and fluorinated alkoxy silane via sol-gel and UV-curing coupled process. *Surface & Coatings Technology* 271, 165–173.
- Polí, R., Colleoni, C., Calvimontes, A., Polášková, H., Dutschk, V., Rosace, G., 2015. Innovative sol-gel route in neutral hydroalcoholic condition to obtain antibacterial cotton finishing by zinc precursor. *Journal of Sol-Gel Science and Technology* 74 (1), 151–160.

- Rojace, R., Fathi, M., Raeissi, K., 2014. Comparing nanostructured hydroxyapatite coating on AZ91 Alloy samples via sol-gel and electrophoretic deposition for biomedical applications. *IEEE Transactions on Nanobioscience* 13 (4), 409–414.
- Sayıllan, F., Asiltürk, M., Kiraz, N., Burunkaya, E., Arpaç, E., Sayıllan, H., 2009. Photocatalytic antibacterial performance of Sn⁴⁺-doped TiO₂ thin films on glass substrate. *Journal of Hazardous Materials* 162 (2), 1309–1316.
- Si, Y.S., Mao, X., Zheng, H.X., Yu, J.Y., Ding, B., 2015. Silica nanofibrous membranes with ultra-softness and enhanced tensile strength for thermal insulation. *RSC Advances* 5 (8), 6027–6032.
- Skoc, M.S., Macan, J., Pezelj, E., 2011. Application of sol-gel process for modifying textile surfaces and properties. *Tekstil* 60 (1), 18–29.
- Skoc, M.S., Macan, J., Pezelj, E., 2014. Modification of polyurethane-coated fabrics by sol-gel thin films. *Journal of Applied Polymer Science* 131 (4), 39914.
- Tadanaga, K., Morinaga, J., Matsuda, A., Minami, T., 2000. Superhydrophobic-superhydrophilic micropatterning on flowerlike alumina coating film by the sol-gel method. *Chemistry of Materials* 12 (3), 590–592.
- Textor, T., Bahners, T., Schollmeyer, E., 1999. Surface modification of textile fabrics by coatings based on the sol-gel process. *Melliand Textilberichte International Textile Reports* 80, E229.
- Tizjang, V., Montazeri-Pour, M., Rajabi, M., Kari, M., Moghadas, S., 2015. Surface modification of sol-gel synthesized TiO₂ photo-catalysts for the production of core/shell structured TiO₂-SiO₂ nano-composites with reduced photo-catalytic activity. *Journal of Materials Science-Materials in Electronics* 26 (5), 3008–3019.
- Toledo-Fernandez, J.A., Mendoza-Serna, R., Morales, V., de la Rosa-Fox, N., Pinero, M., Santos, A., Esquivias, L., 2008. Bioactivity of wollastonite/aerogels composites obtained from a TEOS–MTES matrix. *Journal of Materials Science—Materials in Medicine* 19 (5), 2207–2213.
- Vasiljevic, J., Gorjanc, M., Tomsic, B., Orel, B., Jerman, I., Mozetic, M., Vesel, A., Simoncic, B., 2013. The surface modification of cellulose fibres to create super-hydrophobic, oleophobic and self-cleaning properties. *Cellulose* 20 (1), 277–289.
- Viard, N., Niznansky, D., Rehspringer, J.L., 1997. Structural evolution of a formamide modified sol—spectroscopic study. *Journal of Sol-Gel Science and Technology* 8 (1–3), 183–187.
- Vilcnik, A., Jerman, I., Vuk, A.S., Kozelj, M., Orel, B., Tomsic, B., Simoncic, B., Kovac, J., 2009. Structural properties and antibacterial effects of hydrophobic and oleophobic sol-gel coatings for cotton fabrics. *Langmuir* 25 (10), 5869–5880.
- Villiers, C., Freitas, H., Couderc, R., Villiers, M.B., Marche, P., 2010. Analysis of the toxicity of gold nano particles on the immune system: effect on dendritic cell functions. *Journal of Nanoparticle Research* 12 (1), 55–60.
- Vince, J., Orel, B., Vilcnik, A., Fir, M., Vuk, A.S., Jovanovski, V., Simoncic, B., 2006. Structural and water-repellent properties of a urea/poly(dimethylsiloxane) sol-gel hybrid and its bonding to cotton fabric. *Langmuir* 22 (15), 6489–6497.
- Wang, X., Romero, M.Q., Zhang, X.Q., Wang, R., Wang, D.Y., 2015. Intumescent multilayer hybrid coating for flame retardant cotton fabrics based on layer-by-layer assembly and sol-gel process. *RSC Advances* 5 (14), 10647–10655.
- Wang, X., Wang, C., 2009. The antibacterial finish of cotton via sols containing quaternary ammonium salts. *Journal of Sol-Gel Science and Technology* 50 (1), 15–21.
- Wang, X.X., Yin, Y.J., Wang, C.X., 2010. New approach to impart antibacterial effect and improve ink jet printing properties with modified SiO₂ sols containing cationic biocides. *Colloids and Surfaces A-Physicochemical and Engineering Aspects* 361 (1–3), 51–55.

- Wedin, P., Svanholm, E., Alberius, P.C.A., Fogden, A., 2006. Surfactant-templated mesoporous silica as a pigment in inkjet paper coatings. *Journal of Pulp and Paper Science* 32 (1), 32–37.
- Yang, H.Y., Zhu, S.K., Pan, N., 2004. Studying the mechanisms of titanium dioxide as ultraviolet-blocking additive for films and fabrics by an improved scheme. *Journal of Applied Polymer Science* 92 (5), 3201–3210.
- Yang, L.X., Feng, J., Zhang, W.G., Qu, J.E., 2010. Film forming kinetics and reaction mechanism of gamma-glycidoxypropyltrimethoxysilane on low carbon steel surfaces. *Applied Surface Science* 256 (22), 6787–6794.
- Yin, Y.J., Guo, N., Wang, C.X., Rao, Q.Q., 2014. Alterable superhydrophobic-superhydrophilic wettability of fabric substrates decorated with ion-TiO₂ coating via ultraviolet radiation. *Industrial & Engineering Chemistry Research* 53 (37), 14322–14328.
- Yin, Y.J., Li, T., Fan, F., Zhao, C.Y., Wang, C.X., 2013. Dynamically modifiable wettability comparisons of the hydrophilic and hydrophobic substrates coated with F/TiO₂ hybrid sol by UV irradiation. *Applied Surface Science* 283, 482–489.
- Yin, Y.J., Wang, C.X., 2011. Multifunctional performances of nanocomposite SiO₂/TiO₂ doped cationic EBODAC film coated on natural cellulose matrix. *Journal of Sol-Gel Science and Technology* 59 (1), 36–42.
- Yin, Y.J., Wang, C.X., 2012a. Organic-inorganic hybrid silica film coated for improving resistance to capsicum oil on natural substances through sol-gel route. *Journal of Sol-Gel Science and Technology* 64 (3), 743–749.
- Yin, Y.J., Wang, C.X., 2012b. Sol-gel synthesis and characterizations of organically modified silica coatings on knitted cellulose for fixation applications. *Progress in Organic Coatings* 73 (1), 14–18.
- Yin, Y.J., Wang, C.X., 2013. Water-repellent functional coatings through hybrid SiO₂/HTEOS/CPTS sol on the surfaces of cellulose fibers. *Colloids and Surfaces A-Physicochemical and Engineering Aspects* 417, 120–125.
- Yin, Y.J., Wang, C.X., Wang, C.Y., 2008. An evaluation of the dyeing behavior of sol-gel silica doped with direct dyes. *Journal of Sol-Gel Science and Technology* 48 (3), 308–314.
- Yin, Y.J., Wang, C.X., Wang, C.X., Wu, M., Tian, A.L., Fu, S.H., 2011. Hydrophobic properties and color effects of hybrid silica spin-coatings on cellulose matrix. *Journal of Materials Science* 46 (20), 6682–6689.
- Yin, Y.J., Wang, C.X., Wang, Y.J., 2012. Fabrication and characterization of self-assembled multifunctional coating deposition on a cellulose substrate. *Colloids and Surfaces A-Physicochemical and Engineering Aspects* 399, 92–99.
- Yu, M., Gu, G.T., Meng, W.D., Qing, F.L., 2007. Superhydrophobic cotton fabric coating based on a complex layer of silica nanoparticles and perfluorooctylated quaternary ammonium silane coupling agent. *Applied Surface Science* 253 (7), 3669–3673.
- Zhang, Y., Dong, H., Wu, C., Yu, L., 2014. Thermophysical properties of binary mixtures of triethoxysilane, methyltriethoxysilane, vinyltriethoxysilane and 3-mercaptopropyltriethoxysilane with ethylbenzene at various temperatures. *The Journal of Chemical Thermodynamics* 76, 45–55.
- Zhu, X.T., Zhang, Z.Z., Ge, B., Men, X.H., Zhou, X.Y., Xue, Q.J., 2014. A versatile approach to produce superhydrophobic materials used for oil-water separation. *Journal of Colloid and Interface Science* 432, 105–108.

Smart coatings for comfort in clothing

14

D. Jovic

University of Belgrade, Belgrade, Serbia

14.1 Introduction

The most traditional area of textile material use is human clothing. Since the dawn of humanity, textile materials have acted as the interface between the wearer and the environment. The aim of clothing has always been to protect the human body against possible injuries such as insect bites, abrasive and harmful substances (physical protection), and adverse climate conditions such as strong sunlight, wind, and intense heat, cold, and precipitation (insulation). Apart from its practical protective function, throughout history the role of clothing has become much more complex as it has gained strong bonds with fashion and specific cultural and social contexts.

The traditional protective role of clothing has been passive, restricted to choosing the proper material for certain physical conditions of the body and the environment, always with the aim of keeping the wearer comfortable and healthy. In most cases, in cold climate conditions, the physiological function of clothing has been limited to preventing air circulation around the skin of the wearer and thus avoiding the exit of air reheated by the skin. In warm and sunny environments, clothing directly protects the wearer from sunburn and extensive heating. In case of precipitation (rain and snow), impermeable clothing protects the wearer from water that could reach the body and cause cold and discomfort.

Nevertheless, these simple physiological functions of clothing cannot meet current consumer demands, which are closely related to the demands of high performance and efficiency. Modern changes in lifestyle and the sophistication of consumer demands create the current situation in which the actual aim of clothing is changing from traditional simple protection to necessary functionality and added value, especially within the areas of work wear, leisure wear, and sportswear.

Therefore, although in the contemporary world practical protection remains the main reason for our need for clothing, currently it often has an active role in adapting to changes in physiological needs in the accordance with the activity of the wearer and changes in the environment. This new functionality is known as ‘active comfort regulation’ and can be achieved by implementing so-called ‘smart technology’.

In the current practice of materials engineering, smart technology is creating a sea change. Because a commonly accepted definition characterising smart materials does not exist, this situation leads to ambiguities in classifying materials in this group. The terms ‘smart’ and ‘intelligent’ are also used frequently in parallel to ones such as

'interactive', 'responsive', and 'adaptive'. No matter how the term is used, it generally refers to a material that reacts (responds or changes) to defined influences (impulses or stimuli) from the local environment (outside or inside) (Mather, 2001; Matilla, 2006; Tao, 2001; Vigo, 1999). Hence, smart textiles are usually defined as textile materials or products that can sense and interpret changes in their local environment and respond appropriately. When considering clothing, the term 'local environment' comprises environmental conditions (outside) and body functions (inside).

Today, functional finishing technology, which includes smart coatings, is considered a specific technology that could provide active comfort regulation function to textile materials. The functional finishing approach is possible as the consequence of enormous growth in supporting technologies, primarily in the areas of surface modification techniques, stimuli-responsive polymers (SRPs), phase change materials (PCMs), and shape memory polymers (SMPs). By redesigning the textile material surface, operating at a microscopic level, new added-value textile material can be created, containing fibres that maintain advantageous conventional properties (eg, mechanical strength, flexibility) but with advanced functionalities and environmental responsiveness implemented by smart coating. This approach enables producers to continue to use conventional textile fibres and, by modifying a very thin surface layer of the material, to create modern smart textile materials that not only keep us warm, dry, and comfortable but are expected to react and interact with a wide range of stimuli and situations.

Facilitated by technological advances in smart coatings, active comfort regulation by smart textiles and clothing has expanded rapidly, providing the consumer with a wide assortment of products from which to choose.

14.2 Principles of comfort in textiles and clothing

14.2.1 General aspects of wear comfort

Wear comfort is the most important property of clothing demanded by users and consumers. It is currently the major sales aspect for clothing. Wear comfort affects the well-being of the wearer but also the wearer's performance and efficiency, so it can be appointed the physiological function of clothing.

There is no single determination of comfort, but it is well-known that thermal resistivity and moisture dissipation in all their forms have a significant role in providing overall comfort. Mecheels (1977, 1998) described wear comfort as a measure of how well clothing assists the function of the body or impairs it to a minimal degree.

In assessing comfort, it must be recognised that it is actually a state of mind, because it comprises subjective weighting of all the different properties of clothing. Therefore, Goldman (2007) stated that it is difficult to identify the numerous factors which affect comfort; for instance, the interaction between the physical demand imposed upon individuals, their physiological status, and their psychological attitudes must be considered together with social customs, tactile perceptions, and the like.

As a complex phenomenon, wear comfort can be divided into four different main aspects (Bartels, 2006; Mecheels, 1998):

1. **Thermophysiological wear comfort**
The attainment of a comfortable thermal and wetness state. It directly influences a person's thermoregulation and is composed of heat and moisture transport processes through the clothing (thermal insulation, breathability, moisture management, etc.).
2. **Skin sensorial wear comfort**
The elicitation of various neural sensations when a textile comes into contact with skin. Characterised by mechanical sensations caused by direct contact of textile material with the skin (smoothness, softness, scratchy, and clinging).
3. **Ergonomic wear comfort**
The ability of a textile to allow freedom of movement, reduced burden, and body shaping, as required. It is influenced by the cut and fit of the clothing (the garment's pattern and the elasticity of the material).
4. **Psychological wear comfort**
The subjective perception of clothing to the eye, hand, ear, and nose, which contributes to the overall well-being of the wearer. It is affected by fashion, personal preferences, social context, and so forth (touch, colour, etc.).

Because clothing is directly in contact with the human body, it interacts with the body continuously and dynamically during wear, which stimulates mechanical, thermal, and visual sensations. Li (2001) termed this 'sensory comfort', which is a relatively new area in clothing comfort research.

Thermophysiological wear comfort is the main aspect of comfort which can be influenced by innovative smart coatings for active comfort regulation in responsive performance apparel (ie, smart clothing). Nevertheless, smart coatings can have also a secondary, mainly worsening, influence on skin sensorial wear comfort (eg, possible irritation) and the ergonomic wear comfort (eg, possible reduced elasticity), which must not be neglected when developing new materials.

14.2.2 Factors of thermal comfort in clothing

A key function of clothing in terms of thermal comfort is insulation. Clothing creates a certain microclimate around the human body, which is mostly determined by the volume of air enclosed in the fabric and between the fabric and skin. In general, thermal comfort depends on the interaction among three sets of factors: environmental, physiological, and clothing.

Main environmental factors in defining thermal comfort are air temperature, air motion, ambient air relative humidity (RH) (or more appropriately, vapour pressure), and mean radiant temperature. These parameters directly affect heat transfer from the body. In terms of environmental parameters, important factors that influence thermoregulation are radiant heat transfer (the difference between mean radiant temperature and skin temperature), convective heat transfer (the difference between skin temperature and ambient air temperature), evaporative heat transfer (the difference between the vapour pressure of sweat at skin temperature and ambient vapour pressure), and directed fluid

transport (eg, of sweat) as well. In general, clothing can serve a protective insulation function by reducing radiant heat gain and thermal stress.

In assessing physiological factors of thermal comfort, it is important to stress that human skin represents a critical structure in the interaction of the human body with the environment (Wollina, Abdel-Naser, & Vermaet, 2006). Hence, thermal wear comfort is directly related to the physiological processes of the individual which occur within the body, but which are mainly reflected through the skin. These processes produce a certain amount of metabolic heat, which is an important element to be considered in thoroughly defining a comfort state. Heat production at rest or at work is different, and it is an essential element in assessing comfort balance.

Because clothing represents a direct barrier between skin and ambient air, it directly influences thermal comfort, so the clothing factor must also be seriously considered. Its influence is mainly recognised through the aspects of insulation (the convective heat exchange between skin and the environment; a linear function of the thickness of the clothing and associated trapped air layers); permeability (evaporative transfer, ie, the moisture permeability of the clothing; the difference between the vapour pressure of sweat at the skin and ambient vapour pressure); clothing design elements (the cut and fit of clothing, the weight of the material, the nature of apertures, the thickness and stiffness of the material, the total number of layers, etc.) which can alter insulation and permeability when the clothing is exposed to an external air motion or generates air and/or clothing movement by activity, ie, wearer motion.

Human performance can be strongly impaired by the poor fit as well as the excessive weight of clothing, which could result in increased energy expenditure for a given activity rate (Laing & Sleivert, 2002). Thus, the wearer can be burdened by increased difficulty in achieving adequate moisture vapour transmission. Taking in consideration main factors of thermal comfort, proper insulation by clothing is obtained by ensuring thermal balance of the human body despite changes in ambient temperature and humidity, as well as in metabolic heat production as the result of wearer activity (Tuğrul Oğulata, 2007). Generally, perception of clothing comfort is positively related to warmth and negatively to dampness (Li, 2005).

Because clothing creates a certain microclimate around the human body which affects the human feeling of comfort, the air temperature between the body and the first layer of clothing is the determining factor for comfort feeling. However, the optimum level of this temperature is determined by human physical activity and is greatly influenced by the level of health, age, physical fitness, and general metabolism of any individual. The more intense the activity of the wearer and the more extreme the environmental conditions are, the higher is the impact of clothing on thermoregulation. This is the real challenge for active comfort regulation by smart clothing, ie, responsive performance apparel, which must be capable of supporting a wide variety of microclimate variations caused by both environmental and physiological factors.

14.2.3 Thermal comfort ability of textile clothing

In the interaction between a clothing system and the person wearing it, the properties of fibres and fabrics used to produce clothing are important. As mentioned, the thermal

insulation of clothing is defined through the resistance to heat transfer by convection, radiation, and conduction. Because air is known as one of the best heat insulators, the most important factor enabling thermal comfort is the volume of trapped still air layers within the garment. This volume is determined by the intrinsic properties of textile material (fibre and yarn type, fabric structure, fabric construction, and mechanical and thermal properties of fabric).

The provision of insulation against the cold environment has traditionally been achieved by resorting to the multilayer system, which is less bulky for a given insulation level than that of a single-layer system. A multilayer system usually offers a greater thermal range and individual layers can carry specific protective properties which can be beneficial.

Apart from thermal insulation, to give complete protection against discomfort caused by precipitation and wind, thermoregulating garments usually include water-resistant and windproof properties. When implementing water resistance at the outer layer of garment, the means of preventing the entry of moisture into and through the clothing layers must not prevent the exhaustion of moisture vapour from the body (breathability property). If an impermeable barrier is imposed, it prevents the transmission of moisture vapour, leading to the risk of heat stress and seriously impairing the activities and efficiency of the wearer. Hence, the breathability must be accomplished through by using vapour-permeable membranes or coatings. A similar approach applies to windproofing. If it is achieved using a tightly constructed woven fabric or by coating the fabric, possible physiological problems must be avoided (Barker, 2002).

To define the degree of thermal comfort of a garment objectively, international standards have been developed based on the objective and representative measuring methods of five properties of textile materials, which have a determining influence on the thermal regulation of garments: (1) thermal insulation; (2) resistance to the transfer of water vapour; (3) permeability to air; (4) resistance to the penetration of water; and (5) wicking. These five methods allow the classification of thermoregulation properties of a garment and are of great importance to the producers of work wear, sportswear, and any kind of thermoregulating garments.

To assess thermophysiological comfort of the entire garment, the insulation and permeability of clothing are usually measured in a static state on a thermal manikin, expressed by the thermal insulation parameter (clo) and permeability index (i_m). The thermal manikin allows thermal insulation and moisture transport of the entire garment to be measured while simulating the body heat and transpiration of a person in action (eg, work, sports, walking), exactly simulating their effects for the wearer in practical use (Holmer, 2004).

The thermal insulation of clothing is measured by the lateral thickness of the total clothing ensemble and is expressed by the unit clo (Yee Yan & Oliver, 1996). The clo is a measure of thermal resistance and it includes the insulation provided by any layer of trapped air between the skin and clothing, as well as the insulation value of the clothing itself. One clo ($1 \text{ clo} = 0.155 \text{ m}^2 \text{ }^\circ\text{C/W}$) corresponds to the insulating value of clothing needed to keep a person indefinitely comfortable (when sitting at rest) in a room at 21°C with air movement at 0.1 m/s and humidity less than 50% – typically a person

wearing a business suit. 0 clo corresponds to a naked person. Very thin fabric layers of clothing vary from 0.02 to 0.20 clo (for example, underwear), thick fabric layers vary from 0.20 to 0.50 clo (for example, sweater), and coats, overjackets, and overtrousers are expressed as 0.50–0.70 clo units. In Europe, a similar value was developed, called the tog, which equals 0.645 clo. The clo is used more commonly than the tog.

Insulation is generally a function of the thickness of the clothing ensemble; this, in turn, is characteristically a function of the number of clothing layers. Thus, each added layer of clothing will tend to exert a characteristic increase in total insulation. The overall insulation or clo value can be calculated simply by taking the clo value for each individual garment worn by the person and adding them together. This is why most two-layer clothing ensembles exhibit similar insulation characteristics, most three-layer systems are comparable, and so forth, regardless of major differences in fibre selection, fabric type, or layer thickness.

Another important parameter in measuring the thermal comfort of clothing is the moisture permeability index (i_m), which is given as a dimensionless unit as a function of ambient vapour pressure, taking values between 0 (impermeable layer) and 1 (totally moisture permeable layer) (Huang, 2006; Spencer-Smith, 1975). A typical i_m value for most permeable clothing ensembles in still air is less than 0.5. Water-repellent treatment, very tight weaves, and protective coatings can reduce the i_m value significantly.

The ultimate evaporative heat transferred from skin through clothing and external air layers to the environment is not simply a function of the permeability index (i_m) but is a function of the ratio of intrinsic moisture permeability to the insulation (ie, permeability index to insulation ratio) (i_m/clo).

14.2.4 Active versus passive thermoregulation

The functional activity (sense – react – adapt) of smart textiles can provide active comfort regulation function to textile materials. Smart textiles can act as both sensors and actuators, so they should not be confused with other existing high-performance or multifunctional textiles that are actually passive materials with advanced properties. The fusion of conventional structural textile materials with advanced properties given by smart technologies offers the possibility of active comfort regulation as a high-added-value product option to producers and consumers.

Based on the ability to respond to environmental parameter changes, textiles with thermoregulation function can be divided into passive and active. Passive thermoregulation is present in conventional textiles (eg, silk or wool) which are able to warm or cool depending on environmental conditions. It can also be achieved with textiles made of special fibres (eg, hollow fibres for warming) or with a special textile structure (eg, three-dimensional-structure constructions), as well as with functional multilayer clothing systems (eg, first layer with good vapour and air permeability, second layer with warmth isolation, third layer with protection from environmental conditions such as wind and rain). Active thermoregulation is the property of smart textiles which can respond to changes in ambient temperature to keep balance in human body microclimate temperatures.

Both passive and active thermoregulation properties are currently main factors for the global market success of performance apparel. As the consequence of a modern lifestyle, performance apparel production now represents one of the fastest-growing sectors of the textile industry. It is a typical 21st-century product that provides consumers with greater levels of comfort, safety, aesthetics, and functional performance. Currently it is mostly used for protective clothing, because in many industrial sectors, military and energy services, and hospital environments, humans are subjected to various types of risks (each sector has its own requirements for protective clothing). Another well-known end use of performance apparel is sportswear, through which it crosses the boundary to everyday fashion. In the case of sports and outdoor textiles, main features required by customers are related to comfort: water repellency to keep the body dry, moisture management (eg, moisture wicking, quick drying), antibacterial/antiodour qualities, ultraviolet (UV) protection, and wind resistance (Anon, 2009, 2010).

High-performance characteristics of apparel are achieved by using innovative technologies. Apart from improving different product properties, innovative technologies incorporate new functionalities with high importance for consumers, with the ultimate goal of improving comfort, increasing protection, and enhancing performance in human activities. To reach these goals, innovative fibres and fabrics, including high-performance and high-functional fibres, smart and intelligent textiles, and coated and laminated textiles have been used (Holme, 2007).

Main drivers for the production of performance apparel emerge from both technical textiles (known for their performance and functionality) and traditional textiles (mainly known for their aesthetics) (Fig. 14.1). The appearance of performance apparel makes it possible to bridge the gap between technical and traditional textiles; thus, the distinction between them is no longer relevant. However, because the actual trend in producing textile materials is to ensure the smart capability of interacting with human and environmental conditions, it is necessary to consider the further development of materials for performance apparel with environmental responsiveness capability. Hence the next step in development are materials for so-called 'responsive performance apparel', in which the specific attribute (function or effect) will not be continuously present (ie, passively), but can be activated on demand. In terms of comfort improvement, that specific attribute is active comfort regulation, which can be activated by sensing ambient stimuli and appropriately reacting to human and environmental conditions. This will enable the spontaneous regulation of clothing performance in a desirable manner when environmental conditions change.

14.3 Technologies for smart textile coatings

To assist the human body in automated thermoregulation, especially in extreme situations of sudden temperature change, novel concepts of smart clothing are constantly being explored. Current systems for adaptive comfort regulation are based on various smart coating technologies which involve the application of PCMs, SMPs, and SRPs.

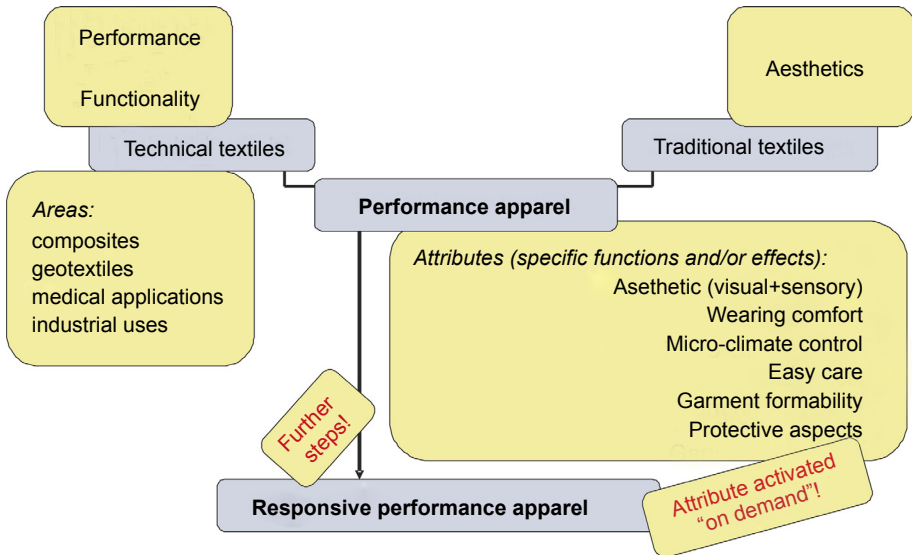


Figure 14.1 Responsive performance apparel as an example of high-added-value textile product.

Adapted from Jovic, D. (2010). Functional finishing of textiles with responsive polymeric systems. In D. Jovic (Ed.), *Surface modification systems for creating stimuli responsiveness of textiles* (pp. 37–59). Enschede, The Netherlands: University of Twente. ISBN: 978-90-365-3122-1.

14.3.1 Phase change materials

PCMs are substances that possess the ability to change their physical state within a narrow temperature range. During phase transitions (ie, as a phase change takes place) PCM store, release, or absorb energy in the form of latent heat. Energy storage (ie, absorbing energy) occurs during the heating process, when PCMs change to a liquid phase; energy release occurs when they change to a solid state. These actions are typically transient; ie, they occur until the latent heat of the PCM is absorbed or released, when the temperature of the PCM does not change. Because the process of phase change requires an unusually high quantity of energy to be transferred to move from one physical state to another, this makes PCM interesting as an efficient source of latent heat storage. In simple words, PCMs are basically materials that absorb lots of heat from their environment when it is warm and then release it when it becomes cold. The ability of PCM to control the heat flow in and out without temperature change makes them suitable as a source of heat storage for smart temperature regulation of textile materials and clothing (Geethamalini, 2006; Mondal, 2008; Sarier & Onder, 2012).

Textiles containing PCMs are able to react immediately to changes in environmental temperatures and the temperatures in different areas of the body. When a rise in temperature occurs, the PCM (usually in form of microcapsules) reacts by absorbing heat and storing this energy in liquefied material. When the temperature falls

again, the PCM releases this stored heat energy and the material solidifies again. In such a way, PCMs are able to produce an active thermal barrier effect by heat absorption or emission, which can regulate heat flux from the human body into the environment when applied in a garment system. In this way, the garment system can adapt itself to thermal needs (ie, the activity level of the wearer and ambient temperature). This exciting property of PCMs is recognised as useful in producing protective garments for all kinds of weather, from the strongest winter to the hottest summer.

A wide spectrum of PCMs is available with different heat storage capacities and phase change temperatures. For the suitable application of PCM in textiles, the phase change temperature must be within the temperature range of human skin. In general, the required properties of PCM to obtain a high efficiency cooling system for specific application in the textile field are a melting point between 15°C and 35°C, a large heat of fusion, a small temperature difference between the melting point and the solidification point, harmlessness to the environment; low toxicity; ability to be noncombustible, stable repeatability of melting and solidification, large thermal conductivity for effective heat transfer, ease of availability, and a low price.

PCMs that fulfil most of these requirements are different kinds of paraffin waxes (a mixture of mostly straight-chain *n*-alkanes) and linear long chain hydrocarbons (eg, *n*-octadecane, *n*-hexadecane, *n*-eicosane), which are usually combined to give the desired physical properties and reach the required temperature stability. Another important PCM for textile applications is low-cost commercial paraffin wax polyethylene glycol (PEG) of variable molecular weights. Other attractive candidates for textile applications are fatty acids and their binary mixtures, polyalcohols and polyalcohol derivatives, and hydrated inorganic salts.

Although they are attractive, organic PCMs have limitations in use, such as low thermal conductivity leading to low charging and discharging rates and a supercooling effect in cooling cycles. Nevertheless, for the application of PCM in the textile field, the major disadvantage is the need for containers to prevent the leakage of PCMs. Therefore, because under certain conditions PCMs are in a liquid state, they are usually not applied directly to textile materials but mostly are first encapsulated and further applied in the form of microcapsules, small polymeric spheres with diameters of only a few micrometres.

Microcapsules are produced by depositing a thin polymer coating onto small solid particles or liquid droplets, or on dispersions of solids in liquids. In this way, the PCM core material is enclosed in a hard polymeric shell, thus forming PCM microcapsules. The PCM content of a capsule is usually 80–85%. The particle size of PCM microcapsules varies from less than 1 µm to more than 300 µm depending on the method of encapsulation, but typically it is 20–40 µm in diameter (Nelson, 2002; Sarier & Onder, 2007).

Applied to textile materials, PCM microcapsules can be either permanently locked in the fibre structure (applied during synthetic fibre forming – spinning) or coated onto the surface of a textile structure (chemical finishing). To apply PCM microcapsules by coating, a coating composition must be prepared, which includes PCM microcapsules, a surfactant, a dispersant, an antifoam agent, and a polymeric mixture (as a thickener and binder). In this way, PCM microcapsules are dispersed in an aqueous system,

which is easily applied by any available industrial coating process (knife-over-roll, knife-over-air, pad-dry-cure, gravure, dip coating, transfer coating, etc.). The polymer binder may be in the form of a solution, dispersion, or emulsion in water or in an organic solvent. For most garment applications, the use of an elastomeric polymer with a glass transition temperature (T_g) varying from about -30°C to about $+12^\circ\text{C}$ is preferable (Sarier & Onder, 2012). Sánchez, Sánchez-Fernandez, Romero, Rodríguez, and Sánchez-Silva (2010) showed that commercially available binders can be used successfully to fix polystyrene microcapsules containing different paraffin wax compositions without modifying the original properties of the textile material, and with acceptable durability.

An alternate method is to incorporate PCM microcapsules in the form of continuous film to the textile material surface by coating with polymers such as acrylic, polyurethane, etc. PCMs can also be applied to the textile material by lamination. In that case, PCM microcapsules are incorporated into a thin polymer film, which is applied to the inner side of the fabric system in the next stage of production by lamination. For protective garments made of nonwovens (surgical gowns, clean room garments, etc.), a useful method of application is to mix PCM microcapsules into a water-blown polyurethane foam mix and apply this foam to a fabric in a lamination process (Pause, 2003). During subsequent drying, water is taken out of the system, which results in an excellent honeycomb porous structure with considerable still air-trapping ability, leading to increased passive insulation.

Besides imparting active comfort regulation to textile materials, PCM microcapsules can affect other comfort-related properties of textiles, especially when coating results in drastic changes in the surface characteristics of materials as the consequence of an increased quantity of microcapsules applied. The fabric can become stiff and moisture-impermeable, consequently reducing fabric softness and flexibility and impairing breathability and moisture transport properties. Therefore, the properties of fabrics treated with PCM microcapsules need to be assessed before they are used in a garment (Shin, Yoo, & Son, 2005; Ying, Kwok, Li, Zhu, & Yeung, 2004).

The thermal storage behaviour of PCM-modified materials is usually represented in terms of the enthalpy of phase change, ie, heat capacity ΔH (kJ/kg) (released or absorbed latent heat within a certain temperature range). Apart from the high enthalpy of phase change (ΔH) and a suitable phase change interval for the practical conditions, to be considered candidates for application to textile materials for apparel use, PCMs should possess reproducibility of phase change and show stable thermal cycling. Moreover, characteristics of high specific heat capacity c_p (J/kg·K) and high thermal conductivity k (W/m·K) are considered advantageous.

Table 14.1 presents a comparison of heat capacity ΔH achieved by industrially applicable coating methods on conventional woven and knitted textile materials (made of cotton, PES-cotton, PES, polyamide, and wool) for apparel use.

As expected, current technologically achievable values of ΔH vary depending on the PCM/binder type used as well as on the coating method. Most ΔH values achieved are below or around 15 kJ/kg, which could ensure the active thermal regulating property of the apparel, but for a limited period of time. On the other hand, as Table 14.1 shows, the PCM add-on levels necessary to achieve active thermal regulation reach

Table 14.1 Heat capacity ΔH (kJ/kg¹) of some different PCM-modified textile materials for use in apparel

Textile material	PCM type/coating	Coating method	Add-on (wt. %)	ΔH (kJ/kg)	References
Cotton	<i>n</i> -Hexadecane modified cotton/polyurethane	Pad-dry-cure	n.a.	6.6	Alay et al. (2011)
Cotton	Paraffin wax modified cotton/commercial binder	Film applicator/dip coating	19	14.4	Sánchez-Silva et al. (2012)
Cotton/PES (50/50)	<i>n</i> -Hexadecane modified cotton/polyurethane	Pad-dry-cure	n.a.	28.6	Alay et al. (2011)
Cotton/PES (60/40)	Paraffin wax modified cotton/commercial binder	Film applicator/dip coating	18.9	14.3	Sánchez-Silva et al. (2012)
PES	<i>n</i> -Octadecane modified cotton/acrylic-urethane	Knife-over-roll	30	7.4	Choi et al. (2004)
PES (knitted)	<i>n</i> -Eicosane modified cotton/polyurethane	Pad-dry-cure	5–33	0.9–4.5	Shin et al. (2005)
PA	Paraffin wax modified cotton/commercial binder	Film applicator/dip coating	17.8	13.5	Sánchez-Silva et al. (2012)
Wool (fluorinated)	PEG 1000	Pad-dry-cure	n.a.	18	Ghahremanzadeh et al. (2010)
Wool (chlorinated)	PEG 1000	Pad-dry-cure	n.a.	10	Ghahremanzadeh et al. (2010)

30%, which implies that the textile material is relatively highly loaded with PCM, which could lead to difficulties in maintaining the durability, moisture vapour permeability, elasticity, and softness of PCM-coated fabrics. Hence, to match high activity levels and longer duration in the use of corresponding garments as well as fulfil all of the requirements of the textile material in apparel application, more research is required to ensure higher heat capacity values of materials coated with PCMs by using a lower quantity of PCM in application.

The composition of the polymeric binder, the binder–PCM microcapsules mass ratio, the type and mechanical stability of the shell material, the binding tendency of the fabric surface with the binder, the curing temperature, and all other process conditions of coating are factors affecting the thermal insulation capability, thermal stability, durability, and tactile comfort properties of the final product.

14.3.2 Shape memory polymers

Shape memory materials (SMMs) are a set of materials that can change their shape, as the result of an external stimulus, from some temporary deformed shape to a previously programmed shape (Honkala, 2006). The shape change is activated most often by changing the surrounding temperature, but with certain materials stress, a magnetic field, an electric field, the pH value, UV light, and even the presence of water can be the triggering stimulus.

Among the variety of available SMMs, SMPs are suitable for producing smart coatings for textiles. Nevertheless, the shape memory effect of SMPs is not related to a specific material property of single polymers but to specific polymer systems that possess shape memory properties. The shape memory effect results from a combination of the polymer structure and the polymer morphology together with applied processing and programming technology (Lenlein & Kelch, 2002; Liu, Qin, & Mather, 2007; Meng & Li, 2013).

The most readily available SMP for use in textiles is segmented polyurethane (SMPU), which is two-phase heterogeneous structure consisting of a rigid fixed phase and a soft reversible phase. The reversed phase is used to hold the temporary deformation and the fixed phase is responsible for memorising the permanent shape. The permanent shape can be memorised and recovered automatically from the temporary deformation with the trigger of heating (Hu, 2007).

Because the most common stimulus in SMP applications is heat (ie, a change in environmental temperature), the most often reported research on their application in textiles is on thermoregulation, ie, active comfort control (Hu & Mondal, 2006a). SMPs can be incorporated in the form of films in multilayer garments for protective clothing, sportswear, or leisure wear. Using a composite film of SMP as an interlining (ie, membrane) in multilayer garments, outdoor clothing can have an adaptable thermal insulation and be used as performance clothing with variable adaptable clo values (Hu & Mondal, 2006b).

The principle of active comfort regulation is based on the ability of SMP film (or coating) to undergo a large change in moisture permeability across the T_g or soft segment crystal melting point temperature (T_{ms}). Based on the T_g/T_{ms} set at room

temperature, the SMP can have low moisture permeability below the T_g/T_{ms} (in the glassy state) and high moisture permeability above T_g/T_{ms} (in the rubbery state).

The same principle applies to SMP-coated textiles. The permeability of the coated fabric changes as the wearer's environment and body temperature change. When the wearer's body temperature is low, the fabric remains less permeable, restricting the loss of body warmth and thus keeping the body warm. When the body temperature rises as the consequence of certain activity (and the wearer starts sweating), the SMP-coated textile allows water vapour to escape into the environment (ie, releasing heat into the environment) because moisture permeability becomes high with increasing body temperature.

As an alternative to the use of films and lamination, an SMP can be used directly as a finishing agent (by coating) for application on textile fabrics. Nevertheless, the area coating SMP on textiles is relatively new and reported developments are scarce. One promising method is based on a highly adhesive resin coating solution by dissolving polyurethane SMP in dimethylacetamide (Stylios, 2006) or grafting onto cotton (Liem, Yeung, & Hu, 2007; Liu, Hu, Zhu, & Yang, 2005) and wool (Dong, Hu, Liu, Liu, & Chan, 2008) fabrics. The coating process is reported to be highly efficient, because a small content of SMP is sufficient to transfer the shape memory effect to the fabric. Hu, Zhu, Huang, & Lu (2012) proposed a general mechanism for coating textiles with SMP, based on cross-linking between the SMP network itself and the fibre, which can form the net points, and the soft segments of the SMP, which can serve as switches. Thus, the shape memory effect from SMP can be transferred to the fabric and maintain durability during washing.

Currently, the application of SMPs on the fabrics and garments to develop smart textiles is a promising area which has tremendous potential. It has attracted enormous attention, but technologically it can still be considered challenging.

14.3.3 Stimuli-responsive polymers

One approach to obtaining active comfort regulation in smart textiles is based on using SRP coatings integrated into the fabric structure. The main challenge of this approach is to integrate SRP durably to a textile material surface in such a way that it retains its responsive behaviour.

An increasing amount of research is being done on the functional finishing of textile materials by incorporating SRP systems. Hu, Meng, Li, & Ibekwe (2012) comprehensively elucidated the applications of SRPs in the textile and clothing sector in a review, together with an assessment of the associated constraints in fabrication processes for textiles and their potential applications in the near future. Another extensive review deals with temperature-responsive SRPs and their application to textiles (Crespy & Rossi, 2007). Both reviews give special attention to systems for improving comfort in clothing by active comfort regulation; apart from reviewing the possibilities of PCMs and SMPs, they pay special attention to thermal/pH-responsive polymeric hydrogels.

Hydrogels are widely used in a variety of applications and are usually defined as three-dimensional cross-linked polymeric networks that can imbibe large amounts

of water (Hoffman, 2001; Peppas & Khare, 1993). If a hydrogel is prepared from SRPs, it has added functionality and display changes in solvation in response to certain stimuli such as temperature, pH, ionic strength, light, and electric fields. Hydrogels responsive to temperature and pH have been the most widely studied systems because these two factors have physiological significance. Versatile dual-responsive hydrogels have been reported mainly for biomedical applications; the reviews in this area address the latest developments (Kopecek & Yang, 2007; Kumar, Srivastava, Galaev, & Mattiasson, 2007; Mano, 2008; Pelton, 2000). Special interest in applying smart textiles occurs because responsive hydrogels exhibit specific volume phase transition (swelling and shrinking) properties which can be triggered by various stimuli (temperature, pH, humidity, etc.). Incorporation of responsive hydrogels (ie, microgels) to the surface of a textile material enables switching (on/off) of various properties of a material (Jocic, 2008).

Efficient incorporation of the surface-modifying system based on a responsive poly-NiPAAm/chitosan microgel to a textile material (cotton, polyamide, or polyester) can be done by aqueous microgel dispersion using a simple pad–dry or pad–dry–cure procedure. Microgel can impart responsive moisture management properties to cotton, transforming it into an advanced material which can improve wear comfort when used for clothing (Kulkarni, Tourrette, Warmoeskerken, & Jocic, 2010; Tourrette et al., 2009). SRP microgel particles exhibit reversible phase transition (expansion–contraction) by varying their size more than threefold between temperatures above and below lower critical solution temperature (LCST) (Jocic, Tourrette, Glampedaki, & Warmoeskerken, 2009).

Once incorporated into a textile material surface, it is likely that SRP microgel particles act as a temperature sensor and a valve to regulate water vapour permeability. Hence, incorporation of a responsive microgel to cotton fabric results in the possibility of controlling moisture content and moisture transmission properties of a modified fabric with small temperature variation in the physiological range (Krizman Lavric, Tomsic, Simoncic, Warmoeskerken, & Jocic, 2012; Krizman Lavric, Warmoeskerken, & Jocic, 2012). Another study with a similar microgel system showed the temperature responsiveness of cotton fabric in terms of higher water vapour permeability at a higher temperature (Wang & Yu, 2015).

Because moisture permeability is the most important criterion to evaluate textile fabric comfort ability, water vapour transmission (WVT) values for cotton and PES fabrics coated with poly-NiPAAm/chitosan microgel at low and high RH and temperatures below and above the LCST of the microgel are presented in Table 14.2 (Glampedaki, Dutschk, Jocic, & Warmoeskerken, 2011; Krizman Lavric, Warmoeskerken, & Jocic, 2010; Tomsic, 2010; Wang & Yu, 2015). For a comparison, the WVT values of untreated (ie, source) materials are also presented.

Because the presence of water is the driving force for the temperature responsiveness of microgels, different behaviours can be observed at low and high RH. At low RH values (50% or 65%), because not enough ambient humidity is available, the microgel particles are in a dry state and the modified textile fabrics do not show an obvious temperature response (or at least it is not macroscopically observable) and thus show similar behaviour in the untreated material. However, at high RH values

Table 14.2 WVT values for different textile materials treated with poly-NiPAAm/chitosan microgel at low and high RH values and temperatures below and above LCST of microgel

Textile material	Fixation system	Application system	WVT (g/m ² day)			
			50% RH		80% RH	
			25°C	40°C	25°C	40°C
Reference: Krizman Lavric, Warmoeskerken and Jovic (2010)						
Untreated cotton	—	—	~ 2200	~ 5700	~ 900	~ 2100
Modified cotton	BTCA	Pad–dry–cure	~ 2100	~ 5300	~ 800	~ 2200
Reference: Tomsic (2010)						
PES (AA activated)	—	—	~ 2300	~ 5200	~ 600	~ 1100
Modified PES	—	Pad–dry–cure	~ 2150	~ 6300	~ 550	~ 1200
Modified PES	VTMS-SO ₂	Sol–gel	~ 2200	~ 6100	~ 450	~ 1400
			65% RH		95% RH	
			20°C	40°C	20°C	40°C
Reference: Glampedaki et al. (2011)						
PES (untreated)	—	—	~ 1000	~ 3600	~ 450	~ 1000
PES (aminated)	—	—	~ 1000	~ 4500	~ 350	~ 1000
Modified PES	Genipin	Padding	~ 1400	~ 6500	~ 370	~ 1100
			50% RH		90% RH	
			25°C	40°C	25°C	40°C
Reference: Wang and Yu (2015)						
Untreated cotton			~ 1200	~ 3300	~ 400	~ 1000
Cotton (with BTCA)			~ 770	~ 3250	~ 300	~ 850
Modified cotton	BTCA	Pad–dry–cure	~ 1300	~ 3600	~ 370	~ 1350

(80%, 90%, or 95%), when enough humidity is available, there are noticeable differences in the behaviour of the modified textile fabric in response to temperature change. Although the differences in WVT can be considered small, they clearly imply the responsive property of materials coated with microgel particles. Nevertheless, WVT values confirm that the moisture permeability of coated fabrics is not continuously present (ie, passively) but can be activated on demand by sensing stimuli (temperature and humidity) in the immediate surroundings, thus reacting to human activity levels or changing ambient conditions.

These properties can meet the demands for better water vapour permeation at higher temperature and humidity for use in clothing and may be considered an important step in the development of materials for so-called responsive performance apparel.

14.4 Functions of smart textile/apparel coatings

Responsive performance apparel is a typical high-added-value textile product adapted to the modern lifestyle of consumers. It provides users with greater levels of comfort, safety, aesthetics, and functional performance. Good thermal sensation and comfort are key factors for the production of responsive performance apparel, both of which are related to the ability of the fabric to maintain thermal equilibrium between the human body and the environment, which is influenced not only by insulation properties but also by the ability of the material to manage moisture and liquid (Li, 2001). Hence, responsive and adaptive functions of smart apparel must be capable of supporting abrupt microclimate changes, especially during exercise or under extreme environmental (cold and heat) conditions. In extreme climatic conditions, particularly in cold weather, in addition to proper thermal insulation, clothing should impart protection against wind, rain, and snow. Cold weather clothing should ideally have the features of being insulating, windproof, and waterproof. The adaptive function of smart apparel is mainly directed toward an insulating function. Nevertheless, some features of smart coatings can positively influence the other two functions, as well.

Thermally active materials made by PCM microcapsules coating are able to improve the wear comfort of the garment by active thermal insulation, ie, controlling heat flux through the garment layers and adjusting it to variable thermal circumstances (activity level and ambient conditions). The functionality of such a material is based on a buffering effect that PCM microcapsules have against temperature changes, which provides an enhanced thermal capacity in addition to the existing passive insulation characteristic of the garment system. However, the clothing layer (or layers) containing PCM must go through the transition temperature range before the phase change in PCM occurs and either release or absorb heat (depending on the ambient conditions). This means that active comfort regulation cannot be achieved under steady-state thermal conditions, so the wearer has to impose some activity to cause a change in the temperature of the PCM-containing fabric. The need of PCM for constant charging and recharging is the main reason why PCM microcapsule-coated clothing is mainly used for active wear, work wear, and outdoor sports apparel.

Enhanced wearer efficiency under extreme weather situations is also reflected in significantly extended wearing times of the garments without the occurrence of heat stress as a serious health risk. The longer wearing times further lead to significantly higher productivity, and the more comfortable wearing conditions result in a reduced number of accidents. This is an important aspect for work wear and outdoor sports apparel.

Thermally active materials made by SMP and SRP coating are able to improve the wear comfort of the garment by active permeability control. This is a fundamental feature of smart breathable fabrics (Mukhopadhyay & Kumar Midha, 2008). To keep the wearer dry and comfortable during sweating, the vapour from sweat must be transmitted through the porous structure of textile material toward the outer layer, where it evaporates. This makes the wearer feel dry and comfortable (Manner, Schuster, Suchomel, Gurtler, & Firgo, 2004; Okubayashi, Griesser, & Bechtold, 2005).

The processes of active permeability control in SMP- and SRP-coated textiles are based on their ability to act as a switch to control the transmission of water vapour (Fig. 14.2). The wearer's comfort can be improved if the material possesses high water vapour permeability at higher temperatures and low water vapour permeability at lower temperatures. At temperatures below the switching temperature, SMP/SRP coating on the material surface exists in a glassy/expanded state, whereas at higher temperatures it exists in a rubbery/collapsed state. Thus, SMP/SRP-coated fabric could have water vapour permeability controlled by closing and opening the permitting

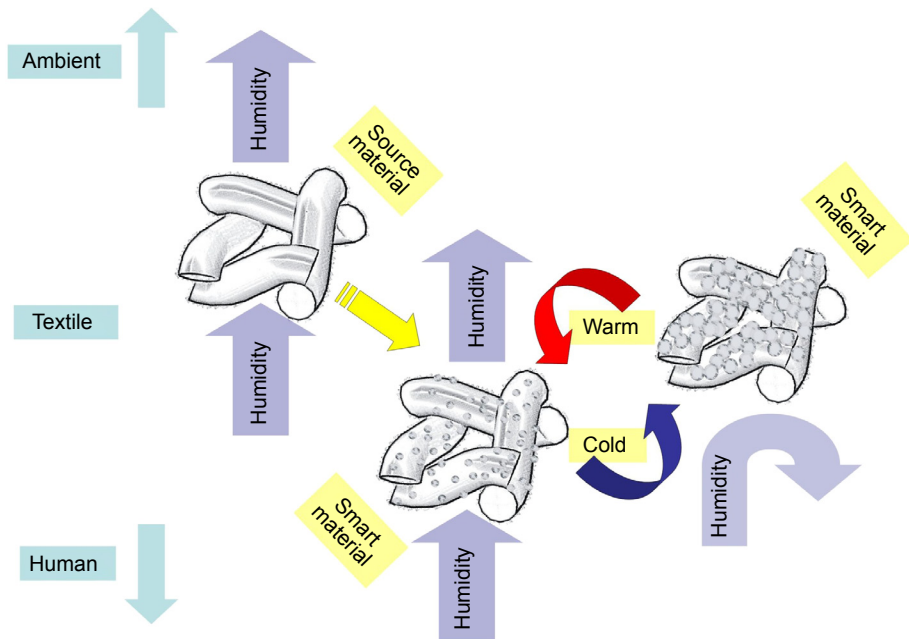


Figure 14.2 Schematic representation of SRP microgel particles as valves for water vapour passage through the textile material.

passages for water vapour transport through the material as a consequence of drastic polymer changes with variations in temperature. Blocking the pores could also form a physical barrier to wind and water, which could be useful for rainwear and foul weather clothing.

Another factor which may influence the overall effect in these thermoregulating systems is changes in water vapour diffusion flux, which are governed by changes in both the diffusion coefficient and diffusion path of water molecules through the coating. As a consequence of these two factors, diffusion flux is likely to decrease at a lower temperature compared with a higher temperature.

14.5 Future trends

Potential future benefits of apparel adaptive comfort regulation by smart coatings involving the application of PCMs, SMPs, and SRPs are significant. Hence, the use of smart coatings to improve comfort will undoubtedly continue to expand into apparel applications. However, all available technologies have limitations and still have the potential to develop.

Although a high level of adaptation to outdoor weather by smart clothing has been achieved, many problems remain in certain areas. Among the challenges remaining, improvement in the efficiency of the systems is the main task, which includes enhancing the response time, improving durability and material processability, and assessing the lifecycle of smart clothing.

In applying PCM to textile materials, a route of important future research may be directed toward improving direct application of PCMs without microencapsulation. Because currently widely accepted microencapsulation methods introduce an amount (15–20%) of ineffective material to the textile substrate (ie, microcapsule shell) a direct application approach would avoid loading the textile material with a significant amount of ineffective material.

Currently, among various types of PCMs (organic, inorganic, and bio-based) organic-based PCMs are mostly used in textile applications because they offer maximal revenue. Nevertheless, strict regulations about being noncombustible and requirements regarding biodegradability are motivating the growth of bio-based PCMs. With a reduction in price, bio-based PCMs can overtake the main role in future treatments of textiles with PCMs.

Future efforts with PCM-treated materials will be applied to enhancing heat capacity over 50 kJ/kg. This will ensure efficient thermal storage by prolonging the period through which the thermoregulation function is available.

Because most novel substances for smart coating appear in the areas of research and industries other than textiles, there is scope for future cooperation and synergies with them, especially because they are usually larger than the textile industry and have larger development budgets. This fact opens the possibility for combining the technologies. In that sense, one possible way is to combine PCM thermal regulation properties with energy storage potential. Other possibilities are the application of advances from nanotechnology and the development of new application systems. Advances from

nanotechnology could involve the use of carbon nanotubes and even graphene to improve the conducting properties of coatings.

Wider and more consistent investigation in SMPs use in apparel adaptive comfort regulation is still required. This especially concerns their transition temperature (at which shape memory effects are triggered), which has to be lowered to meet the needs of human body regular temperature. This could be done by further tailoring hard and soft segments, as they directly affect the shape recovery temperature. In addition, further investigation is needed to improve hand feel and durability to produce practical and reliable materials.

SRPs provide potential and enormous current opportunities to provide adaptive comfort regulation to textiles and apparel. This especially relates to responsive microgel, which could enable microstructural changes in smart apparel in response to stimuli (temperature and humidity) and thus achieve active moisture management with improved feelings of comfort. However, there is still much space for new investigation in this area, especially in providing novel strategies for the integration of SRPs to textile structures with the aim of achieving satisfying compatibility with textile materials.

The introduction of advanced coating techniques is foreseen. This is directed to moving the coating level from traditional fabric coating to an advanced yarn and fibre/filament coating. Among new application systems, inkjet printing may have special attention because its special advantage may be the application of a smart coating to certain (eg, most exposed) areas of a ready-made garment. Other available advanced coating systems include atomic layer deposition and atmospheric plasma coating, which still have to be investigated for application to smart fabrics and apparel.

In finding solutions for these challenges, researchers involved in the smart coating of textiles should involve more lateral thinking and keep up to date with the world around them. This will enable them to spot opportunities for new solutions which may arise at any time. Nevertheless, current potential and future opportunities in smart coatings could ultimately lead to the production of a single garment suitable for all weather, hot or cold, dry or wet, with additional functionalities such as self-cleaning, which may well be possible in the near future.

14.6 Conclusion

Responsive performance apparel is a typical high-added-value textile product adapted to the modern lifestyle of the consumer in the 21st century. Good thermal sensation and comfort are key factors for the production of responsive performance apparel, both of which are related to the ability of the garment to maintain thermal equilibrium between the human body and the environment. Hence, responsive and adaptive functions of smart apparel must be capable of supporting abrupt microclimate changes, especially during exercise or under extreme environmental (cold and heat) conditions, thus enabling enhanced wearer efficiency.

Smart coatings currently provide great potential in obtaining textile materials (ie, apparel) with active comfort regulation properties. Technologies for the smart coating of textile materials are based on applying different smart polymeric materials, such as

PCMs, SMPs, and SRPs. These coatings successfully impart stimuli responsiveness to the textile material, making it an adequate raw material for the production of responsive performance apparel.

Thermophysiological wear comfort is the main aspect of comfort which can be influenced by innovative smart coatings for active comfort regulation in responsive performance apparel (ie, smart clothing). Nevertheless, smart coatings also can have a secondary, mainly worsening, influence on skin sensorial wear comfort (eg, possible irritation) and the ergonomic wear comfort (eg, possible reduced elasticity), which must not be neglected when developing new materials. This is an important aspect for work wear and outdoor sports apparel.

Despite worldwide research and industrial efforts to show the good compatibility of smart polymeric materials with a variety of textile materials, the use of smart coatings in textile apparel applications remains largely underestimated. This is the consequence of strict requirements and regulations imposed by the textile/clothing industry and consumers, and it is a challenge to be overcome. Among these properties to be addressed, the most important are safety in use, durability, and the need for adequate maintenance procedures.

In the 21st century, we have entered the exciting age of smart fabrics and smart clothing. In addition to smart coating substances mentioned in this text (PCMs, SMPs, and SRPs), new materials continuously appear, for which new applications are still being developed. With the tremendous variety of conventional textile fabrics and novel coating substances, there has never been a better time to innovate in the area of smart coatings for the improvement of comfort in apparel.

Sources of further information

- Fung, W. (2002). *Coated and laminated textiles*. Cambridge, UK: Woodhead Publishing Ltd.
- Hu, J. (Ed.). (2007). *Shape memory textiles*. Cambridge, UK: Woodhead Publishing Ltd.
- Jocic, D. (Ed.). (2010). *Surface modification systems for creating stimuli responsiveness of textiles*. Enschede, The Netherlands: University of Twente. Available through the University of Twente Website: <http://www.utwente.nl/ctw/efsm/advanbiotex/workshop/proceedings/>.
- Mattila, H.R. (Ed.). (2006). *Intelligent textiles and clothing*. Cambridge, UK: Woodhead Publishing Ltd.
- Paul R. (Ed.). (2015). *Functional finishes for textiles*. Cambridge, UK: Woodhead Publishing Ltd.
- Tao, X. (Ed.). (2001). *Smart fibres, fabrics and clothing*. Cambridge, UK: Woodhead Publishing Ltd.

References

- Alay, S., Alkan, C., & Göde, F. (2011). Synthesis and characterization of poly(methyl methacrylate)/*n*-hexadecane microcapsules using different crosslinkers and their application to some fabrics. *Thermochimica Acta*, 518, 1–8.

- Anon. (May 2009). *Athletic apparel: A market opportunity*. Cotton Incorporated Supply Chain Insights. Available through the Cotton Incorporated website: <http://www.cottoninc.com>. Accessed 17.05.15.
- Anon. (2010). *Innovations in sports textiles*. CENTEXBEL Info, No.7. Available through the Centexbel website: <http://www.centexbel.be/>. Accessed 17.05.15.
- Barker, R. L. (2002). From fabric hand to thermal comfort: the evolving role of objective measurements in explaining human comfort response to textiles. *International Journal of Clothing Science and Technology*, 14, 181–200.
- Bartels, V. T. (2006). Physiological comfort of biofunctional textiles. In U.-C. Hipler, & P. Elsner (Eds.), *Biofunctional textiles and the skin. Current Problems in Dermatology*, Vol. 33 (pp. 51–66). Basel: Karger.
- Choi, J. K., Cho, G., Kim, P., & Cho, C. (2004). Thermal storage/release and mechanical properties of phase change materials on polyester fabrics. *Textile Research Journal*, 74(4), 292–296.
- Crespy, D., & Rossi, M. R. (2007). Temperature-responsive polymers with LCST in the physiological range and their applications in textiles. *Polymer International*, 56, 1461–1468.
- Dong, Z. E., Hu, J. L., Liu, Y., Liu, Y., & Chan, L. K. (2008). The performance evaluation of the woven wool fabrics treated with shape memory polymers. *International Journal of Sheep and Wool Science*, 56(1), 9–18.
- Geethamalani, R. (2006). The role of phase change material in textiles. *Melliand International*, 12(2), 118–121.
- Ghahremanzadeh, F., Khoddami, A., & Carr, C. M. (2010). Improvement in fastness properties of phase-change material applied on surface modified wool fabrics. *Fibers and Polymers*, 11(8), 1170–1180.
- Glampedaki, P., Dutschk, V., Jovic, D., & Warmoeskerken, M. M. C. G. (2011). Functional finishing of aminated polyester using biopolymer-based polyelectrolyte microgels. *Biotechnology Journal*, 6, 1219–1229.
- Goldman, R. F. (2007). Biomedical effects of clothing on thermal comfort and strain. In R. F. Goldman, & B. Kampmann (Eds.), *Handbook of clothing; Biomedical effects of military clothing and equipment systems* (2nd ed.) [e-book]. Available through the ICEE website: <http://www.lboro.ac.uk/microsites/lds/EEC/ICEE/>. Accessed 17.05.15.
- Hoffman, A. S. (2001). Hydrogels for biomedical applications. *Annals of the New York Academy of Sciences*, 944(1), 2–73.
- Holme, I. (2007). Innovative technologies for high performance textiles. *Coloration Technology*, 123, 59–73.
- Holmer, I. (2004). Thermal manikin history and applications. *European Journal of Applied Physiology*, 92, 614–618.
- Honkala, M. (2006). Introduction to shape memory materials. In H. R. Mattila (Ed.), *Intelligent textiles and clothing* (pp. 85–103). Cambridge: Woodhead Publishing Limited.
- Hu, J. (2007). Shape memory textiles. In J. Hu (Ed.), *Shape memory polymers and textiles* (pp. 305–337). Cambridge: Woodhead Publishing Limited.
- Hu, J., & Mondal, S. (2006a). Temperature sensitive shape memory polymers for smart textile applications. In H. R. Mattila (Ed.), *Intelligent textiles and clothing* (pp. 104–123). Cambridge: Woodhead Publishing Limited.
- Hu, J., & Mondal, S. (2006b). Study of shape memory polymer films for breathable textiles. In H. R. Mattila (Ed.), *Intelligent textiles and clothing* (pp. 143–164). Cambridge: Woodhead Publishing Limited.

- Hu, J., Meng, H., Li, G., & Ibekwe, S. I. (2012a). A review of stimuli-responsive polymers for smart textile applications. *Smart Materials and Structures*, 21(5), 1–23.
- Hu, J., Zhu, Y., Huang, H., & Lu, J. (2012b). Recent advances in shape-memory polymers: structure, mechanism, functionality, modeling and applications. *Progress in Polymer Science*, 37, 1720–1763.
- Huang, J. (2006). Thermal parameters for assessing thermal properties of clothing. *Journal of Thermal Biology*, 31(6), 461–466.
- Jocic, D. (2008). Smart textile materials by surface modification with biopolymeric systems. *Research Journal of Textile and Apparel*, 12(2), 58–65.
- Jocic, D., Tourrette, A., Glampedaki, P., & Warmoeskerken, M. M. C. G. (2009). Application of temperature and pH responsive microhydrogels for functional finishing of cotton fabric. *Materials Technology: Advanced Performance Materials*, 24, 14–23.
- Kopecek, J., & Yang, J. (2007). Hydrogels as smart biomaterials. *Polymer International*, 56, 1078–1098.
- Krizman Lavric, P., Warmoeskerken, M. M. C. G., & Jocic, D. (2010). Microgel functionalized textiles responsive to ambient conditions. In *Proceedings (CD-Rom) of the 10th World Textile conference (AUTEX2010)*. Vilnius, Lithuania, 21–23 June 2010 (4 pages).
- Krizman Lavric, P., Tomsic, B., Simoncic, B., Warmoeskerken, M. M. C. G., & Jocic, D. (2012). Functionalization of cotton with poly-NiPAAm/chitosan microgel: Part II. Stimuli-responsive liquid management properties. *Cellulose*, 19, 273–287.
- Krizman Lavric, P., Warmoeskerken, M. M. C. G., & Jocic, D. (2012). Functionalization of cotton with poly-NiPAAm/chitosan microgel. Part I. Stimuli-responsive moisture management properties. *Cellulose*, 19, 257–271.
- Kulkarni, A., Tourrette, A., Warmoeskerken, M. M. C. G., & Jocic, D. (2010). Microgel-based surface modifying system for stimuli-responsive functional finishing of cotton. *Carbohydrate Polymers*, 82, 1306–1314.
- Kumar, A., Srivastava, A., Galaev, I. Y., & Mattiasson, B. (2007). Smart polymers: physical forms and bioengineering applications. *Progress in Polymer Science*, 32, 1205–1237.
- Laing, R. M., & Sleivert, G. G. (2002). Clothing, textiles and human performance. *Textile Progress*, 32(2), 1–122.
- Lenlein, A., & Kelch, S. (2002). Shape-memory polymers. *Angewandte Chemie International Edition*, 41, 2034–2057.
- Li, Y. (2001). The science of clothing comfort. *Textile Progress*, 31(1), 1–135.
- Li, Y. (2005). Perceptions of temperature, moisture and comfort in clothing during environmental transients. *Ergonomics*, 48, 234–248.
- Liem, H., Yeung, L. Y., & Hu, J. L. (2007). A prerequisite for the effective transfer of the shape-memory effect to cotton fibers. *Smart Materials and Structures*, 16, 748–753.
- Liu, Y. Q., Hu, J. L., Zhu, Y., & Yang, Z. H. (2005). Surface modification of cotton fabric by grafting of polyurethane. *Carbohydrate Polymers*, 61, 276–280.
- Liu, C., Qin, H., & Mather, P. T. (2007). Review of progress in shape-memory polymers. *Journal of Materials Chemistry*, 17, 1543–1558.
- Manner, J., Schuster, K. C., Suchomel, F., Gurtler, A., & Firgo, H. (2004). Higher performance with natural intelligence. *Lenzinger Berichte*, 83, 99–110.
- Mano, J. F. (2008). Stimuli-responsive polymeric systems for biomedical applications. *Advanced Engineering Materials*, 10, 515–527.
- Mather, R. R. (2001). Intelligent textiles. *Review of Progress in Coloration and Related Topics*, 31, 36–41.
- Matilla, H. R. (Ed.). (2006). *Intelligent textiles and clothing*. Cambridge, UK: Woodhead Publishing Limited.

- Mecheels, J. (1977). Körper-klima-kleidung-textil. *Melliand Textilberichte*, 58, 773–776, 857–860, 942–946.
- Mecheels, J. (1998). *Körper-klima-kleidung: Wie funktioniert unsere Kleidung?* Berlin: Schiele & Schön.
- Meng, H., & Li, G. (2013). A review of stimuli-responsive shape memory polymer composites. *Polymer*, 54, 2199–2221.
- Mondal, S. (2008). Phase change materials for smart textiles – an overview. *Applied Thermal Engineering*, 28, 1536–1550.
- Mukhopadhyay, A., & Kumar Mitha, V. (2008). A review on designing the waterproof breathable fabrics. Part I: fundamental principles and designing aspects of breathable fabrics. *Journal of Industrial Textiles*, 37, 225–262.
- Nelson, G. (2002). Application of microencapsulation in textiles. *International Journal of Pharmaceutics*, 242, 55–62.
- Okubayashi, S., Griesser, U. J., & Bechtold, T. (2005). Moisture sorption/desorption behaviour of various manmade cellulosic fibers. *Journal of Applied Polymer Science*, 97, 1621–1625.
- Pause, B. (2003). Nonwoven protective garments with thermo-regulating properties. *Journal of Industrial Textiles*, 33(2), 93–99.
- Pelton, R. (2000). Temperature-sensitive aqueous microgels. *Advances in Colloid and Interface Science*, 85, 1–33.
- Peppas, N. A., & Khare, A. R. (1993). Preparation, structure and diffusional behaviour of hydrogels in controlled release. *Advanced Drug Delivery Reviews*, 11, 1–35.
- Sánchez, P., Sánchez-Fernandez, M. V., Romero, A., Rodríguez, J. F., & Sánchez-Silva, L. (2010). Development of thermo-regulating textiles using paraffin wax microcapsules. *Thermochimica Acta*, 498, 16–21.
- Sánchez-Silva, L., Rodríguez, J. F., Romero, A., & Sánchez, P. (2012). Preparation of coated thermo-regulating textiles using Rubitherm-RT31 microcapsules. *Journal of Applied Polymer Science*, 124(6), 4809–4818.
- Sarier, N., & Onder, E. (2007). The manufacture of microencapsulated phase change materials suitable for the design of thermally enhanced fabrics. *Thermochimica Acta*, 452, 149–160.
- Sarier, N., & Onder, E. (2012). Organic phase change materials and their textile applications: an overview. *Thermochimica Acta*, 540, 7–60.
- Shin, Y., Yoo, D. I., & Son, K. (2005). Development of thermoregulating textile materials with microencapsulated phase change materials (PCM). IV. Performance properties and hand of fabrics treated with PCM microcapsules. *Journal of Applied Polymer Science*, 97, 910–915.
- Spencer-Smith, J. L. (1975). The limitations of Woodcock's "Moisture permeability index". *Textile Research Journal*, 45, 220–222.
- Stylios, G. K. (2006). Engineering textile and clothing aesthetics using shape changing materials. In H. R. Mattila (Ed.), *Intelligent textiles and clothing* (pp. 165–189). Cambridge: Woodhead Publishing Limited.
- Tao, X. (Ed.). (2001). *Smart fibres, fabrics and clothing*. Cambridge, UK: Woodhead Publishing Limited.
- Tomsic, B. (2010). Modification of PES fabric by stimuli responsive microgel using sol-gel technology. In D. Jovic (Ed.), *Surface modification systems for creating stimuli responsiveness of textiles* (pp. 107–122). Enschede, The Netherlands: University of Twente. Available through the University of Twente website: <http://www.utwente.nl/ctw/efsm/advanbiotex/workshop/proceedings/>. Accessed 17.05.15.

- Tourrette, A., De Geyter, N., Jovic, D., Morent, R., Warmoeskerken, M. M. C. G., & Leys, C. (2009). Incorporation of poly(N-isopropylacrylamide)/chitosan microgel onto plasma functionalized cotton fibre surface. *Colloids and Surfaces A: Physicochemical and Engineering Aspects*, 352, 126–135.
- Tuğrul Oğulata, R. (2007). The effect of thermal insulation of clothing on human thermal comfort. *Fibres & Textiles in Eastern Europe*, 15(2), 67–72.
- Vigo, T. L. (1999). Intelligent fibrous materials. *The Journal of the Textile Institute, Part 3*, 90, 1–13.
- Wang, W., & Yu, W. (2015). Preparation and characterization of CS-g-PNIPAAm microgels and application in a water vapour-permeable fabric. *Carbohydrate Polymers*, 127, 11–18.
- Wollina, U., Abdel-Naser, M. B., & Verma, S. (2006). Skin physiology and textiles – consideration of basic interactions. In U.-C. Hipler, & P. Elsner (Eds.), *Biofunctional textiles and the skin. Current Problems in Dermatology*, Vol. 33 (pp. 1–16). Basel: Karger.
- Yee Yan, Y., & Oliver, Y. E. (1996). The clo: a utilitarian unit to measure weather/climate comfort. *International Journal of Climatology*, 16, 1045–1056.
- Ying, B., Kwok, Y., Li, Y., Zhu, Q., & Yeung, C. (2004). Assessing the performance of textiles incorporating phase change materials. *Polymer Testing*, 23, 541–549.

Smart coatings for sportswear

15

M. Manshahia¹, A. Das², R. Alagirusamy²

¹Amity University, Noida, Uttar Pradesh, India; ²Indian Institute of Technology Delhi, Delhi, India

15.1 Introduction

Sports have become highly competitive due to increased participation across the world, and the sportswear market has seen enormous growth in the past two decades. Due to increasing participation in sports and fitness events, the sportswear market has seen its highest growth of 7% in the last 5 years with a total global share of US\$270 billion in 2014 (Research and Markets, 2015). As per the market, sportswear can be broadly classified into three categories: performance sportswear, leisure and outdoor sportswear, and sportswear-inspired clothing. Among these categories, performance sportswear has the highest share, at US\$120 billion in 2014 (Euromonitor, 2015). Performance sportswear enhances the performance of athletes by imparting special functionality like reducing drag resistance as well as providing maximum wear comfort and protection in extreme weather conditions such as rain, snow, extreme cold, and heat.

Innovative materials and remarkable technologies are emerging very fast in this area to provide that extra benefit to players for enhanced performance. Performance swimwear like Speedo[®] became highly popular in the 2004 Olympics and completely changed the scenario of the swimwear market. Lightweight shield by Gore-Tex[®] has completely replaced bulky multilayered protective sportswear. Outlast[®] offered the smart solution for extreme cold clothing with phase changing materials (PCMs). Nike[®] sphere shirt open completely new avenues of moisture-sensitive clothing.

Smart coatings can be defined as those that enable the textile material to sense and respond to any external stimuli, like change in temperature, moisture, strain, etc. This response either could be direct and evidently visible, like change in shape, color, or size, or it could be indirect, like change in molecular configuration, electrical response, etc. (Tang and Stylios, 2006). Phase change materials respond to any temperature change by changing their physical state. Shape memory materials change their shape in response to external stimuli like heat, moisture, light, and electricity. Shape change at the macro level is visible to the naked eye like shrinking and curling of fibers, whereas shape change at the microlevel is not physically visible but may change material porosity. Conductive coatings enable the textile material to sense any mechanical strain and respond in the form of electrical signals.

15.2 Smart coating and functional requirements of sportswear

Functional requirements of sportswear depend on many factors such as the nature and duration of sports, amount of physical activity involved, and atmospheric conditions. All sportswear should provide basic functions like comfort, protection, stretchability, light weight, and dimensional stability. According to the nature of sport, sportswear may provide some special functions such as low aerodynamic and hydrodynamic drag force, compression, and having waterproof, windproof, and health-monitoring capabilities, etc.

One of the basic functional requirements for all types of sportswear is the wear comfort. Wear comfort is important for players as it may enhance performance by providing suitable physiological conditions in all climatic extremities. Wear comfort is comprised of thermophysiological comfort, skin sensorial comfort, ergonomic comfort, and psychological comfort (Das and Aliguruswamy, 2010). Thermophysiological comfort depends on moisture and heat transmission through textile fabric. It determines the microclimatic condition of the player during the course of a game as well as after the completion of the game. In active sports like soccer, tennis, and rugby, sweat rate is extremely high. Therefore, the moisture transmission aspect of thermophysiological comfort becomes a most important functional requirement (Manshahia and Das, 2014). In cold climate sports like skiing, snowboarding, and mountaineering, temperatures may fall to subzero conditions. To maintain the body temperature in these conditions, thermal insulation becomes one of the functional requirements for fabric. Strenuous physical activity is performed in these sports, so high moisture vapor transmission is also required to avoid sweat condensation at the skin. Skin sensorial comfort depends on surface properties, surface friction, roughness, and softness (Bartels, 2005). It may affect skin abrasion, chafing, and skin injury during the course of a game. Ergonomic comfort depends on the fit and freedom of movement. It may affect the air drag in high-speed games, so it becomes very important in aerodynamic sports like cycling, running, skiing, and swimming (Brownlie, 1992).

Another required functionality of sportswear is protection against climate extremes like wind, rain, and snow in sports such as skiing, mountaineering, snowboarding, and alpine running. Protection against ultraviolet (UV) rays also becomes an important functional requirement for someone spending long hours at outdoor sports like golf, cricket, and tennis. As lot of moisture and heat is involved in all sports, and protection against bacteria becomes a required functionality for almost all type of sportswear.

Special functionality is also imparted in sportswear by incorporating smart material and smart coatings. In high-speed games, a little reduced drag force may enhance the performance (Benjanuvatra et al., 2002) and make a difference in this high competition arena. Motion capturing and health monitoring by textiles during sports training may give accurate and elaborate data for performance enhancement (Husain and Kennon, 2014).

15.3 Smart coatings to enhance comfort in sportswear

15.3.1 Phase changing material coating

Phase change process is the change of material physical state from one state to another like solid to liquid and vice versa. Material utilizes its latent heat during phase change processes. PCM changes its physical state within a certain range of temperature. When temperature starts rising, PCM melts and heat is absorbed during melting without any significant change in temperature of the PCM. When temperature starts decreasing, this stored heat is released as a result of solidification of the PCM (Mondal, 2008). This property of PCM enables it to act as a heat storage unit and absorb or release heat while maintaining a nearly constant temperature (Kürklü, 1997; Pause, 2001a,b). Phase change process of PCM is shown in Fig. 15.1.

To utilize the thermal storage capacity of PCM in apparels, PCM should have a melting point between 15°C and 35°C with a small temperature difference between the melting and solidification point. PCM should be stable enough to have a repeated phase change process from solid to liquid and vice versa (Tyagi et al., 2011). To attain this stability, PCM needs to be encapsulated in small spheres by microencapsulation (Buddhi et al., 1987).

These microcapsules are either locked in the fiber or coated on the textile surface. The coating techniques, which can be used for PCM applications, are knife-over-roll coating, transfer coating, or dip coating (Kim and Cho, 2003; Chung and Cho, 2004). In continuous coating, a binder layer used for coating reduces the water vapor permeability of fabric so PCM can be applied in discrete dots by using a screen printing method (Pause, 2010).

Human body core temperature is 37°C and it should be always be maintained in a narrow range of 37°C ± 1°C. Any change in the body core temperature creates thermal discomfort and may lead to various health problems like hypothermia and frostbite in extreme conditions. In active sports, a large amount of metabolic heat is generated due to strenuous physical activity. Heat loss is mainly achieved by evaporation of moisture from human skin. Clothing determines the heat transfer between the body and environment and maintains the thermal balance to attain thermal comfort

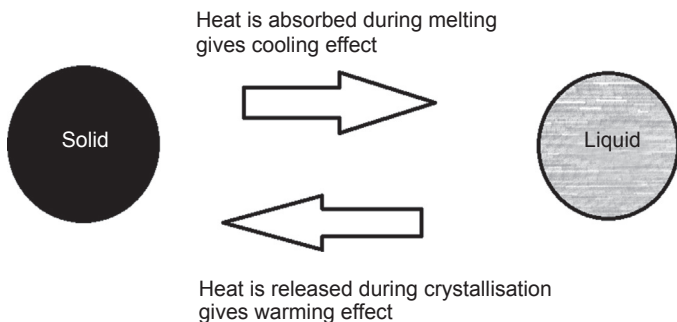


Figure 15.1 Phase change process.

(Das and Aliguruswamy, 2010). Textile structure with PCM microcapsules provides the following benefits (Morikawa and Hashimoto, 2000):

- Cooling effect: when PCM layer temperature rises above 29°C, then it starts melting and becomes liquid. Thermal energy is absorbed during this transition, which provides a cooling effect to the surroundings.
- Heating effect: when PCM layer temperature goes below 27°C, then solidification of PCM occurs and stored thermal energy is released and provides a heating effect to the surroundings.
- Acts as active thermal barrier and adopts itself to thermal needs of human body (Buddhi et al., 1987).
- Acts as a thermoregulating body by keeping the surrounding temperature constant either by heat absorption or by heat emission.

In cold climate sports like skiing, traditional sports clothing is a multilayer ensemble that is passive heat insulating material. Heat transmission through clothing depends on thermal resistance of fabric layers and air layers. During activity, if heat generation exceeds the heat flux from human body to environment, a player feels the thermal discomfort. Moisture vapor condensation may worsen the situation and result in a sudden and large reduction in thermal resistance, which may cause postexercise chill to the player. In these conditions, PCM provides an active thermal insulation system by absorbing and storing excess heat generated during activity. At the end of a game, when metabolic heat generation falls sharply, PCM releases stored heat and maintains the heat flux through the multilayer (Pause, 2001a,b).

In skiwear, textile fabrics dotted with a coating of PCM microcapsules are preferred to attain breathable and lightweight garments. In the multilayer clothing of skiwear, a temperature gradient exists through different layers of a garment ensemble. Temperature decreases from skin through layers of ensemble into environment. Selection of PCM should correspond to the ambient temperature of the layer. The phase transition temperature of PCM applied on the innermost layer should be higher than those applied on outermost layer (Pause, 2001a,b). In skiwear, the preferred location of PCM microcapsule coating is between the inner liner and insulation layer of the suit.

Fabric coating with microencapsulated PCM has been exploited by *Outlast Technology* (n.d.). Products with *Outlast*[®] technology buffer the changes in humidity and temperature in microclimate and external environment. They maintain constant body temperature by absorbing excess body heat when the temperature starts rising due to heat production and releasing it when the temperature falls during cooling (Anon., 2007).

Lower heat stress has been reported for PCM-incorporated helmets. In this helmet, PCM Octadecane polymer with T_m 28.2°C and heat storage capacity 244 J/g has been used in the form of aluminum foil pouches. The embedded PCM is reported to provide cooling for 20 min as compared to the conventional helmet (Halimi et al., 2012).

A polyester vest with 21 pieces of incorporated PCM shows better cooling effect, which lasts for 8 h as compared to a vest without PCM. After strenuous cycling activity, human subjects wearing a PCM vest have chest skin temperature lower by 3°C and body core temperature lower by 0.5°C in comparison to human subjects without these vests (Gao et al., 2007).

15.3.2 Shape memory polymers

Shape memory polymers (SMPs) have the ability to change their shape when exposed to external stimuli like heat, moisture, light, and electricity (Hu, 2013). SMPs are set to a permanent shape that is maintained by cross-links or net points of morphological structure. When SMPs are subjected to deformation, a temporary shape is achieved. This temporary shape is created and maintained by switchable segments (Hu et al., 2012).

In permanent shape, internal stresses are zero. When SMPs are deformed, internal stresses are developed and stored in a structure and temporarily get fixed. The switch to maintain this shape may be crystallization, glass transition, or liquid crystals phase. On exposure to external stimuli, these internal stresses are released and the material recovers to its original shape (Takahashi et al., 1996).

15.3.2.1 Temperature responsive shape memory polymers

Temperature acts as external stimuli for shape recovery for temperature responsive SMPs. In sportswear applications, shape memory polymer-based polyurethane (SMPU) with temperature sensitive moisture vapor permeability is used. Switching temperature (T_{Trans}) is chosen close to human body temperature and provides higher thermophysiological comfort by altering moisture vapor transmission according to skin temperature (Hu et al., 2002). During physical activity body temperature increases, and when it exceeds the T_{Trans} of SMPU, free space within the structure increases, which increases the moisture vapor flow across the fabric and keeps the body cool and comfortable (Hyashi, 1993). At rest, when the body temperature falls below the T_{Trans} of SMPU, free space decreases, which further reduces the moisture vapor flow and keeps the body warm. SMPU-based commercial product “Diaplex” fabrics have been developed (Hayashi et al., 2004), which change the free volume within fabric with the change in temperature. It has been suggested that intermolecular bonds relax above a switching temperature and micro-Brownian motion is achieved. Fabric resistance to air and moisture vapor changes according to skin temperature. Other products like “Membrain” (Maramot, n.d.) also claimed to use micro-Brownian motion to show temperature-dependent water vapor permeability. SMPU-coated fabrics can be used in various types of sportswear like cycling gear, diving suits, and mountaineering clothing.

15.3.2.2 Moisture responsive shape memory polymer

Moisture acts as external stimuli for moisture responsive SMPs. Moisture increases the molecular flexibility and acts as a switch for shape transformation in these SMPs (Huang et al., 2005; Hu and Zhuo, 2010). Moisture-responsive SMPs are used to make activewear with intelligent moisture management. Dawson et al. (1997) has developed an SMP-incorporated moisture sensitive textile that is biomimetic of the pinecone mechanism.

Trees that produce pinecones are moisture-sensitive plants that change their flower opening (the pinecones) according to the moisture content. Moisture-responsive

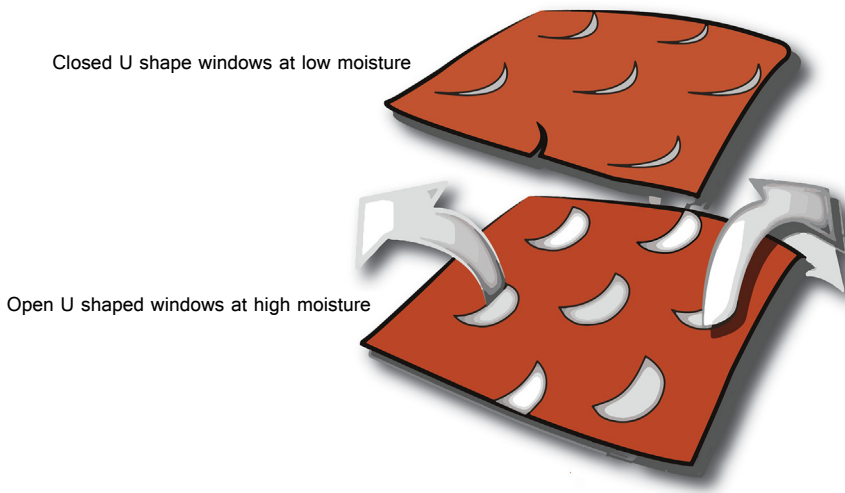


Figure 15.2 Nike sphere react shirt.

Adapted from Nike Innovations, 2013. Sustainable Innovations (Online). Available at: <http://www.nikeresponsibility.com/innovations> (accessed 22.08.15.).

shape-memory fabric shows a similar behavior. These moisture-responsive fabrics are single or composite textile structures with many tiny spikes on the outer layer that will open to cool down the body in hot temperatures and then again flatten down to trap air and provide insulation in cold temperatures (Pine cone cloths, 2004).

Nike has developed a smart shirt, “Sphere react shirt,” based on a similar principle (US 20050208860, 2005; Fig. 15.2). It is a bilayer structure with different swelling properties of each layer. The outer layer is nonswelling and nonhygroscopic, whereas the next-to-skin layer is hygroscopic in nature. U-shaped cuts are created on the outer layer using laser cutting. During activity excess sweat is generated, which causes the inner layer to swell whereas the outer layer remains unaffected. Moisture acts as stimuli for moisture responsive SMPs and causes the U-shaped windows to curl back. These open windows increase the air permeability and cool down the body with faster drying. When the player is at rest, the windows close and increase the fabric insulation to keep the player warm (Hu and Meng, 2011).

Moisture-responsive shape memory fiber has been patented by Teijin Ltd that shows a self-crimping behavior (JP2003239141, 2013). In higher sweat conditions, fibers get crimped, which increases the surface roughness. This shape transformation reduces the contact points between fabric and skin, which enhances the sensorial comfort of the player.

15.3.3 Moisture management hydrophilic coatings

In active sports the sweat generation rate is very high, so moisture management becomes a very important functional requirement of high active sportswear. Moisture management

may improve the performance of players by providing better sweat transmission, quick drying, reduced “sticky” tactile sensations, and enhanced comfort. Moisture transmission takes place via three processes: absorption, wicking, and evaporation. For active sportswear, higher wicking and faster evaporation are required to enhance comfort and performance (Manshahia and Das, 2014). Moisture management mainly depends on the surface energy of the material, which further depends on the chemical structure of the surface. Chemical finishes change the surface chemistry, hence change the surface energy. Special finishes can create different surface energy on either side of the fabric to promote rapid moisture transmission along the fabric.

Functional sportswear with distinct hydrophilicity was developed by graft polymerization process (Okubo and Saeki, 2008). Polyester fabric, with a hydrophobic inner side and hydrophilic outer side, was created with graft polymerization of acrylic acid on its surface. This type of structure is reported to have superior moisture management with effective dispersion of sweat along the fabric thickness.

Active carbon-coated polyester fabric has been found to have improved moisture comfort due to absorption of sweat impulses by carbon particles (Splendore et al., 2010). However, this structure is reported to have a slow drying rate, which restricts its use in mild physical activity, with a low amount of sweat, but not in high strenuous exercise (Splendore et al., 2011).

Hydrophilic finishes, like MMF Resil HJHP, are used to increase the absorbency in polyester, whereas other finishes, like Resil Nanocelle G6, increase the wicking along with absorbency (Manickam, 2006). The nano dry finish for Nanotex LLC has polyethylene glycol and amino silicone in nano form. This finish is reported to improve absorbency of sweat in high active sportswear (Holmes, 2007).

Polyester fabric contact angle can be reduced to zero by surface modification using UV irradiation/nano-TiO₂. Modified polyester fabric became highly hydrophilic with improved wettability (Liang et al., 2013). Microdenier polyester fabric treated with moisture management finish (MMF), composed of a combination of hydrophilic polymer and amino silicon polyether copolymer, is reported to show better wicking, absorbency, and quicker absorption as compared to untreated fabric (Sampath and Senthilkumar, 2009).

15.4 Smart coating to provide protection

15.4.1 Protection against weather by waterproof, breathable coating

Waterproofing is a required functionality of sportswear in many sports like mountaineering, skiing, diving, rafting, cycling, and golfing. Human body core temperature should be well maintained within its narrow limits, and inclusion of water or wind reduces the thermal insulation of a clothing system and may lead to drastic temperature fall. So sportswear must protect athletes against wind and rain and maintain the body core temperature. In earlier days, rubber coating and PVC coating were used to

waterproof fabrics, but these coatings also make the fabric impermeable to water vapors. These rubber coatings completely fill the fabric pores and make the fabric unbreathable and uncomfortable to wear. This led to development of waterproof yet breathable coatings.

One of the techniques is using a microporous membrane, in which very fine pores are created in an impermeable membrane. The size of pores is much smaller than a water droplet but large enough for water vapor to pass through. Gore-Tex[®] is the most revolutionary product in this category, which is made up of stretched polytetrafluoroethylene (PTFE) membrane. This microporous PTFE film has 9 billion pores per square inch, where pore size is 700 times than that of water vapor but 1/20,000 of a water droplet (Gore-Tex, n.d.). Gore-Tex[®] membrane is laminated to the outer side of fabric and makes it impermeable to water and wind but allows perspiration to pass through. The maximum pressure that Gore-Tex[®] (2012) can sustain without getting wet is of 30 psi. Gore-Tex[®] fabric is a two-layer construction in which Gore-Tex[®] membrane is laminated to the outer material and the lining is independently placed under it. This product provides protection and comfort in many sports like, golfing, cycling, running, skiing, and snowboarding. Gore-Tex Pro[®] is a three-layer construction in which Gore-Tex[®] membrane is sandwiched between an outer layer and inner lining. This is a very durable product used for sports in extreme conditions like winter climbing, mountaineering, snowboarding, and sailing. Gore-Tex Active[®] is an ultralightweight microdenier three-layer system in which lining is integrated as backing to finer and lighter Gore-Tex[®] membrane. It provides maximum breathability as compared to two other products with similar protection. It is preferred in active sports like alpine running, endurance running, and fast-ascent mountaineering.

Polyurethane (PU) microporous membranes are also used in waterproof breathable fabrics. Porelle Dry[®] is a microporous PU membrane (Porelle Membranes, n.d.) with micropores of less than 1 μm , which help to diffuse water vapor from the skin to the outside environment. It claims to provide a super dry feel even after repeated washing due to hydrophobic nature of PU. Breathable PU membranes have been developed by electrospinning the polymer using a metal mesh conductor. It shows high moisture vapor transfer due to larger pores as compared to membranes made using a conventional collector electrode (Hong et al., 2007).

Dermizax NX[®] is the latest waterproof breathable PU membrane developed by Toray Industries (Torayentrant, n.d.). It claims to minimize the condensation with double breathability and super stretch than its previous product, Dermizax EV[®].

The other method to achieve waterproof yet breathable function is using a hydrophilic membrane, which is a nonporous film composed of hard segments (urethane chains) with soft segments (hydrophilic molecules, ie, $-\text{O}-$, $-\text{OH}$, $\text{CO}-$, $-\text{NH}_2$) as a block copolymer. Hard segments make the waterproof and soft segment is responsible for water vapor transfer. The water vapor makes a weak bond with a hydrophilic molecule and remain there until replaced by another water molecule. This type of chain action causes the water vapor to diffuse through the membrane (Painter, 1996). Temperature and relative humidity difference is the driving force for water vapor transfer. Hydrophilic molecules act as transfer agents and moisture vapor transfer takes place by adsorption, diffusion, and desorption (Lomax, 1990).

Breathable nonporous PU film was developed by copolymerization of low molecular difunctional compound, polyethylene glycol (PEG) and diisocyanate, whereas PEG is soft segment and incorporated as 25–40% by weight (US 4367327, 1983). Smart temperature-controlled PU film with PBA/PEG multiple polyol as soft segments has been developed. Water vapor transmission of film drastically increases above its glass transition temperature. It has been reported that WVP (water vapor permeability) of film increases but mechanical strength decreases with increase in PEG content (Lin and Siao, 2007). Sympatex is the commercial hydrophilic solid film that is based on the copolymer of polyester and polyether and has thickness in the range of 5–25 μm (Sympatex).

It has been reported that two-layer microporous membranes perform better and are more permeable to water vapors as compared to hydrophilic membranes and coatings in isothermal conditions, whereas hydrophilic solid film is more breathable in nonisothermal conditions (Ren and Ruckman, 2003). Microporous films are less durable and their performance deteriorates due to blockage of pores with contamination, body oils, dirt, etc., as well as waterproofing characteristics may be affected when film is stretched at knees and elbows. Hydrophilic films and coatings are not affected by washing or stretching (Desai and Athawale, 1995). The presence of rain causes saturation of hydrophilic sites in hydrophilic membranes or coatings, causing a wet and clammy sensation (Holmes, 2000; Weder, 1997).

A wetsuit for water sports has been developed in which waterproof breathable fabric panels are systematically placed on the suit to cover areas of high heat generation like armpits, inner thighs, behind the neck, and chest portions. This is reported to provide more stretch and improved comfort of the wearer due to better heat dissipation (US 2012/0023631 A1, 2011).

15.4.2 Protection against ultraviolet radiation

Protection against the sun's rays has become very important nowadays as players have to face long exposures to sunlight in outdoor games. Due to depletion of the ozone layer, these long sun exposures become very detrimental to human skin and may cause skin-related diseases like sunburn, blotching, premature aging of skin, and skin cancers (Pailthorpe and Chriskis, 1995). Effects of UV radiation depend on many factors such as geographical location, altitude, cloud cover, environmental conditions, and skin type (Dornelles et al., 2004). UVB rays are short-frequency radiation (290–320 nm) and are more harmful as compared to UVA radiation (320–400 nm). Effects of UV radiation on human skin can be measured by UV protection factor (UPF) and sun protection factor (SPF). UPF is the ratio of risk in case of unprotected surface to risk involved in protected surface, whereas SPF is defined as threshold time for an effect to take place with protection to time taken without protection (Ilefiker et al., 1996).

To attain UVR protection in textile materials, UV absorbers are incorporated in textile material either at extrusion stage (Gantz, 2003) or applied on fabric surface using coating (Rupp et al., 2001). These are colorless compounds that absorb UV rays in the range of 290–360 nm. These compounds absorb shortwave UV energy and convert it to longwave thermal energy or break into nonabsorbing fragments (Holme, 2003). Commonly used UV absorbers in coating and padding are

benzotriazole, phenyltriazene, and hydroxybenzophenone. Benzophenone derivatives are easily diffusible but have low sublimation fastness, whereas diphenyltriazine derivatives have a self-dispersing property with excellent sublimation fastness, which makes them suitable for high-temperature dyeing and printing (Achwal, 1994). It has been reported that the introduction of a sulfonic group in benzophenone and benzotriazole moiety shows extremely high UVR protection (Oda, 2011). Titanium dioxide added as dope additive shows good UVR absorption in the spectrum range of 290–400 nm (Joshi and Reddy, 2005). Zinc oxide (ZnO) nanoparticles are reported to have good UV protection when applied in a narrow range of size with minimum aggregation (Antaria, n.d.). TiO₂ nanoparticles applied on cotton fabric are reported to have higher UPF (50+) as compared to ZnO nanoparticles (Paul et al., 2010). UV protection is reported to be further enhanced for nylon with a mixture of TiO₂ and ZnO in ratio of (2:1) instead of 100% ZnO (Gupta et al., 2002). In swimwear fabrics, polyamide elastane fabric is found to give better UV protection as compared to polyester elastane fabrics. Further, it was found that optical bleaching pretreatment increases the UPF factor of swimwear fabric.

15.4.3 Protection against microorganisms

In active sports, the presence of moisture on fabric and heat generates ideal conditions for microbial growth and propagation. Most of the sportswear is made up of synthetic fibers and stale perspiration in fabric pores encourages microbial growth as reported by higher foot infections in people who wear synthetic socks as compared to cotton socks. Polyester is reported to increase bacterial adherence and bacteria persist for longer duration with an increase in polyester content in fabric (You and Merry, 1986). Microbial growth causes various health problems like pyrogenic infection, skin infections, and foul body odors, as well as fabric degradation (Kloos and Musselwhite, 1975). Body odor is produced by the metabolism of various gram-positive or gram-negative bacteria. For example, during metabolism action of gram-positive bacteria *Staphylococcus aureus*, it converts human sweat into odor-producing molecules like carboxylic acid and amines (Mao and Murphy, 2001). Microbial attack may also cause the degradation of synthetic fiber-like nylon, polypropylene, and PU (Yau, 1988).

A living microbe has a cell wall that protects the integrity of its cellular components and protects them from extracellular environment. Antimicrobial agents destroy this cell wall and inhibit the enzyme and lipid activity required for cell survival (Gao and Cranston, 2008). Heavy metals are very effective for killing microorganisms and bacteria, and silver, in particular, is very effective in warm and moist environments. Silver ions attach themselves to the cell wall and inhibit the cell respiration and cell reproduction. Silver can be incorporated during extrusion (Yeo et al., 2003), during electrospinning (Son et al., 2006), or can be applied as a coating of nano-sized silver colloidal solution (Williams et al., 2005). Ultra Fresh[®] and Silphure[®] developed by Thomson Research Associates are based on a coating of ultrafine silver particles and are mainly used for polyester fabrics. AgION technologies developed antimicrobials with silver particles in a zeolite carrier, which works on the ion exchange mechanism. In moist conditions, silver ions are exchanged with sodium

ions of sweat and control the bacterial growth (Bio Shield Tech, n.d.). Polymer nanocomposites with nanosilver particles are reported to have excellent antimicrobial action against both gram-positive and gram-negative bacteria. Hybrid (SiO₂/AG) coatings create good dispersion of silver nanoparticles in silica polymer matrix and have been found to have good antibacterial properties (Marek et al., 2009). TiO₂/AG nanocomposite synthesized by sol–gel technique showed excellent antimicrobial activity against gram-negative bacteria *Escherichia coli* (Amin et al., 2009).

15.5 Smart coating for performance enhancement

15.5.1 Drag in sports

In speed sports, like cycling, skiing, sprinting, and swimming, there are mainly three forces acting against the athlete's movement: drag, friction, and inertia. Drag force is determined by using Eq. [15.1] (White, 1991):

$$D = \frac{1}{2}AC_d\rho V^2 \quad [15.1]$$

where D is drag force, A is frontal area, C_d is drag coefficient, ρ is air density, and V is the wind speed. Power required to overcome drag is proportional to the cube of speed, so in speed sports like cycling, the component of drag force can be as high as 80% of total forces acting on the athlete. Total drag acting on anybody is composed of skin friction drag and pressure drag. In flat bodies, skin friction is the main component, whereas in bluff bodies like cylinders, pressure drag contributes up to 90% of total drag. During flow transition from laminar to turbulent for bluff bodies, skin friction drag increases but pressure drag reduces to a great extent due to shifting of separation point to back (White, 1991).

Drag coefficient is a function of motion, shape, and surface. Motion and shape depend on speed, acceleration, body size, body shape, and body posture, whereas surface depends on surface roughness, surface coating, and surface porosity.

Aerodynamic optimization of an athlete in any sport depends on many factors, which are as follows (Lukes et al., 2005):

- Speed: Speed is an important factor in affecting the aerodynamic efficiency of an athlete. Average speeds for different aerodynamic sports are 30–60 km/h for cycling, 90–100 km/h for ski jumping, 80–120 km/h for downhill skiing, 112 km/h for swimming. Speed determines the flow transition from laminar to turbulent (Chowdhury et al., 2010).
- Body position: Body position of an athlete also influences the aerodynamic efficiency. Body position decides the angle of attack, which further determines the drag and lift generation (Grappe et al., 1997).
- Fabric properties: Aerodynamic characteristics of sportswear are influenced by fabric parameters like fabric surface roughness, fabric grain, and fabric air permeability. Aerodynamic drag and lift is significantly influenced by surface roughness due to transitional properties of the boundary layer of sportswear. Aerodynamic drag is found to be directly related to air permeability of fabric (Brownlie, 1992).

- Garment construction: In sportswear construction, various pieces of fabric are joined together with seams or fasteners. Type and placement of seams influence the airflow regime and aerodynamic drag. Fabric grain and wale orientation in different parts of a garment are also reported to influence the aerodynamic behavior of sportswear.
- Fitting of garments: Skin suits reduce the drag as compared to loose-fitting sportswear. A two-size large suit is reported to increase the drag by 3% in a skiing suit as reported by [Kyle et al. \(2004\)](#).

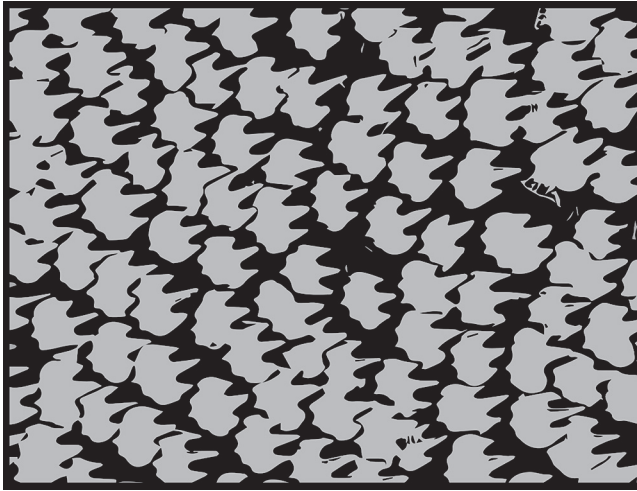
15.5.2 Drag reduction in swimwear

In swimming, three types of drag are offered; skin friction drag, pressure drag and wave making drag ([Wu, 2011](#)). Skin friction drag is the drag between surface and water. Pressure drag is the resistance generated due to differential pressure along the swimmer body. Wave drag is the drag offered due to swimmer movement in wave form over and under water. Surface smoothness and roughness influence the skin friction drag which can be reduced by using better design of swimwear.

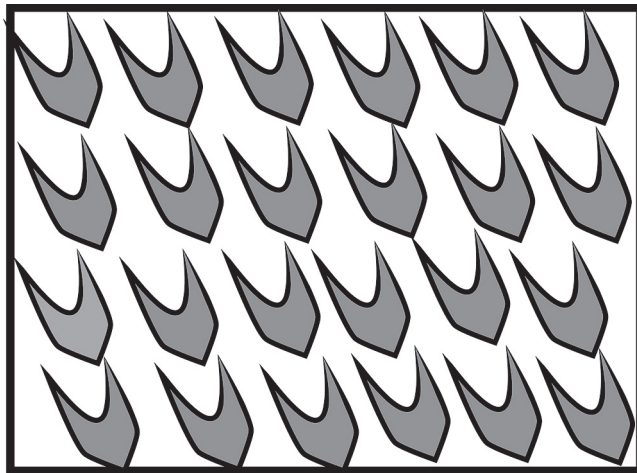
Biomimetic swimsuit *Fastskin*[®] developed by *Speedo*[®] is inspired from shark skin (see [Fig. 15.3](#)). The denticles of shark's skin and super stretch property of fabric can enhance the performance of swimmer by shape retention, muscle compression and reduced drag coefficient ([Benjanuvatrat et al., 2002](#)). On shark skin, there are V shaped ridges known as denticles. These denticles create turbulence on shark's skin and reduce the surface drag. In *Fastskin*[®] and second version of *Fastskin*[®] FSII, similar structure is created by peaks and valleys. During flow, only peaks comes in contact with water and allow water to pass more effectively by reducing the skin friction drag.

Speedo introduced its next generation swimsuit, *LZR pulse* fabric, which is woven fabric composed of 65% of chlorine resistant ultrafine nylon and 35% of elastane with water repellent plasma coating. Seams have been replaced with ultrasonic welding to reduce the flow disturbance around joints of suit. PU panels have been placed in selected portion of suit which faces higher drag during swimming stroke. Higher elastane content creates the necessary compression and increase the muscle power ([Frickle, 2010](#)). This suit has gained enormous popularity in Olympics games in 2008. Polyamide elastane fabric with mechanochemical coating reported to have higher contact angle and lower drag force as compared to polyamide fabric. This coating makes the fabric water repellent and reduces the spreading asymmetry. Better performance and high hip linear velocity has been reported with coated professional swimsuit in butterfly stroke of swimming ([Rogowski et al., 2006](#)).

Innovative swimwear reduces the drag and imposes less physiological stress on swimmer. Lower VO_2 level ([Smith et al., 2007](#)), lower heart ([Tiozzo et al., 2009](#)) rate and higher blood lactate ([Roberts et al., 2003](#)) has been reported with this swimwear as compared to conventional swimwear. All these parameter reduce the swimmer fatigue and increase the performance. With Innovative swimwear, Higher swimming speed ([de Lucas et al., 2000](#)) and the higher stroke distance has been reported.



Denticles on shark skin



Speedo Fastskin swimwear mimicking the shark denticles

Figure 15.3 Speedo Fastskin fabric surface inspired form shark denticles.

Adapted from Speedo, 2015. Speedo Fastskin (Online). Available at: <http://www.speedo.co.uk/technology/fastskin> (accessed 22.08.15.).

15.5.3 Drag reduction in skiing, cycling

In high-speed sports like skiing, cycling, and sprinting, drag reduction can be achieved by optimizing the surface roughness. In textile materials, roughness can be optimized at different levels (Wieland et al., 2000): at the macrostructure where surface modification can be done like a dimpled surface; at the microstructure where roughness is

induced by fabric structure like being knitted or woven; and at third level is the yarn fuzziness. It has been reported that rough macrostructure with no microscale roughness reduces the drag coefficient. This type of structure was used in a dimpled sprinting suit in the 2012 Olympics (Oggiano et al., 2013).

Aerodynamic characteristics of fabric depend on fabric cover factor and surface roughness. Smooth fabric reduces the drag at low angle of attack and at high speed range, whereas, rough fabrics show lower drag coefficient at lower range of speed (Oggiano et al., 2009) at angle of attack greater than 45 degree. At higher roughness, flow transition shifts early at lower speed resulting in lower drag at lower speed but higher drag at higher speed. So rough fabric would be beneficial for long distance sports and smooth fabric should be used for short distance events where average speed is higher (Oggiano and Sætran, 2008).

PU coating delays the flow transition. In speed skiing where early transition is not required, PU coating increases the smoothness and reduces the skin friction. Sublimation printing on coated fabric changes the surface topology and permeability of fabric and is reported to increase the fabric smoothness. In sprinting, significant increase in performance has been reported by reducing the aerodynamic drag. Timing improved by 0.01 s for 100 m sprint and 5.7 s in marathon by 2% reduction in drag resistance (Kyle and Caiozzo, 1986).

Fabric with lower cover factor and higher air permeability shows higher drag as compared to fabric with lower permeability (Holden, 1988). This may be due to the trapped air in permeable structure, which increases the skier mass and increases the drag. Tight-fitting skin suits reduce the frontal area and reduce the drag.

15.6 Smart textiles for health and motion monitoring in sportswear

In sports training, human motion capturing and health monitoring are useful tools to measure the athlete's well-being and improve his performance. As textiles cover most of the athlete's body, so they can act as an interactive interface for sensing by imparting sensors and electrical conductivity in an appropriate way (Paradiso et al., 2014). Electrical conductivity is the main functional requirement for any textile to perform as a sensor for biomechanical sensing and health monitoring. Various methods can be found in the literature to impart electrical conductivity in textiles, such as metallic fiber blending at pre-spinning stage, bicomponent fibers with polymer matrix embedded in conductive layer of metal compounds or carbon black, and metallic or galvanic coating of fibers (Paradiso et al., 2014).

For biomechanical sensing, a sensor based on piezoresistive principle is used, which is based on measuring the change in electrical resistance when induced to mechanical strain. During human body movement, small fabric deformation occurs, which changes the current path in conductive filament of fabrics and hence electrical resistance. This type of sensor can be used to monitor a wide range of human movement configurations like elbow, wrist, knee, and ankle articulations

(Pacelli et al., 2006). Mechanical signals generated by body movement can also be used to measure some physiological parameters like breathing rate. Low-frequency mechanical signals are generated during breathing, which can be measured by strain gauge. One approach uses silver-plated fibers for manufacturing conductive fabric sensor electrical conductive yarns that measure the resistance change during breathing movement (Frydrysiak and Zi Öba, 2012). The SuperNova® Glide Bra developed by Adidas is based on same signals, which is used to monitor heart rate (Styletime, n.d.). In another approach, screen printing with conductive paste was used to apply strain sensors which produce similar results as the first method (Furtak et al., 2013). Fabric coated with a thin, conductive polymer layer of polypyrrole is reported to have temperature- and strain-sensing capabilities (De Rossi et al., 1999). The Hetero optical wire-based sensor is also used to capture body motion. The developed system has sensors sewn to cloth and used to measure the athlete's trunk movement, such as when a golf swing is performed (Koyama et al., 2013).

Temperature-sensing fabrics have also been developed by combining temperature-sensitive metallics wired with textile yarns on a flatbed knitting machine. This sensor is based on a resistance temperature detector and measures the temperature change by measuring the corresponding change in electrical resistance (Husain and Kennon, 2014). Biotex projects have developed a sweat analysis system to analyze various parameters related to sweat like sweat quantity, composition, salinity, pH, and oxygen saturation of blood (Coyle et al., 2010). In this system various sensors based on electrical, electrochemical, and optical principles are positioned on various places of clothing.

15.7 Conclusions

Sportswear has emerged as a fast-growing textile sector with innovative materials and the latest technologies. Sportswear is a niche market, where price is not usually a considerable factor, because the strong emphasis is on performance enhancement. In highly competitive sports, when the human body reaches its upper limit of endurance, technology can play its part to provide that special winning edge. With special functionality and smart technologies, sportswear is considered as power skin instead of second skin. It may reduce the muscle fatigue and improve the physical endurance while maintaining the athlete's well-being in the toughest climatic conditions.

Smart coating like PCM, SMP, conductive coating, and nanocoating are being well exploited to develop new sportswear products. SMP opens up new opportunities to develop smart sportswear, which functions according to the physiological condition of the player. PCM enables development of smart sports gear, which adapt per the changes in atmospheric conditions. Conductive coatings can be used to develop more flexible textile sensors for motion capturing and health monitoring in sports training. All these smart coatings provide required functions as per the design, but the biggest challenge is to increase their durability with repeated laundering. Innovative special functional sportswear can be designed with better understanding of performance affecting parameters, and finding solutions with smart textiles and smart coatings.

References

- Achwal, L.W.B., 1994. Use of UV absorbers for minimising photodegradation of disperse dyes as well as polyester fibres. *Colourage* 6, 21–22.
- Amin, S.A., Pazouki, M., Hosseinnia, A., 2009. Synthesis of TiO₂–Ag nanocomposite with sol–gel method and investigation of its antibacterial activity against *E. coli*. *Powder Technology* 196, 241–245.
- Anon., November 2007. Smart sportswear signs with outlast. *Apparel Magazine* 44.
- Antaria, n.d. Zinclear (Online). Available at: <http://www.antaria.com/irm/content/zinclear-range.aspx?RID=295&RedirectCount=1> (accessed May 2015).
- Bartels, V.T., 2005. Part III: sportswear and comfort. In: Bartels, V.T. (Ed.), *Textile in Sports*. Woodhead Publication, Cambridge, UK, pp. 177–200.
- Benjanuvatra, N., Dawson, G., Blanksby, B.A., Elliott, B.C., 2002. Comparison of buoyancy, passive and net active drag forces between Fastskin™ and standard swimsuit. *Journal of Science and Medicine in Sport* 5, 115–123.
- Bio Shield Tech, n.d. The AgION® Technology Behind the Performance (Online). <http://www.bioshieldtech.com/tech.html> (accessed 2015).
- Brownlie, L.W., 1992. *Aerodynamic Characteristics of Sports Apparel* (Ph.D. thesis). University of British Columbia, Canada.
- Buddhi, D., Sawhney, R., Sehgal, P.N., Bansal, N., 1987. A simplification of the differential thermal analysis method to determine the latent heat of fusion of phase change materials. *Journal of Physics D: Applied Physics* 20, 1601–1605.
- Chowdhury, H., Alam, F., Subic, A., 2010. Aerodynamic performance evaluation of sports textile. *Procedia Engineering* 2 (2), 2517–2522. Elsevier, UK.
- Chung, H., Cho, G., 2004. Thermal properties and physiological response of vapour-permeable water-repellent fabrics treated with microcapsule-containing PCMs. *Textile Research Journal* 74 (7), 571–575.
- Coyle, S., et al., 2010. *IEEE Transactions on Information Technology in Biomedicine* 14 (2), 364–371.
- Das, A., Aliguruswamy, R., 2010. In: Das, A., Aliguruswamy, R. (Eds.), *Science in Clothing Comfort*. Woodhead Publishing, New Delhi, India.
- Dawson, C., Vincent, J.F.V., Rocca, A., 1997. How pine cones open. *Nature* 390, 668–675.
- Desai, V.M., Athawale, V.D., 1995. Water resistant breathable hydrophilic polyurethane coatings. *Journal of Coated Fabrics* 25 (1), 39–46.
- Dornelles, S., Goldim, J., Cestari, T., 2004. Determination of the minimal erythema dose and colorimetric measurements as indicators of skin sensitivity to UV B radiation. *Photochemistry and Photobiology* 79 (6), 540–544.
- Euromonitor, 2015. *New Insight in Apparel and Footwear Market in 2015* (Online). Euro-monitor International. Available at: <http://www.euromonitor.com/sportswear> (accessed June 2015).
- Frickle, 2010. Speedo's LZR: The World's Fastest Swimsuit (Online). Available at: http://www.stc-orlando.org/education/highsch/winning_entries/2010_rfricke.pdf (accessed May 2015).
- Frydrysiak, M., Zi Ōba, J., 2012. Textronic sensor for monitoring respiratory rhythm. *Fibres and Textiles in Eastern Europe* 20 (2), 74–78.
- Furtak, N.T., Skrzetuska, E., Krucińska, I., 2013. Development of screen-printed breathing rate sensors. *Fibres and Textiles in Eastern Europe* 21 (6), 84–88.
- Gantz, G.M., 2003. Stable ultraviolet light absorbers. *Textile Research Journal* 27 (3), 244–251.

- Gao, Y., Cranston, R., 2008. Recent advances in antimicrobial treatments of textiles. *Textile Research Journal* 78 (1), 60–72.
- Gao, H., Kuklane, K., Holmér, I., 2007. Cooling effect of a PCM vest on a thermal manikin and on humans exposed to heat. In: Mekjavic, I.B., Kounalakis, S.N., Taylor, N.A.S. (Eds.), *Environmental Ergonomics XII*. © BIOMED, Ljubljana.
- Gore-Tex, 2012. Gore-Tex Retails Training Manual (Online). Available at: <http://www.gore-tex.com/remote/Satellite/content/our-fabrics#sec-waterproof> (accessed May 2015).
- Gore-Tex, n.d. Gore-Tex Technology (Online). Available at: <http://www.gore-tex.com/remote/Satellite/content/our-fabrics#sec-waterproof> (accessed May 2015).
- Grappe, F., Candau, R., Belli, A., Rouillon, J.D., 1997. Aerodynamic drag in field cycling with special references to the Obree's position. *Ergonomics* 40 (12), 1299–1311.
- Gupta, K.K., Tripathi, V.S., Ram, H., Raj, H., 2002. Sun protective coatings. *Colourage* 6, 35–40.
- Halimi, M.T., Hassen, T.B., Sakli, F., 2012. Design of a novel comfort liner for a motorcycle helmet. *International Journal of Sustainable Engineering* 5 (2), 128–134.
- Hayashi, S., Tasaka, Y., Hayashi, N., Akita, Y., 2004. Development of Smart Polymer Materials and Its Various Applications, vol. 41. Mitsubishi Heavy Industries, Ltd, pp. 1–3 (Technical Review).
- Holden, M., 1988. The aerodynamic of skiing. *The Technology of Winning* 258.
- Holme, I., 2003. UV absorbers for protection and performance. *International Dyer* 9–10.
- Holmes, 2000. Performance characteristics of waterproof breathable fabrics. *Journal of Industrial Textiles* 29 (4), 306–316.
- Holmes, J., 2007. Innovative technologies for high performance textiles. *Coloration Technology* 123, 59–73.
- Hong, S.K., Lim, G., Cho, S.J., 2007. Breathability enhancement of electrospun microfibrinous polyurethane membranes through pore size control for outdoor sportswear fabric. *Sensors and Materials* 27 (1), 77–85.
- Hu, J., 2013. Introduction to shape memory polymers. In: Hu, J. (Ed.), *Advances in Shape Memory Polymers*. Woodhead Publishing, Cambridge, UK, pp. 1–22.
- Huang, W.M., Yang, B., Li, C.L., Chan, Y.S., 2005. Water-driven programmable polyurethane shape memory polymer: demonstration and mechanism. *Applied Physical Letter* 86, 11410501–11410503.
- Hu, J.L., Ding, X.M., Tao, X.M., 2002. Shape memory polymers and their applications to smart textile products. *Journal of China Textile University* 19, 89–93.
- Hu, J., Meng, Q., 2011. Functional shape memory textiles. In: *Functional Textiles for Improved Performance, Protection and Health*. Woodhead Publishing Limited, New York, pp. 131–161.
- Husain, M.D., Kennon, R., 2014. Design and fabrication of temperature sensing fabric. *Journal of Industrial Textile* 44 (3), 398–417.
- Hu, J., Zhu, Y., Huang, H., Lu, J., 2012. Recent advances in shape-memory polymers: structure, mechanism, functionality, modeling and applications. *Progress in Polymer Science* 37, 1720–1763.
- Hu, J., Zhuo, H., 2010. Shape memory polymers in coatings and laminates for textiles. In: *Smart Textile Coatings and Laminates*. Woodhead Publishing Limited, Cambridge, UK, pp. 222–236.
- Hyashi, S., 1993. Properties and applications of polyurethane. *International Progress in Urethanes* 6, 90–115.
- Ilfiker, R.H., Aufmann, W.K., Einert, G., Erika, S., 1996. Improving sun protection factors of fabrics by applying UV-absorbers. *Textile Research Journal* 66 (2), 61–70.

- Joshi, M., Reddy, G., 2005. UV protection textiles – options and opportunities. *Asian Dyer* (9–10), 76–81.
- Kim, J., Cho, G., 2003. Thermal storage/release, durability, and temperature sensing properties of thermostatic fabrics treated with octadecane-containing microcapsules. *Textile Research Journal* 72 (12), 1093–1098.
- Kloos, W.E., Musselwhite, M.S., 1975. *Applied Microbial Attack* 381–391.
- Koyama, Y., Nishiyama, M., Watanabe, K., 2013. A motion monitor using hetero-core optical fiber sensors sewed in sportswear to trace trunk motion. *IEEE Transactions on Instrumentation and Measurement* 62 (4), 828–831.
- Kürklü, A., 1997. Thermal performance of a tapered store containing tubes of phase change material: cooling cycle. *Energy Conversion and Management* 38 (4), 333–340.
- Kyle, C.R., Brownlie, L.W., Harber, E., MacDonald, R., Nordstrom, M., 2004. The Nike swift spin cycling project: reducing the aerodynamic drag of bicycle racing clothing by using zoned fabrics. In: *The Engineering of Sport 5*. International Sports Engineering Association, UK.
- Kyle, C., Caiozzo, V., 1986. The effect of athletic clothing aerodynamics upon running speed. *Medicine and Science in Sports and Exercise* 18 (5), 509–515.
- de Lucas, R.D., et al., 2000. The effects of wet suits on physiological and biomechanical indices during swimming. *Journal of Science and Medicine in Sport* 3, 1–8.
- Liang, H., Zhang, G., Zhang, F., Wu, D., 2013. Preparation of highly hydrophilic polyester fabrics via UV irradiation/nano-TiO₂ modification. *Journal of Textile Research* 3–15.
- Lin, C.Y., Siao, K.H., 2007. Smart temperature-controlled water vapor permeable polyurethane film. *Journal of Membrane Science* 91–96.
- Lomax, G.R., 1990. *Journal of Coated Fabrics* 20 (2), 88–107.
- Lukes, R.A., Chin, S.B., Haake, S.J., 2005. The understanding and development of cycling aerodynamics. *Sports Engineering* 8 (2), 59–74.
- Manickam, M.M., 2006. Moisture management: its conquering techniques. *Colourage* 53, 105–108.
- Manshahia, M., Das, A., 2014. High active sportswear: a critical review. *Indian Journal of Fibre and Textile Research* 39, 441–449.
- Mao, J., Murphy, L., 2001. *AATC Review* 9, 28–40.
- Marmot, n.d. Marmot Membrain (Online). Available at: <http://marmot.com/content/technology/the-elements/water/marmot-membrain> (accessed June 2015).
- Marek, J., Leszkiewicz, A., Stefen, B., Polskoviska, G.B., 2009. In: *5th International Conference on Sol-Gel Materials*. Trzebieszowice, Poland.
- Mondal, S., 2008. Phase change materials for smart textiles – an overview. *Applied Thermal Engineering* 28, 1536–1550.
- Morikawa, J., Hashimoto, T., 2000. Simultaneous measurement of heat capacity and thermal diffusivity in solid–solid and solid–liquid phase transitions of nalkane. *Thermochimica Acta* 352, 291–296.
- Nike Innovations, 2013. Sustainable Innovations (Online). Available at: <http://www.nikeresponsibility.com/innovations> (accessed 22.08.15.).
- Oda, H., 2011. Development of UV absorbers for sun protective fabrics. *Textile Research Journal* 81 (20), 2139–2148.
- Oggiano, L., et al., 2013. A review on skin suits and sport garment aerodynamics: guidelines and state of the art. *Procedia Engineering* 60, 91–98.
- Oggiano, L., et al., 2009. Aerodynamic behaviour of single sport jersey fabrics with different roughness and cover factors. *Journal of Sport Engineering* 12 (1), 1–16.

- Oggiano, L., Sætran, L.R., 2008. Effect of different skin suits on speed skating performances. *Computer Science in Sports* 163–173.
- Okubo, M., Saeki, N., Yamamoto, T., 2008. Development of functional sportswear for controlling moisture and odor prepared by atmospheric pressure nonthermal plasma graft polymerization induced by RF glow discharge. *Journal of Electrostatics* 66, 381–387.
- Outlast, n.d. Outlast Technology (Online). Available at: <http://www.outlast.com/en/applications/matrix-infusion-coating> (accessed 25.05.15.).
- Pacelli, M., Caldani, R., Paradiso, 2006. Textile piezoresistive sensors for biomechanical variables monitoring. *Conference Proceedings: IEEE Engineering in Medicine and Biology Society* 5358–5361.
- Pailthorpe, M.T., Chriskis, J.I., 1995. Sun protection of apparel textiles. In: 3rd Asian Textile Conference.
- Painter, C.J., 1996. Waterproof, breathable fabric laminates: a perspective from film to market place. *Journal of Coated Fabrics* 26 (2), 107–130.
- Paradiso, R., Caldani, L., Pacelli, M., 2014. Knitted electronic textiles. In: *Wearable Sensors*. Elsevier Inc, pp. 153–175.
- Paul, R., Bautista, M., Varga, M.D., 2010. Nano-cotton fabrics with high ultraviolet protection. *Textile Research Journal* 80 (5), 452–462.
- Pause, B., 2001a. Development and application of textiles with phase change. In: *Textile International Forum and Exhibition 2001*. ROC, Taipei.
- Pause, B., 2001b. Textiles with improved thermal capabilities through the application of phase change material (PCM) microcapsules. *Melliands Textilberichte* 1 (1), 753–754.
- Pause, B., 2010. Phase change materials and their application in coatings and laminates for textiles. In: *Smart Textile Coatings and Laminates*. Woodhead Publishing Limited, pp. 236–250.
- Pine cone cloths, 2004. *The Engineer* (online). Available at: <http://www.theengineer.co.uk/news/pine-coneclothes/267046.article> (assessed on 25.05.15.).
- Porellemembranes, n.d. Microporous Membranes (Online). Available at: <http://www.porellemembranes.com/en/microporous-membranes> (accessed May 2015).
- De Rossi, D., Santa, A.D., Mazzoldi, A., 1999. Dressware: wearable hardware. *Materials Science and Engineering: C* 7 (1), 31–35.
- Ren, Y.N., Ruckman, J.E., 2003. Water vapour transfer in wet waterproof breathable fabrics. *Journal of Industrial Textiles* 32, 165–175.
- Research and markets, 2015. *Global Sportswear Market Size 2015 Industry Trend and Forecast 2020* (Online). Orbis Research, USA. Available at: http://www.researchandmarkets.com/research/828j6s/global_sportswear.
- Roberts, B.S., Kamal, K.S., Hedrick, C.E., McLean, S.P., Sharp, R.L., 2003. Effect of a Fast-Skin™ suit on submaximal freestyle swimming. *Medicine and Science in Sports and Exercise* 35, 519–524.
- Rogowski, I., Monteil, K., Legreneur, P., Lanteri, P., 2006. Influence of swimsuit design and fabric surface properties on the butterfly kinematics. *Journal of Applied Biomechanics* 22, 61–66.
- Rupp, J., Bohringer, J., Yonenaga, A., Hilden, J., 2001. Textiles for protection against harmful. *International Textile Bulletin* 6, 8–20.
- Sampath, Senthilkumar, 2009. Effect of moisture management finish on comfort characteristics of microdenier polyester knitted fabrics. *Journal of Industrial Textiles* 39 (2), 163–173.
- Smith, J.W., Molloy, J.M., Pascoe, D.D., 2007. The influence of a compressive laminar flow body suit for use in competitive swimming. *Journal of Swimming Research* 17, 10–16.

- Son, W.K., Youk, J.H., Park, W.H., 2006. Antimicrobial cellulose acetate nanofibers containing silver nanoparticles. *Carbohydrate Polymers* 65, 430–434.
- Speedo, 2015. Speedo Fastskin (Online). Available at: <http://www.speedo.co.uk/technology/fastskin> (accessed 22.08.15).
- Splendore, R., Dotti, F., Cravello, B., Ferri, A., 2010. *International Journal of Clothing Science and Technology* 22 (5), 333–342.
- Splendore, R., Dotti, F., Cravello, B., Ferri, A., 2011. Thermo-physiological comfort of a PES fabric with incorporated activated carbon, Part II: wear trials. *International Journal of Clothing Science and Technology* 23 (5), 283–293.
- Styletime, n.d. Supernova Glide Bra (Online). Available at: <http://style.time.com/2012/05/29/a-fashionable-fit/slide/adidas-supernova-glide-bra/> (accessed June 2015).
- Sympatex. Sympatex Membrane Properties (Online). Available at <http://sympatex.com/en/membrane/225/properties> (accessed May 2015).
- Takahashi, T., Hayashi, N., Hayashi, S., 1996. Structures and properties of shape- memory polyurethane block copolymers. *Journal of Applied Polymer Science* 60, 1061–1072.
- Tang, S.L.M., Stylios, G.K., 2006. An overview of smart technologies for clothing design and engineering. *International Journal of Clothing Science and Technology* 18 (2), 108–128.
- Tiozzo, E., Leko, G., Ruzic, L., 2009. Swimming bodysuit in all-out and constantpace trials. *Biology of Sport* 26, 149–156.
- Torayentrant, n.d. Dermizax (Online). Available at: http://www.torayentrant.com/en/products/dermizax/der_003.html (accessed May 2015).
- Tyagi, V., Kaushik, S., Tyagi, S.K., Akiyama, T., 2011. Development of phase change materials based microencapsulated technology for buildings: a review. *Renewable and Sustainable Energy Reviews* 15, 1373–1392.
- Weder, M., 1997. Performance of rainwear material with respect to protection, physiology, durability and ecology. *Journal of Coated Fabrics* 27 (2), 146–168.
- White, F.M., 1991. *Viscous Fluid Flow*, second ed. McGraw-Hill, New York.
- Wieland, M., et al., 2000. Wavelength-dependent measurement and evaluation of surface topographies: application of a new concept of window roughness and surface transfer function. *Wear* 237, 231–252.
- Williams, J.F., HaloSource, V., Cho, U., 2005. Antimicrobial functions for synthetic fibers: recent developments. *AATCC Review* 5, 17–21.
- Wu, J., 2011. Development and design of performance swimwear. In: *Functional Textiles for Improved Performance, Protection and Health*. Woodhead Publishing Limited, pp. 226–249.
- Yau, L., 1988. *Canadian Textile Journal* 36–45.
- Yeo, S.Y., Lee, H., Jeong, S.H., 2003. Preparation of nanocomposite fibers for permanent antibacterial effect. *Journal of Materials Science* 38, 2143–2147.
- You, H.L., Merry, J., 1986. *Journal of Applied Bacteria* 60, 535–545.

Smart coatings for protective clothing

16

H. Cao

University of Delaware, Newark, DE, United States

16.1 Introduction

A coating is the application of a liquid material onto the surface of a solid substrate and appears as a continuous or discontinuous film after drying (Ghosh, 2006). Textile fabrics are commonly used substrates for coating and coated textiles are widely used in a variety of applications such as protective clothing, sportswear, and outdoor equipment. Coating formulations usually contain polymer materials, ie, polyvinyl chloride, polyurethane, acrylic, rubber, and polytetrafluoroethylene, to incorporate useful waterproof, soil release, chemical protection, thermal resistance, and insulation functions into textiles. Coatings can be applied to textiles made from any fiber (natural, regenerated, or synthetic) or structure (woven, knit, or nonwoven), which makes coating a diverse technique to enhance the value and performance of textile materials and products such as apparel, upholstery, carpet, airbags, and belts (Singha, 2012).

In many industrial sectors, military and energy service, law enforcement, and hospital environments, millions of people encounter various types of risks. Protective clothing can provide necessary protection against chemicals, microorganisms, fire, heat, ballistics, and punctures. Many new developments in protective clothing and materials are aimed at solving a set of problems such as improved protection, maintenance of thermophysiological comfort, and reduction in weight and bulk (Shishoo, 2002).

A smart coating can change its properties in response to an environmental stimulus (Makhlouf, 2014). The environmental stimulus may be a change in temperature, humidity, pH, light, mechanical damage, or contact with chemicals. Applying smart coating to textiles is a major method to produce smart textiles that enhance the protection and comfort of a textile system and protective clothing. New advancements in nanotechnology have launched many new smart coating materials and processes. This chapter discusses new developments in smart coatings on textiles that can be used in protective clothing such as body armor, hazardous material (HAZMAT) suits, health care clothing, and firefighter turnout coats.

16.2 Smart coating for body armor application

16.2.1 Bullet-resistant body armor

Body armor is one of the most important and effective pieces of equipment to protect military and law enforcement personnel. Depending on the ballistic materials used, body armor includes soft armor which uses lightweight, flexible textiles and hard armor which combines ballistic textile materials and rigid insert plates made from ceramics, metals, and/or fiber-reinforced composites. Flexible ballistic textile materials include aramid, eg, Kevlar[®] (DuPont), Twaron[®] (Teijin), Technora[®] (Teijin); highly oriented polyethylene, eg, Spectra[®] (Honeywell), Dyneema[®] (DSM); and polybenzobisoxazole (PBO), eg, Zylon[®] (Toyobo) (Phoenix & Porwal, 2003). Approximately 20–50 layers of ballistic fabrics are used in a soft body armor to meet protection requirements for different ballistic threats (Lee, Wetzel, & Wagner, 2003). Soft armor made from ballistic fabrics effectively protects the wearer against shrapnel but cannot provide sufficient protection against high-speed bullets, which can pierce the fabric even if multiple layers are used. Hard armor with rigid ceramic plates inserted in the front and back provides sufficient protection against bullets (Gadow & von Niessen, 2006; Kosashvili et al., 2005).

For law enforcement personnel, the National Institute of Justice (NIJ) Standard 0101.06, Ballistic Resistance of Body Armor, specifies minimum performance requirements and test methods for the ballistic resistance of personal body armor intended to protect the torso against gunfire (National Institute of Justice, 2008). According to NIJ Standard 0101.06 (NIJ, 2008), personal body armor is classified into five types by level of ballistic performance: type IIA (9 mm; 40 Smith and Wesson), type II (9 mm; 0.357 Magnum), type IIIA (0.357 Sig Sauer; 0.44 Magnum), type III (rifles), and type IV (armor-piercing rifle).

The development and use of body armor has significantly protected safety law enforcement officers and military personnel. The use of soft body armor has saved over 2900 lives since its inception in 1972, and it is estimated that an officer is 14 times more likely to survive a gunshot to the torso if body armor is worn (Wilhelm & Bir, 2008). However, wearing body armor also affects comfort, mobility, and other performance of those who wear it. Wearers often experience excessive thermal stress from heavy body armor. Although a single layer of Kevlar woven fabric is breathable, as indicated by the evaporative resistance (R_{et}) value of 17.25 Pa m²/W, 32 layers of Kevlar, which can provide a certain level of ballistic protection, are not breathable with an R_{et} value greater than 999 Pa m²/W (Kamenidis, 2009).

Increasing the protection performance of ballistic materials has the potential to reduce the layers of material used for certain protection requirement and thus improve the comfort and mobility of armor users. Shear thickening fluid (STF) has non-Newtonian flow behavior in which the viscosity of concentrated colloidal dispersion significantly and abruptly increases once the shear rate or applied stress increases to a critical level. This shear thickening behavior is reversible and when the impact force disappears, the viscosity will reduce accordingly (Lee et al., 2003; Sun, Xiong, & Xu, 2013). One proposed mechanism of the reversible shear thickening behavior is

the hydrocluster mechanism. The formation of particle aggregates or hydroclusters induced by the shear rate dramatically increases the viscosity of the fluid and transforms the flowing liquid into a solid-like material (Hassan, Rangari, & Jeelani, 2010; Lee et al., 2003). This property of an abrupt increase in viscosity makes STF an ideal smart coating material for body armor applications because the shear stress from a bullet can trigger the material to convert from a fluid-like flexible status to a solid-like rigid status and enhance protection. Moreover, the fluid thickening transition is reversible. The STF can be stable in fabric in the liquid form and does not affect the material's flexibility under ordinary conditions (Sun et al., 2013).

A research group led by Norman Wagner of the University of Delaware was the first to apply STF technology to ballistic materials and develop liquid body armor (Wagner & Wetzel, 2004). Lee et al. (2003) impregnated Kevlar[®] woven fabric by colloidal silica-ethylene glycol STF. They found that four layers of STF-Kevlar[®] have weight and ballistic protection performance similar to 10 layers of neat Kevlar[®]. However, the thickness and flexibility of four layers of STF-Kevlar[®] were similar to 4 layers of neat Kevlar[®] and significantly less than 10 layers of neat Kevlar[®]. Lee et al. (2003) identified that the possible mechanism of enhanced ballistic performance of STF-impregnated Kevlar[®] resulted from an increase in yarn pullout force when STF transitioned from a rigid state during ballistic impact.

Srivastava, Majumdar, and Butola (2011) coated Kevlar[®] fabric with silica-polyethylene glycol STF and further studied the padding pressure and silica concentration in STF on add-on percentage, Kevlar[®] yarn pullout force, and impact energy absorption. Although the maximum STF weight add-on percentage and maximum yarn pullout force occurred at minimum padding pressure and maximum SFT concentration, the maximum impact energy absorption was achieved at maximum padding pressure and maximum SFT concentration. Higher padding pressure reduced SFT add-on percentage (lower total weight of the coated fabric) but increased impact energy absorption. This indicated that better penetration and uniform distribution of the STF within the yarn structure resulting from higher padding pressure helped improve impact energy absorption (Srivastava et al., 2011).

16.2.2 Stab-resistant body armor

Because of its lightweight and sufficient protection against handgun threats, soft body armor is most widely used by law enforcement personnel. According to the National Institute of Justice (2008), type II, IIA, and IIIA armor (usually soft armor) is suitable for full-time wear throughout an entire shift of duty whereas type III and IV (usually hard armor to protect against rifle rounds) is generally used only in tactical situations or when the threat warrants such protection. However, ballistic fibers have a limited level of protection against nonballistic threats such as knives, sharp blades, or sharp-tipped weapons (Gadow & von Niessen, 2006). Incorporating stab-resistant properties into soft ballistic materials would provide protection for law enforcement personnel against multiple threats.

Coating a hard material on soft ballistic fabric would enhance stab and cut resistance while retaining fabric flexibility. Gadow and von Niessen (2006) coated cermet

(WC Co 83/17) and oxide ceramics aluminum oxide (Al_2O_3) and titanium oxide (TiO_2) on aramid Twaron[®] fabric using a thermal spray process. For ceramics coating, AlSi 12 was used as additional bond coat to improve the bonding strength of ceramic (Al_2O_3 and TiO_2) coating on fabric. Among the coating systems, Al_2O_3 –AlSi 12 and the WC Co 83/17 showed high bonding strength and the highest microhardness. Table 16.1 compares weight and stab resistance of Twaron[®] fabrics without a coating and those coated with multilayer Al_2O_3 –AlSi 12 (30- μm AlSi 12 and 75- μm top coat of Al_2O_3), and single-layer WC Co 83/17 (75 μm). The weight gain was less than 150% but the stab penetration work increased by a factor of 4 (Al_2O_3 –AlSi 12) or 5 (WC Co 83/17) (Gadow & von Niessen, 2006). Atanasov et al. (2014) used an atomic layer deposition (ALD) process to coat conformal dielectric Al_2O_3 and TiO_2 thin films on Kevlar[®] fibers. Compared with untreated Kevlar[®] fabric, coating a single layer of Al_2O_3 on fabric reduced the fabric's cut resistance whereas coating a single layer of TiO_2 moderately increased cut resistance. However, coating a conformal 50–50 Å bilayer of TiO_2 – Al_2O_3 thin film on Kevlar fabric increased 30% of cut resistance, with a negligible weight gain of 0.87%. The Kevlar fabric with ALD coatings also retained good durability and flexibility (Atanasov et al., 2014). In these studies (Atanasov et al., 2014; Gadow & von Niessen, 2006), the property of coating materials did not change in response to an environmental stimulus, ie, stab or cut. Thus, coating hard materials cermet, Al_2O_3 , and TiO_2 on ballistic fabrics is not a smart coating although the coating effectively enhanced stab and cut resistance.

Rosen, Laufer, Kalman, Wetzell, and Wagner (2007) treated Kevlar[®] fabrics with kaolin clay–glycerol (mean size of kaolin particles, 500 nm) STF (K-STF) and spherical silica STF (S-STF), and conducted quasistatic stab tests using three different threats, ie, NIJ knife (type S1), NIJ spike, and stainless-steel Sharpvet hypodermic needles (HN) on four layers of fabric (neat Kevlar[®] or STF-impregnated Kevlar[®]). Their results, as shown in Table 16.2, indicated that Kevlar[®] fabrics coated with K-STF and S-STF significantly increased stab resistance against knives, spikes, and needles, with low weight gain (16.7% for K-STF and 20% for S-STF) (Rosen et al., 2007). Hassan et al. (2010) coated Kevlar[®] and nylon fabrics with nanoparticle silica (40%)–polyethylene

Table 16.1 Weight and stab resistance of neat and coated Twaron[®]

Sample	Weight (g/m^2)	Stab penetration work ($\text{N}\cdot\text{mm}$)	
		At the 1st stab	After six stabs
Twaron [®] without coating	220	~ 200	~ 300
Twaron [®] coated with Al_2O_3 –AlSi 12	480	1000	~ 1400
Twaron [®] coated with WC Co 83/17	520	1200	1500

Data from Gadow, R., and von Niessen, K. (2006). Lightweight ballistic with additional stab protection made of thermally sprayed ceramic and cermet coatings on aramide fabrics. *International Journal of Applied Ceramic Technology*, 3(4), 284–292.

Table 16.2 Weight and stab resistance of neat Kevlar and STF-impregnated Kevlar

Material	One-layer weight (g/m ²)	Quasistatic loads at 20 mm		Quasistatic needle resistance energy absorbed			
		Spike (N)	Knife (N)	12 gauge HN (J)	16 gauge HN (J)	18 gauge HN (J)	22 gauge HN (J)
Neat Kevlar	180	35	80	150	9	8	11
K-STF Kevlar	210	160	120	760	155	76	39
S-STF Kevlar	216	180	120	810	150	62	36

Data from Table 1 of Rosen, B.A., Laufer, C.H.N., Kalman, D.P., Wetzel, E.D., and Wagner, N.J. (2007). Multi-threat performance of kaolin-based shear thickening fluid (STF)-treated fabrics. In *Proceedings of SAMPE 2007, Baltimore, MD, June 3–7, 2007*.

glycol (60%) STF and conducted dynamic (using a drop tower) and quasistatic (using a Zwick-Roell materials testing machine) stab resistance tests against knife (S1 knife blade) and spike (engineered spike) threats. They found that coating STF on fabric did not change the thickness and flexibility of Kevlar[®] fabric but slightly increased thickness and reduced flexibility for nylon fabric. With similar fabric weight (15 layers of neat Kevlar versus 11 layers of STF/Kevlar; and 6 layers of neat nylon versus 5 layers of STF–nylon), SFT-coated Kevlar[®] and nylon fabrics showed better stab resistance against knives and spikes in both dynamic and quasistatic tests (Hassan et al., 2010). The improvement in stab resistance with the STF coating was more significant for a spike threat, as shown in Table 16.3.

Table 16.3 Stab resistance results of neat and STF-coated Kevlar and nylon fabrics

Materials	Dynamic (no. of penetrated witness paper under 5.4 J of impact energy)		Quasistatic (load [N] at 30-mm displacement)	
	Knife	Spike	Knife	Spike
Neat Kevlar (15 layers)	5	5	286	85
SFT/Kevlar (11 layers)	4	4	530	575
Neat Nylon (6 layers)	4	5	284	100
STF/Nylon (5 layers)	3	4	406	548

Data from Hassan, T.A., Rangari, V.K., and Jeelani, S. (2010). Synthesis, processing, and characterization of shear thickening fluid (STF) impregnated fabric composites. *Materials Science and Engineering A*, 527, 2892–2899.

Sun et al. (2013) coated silica–ethylene glycol (EG) STF on ultrahigh-molecular-weight polyethylene (UHMWPE) and used a self-made fabric dynamic puncture tester to evaluate stab resistance against knife and spike threats. Eight layers of STF-coated UHMWPE fabric (38% STF) showed comparable protection against a spike threat as did 16 layers of neat UHMWPE fabric but it had significantly lower weight and thickness (37% lower for weight and 36% lower for thickness), and significantly better flexibility (Sun et al., 2013). Similar to the findings of Rosen et al. (2007) and Hassan et al. (2010) on STF-coated Kevlar® and nylon, STF-coated UHMWPE showed higher improvement of stab resistance under a spike threat than a knife threat. Under a high-speed impact, STF particles quickly gathered together to increase the compactness of the fabric structure, whereas the breaking strength of the fiber was less affected. The increased fabric structure compactness restricted the movement of fiber bundles and made it difficult for spike penetration, in which fiber bundles were pushed away. For a knife puncture, the knife blade cut the fibers to penetrate. However, the STF coating could not significantly increase the breaking strength of the fiber. This may be why STF coating showed higher improvement in stab resistance under a spike threat than under a knife threat (Sun et al., 2013).

16.3 Smart coating for hazardous material protective clothing

To protect against chemical and biological threats, military and law enforcement personnel and first responders, ie, firefighters and HAZMAT workers, wear HAZMAT protective clothing on a variety of occasions such as urban combat, terrorism attacks, and chemical spills and pollution. HAZMAT protective clothing usually contains multilayer laminated fabric that functions as a barrier to absorb or block contaminants (toxin chemicals or microorganisms) (Schreuder-Gibson et al., 2003). Absorbed toxic chemicals may cause secondary contamination as they leave the fabric surface during use or decontamination (Chen et al., 2009). Biological warfare agents do not typically penetrate the skin but they can attach to HAZMAT protective clothing in high concentrations and leave the fabric surface as aerosols to endanger nearby unprotected personnel (Schreuder-Gibson et al., 2003). Smart coating on fabrics that can detoxify chemicals and/or kill biological warfare agents provide HAZMAT clothing with better protection, and there has been much research and development effort in this area.

A high surface area with more reactive sites is important for smart coatings used for HAZMAT protective clothing. Therefore, nanotechnology has been extensively investigated. Sundarajan, Chandrasekaran, and Ramakrishna (2010) considered electrospinning to be the most promising nanotechnology to produce continuous fibers in nanometer size and with a high surface area. Lee et al. (2009) expected that coating nanoparticles on nanoscale electrospun fibers would remarkably increase reactive sites. Layer-by-layer (LbL) assembly formed thin films with nanoscale composition and structure via alternating adsorption of positively and negatively charged species from aqueous solution. LbL assembly has a low cost compared with other

nanofabrication methods such as chemical vapor deposition, ALD, colloidal assembly, and molecular beam epitaxy; and it has a unique ability to incorporate a number of different materials into layers (Hammond, 2004).

Enzyme organophosphorus hydrolase (OPH) can rapidly hydrolyze and detoxify organophosphorus-based toxins, ie, pesticides and nerve agents. Singh, Lee, and Dressick (2004) used a dip-coating process to deposit polyelectrolyte multilayers (PEMs) of branched polyethylenimine (BPEI) and OPH encapsulation on fiberglass (FG) and cotton (CC) fabrics in the form of FG-BPEI_w-OPH_b-BPEI_b or CC-BPEI_w-OPH_b-BPEI_b (the subscripts “w” and “b” indicate layer deposition from aqueous and *bis-tris*-propane buffer solutions, respectively). The purpose of the PEM process using LbL electrostatic adsorption was to immobilize OPH on solid supports and extend its bioactivity. Both FG-BPEI_w-OPH_b-BPEI_b and CC-BPEI_w-OPH_b-BPEI_b systems can effectively catalyze the hydrolysis of organophosphorus chemical methyl parathion (MPT), and MPT hydrolysis by CC-BPEI_w-OPH_b-BPEI_b was 2.4 ± 0.3 times the equivalent weight of FG-BPEI_w-OPH_b-BPEI_b owing to the adsorption of large quantities of OPH on cotton (Singh et al., 2004). Using track line manufacturing conditions, spray coating was used to produce CC-BPEI_w-OPH_b-BPEI_b. The MPT hydrolysis activity of CC-BPEI_w-OPH_b-BPEI_b made from spray coating was about 15% of the material made from dip coating. The lower detoxification efficiency of spray coating was related to the shorter contact time with cotton fabric in spray coating (2 min) compared with dip coating (10 min) and the lower amount of reagents available in the spray coating aerosol (Singh et al., 2004).

TiO₂ has the photocatalysis capability to decompose chemicals effectively (Fujihira, Satoh, & Osa, 1981; Fujishima & Honda, 1972). Coating TiO₂ on textiles to degrade harmful organic chemicals and enhance HAZMAT protection has been investigated (Grandcolas, Louvet, Keller, & Keller, 2009; Krogman, Lowery, Zacharia, Rutledge, & Hammond, 2009; Lee et al., 2009). Grandcolas et al. (2009) used LbL deposition method to coat cotton fibers with WO₃-titanate nanotube (WO₃-TiNT) by alternately immersing the fabric into either a polyethylenimine solution or a colloidal solution of WO₃-TiNT until the desired number of layers was attained. Under 24-W simulated solar light, the WO₃-TiNT-coated cotton fabric can photocatalytically degrade or detoxify an organophosphonate simulant dimethyl methylphosphonate and yperite warfare agent (mustard gas) within a few minutes (Grandcolas et al., 2009). Lee et al. (2009) electrospun poly(dimethylsiloxane-*b*-etherimide) (PSEI) fibers with diameters ranging from 400 to 1300 nm (average diameter, 650 nm; standard deviation, 180 nm) to produce a nonwoven mat. TiO₂ nanoparticles (mean diameter, 7 ± 1 nm) were coated on the PSEI nonwoven mat via LbL deposition, in which the PSEI nonwoven mat was treated with low-pressure air plasma to introduce negatively charged surface groups and then coated with alternating layers of positively charged octa(3-ammonium-propyl)octasil-sesquioxane octachloride (POSS-NH₃⁺) and negatively charged TiO₂ nanoparticles using a dipping process. Illuminated with UV light, the TiO₂-coated PSEI sample can photocatalytically degrade ally alcohol. It was also shown that the flexibility of the fiber was retained after the LbL TiO₂ nanoparticle coating, and the PSEI nonwoven mat coated with POSS-NH₃⁺-TiO₂ nanoparticles pairs via LbL deposition was stable under UV illumination (Lee et al., 2009). Krogman et al. (2009) used a vacuum-assisted spray

LbL process to coat 25 bilayers of positively charged poly(dimethyldiallyl ammonium chloride) (PDAC) and negatively charged TiO_2 nanoparticles on an electrospun nylon (ES) mat. The mat was then flipped and sprayed with 50-bilayer coatings of a polyelectrolyte system of poly(amidoamine) (PAMAM) and poly(acrylic acid) (PAA). The resulting ES + vac(PDAC– TiO_2)₂₅ + (PAMAM–PAA)₅₀ LbL coating system maintained a water vapor-permeable property (similar to that of cotton materials) while it effectively blocked and photocatalytically degraded chloroethyl ethyl sulfide (CEES), a simulant for the chemical warfare agent HD mustard gas (74% CEES degradation with the aid of UV light) (Krogman et al., 2009).

Chen et al. (2010) reported the application of an LbL assembly to develop a multi-functional protective fabric that can simultaneously detoxify and decontaminate both toxic chemical and biological agents. They produced an electrospun polyacrylonitrile (PAN) fiber mat and used an LbL electrostatic assembly technique to deposit multi-layer polyelectrolyte coatings on the fiber mat by alternately dipping the fiber mat in bactericidal polycation poly(*N*-vinylguanidine) (PVG) and chemically reactive polyanion poly(hydroxamic acid) (PHA) aqueous solutions. PHA can hydrolyze diisopropyl fluorophosphates (DFP), a close analog of the chemical warfare agent sarin. It was demonstrated that the PAN fiber mat coated with PVG–PHA layers was capable of degrading a DFP mist (with DFP hydrolysis rates 60-fold higher than untreated fabrics) and had bactericidal capability against *Escherichia coli* and *Staphylococcus epidermidis* strains. The LbL-functionalized PAN fiber mats coated with 20 or 30 bilayers of PVG–PHA exhibited water vapor diffusion resistivity comparable to that of untreated PAN fiber mats, which indicated that the LbL coating did not affect the fabric's breathability (Chen et al., 2010).

16.4 Smart coating for health care protective clothing

The chemical degradation and biocidal coating discussed in the previous section (HAZMAT protective clothing) can also be applied to protective clothing for health care workers and patients. The focus on chemical degradation and antimicrobials for health care protective clothing is to incorporate a self-cleaning function. Compared with HAZMAT protective clothing, reusable health care protective clothing such as surgical gowns requires a higher level of durability, especially durability against chemical degradation and with antimicrobial function after washing. Moreover, fibers such as cotton or polyester are more commonly used in health care protective clothing to enhance comfort. The research group of John Xin at the Hong Kong Polytechnic University used the photocatalytic property of TiO_2 to develop self-cleaning textiles (Qi et al., 2006; Qi, Wang, & Xin, 2011; Qi, Xin, & Daoud, 2007). Qi et al. (2006) used the low-temperature sol–gel process of mixing titanium tetraisopropoxide and acid to prepare TiO_2 sols, and used a dip–pad–dry–cure process to coat cotton fabrics with nanocrystalline anatase TiO_2 thin film. Under UV irradiation, the TiO_2 -coated cotton fabric has self-cleaning property to kill gram-positive bacterium *Staphylococcus aureus* and degrade colorant stains from Neolan Blue 2G, Cibacron Blue F-R, red wine, and coffee (Qi et al., 2006). The researchers further modified the sol–gel process with a small amount of acid to prevent the loss of tensile and tearing strength of cotton fabrics

owing to the TiO₂ coating. The TiO₂ thin-film-coated cotton fabric has good air permeability, handling, and fastness after 20 home launderings and has the self-cleaning property to decompose red wine, coffee, and curry stains under UV irradiation (Qi et al., 2011). In addition to cotton fabric, Xin's group applied similar technology to develop an anatase TiO₂ thin-film-coated polyester fabric that has the self-cleaning properties to kill bacteria *S. aureus* and decompose colorant stains from Neolan Blue 2G, red wine, and coffee under UV irradiation. It was also found that pretreating polyester with oxygen plasma would increase the self-cleaning performance of TiO₂-coated polyester fabric because of the greater deposition of TiO₂ particles, and to increase the adhesion between TiO₂ layers and polyester, resulting in better self-cleaning performance after home washing five times (Qi et al., 2007).

Silver has long been used as an antimicrobial agent. Silver is known to be an efficient antimicrobial agent against nearly 650 types of bacteria (Dubas, Kumlangdudsana, & Potiyaraj, 2006). Although the exact mechanism of silver's antimicrobial property is not known, Rai, Yadav, and Gade (2009) summarized the possible antimicrobial mechanisms of metallic silver, silver ions—AgNO₃, silver zeolite, and silver nanoparticles. Mahltig, Fiedler, and Böttcher (2004) embedded biocides AgNO₃, quaternary ammonium salts (octenidine and cetyltrimethylammonium bromide) in silica sol, and coated the silica sol on cotton-polyester fabric. The silica sol-gel coating demonstrated the slow release of biocides. The fabrics treated with a silica sol-gel coating embedded with octenidine and AgNO₃ exhibited long-term stability and antimicrobial efficiency to inhibit the growth of *Aspergillus niger* fungus, *E. coli* bacterium, and airborne germs (Mahltig et al., 2004).

Silver nanoparticles have gained researchers' interest because of their efficient antimicrobial property when large surface areas are in contact with microorganisms (Rai et al., 2009). Dubas et al. (2006) used the LbL deposition technique to coat 20 bilayers of poly(diallyl dimethyl ammonium chloride) and silver nanoparticles capped with poly(methacrylic acid) on nylon and silk fibers, and demonstrated that the coated silk and nylon fibers can reduce 80% and 53% of *E. coli*, respectively. To increase the wash fastness of silver nanoparticles on textile fabrics, Xu, Shi, Ma, Lv, and Mao (2013) and Xu et al. (2011) treated cotton and polyester fabrics with dopamine, a low-molecular-weight catecholamine that can self-polymerize on the surface of a variety of materials, to coat a polydopamine film on the fabrics. Dopamine mimics an adhesive protein and its catechol group has metal reduction capability. The polydopamine-coated fabrics were then immersed into an AgNO₃ solution and silver nanoparticles were generated on the fabric surface owing to the in situ reduction of Ag⁺ to Ag⁰ by dopamine. After washing 30 times, the silver- and dopamine-coated cotton and polyester fabrics still reduced 99.99% of bacteria *E. coli* (Xu et al., 2011, 2013).

16.5 Smart coating for firefighter protective clothing

During firefighting, firefighters experience extensive thermal strain as a result of the metabolic heat produced by working muscles; the heavy, insulating, nonpermeable protective gear they wear; and the radiant heat associated with the fire

(Smith, Manning, & Petruzzello, 2001). In 2013, the leading cause of firefighters' fire-ground injuries was overexertion and strain, which accounted for 26.5% of the 29,760 total fire-ground injuries (Karter & Molis, 2014). Rossi (2003) reviewed the literature on heat exposure when fighting fire, and conducted experiments to measure temperatures and radiant heat loads during simulated firefighting situations in training buildings and in heated rooms. Firefighters were typically exposed to radiant heat flux of 5–10 kW/m², and in one case 42 kW/m² was measured, corresponding to the highest value obtained during domestic fires. Skin temperature was measured with six firefighters; values were between 39°C and 45.5°C, which reached or exceeded the pain threshold of around 44°C skin temperature (Rossi, 2003). Therefore, it has always been necessary to provide cooling and reduce heat stress for firefighters.

A phase change material (PCM) can absorb a large quantity of latent heat when it changes state from a solid to a liquid, and transfer the energy to the environment and change its state back to a solid in a cooling process. During phase change, the volume and temperature of the PCM, as well as the temperature of the surrounding environment, remain nearly constant. This property makes PCM a useful material for thermal regulation, including applications in textiles and clothing. Mondal (2008) and Sarier and Onder (2012) provided good reviews of PCMs and the applications of PCM in textiles. There are more than 500 PCMs; the commonly used types include hydrated inorganic salts, paraffin waxes, polyethylene glycols, fatty acids and fatty acid derivatives, polyalcohols, and polyalcohol derivatives. PCMs are often enclosed in thin and resilient polymer shells (microcapsules) so that the material can change from solid to liquid and vice versa within the microcapsules (Shin, Yoo, & Son, 2005). PCMs can be incorporated into textiles by coating, lamination, finishing, melt spinning, bicomponent synthetic fiber extrusion, injection molding, and foam techniques (Mondal, 2008). The fact that temperature change can trigger the phase change of PCMs and store large quantity of energy makes PCMs ideal smart materials for textile coating. Coating methods to apply PCM microcapsules to fabrics include knife over roll, screen printing, pad-dry-cure, and dip coating (Sarier & Onder, 2012). Shin et al. (2005) used a pad-dry-cure process to treat polyester knit fabrics with melamine-formaldehyde microcapsules containing PCM paraffin wax eicosane and reported that the fabrics had a heat storage capacity of 0.91–4.41 J/g and retained 40% of their heat storage capacity after five launderings. Sánchez, Sánchez-Fernandez, Romero, Rodríguez, and Sánchez-Silva (2010) coated cotton fabrics with paraffin wax encapsulated in polystyrene using polymer binders. The cotton fabric coated with 35 wt% of PCM microcapsules and WST SUPERMOR[®] binder had an energy storage capacity of 7.6 J/g and thermoregulatory effects of 8.8, 6.3, 5.6, and 2.5°C difference for 6, 12, 44, and 75 s, respectively compared with a coated fabric without PCM microcapsules. The PCM-coated cotton fabric retained 47.4%, 63.2%, and 79.7% of energy storage capacity after washing, rubbing, and ironing, respectively (Sánchez et al., 2010).

A firefighter's turnout coat is made of four basic components. The exterior component is the outer shell, which protects against flames and heat. Underneath the outer shell is the moisture barrier to keep water out while allowing a limited

amount of moisture vapor to exit. The innermost two components are the face cloth and thermal liner combination that protect against heat penetration (Brown, 2005). Rossi and Bolli (2005) coated the liner of firefighter protective clothing with micro-encapsulated PCM paraffin (adding about 180 g/m^2 weight to the linings) and investigated whether the PCM coating could provide thermal protection and increase the firefighter's pain alarm time, the time between feeling pain and experiencing irreversible burns. A longer pain alarm time would give a firefighter more time to escape the danger zone. Rossi and Bolli (2005) prepared material samples consisting of three to four layers simulating a real firefighter's turnout coat and measured heat protection performance during radiant and convective heat exposure in accordance with ISO 6942 (Protective clothing—Protection against heat and fire—Method of test: Evaluations of materials and material assemblies when exposed to a source of radiant heat) and ISO 9151 (Protective clothing—Protection against heat and fire—Determination of heat transmission on exposure to flame) standards. According to ISO 6942, the combinations of material were exposed to different heat sources and the times for the rise in temperature from 12°C to 24°C behind the innermost layer were registered as radiant heat transfer indices RHTI12 and RHTI24, respectively. The time difference of RHTI24 to RHTI12 gave a good indication of the pain alarm time. They found that PCM coatings on the lining had a positive effect on heat protection, the effect of PCM was more pronounced when the PCM-coated layer was placed in the inner rather than the outer layer, and the efficiency of heat protection was related to the incident heat intensity. The average RHTI12 increased 43.5%, 40.7%, and 38.5% when the radiant heat exposure was 40, 10, and 5 kW/m^2 , respectively. For a three-layer (outer shell, moisture barrier, thermal liner) material combination, RHTI24 to RHTI12 was 38.3 s when the liner was not coated with PCM. For a liner coated with PCM, RHTI24 to RHTI12 increased to 47.2 s when the PCM layer was directed toward the outside and increased to 48.4 s when the PCM layer was directed toward the inside (closer to the firefighter's skin). The increase in RHTI24 to RHTI12 indicated that PCM coating in the liner of the firefighter's turnout coat increased the pain alarm time and gave the firefighter more time to escape the danger zone (Rossi & Bolli, 2005). Rossi and Bolli (2005) also pointed out that the paraffin PCM's phase change temperature of 50°C was low for the use in firefighter protective clothing and the burning behavior of paraffin restricted its use in firefighter protective clothing. To address these problems, Bühler, Popa, Scherer, Lehmeier, and Rossi (2013) prepared flexible blister foils embedded with nonflammable PCM salt hydrates ($\text{Mg}[\text{SO}_4]_2 \cdot 7\text{H}_2\text{O}$ and $\text{Na}[\text{CH}_3\text{COO}] \cdot 3\text{H}_2\text{O}$) and a water-saturated zeolite, and compared their heat protection performance with paraffin wax. Irradiated with a heat flux of 1.5 kW/m^2 , the heat buffering capacity of these inorganic nonflammable materials was higher than paraffin. For irradiation times up to 9 min, $\text{Na}[\text{CH}_3\text{COO}] \cdot 3\text{H}_2\text{O}$ exhibited the lowest temperature increase, whereas irradiating more than 9 min, zeolite showed the lowest temperature increase of up to 36°C compared with a reference with no PCM. This research indicated these nonflammable PCMs are better suited in textiles for heat protection (Bühler et al., 2013).

16.6 Future trends

Many new smart coating materials, formulations, and application processes have been developed to introduce new functions to textiles and enhance the performance of protective clothing. The smart coatings for protective clothing applications that have been discussed in this chapter are mainly academic research. To make these new technologies commercially successful, it is necessary to test the durability of the coated textile against the conditions of use and care associated with the protective clothing, such as abrasion, washing, perspiration, and weathering. In addition, many of the smart coating techniques apply nanotechnology and use the nanosize coating materials. It is necessary to evaluate and understand biophysicochemical interactions at the nano–bio interface from the perspective of safe use of nanomaterials (Nel et al., 2009).

It is easy to apply multiple layers of coating onto a textile substrate to incorporate multiple functions. Multilayer coatings may help solve important problems related to protective clothing. Because it was the first fiber used in body armor, Kevlar[®] polymer degradation resulting from aging, ie, UV instability, has been known for a long time (Holmes, Rice, & Snyder, 2006). Chin et al. (2007) conducted an accelerated aging study on PBO fabric, another important ballistic material, and found that PBO yarns lost approximately 40% of tensile strength after a 157-day testing period with elevated temperature and humidity. One of the main mechanisms in PBO fiber degradation was initiated by moisture. A review by Holmes et al. (2006) indicated that moisture, UV, and heat may degrade PBO fiber. Coating can introduce UV blocking and water-repellent properties to textiles. Nanoparticle ZnO coating has been proved an effective method to enhance the UV blocking property of textiles (Mao, Shi, Zhang, & Cao, 2009; Wang, Xin, & Tao, 2005) and silica coating can increase a water-repellent property to textiles (Daoud, Xin, & Tao, 2004; Mahltig & Böttcher, 2003). Coating with UV protection nanoparticles containing ZnO can prevent the degradation of Kevlar[®] (Katangur, Patra, & Warner, 2006) and PBO (Zhang, Huang, Yuan, & Zhang, 2011) textiles. A combination of multilayer smart coatings such as STF, UV protection, and water repellency on ballistic materials will enhance protection, comfort, and mobility for users and prolong the time of use. Similarly, multilayer water-repellent and antimicrobial coatings will be useful in protective clothing for health care employees to enhance protection against blood-borne microorganisms. Multilayer smart coatings to enhance protection synergistically need to be further investigated for protective clothing applications.

References

- Atanasov, S. E., Oldham, C. J., Slusarski, K. A., Taggart-Scarff, J., Sherman, S. A., Senecal, K. J., et al. (2014). Improved cut-resistance of Kevlar[®] using controlled interface reactions during atomic layer deposition of ultrathin (<50 Å) inorganic coatings. *Journal of Materials Chemistry A*, 2, 17371–17379.

- Brown, H. (2005). *Firefighter turnout coat configurations: Performance data for acquisition decisions*. NISTIR 7141. Gaithersburg, MD: National Institute of Standards and Technology. <http://nvlpubs.nist.gov/nistpubs/ir/2005/ir7141.pdf> Accessed 20.06.15.
- Bühler, M., Popa, A. M., Scherer, L. J., Lehmeier, F. K. S., & Rossi, R. M. (2013). Heat protection by different phase change materials. *Applied Thermal Engineering*, *54*, 359–364.
- Chen, L., Bromberg, L., Lee, J. A., Zhang, H., Schreuder-Gibson, H., Gibson, P., et al. (2010). Multifunctional electrospun fabrics via layer-by-layer electrostatic assembly for chemical and biological protection. *Chemistry of Materials*, *22*, 1429–1436.
- Chen, L., Bromberg, L., Schreuder-Gibson, H., Walker, J., Hatton, T. A., & Rutledge, G. C. (2009). Chemical protection fabrics via surface oximation of electrospun polyacrylonitrile fiber mats. *Journal of Materials Chemistry*, *19*, 2432–2438.
- Chin, J., Forster, A., Clerici, C., Sung, L., Oudina, M., & Rice, K. (2007). Temperature and humidity aging of poly(p-phenylene-2,6-benzobisoxazole) fibers: chemical and physical characterization. *Polymer Degradation and Stability*, *92*, 1234–1246.
- Daoud, W. A., Xin, J. H., & Tao, X. M. (2004). Superhydrophobic silica nanocomposite coating by a low-temperature process. *Journal of the American Ceramic Society*, *87*, 1782–1784.
- Dubas, S. T., Kumlangdudsana, P., & Potiyaraj, P. (2006). Layer-by-layer deposition of antimicrobial silver nanoparticles on textile fibers. *Colloids and Surfaces A: Physicochemical and Engineering Aspects*, *289*, 105–109.
- Fujihira, M., Satoh, Y., & Osa, T. (1981). Heterogeneous photocatalytic oxidation of aromatic compounds on TiO₂. *Nature*, *293*, 206–208.
- Fujishima, A., & Honda, K. (1972). Electrochemical photolysis of water at a semiconductor electrode. *Nature*, *238*, 37–38.
- Gadow, R., & von Niessen, K. (2006). Lightweight ballistic with additional stab protection made of thermally sprayed ceramic and cermet coatings on aramide fabrics. *International Journal of Applied Ceramic Technology*, *3*(4), 284–292.
- Ghosh, S. K. (2006). Functional coatings and microencapsulation: a general perspective. In S. K. Ghosh (Ed.), *Functional coatings by polymer microencapsulation* (pp. 1–28). Wiley-VCH Verlag GmbH & Co.
- Grandcolas, M., Louvet, A., Keller, N., & Keller, V. (2009). Layer-by-layer deposited titanate-based nanotubes for solar photocatalytic removal of chemical warfare agents from textiles. *Angewandte Chemie*, *121*, 167–170.
- Hammond, P. T. (2004). Form and function in multilayer assembly: new applications at the nanoscale. *Advanced Materials*, *16*, 1271–1293.
- Hassan, T. A., Rangari, V. K., & Jeelani, S. (2010). Synthesis, processing, and characterization of shear thickening fluid (STF) impregnated fabric composites. *Materials Science and Engineering A*, *527*, 2892–2899.
- Holmes, G. A., Rice, K., & Snyder, C. R. (2006). Review ballistic fibers: a review of the thermal, ultraviolet and hydrolytic stability of the benzoxazole ring structure. *Journal of Materials Science*, *41*, 4105–4116.
- Kamenidis, P. (2009). *Effect of trapped air on heat and moisture resistance of multilayered soft body armors* (Unpublished M.S. thesis). Stillwater, OK: Oklahoma State University.
- Karter, M. J., Jr., & Molis, J. L. (2014). *U.S. firefighter injuries – 2013*. Quincy, MA: National Fire Protection Association. <http://www.nfpa.org/research/reports-and-statistics/the-fire-service/fatalities-and-injuries/firefighter-injuries-in-the-united-states> Accessed 17.06.15.
- Katangur, P., Patra, P. K., & Warner, S. B. (2006). Nanostructured ultraviolet resistant polymer coatings. *Polymer Degradation and Stability*, *91*, 2437–2442.

- Kosashvili, Y., Hiss, J., Davidovic, N., Lin, G., Kalmivic, B., Melamed, E., et al. (2005). Influence of personal armor on distribution of entry wounds: lessons learned from urban-setting warfare fatalities. *The Journal of Trauma*, *58*, 1236–1240.
- Krogman, K. C., Lowery, J. L., Zacharia, N. S., Rutledge, G. C., & Hammond, P. T. (2009). Spraying asymmetry into functional membranes layer-by-layer. *Nature Materials*, *8*, 512–518.
- Lee, J. A., Krogman, K. C., Ma, M., Hill, R. M., Hammond, P. T., & Rutledge, G. C. (2009). Highly reactive multilayer-assembled TiO₂ coating on electrospun polymer nanofibers. *Advanced Materials*, *21*, 1252–1256.
- Lee, Y. S., Wetzel, E. D., & Wagner, N. J. (2003). The ballistic impact characteristics of Kevlar woven fabrics impregnated with a colloidal shear thickening fluid. *Journal of Materials Science*, *38*, 2825–2833.
- Mahltig, B., & Böttcher, H. (2003). Modified silica sol coatings for water-repellent textiles. *Journal of Sol-Gel Science and Technology*, *27*(1), 43–52.
- Mahltig, B., Fiedler, D., & Böttcher, H. (2004). Antimicrobial sol-gel coatings. *Journal of Sol-Gel Science and Technology*, *32*, 219–222.
- Makhlouf, A. S. H. (2014). *Handbook of smart coatings for materials protection*. Cambridge, UK: Woodhead Publishing.
- Mao, Z., Shi, Q., Zhang, L., & Cao, H. (2009). The formation and UV-blocking property of needle-shaped ZnO nanorod on cotton fabric. *Thin Solid Films*, *517*, 2681–2686.
- Mondal, S. (2008). Phase change materials for smart textiles – an overview. *Applied Thermal Engineering*, *28*, 1536–1550.
- National Institute of Justice. (2008). *Ballistic resistance of body armor*. NIJ Standard 0101.06. <https://www.ncjrs.gov/pdffiles1/nij/223054.pdf> Accessed 20.06.15.
- Nel, A. E., Mädler, L., Velegol, D., Xia, T., Hoek, E. M. V., Somasundaran, P., et al. (2009). Understanding biophysicochemical interactions at the nano-bio interface. *Nature Materials*, *8*, 543–557.
- Phoenix, S. L., & Porwal, P. K. (2003). A new membrane model for the ballistic impact response and V₅₀ performance of multi-ply fibrous systems. *International Journal of Solids and Structures*, *40*, 6723–6765.
- Qi, K., Daoud, W. A., Xin, J. H., Mak, C. L., Tang, W., & Cheung, W. P. (2006). Self-cleaning cotton. *Journal of Materials Chemistry*, *16*, 4567–4574.
- Qi, K., Wang, X., & Xin, J. H. (2011). Photocatalytic self-cleaning textiles based on nanocrystalline titanium dioxide. *Textile Research Journal*, *81*, 101–110.
- Qi, K., Xin, J. H., & Daoud, W. A. (2007). Functionalizing polyester fiber with a self-cleaning property using anatase TiO₂ and low-temperature plasma treatment. *International Journal of Applied Ceramic Technology*, *4*, 554–563.
- Rai, M., Yadav, A., & Gade, A. (2009). Silver nanoparticles as a new generation of antimicrobials. *Biotechnology Advances*, *27*, 76–83.
- Rosen, B. A., Laufer, C. H. N., Kalman, D. P., Wetzel, E. D., & Wagner, N. J. (2007). Multi-threat performance of kaolin-based shear thickening fluid (STF)-treated fabrics. In *Proceedings of SAMPE 2007, Baltimore, MD, June 3–7, 2007*.
- Rossi, R. M. (2003). Firefighting and its influence on body. *Ergonomics*, *46*, 1017–1033.
- Rossi, R. M., & Bolli, W. P. (2005). Phase change materials for improvement of heat protection. *Advanced Engineering Materials*, *7*, 368–373.
- Sánchez, P., Sánchez-Fernandez, M. V., Romero, A., Rodríguez, J. F., & Sánchez-Silva, L. (2010). Development of thermos-regulating textiles using paraffin wax microcapsules. *Thermochemica Acta*, *498*, 16–21.

- Sarier, N., & Onder, E. (2012). Organic phase change materials and their textile applications: an overview. *Thermochimica Acta*, *540*, 7–60.
- Schreuder-Gibson, H. L., Truong, Q., Walker, J. E., Owens, J. R., Wander, J. D., & Jones, W. E., Jr. (2003). Chemical and biological protection and detection in fabrics for protective clothing. *MRS Bulletin*, *28*, 574–578.
- Shin, Y., Yoo, D.-I., & Son, K. (2005). Development of thermoregulating textiles with microencapsulated phase change materials (PCM). II. Preparation and application of PCM microcapsules. *Journal of Applied Polymer Science*, *96*, 2005–2010.
- Shishoo, R. (2002). Recent developments in materials for use in protective clothing. *International Journal of Clothing Science and Technology*, *14*, 201–215.
- Singh, A., Lee, Y., & Dressick, W. J. (2004). Self-cleaning fabrics for decontamination of organophosphorous pesticides and related chemical agents. *Advanced Materials*, *16*, 2112–2115.
- Singha, K. (2012). A review on coating & laminations in textiles: processes and applications. *American Journal of Polymer Science*, *2*, 39–49.
- Smith, D. L., Manning, T. S., & Petruzzello, S. J. (2001). Effect of strenuous live-fire drills on cardiovascular and psychological responses of recruit firefighters. *Ergonomics*, *44*, 244–254.
- Srivastava, A., Majumdar, A., & Butola, B. S. (2011). Improving the impact resistance performance of Kevlar fabrics using silica based shear thickening fluid. *Materials Science and Engineering A*, *529*, 224–229.
- Sun, L.-L., Xiong, D.-S., & Xu, C.-Y. (2013). Application of shear thickening fluid in ultra high molecular weight polyethylene fabric. *Journal of Applied Polymer Science*, *129*, 1922–1928.
- Sundarrajan, S., Chandrasekaran, A. R., & Ramakrishna, S. (2010). An update on nano-materials-based textiles for protection and decontamination. *Journal of American Ceramic Society*, *93*(12), 3955–3975.
- Wagner, N., & Wetzel, E. (2004). *Advanced body armor utilizing shear thickening fluids*. U.S. Patent No. 7498276, Filing date May 2004, Publication date March 2009.
- Wang, R. H., Xin, J. H., & Tao, X. M. (2005). UV-blocking property of dumbbell-shaped ZnO crystallites on cotton fabrics. *Inorganic Chemistry*, *44*, 3926–3930.
- Wilhelm, M., & Bir, C. (2008). Injuries to law enforcement officers: the backface signature injury. *Forensic Science International*, *174*, 6–11.
- Xu, H., Shi, X., Ma, H., Lv, Y., & Mao, Z. (2013). The preparation and antibacterial activity of polyester fabric loaded with silver nanoparticles. *Textile Research Journal*, *83*, 321–326–6803.
- Xu, H., Shi, X., Ma, H., Lv, Y., Zhang, L., & Mao, Z. (2011). The preparation and antibacterial effects of dopa-cotton/AgNPs. *Applied Surface Science*, *257*, 6799–6803.
- Zhang, C.-H., Huang, Y.-D., Yuan, W.-J., & Zhang, J.-N. (2011). UV aging resistance properties of PBO fiber coated with nano-ZnO hybrid sizing. *Journal of Applied Polymer Science*, *120*, 2468–2476.

Smart medical textiles based on cyclodextrins for curative or preventive patient care

17

L. Leclercq

Lille University, Science and Technology, Villeneuve d'Ascq Cedex, France

17.1 Introduction

Cyclodextrins (CDs), also called Schardinger dextrins, are nonreducing cyclic oligomers of 1,4-linked α -D-glucopyranose. The most important native CDs are six-, seven-, or eight-membered oligomers, named, respectively, α -, β -, and γ -CD (Szejtli, 1998). These cyclic oligosaccharides have a shallow truncated cone shape with hydrophilic annulus owing to the primary and the secondary hydroxyl groups of the glucoses that face the exterior ends of the molecule. In contrast, the cavity has a hydrophobic character as a result of carbons and ethereal oxygen atoms and allows the formation of reversible inclusion complexes with polar compounds (amines, acids, esters, etc.), aliphatic or aromatic hydrocarbons, and so on (Szejtli, 1998). More than a century after their discovery by French chemist Villiers (1891), CDs are among the most widely used host molecules in the supramolecular chemistry domain (Dietrich et al., 1991). They are widely applied in agriculture (Campos et al., 2014), food technology (Szente and Szejtli, 2004), pharmacy (Funasaki et al., 2008), biotechnology (Singh et al., 2002), chemical and biological analysis (van de Manakker et al., 2009), chemical synthesis (Bjerre et al., 2008), catalysis (Leclercq et al., 2007, 2009), the cosmetics industry (Buschmann and Schollmeyer, 2002), environmental protection technologies (Baudin et al., 2000), the textile industry (Szejtli, 2003), and many other industrial applications (Hedges, 1998). The main reasons why CDs are so popular are that: (1) they are produced from a renewable raw material (ie, starch), (2) their preparation applies only enzymatic environmentally friendly technologies, (3) they are relatively cheap and are produced in amounts of thousands of tons per year, (4) their numerous chemical modifications are relatively easy, (5) they are biocompatible in consumable concentrations, and (6) they are biodegradable (Nardello-Rataj and Leclercq, 2014). Taking into account the increasing demand on the world textile market and the need for highly smart performing materials, the amelioration of textile materials remains open for new applications. In this context, the use of CD inclusion complexes is particularly interesting to improve the performance and obtain new functionalities of medical textiles (Bhaskara-Amrit et al., 2011). One of the most important and well-documented uses of CDs is the encapsulation of biocides (eg, bactericides, fungicides, virucides). For instance, the grafting of CDs on fabrics can be used to achieve antiseptic textiles to avoid skin disease with superinfection hazards. Under appropriate

conditions, the complexation of medications by CD improves their (1) physicochemical properties (eg, reduced vapor pressure), (2) controlled release and bioavailability, (3) shelf-life, (4) their storage conditions and environmental toxicity, and (5) resistance to repeated washing (Nardello-Rataj and Leclercq, 2014). The second well-documented use of CDs in the literature is probably the loading of insecticides to diminish the hazard of infections transmitted by insect bites. The third application is cosmetotextiles, on the borderline between cosmetic and medicine. Finally, some promising future directions of applications are still in development to obtain new functionalized textile products with advanced properties. In the following sections, all of these applications are illustrated by some references taken from the literature after a general presentation of CDs.

17.2 Cyclodextrin production, binding properties, and applications

17.2.1 Synthesis and characteristics

Starch degradation by enzymes results in dextrin (a mixture of low-molecular-weight polysaccharides), oligosaccharides containing a small number of glucose units (typically three to nine), and finally glucose. For instance, α -amylase, which is found in human saliva, is responsible for this degradation. The production of CDs, which are cyclic oligosaccharides, is relatively simple and involves the treatment of ordinary starch (eg, cornstarch) by enzymatic degradation in the presence of CD glycosyl transferase (CGTase) (EC 2.4.1.19). This enzyme is produced by numerous microorganisms: *Bacillus macerans*, *Klebsiella oxytoca*, *Alkalophylic bacillus*, *Bacillus circulans*, etc. (Fig. 17.1, Szejtli, 1998). In addition to CGTase, the industrial production of CDs requires large quantities of cornstarch. In this context, Wacker Chemie AG, which has produced CDs since the 1980s, built its latest production plant in Eddyville, Iowa next to cornfields in 1999. On the whole, Wacker produces up to 7500 metric tons/year of CDs and is the world's largest producer (Wacker Website, 2009).

From a historical point of view, CD synthesis occurs in two steps: starch hydrolysis by CGTase, resulting in a mixture of α -, β -, and γ -CD with six, seven and eight glucose units per molecule owing to the helical structure of the starch, and separation and purification of the three natural CDs. The simplest method to separate α -, β -, and γ -CD from the reaction mixture is selective precipitation by forming inclusion complexes with an adequate guest molecule (eg, α -, β -, and γ -CD crystallize with 1-decanol, toluene, and cyclohexadec-8-en-1-one, respectively). However, this kind of production was associated with considerable cost because of the separation process. Currently, elucidation of the DNA sequence involved in the production of CGTase allows isolation of the selective α -, β -, and γ -CGTase, which further increases the yield while decreasing the production cost (Toth, 2005).

From a structural point of view, the glucopyranosyl residues of the three common CDs are linked in a ring by α -1,4-glycosidic bonds. All glucose residues are in a 4C_1 (chair) conformation (Fig. 17.2, Szejtli, 1998).

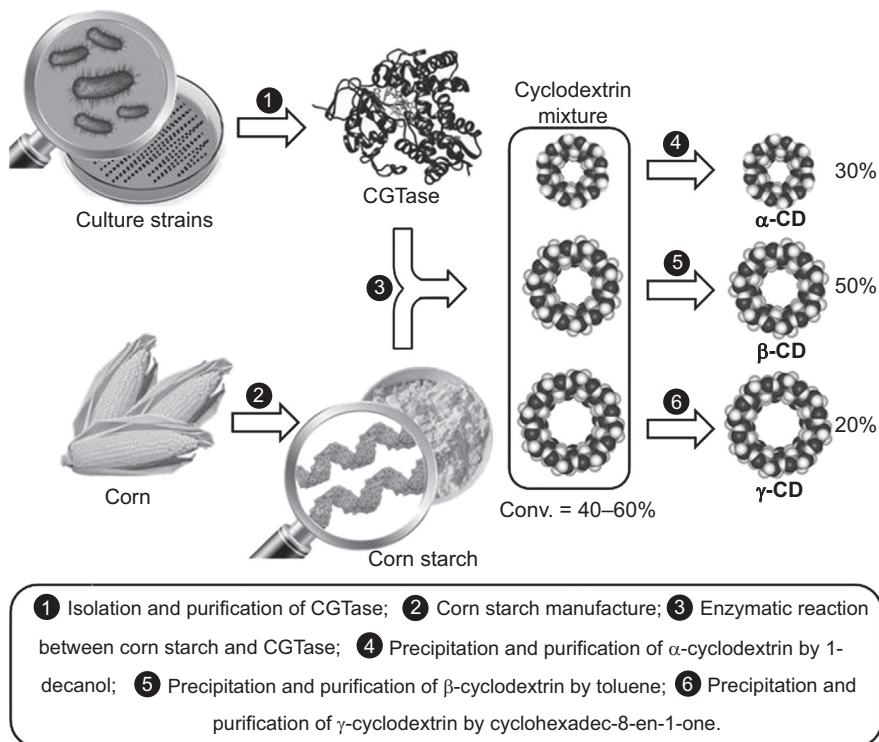


Figure 17.1 Enzymatic production of native cyclodextrins from cornstarch.

These three CDs have similar structures (in terms of bond lengths and orientations) apart from the structural necessities of accommodating a different number of glucose residues. CDs can be topologically represented as a truncated cone (eg, bottomless bowl-shaped) stiffened by H-bonds between the secondary hydroxyl groups (eg, 3OH and 2OH) around the outer rim. The H-bond strengths are α -CD < β -CD < γ -CD. The flexible primary hydroxyl groups are also capable of forming linking H-bonds around the bottom rim, but these are destabilized by dipolar effects, easily dissociated in aqueous solution and not normally found in crystalline structures. In α -CD, the 3OH groups have the role of H-bond donor whereas the 2OH groups are acceptor. In contrast, an inversion is observed for β - and γ -CD (Saenger et al., 1998).

In solution, the larger and the smaller openings of the cone expose the secondary and the primary hydroxyl groups, respectively, to the solvent. This arrangement allows variation in the polarity between the exterior and the interior of the truncated cone: CD rings are amphipathic. Indeed, the primary and the secondary hydroxyl groups, oriented to the narrow and the wider edge of the cone, allow a hydrophilic exterior. In contrast, the cavity has a hydrophobic character owing to carbons (eg, C₃–H and C₅–H) and ethereal anomeric oxygen atoms. Therefore, CDs have good aqueous solubility with the possibility to complex hydrophobic residues of molecules with remarkably sensitivity and selectivity depending on the cavity size (Table 17.1).

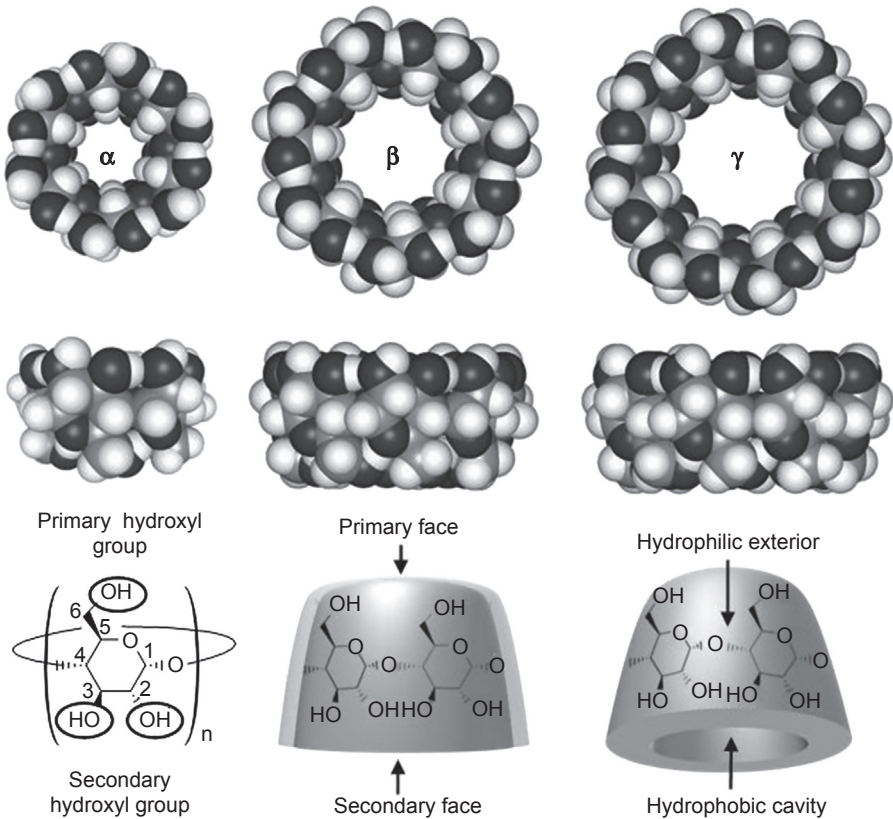
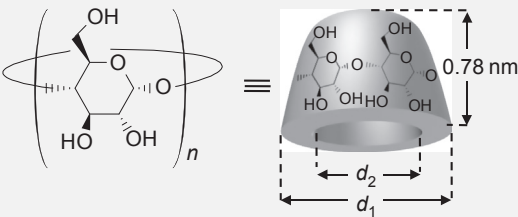


Figure 17.2 Molecular structure and schematic representation of native cyclodextrins.

Indeed, in aqueous solution, the hydrophobic cavity of α -, β -, and γ -CD contains about two, six, or nine poorly held water molecules which can be easily displaced to accommodate hydrophobic molecules (eg, aroma compounds or lipophilic drugs) (Uekama et al., 1998; Loftsson and Brewster, 2013). For instance, α -CD forms inclusion complexes with aliphatic residues (eg, decanoic acid) whereas β -CD prefers small aromatic, bicyclic, or tricyclic compounds (eg, adamantane) and γ -CD easily accommodates larger hydrophobic molecules (eg, the partial inclusion of fullerene C_{60}). The most commonly reported host–guest ratios are 1:1, 2:1, and 1:2 (Rekharsky and Inoue, 1998). Binding is an exothermic process (ie, $\Delta H < 0$). However, binding is also entropy-driven owing to the reduction of the hydrophobic surface in contact with water and the release of water molecules from the cavity to the bulk phase (Table 17.1).

Formation of the inclusion compounds allows CDs to be used to greatly improve the water solubility of hydrophobic compounds. This is why CDs have attracted much interest for pharmaceutical applications (see subsequent discussion). Because the water solubility of native CDs ranges from 18 to 232 g/L, a variety of modified

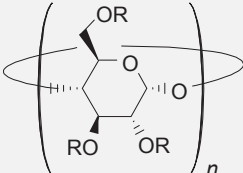
Table 17.1 Main properties of native cyclodextrins


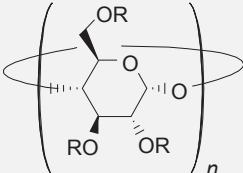
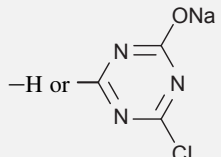
	<i>n</i>	Mass	<i>d</i> ₁ (nm)	<i>d</i> ₂ (nm)	Cavity volume (nm ³)	Aqueous solubility (g/L) ^a	Hydrate H ₂ O (cavity) ^a	Indicative price (€/g) ^b
α-CD	6	972	1.37	0.50	0.174	129.5	6.4 (2.0)	0.73
β-CD	7	1134	1.53	0.65	0.262	18.4	9.6 (6.0)	0.48
γ-CD	8	1296	1.69	0.85	0.472	249.2	14.2 (8.8)	4.76

^aTaken from Sabadini, E., Cosgrove, T., Egidio Fdo C., 2006. Solubility of cyclomaltooligosaccharides (cyclodextrins) in H₂O and D₂O: a comparative study. Carbohydrate Research 341 (2), 270–274.

^bFine chemical grade price obtained from CycloLab Cyclodextrin Research and Development Laboratory Ltd., Budapest, Hungary. The price depends on the purity and technological grade of the CD.

CDs have been developed to improve the formation of inclusion complexes and their solubility. Indeed, the hydroxyl groups allow the introduction of various functional groups (Khan et al., 1998). For instance, some native and chemically modified CDs are presented in Table 17.2.

Table 17.2 Structures and acronyms of some modified cyclodextrins^a


	Abbreviation	Substituent
	ME	–H or –CH ₃
	HP	–H or –CH ₂ CH(OH)CH ₃
	S	–H or –SO ₃ Na
	SBE	–H or –(CH ₂) ₄ SO ₃ Na
	CM	–H or –CH ₂ CO ₂ Na
	MCT	–H or 

^aME, methyl; HP, 2-hydroxypropyl; S, sulfo; SBE, sulfobutyl ether; CM, carboxymethyl; MCT, monochlorotriazinyl.

17.2.2 Toxicological properties

In the literature, detailed studies on toxicology, mutagenicity, teratogenicity, and carcinogenicity were carried out for native CDs (Stella and He, 2008). Cellular toxicity is directly correlated to the ability to complex membrane phospholipids and cholesterol. In consequence, CDs have *in vitro* hemolytic activity in the order β -CD > α -CD > γ -CD (Irie and Uekama, 1997). However, the toxicological implication *in vivo* is considered negligible. General toxicity on laboratory animals has been also reported in the literature (Saenger, 1980). The results support no acute intoxications (ie, no inflammatory response, no cell death, and no cell degeneration). The effect on the human gastrointestinal tract is also minimal (Stella and He, 2008). However, α - and β -CD cause renal damage and dysfunction but only at high concentrations (Thompson, 1997). A standard battery of reproductive and developmental tests was performed and indicated that none of the tested CDs are genotoxic, embryotoxic, teratogenic, or mutagenic (Stella and He, 2008). All of the human clinical experiences indicate that CDs can affect the human organism only at extremely high concentrations. Finally, various products using CDs are approved or undergo evaluation by regulatory agencies for use in food and pharmaceuticals. Indeed, β -CD was admitted in some countries as food additives (E 459) in the form of pellets and pills, with the restriction “only as necessary” (Buschmann et al., 2001).

For textile finishing, CDs modified with reactive groups are used. The most commonly used anchor group is the monochlorotriazinyl (MCT) residue (Reuscher and Hirsenkorn, 1996), which reacts with the cellulose hydroxyl groups leading to permanent covalent bonds between the fibers and the CDs (see subsequent discussion). For these MCT- β -CDs, the toxicological properties are important because most times the human skin is in permanent contact with textiles during various activities of everyday life when touching or wearing fabric. According to Organization for Economic Co-operation and Development (OECD) tests, MCT- β -CD derivatives have a neutral effect on the human body. Indeed, the median lethal dose is greater than 2 g/kg (Reuscher and Hirsenkorn, 1996). Moreover, MCT- β -CD derivatives have no effect on skin (ie, OECD tests 404 and 406 indicate no dermal irritation or corrosion and no skin sensitization, respectively). No mutagenic evidence was found in studies carried out on bacteria for MCT- β -CD (OCDE test 471). Comparable results were also obtained for textile products finished with this type of derivative; these results were backed up by the first clinical tests with T-shirts, which detected no human skin irritation (Buschmann et al., 2001). Finally, α -, β -, and γ -CD are also all generally recognized as safe by the Food and Drug Administration (Stella and He, 2008).

17.2.3 Binding properties

As mentioned, CDs are typical host molecules which can form inclusion complexes with various hydrophobic molecules. These guest molecules can be completely or partly accommodated inside the cavity. The inclusion complexes exist in solid state as well as in solution. In an aqueous solution, solubilized CDs accommodate some water molecules inside the cavity with energetically unfavorable interactions

(Szejtli, 1998). On the other hand, these water molecules are expelled outside and favorable interactions take place between the host and the guest molecule (Fig. 17.3). In other words, the well-known hydrophobic effect is the driving force of the complexation process: complexation is entropy-driven (Junquera et al., 1999). Indeed, pure water molecules adopt a structure that maximizes the entropy owing to the formation of a highly dynamic three-dimensional (3D) hydrogen bonding network. In the presence of hydrophobic molecules (or apolar residues), the H-bonds are partially disrupted around the nonpolar solute. Indeed, the nonpolar molecules are unable to form H-bonds with water. As consequence, a cavity is created in which water molecules form a cage around the solute (ie, the hydrophobic molecule is locked in a clathrate-like basket shape). In this clathrate, the H-bonds are reoriented tangentially to such a surface to minimize the number of disrupted H-bonds. The same behavior can be invoked for water molecules inside the CD cavity. In this case, there are fewer mobile water molecules in the system. To maximize the entropy of the system, water molecules are expelled from the CD cavity whereas the hydrophobic molecule shifts inside the CD cavity to form the inclusion complex. Upon complexation, the surface area exposed to water is reduced and the disruptive effect is minimized. Indeed, a smaller surface area is obtained for the inclusion complex than the total surface area created by the hydrophobic cavity and the nonpolar molecule. Some water molecules are now available to recreate the dynamic 3D hydrogen bonding network. Thus, the final entropy of the system is higher than the initial one (ie, $\Delta S > 0$) (Junquera et al., 1999). Therefore, the complexation was found to be entropy-driven at room temperature because of the reduced mobility of water molecules in the solvation shell of the nonpolar solute. However, at higher temperature, when water molecules become more mobile, this energy gain decreases along with the entropic component (Rekharsky and Inoue, 1998).

Moreover, some complementary interactions (ie, van der Waals forces and H-bonds) appear between the guest and the CD molecule. In addition, the cycle stress decreases, leading to a low-energy steady state. All of these noncovalent interactions ensure complex cohesion. The presence of a substituent can be used to maximize recognition between the guest and the CD. For instance, the introduction of ionic residues on the CD can be used to create an ionic interaction between complementary

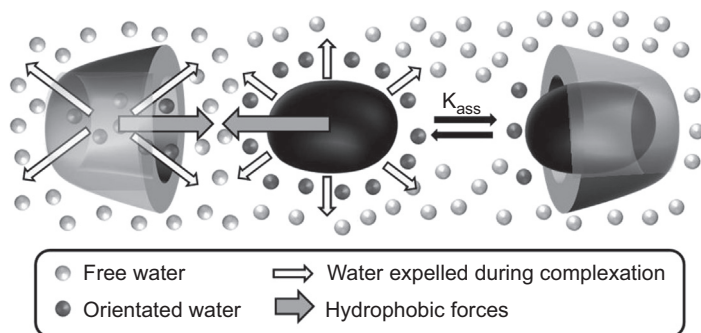


Figure 17.3 Cyclodextrin–guest inclusion complex formation upon a hydrophobic effect.

ionic regions. In other words, the number of binding sites of the CD host can be adjusted as a function of the guest structure. Binding constants and stoichiometries can easily be determined by various methods such as nuclear magnetic resonance (NMR), phase solubility, ultraviolet (UV)–visible imaging, potentiometry, and surface tension measurements (Rekharsky and Inoue, 1998; Leclercq et al., 2013b). Classically, the CD–guest molar ratio is 1:1. However, various stoichiometries can be obtained (see earlier discussion). The mechanism for higher stoichiometries involves a sequential stepwise complexation process depending on various factors: (1) the CD used (ie, the macrocycle size and the nature of substituent); (2) variations in temperature, concentration, and pH; (3) the solvent polarity; and (4) the presence of other compounds (eg, competition between various guests). Based on the Le Chatelier’s principle, which states that a system always acts to oppose changes in chemical equilibrium, the inclusion complexes can easily be separated by preferential complexing, ultrasound, or heating (see subsequent discussion) (Hirsch et al., 1985).

17.2.4 Applications in free form

The binding properties of CDs are useful for numerous applications. Some of them are presented in Fig. 17.4 (Del Valle, 2004).

From an academic point of view, CDs are potentially interesting for performing chemical and catalytic reactions. Indeed, they can control the regioselectivity of reactions while improving performance (Leclercq et al., 2005). They act as carriers or emulsifiers of hydrophobic substrates in aqueous phase (Leclercq et al., 2013a). They are often used to develop artificial enzymes (Breslow and Dong, 1998).

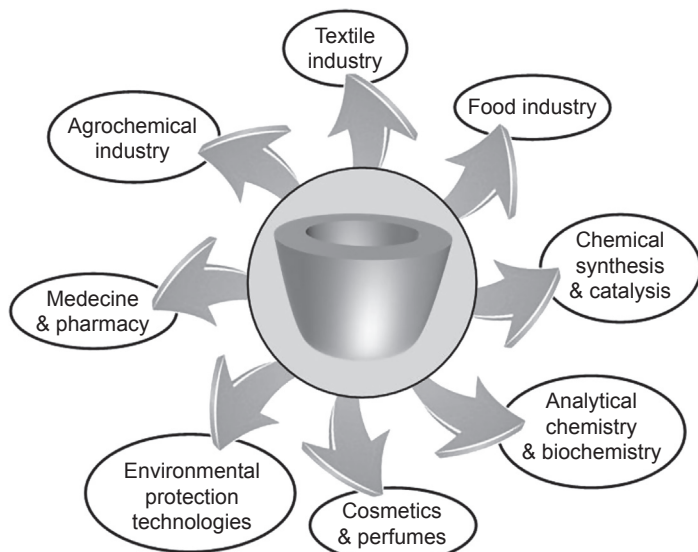


Figure 17.4 Principal applications of cyclodextrins.

CDs are also increasingly used in analytical chemistry and biochemistry, including high-performance liquid chromatography. Indeed, CDs change the affinity of the injected molecules for the stationary phase, and thus alter their retention time (Xiao et al., 2012). Moreover, CDs allow the separation of enantiomers because of their chirality. The exaltation of the responsiveness of photosensitive molecules upon complexation is used in fluorimetry (Hamasaki et al., 1993).

From an industrial point of view, three factors have long prevented their industrial use: the cost of production, incomplete toxicological studies, and the lack of knowledge pharmaceutically (Del Valle, 2004). Because this information is now available (see earlier discussion), CDs in free form (ie, in solid or in solution) are commonly used on an industrial scale. Thus, in the agrochemical field, the CDs are used to improve the efficiency of fertilizers, herbicides, insecticides, repellents, etc., and to solidify liquid biocides to achieve better stability during storage (Nardello-Rataj and Leclercq, 2014). The industrial applications of CDs are also important in cosmetics. Indeed, they improve the solubility of vitamins A and E, they stabilize the taste and colors of toothpaste, they are antiplaque compounds, they reduce irritation caused by shampoo formulations, and they protect perfumes and allow long-lasting fragrance release (Buschmann and Schollmeyer, 2002). In environmental protection technologies, CDs are used for soil remediation or to reduce oxidizer requirements in paper production (Boyle, 2006). CDs are also commonly used in the food industry to preserve aromas, extend the duration of chewing gum taste, trap odor molecules, protect molecules against oxidation or thermal decomposition, prepare cholesterol-free products (from milk, butter, eggs, etc.), and emulsify mayonnaise, desserts, and sweets (Szente and Szejtli, 2004). In the paint industry, CDs improve the compatibility of ingredients, the stability of paint, as well as the range of colors and the quality of dyes (Szejtli, 2004).

However, the first global consumer of CDs is undoubtedly the pharmaceutical industry (Loftsson and Brewster, 2011). Indeed, because of their hydrophobic cavity and hydrophilic outside, they can form inclusion complexes with a wide range of hydrophobic drugs. Upon complexation, biologically active molecules solubility is improved. Moreover, CDs act as carriers in which hydrophobic drugs can be released under specific conditions on a specific target. In most cases, the mechanism of controlled degradation of such complexes is based on a change in pH, leading to the loss of hydrogen between the host and the guest molecules (Zhang and Ma, 2013). Alternative means for the disruption of the complexes take advantage of heating or enzymatic cleavage of α -1,4 links between glucoses (see previous discussion). In consequence, the complexation enhances the bioavailability of medications. For instance, the controlled release of nicotine in smoking cessation treatment occurs by the use of β -CD/nicotine (Nicorette[®] sublingual tablets). Numerous formulations that use CDs are commercialized worldwide to complex fungicides, bactericides, anti-inflammatories, etc. For instance, β -CD/piroxicam, a nonsteroidal antiinflammatory drug (NSAID), is also used in various formulations distributed under various commercial names (eg, Brexin[®], Flogene[®] and Cicladon[®]) (Loftsson and Duchêne, 2007). In addition, side effects of the active ingredients may be reduced (eg, irritation of the intestinal mucosa). For instance, they can be used to decrease by sixfold propylene glycol,

which is responsible for greasy and sticky effects, in antialopecia formulation (Alopecy[®] 2%) (Delaunois and Navarro, 1997). They also reduce the sensitivity of active ingredients to light, heat, hydrolysis, and oxidation. Moreover, aqueous CD solutions can generate aerosols suitable for pulmonary deposition. α -CD has been authorized for use as “a novel food ingredient” (eg, dietary fiber) (Furune et al., 2014) in the European Union since 2008 to reduce blood sugar peaks after a high-starch meal (Decision 258/97/EC of the European Parliament and of Council, May 26, 2008). α -CD is also used in weight loss supplements and antiobesity medications to bind fat (Buckley et al., 2006). They can also transform liquid compounds in solids (powder or tablets) by precipitating inclusion complexes. For instance, CDs are used to encapsulate ethanol and produce alcoholic beverages when mixed with water. Other applications of CDs are for treating inflammation or throat infection (with iodine), coronary dilatation (with nitroglycerin), as an antiulcerate (with benexate), for complexation (eg, vectors) for vitamins or hormones, and to reduce side effects and increase the efficiency of anticancer drugs (Calleja et al., 2012).

The wide use of CDs for pharmaceutical purposes can be explained by the reversibility of host–guest binding. However, when the complexes are dissociated, the reverse process occurs according to the binding constant value (K_{ass}). For solid complexes, dissociation occurs quickly when water is added. Despite the initial dissociation energetic barrier resulting from interactions between guest and host molecules, the concentration gradient prevails, and the guest drugs leave the host molecules. Given the small concentration in solution, complex reformation is impossible; the released molecule remains in solution and can interact with the biological target with a controlled release (Challa et al., 2005). For solutions, the complexes act as a reservoir of drugs which are readily available for adsorption onto the biological target. Indeed, because the free drug concentration is in equilibrium with the drug adsorbed onto the target and with CD–drug complexes, the decrease in free drug concentration, owing to drug adsorption by the target, alters the equilibrium between free and complexed drug; the drug is progressively released in solution (Fig. 17.5).

The last, but one of the main fields of application of CD complexes, is the creation of smart textiles. Indeed, the applications presented earlier can be transposed to the textile technology, in which the CDs are used to fix various active compounds on the textile fibers: eg, antipathogens, antiinflammatories, insecticides, essential oils, venotonic molecules (Szejtli, 2003). Before we move on to look at CD–drug complexes and their applications, the first step to obtaining these new and smart textiles is the binding of CDs on fabrics.

17.2.5 Interaction with textile support

From a general point of view, CDs can be fixed on textile materials by means of various methods including spraying, printing, padding, grafting, surface coating, impregnation, and inkjet printing (Table 17.3) (Bhaskara-Amrit et al., 2011). These methods can be divided into physisorption and chemisorption. Compared with chemisorption, in which the electronic structure of bonding molecules is changed and covalent or ionic bonds are formed, physisorption can be observed only in the environment

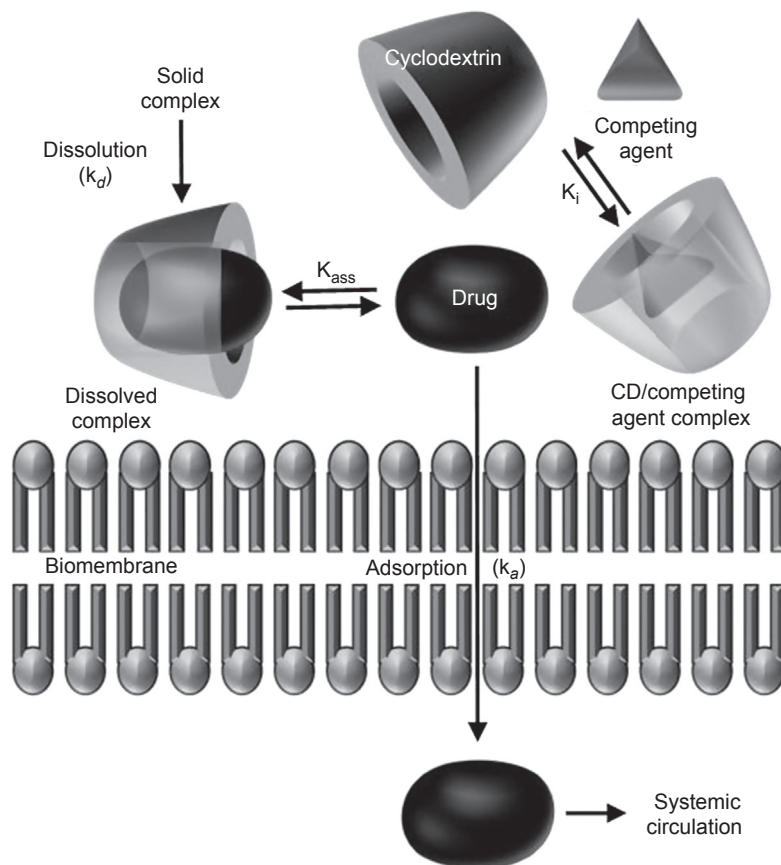


Figure 17.5 Mechanism of controlled release of drug from free cyclodextrin inclusion complex to a given biological target.

Table 17.3 Possible interactions between cyclodextrins and some textile fibers

Interactions	Natural fibers		Synthetic fibers		
	Cotton	Wool	PES	PA	PAN
van der Waal forces	✗	✗	✓	✓	✓
Ionic interactions	✗	✓	✗	✓	✓
Covalent bonds	✓	✓	✗	✓	✗
Cross-linking agents	✓	✓	✓	✗	✗
Graft polymerization	✓	✓	✓	✓	✓

PES, polyester; *PA*, polyamide; *PAN*, polyacrylonitrile.

Adapted from Andreus, J., Dalmolin, M.C., de Oliveira I.B.J.R., Barcellos, I.O., 2010. Aplicação de ciclodextrinas em processos têxteis. *Química Nova* 33(4), 929–937.

of low temperature (at room temperature) and in the absence of strong chemisorptions. For instance, physical adsorption is based on the use of hydrophobic groups which penetrate the polymer surface (Fig. 17.6(a)).

This method is particularly useful for hydrophobic nonionic CDs that can be fixed to hydrophobic textiles (eg, polyamide, polyester, and polyacrylonitrile) through apolar interactions. This physisorption can be useful for removing unpleasant smells. Indeed, the textile is treated by spraying with a solution of CD. Because CDs do not bind to the fibers, the undesirable complexes can be removed by washing (Trinh et al., 1997). In this case, CDs are not reused and the application of this system is limited to deodorizing. In contrast, permanent fixation of CDs on the fabrics can be achieved by chemisorption. Here, fixation, which involves a chemical reaction between the surface and the adsorbate, allows the generation of chemical bonds at the adsorbent surface (Fig. 17.6(b)).

In a more detailed way, grafting of CDs on cellulose fibers is common and generally easy to perform. The first cellulose-CD copolymer was described in 1980 (Szejtli et al., 1980). This method involves the use of epichlorohydrin as a cross-linking reagent to fix CDs to alkali-swollen cellulose fibers. However, most chemical adsorption requires the prior addition of reactive residues on native CDs. Since 1996, one of the most widely used residues has probably been MCT binding to CD (eg, MCT- β -CD) (Reuscher and Hirsenkorn, 1996). This kind of CD is obtained by (1) treatment of 2,4,6-trichloro-1,3,5-triazine in the presence of sodium hydroxide to obtain 2,4-dichloro-6-hydroxytriazine sodium salt and (2) the addition of native CDs to this derivate in the presence of sodium hydroxide, which allows the formation of

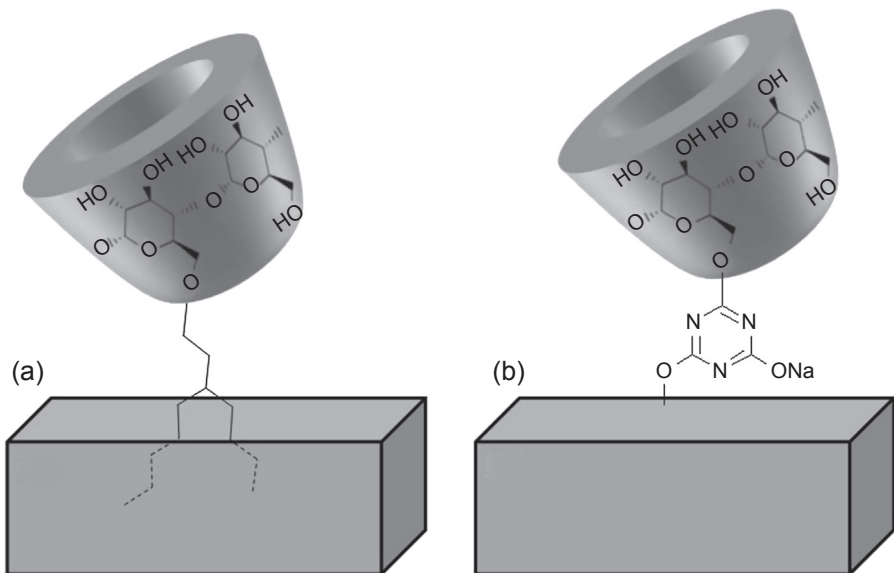


Figure 17.6 Schematic representation of physisorption (a) and chemisorption (b) of modified cyclodextrins at the polymer surface.

MCT-CD. Finally, the CD-grafted fibers are easily obtained by immersing the textile material in a bath containing the MCT-CD through a simple nucleophilic substitution (Fig. 17.7). The fixed CDs can be used to complex smells or perfumes. In contrast to textile spraying with a solution of CD, CDs can be reused and new substances can be reloaded inside the CD cavities. For instance, odor can be controlled by applying an antimicrobial finish (see subsequent discussion). Upon humidity, the biocide is progressively released and the odor molecules can be trapped in the cavities of the CDs and removed during laundering. This system can be used on T-shirts and other sports apparel.

The grafting of CDs on synthetic fibers (eg, polyester, polyamide) is also common and generally easy to perform. For instance, polyamide fibers, which are used in the medical field for different prostheses, can be modified by incorporating CDs which complex antibiotic molecules. In this case, controlled release of the antibiotic is obtained to avoid hazardous infections (see subsequent discussion). From a synthetic point of view, the CDs are attached by using citric acid (CTR) as a reticulating agent (Fig. 17.8, Martel et al., 2002a,b). The reaction occurs between CDs and CTR to form polyester (ie, poly[CTR-CD]). Finally, this polyester interacts with the polyamide fabric to form a continuous film. Another, similar method of grafting uses 1,2,3,4-butanetetracarboxylic acid (BTCA) as a cross-linking agent (Martel et al., 2002a,b). This method can be used with cotton, wool, polyester, polyamide, polyethylene terephthalate, etc. In this method, the fibers are treated with β -CD and BTCA in an aqueous solution. BTCA molecules react via anhydride formation with hydroxyl groups of β -CD and form a nano-assembly which can be physically attached to the fibers surface at an elevated temperature. Such an assembly is schematically presented in Fig. 17.9.

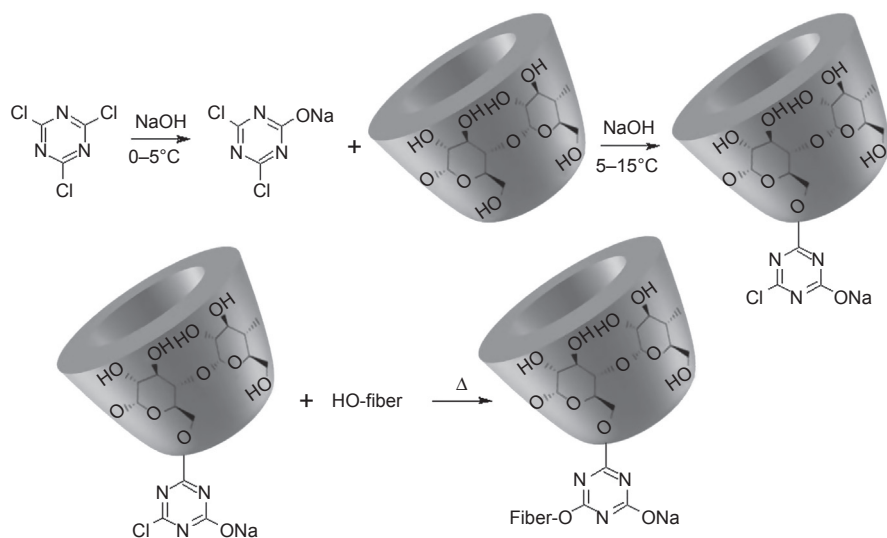


Figure 17.7 Synthesis of monochlorotriazinyl-cyclodextrin (MCT-CD) and its grafting on fabric.

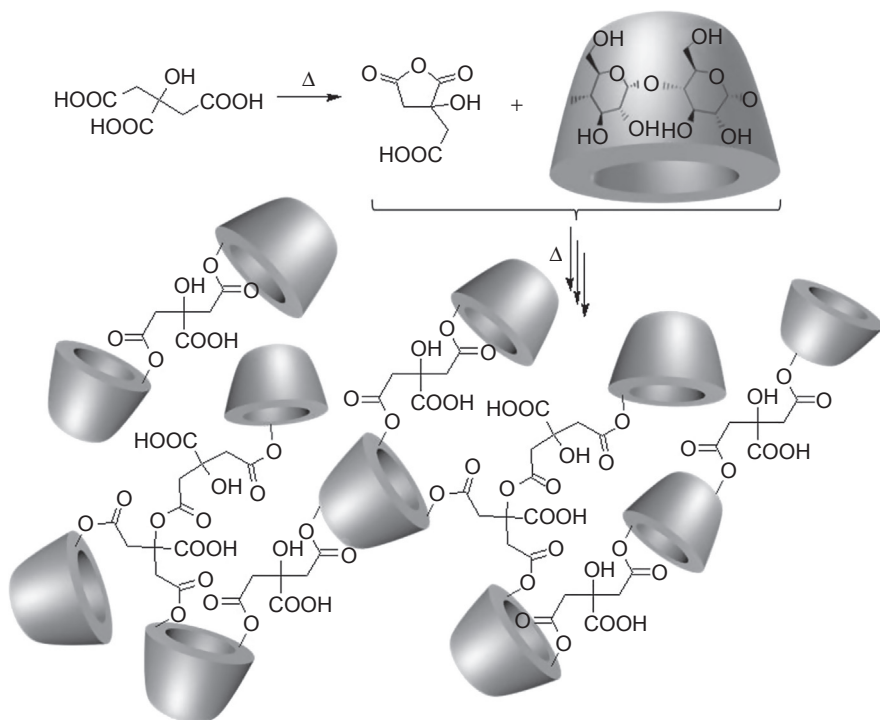


Figure 17.8 Reaction of cyclodextrins with citric acid to form poly(citric acid–cyclodextrin).

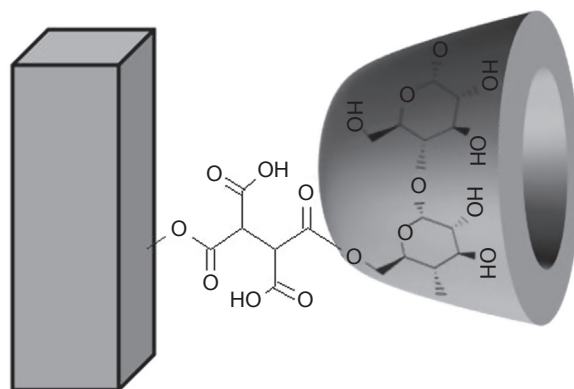


Figure 17.9 Nano-assembly of β -cyclodextrin via 1,2,3,4-butanetetracarboxylic acid onto cotton textile.

Finally, newer methods are reported in the literature. For instance, 6-monodeoxy-6-mono(*N*-tyrosinyl)- β -CD can be fixed on a cotton surface by enzymatic reactions (Agrawal et al., 2010a,b). In conclusion, a large variety of modified fabrics can easily be obtained and the number of binding sites on textile can easily be controlled by the number of CDs that are incorporated.

17.2.6 General applications of cyclodextrins in textile industry

CDs are generally used in the textile industry, as in free form, to improve (1) the physicochemical properties of the various guest molecules (eg, wettability, reduced vapor pressure), (2) controlled release and bioavailability, (3) shelf-life, (4) storage conditions, and (5) biodegradability (Nardello-Rataj and Leclercq, 2014). Under such conditions, four main fields can be highlighted: (1) their use as auxiliary substances in laundering, (2) their use in fiber dyeing, (3) their use in textile finishing, and (4) their use in medication delivery. In this section, these key advantages are illustrated by some typical examples. However, the separation of CDs applications is purely made up, because a combination of advantages is often reported.

CDs can be used in washing liquids for various reasons. Indeed, in the literature it is known that CDs form inclusion complexes with detergent molecules. Because surfactants have potential drawbacks for the human body and the environment (eg, skin irritation, hemolysis, protein denaturation), the addition of CDs to the final rinse water reduces the residual surfactant content on the laundered fabric from 209 to 134 parts per million (Dehmer et al., 1998). In other words, CDs reduce the potential harmful interaction of detergent molecules with the human skin. In addition, CDs can act as defoaming agents and may be used to reduce water consumption. Moreover, CDs may be used to prevent colors from running in textiles during washing or rinsing (Weiss et al., 1998). Finally, CDs can be used to avoid fragrance evaporation during the storage of washing powders. Indeed, perfumes complexed by CDs are more stable and are easily displaced by detergent molecules during the washing process.

CDs can be also used in textile dyeing. Indeed, CDs increase the affinity of the dyestuff to the textile but decrease the diffusion coefficient into the fabric. For instance, disperse dye-printed cotton and cotton–polyester fabrics, with improved dye absorption, were prepared by treating the fabric with α - or β -CD and printing the fabric with pastes containing a disperse dye (Okano, 1978). Moreover, the light stability of the textiles was improved by using UV-filter–ME- β -CD complexes and textile dyes (Remi et al., 1996).

Physically adsorbed CDs are used to remove sweat or sweat degradation from the textile by preventing their penetration into the fiber interior (see earlier discussion) (Poulakis et al., 2002). In these formulations, complexes can easily be removed by simple washing. CDs can be also used to incorporate fragrance in synthetic fiber polymers. Under appropriate conditions, wash-resistant fragrant fabrics can be obtained (Fujimura, 1985). Indeed, in the presence of CDs, the vapor pressures of perfumes are reduced. As a consequence, the properties of fragrant textiles are clearly improved.

CDs and their inclusion complexes can be also employed for some miscellaneous uses: to reinforce rubber, to remove harmful organic pollutant substances from the textile finishing process by forming inclusion complexes, and to prevent starch from depositing on an iron (Szejtli, 2003).

However, the most important application of CDs in the textiles industry is to obtain textiles with pharmacological properties. Indeed, the chemically bound CD retains a complex-forming ability and can be loaded with biologically active guests (drugs, insect repellents, antimicrobial agents, etc.). Fabrics made from such fibers ensure drug release upon contact with skin. The following section is devoted to this topic.

17.3 Cyclodextrins grafted on textiles for medical purposes

As presented in the previous section, upon CD encapsulation, the physicochemical properties of the guest molecules are changed (eg, the solubility of drugs increases, vapor pressure is reduced, stability against light and oxygen increases). When CDs are anchored to textile fibers, we obtain new smart medical products which allow the simple and controllable administration of various medication molecules via complexation (see previous discussion). Indeed, the sustained drug delivery results from the equilibrium between the drug complexed by CDs and the drug released in perspiration before the diffusion in dermis (Radu et al., 2014). A scheme of this diffusion process is illustrated in Fig. 17.10.

17.3.1 Antipathogen textiles

A pathogen describes an infectious agent, including bacteria, virus, prion, fungus, or protozoan. The host may be an organism such as a vertebrate, insect, plant, fungus, or bacterium. To prevent and treat these infections, antipathogen agents, defined as “active substances and preparations containing one or more active substances, put up in the form in which they are supplied to the user, intended to destroy, render harmless, prevent the action of, or otherwise exert a controlling effect on any harmful organism by chemical or biological means” (Directive 98/8/EC of the European Parliament and Council of February 16, 1998, Article 2.1.a), are commonly used. Antipathogen agents in the textile industry for health care and hygiene applications have received a lot of attention. Indeed, to prepare medical bandages, the complexation of antipathogen agents is useful to achieve sustained drug release from the fabrics upon contact with skin. However, for the sake of clarity, only some typical examples

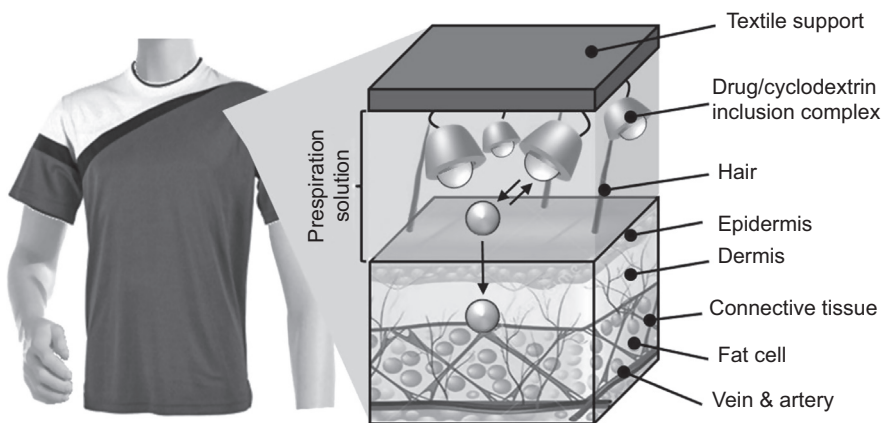


Figure 17.10 Diffusion principle of drug from cyclodextrin inclusion complexes grafted onto the textile to dermis.

of CD–biocide inclusion complexes on textile are reported. The chemical structures of the active biocides mentioned in this section are presented in Fig. 17.11.

Antipathogen medications based on iodine, in various forms (eg, elemental iodine or water-soluble triiodide), are active in treating superficial skin infections. The water-soluble triiodide anion I_3^- is generated in situ by adding iodide to poorly water-soluble elemental iodine. In this case, the reverse chemical reaction releases free elemental iodine available for antiseptics. Various topical solutions have been developed including tincture of iodine (eg, iodine in ethanol, or iodine and sodium iodide in a mixture of ethanol and water); Lugol's iodine (iodine and iodide in water, forming mostly triiodide); and povidone–iodine (a stable chemical complex of polyvinylpyrrolidone). Because CDs are known to complex iodine, a cellulose fabric containing chemically bound β -CD (0.27 equivalent of β -CD/g) using epichlorhydrin was patented in 1991. To obtain a smart medicated bandage, this fabric was treated with 50 mL solution of 1% I_2 and 0.7% KI in 75% ethanol (Szejtli et al., 1991).

In 1997, Yamamoto and Saeki reported on antiinfective bed sheets containing CD inclusion compounds of antimicrobial agents for controlling infections in hospitals, nursing homes, etc. Because the allyl isothiocyanate (bactericide) is particularly volatile, its encapsulation by CDs is a smart solution to obtain antiinfective sheets (Fig. 17.11, Yamamoto and Saeki, 1997). Antiinfective sheets were easily prepared

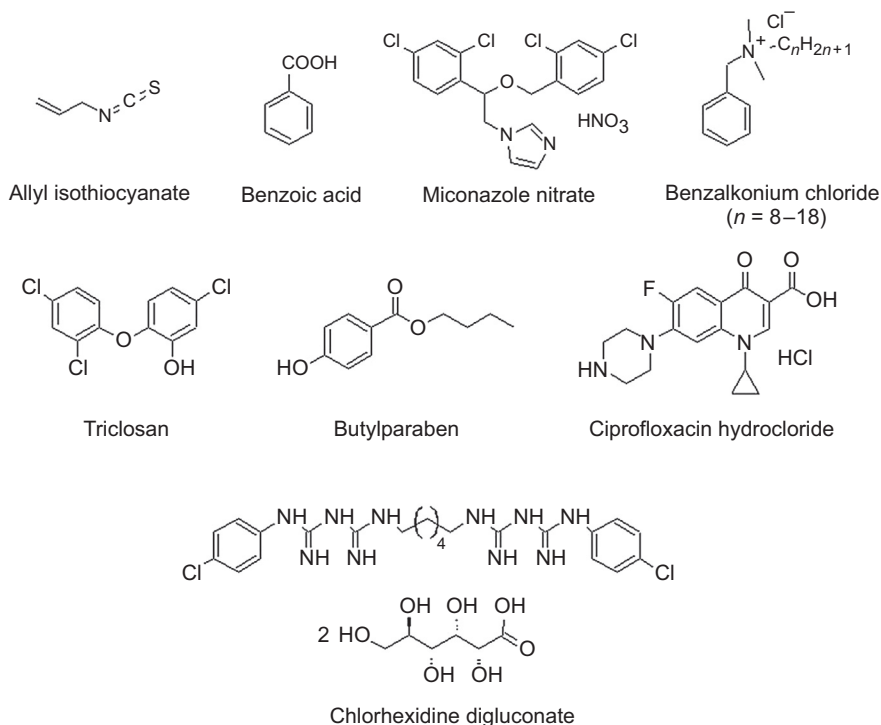


Figure 17.11 Chemical structures of active biocides mentioned in this section.

by mixing the inclusion complex particles with thermoplastic resin, followed by molding so that the average particle size of the particles is larger than the average thickness of the sheets. Particles of allyl isothiocyanate/ β -CD inclusion complex ($\approx 25 \mu\text{m}$) showed antimicrobial activity against various common pathogen strains (eg, *Candida albicans*, *Salmonella enteritidis*, *Staphylococcus aureus*, *Escherichia coli*) whereas control particles of inclusion complex were not effective on *E. coli*. The antimicrobial particles were mixed with low-density polyethylene and the mixture was extrusion-molded, followed by stretching to give a 20- μm -thick antiinfective sheet. In 1998, the same authors reported on bed sheets containing noncrystalline calcium phosphate and CD inclusion compounds of allyl isothiocyanate as antimicrobial agents active against *C. albicans* and *S. aureus* (Yamamoto and Saeki, 1998).

In 2000, grafting onto cotton fiber with acrylamidomethylated- β -CD (AAM- β -CD) was reported in the literature (Fig. 17.12, Lee et al., 2000).

First, the authors synthesized the chemically modified CD by the reaction of *N*-methylolacrylamide (NMA) with β -CD in the presence of formic acid as a catalyst. After purification and initiation of the cotton cellulose backbone with ceric ion, the modified β -CD was grafted. The amount of grafted CD was determined by fluorescence measurements. The possibility of textile finishing of CD-containing cotton fibers was investigated using an archetypal antibacterial agent (eg, benzoic acid) (Fig. 17.11). Antibacterial activity against *S. aureus* of benzoic acid-treated samples was retained even after 10 laundering cycles, which suggests that the use of CD in functional textile finishing is promising.

The previous results were used to modify cellulosic fabric (Tencel[®]) with β -CD to obtain biocidal textiles (Lo Nostro et al., 2002). The authors used two β -CD

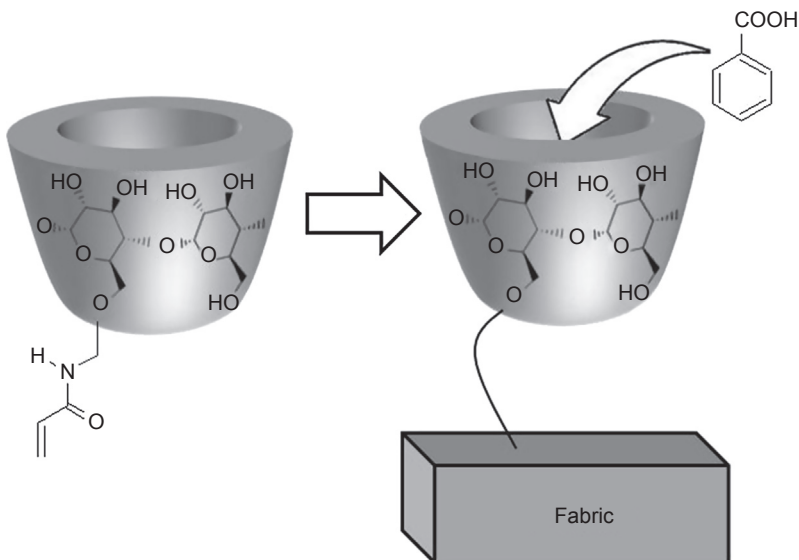


Figure 17.12 Structure of acrylamidomethylated- β -cyclodextrin (AAM- β -CD) and schematic representation of an inclusion compound formed on the fabric's surface.

derivatives: the well-known MCT- β -CD and AAM- β -CD. After grafting, benzoic acid and iodine were included in β -CD cavities at the textile's surface. The untreated and treated fabrics were evaluated through scanning electron microscopy (SEM) imaging, differential scanning calorimetry, UV-visible spectra, X-ray diffractometry, water absorbency, and breaking load loss. The results proved the inclusion of the biocidal compounds in the CD cavities. Moreover, the fabric's surface properties were not significantly modified by the chemical treatments. Finally, the biocidal properties of finishing fabrics were evaluated. The best activity was observed for benzoic acid included in AAM- β -CD-Tencel[®], particularly against *S. aureus* and *C. albicans*. This cellulose fabric may be suitable for medicinal bandages.

In this context, the encapsulation of miconazole nitrate salt into the cavity of MCT- β -CD covalently bound onto textile fibers was reported in 2008 (Fig. 17.11, Wang and Cai, 2008). Miconazole salt is an imidazole antifungal agent used topically on skin or the mucous membranes to cure fungal infections. Additional antibacterial and antiparasitic actions are also reported owing to the inhibition of ergosterol synthesis, a critical component of cell membranes. A grafting yield of about 5% was obtained when MCT- β -CD (60–100 g/L) and Na₂CO₃ (50–60 g/L) reacted at 150–160°C for 5–8 min. To know the quantity of miconazole nitrate entrapped in the functionalized textile with MCT- β -CD, UV spectrophotometry on modified and unmodified fabrics was performed. The functionalized textile with MCT- β -CD was richer than the unmodified one (up to 8.2-fold). As expected, biocidal activity against *C. albicans* was enhanced for the MCT- β -CD-modified textile impregnated with the antifungal drug. The finished fabric retained its antifungal property after 10 washes, unlike the unmodified textile.

The immobilization of butylparaben and triclosan with the use of a cationic- β -CD polymer was developed (Fig. 17.11, Qian et al., 2009). Butylparaben is known to be an antimicrobial agent used in pharmaceutical suspensions, whereas triclosan is an antibacterial and antifungal molecule. Butylparaben is known to act by inhibiting DNA, RNA, and enzymes (eg, ATPase and phosphotransferase) synthesis. The biocidal mechanism of triclosan is greatly influenced by its concentration. Indeed, at high concentrations triclosan acts as a biocide with multiple cytoplasmic and membrane targets, whereas at lower concentrations, triclosan is essentially bacteriostatic (Russel, 2004). In the last case, the cell membrane fatty acid synthesis of bacteria is inhibited owing to the formation of a stable complex between enoyl-acyl carrier protein reductase, nicotinamide adenine dinucleotide, and triclosan. One-step condensation of β -CD, epichlorohydrin, and choline chloride (1/5/2) was used to synthesize the cationic- β -CD polymer (CP- β -CD). The aqueous solubility of butylparaben and triclosan encapsulated in the CP- β -CD polymer improved from 0.001 to 2.80 and to 1.64 g/L, respectively. The aqueous solubility of butylparaben greatly improved in the CP- β -CD cavities owing to its smaller volume. The CP- β -CD polymers loaded with triclosan and butylparaben were adsorbed on cellulose fibers and the antimicrobial activities against *E. coli* and *Salmonella* were reported. The best activity was obtained for the triclosan loaded inside the CP- β -CD cavities. The biocidal mechanism of the CP- β -CD polymers was investigated by observing the morphology of *E. coli* with atomic force microscopy. Because the cell membrane was not affected by the CP- β -CD

polymer loaded with butylparaben or triclosan, the authors proposed that the biocide–CP- β -CD complexes inhibit only cell metabolism. The authors concluded that the cationic groups of the CP- β -CD polymer facilitate biocide delivery as a result of the binding of polymer on the negatively charged cell membrane.

In 2013, cellulosic medical bandages functionalized with CDs were reported for the prolonged release of chlorhexidine digluconate (Fig. 17.11, Cusola et al., 2013). Surface functionalization was performed using CTR as a cross-linker agent. SEM and Fourier transform infrared (FTIR) spectroscopy analyses were used to characterize the bandage. The drug-delivery kinetics of the encapsulated antibacterial agent was carried out by immersing the medical bandage into an aqueous medium, and the quantity of the released biocide was measured as a function of time by UV spectroscopy. The retention of the biocide after 12 h was around 30% and 10% for the grafted and nongrafted samples, respectively. After 2 days, nongrafted samples no longer released the biocide, whereas for grafted samples this delay was extended to 4 days. These results support the potential use of this cellulosic bandage in the medical domain.

Ciprofloxacin is an antibiotic that can treat a number of respiratory, urinary tract, gastrointestinal, and abdominal infections. It has excellent human tissue penetration and is classified as a broad-spectrum antibiotic. Indeed, it is active against gram-negative (*E. coli*, *Haemophilus influenzae*, *Klebsiella pneumoniae*, *Legionella pneumophila*, *Pseudomonas aeruginosa*, etc.), and gram-positive (*S. aureus*, *Staphylococcus epidermidis*, *Streptococcus pneumoniae*, *Enterococcus faecalis*, etc.) bacterial pathogens. Therefore, scientists drew attention to its inclusion in β -CD grafted on cellulose fabrics (Fig. 17.11, Dong et al., 2014). β -CD-grafted cellulose was prepared by forming CTR- β -CD (see previous description). The CTR- β -CDs were covalently bound to the hydroxyl groups of cellulose. Under the best conditions ([CTR- β -CD] = 300 g/L, pH 3.4, 15 min, 160°C), the grafted ratio of β -CD onto cellulose fibers was 9.7%. The ciprofloxacin hydrochloride was encapsulated and the release behavior from cellulose fibers was studied. Prolonged release of the biocide from the cellulose was clearly observed. Indeed, the cumulative release from the virgin fibers was 90% within the first 30 min, whereas the modified ones reached the same level after 240 min owing to the formation of inclusion complexes. However, the presence of β -CD and its inclusion complexes modified the cellulose microstructure and its mechanical properties. As expected, the activity against *E. coli* and *S. aureus* was excellent for grafted fibers loading ciprofloxacin compared with virgin ones; virgin fibers loading biocide were active for 4 days whereas the grafted fibers were active for 15 days.

As a response to imposed pressures, resistance of microorganisms to classical organic biocides increases (Fig. 17.13).

As a consequence, the use of metal nanoparticles as alternative biocidal agents has emerged in the past decade (Maillard, 2005). Metal nanoparticles have high thermal stability, low toxicity to human cells, and effective broad-spectrum activity, which makes them good candidates for inhibiting bacterial growth. Their antibacterial activity results from their rapid breakdown, which releases ionic metal that interact with the thiol or *N*-end amine residues of bacterial enzymes, leading to the inhibition of DNA replication (Stobie et al., 2008). Moreover, bacterial cytoplasmic membranes can be damaged, leading to cell lysis (Feng et al., 2000).

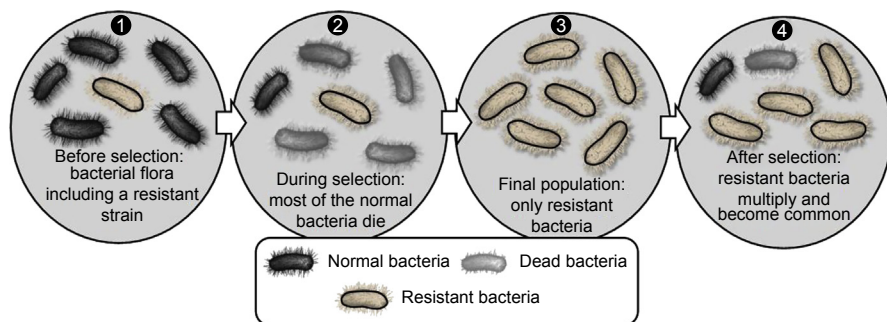


Figure 17.13 Principle of resistance mechanisms through the selection of the most resistant pathogens.

In this context, silver ions (Ag^+) were loaded on CD grafted onto cotton fabrics (Bajpai et al., 2010). Owing to the prolonged release of silver ions for a period of 7 days, correct antibacterial activity was obtained against *E. coli*. The antibacterial action of silver applied to cellulose fibers grafted with MCT- β -CD was reported in the literature (Popescu et al., 2013). Through a completely ecological process, without dispersants, the authors could link the silver nanoparticles (Ag^0) or silver ions (Ag^+) because of interactions between the hydroxyl groups of the grafted CD and the silver ions or nanoparticles. These interactions are supported by FTIR spectra and by the value of the binding constants (360 and $3.07 \times 10^6 \text{ M}^{-1}$ for Ag^0 and Ag^+ , respectively). The antibacterial activities against *E. coli* and *S. aureus* were similar for the two fabrics grafted with CD and treated with Ag^0 or Ag^+ . This suggests that the silver nanoparticles (Ag^0) were dissociated into silver (I) cations which act as active species (Fig. 17.14). Finally, the authors established a relationship between the binding constants of the CD with Ag^0 and Ag^+ and antibacterial activity as well as resistance to washing. The antibacterial effect of grafted fabrics washed 10 times was equal to that of the unwashed original fabric.

In 2011, the use of carbon nanotubes with copper or silver nanoparticles embedded on water-insoluble CD polyurethane polymers was explored (Lukhele et al., 2011). After characterization, the resulting material was tested for water disinfection. The authors determined the antibacterial properties of the material against *Salmonella typhi* and *E. coli* using water samples containing an organic pollutant (eg, *p*-nitrophenol) in addition to bacteria. The material based on polyurethanes adsorbed up to 55% of *p*-nitrophenol pollutant and reduced up to three logs the bacteria titers. The mechanism is the result of a synergism between the metal nanoparticles and the carbon nanotubes. Carbon nanotubes exhibit strong antimicrobial activity because of piercing of the bacterial cell membranes (Liu et al., 2009). This type of material may be suitable for avoiding water-related diseases (eg, leptospirosis, malaria, dengue, typhoid fever).

In 2013, the synthesis of sulfated- β -CD/cotton-ZnO nanocomposite was reported (Sundrarajan et al., 2013). Sulfo- β -CD (S- β -CD) was cross-linked with cotton fabric using ethylenediaminetetraacetic acid. Next, the fabric surface was padded with ZnO nanoparticles. The synthesized β -CD/ZnO cotton fabrics were fully characterized

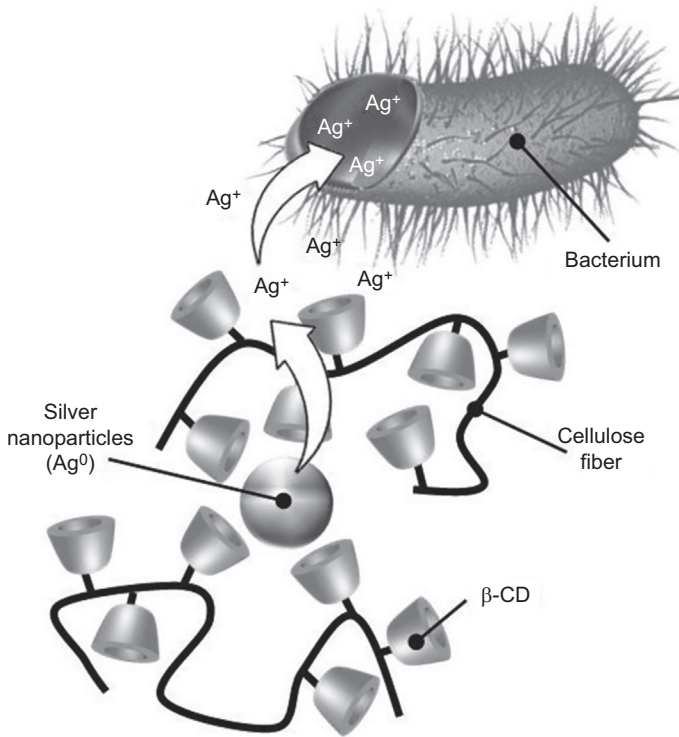


Figure 17.14 Proposed antibacterial mechanism of silver nanoparticles capped by β -CD grafted onto cellulose fibers.

using FTIR, X-ray diffraction, granulometric analysis, and transmission electron microscopy (TEM). The antibacterial efficiencies were very high (99% and 97% against *S. aureus* and *E. coli*). Following the same protocol, the authors extended the coating of S- β -CD polymer cross-linked with cotton fabric by TiO₂ and Ag nanoparticles (Selvam et al., 2012). Biocidal efficiency against *S. aureus* and *E. coli* decreased in the order ZnO > Ag > TiO₂. Because the best biocidal activity obtained for the S- β -CD/ZnO cotton fabric also had the low production cost, this type of cellulose fabric may be suitable for medicinal bandages, etc.

In 2014, the synthesis of β -CD–polyacrylonitrile–copper nanorod composite fibers was performed to obtain antibacterial textiles (Li et al., 2014). The synthesis required the preparation of β -CDs/polyacrylonitrile composite fibers by electrospinning followed by the preparation of β -CDs/polyacrylonitrile–copper nanorod composite fibers by adsorption and reduction. The composite fibers were fully characterized by FTIR, SEM, TEM, energy-dispersive spectroscopy, and X-ray photoelectron spectroscopy. Results indicated that the copper nanorods were not only successfully synthesized on the surface of the composite fibers, they were distributed without aggregation on the composite fibers. The antibacterial efficacy of the composite fibers against *E. coli* indicated that they have bactericidal effects only in the

presence of copper nanorods. Based on the literature, the authors mentioned that the loaded copper ions interact with bacterial cell membranes which induced structural change and led to cell death. The proposed system can be used for water purification systems as a filtration membrane.

A more sustained release can be obtained when CDs are trapped inside matrix networks. In this context, hydrogels based on CDs can be useful for creating robust networks with switchable mechanical properties capable of serving as device coatings. As expected for affinity-based mechanisms, the release of drugs from CD-based hydrogels was slower than classical diffusion-based release from dextran gels owing to the complexation of the drug inside the CD cavity (Thatiparti et al., 2010). In affinity-controlled release kinetics, the guest drug released from one CD may become available to form new complexes with other free CDs during diffusion through the hydrogel matrix (Fig. 17.15, Concheiro and Alavarez-Lorenzo, 2013). The slow, sustained, affinity-based release of antibiotics from the CD-based hydrogels is of potential interest as a delivery platform.

To prevent and manage wound infections, the use of HP- β -CDs as main components of hydrogels and gauzes was proposed for the prolonged release of benzalkonium chloride (Garcia-Fernandez et al., 2013). Benzalkonium chloride (Fig. 17.11) is a classical antiseptic used in many consumer products such as eye, ear, and nasal

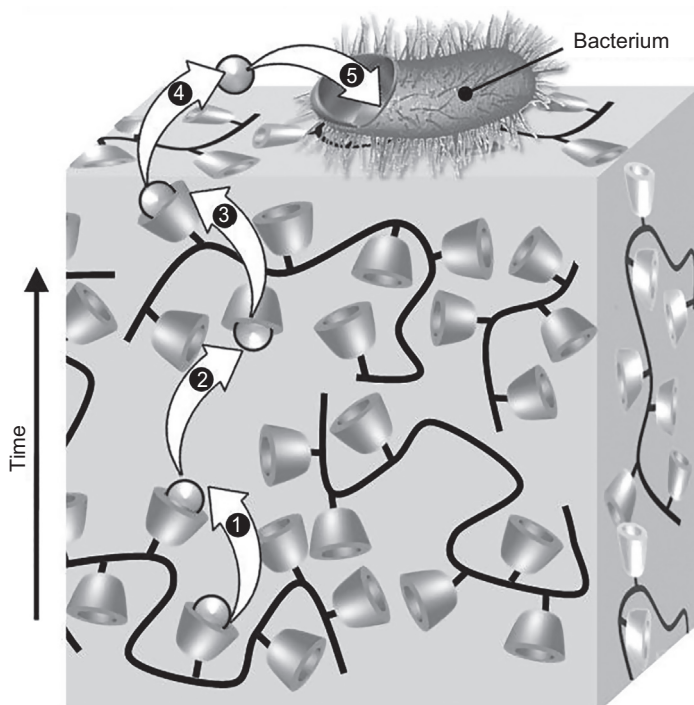


Figure 17.15 Proposed mechanism of biocide release from a CD-based hydrogel.

drops or sprays; skin antiseptics (Bactine[®] and Dettol[®]); throat lozenges and mouthwashes; treatment for fever blisters (Viroxyn[®]); burn and ulcer treatment; and cleaners for hard surfaces (Lysol[®]). Because benzalkonium chloride is known to form inclusion complexes easily with various CDs, the authors grafted CDs onto cotton gauze using CTR as a cross-linker (190°C for 15 min). In parallel, the authors formed hydrogels based on HP- β -CD and hydroxypropyl methylcellulose. Biocidal activity against *S. epidermidis* and *E. coli* revealed that benzalkonium chloride in hydrogels and gauze inhibited growth and reduced the number of living bacterial cells. The results and the slow and sustained affinity-based release of benzalkonium from the CD-based networks highlight the role of CDs as main components of hydrogels and gauze for the efficient delivery of antiseptics.

17.3.2 Antiinflammatory textiles

As seen in the previous section, CDs grafted onto textile fibers are useful for delivering antibiotics. Therefore, if the antiseptic is replaced by an antiinflammatory, an antiinflammatory textile is obtained. The advantages of these fabrics are similar to those based on antiseptics. However, for inflammation treatment, textiles based on CDs offer favorable solutions to the sensitivity of certain patients to oral administration, possible omission by children and old people, and the frequent change of bandages in the case of conventional bandages. To stop swelling, a bandage able to release medication gradually (eg, diclofenac, ibuprofen (IBU) or aspirin) (Fig. 17.16) directly to the inflamed region avoids all of these difficulties. As a consequence, in the current section, some typical examples of textiles based on CDs are reported.

In 2010, a bandage capable of releasing diclofenac sodium was developed (NSAID) (Fig. 17.16, Montazer and Mehr, 2010). The bandage was executed in two steps: the complexation of diclofenac sodium by β -CD, followed by complex grafting onto cotton wound dressing using a cross-linking agent (eg, dimethyldihydroxyethylene urea) (Fig. 17.17).

The complexation of β -CD and diclofenac sodium was proven by UV spectrophotometry and NMR spectroscopy. The surface morphology and drug release were studied by SEM and dissolution kinetic measurements, respectively. The results revealed that the cross-linking agent prolongs the drug release time. The authors proved that the increase in the medicine release rate is not proportional to its initial concentration. Moreover, if the textile is impregnated in a vat containing ethanol, the drug release

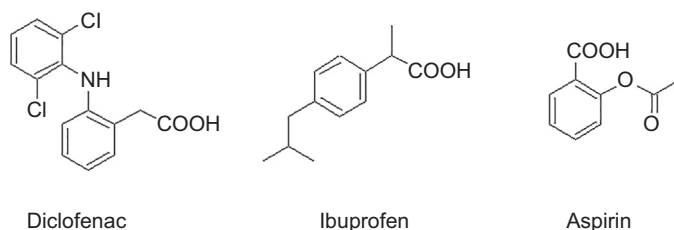


Figure 17.16 Chemical structure of diclofenac, ibuprofen, and aspirin.

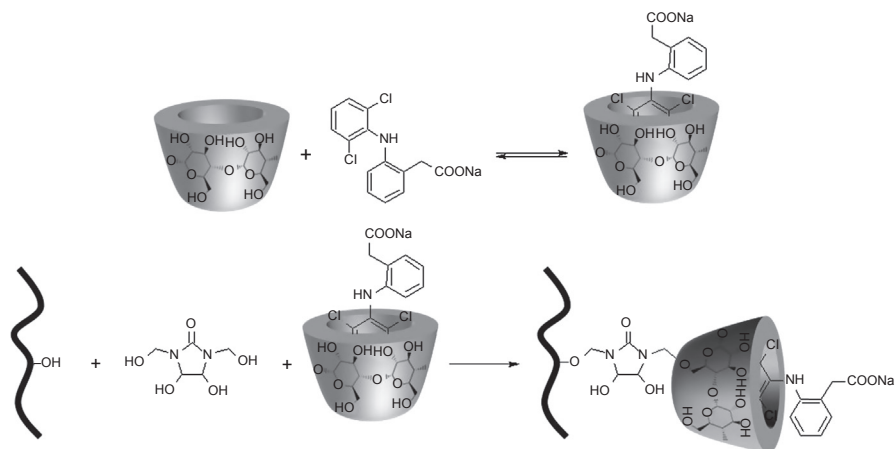


Figure 17.17 Synthesis of cotton bandage impregnated with CD–diclofenac complex by means of dimethyldihydroxyethylene urea.

increased during the initial hours. However, if the bandage was not treated with ethanol, the initial release of medication was slow. Therefore, the bandage containing ethanol can be useful when inflammation is severe. In other words, the drug release of these bandages is switchable according to the concentration of ethanol.

Another method is possible to obtain the prolonged release of antiinflammatory agents indirectly. Because gels or hydrogels can be impregnated in gauze for medical bandages, the work of [Pose-Vilarnovo et al. \(2004\)](#) can be fruitful in this field. In that article, the authors reported on the effect of β - and HP- β -CD on the diffusion and release behavior of diclofenac sodium from hydroxypropyl methylcellulose gels. These gels were prepared with 0.5–2.0% polymer and different drug–CD molar ratios. The viscosity of the gels strongly depended on the hydroxypropyl methylcellulose proportions (from 0.7 to 100 mPa s), which affected to a lesser extent the resistance to the diffusion of the drugs (D from 60 to 5×10^{-6} cm²/s). The influence of CD on diffusion was particularly evident in gels prepared with polymer proportions above its entanglement concentration, 2.0% hydroxypropyl methylcellulose. In these systems, whereas high drug–CD proportions enhanced the diffusivity, preventing polymer–drug hydrophobic interactions, low drug–CD ratios hindered it. This system may be particularly useful to modulate drug release from gels. The influence of CDs depends on the nature of the drug and the molecular size and hydrophilic character of the CD used.

On the other hand, because IBU and aspirin ([Fig. 17.16](#)) are widely used NSAIDs to treat fever, mild to moderate pain, painful menstruation, osteoarthritis, dental pain, headaches, and arthritis, and because these two drugs are known to form inclusion complexes with various CDs, their inclusion in CDs grafted onto cotton fabric is promising. In this context, fabric functionalized with MCT- β -CD was developed for their controlled release ([Agrawal et al., 2010a,b](#)). The maximum amount of MCT- β -CD achieved on the cotton fabric sample was 2.585 g/m² out of 3.2 g/m² delivered on

the surface by drop-on-demand inkjet print head. The release kinetics of aspirin and IBU with these textiles is switchable depending on several external stimuli (eg, pH, electrolyte).

Similar to diclofenac sodium, it is possible to obtain sustained IBU release by incorporating CDs inside polyvinylpyrrolidone–poly(ethylene glycol) dimethacrylate (PVP–PEG–DMA) hydrogels (Nielsen et al., 2009). To retard the release of water-soluble sodium ibuprofenate, the three native CDs (4–5 w/w%) were covalently grafted onto the vinylpyrrolidone–ethyleneglycol dimethacrylate copolymer matrix in the presence of NMA and under UV radiation (see earlier discussion). The IBU salt was loaded by swelling in various IBU–CD ratios. Because the release rate and the release profile of ibuprofen can be modified by the CD used, the best compromise for sustained drug release was obtained with the β -CD hydrogel. These hydrogels show promising wound care properties when they are applied on a textile surface for medical bandages.

17.3.3 Insect repellent and insecticide textiles

Insects are common vectors of various diseases. Insects spread pathogens (eg, bacterial, viral, and protozoan) from one host to another. Two main mechanisms can be highlighted: via their bite (eg, malaria spread by mosquitoes) or via their feces (eg, Chagas disease spread by *Triatoma* bugs). Mosquitoes are perhaps the best known vector. They transmit a wide range of tropical diseases including yellow fever, dengue fever, and malaria. For instance, malaria is caused by parasitic protozoans belonging to the genus *Plasmodium*. Common symptoms include fever, fatigue, vomiting, and headaches. However, in severe cases, seizures, coma or death is possible. Although this disease poses a particular threat on the continents of Africa, Asia, and South America, malaria can be controlled with the use of mosquito nets, insect repellents, and insecticides. Malaria prevention is more cost-effective than treatment of the disease in the long run by chloroquine or mefloquine. Under such conditions, the use of textiles with insect-repellent properties comprising a natural or synthetic fabric and an encapsulated active ingredient with insecticide or insect-repellent properties can be useful. Therefore, the ability of CDs to include various hydrophobic molecules can be exploited to produce new grafted textiles with insecticidal or insect-repelling performance. These are particularly promising and not only for malaria. In this section, only a few typical examples taken from the literature are discussed. The chemical structures of the insecticides and insect repellents mentioned in this section are presented in Fig. 17.18.

In 1992, wash-resistant and insecticidal fibers were developed (Akasaka et al., 1992). These fibers were prepared by treating fibers with an organic insect-proofing agent, a molecular CD, or an oligomer ($M_w \leq 3000$), and a siloxane. For instance, acrylic fibers were treated with a solution containing 0.34% β -CD, 0.14% isobornyl thiocyanacetate (Fig. 17.18) and 0.5 g/L aminosiloxane (based on the fiber mass). After 45 min at 90°C in a package dyeing machine and heat treatment for 10 min at 100°C, the mixture was blended with untreated fibers and a woven fabric was produced which, even after 20 washings, had insecticidal properties.

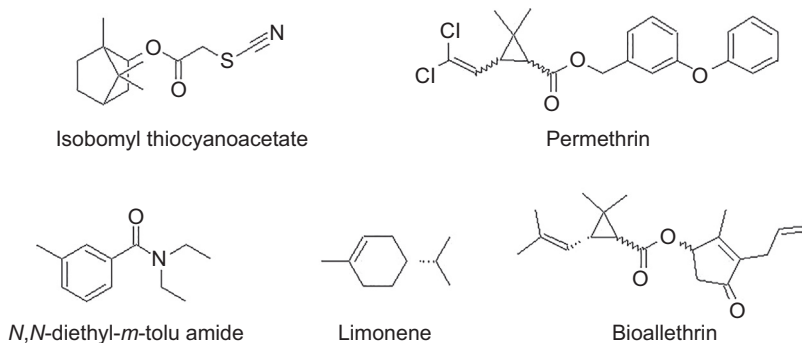


Figure 17.18 Chemical structures of insecticides and insect repellents mentioned in this section.

In 2005, the use of MCT- β -CD grafted onto cellulosic textiles through covalent bonds was proposed for entrapping hydrophobic insecticides on the surface of the fabric and releasing them progressively (Romi et al., 2005). In this work, the authors used permethrin (insecticide) and *N,N*-diethyl-*m*-toluamide (insect repellent) (Fig. 17.18). UV-visible spectrophotometry and thermal analysis confirmed the presence of the guest molecules in the β -CD molecules grafted on the cotton fabric surface. Bioassays against *Aedes aegypti* and *Anopheles stephensi* (two mosquito species of medical importance) repellency and irritancy were performed. *N,N*-diethyl-*m*-toluamide appears to be unsuitable for the direct treatment of cotton fabrics; its activity remained only a short time after treatment. In contrast, fabrics grafted with MCT- β -CD and loaded with permethrin kept insecticidal/irritant efficacy even for a long time after treatment. In other words, permethrin treatment of bed nets or curtains made with this textile can be useful to avoid malaria.

In 2008, Hebeish et al. used an insecticide against anopheles (eg, limonene) (Fig. 17.18) applied to cotton fabrics with conventional impregnation and coating methods in addition to a functionalized fabric obtained via grafting with MCT- β -CD. For the conventional methods, an emulsion of limonene and polymeric binder was used, whereas limonene inclusion inside the MCT- β -CD cavities was used with the functionalized fabric (Hebeish et al., 2008). Bioassay test results expressed as repellency, knockdown, and mortality were very good. Moreover, good washing and storage results were reported.

In 2014, a new textile consisting of cotton/poly(glycidyl methacrylate) copolymer containing β -CD allowed the introduction of two insecticides (permethrin and bioallethrin) (Fig. 17.18) against blood-sucking insects (Hebeish et al., 2014). The chemical functionalization of cotton was realized by grafting glycidyl methacrylate alone or combined with β -CD by irradiation using fast electron beam. The retreatment of the obtained modified cotton increased the amount of CDs. The inclusion of the two insecticides was performed and gas chromatography was used to quantify the insecticides in the finished fabrics. The untreated and treated fabrics were fully characterized through FTIR, SEM, and physical testing. The toxic activity properties directly correlated with the amount of loaded insecticide and the bioassay test revealed fast action against mosquitoes.

17.3.4 Cosmetotextiles

By definition, a cosmetotextile is a technology that merges cosmetics and textiles through the process of encapsulation. These textiles are consumer articles containing cosmetic products for the controlled release of these cosmetics. These textiles are sometimes borderline medical applications. Most of them use essential oils, herbal oils, and oils from flower seeds which have skin care benefits in that they provide an occlusive layer that lubricates the epidermis, together with a moisturizing effect. Most contain bioactive molecules and have been used medicinally in history. However, use of essential oils has declined because modern medicine is based on molecules rather than “essential oils” as a class of medication. However, essential oils may have pharmaceutical effects such as sedation, antidepressant, or insect repellent (Voncina and Vivod, 2013). Some are fungicides, bactericides, and insecticides. In contrast to the previous sections that discussed molecular drugs, essential oils (ie, mixtures of molecules) are used directly to obtain cosmetotextiles. Here, only borderline cases between cosmetics and medicine are presented.

Essential oils have been used as insect repellents to discourage insects from landing or climbing on a surface. Some synthetic repellents have been presented previously in this chapter. These synthetic repellents tend to be more effective than natural repellents. However, synthetic insect repellents are highly toxic. Some of them result in dermatitis and other skin problems. In this context, cedar oil is often used as a natural insect repellent because of its low toxicity. Because essential oil repellents tend to be short-lived owing to their volatile nature, their encapsulation with β -CD is a smart solution. In 2013, the encapsulation of cedar oil in wool and PET–wool-blend fibers with β -CD was reported in the literature (Voncina and Vivod, 2013). The complex formation between cedar oil and β -CD was determined by FTIR spectroscopy. After treatment with β -CD–cedar oil complexes, this textile fabric showed prolonged moth repellence compared with textile materials treated only with cedar oil. After β -CD–cedar oil-treated wool was exposed to a moth’s colony for 2 months, no visible damage was observed by the naked eye. In contrast, wool samples treated only with cedar oil were protected only during the first days because the cedar oil evaporated. In this example, the cedar oil encapsulated in the β -CD cavity avoids oil evaporation and improves its gradual release.

In 2011, Cravotto et al. used cosmetotextiles in the treatment of chronic venous insufficiency in the legs by means of elastic bandages loaded with natural products which possess phlebotonic properties. One of these compounds is aescin, the main active principle of the horse chestnut tree (*Aesculus hippocastanum* L.), which has shown marked antiinflammatory, vasoprotecting, and circulation-boosting properties. The efficient synthetic procedure developed by the authors to prepare β -CD–grafted viscose uses a two-step ultrasound-assisted reaction. Viscose fabric soaked in a mixture of DMF and hexamethylene diisocyanate was sonicated at 80°C. Then the viscose fabric, soaked in a solution of β -CD in DMF, was sonicated for 2 h at 70°C. The fabric was washed and dried to perform aescin complexation. The grafted fabric was characterized by FTIR and cross-polarization magic angle spinning NMR spectra and by an empiric colorimetric method which used phenolphthalein as the

CD guest. The efficacy of the new cosmetotextile was corroborated by in vitro studies of diffusion through membranes, cutaneous permeation, and accumulation in porcine skin. Aescin in the cosmetotextile showed excellent application compliance and was easily recharged. The authors mentioned the possibility of producing this grafted textile industrially.

17.3.5 Other smart opportunities

In this section, miscellaneous applications of grafted textiles are presented. In 2001, the use of CDs grafted onto fabrics was used to collect perspiration to establish medical diagnostics (Buschmann et al., 2001). To date, blood and urine tests are normally used because of problems with taking a sweat probe from a patient. This becomes easy when MCT- β -CDs are grafted onto textiles. CDs are able to complex various organic molecules from perspiration. Gas chromatography can be easily performed after extracting substances from a textile functionalized with CDs. Under such conditions, because the organic substances are preconcentrated owing to the presence of CDs compared with untreated textiles, identification becomes easier (Fig. 17.19).

In 2008, polyethylene terephthalate vascular prostheses coated with a CD polymer were proposed to replace damaged arteries (Blanchemain et al., 2008). The prostheses involve the complexation of antibiotics (eg, ciprofloxacin, vancomycin, and rifampicin) to minimize the risk of infection during and after surgical interventions via their controlled release. The epithelial cell was used to determine the viability of antibiotics, whereas human pulmonary microvascular endothelial cells were used for cell proliferation. Some pathogen strains (eg, *S. aureus*, *E. coli*) were used to determine the antimicrobial activity of the antibiotic loaded in prostheses coated with CD polymer and to compare it with the virgin one. A larger amount of antibiotics was adsorbed onto prostheses coated with CD polymer compared with the virgin one (26.7 vs 35.3 mg/g, 51.1

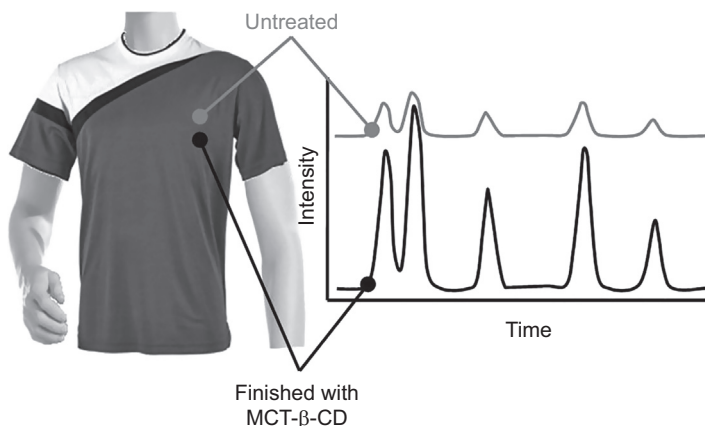


Figure 17.19 T-shirt partially finished with and without cyclodextrins and schemes of corresponding gas chromatograms obtained after extraction.

vs 72.4 mg/g, and 4.1 vs 21.0 mg/g for rifampicin, vancomycin, and ciprofloxacin, respectively). Therefore, better microbiological activity was shown for prostheses coated with CD polymer and loaded with antibiotics. Rifampicin and ciprofloxacin were toxic (22 and 35 mg/L, respectively) but vancomycin is nontoxic. The poor viability and proliferation of the human microvascular endothelial pulmonary cells when the prosthesis was coated with CD polymer containing antibiotic resulted from the cytotoxicity of the antibiotic itself. This kind of property can be exploited to fight intracellular bacteria without compromising the in vivo applications of the functionalized prosthesis. Moreover, because polyethylene terephthalate is used in fibers for clothing, some fruitful developments are expected for other textile applications.

In 2013, the use of cellulose supports was proposed to obtain antiallergic pajamas (Hritcu et al., 2013; Radu et al., 2013). The cotton was grafted with MCT- β -CD as a support for an inclusion compound with natural antiallergic active principles: extract of *Viola tricolor*, a solution of propolis and of menthol, as well as pharmacologic products: methylprednisolone aceponate, hydrocortisone, and pimecrolimus. The fabric was characterized by FTIR and SEM analyses. The antimicrobial properties of the textile material grafted with MCT- β -CD and with *V. tricolor*, propolis, and menthol absorbed onto the cotton was tested. Results proved that these modified textiles inhibited the microbial development of *Rhizopus* and *Trichoderma* and avoided encouragement of an allergic reaction. These textiles can be useful for improving curative properties and for comfortable pajamas for patients with contact and atopic dermatitis.

17.4 Conclusion and perspectives

This chapter presents an analysis of current and potential applications of smart textiles based on CDs for curative or preventive patient care. Because of their molecular structure, CDs are topologically represented as toroids in which the openings expose the hydroxyl groups. As consequence, hydroxyl residues can be easily modified to introduce reactive groups and be grafted onto natural or synthetic fibers. Moreover, the interior of the toroid is sufficiently hydrophobic to host nonpolar medications. Indeed, CDs allow to the encapsulation of antibiotics, antiinflammatories, insecticides, insect repellents, essential oils, antihistaminics, phlebotonics, etc. on fabric surfaces. Because the formation of the inclusion compounds greatly modifies the physical and chemical properties of the guest molecule, mostly in terms of the delivery kinetic rate, the drug bioavailability is clearly modified. This modification offers the possibility of controlled release, which is one of the most important advantages for the textile industry in addition to their reuse (Fig. 17.20). Because host–guest systems are reversible, textiles with grafted CDs behave as kinetic retardants. For most inclusion complexes, the complexation kinetics is extremely fast. Accordingly, the delayed release generally observed in the presence of CDs is not linked to the kinetics of inclusion but rather is induced by thermodynamic control. At a given time, only a small percentage of the drug is free and really bioavailable. Thus, prolonged release comes from displacing

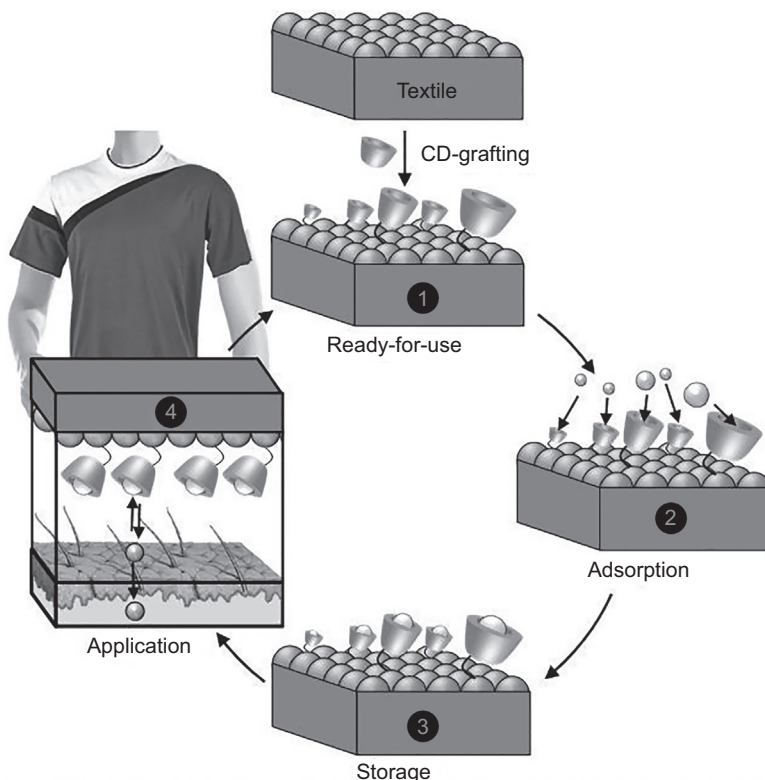


Figure 17.20 Preparation and life cycle of CD-grafted medical textile.

the inclusion equilibrium. However, the releasing kinetics of guest substances from CD cavities as well as the study of key parameters that influence this phenomenon must be rationalized. This rationalization combined with their capacity to form inclusion complexes with numerous drugs offers unrestricted possibilities, and we may suppose that in the near future new smart medical textiles will emerge and open up a new approach for designing novel drug delivery systems.

Acknowledgment

This chapter is dedicated to the memory of my father, Gérard Leclercq (1948–2015).

References

- Agrawal, P.B., Ali, K., Warmoeskerken, M.M.C.G., 2010a. Digitally finished cyclodextrin based controlled release functionality for cotton textiles. NIP & Digital Fabrication Conference 2, 670–672.

- Agrawal, P.B., Ali, K., Warmoeskerken, M.M.C.G., 2010b. Inkjettable β -cyclodextrin based release system for cotton textiles. In: Autex World Textile Conference, Vilnius, Lithuania.
- Akasaka, M., Sawai, Y., Iwase, K., Moriishi, H., 1992. Insectproofing Fibers and Method for Preparing the Same. Patent No. EP 488294.
- Andreas, J., Dalmolin, M.C., de Oliveira, I.B.J.R., Barcellos, I.O., 2010. Aplicação de ciclodextrinas em processos têxteis. *Química Nova* 33 (4), 929–937.
- Bajpai, M., Gupta, P., Bajpai, S.K., 2010. Silver(I) ions loaded cyclodextrin-grafted-cotton fabric with excellent antimicrobial property. *Fibers and Polymers* 11 (1), 8–13.
- Baudin, C., Pean, C., Perly, B., Goselin, P., 2000. Inclusion of organic pollutants in cyclodextrin and derivatives. *International Journal of Environmental Analytical Chemistry* 77 (3), 233–242.
- Bhaskara-Amrit, U.R., Agrawal, P.B., Warmoeskerken, M.M.C.G., 2011. Applications of β -cyclodextrins in textiles. *Autex Research Journal* 11 (4), 94–101.
- Bjerre, J., Rousseau, C., Marinescu, L., Bois, M., 2008. Artificial enzymes, “Chemzymes”: current state and perspectives. *Applied Microbiology and Biotechnology* 81 (1), 1–11.
- Blanchemain, N., Laurent, T., Chai, F., Neut, C., Haulon, S., Krump-Konvalinkova, V., Morcellet, M., Martel, B., Kirkpatrick, C.J., Hildebrand, H.F., 2008. Polyester vascular prostheses coated with a cyclodextrin polymer and activated with antibiotics: cytotoxicity and microbiological evaluation. *Acta Biomaterialia* 4 (6), 1725–1733.
- Boyle, D., 2006. Effects of pH and cyclodextrins on pentachlorophenol degradation (mineralization) by white-rot fungi. *Journal of Environmental Management* 80 (4), 380–386.
- Breslow, R., Dong, S.D., 1998. Biomimetic reactions catalyzed by cyclodextrins and their derivatives. *Chemical Reviews* 98 (5), 1997–2011.
- Buckley, J.D., Thorp, A.A., Murphy, K.J., Howe, P.R., 2006. Dose-dependent inhibition of the post-prandial glycaemic response to a standard carbohydrate meal following incorporation of alpha-cyclodextrin. *Annals of Nutrition and Metabolism* 50 (2), 108–114.
- Buschmann, H.-J., Knittel, D., Schollmeyer, E., 2001. New textile applications of cyclodextrins. *Journal of Inclusion Phenomena and Macrocyclic Chemistry* 40 (3), 169–172.
- Buschmann, H.-J., Schollmeyer, E., 2002. Applications of cyclodextrins in cosmetic products: a review. *Journal of Cosmetic Science* 53 (3), 185–191.
- Calleja, P., Huarte, J., Agüeros, M., Ruiz-Gatón, L., Espuelas, S., Irache, J.M., 2012. Molecular buckets: cyclodextrins for oral cancer therapy. *Therapeutic Delivery* 3 (1), 43–57.
- Campos, E.V.R., de Oliveira, J.L., Fraceto, L.F., 2014. Applications of controlled release systems for fungicides, herbicides, acaricides, nutrients, and plant growth hormones: a review. *Advanced Science, Engineering and Medicine* 6 (4), 373–387.
- Challa, R., Ahuja, A., Ali, J., Khar, R.K., 2005. Cyclodextrin in drug delivery: an updated review. *AAPS PharmSciTech* 6 (2), E329–E357.
- Concheiro, A., Alvarez-Lorenzo, C., 2013. Chemically cross-linked and grafted cyclodextrin hydrogels: from nanostructures to drug-eluting medical devices. *Advanced Drug Delivery Reviews* 65 (9), 1188–1203.
- Cravotto, G., Beltramo, L., Sapino, S., Binello, A., Carlotti, M.E., 2011. A new cyclodextrin-grafted viscose loaded with aescin formulations for a cosmeo-textile approach to chronic venous insufficiency. *Journal of Materials Science: Materials in Medicine* 22 (10), 2387–2395.
- Cusola, O., Tabary, N., Belgacem, M.N., Bras, J., 2013. Cyclodextrin functionalization of several cellulosic substrates for prolonged release of antibacterial agents. *Journal of Applied Polymer Science* 129 (2), 604–613.
- Dehmer, M., Schleinig, C.H., Merz, T., Everts, F., 1998. Cyclodextrins as Washing or Laundering Rinse Aids and Their Use. Patent No. WO 9813456.

- Del Valle, E.M.M., 2004. Cyclodextrins and their uses: a review. *Process Biochemistry* 39 (9), 1033–1046.
- Delaunois, M., Navarro, R., 1997. Composition capillaire à base de minoxidil à faible teneur en solvant gras. Patent No. WO 1997003638.
- Dietrich, B., Viout, P., Lehn, J.-M., 1991. Aspects de la chimie des composés macrocycliques. EDP Sciences, Paris.
- Dong, C., Ye, Y., Qian, L., Zhao, G., He, B., Xiao, H., 2014. Antibacterial modification of cellulose fibers by grafting β -cyclodextrin and inclusion with ciprofloxacin. *Cellulose* 21 (3), 1921–1932.
- Feng, Q.L., Wu, J., Chen, G.Q., Cui, F.Z., Kim, T.N., Kim, J.O., 2000. A mechanistic study of the antibacterial effect of silver ions on *Escherichia coli* and *Staphylococcus aureus*. *Journal of Biomedical Materials Research* 52 (4), 662–668.
- Fujimura, T., 1985. Fragrant Fabrics. Patent No. JP 60259648.
- Funasaki, N., Ishikawa, S., Neya, S., 2008. Advances in physical chemistry and pharmaceutical applications of cyclodextrins. *Pure and Applied Chemistry* 80 (7), 1511–1524.
- Furune, T., Iikuta, N., Ishida, Y., Okamoto, H., Nakata, D., Terao, K., Sakamoto, N., 2014. A study on the inhibitory mechanism for cholesterol absorption by α -cyclodextrin administration. *Beilstein Journal of Organic Chemistry* 10, 2827–2835.
- Garcia-Fernandez, M.J., Brackman, G., Coenye, T., Concheiro, A., Alvarez-Lorenzo, C., 2013. Antiseptic cyclodextrin-functionalized hydrogels and gauzes for loading and delivery of benzalkonium chloride. *Biofouling* 29 (3), 261–271.
- Hamasaki, K., Ikeda, H., Nakamura, A., Ueno, A., Toda, F., Suzuki, I., Osa, T., 1993. Fluorescent sensors of molecular recognition. Modified cyclodextrins capable of exhibiting guest-responsive twisted intramolecular charge transfer fluorescence. *Journal of the American Chemical Society* 115 (12), 5035–5040.
- Hebeish, A., EL-Sawy, S.M., Ragaai, M., Hamdy, I.A., El-Bisi, M.K., Abdel-Mohdy, F.A., 2014. New textiles of biocidal activity by introduce insecticide in cotton-poly (GMA) copolymer containing β -CD. *Carbohydrate Polymers* 99 (2), 208–217.
- Hebeish, A., Fouda, M.M.G., Hamdy, I.A., EL-Sawy, S.M., Abdel-Mohdy, F.A., 2008. Preparation of durable insect repellent cotton fabric: limonene as insecticide. *Carbohydrate Polymers* 74 (2), 268–273.
- Hedges, A.R., 1998. Industrial applications of cyclodextrins. *Chemical Reviews* 98 (5), 2035–2044.
- Hirsch, W., Fried, V., Altman, L., 1985. Effect of cyclodextrins on sparingly soluble salts. *Journal of Pharmaceutical Sciences* 74 (10), 1123–1125.
- Hritcu, M., Radu, C.-D., Ferri, A., Grigoriu, A., Oproiu, L.-C., 2013. Anti-allergic cellulose support at the epidermis–environment interface. *Cellulose Chemistry and Technology* 47 (3–4), 257–266.
- Irie, T., Uekama, K., 1997. Pharmaceutical applications of cyclodextrins. III. Toxicological issues and safety evaluation. *Journal of Pharmaceutical Sciences* 86 (2), 147–162.
- Junquera, E., Ruiz, D., Aicart, E., 1999. Role of hydrophobic effect on the noncovalent interactions between salicylic acid and a series of β -cyclodextrins. *Journal of Colloid and Interface Science* 216 (1), 154–160.
- Khan, A.R., Forgo, P., Stine, K.J., D'souza, V.T., 1998. Methods for selective modifications of cyclodextrins. *Chemical Reviews* 98 (5), 1977–1996.
- Leclercq, L., Bricout, H., Tilloy, S., Monflier, E., 2007. Biphasic aqueous organometallic catalysis promoted by cyclodextrins: can surface tension measurements explain the efficiency of chemically modified cyclodextrins? *Journal of Colloid and Interface Science* 307 (2), 481–487.

- Leclercq, L., Compagny, R., Mühlbauer, A., Mouret, A., Aubry, J.-M., Nardello-Rataj, V., 2013a. Versatile eco-friendly pickering emulsions based on substrate/native cyclodextrin complexes: a winning approach for solvent-free oxidations. *ChemSusChem* 6 (8), 1533–1540.
- Leclercq, L., Hapiot, F., Tilloy, S., Ramkisoensing, K., Reek, J.N.H., van Leeuwen, P.W.N.M., Monflier, E., 2005. Sulfonated xantphos ligand and methylated cyclodextrin: a winning combination for rhodium-catalyzed hydroformylation of higher olefins in aqueous medium. *Organometallics* 24 (9), 2070–2075.
- Leclercq, L., Lacour, M., Sanon, S.H., Schmitzer, A.R., 2009. Thermoregulated microemulsions by cyclodextrin sequestration: a new approach to efficient catalyst recovery. *Chemistry – A European Journal* 15 (26), 6327–6331.
- Leclercq, L., Lubart, Q., Aubry, J.-M., Nardello-Rataj, V., 2013b. Modeling of multiple equilibria in the self-aggregation of di-*n*-decyldimethylammonium chloride/octaethylene glycol monododecyl ether/cyclodextrin ternary systems. *Langmuir* 29 (21), 6242–6252.
- Lee, M.H., Yoon, K.J., Ko, S.-W., 2000. Grafting onto cotton fiber with acrylamidomethylated β -cyclodextrin and its application. *Journal of Applied Polymer Science* 78 (11), 1986–1991.
- Li, H., Li, C., Zhang, C., Bai, J., Xu, T., Sun, W., 2014. Well-dispersed copper nanorods grown on the surface-functionalized PAN fibers and its antibacterial activity. *Journal of Applied Polymer Science* 131 (21), 41011.
- Liu, S., Wei, L., Hao, L., Fang, N., Chang, M.W., Xu, R., Yang, Y., Chen, Y., 2009. Sharper and faster “nano darts” kill more bacteria: a study of antibacterial activity of individually dispersed pristine single-walled carbon nanotube. *ACS Nano* 3 (12), 3891–3902.
- Lo Nostro, P., Fratoni, L., Baglioni, P., 2002. Modification of a cellulosic fabric with β -cyclodextrin for textile finishing applications. *Journal of Inclusion Phenomena and Macrocyclic* 44 (1–4), 423–427.
- Loftsson, T., Brewster, M.E., 2011. Pharmaceutical applications of cyclodextrins: effects on drug permeation through biological membranes. *Journal of Pharmacy and Pharmacology* 63 (9), 1119–1135.
- Loftsson, T., Brewster, M.E., 2013. Drug solubilization and stabilization by cyclodextrin drug carriers. In: Douroumis, D., Fahr, A. (Eds.), *Drug Delivery Strategies for Poorly Water-soluble Drugs*. John Wiley & Sons, Chichester, pp. 67–101.
- Loftsson, T., Duchêne, D., 2007. Cyclodextrins and their pharmaceutical applications. *International Journal of Pharmaceutics* 329 (1–2), 1–11.
- Lukhele, L.P., Krause, R.W.M., Nhlabatsi, Z.P., Mamba, B.B., Momba, M.N.B., 2011. Copper and silver impregnated carbon nanotubes incorporated into cyclodextrin polyurethanes for the removal of bacterial and organic pollutants in water. *Desalination and Water Treatment* 27 (1–3), 299–307.
- van de Manakker, F., Vermonden, T., van Nostrum, C.F., Hennink, W.E., 2009. Cyclodextrin-based polymeric materials: synthesis, properties, and pharmaceutical/ biomedical applications. *Biomacromolecules* 10 (12), 3157–3175.
- Maillard, J.-Y., 2005. Antimicrobial biocides in the healthcare environment: efficacy, usage, policies, and perceived problems. *Therapeutics and Clinical Risk Management* 1 (4), 307–320.
- Martel, B., Morcellet, M., Ruffin, D., Ducoroy, L., Weltrowski, M., 2002a. Finishing of polyester fabrics with cyclodextrins and polycarboxylic acids as crosslinking agents. *Journal of Inclusion Phenomena and Macrocyclic* 44 (1–4), 443–446.

- Martel, B., Wetrowski, M., Ruffin, D., Morcellet, M., 2002b. Polycarboxylic acids as crosslinking agents for grafting cyclodextrins onto cotton and wool fabrics: study of the process parameters. *Journal of Applied Polymer Science* 83 (7), 1449–1456.
- Montazer, M., Mehr, E.B., 2010. Na-diclofenac β -cyclodextrin inclusion complex on cotton wound dressing. *Journal of the Textile Institute* 101 (5), 373–379.
- Nardello-Rataj, V., Leclercq, L., 2014. Encapsulation of biocides by cyclodextrins: toward synergistic effects against pathogens. *Beilstein Journal of Organic Chemistry* 10, 2603–2622.
- Nielsen, A.L., Madsen, F., Larsen, K.L., 2009. Cyclodextrin modified hydrogels of PVP/PEG for sustained drug release. *Drug Delivery* 16 (2), 92–101.
- Okano, S., 1978. Printing of Cellulosic Fibers and Their Blends. Patent No. JP 53114987.
- Popescu, O., Dunca, S., Grigoriu, A., 2013. Antibacterial action of silver applied on cellulose fibers grafted with monochlorotriazinyl- β -cyclodextrin. *Cellulose Chemistry and Technology* 47 (3–4), 247–255.
- Pose-Vilarnovo, B., Rodríguez-Tenreiro, C., Rosa Dos Santos, J.F., Vázquez-Doval, J., Concheiro, A., Alvarez-Lorenzo, C., Torres-Labandeira, J.J., 2004. Modulating drug release with cyclodextrins in hydroxypropyl methylcellulose gels and tablets. *Journal of Controlled Release* 94 (2–3), 351–363.
- Poulakis, K., Buschmann, H.-J., Schollmeyer, E., 2002. Textile Material Permanently Finished with Polymeric Cyclodextrins, and Method for its Manufacture. Patent No. WO 2002046520.
- Qian, L., Guan, Y., Ziaee, Z., He, B., Zheng, A., Xiao, H., 2009. Rendering cellulose fibers antimicrobial using cationic β -cyclodextrin-based polymers included with antibiotics. *Cellulose* 16 (2), 309–317.
- Radu, C.-D., Popa, M., Parteni, O., Salariu, M., Lupșoru, E.-C., Ghiciuc, C., Foia, L., Chiriac, A., Lupșoru, R., Oproiu, L., Ulea, E., 2014. Achievements and limits on the controlled release of a drug from a textile fabric to dermis. *Open Conference Proceedings Journal* 5, 1–8.
- Radu, C.-D., Salariu, M., Avadanei, M., Ghiciuc, C., Foia, L., Cătălina Lupșoru, E., Ferri, A., Ulea, E., Lipsa, F., 2013. Cotton-made cellulose support for anti-allergic pajamas. *Carbohydrate Polymers* 95 (1), 479–486.
- Rekharsky, M.V., Inoue, Y., 1998. Complexation thermodynamics of cyclodextrins. *Chemical Reviews* 98 (5), 1875–1918.
- Remi, E., Fenyvesi, É., Ruzsna, I., Vig, A., 1996. The action of lipophilic UV absorbers – solubilized by cyclodextrin – on photofading of aqueous solution of azo reactive dyes. *Journal of Inclusion Phenomena and Macrocyclic Chemistry* 25 (1–3), 203–207.
- Reuscher, H., Hirsenkorn, R., 1996. Beta W7 MCT – new ways in surface modification. In: *Proceedings of the Eighth International Symposium on Cyclodextrins*, pp. 553–558.
- Romi, R., Lo Nostro, P., Bocci, E., Ridi, F., Baglioni, P., 2005. Bioengineering of a cellulosic fabric for insecticide delivery via grafted cyclodextrin. *Biotechnology Progress* 21 (5), 1724–1730.
- Russell, A.D., 2004. Whither triclosan? *Journal of Antimicrobial Chemotherapy* 53 (5), 693–695.
- Sabadini, E., Cosgrove, T., Egídio Fdo, C., 2006. Solubility of cyclomaltooligosaccharides (cyclodextrins) in H₂O and D₂O: a comparative study. *Carbohydrate Research* 341 (2), 270–274.
- Saenger, W., 1980. Cyclodextrin inclusion compounds in research and industry. *Angewandte Chemie International Edition* 19 (5), 344–362.

- Saenger, W., Jacob, J., Gessler, K., Steiner, T., Hoffmann, D., Sanbe, H., Koizumi, K., Smith, S.M., Takaha, T., 1998. Structures of the common cyclodextrins and their larger analogues – beyond the doughnut. *Chemical Reviews* 98 (5), 1787–1802.
- Selvam, S., Rajiv Gandhi, R., Suresh, J., Gowri, S., Ravikumar, S., Sundrarajan, M., 2012. Antibacterial effect of novel synthesized sulfated β -cyclodextrin crosslinked cotton fabric and its improved antibacterial activities with ZnO, TiO₂ and Ag nanoparticles coating. *International Journal of Pharmaceutics* 434 (1–2), 366–374.
- Singh, M., Sharma, R., Banerjee, U.C., 2002. Biotechnological applications of cyclodextrins. *Biotechnology Advances* 20 (5–6), 341–359.
- Stella, V.J., He, Q., 2008. Cyclodextrins. *Toxicologic Pathology* 36 (1), 30–42.
- Stobie, N., Duffy, B., McCormack, D.E., Colreavy, J., Hidalgo, M., Mchale, P., Hinder, S.J., 2008. Prevention of *Staphylococcus epidermidis* biofilm formation using a low-temperature processed silver-doped phenyltriethoxysilane sol–gel coating. *Biomaterials* 29 (8), 963–969.
- Sundrarajan, M., Selvam, S., Ramanujam, K., 2013. Synthesis of sulfated β -cyclodextrin/cotton/ZnO nano composite for improve the antibacterial activity and dyeability with *Azadirachta indica*. *Journal of Applied Polymer Science* 128 (1), 108–114.
- Szejtli, J., 1998. Introduction and general overview of cyclodextrin chemistry. *Chemical Reviews* 98 (5), 1743–1754.
- Szejtli, J., 2003. Cyclodextrins in the textile industry. *Starch–Stärke* 55 (5), 191–196.
- Szejtli, J., 2004. Cyclodextrins: applications. In: Atwood, J.L., Jonathan Steed, W. (Eds.), *Encyclopedia of Supramolecular Chemistry*, vol. 1. Marcel Dekker, New York, pp. 405–413.
- Szejtli, J., Zsardon, B., Fenyvesi, É., Otta, K., Tudos, F., 1980. Cellulose Derivatives Capable of Forming Inclusion Complexes. Patent No. HU 181733.
- Szejtli, J., Zsardon, B., Horvath, O.K., Ujhazy, A., Fenyvesi, É., 1991. Cellulose-bound Cyclodextrin Drug Complexes. Patent No. HU 54506.
- Szente, L., Szejtli, J., 2004. Cyclodextrins as food ingredients. *Trends in Food Science & Technology* 15 (3–4), 137–142.
- Thatiparti, T.R., Shoffstall, A.J., von Recum, H.A., 2010. Cyclodextrin-based device coatings for affinity-based release of antibiotics. *Biomaterials* 31 (8), 2335–2347.
- Thompson, D.O., 1997. Cyclodextrins-enabling excipients: their present and future use in pharmaceuticals. *Critical Reviews in Therapeutic Drug Carrier Systems* 14 (1), 1–104.
- Toth, B., 2005. Outstanding technology. *Wacker World Wide Corporate Magazine* 3.5, 28–33.
- Trinh, T., Cappel, J.P., Geis, P.A., Mccarty, M.L., Pilosof, D., Schmaedecke Zwerdling, S., 1997. Uncomplexed Cyclodextrin Solutions for Odor Control on Inanimate Surfaces. Patent No. US 5668097.
- Uekama, K., Hirayama, F., Irie, T., 1998. Cyclodextrin drug carrier systems. *Chemical Reviews* 98 (5), 2045–2076.
- Villiers, A., 1891. Sur la fermentation de la fécule par l'action du ferment butyrique. *Comptes Rendus* 112, 536–538.
- Voncina, B., Vivod, V., 2013. Cyclodextrins in textile finishing. In: Günay, M. (Ed.), *Eco-friendly Textile Dyeing and Finishing*. InTech, pp. 53–75.
- Wacker Website, 2009. Cyclodextrin Production Expanded in Eddyville. Available from: <http://www.wacker.com/>.
- Wang, J.-H., Cai, Z., 2008. Incorporation of the antibacterial agent, miconazole nitrate into a cellulosic fabric grafted with β -cyclodextrin. *Carbohydrate Polymers* 72 (4), 695–700.
- Weiss, A., Maurer, K.-H., Kasten, G.W., 1998. Method for Preventing Colors from Running in Textiles during Washing. Patent No. WO 9850511.

-
- Xiao, Y., Ng, S.-C., Tan, T.T.Y., Wang, Y., 2012. Recent development of cyclodextrin chiral stationary phases and their applications in chromatography. *Journal of Chromatography A* 1269 (21), 52–68.
- Yamamoto, K., Saeki, T., 1997. Anti-Infective Sheets Containing Inclusion Compounds of Microbicides With Cyclodextrin and Prevention of Infection. Patent No. JP 09299458.
- Yamamoto, K., Saeki, T., 1998. Sheets for Infection Control in Hospitals. Patent No. JP 10007591.
- Zhang, J., Ma, P.X., 2013. Cyclodextrin-based supramolecular systems for drug delivery: recent progress and future perspective. *Advanced Drug Delivery Reviews* 65 (9), 1215–1233.

Smart coatings for textiles in architecture

18

A. Ritter

Ritter Architekten, Germany

18.1 Introduction

About 10 years ago was the first time that books about using smart materials in architecture were published (Ritter, 2006, and others), and we had only a few useful smart materials and only a few applications in this field.

Since this time there have been remarkable changes. Several significant inventions and further developments in these materials have been made. Now you can find several interesting applications using these fascinating functional materials and products. It has become popular to use them, whether in buildings where people want to live, in office buildings, or in buildings used for industry. Depending on the properties and the size, you can use them differently, for example, in colour-changing and passive-cooling facades, in or as actuators, for example as positioning devices, for creating new geometries, etc. The application possibilities are huge.

Using smart textiles in architecture is relatively new. About 10 years ago, we had smart textile products that were able to react to stimuli such as light and moisture — these products are still on the market and still in use. Today we use smart textiles where the fibres of the textiles are able to react. These textiles can be combined with passive and active components, for instance, special coatings, etc. And we also have smart textiles where the fibres of the textiles are more or less not sensitive to one or more than one stimulus. Besides the possibility of combination, you can also create new types of smart textiles through new developments like the 3D-printer and inventions in the field of smart or other components.

18.2 Current trends in advanced architecture and smart textiles for architectural applications

Contemporary modern architecture can be characterized as sometimes green and sustainable, lightly adaptive and sometimes changeable, can have automation and little intelligence, and can be simple but also be complex.

In comparison to this architecture, advanced architecture is more extreme, more progressive. This means, for example, that this type of architecture uses more new techniques, more new materials, more new structures, can have one or more than one novelty, often has multiple functions, and is perhaps more dynamic.

Additionally, advanced architecture can be able, for example, to be protective and to improve conditions, often communicates and interacts, and is preferably really new.

Accordingly, a number of current trends in this field of architecture and smart textiles for architectural applications include the following concepts:

- sustainability
- adaptability
- intelligence

18.2.1 Current trends in advanced architecture

Sustainability in advanced architecture means on the one hand that building materials and products are preferably natural, fully recyclable or both. On the other hand, it means that buildings are able to harvest, generate and store energy, and are able to harvest and store matter. By absorbing, for example, sun heat and rainwater through the use of special materials and facilities, this architecture is essentially independent from the local distribution grids.

Adaptability is another trend here. Advanced adaptive buildings need special materials and/or structures that are able to react to stimuli by changing one or more than one property. Therefore, it is possible to use smart materials, for example, colour-changing materials, to create adaptive, temperature-sensitive colour-changing facades. Another possibility is using special weight-sensitive structures, for example, person-weight-sensitive structures (Fig. 18.1(a) and (b)), to create adaptive, weight-sensitive geometry-changing rooms.

Another current trend is so-called intelligent architecture, which has become increasingly important. Intelligence has to do with data processing, and with learning. Most smart materials do not have these properties, but smart materials are able to react when they are stimulated. This behaviour is comparable to the behaviour of plants.

To create real intelligent architecture, you normally have to use electrically or pneumatically powered devices. In some cases you can use also systems based on fluids. Home automation, for example, normally works with electricity. New adaptive structures like *dynaflex p01* and *Transformacer p02* (both developed by the author of this chapter) are generally suitable for generating electrical power, which again can be used for such automation.

The *dynaflex p01* (1995) is the first building structure in the world that is able to react on internal and external weight loads by changing its geometry reversibly. Depending on the height and the location of the produced (gravitational) forces, for example, produced by persons (the loads of furniture and other stuff are also usable), the mechanical structure expands linearly or curved (Fig. 18.1(a)). If there is no additional load, the structure is small, and has its normal geometry. It consists of seven modules. Each module has two inner oval rings, which are connected to a weight-sensitive platform section, and one outer oval ring, where a large number of glass elements are mounted, using special bendable carriers, each equipped with a bendable piezo element that is able to convert vibrations into electricity, caused by,

for example, people walking; in this case, the vibrations switch processes in the glass elements, reversibly turning from transparent to colourful, which is quite similar to leaves in a forest (Ritter, 1995, 1996).

Transformacer p02 from 2011 is also a weight-sensitive building structure, but also includes a new type of actuator, where water-swollable polymer strips are used. Depending, for example, on rainwater, these strips produce the needed forces to move two special scissors, which are in contact with a flexible overlying room. The original draft, shown in Fig. 18.14(a), differs from the realized draft, which shows the lower part of the structure, without the weight-sensitive platform and without the room.

In both cases, natural influences are used.

More detailed information on these and other smart and kinetic structures introduced by the author can be found in his book *smart materials in architecture, interior architecture and design* (Ritter, 2006), his doctoral thesis *smart und kinetisch!* (Ritter, 2012a, 2014a) and his e-book *smart and kinetic!* (Ritter, 2014b).

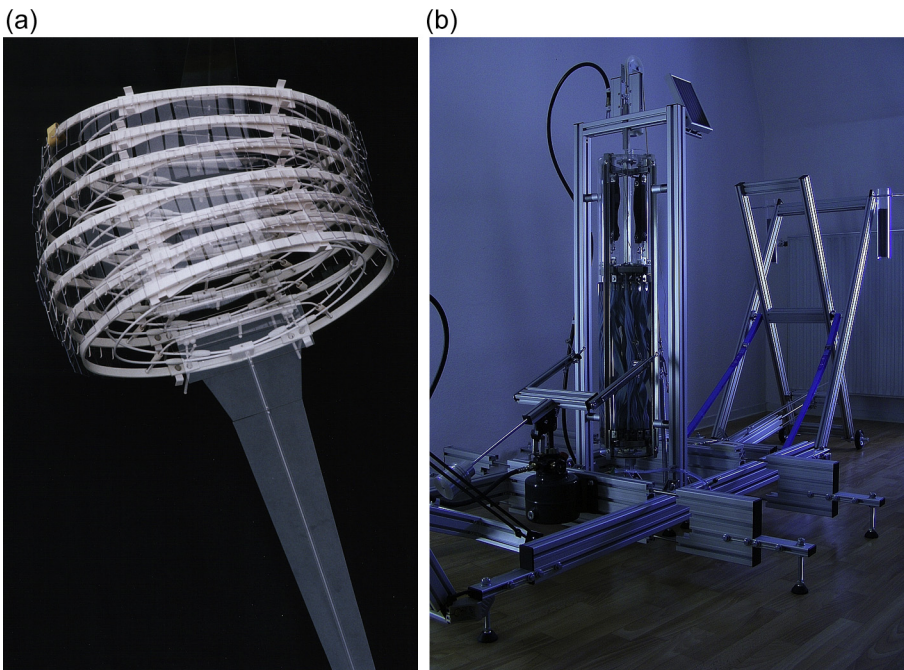


Figure 18.1 Examples of advanced architecture: (a) The first person-weight-sensitive structure in the world: *dynaflex p01*; (b) lower part of the water- and person-weight-sensitive structure *Transformacer p02*, equipped with a large-scale actuator powered by water-swollable polymer strips.

Ideas, realizations and photos by Axel Ritter.

18.2.2 Current trends in smart textiles for architectural applications

Sustainability in smart textiles for architectural applications means that the main materials and perhaps also additional components are preferably natural, fully recyclable, or both. Further, it can mean that textiles are able to absorb, generate and store energy, in some cases matter.

Fig. 18.2(a) shows an example of a complex smart textile – here without the normally needed outer textile membrane – called *Polyreagible Mechanomembran*, which

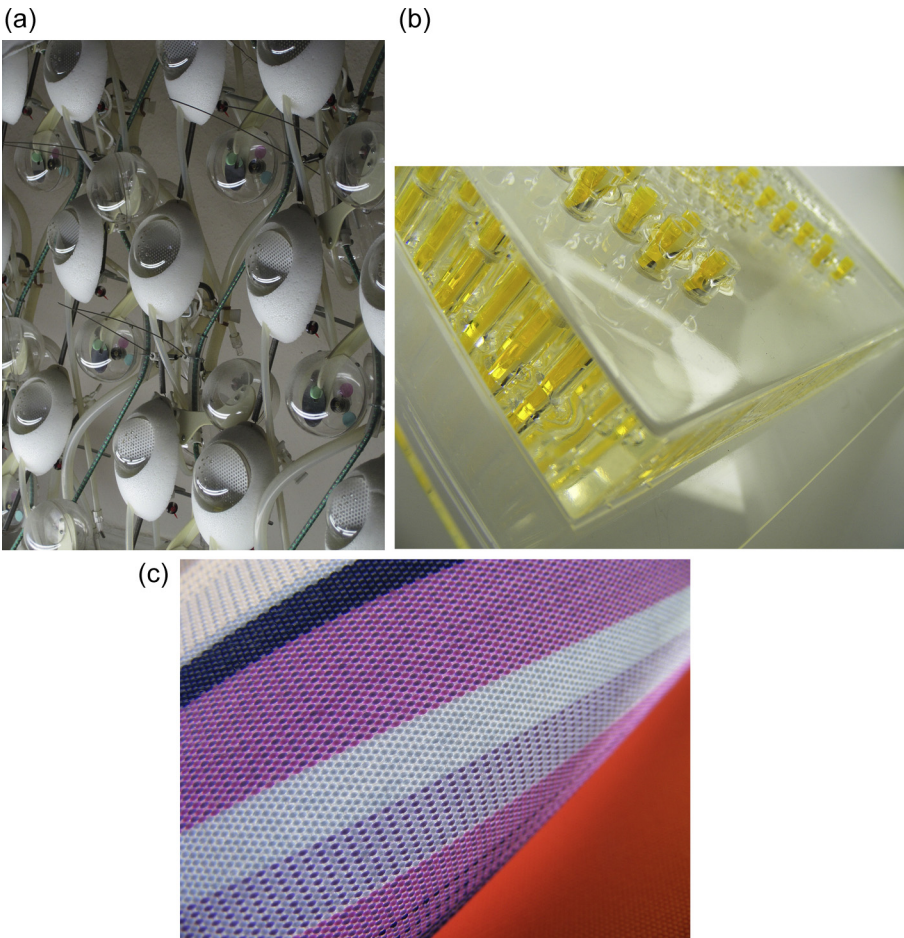


Figure 18.2 Examples of smart textiles: (a) *Polyreagible Mechanomembran* with water-absorbing and storing balls and among others thermobimetal springs as part of the smart component system; (b) luminescent skin called *glowingSkin I* made of silicone and embedded fluorescent and phosphorescent sticks, preferably mounted on a translucent textile (Ideas, realizations and photos by Axel Ritter.); (c) smart awning fabric, which is able to regain its original shape after a thermal stimulus (Product of weinor GmbH, photo by Axel Ritter.).

attempts to mimic the behaviour of human skin. It is able to collect rainwater, store it and use it to regulate the temperature of the surface of the whole membrane. It also has the property to change colour depending on the temperature of the surrounding air. For that, it is equipped with water-absorbing and storing balls, thermobimetal and hygro-bicomposite springs, moveable carrier arms with little mirrors, as well as rubber cords and flexible water lines made from silicone. Some of the thermobimetal springs work as tiny actuators, connecting the water-filled storing balls with the so-called *Transpirator-Ringe*, which surround the absorbing balls, depending on specific high air temperatures, while other thermobimetal springs work together with the humidity-sensitive springs by positioning two coloured areas (one of them is a colour filter) to create temperature and humidity depending on the colour changes (Ritter, 2002, 2006).

This artificial skin is therefore also essentially an example of an adaptive textile.

Other adaptive products are *glowingSkin I* (Fig. 18.2(b); Ritter, 2012b), which is able to be luminescent, because of the fluorescent and phosphorescent sticks embedded in a transparent layer of silicone, and a woven textile (Fig. 18.2(c)) that is able to react to thermal stimuli by retaking its original shape (although in this case we do not have a smart coating, the unusual property has to do only with the fibre). In some cases we call the property of the woven textile intelligent because of the memory effect.

18.3 Current components and types of smart-coated textiles for architectural applications

To create smart textiles for architectural applications it is possible, for example, to combine passive with active components.

One possibility here is to use a conventional fabric made of, for example, polyester or glass fibre and cover this with an active, specific stimulus-sensitive layer, such as a photocatalytic layer; in this case additional layers could be required.

Another possibility is to cover a smart fabric made of, for example, temperature-sensitive fibre with a specific stimulus-sensitive layer, such as a water-sensitive layer; in this case an additional layer could also be required.

Coatings can cover each single fibre and/or can cover the fabric itself.

18.3.1 Passive and active components

Next we discuss some examples of passive and active components for use in and/or on smart textiles. For example, conventional two-dimensional passive membranes, like many building membranes, such as square hole raster equipped membranes (see Fig. 18.3(a)), can be used as carrier components, where active components can be mounted on, for example, by affixing them with specific adhesives and/or mechanical fasteners. In comparison, three-dimensional membranes can be filled with solid components, as sticks or plates, for example, powdered, granulated and/or liquid components. Furthermore, you can cover the outer and inner surfaces with additional

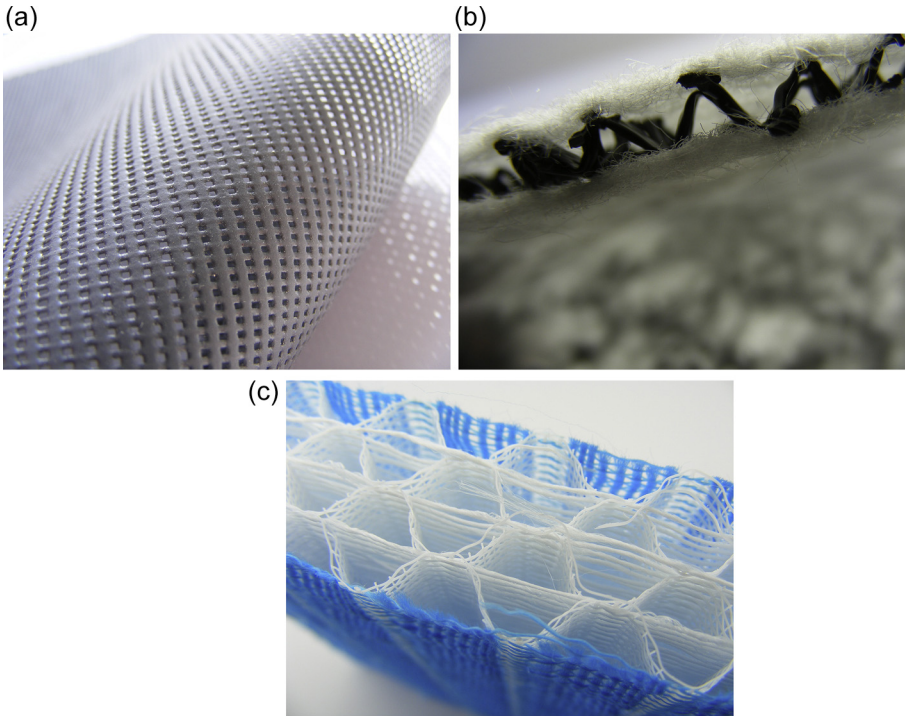


Figure 18.3 Examples of passive usable components in smart textiles: (a) A square hole raster equipped membrane, normally used as building shades (*Product of Serge Ferrari S.A.S.*); (b) a three-dimensional plastic mat, both sides covered with a white, translucent synthetic fleece, normally used to protect against surface erosion (*Product of NAUE GmbH.*); (c) a three-dimensional multilayer fabric cushion (*unknown manufacturer*). All photos by Axel Ritter.

components. Besides the options already described, in some cases components can be connected by sewing them together.

Normally two-dimensional active components, which have, for example, a shape-changing effect, such as shape memory alloy (SMA) wires ([Fig. 18.4\(a\)](#)), as thermobimetal plates, can be used as actuators, for example, to move passive components like yarns and/or fabrics. Depending on the desired effect, you can connect them through interweaving and other ways of traditional mechanical and/or chemical fixing. Some active components can have different phases, like phase change materials (PCMs), as for example salt hydrates ([Fig. 18.4\(b\)](#)). If you want to use such materials, you have to ensure, that, among other things, no material can leak in any phase. Therefore, it may be necessary to use encapsulations, which in turn should have good thermal conductivity. Some three-dimensional active components also have a shape-changing effect, such as water-swellaible strips. Some of them were developed

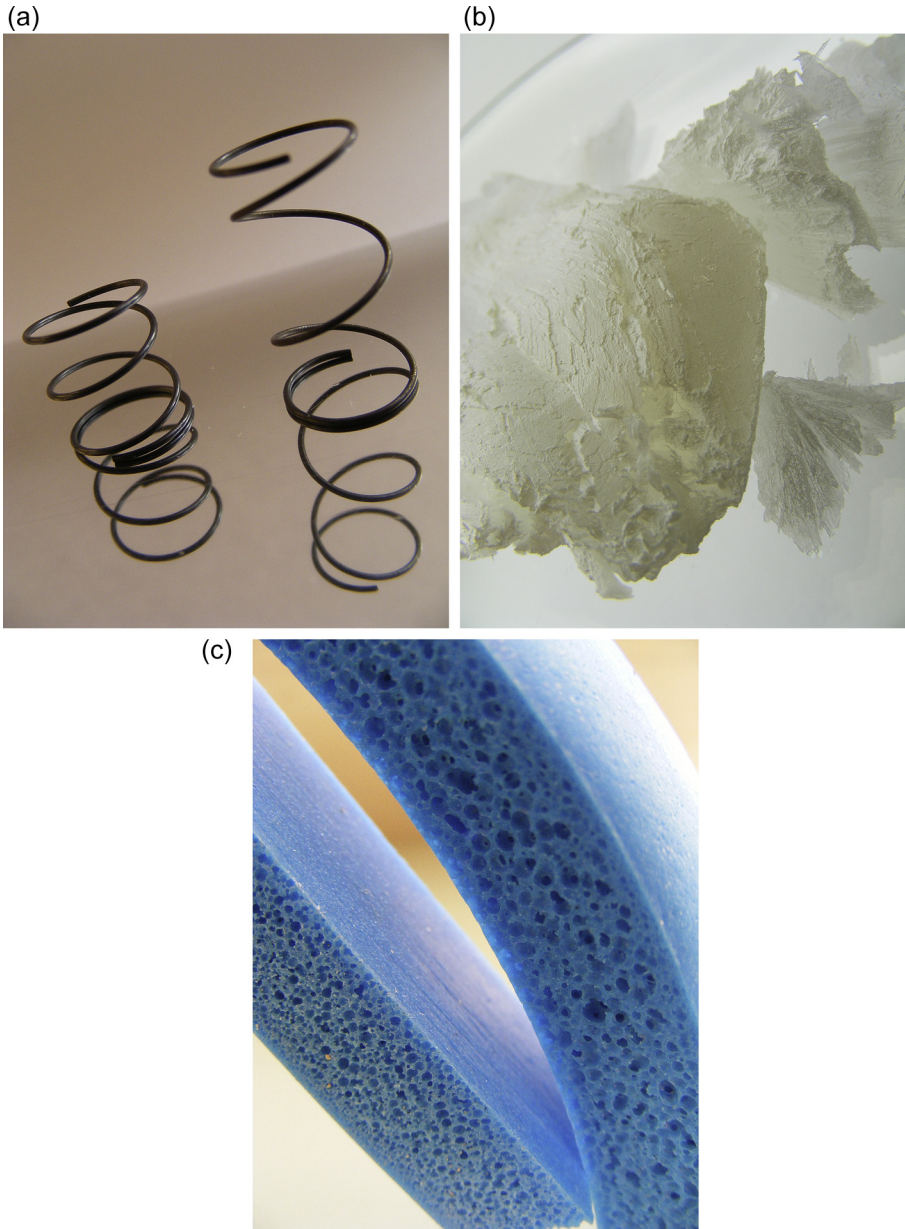


Figure 18.4 Examples of active usable components in smart textiles: (a) Shape memory alloy (SMA) products, here: two springs showing a two-way effect; (b) a phase change material (PCM), here: salt hydrate; (c) two water-swollable polymer strips, the left one is not activated, the right one is activated.

All photos by Axel Ritter.

as sealing elements for use in cellars and other building construction; for example, in tunnels (Fig. 18.4(c)). Notwithstanding, these also could be used as variable stiffening and/or as variable load components (Ritter, 2013, 2014).

Through new combination of a known smart material, like the PCM *Micronal* (product of BASF SE), with a known conventional material, like limewash, new smart coatings (Fig. 18.5(a–c)) can be created for use on textiles or other surfaces. In this case the mixture can be applied, for instance, on armed loam plaster boards mounted as building walls by using a brush.

We often call these smart materials because they are able to change one or more than one property depending on one or more than one stimulus (Ritter, 2006).

18.3.2 Smart-coated property-changing textiles

In some cases, depending on a desired effect, it is helpful to have textiles that are able to change one or more than one property. To achieve such textiles, you need special active components, so-called smart components – this is analogous to the definition

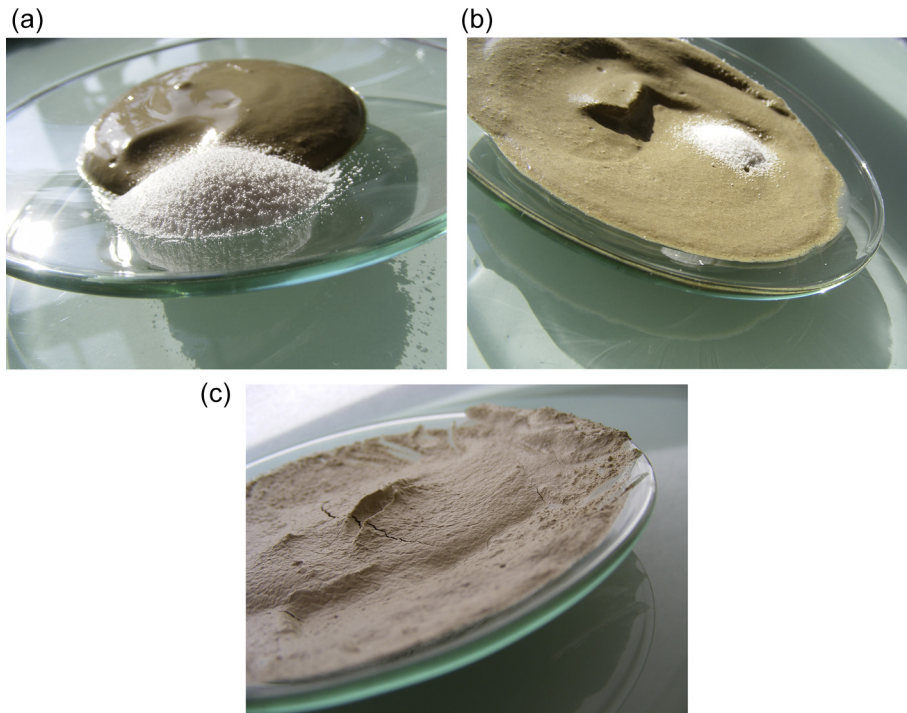


Figure 18.5 Example of how you can create a new coating for smart textiles: Combine, for example, a powdered smart material with a fluid passive material: (a) Powdered PCM (*Micronal*) and lime wash on a watch glass, (b) mixed and (c) in dry condition. Idea, realization and all photos by Axel Ritter.

of smart materials (see chapter: Smart medical textiles based on cyclodextrins for curative or preventive patient care).

In general you can find coatings that are in a solid state, such as tubes. These can cover, for example, one single piece of yarn. Smart tubes are made, for example, from an SMA, which makes the tubes shorter and longer depending on specific temperatures.

You also can find coatings that are pasty before their application. Only after a certain time do they become more solid (not activated). An example of such a coating is a water-swellaible single-component material (Fig. 18.6(a)), which allows different applications.

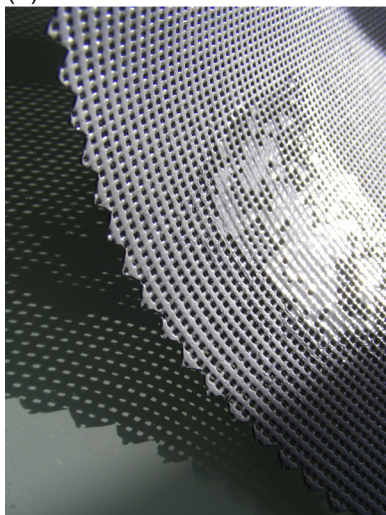
In addition, you can find coatings that are normally liquid before application. These dry during contact with the surrounding air.

Many coatings can be applied by hand and machines.

Depending on a significant changing property, you can select from:

- smart-coated shape-changing textiles
- smart-coated colour-changing textiles
- smart-coated permeability-changing textiles
- smart-coated self-cleaning textiles
- smart-coated self-healing textiles

(a)



(b)



Figure 18.6 Examples of smart-coated shape-changing textiles and their components: (a) A square hole raster equipped textile membrane with a water-swellaible original pasty coating; (b) the same membrane with a water-swellaible polymer strip mounted on the surface; for that you can use an adhesive compound based on silane terminated polypropylenoxide (SPPO). All photos by Axel Ritter.

In several cases there are textiles with more than one changing property (see, eg, Fig. 18.6(a,b)).

Because of the water-swellaable properties of the active components, both textiles are self-healing. This means that in case of mechanical treatments, injuries will be healed by closing the emerging openings through the volume increase of the active material.

Also water sensitive is the following smart-coated textile (Fig. 18.7(a–c)), mounted on the foldable carrying structure of an umbrella. In this case a woven fabric was treated by water-sensitive colour-changing coatings, here in the shape of butterflies, which look white when dry. In contact with water, however, the areas change from white into green, yellow, or pink in seconds. The time for the reverse process, going back to white, depends on the time for drying the pattern. This special fabric is also suitable for architectural applications, for example, as temporarily used foldable roofs and as awnings.

Some existing textiles are sensitive to moisture, especially humidity. Following (Fig. 18.8(a)) you see an actuator, normally mounted on a window frame to control air passage, consisting of eight hygroactive strips that are able to change their length, depending on the humidity of the surrounding air. In this case the textile strips have no special active coating. The length changes are based solely due to the used synthetic yarn.

Fig. 18.8(b) and (c) show two different, relatively new climate membranes for buildings that have the ability to change their permeability due to moisture. They can be used as variable vapour barriers and as variable air sealing membranes, for example, in the field roofs and exterior walls. In both cases the textiles are fleeces made of polypropylene; in one case the fleece is additionally reinforced by a grid-like fabric also of polypropylene. These are coated with transparent, humidity-sensitive foils that are able to change the pore size, depending on the humidity of the surrounding air. One is made of a modified polyamide (Fig. 18.8(b)), the other made of a polyethylene copolymer (Fig. 18.8(c)). The so-called dynamic diffusion-equivalent air layer thickness (S_d) ranges here between 0.25 and >25 m (metres) (see additional information in Fig. 18.8 caption).

An example of a smart-coated self-cleaning textile is shown in Fig. 18.9. For an actual architectural application for this textile, see Fig. 18.16(a). Responsible for the self-cleaning process is the photosensitive titanium dioxide (TiO_2), a white active coating, which is on the top of the multilayered, PVC-based textile membrane. The membrane itself consists of polyester or glass fibres.

18.3.3 Smart-coated energy-generating and exchanging textiles

Sometimes textiles that are able to generate energy are needed. Besides existing products, there are now textiles printed with organic light-emitting diodes (OLEDs). These OLEDs are able to convert light – like the well-established silicon-based solar cells

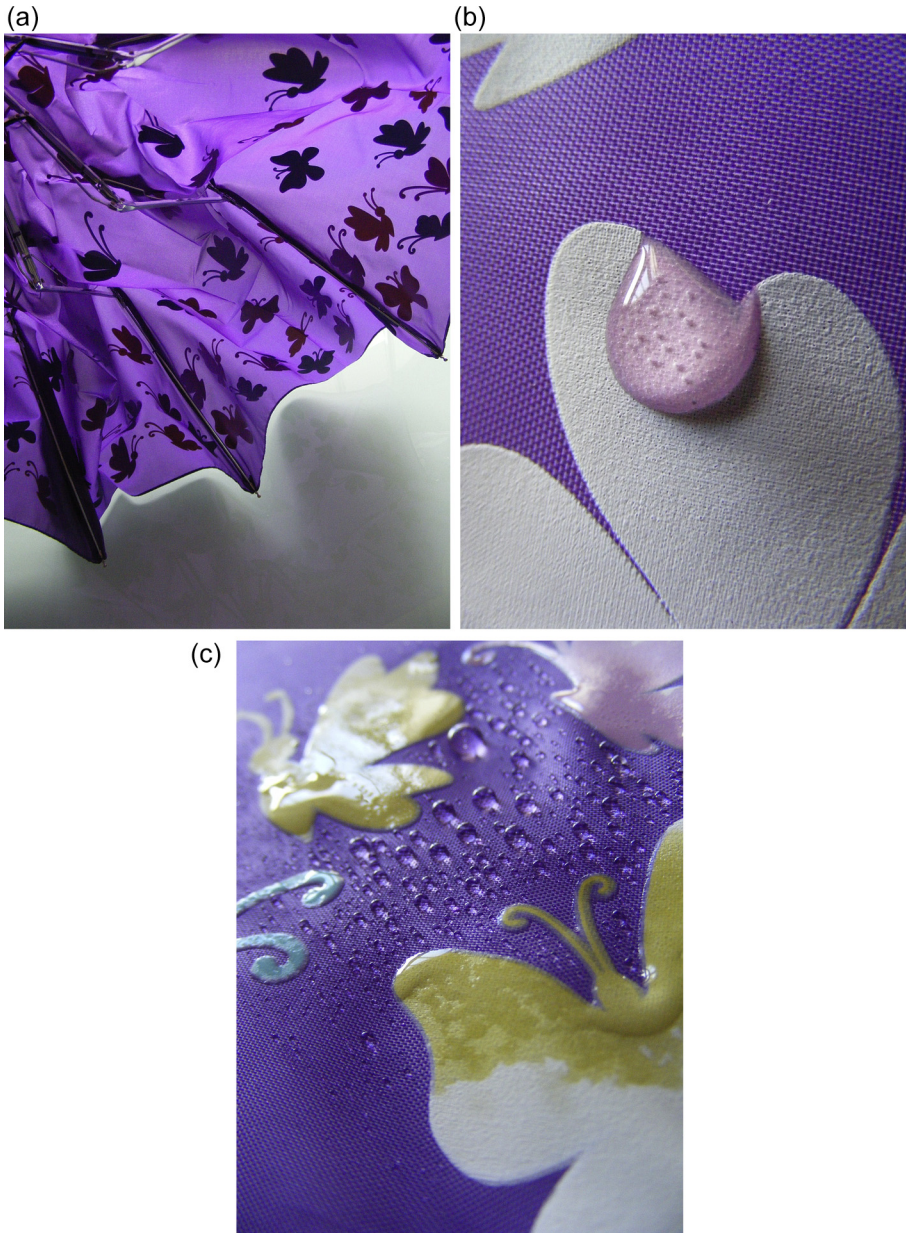


Figure 18.7 Example of a smart coated colour-changing textile and its components: (a) Umbrella, equipped with printed, water-sensitive colour-changing butterflies as a stylish pattern; (b) detail of the fabric with the smart printings and a water drop, which is activating the colour-changing-effect – here into pink; (c) several activated butterflies with water drops on the hydrophobic-treated fabric.

Unknown manufacturer, all photos by Axel Ritter.

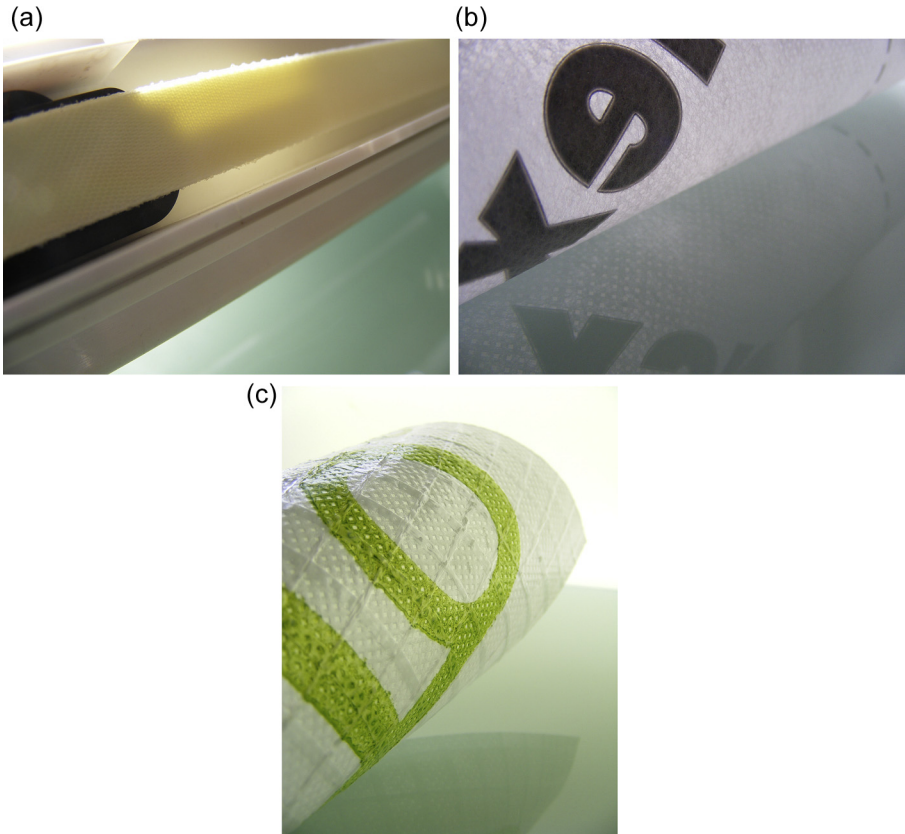


Figure 18.8 Examples of humidity-sensitive textiles, one not smart coated, two smart coated: (a) Detail of an actuator, consisting of eight hygroactive textile strips (Product of Aereco GmbH.); (b) detail of a moist variable, permeability-changing climate membrane – $S_d = 0.3$ to 5 m (Product of SAINT-GOBAIN ISOVER G + H AG.); (c) detail of a moist variable, permeability-changing climate membrane – $S_d = 0.25$ to >25 m (Product of MOLL GmbH.). All photos by Axel Ritter.

do – into electricity. An advantage of these smart materials is, among the printability and other features, is that they are flexible.

Another possibility to create energy-generating textiles is to use thermo-, piezo- and/or mechanoelectrically operating systems, for example, in the shape of strips, as active layers.

Smart-coated energy-exchanging textiles are well established on the market. More or less everyone today can create, for example, light-emitting textiles by using available fluorescent and phosphorescent sprays and textile dyes.

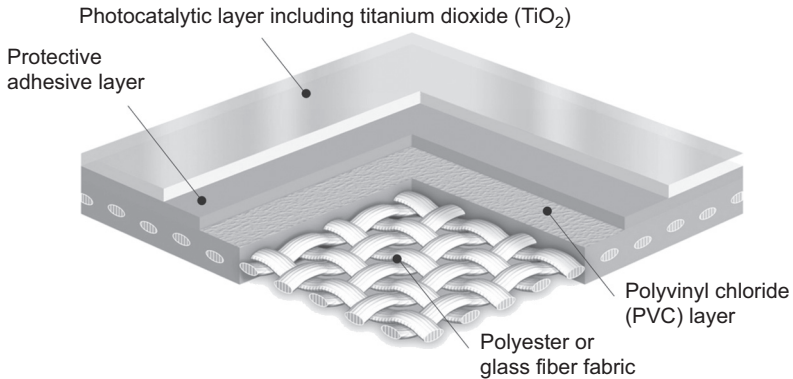


Figure 18.9 Example of a smart-coated self-cleaning textile and its components: PVC-based membrane covered with a photocatalytic layer that has embedded TiO_2 . Drawing courtesy of Taiyo Kogyo Group.

Section 18.5.1, Fig. 18.15, shows a new application for a smart-coated light-emitting textile.

18.3.4 Smart-coated energy-storing textiles

Sometimes it is desirable to have textiles that are able to store energy. To realize such textiles so-called PCMs such as water, salt hydrate and paraffin can be used (see also Section 18.3.1). To use paraffin in buildings it is required that this material cannot burn, because paraffin is flammable. Therefore, and for better handling, this PCM is normally microencapsulated; on the market it is available as a white powder, which can be mixed with different materials like gypsum, plaster, loam, etc. Fig. 18.5 shows in different stages how to make a new active coating by using such a powdered PCM, mixing it with a conventional material, like lime wash.

Two other examples of smart-coated energy-storing textiles, both currently available, are shown in Fig. 18.10(a) and (b). In these cases the textiles are the passive components and the loam and the embedded PCM are the active components. Loam has the ability to absorb humidity and water by changing its volume and its weight as what is usable for different applications, for example, as part of weight-sensitive structures (see, eg, Section 18.2.1 and Fig. 18.1(a) and (b)).

18.3.5 Smart-coated matter-exchanging textiles

There also can be cases that desired or need textiles that are able to exchange matter. Especially in the field of architecture we can find several interesting applications for such textiles.

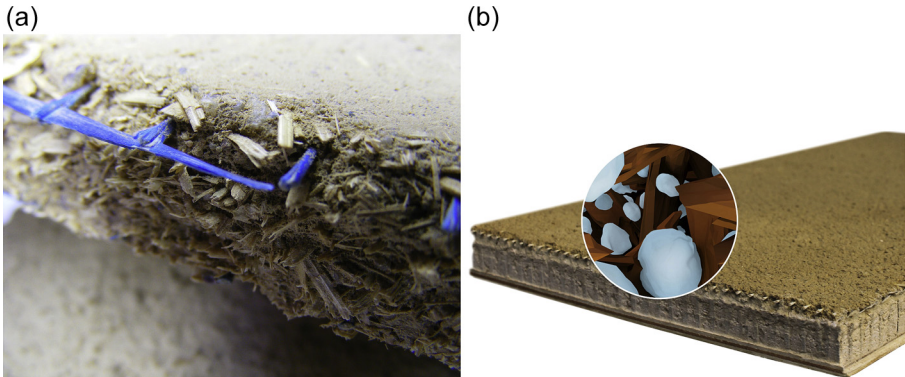


Figure 18.10 Examples of smart-coated energy-storing textiles and their components: (a) Detail of two loam boards with embedded microencapsulated PCM and glass textiles. (b) new type of a loam board with PCM and a glass textile.

Photo left by Axel Ritter, photo right by lehmorange.

Smart-coated matter-exchanging textiles can be useful for planning textiled buildings that are able to heal themselves. Conventional building membranes can be used as the passive components and these can then be equipped them with active water-swallowable products. In this case rainwater and/or groundwater are the needed solvents.

Fig. 18.11(a) and (b) shows two such textiles. Here the active components consist of the natural product bentonite, which is a clay mineral. Normally these textiles are used as sealing products, for example, to protect the basements of buildings against ground and/or pressing water.

Smart-coated matter-exchanging textiles can also be useful, if variable loads are desired (see, eg, Section 18.2.1 and Fig. 18.1(a) and (b)). Fig. 18.11(a) and (b) shows water-swallowable textiles; the following two types of textiles are capable of swelling as such. In one of them, you use textiles with fibres that are susceptible to electrostatic charging due to, for example, mechanical friction. It is well known that specific fibres and fabrics, especially those made of synthetic components, can have good charge and discharge due to mechanical friction. For those, we use fibres and fabrics made of, for example, polypropylene, polyvinylchloride (PVC) and polytetrafluoroethylene. Carpets made of these components charge if someone walks on them with shoes with rubber soles and discharge if a charge equalization can occur, for example, through subsequent contact with the ground.

Another possibility to get smart-coated textiles, which are susceptible to electrostatic charging, are textiles that have electrically conductive components, like fibres made from metal.

Both types of textiles have the ability to attract dust, and therefore can be used where dust can occur, for example, in cities.

See also Section 18.3.2, Fig. 18.6.

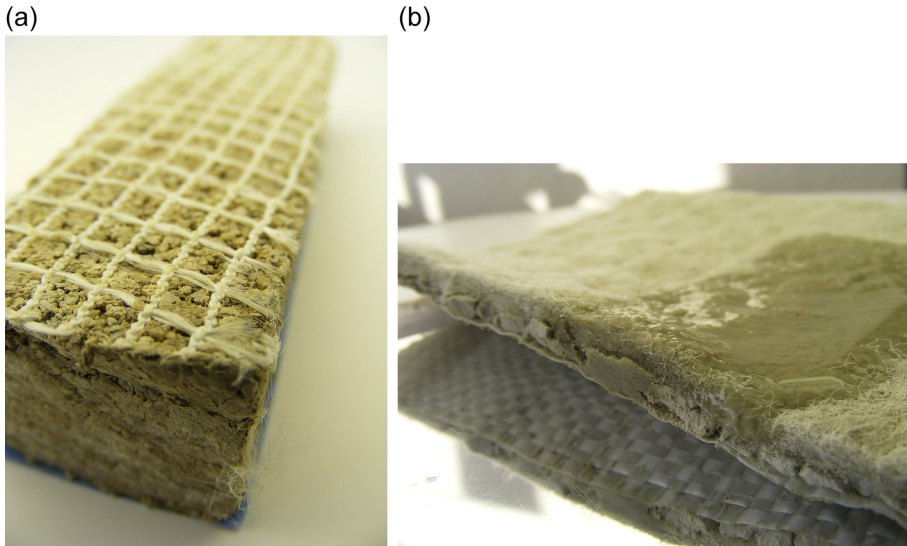


Figure 18.11 Examples of smart-coated matter-exchanging textiles and their components: (a) Sealing strip with water-swellable bentonite between two textiles, (b) geotextile with water-swellable bentonite embedded in a synthetic fleece; the bentonite here is partly activated through contact with water.

Product of NAUE GmbH, photos by Axel Ritter.

18.4 Future trends in advanced architecture and smart textiles for architectural applications

Looking to the future there are a number of interesting trends in advanced architecture as well as in smart textiles for architectural applications.

18.4.1 *Future trends in advanced architecture*

Interesting trends in advanced architecture for the future could be

- gestures-controlled buildings
- totally transformable/transforming buildings
- real thinking buildings
- real living buildings

The possibilities for interacting with buildings or parts of buildings are becoming increasingly interesting. We speak of so-called smart homes, where, for example, our smartphone becomes more and more important, connecting us with our home, controlling household functions with special apps.

In this context, it is also interesting to control buildings or parts of buildings by gestures, which partly are already in development and in a demonstration phase. Here, for example, the software of game consoles can be used.

Totally transformable buildings could be another trend; some architects and engineers are working intensively in this field (for example, this is one of my interests). This requires a wide range of different, in some cases very special materials and structures. Here it is necessary to have kinetic structures. If the transformations should be energy and/or matter self-sufficient, you usually need smart materials as well as smart components.

A next step to creating fully autonomous architecture is real thinking buildings. This means that homes, offices and factories not only operate due to a more or less simple program but that the building becomes its own character, interacting with real people inhabiting or working inside of them. For this you need new hardware and software. The possibilities could be very interesting, for example, for people who live alone and may need help, for example, because they have impaired perception.

Another trend could be real living buildings. This could have numerous advantages: one could be the ability to be energy and/or matter self-sufficient, a second the ability to self-repair, another the ability of adaption. Real living buildings could have the behaviour of plants or of animals — perhaps also of humans, if it is wanted (see also chapter: Smart medical textiles based on cyclodextrins for curative or preventive patient care, in: *Multidisciplinary know-how for smart-textiles developers*, Kirstein et al., 2013).

18.4.2 Future trends in smart textiles for architectural applications

Interesting trends in smart textiles for architectural applications could be

- biomonitoring textiles (bacteria-based textiles)
- (variable) protective textiles
- polymorphic textiles (nanometre-sized units-based textiles)
- stimulating textiles

One important trend in the future of textiles for architectural applications could be biomonitoring. That could mean that textiles are able to indicate, for example, the quality of surrounding air by showing a special pattern and/or signal colours. Possible are also textiles that smell good if all is okay and smell bad if one or more than one parameter is far from a wanted value.

For this type of function you could use an existing living organism like bacteria and mold fungus in the air by, for example, equipping a room-forming textile with a coating that is or has a suitable culture medium (substrate) like gelatin.

Fig. 18.12 shows such a coating, which can be applied on different types of textiles. To ensure that such textiles work for a long period of time, it is required that the culture mediums do not fall down and do not get consumed (Kirstein et al., 2013).

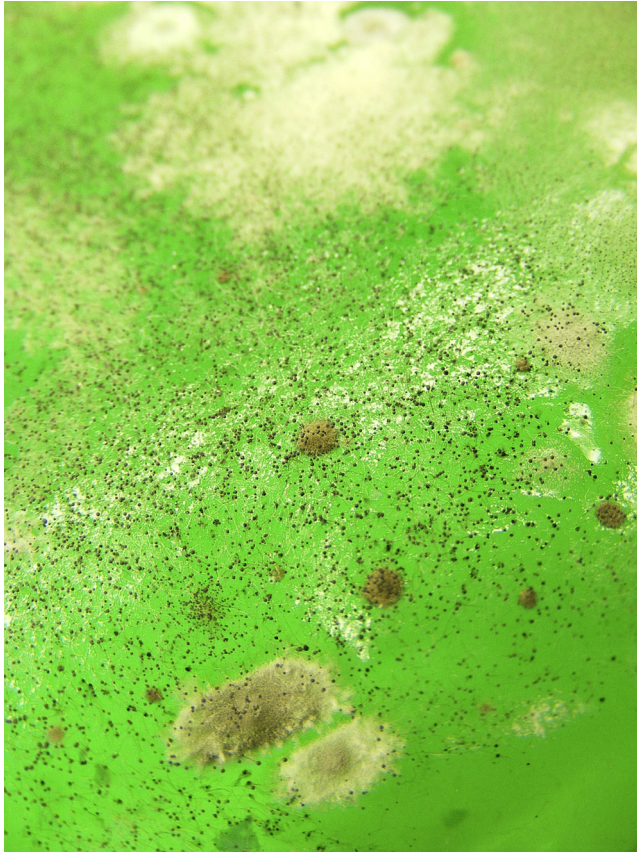


Figure 18.12 Example of a biomonitoring coating for use in textiles (from 2011): Detail of a green gelatin surface with mold fungus, indicating an actual population of mold fungus in a room. Idea, realization and photo by Axel Ritter.

Increasingly interesting could be another trend in smart textiles: the (variable) protection of people, goods and buildings. This may involve protection against cosmic radiation, rainfall, hail, fire, vandalism, terrorism, etc.

From a wide range of options, one example for that could be textiles that are able to change the transmission of sunlight due to a room temperature and/or the well-being of people. For that one can possibly use new electrooptically switchable gels, embedded between two layers of transparent textiles. Transparent textiles can be transparent foils, armed with textiles.

Another example could be textiles that are normally stiff and are able to be stiff when they are quickly be pierced with something, for example, a knife, and then be flexible and/or bendable when they are under the influence of other mechanical treatment, for example, vibrations. For that you can use textiles that include thixotropic fluids (TFs). TFs can be, among others, mixtures of sand with water. That these fluids are normally stiff has to do with gravity.

Other useful components can be electrorheological fluids (ERFs) and magnetorheological fluids (MRFs). These fluids are able to reverse their viscosity, their stiffness, depending on an electrical respectively magnetic field. These consist of electrically respectively magnetically polarizable particles in a nonpolarizable carrier liquid (Ritter, 2006).

In some cases, especially TFs and MRFs could be applied directly as smart coatings of textiles without using additional fixing devices, because here the carrier liquid can consist of water, which is nontoxic, if somehow it would leak into the soil.

Due to progressive developments in the field of materials, the wish to realize polymorphic materials, in the future we may also look forward to polymorphic textiles. Polymorphic textiles would be probably be made from nanometre-scale substances, probably based on programmable mechanical nanometre-sized units. Such materials and textiles can take up a wide range of physical and optical stages; they can, for example, convert from wood to plastic, from solid to liquid, etc. A visionary polymorphic smart material is the *Utility Fog* of J. Storrs Hall, conceived at the beginning of the 1990s by using so-called *nanobots* (Fig. 18.13) (Ritter, 2006).

In this case, it could be interesting to combine conventional textiles with smart coatings made from such polymorphic materials. In this way, it could be possible that the active layer influences the passive layer, for example, by changing the geometry of the whole textile system, the external form, the light and/or heat transmission, etc.

The trend towards stimulating textiles. This means, for example, textiles that have the ability to repeatedly smell depending on a specific room temperature or depending on the touch of shoes (pressure and/or friction-sensitive textiles), and/or that have the ability to repeatedly change colour, showing a specific pattern, depending on,

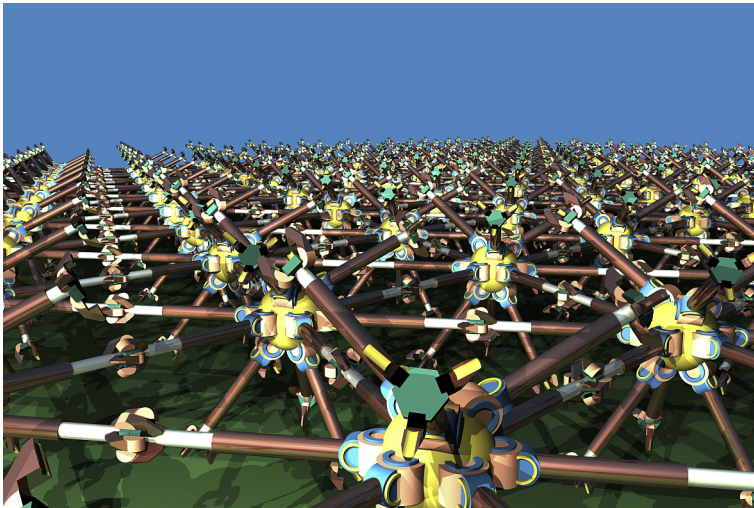


Figure 18.13 Proposal of a polymorphic smart material that could be used as an active coating of smart textiles: Flat structure constructed with *nanobots*.

Photo courtesy of J. Storrs Hall, USA.

for example, the mood of people. A scenario could be: If you are stressed, your smart watch detects this and sends information to a little processor through which an electrical current will pass through an accordingly heated textile, which in turn releases a desired perfume and shows at the same time a desired image, for example, of your family or your pet.

Another possibility could be the release of oxygen respective to the outflow of natural air through specific textiles if there is too little oxygen in a room and/or the air composition is insufficient, or there are high levels of pollution.

Stimulating components, especially scents, are normally placed in the coatings. From there it is relatively easy to release them (see previous description). Now, we often use PVC-based coatings, where the components are embedded. The disadvantage here is that PVC is toxic. In the future, we will hopefully have new, nontoxic coatings with nontoxic stimulating components.

18.5 Applications for interior, exterior use and for actuators

In this section is a discussion of some applications of smart-coated textiles for interior and exterior use as well as for actuators.

18.5.1 Applications for interior use

Smart-coated textiles that can be used in the interior of rooms include:

- curtains
- shades
- ceilings
- walls
- rooms
- furniture fabrics

Examples of these applications are the following two textiles. The first example (see Fig. 18.14) is a white curtain textile with a square grid of a conductive yarn and an attached light-emitting diode (Kirstein et al., 2013).

The second example (see Fig. 18.15) shows a strip curtain, a special shade, that consists of vertical lamellae, one side covered with a phosphorescent coating. During the day the active coated lamellae are orientated to the sun, while during the night these are orientated to the room to illuminate it. The coating itself can consist of a phosphorescent dye that can be applied as a spray or by screen printing. In both cases it is necessary to make sure that there will be a high density of active components in the coating. Furthermore, it is important to use high-quality components, preferably those that have good brightness and a long afterglow property, so the material can give good illumination after it is stimulated. To give the lamellae a specific design, you can spray and

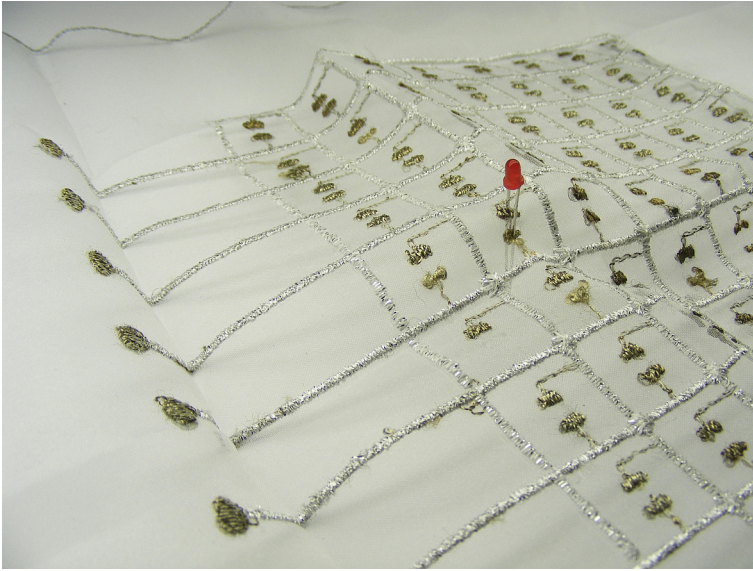


Figure 18.14 Part of a curtain textile with a conductive yarn and one (red) LED. Modification of the textile and photo by Axel Ritter.

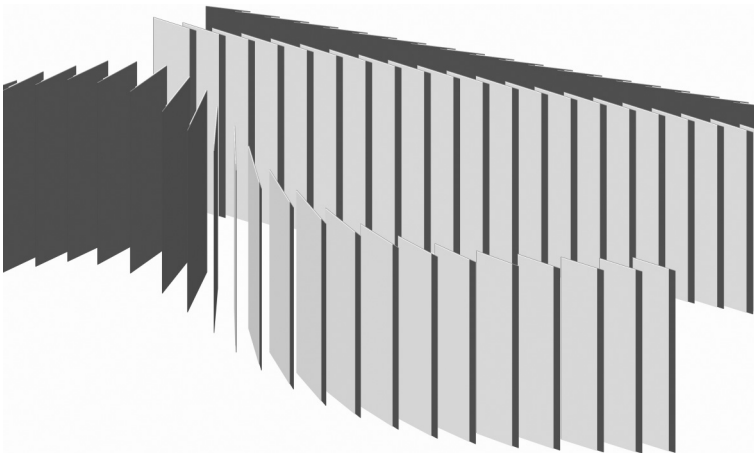


Figure 18.15 Example of a smart-coated illuminating textile shade (from 2011): One side of the lamellae was treated by a phosphorescent coating. In the background you see first the lamellae oriented with the phosphorescent coating to the sun, and behind it, the active, illuminating coating oriented to a room (both lamellae are straight). In the front you see the turning process, represented by the relocation of individual lamellae (lamellae are arranged wavy). Idea and drawing by Axel Ritter.

print the coatings in the form of patterns on the textiles – in this case the brightness of the active coating will decrease slightly to strongly.

Other useful coatings could be colour-changing coatings to indicate, for example, worsening quality of the ambient air or using too hot water while showering. More in the context of architecture applicable coatings and smart textiles for interior can be found in the books *smart materials in architecture, interior architecture and design* (Ritter, 2006) and *smart und kinetisch!* and *smart and kinetic!* (Ritter, 2012a, 2014a,b).

18.5.2 Applications for exterior use and for actuators

Smart-coated textiles, which can be used for exteriors and for actuators, include

- curtains
- shades
- ceilings
- walls, facades
- furniture fabrics
- buildings
- actuators

Following are some examples for architectural applications (Fig. 18.16(a) and (b)) with smart-coated textiles, discussed in Sections 18.3.2–18.3.5.

The first application here is a building, where a PVC-based, with photocatalytic TiO_2 -equipped textile membrane is used as a self-cleaning facade (Fig. 18.15(a)).

The second application is the Shanghai Airport, using a geotextile with water-swallowable bentonite (Fig. 18.16(b)) on the walls of the basements, to protect them from water and water damage.

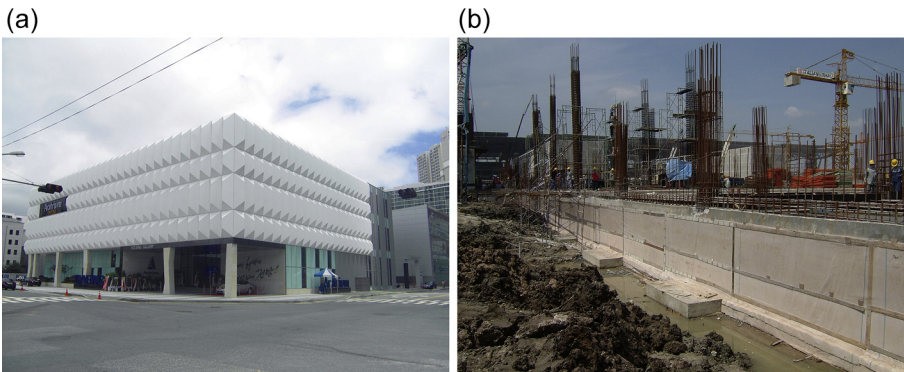


Figure 18.16 Realized applications of smart-coated textiles for exterior use: (a) *Busan Bando Model House*, using a PVC-based photocatalytic membrane (Photo courtesy of *Taiyo Kogyo Group*); (b) *Shanghai Airport* using a geotextile with water-swallowable bentonite (Photo courtesy of *NAUE GmbH*).

An example for an adaptive building structure, where the flexible textile room can be covered by two out and in rollable smart-coated textiles, is shown in Fig. 18.17(a). In the middle of the structure you can find a large-scale actuator. The mounted textiles could be replaced by smart, specific stimuli-sensitive textiles; for example, to control the behaviour of the actuator depending on a stimulus.

A relatively new actuator using smart-coated textiles is shown in Fig. 18.18(a–c). This has the property to contract and expand depending on an absorbed amount of water. If it is not activated, we do not have a smart coating. This appears in the case that the device is fully contracted and superabsorbing polymers, here so-called crystals, penetrate the double-layered textile membrane and come to its surface.

Other information on useful coatings and applications for exterior use and for actuators can be found in the books *smart materials in architecture, interior architecture and design* (Ritter, 2006), and *smart und kinetisch!* and *smart and kinetic!* (Ritter, 2012a, 2014a,b).

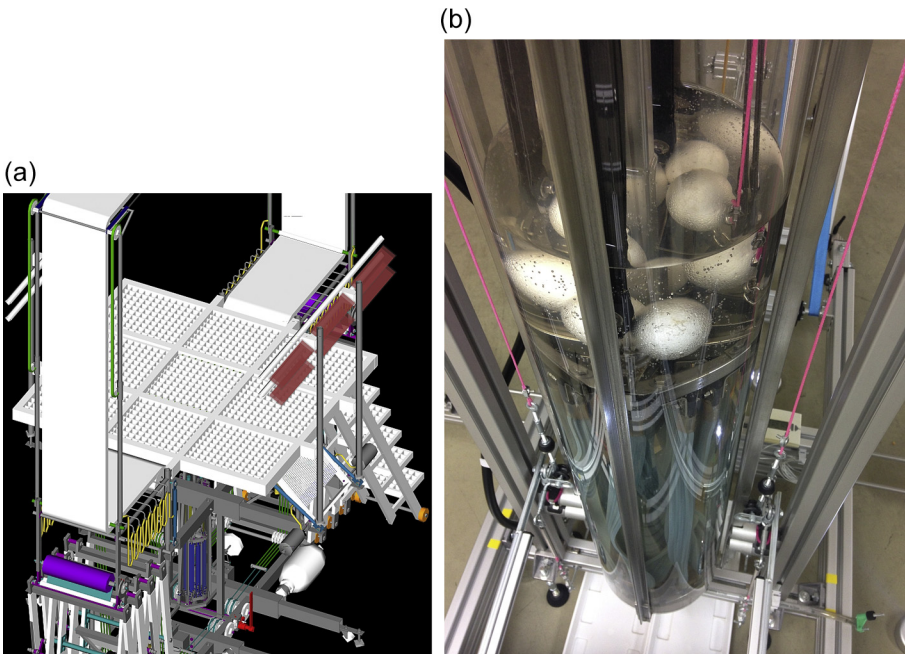


Figure 18.17 Partly realized application of smart-coated textiles for exterior use: (a) Drawing of the water- and person-weight-sensitive structure *Transformacer p02*, equipped with a flexible textile room, two out and in rollable smart-coated textiles and a large-scale actuator powered by water-swellaible polymer strips; (b) realized actuator with elastic textile strips (see also Fig. 18.1).

Idea, realization, drawing and photo by Axel Ritter.

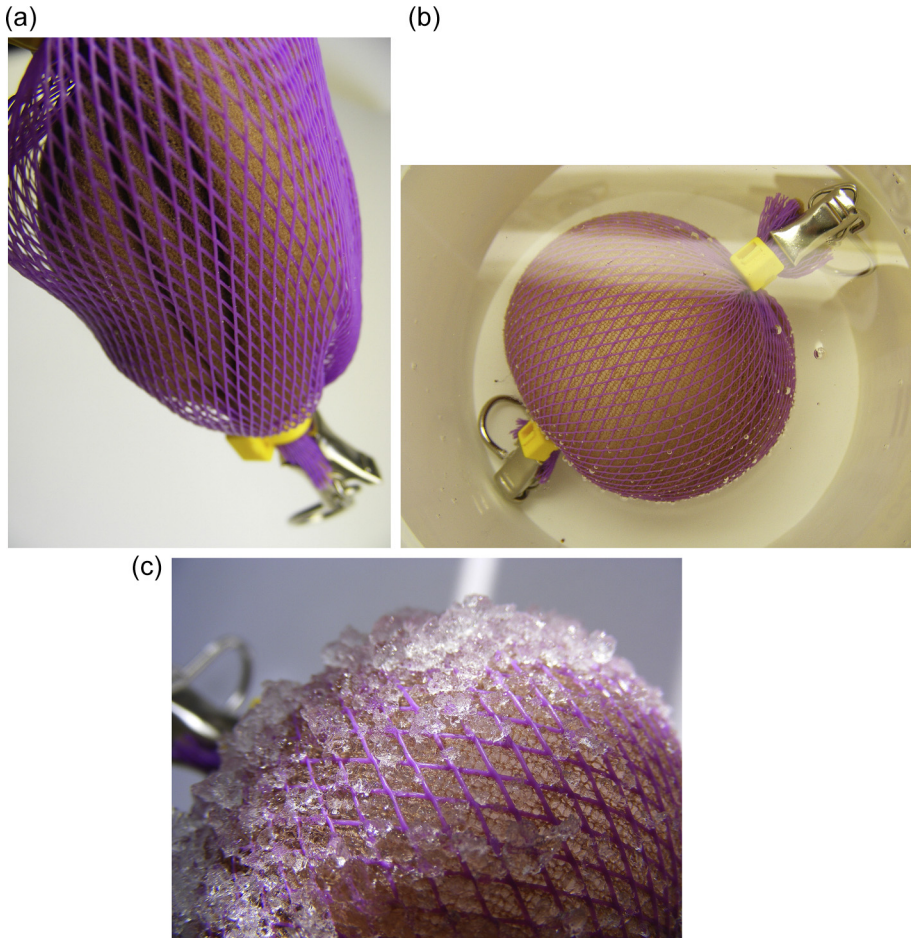


Figure 18.18 Realized application of a smart-coated textile for a new actuator (from 2012): (a) Detail of *Antriebsstrang II* equipped with superabsorbing polymers (SAPs), when not activated and at normal length; (b) the actuator in contact with water, which has activated it, and the actuator is nearly fully contracted; (c) detail of the activated surface with the double-layered textiles, which are mostly covered by activated SAP crystals. Idea, realization and photos by Axel Ritter.

References

- Kirstein, T., Ritter, A., et al., 2013. Multidisciplinary know-how for smart-textiles developers. Woodhead Publishing Limited, Oxford, Cambridge, Philadelphia, New Delhi.
 N.N. (unknown), December 2002. Polyreagible Mechanomembran. Wallpaper 54, 67.
 Ritter, A., December 1995. Flexible Tragstruktur aus Glasfaserkunststoff. Arch + 129, 136.

- Ritter, A., March 1996. "Es" bewegt sich – Reagible Tragstruktur aus Glasfaserkunststoff. AIT Spezial – Intelligente Architektur 4, 70–71.
- Ritter, A., 2002. Lektionen aus der Natur – Polyreagible Mechanomembran. Intelligente Architektur 36, 16–17, 09/10.
- Ritter, A., 2006. Smart materials in architecture, interior architecture and design. Birkhäuser, Basel, Berlin, Boston.
- Ritter, A., 2012a. Smart and kinetisch! (Doctoral thesis) Universität/University of Duisburg-Essen/Campus Essen.
- Ritter, A., 2012b. Smart and kinetic! – intelligent and adaptive building skins through the use of smart materials, adaptive and kinetic structures. In: Solar Building Skins – Conference Proceedings of the 7th Energy Forum, 06–07 December 2012, Bressanone/Italy. EF Economic Forum Ltd., Munich, Bozen.
- Ritter, A., 2014a. Smart und kinetisch! (Printed book, ebook). Shaker Verlag, Aachen.
- Ritter, A., 2014b. Smart and kinetic! (Ebook). Shaker Verlag, Aachen.

Further reading

- Geotechnik mit Geokunststoffen*, product information of NAUE GmbH & Co. KG, Germany.
- TiO₂ Photocatalytic Membrane*, product information of Taiyo Kogyo Group, Japan.
- Ritter, A., 2007. Material world – advanced materials have many potential applications in design and architecture, both practical and futuristic. *Engineering* 248 (1), 56–57.
- Ritter, A., April 2008a. Advanced Materials – Neue Materialien für das Interior-Design. *medAmbiente* 2, 30–31.
- Ritter, A., 2008b. Innovative building materials: green smart materials – an international perspective. In: Lecture on the Event Green Building Fest in Toronto/Canada, 09.10.2008 invitation through: Sustainable Buildings Canada.
- Ritter, A., 2009a. Green smart materials in architecture and interior architecture. In: Lecture on the Event Green Building and Design Conference 2009 – Green Materials in Melbourne (Convention Centre)/Australia, 09.09.2009 invitation through: Centre for Design at RMIT University, Melbourne.
- Ritter, A., 2009b. Designing zero and plus energy buildings through the use of smart materials. In: Solar Architecture and Urban Planning – Conference Proceedings of the 4th Energy Forum, 02–04 December 2009, Bressanone/Italy. EF Economic Forum Ltd., Munich, Bozen.
- Ritter, A., 2009c. Progettare Edifici Zero Energy e Energy Plus utilizzando Materiali Intelligenti. In: Architettura & Urbanistica Solare – Documentazione, 4^o Energy Forum, 02–04 dicembre 2009, Bressanone/Alto Adige. EF Economic Forum Ltd., Munich, Bozen.
- Ritter, A., 2009d. Smart Materials – Der Einsatz von Materialien mit Wechseleigenschaften in der Architektur als ein Ansatz zur Lösung aktueller Klima- und Energieproblematiken. In: Lecture on the event Montagsgespräche – Positionen: Junge Architekten gesucht in the Domforum Köln, 12.14.2009 invitation through: Bund Deutscher Architekten (BDA), Cologne.
- Ritter, A., April 2010a. Powered by Nature: Energie- und materieautonome Räume. *medAmbiente* 2, 22–23.
- Ritter, A., June 2010b. Desarrollado por la naturaleza: zero and plus energy buildings mediante el uso de materiales inteligentes/powerd by nature: zero and plus energy buildings through

- the use of smart materials. In: European Conference on Energy Efficiency and Sustainability in Architecture and Planning/Jornadas Europeas sobre Eficiencia Energetica y Sostenibilidad en la Arquitectura y el Urbanismo – proceedings. Universidad del Pais Vasco (UPV/EHU), Espania.
- Ritter, A., 2010c. Powered by nature – Energie- und materieautonome Gebäude durch den Einsatz von Smart Materials und adaptiven Konstruktionen. In: Bauhaus.SOLAR Proceedings (incl. CD-ROM), 3. Internationaler Kongress Technologie – Design – Umwelt, 10–11 November 2010. Messe Erfurt.
- Ritter, A., 2011a. Materialet inteligjente ne arkitekture, interier dhe projektim. Ars Lamina, Skopje, Macedonia.
- Ritter, A., 2011b. Smart materials in architektur, innenarchitektur und design (in Serbian). Ars Lamina, Skopje, Macedonia.
- Ritter, A., 2012. Smart Building Systems – Innovative Energie- und Materiespeicher in der Architektur durch den Einsatz von Smart Materials, adaptiven und kinetischen Konstruktionen/Smart building systems – innovative energy and matter storage in architecture through the use of smart materials, adaptive and kinetic structures. In: Bauhaus. SOLAR Proceedings (incl. CD-ROM), 5. Internationaler Kongress Technologie – Design – Umwelt, 13–14 November 2012. Messe Erfurt.

Index

‘*Note:* Page numbers followed by “f” indicate figures, “t” indicate tables.’

A

Abrasion resistance, 121
Active carbon-coated polyester fabric, 361
Adaptive polymeric particles, 4–5
Aerodynamic optimization, 365–366
Alcedo atthis, 145–146
Anthraquinone sulfonic acid
(AQSA) — doped PPy, 114, 114f
Antimicrobial/antifouling coatings
 aldehyde compounds, 59
 antifouling, 60–61, 61f
 bio-based products, 59–60
 halogen compounds, 58–59
 metal-based antimicrobials, 58
 nitrogen compounds, 59
 phenolic compounds, 59
Antimicrobial finishing, 208–209
Antimicrobial textiles, 231–232
Antipathogen medications, 407
APGD. *See* Atmospheric pressure glow
 discharge (APGD)
Application procedures, microencapsulation
 technology, 194–199
 atmospheric plasma treatment,
 197–198
 chemical grafting, 195–196
 coating, 196–197
 conventional finishing treatment,
 194–195
 double-layered shell, 199
 electrostatic interactions, 198–199
 laminating, 197
 ultraviolet curing, 198
Architectural applications
 current trends in, 429–442, 432f
 exterior use and actuators, 449–450,
 449f–451f
 future trends, 443–447
 smart textiles, 444–447, 445f–446f

 interior use, 447–449
 smart-coated textiles, components and
 types of, 433–436, 434f–435f
 passive and active components,
 433–436, 434f–436f
 smart-coated energy-generating and
 exchanging textiles, 438–441,
 439f–441f
 smart-coated matter-exchanging textiles,
 441–442, 442f–443f
 smart-coated property-changing textiles,
 436–438, 436f–437f
Atmospheric pressure glow discharge
(APGD), 120
Atomic force microscopy (AFM), 121

B

Biomechanical sensing, 368–369
Biomimetic structural coloration
 characterization, 270–271, 270f
 photonic crystals, structural colors of,
 284–295
 application, 286–295
 concept, 284
 fabrication, 284–285
 structural color principles, 285–286,
 285f
thin-film interference
 electrostatic self-assembly, basics of,
 272–273
 multilayer interference, 272, 272f
 principle, 271–272, 271f–272f
 silica–polyethylenimine-coated
 surfaces. *See* Silica–polyethylenimine-
 coated surfaces
Bragg’s equation, 285–286
Breathable fabrics, 23–25
1,2,3,4-Butanetetracarboxylic acid (BTCA),
 249–251, 250f, 315, 403

- C**
- Carboxymethylation, 43
- CD. *See* Cyclodextrins (CD)
- Cellulose, 44
- Centexbel, 64–65
- Cetyltrimethylammonium bromide (CTAB), 312
- Chemical etching, 226
- Chemical processes
- interfacial polymerisation, 185–187, 187t–188t
 - in situ polymerisation, 187–189, 188t
 - suspension polymerisation, 189–191, 190t
- Chemical vapour deposition (CVD), 251
- Chitosan, 232
- γ -Chloropropyltriethoxysilane (CPTS), 302
- Ciprofloxacin, 410
- Coating methods, 93–97
- foam coating, 95
 - mechanical fibrillation, 94
 - melt-blown/hot melt technology, 96–97
 - mixture, solubilising one component in, 96
 - nanofibres, 97
 - point-bonding technology, 97
 - radio frequency/ion/UV and E beam radiation, 96
 - solvent extraction, 95–96
 - thermocoagulation, 95
 - wet coagulation process, 94–95
- Coating processes, 5
- future trends, 173–174
 - overview, 162–163
 - smart textiles, coating for, 167–173, 168f–169f, 171f
 - substrate and coating interactions, 160–162, 160f–161f
 - traditional processes, 163–167, 164f–167f
- Colored stains, self-cleaning of, 42
- Colour change technology, 204
- Comfort clothing
- functional finishing technology, 332
 - future trends, 348–349
 - physiological functions, 331
 - principles
 - active *versus* passive thermoregulation, 336–337, 338f
 - textile clothing, thermal comfort ability of, 334–336
 - thermal comfort, factors of, 333–334
 - wear comfort, general aspects of, 332–333
 - smart technology, 331
 - smart textile coatings, technologies for, 337–346
 - functions of, 346–348, 347f
 - phase change materials (PCM), 338–342, 341t
 - shape memory materials (SMM), 342–343
 - stimuli-responsive polymers, 343–346, 345t, 347f
- Conducting polymer actuators, 129–132, 131f–132f
- Conductive polymer coatings
- electrical degradation, 132–134, 134f
 - properties and applications
 - conducting polymer actuators, 129–132, 131f–132f
 - heated fabrics, 128–129, 129f–130f
 - microwave properties, 123–128, 126f–128f
 - soluble conducting poly(3-alkylpyrrole) polymers, 118–119, 118f–120f, 122f–123f
 - textile coating, 113–123
 - continuous vapor-phase polymerization, 116–117, 117f
 - solution polymerization, 113–116, 114f–115f
- Conductive yarns, 116
- Continuous vapor-phase polymerization, 116–117, 117f
- Conventional finishing treatment, 194–195
- Cooling effect, 358
- Corrosion inhibitor, 257–258, 258f
- Cosmetotextiles, 418–419
- Cross-linking method, 249–251, 250f
- Cross-linking netpoints, 17–18
- Cyclodextrins (CD)
- binding properties and applications
 - binding properties, 396–398, 397f
 - free form, applications in, 398–400, 398f
 - general applications, 405
 - synthesis and characteristics, 392–395, 393f–394f, 395t

- textile support, interaction with, 400–404, 401f, 401t, 402f–404f
 - toxicological properties, 396
 - cosmetotextiles, 418–419
 - insect repellent and insecticide textiles, 416–417, 417f
 - medical purposes, textiles for, 406–420
 - antiinflammatory textiles, 414–416, 414f–415f
 - antipathogen textiles, 406–414, 406f–408f, 411f
 - other smart opportunities, 419–420, 419f
- D**
- Dermizax NX[®], 362
 - Detachment process, 222–223
 - Diffusion process, 223
 - Dimethylformamide (DMF), 246
 - Double-layered shell, 199
 - Drag coefficient, 365
 - Durability-enhancing coatings, properties of textiles with
 - antibacterial and antifungal properties, 65–68, 66t–67t, 69t
 - Centexbel, 64–65
 - scratch resistance, 64–65, 65f
 - ultraviolet resistance, 68, 70f–71f
- E**
- Electrical conductivity, 368
 - Electromagnetic interference (EMI), 252–253
 - Electron–hole recombination, 49
 - Electrospun nanofibre coating application
 - corrosion inhibitor, 257–258, 258f
 - membrane coatings, 260–261
 - sensors, 258–260, 259f–260f
 - solid-phase microextraction, 255–257, 255f–257f
 - textile coatings, 261
 - Electrospun nanofibres, 260–261
 - Electrostatic interactions, 198–199
 - Energy-dispersive spectroscopy (EDS), 46, 47f
 - Environmentally responsive/stimuli-responsive materials
 - pH responsive, 229
 - temperature responsive, 230
 - Ergonomic wear comfort, 333, 356
- Ethylene-bis(octadecyl dimethyl ammonium chloride) (EBODAC), 308
 - External stimuli, structural-colored sensors by, 149–153
 - humidity, 149, 151f
 - light, 153, 154f
 - pH, 153, 153f
 - solvents, 149, 150f
 - stress, 151–153, 152f
 - temperature, 151, 152f
- F**
- Fabric coating, 358
 - Finishing, 1
 - Flame retardant
 - coating with, 203–204
 - microencapsulation, 203
 - Fluorinated-decyl polyhedral oligomeric silsequioxane (FD-POSS), 23
 - Fluoroalkyl silane (FAS), 23
 - Fourier transform infrared (FTIR) spectroscopy, 410
 - Functional coating, 181–182
 - Functional sportswear, 361
- G**
- Gemini quaternary ammonium salt, 312
 - Gravitational sedimentation, 295
- H**
- Heated fabrics, 128–129, 129f
 - Heating effect, 358
 - High-resolution electron microscopic image (HRTEM), 39
 - Humidity, 149, 151f
 - Hybrid sols containing triethoxysilane (HTEOS), 302
 - Hydrogel active coating application, 4
 - Hydrophilic breathable coatings, 86–87, 87f, 88t
 - Hydrophilicity, 227–229
 - Hydrophobic surface, 18–19
- I**
- Immobilised growth factors (IGFs), 232
 - Infrared, 61f, 62–64
 - Innovative swimwear, 366
 - Insect repellent, 207–208
 - In situ polymerisation, 187–189, 188t

- Insulation, 336
Intelligent materials, 2
Interfacial charge transfer mechanism, 51, 51f
Interfacial polymerisation, 185–187,
187t–188t
Intrinsically conductive polymers (ICPs),
252–253
Ion-enhanced energetic etching, 226
Ion-enhanced protective etching, 226
Ionisation reactions, 222–223
- L**
Laminating, 197
Light scattering, 144, 153, 154f
Light-sensitive memory polymer, 12–13
Liquid crystalline elastomers (LCEs), 14
Lower critical solution temperatures
(LCST), 230
- M**
Membrane coatings, 260–261
Memory polymer coatings
classifications of, 16–18
defined, 12–18
functions
aesthetic surface, 25–28, 26f–27f
breathability, 23–25, 25f
self-healing liquid repellent, 21–23, 24f
smart wettability control, 18–21, 20f,
22f
liquid crystalline elastomers (LCEs), 14
nematic/smectic phase, 14–16
reversible supramolecular units, 16
structures and mechanisms, 12–16,
12t–13t
supramolecular switches, 16
Methyltriethoxysilane (MTEOS), 302
Microcapsules, 339
Microencapsulation technology, 6
application procedures, 194–199
atmospheric plasma treatment, 197–198
chemical grafting, 195–196
coating, 196–197
conventional finishing treatment,
194–195
double-layered shell, 199
electrostatic interactions, 198–199
laminating, 197
ultraviolet curing, 198
background, 179–180
benefits, 183–184
compatibility, 183–184
controlled release, 183
protection and shelf life enhancement,
183
chemical processes
interfacial polymerisation, 185–187,
187t–188t
in situ polymerisation, 187–189, 188t
suspension polymerisation, 189–191,
190t
defined, 179–181, 184–194, 185f
generalities, 180–181
functional coating, 181–182
objective, 182
other methods, 193–194, 193t
physicochemical processes
phase coacervation, 191–192,
191t–192t
solvent evaporation, 192–193,
192t
textile substrates containing microcapsules,
smart end uses of, 199–209
antimicrobial finishing, 208–209
flame retardant. *See* Flame retardant
insect repellent, 207–208
printing/dyeing. *See* Printing/dyeing
thermal comfort and cooling effects. *See*
Thermal comfort, cooling effects
well-being. *See* Well-being
Micropatterns, 18–19
Microporous coatings, 85–86, 86f
Microwave properties, 123–128,
126f–128f
Molecular design method, 14
Monochlorotriazinyl (MCT), 396
Multilayer films, 272
Multilayer interference, 141, 272
- N**
Nanopatterns, 18–19
Nanotechnology-based coating, 5
future trends, 261–263, 262f
nanofibre coating, electrospinning,
255–261
electrospun nanofibre coating
application. *See* Electrospun nanofibre
coating application

- size uniformity, 243
- types and classifications
- cross-linking method, 249–251, 250f
 - sol–gel method, 244–248, 245f
 - thin-film deposition technique. *See* Thin-film deposition technique
- Natural photonic materials
- colloidal crystals, photonic crystals based
 - fabrication on, 138–139, 138f
 - external stimuli, structural-colored sensors by, 149–153
 - humidity, 149, 151f
 - light, 153, 154f
 - pH, 153, 153f
 - solvents, 149, 150f
 - stress, 151–153, 152f
 - temperature, 151, 152f
 - photonic materials, typical optical process of, 137
 - textile coatings
 - characterization of, 139
 - photonic structures brought to, 147–148, 148t, 149f
 - types and classifications, 139–147
 - biological photonic crystals, 143–144, 143f
 - multilayer interference, 140f–142f, 141–143
 - noniridescent colorations, 144–146, 145f
 - structural color mixing, 146–147, 146f–147f
 - thin-film interference, 139–141, 140f, 140t
- Nematic phase, 14–16
- N*-methylolacrylamide (NMA), 408
- O**
- Octyltriethoxysilane (OTEOS), 302
- Oleophobicity, 227–229
- Organization for Economic Co-operation and Development (OECD), 396
- P**
- Papilio blumei*, 146–147
- Papilio ulysses*, 146–147
- Paracheirodon innesi*, 272
- Pavo muticus*, 143–144
- Penetration pressure tests, hydrostatic pressure test, 99–100, 100f
- Phase change materials (PCM), 338–342, 341t
- Phase change materials, commercial applications of, 201–202
- Phase coacervation, 191–192, 191t–192t
- Photocatalytic TiO₂-modified cotton, 43
- Photochromism, textile applications of, 205–206
- Photonic crystals, structural colors of, 284–295
 - application, 286–295
 - colloidal microspheres, self-assembly of, 287–289, 288f–290f
 - monodisperse colloidal microspheres, preparation and characterization of, 286, 287f–288f
 - textile fabrics, color properties of, 290–295, 291f–294f, 296f
 - concept, 284
 - fabrication, 284–285
 - structural color principles, 285–286, 285f
- Photoreponsive hydrogels, 18
- Physical vapour deposition (PVD), 251
- Physicochemical processes
 - phase coacervation, 191–192, 191t–192t
 - solvent evaporation, 192–193, 192t
- Plasma ablation
 - chemical etching, 226
 - ion-enhanced energetic etching, 226
 - ion-enhanced protective etching, 226
 - sputtering, 225
- Plasma-deposited films, 224
- Plasma surface treatments
 - applications, 227–235
 - antibiofouling, 233, 234f
 - antimicrobial textiles, 231–232
 - biomedical application, textiles for, 230–231
 - enhancing dyeability, 233–235
 - environmentally responsive/stimuli-responsive materials, 229–230
 - hydrophilicity and oleophobicity, 227–229, 228f
 - tissue regeneration therapeutics, growth factor immobilisation for, 232–233, 233f

- Plasma surface treatments (*Continued*)
 gas pressure, 221
 corona discharge, 221
 glow discharge, 221
 plasma–substrate interactions, 223–227
 functionalisation, 226–227
 plasma ablation. *See* Plasma ablation
 polymerisation, 224–225, 224f
 principles, 222–223
 ionisation and detachment, 222–223
 recombination/detachment and diffusion, 223
- PNIPAAm, 21
- Poly(acrylic acid) (PAA), 230, 260
- Poly(caprolactone) (PCL), 14
- Poly(*N*-isopropyl acrylamide) (PNIPAM), 230
- Poly(sodium 4-styrene-sulfonate) (PSS), 311
- Poly(styrene sulfonate) (PSS), 310
- Poly(styrene-methyl methacrylate-acrylic acid), 21
- Polydimethylsiloxane (PDMS), 257
- Polyester fabric contact angle, 361
- Poly(3-alkylpyrrole) polymers, 118–119
- Polytetrafluoroethylene (PTFE) membrane, 362
- Polyurethane (PU) microporous membranes, 362
- Polyvinylidene fluoride (PVDF), 129–131
- Porous membranes, 260
- Printing/dyeing
 colour change technology, 204
 photochromism, textile applications of, 205–206
 thermochromism, textile application of, 204–205
- Protective clothing
 body armor application, smart coating for, 376–380
 bullet-resistant body armor, 376–377
 stab-resistant body armor, 377–380, 378t–379t
 forefighter protective clothing, smart coating for, 383–385
 future trends, 386
 hazardous material (HAZMAT), 375
 hazardous material protective clothing, smart coating for, 380–382
 health care protective clothing, smart coating for, 382–383
 National Institute of Justice (NIJ), 376
 shear thickening fluid (STF), 376–377
- Psychological wear comfort, 333
- Q**
 Quartz crystal microbalance (QCM), 258–260
- R**
 Recombination process, 223
 Redox reactions, 42
 Retroreflective microbeads, 88
 Reversible supramolecular units, 16
- S**
 Scanning electron microscopy (SEM), 142–143, 230–231, 280
 Scratch resistance, 64–65, 65f
 Segmented polyurethane (SMPU), 342
 Self-cleaning processes
 artificial fibers, colloidal titanium dioxide of
 photocatalytically modified titanium dioxide artificial textiles, surface characterization of, 39–40, 40f–41f
 polyamide/polyester and nylon fabrics, 37–39, 38f–39f
 faster stain discoloration, enhanced copper-binary oxides leading to, 46–51, 48f, 50f–51f
 mild environmental sunlight-activated processes, 35
 natural fibers, colloidal titanium dioxide of, 41–43, 42f–43f
 silicon dioxide-protective layers, titanium dioxide-modified by, 45–46, 46f–47f
 surfaces pretreatment and functionalization, radiofrequency plasma and ultraviolet-C, 36–37, 36f
 titanium dioxide clusters, cotton self-cleaning by, 43–45, 44f–45f
- Self-healing liquid repellent, 21–23
 Self-healing property, 23
 Self-healing textile coatings, 55–57, 56f–57f, 57t
- Sensors, 258–260, 259f–260f
 Shape memory materials (SMM), 342–343

- Shape memory polymers (SMPs), 88–89, 89f–90f, 332
- moisture management hydrophilic coatings, 360–361
 - moisture responsive shape memory polymer, 359–360, 360f
 - temperature responsive shape memory polymers, 359
- Silica-polyethylenimine-coated surfaces
- optical properties, 273–276, 273f–275f, 277f, 278t
 - polyester fabrics, property evaluation of, 283–284, 283f
 - polyester fabric surface, self-assembly process on, 281–283, 282f
 - structural colors, generating mechanism of, 276–281
- Simulated rain tests
- bundesmann rain tester, 99, 100f
 - impact penetration, 99
 - rain test, 98–99, 99f
 - spray test, 98, 98f
- Skin sensorial wear comfort, 333
- Smart breathable coatings
- applications, 104–106, 104f, 105t
 - breathable fabrics, 84
 - breathable garment, construction of, 84
 - classification, 81, 82f
 - coated textile materials, 83–84
 - coating methods, 93–97
 - foam coating, 95
 - mechanical fibrillation, 94
 - melt-blown/hot melt technology, 96–97
 - mixture, solubilising one component in, 96
 - nanofibres, 97
 - point-bonding technology, 97
 - radio frequency/ion/UV and E beam radiation, 96
 - solvent extraction, 95–96
 - thermocoagulation, 95
 - wet coagulation process, 94–95
 - impermeable coated fabrics, 83–84, 83t
 - materials for, 90–92, 92f
 - suitable coating material, choice of, 84–85
 - testing and evaluation, 97–104
 - water penetration and absorption, resistance to. *See* Water penetration and absorption, resistance to
 - water vapour permeability, 101–104
 - wind resistance, 100–101
- waterproof breathable material, development of, 82–83
- waterproof/water-repellent coatings, 82
- working principles of, 85–90
- hydrophilic breathable coatings, 86–87, 87f, 88t
 - microporous coatings, 85–86, 86f
 - retroreflective microbeads, 88
 - temperature-responsive breathable coating. *See* Temperature-responsive breathable coating
- Smart coatings, types and classifications of, 55–64
- antimicrobial and antifouling coatings. *See* Antimicrobial/antifouling coatings
 - infrared, 61f, 62–64
 - self-healing textile coatings, 55–57, 56f–57f, 57t
 - ultraviolet, 62, 63f, 63t
- Smart sols contain quaternary ammonium salts, 313
- Smart textile coatings, technologies for, 337–346
- functions of, 346–348, 347f
 - phase change materials, 338–342, 341t
 - shape memory polymers, 342–343
 - stimuli-responsive polymers, 343–346, 345t
- Smectic phase, 14–16
- SMPU. *See* Segmented polyurethane (SMPU)
- Sodium hypophosphate (SHP), 249–250
- Sol-gel method, 244–248, 245f
- Sol-gel process
- antibacterial finishing, 312–316
 - antibacterial cationic hybrid sol, 312–313, 313f
 - metallic oxide hybrid sol, antibacterial activity of, 313–316, 314f, 314t–315t, 316f
 - dyes and fixation property, solegel silica doped with, 318–319
 - fiber and anti-ultraviolet property, layer-by-layer self-assembly deposition on, 310–311, 311f
 - hydrophobic and oleophobic modifications, 302–307

- Sol-gel process (*Continued*)
 hydrophobic silane coupling agent
 hybrid sol modification, 302–304
 silane coupling agent hybrid sol,
 oleophobic modifications with,
 304–307, 305t, 306f–307f
 smart silane coupling agent hybrid sol,
 color fixation using, 316–322, 317f,
 318t
 self-assembled deposition, color fixation
 analysis of, 319–322, 322f
 titanium dioxide hybrid sol, anti-ultraviolet
 property using, 307–311
 properties, 308–310, 309f
- Solid-phase microextraction (SPME),
 255–257, 255f–257f
- Soluble conducting poly(3-alkylpyrrole)
 polymers, 118–119, 118f–120f,
 122f–123f
- Solution polymerization, 113–116,
 114f–115f
- Solvents, 149, 150f
 evaporation, 192–193, 192t
- Spin-coating method, 19
- SPME. *See* Solid-phase microextraction
 (SPME)
- Sportswear
 comfort enhancing
 phase changing material (PCM),
 357–358, 357f
 shape memory polymers (SMPs). *See*
 Shape memory polymers (SMPs)
 health and motion monitoring, smart
 textiles for, 368–369
 innovative materials, 355
 performance enhancement,
 smart coating for
 skiing/cycling, drag reduction in,
 367–368
 sports, drag in, 365–366
 swimwear, drag reduction in, 366, 367f
 protection, smart coating to
 microorganisms, 364–365
 ultraviolet radiation, 363–364
 waterproof and breathable coating,
 361–363
 smart coating and functional requirements,
 356
- Sputtering, 225
- Stain discoloration, mechanism of, 38
- Staphylococcus aureus*, 364
- Starch degradation, 392
- Stimuli-responsive polymers (SRPs), 332,
 343–346, 345t, 347f
- Stress, 151–153, 152f
- Surface modification, 233–235
- Surface resistivity, 125–126
- Suspension polymerisation, 189–191, 190t
- T**
- Temperature, 151, 152f
- Temperature-responsive breathable coating
 biomimetics, fabrics based on, 89–90,
 91f
 shape memory polymers, 88–89,
 89f–90f
- Temperature-sensing fabrics, 369
- Temperature-sensitive membranes, 230
- Temperature-sensitive polymeric gels, 18
- Tetraethyl orthosilicate (TEOS), 244–245
- Textile coatings, 113–123, 261
 continuous vapor-phase polymerization,
 116–117, 117f
 solution polymerization, 113–116,
 114f–115f
- Textile finishing, 396
- Textiles durability
 applications
 architectural fabrics, new generation of,
 71–72, 72f
 protective clothing, 72–74, 73f, 74t
 securing cargo, 74–75
 durability-enhancing coatings, properties of
 textiles with
 antibacterial and antifungal properties,
 65–68, 66t–67t, 69t
 Centexbel, 64–65
 scratch resistance, 64–65, 65f
 ultraviolet resistance, 68, 70f–71f
 future trends, 75–76
 smart coatings, types and classifications of,
 55–64
 antimicrobial and antifouling coatings.
 See Antimicrobial/antifouling coatings
 infrared, 61f, 62–64
 self-healing textile coatings, 55–57,
 56f–57f, 57t
 ultraviolet, 62, 63f, 63t

- Textile substrates containing microcapsules,
199–209
antimicrobial finishing, 208–209
flame retardant. *See* Flame retardant
insect repellent, 207–208
printing/dyeing. *See* Printing/dyeing
thermal comfort and cooling effects. *See*
Thermal comfort, cooling effects
well-being. *See* Well-being
- Thermal comfort, cooling effects
background, 200–201
microcapsules for, 202
phase change materials, commercial
applications of, 201–202
textiles, performance in, 201
- Thermochromism, textile application of,
204–205
- Thermophysiological wear comfort, 333
- Thin-film deposition technique
ion implantation, 254
physical vapour deposition, 251, 252f
sputter coating, 253–254
vacuum evaporation, 252–253
- Thin-film interference
electrostatic self-assembly, basics of,
272–273
multilayer interference, 272, 272f
principle, 271–272, 271f–272f
silica–polyethylenimine-coated surfaces.
See Silica–polyethylenimine-coated
surfaces
- Titanium dioxide (TiO₂) particles, 308
- Titanium tetraisopropoxide (TTIP),
244–245
- Traditional optical methods, 140
- Traditional textile coatings, 1
- Transmission electron microscopy (TEM),
142–143, 142f, 411–412
- U**
Ultraviolet, 62, 63f, 63t
curing, 198
UV radiation transmittance (URT),
308–310
- V**
Vertical deposition, 295
- W**
Water contact angle (WCA), 250–251
Water penetration/absorption, resistance to
penetration pressure tests
hydrostatic pressure test, 99–100,
100f
simulated rain tests
bundesmann rain tester, 99, 100f
impact penetration, 99
rain test, 98–99, 99f
spray test, 98, 98f
Waterproofing, 361–362
Water vapor permeability (WVP),
23–25
cup method, 101–102, 102f
desiccant inverted cup method, 102
sweating guarded hot plate method,
102–104, 103f
Well-being
aromatherapy, 206–207
dermocosmetics, 206
Wrinkles, 18–19
- X**
X-ray diffraction imaging (XRD), 39–40
X-ray photoelectron spectroscopy (XPS), 36